Dissection of the differential mechanisms of apoptosis used during B cell maturation

Natalie Annis Carter

A thesis submitted for the degree of Doctor of Philosophy at the University of Glasgow

Faculty of Biomedical and Life Sciences

Submitted: December 2005

ProQuest LLC.
789 East Eisenhower Parkway
P.O. Box 1346
Ann Arbor, MI 48106 – 1346

Summary

Ligation of the B cell receptor (BCR) on B lymphocytes results in differential biological outcomes depending on the maturation state of the cell. Thus, mature B lymphocytes become activated and proliferate (clonal expansion) in response to BCR crosslinking, whilst immature B cells either become unresponsive, alter the specificity of their BCR, or undergo apoptosis (clonal deletion). Furthermore, mature B cells can be induced to undergo growth arrest and apoptosis following coligation of the BCR and FcγRIIb by immune complexes during negative feedback of B cell responses. The precise molecular events downstream of BCR signalling that are responsible for these distinct outcomes remain to be established. This study has focused upon identifying the important signalling mechanisms linking BCR ligation with regulation of the cell cycle and induction of apoptosis in immature and mature B lymphocytes.

The murine B cell line WEHI 231 is widely used as a model for clonal deletion of immature B lymphocytes. This is because it has the cell surface phenotype of an immature B lymphocyte, and as such responds to BCR ligation by undergoing growth arrest and apoptosis. Moreover, WEHI 231 cells can be rescued from BCR-mediated apoptosis by co-engagement of CD40, mimicking T cell help. Such BCR-mediated apoptosis has previously been associated with both mitochondrial translocation and activation of PLA_2 and a loss of mitochondrial membrane integrity. This study extended these findings by identifying that the product of PLA_2, arachidonic acid, acts as the causal metabolite in the initiation of such BCR-mediated apoptosis. Furthermore, it demonstrated that the metabolism of arachidonic acid can provide a dynamic switch from apoptotic to proliferative signalling. For example, ligation of the BCR leads to the build up of arachidonic acid which leads to disruption of the mitochondrial membrane potential (MMP) and hence apoptosis. Whereas, in contrast to this, co-engagement of CD40 leads to the induction of COX2 and hence the metabolism of arachidonic acid to prostaglandin E_2 (PGE_2) which promotes proliferative signalling. Therefore arachidonic acid metabolism acts as a dynamic, molecular switch from apoptotic to proliferative signalling.

This study also demonstrated that upregulation of $BclX_L$ (as induced by CD40) acts to protect from arachidonic acid-mediated loss of mitochondrial membrane integrity and apoptosis. Furthermore, co-engagement of CD40 was found to increase the association of Bak with $BclX_L$ indicating that $BclX_L$ may act to sequester the pro-apoptotic Bak and hence inhibit the opening of the mitochondrial permeability pore. These data suggest that modulation of Bcl-2 family member induction and function is integral to such BCR-mediated apoptosis and T cell-derived rescue. In addition, it has been demonstrated that upregulation of $BclX_L$ can additionally function to downmodulate BCR-induced calcium signals providing an additional mechanism for the downregulation of $mPLA_2$ activation and hence consequent apoptotic signalling.

Previous work in this laboratory had highlighted the importance of dynamic ERK signalling in both proliferation and apoptosis of immature B cells. Thus, during BCR-mediated growth arrest and apoptosis the sustained ERK signalling, found in proliferating WEHI 231 cells, is abrogated. Therefore a causal role for such sustained ERK signalling in immature B cell proliferation was investigated by manipulating endogenous ERK activation by expressing constitutively active RasV12 constructs in WEHI 231 cells. Such RasV12 expressing WEHI 231 cells were refractory to both BCR-mediated growth arrest and apoptosis for up to 24 h emphasising the importance of the uncoupling of ERK signalling in BCR-mediated cell cycle arrest and apoptosis. In an attempt to identify key regulatory elements involved, the role of SHIP and Dok in targeting the ERKMAPK pathway was explored by expressing dominant negative constructs. However, these constructs did not provide release from BCR-mediated apoptosis.

Finally, as BCR-stimulated PKC activity is widely established to be suppressed in immature relative to mature B cells and pharmacological activation of PKC can rescue BCR-mediated apoptosis of WEHI 231 cells, it was decided to investigate the effects of expressing constitutively active and kinase dead constructs of various PKC isoforms on BCR-mediated apoptosis and CD40-mediated rescue of WEHI 231 cells. Rather disappointingly, although expression of such constructs afforded some protection against BCR-mediated growth arrest and apoptosis, all of the constitutively active and kinase dead

forms of PKC α, δ, ε and ζ provided similar responses. However the fact that these constructs could rescue WEHI 231 cells from BCR-mediated apoptosis may imply that regulation of PKC activity may be involved in BCR-mediated growth arrest and apoptosis.

By contrast to immature B cells, ligation of the BCR on mature B cells results in growth and proliferation. Previous studies had indicated that ERKMAPK and PI-3 kinase cascades are associated with early BCR-mediated proliferative signals. This study has now demonstrated that such ERK and PI-3 kinase signals are maintained for up to 48 h post BCR-ligation and are important for both survival and proliferation. Moreover, it has shown that PI-3 kinase provides a pro-survival signal by activation of AKT and hence maintenance of a phospho-Bad signal which acts to sustain mitochondrial homeostasis. By contrast, ERK signalling appears to act at least in part, by suppressing p53 induction and hence, growth arrest and apoptosis.

The data in this thesis have also demonstrated that negative feedback inhibition, by immune complex coligation of the BCR and FcγRIIb, not only induces cell cycle arrest but also induces an apoptotic phenotype. This is the only study to date that has attempted to characterise this form of apoptosis. It has been demonstrated that the dissipation of MMP, and hence the breakdown of mitochondrial membrane integrity is essential for such FcγRIIb-mediated apoptosis. This appears to involve FcγRIIb acting to inhibit PI-3 kinase signalling, resulting in the sequestration of the anti-apoptotic $BclX_L$ by Bad, allowing for the opening of the permeability transition pore. Furthermore, caspase 8 activation is central to this form of apoptosis. Caspase 8 acts upstream of the loss of mitochondrial membrane integrity and is proximal to the activation of executioner proteases including caspase 3, cathepsin B and calpains. Caspase 8 is also likely to be involved in the activation of Bid which is shown to be upregulated by FcγRIIb signalling, although no clear evidence is presented that this represents the active truncated form, tBid. Finally, the transcription factor p53 is also activated by FcγRIIb coligation and this involves the inhibition of ERKMAPK which appears to act, at least in part, to suppress p53 induction. p53 is known to act like a pro-apoptotic Bcl-2 family member or

may mediate its effects via the upregulation of Bid, Bak or Bax expression. Collectively, the interaction of these pro-apoptotic signalling elements induced by FcγRIIb results in cytochrome c release due to the loss of mitochondrial membrane integrity, activation of executioner proteases and commitment of the cell to apoptosis.

Declaration

This work represents original work carried out by the author and has not been submitted in any form to any other University.

Natalie Annis Carter
December 2005

"Life is the shape it is for a reason and when you see how things really are, all the waste falls away, and what you are left with is beauty."

Rosalind Elsie Franklin

1920- 1958

Acknowledgements

First, and foremost, I would like to thank my supervisor, Professor Maggie Harnett. Her help and support has been invaluable in both the research undertaken and the writing of this manuscript. I have been given all the assistance I needed and furthermore, been allowed the freedom to take this project in the direction I am interested in. The 4 years I have spent in Professor Harnett's lab have been extremely enjoyable and have given me the inspiration to pursue a career in science. I would also like to thank all the members of the Harnett and Michie labs- past and present- for their friendship and practical expertise. I would particularly like to thank Dr Derek Blair, for teaching me how to isolate and work with mature B cells, and Dr Catriona Ford for imparting all of her Western Blotting knowledge. I would also like to thank Dr Andres Floto for all of his help in measuring cytosolic calcium levels and Dr John M^{c}Carron for allowing me to use his equipment for the real time calcium imaging.

Finally, I would like to thank my parents whose unwavering belief in me has maintained my sanity whilst writing this manuscript.

Contents

	Page
Summary	ii
Declaration	vi
Acknowledgements	viii
List of contents	ix
List of figures	xvi
List of Tables	xxiv
Abbreviations	xxv

Chapter 1: Introduction

1.1 The Humoral Immune System	1
1.2 B cell Development	2
1.2.1 B cell Development	2
1.2.2 Pro-B and Pre-B cells	3
1.2.3 Immature B cells	5
1.2.4 Mature B cells	6
1.3 B cell Signalling	
1.3.1 Initiation of BCR signalling	7
1.3.2 Cell Signalling cascades activated by the BCR	9
1.3.2.1 The PI-3 kinase pathway	9
1.3.2.2 The RasMAPKinase pathway	12
1.3.2.3 The ERK1/2 Module	13
1.3.2.4 The p38 Module	14
1.3.2.5 The JNK Module	14
1.3.2.6 The PLC pathway	15
1.3.2.6.1 PLC generates DAG and IP_3	15
1.3.2.6.2 The PKC family	15
1.3.2.6.3 Isoform specific activation of PKC	16
1.3.2.6.4 The generation of Calcium	17
1.3.2.7 p53	18
1.3.2.8 NF-κB signalling	19
1.4 Cell Cycle and Apoptosis	20
1.4.1 The Cell Cycle	20

1.4.2 Apoptosis: There are many routes to cell death 22
1.4.2.1 Caspase-mediated apoptosis 24
1.4.2.2 Caspase 8 24
1.4.2.3 Caspase 9 25
1.4.3 The Bcl-2 family 26
1.4.3.1 Bcl-2 family members can form channels in intracellular membranes 27
1.4.3.2 Bcl-2 family members can interact and sequester other Bcl-2 family members 27
1.4.3.3 Bcl-2 family members may interact with other cell signalling proteins 28
1.4.3.4 Bcl-2 family members have anti-oxidant properties 28
1.4.3.5 Activation of Bax and Bak 29
1.4.3.6 The BH3-only members modulate apoptosis 30
1.4.3.6.1 The BH3-only modulator Bid 31
1.4.3.6.2 The BH3-only enabler Bad 32
1.5 Alternative executioner Proteases 34
1.5.1 Cathepsins 34
1.5.2 Calpains 36
1.6 Negative feedback inhibition in mature B cells 38
1.6.1 Negative feedback inhibition is mediated by FcRs 38
1.6.2 Signalling mechanisms underlying FcγRIIb-mediated growth arrest and apoptosis 40
1.6.2.1 SHP1/2 40
1.6.2.2 SHIP 41
1.7 Aims and Objectives of thesis 44

Chapter 2: Materials and Methods

2.1 Cell Culture, Antibodies and Inhibitors 66
2.2 Animals 67
2.3 Purification of murine splenic B cells 67
2.4 Cell Lines 68
2.4.1 WEHI 231 Immature B cell line 68
2.4.2 BclX_L WEHI 231 cells 68
2.4.3 Retroviral transfection of WEHI 231 cells with SHIP and Dok 69

2.4.4 Generation of PKC, Ras and ΔMEKK3 mutants 69
2.5 Purification of antibodies from hybridoma cell lines 70
2.6 DNA synthesis assay 70
2.7 Flow Cytometry 71
2.7.1 Flow cytometric analysis of cell cycle and DNA content 71
2.7.2 Cell Cytometric analysis of MMP 71
2.7.2.1 $DiOC_6$ 71
2.7.2.2 JC1 72
2.7.3 Cell Cytometric analysis of caspase activation 72
2.7.4 Flow cytometric analysis of cell proliferation by CFSE 73
2.8 Western Blotting 73
2.8.1 Cell stimulation and whole cell lysate preparation 73
2.8.2 Immunoprecipitation 74
2.8.3 Gel electrophoresis 74
2.8.4 Western Blot Analysis 75
2.8.5 Stripping Western Blots 75
2.9 DNA analysis using DAPI staining 75
2.10 Fast Activated cell based ELISA (FACE) 76
2.10.1 Plating out for the cell based assay 76
2.10.2 Addition of primary and secondary antibodies 76
2.10.3 Colorimetric reaction 77
2.11 TransAM Nuclear Transcription Factor ELISA 77
2.11.1 Nuclear Extraction 77
2.11.2 TransAM ELISA assay 78
2.12 Cytochrome c Function ELISA 78
2.12.1 Preparation of cytosolic and mitochondrial fractions 78
2.12.2 Cytochrome c ELISA procedure 79
2.13 Calcium Imaging and Measurements 80
2.13.1 Real time recordings of single WEHI 231 cells 80
2.13.2 Measurement of cytosolic calcium in WEHI 231 populations 80
2.14 Supplier's addresses 82

Chapter 3: Dissection of the signalling mechanisms involved in BCR induced growth arrest and apoptosis and CD40 mediated rescue in the immature B cell line WEHI 231

3.1 Introduction 91

3.1.1 WEHI 231: a good model for immature B cells 91

3.1.2 ERKMAP kinase acts as an essential regulator of both proliferation and apoptosis in WEHI 231 cells 91

3.1.3 Ras acts to modulate both the ERKMAP kinase and PI-3 kinase cascades 93

3.1.4 Dok 95

3.1.5 SHIP 96

3.1.6 The PKC family 97

3.1.6.1 The Importance of the PKC family in B lymphocytes 97

3.1.6.2 PKC α 98

3.1.6.3 PKC β 98

3.1.6.4 PKC δ 99

3.1.6.5 PKC ε 101

3.1.6.6 PKC ζ 102

3.2 Aims and Objectives 103

3.3 Results 105

3.3.1 Crosslinking of the BCR in WEHI 231 cells leads to growth arrest and apoptosis 105

3.3.2 Ligation of the BCR and CD40 simultaneously leads to increased cell survival and proliferation 106

3.3.3 Bcl-2 family members are regulators of both anti-Ig –induced apoptosis and anti-CD40-mediated rescue 107

3.3.4 Overexpression of $BclX_L$ can protect from either anti-Ig or arachidonic acid induced apoptosis however it cannot overcome growth arrest induced by these stimuli 110

3.3.5 Is BCR-stimulated apoptosis in WEHI 231 cells dependent on the activation of PLA_2? 111

3.3.6 Anti-Ig stimulated growth arrest and apoptosis in WEHI 231 cells is dependent on the generation of arachidonic acid 112

3.3.7 Overexpression of $BclX_L$ protects the cells from arachidonic acid-induced dissipation of the MMP and resultant apoptosis 113
3.3.8 BCR-induced calcium release is decreased in WEHI 231 $BclX_L$ cells as compared to wild type WEHI 231 cells 113
3.3.9 Ligation of the BCR on WEHI 231 cells induces a cellular calcium oscillation 115
3.3.10 The constitutively active Ras mutations rescue cells from growth arrest at 24 hours 116
3.3.11 The Ras V12 mutation increases apoptosis 48 h post BCR ligation 118
3.3.12 Constitutively active Ras mutants have a protective effect on the BCR-induced dissipation of the MMP in WEHI 231 cells 119
3.3.13 The ΔMEKK3 mutant increases growth arrest in response to anti-Ig 120
3.3.14 The mechanism of Ras V12 and ΔMEKK3 rescue from BCR-induced apoptosis involves AKT activation 121
3.3.15 Expression of the Dok PH/PTB domain does not protect from anti-Ig induced growth arrest 122
3.3.16 Expression of SHIP CI and SHIP SH2 constructs does not rescue cells from anti-Ig induced growth arrest 124
3.3.17 Downregulation of active SHIP results in an alteration of the caspase 3 activation profiles 124
3.3.18 Transfection of WEHI 231 cells with PKC mutants 125
3.3.19 Effect of PKC α CAT and KR expression and activation on anti-Ig induced growth arrest in WEHI 231 cells 126
3.3.20 Effect of PKC α CAT and KR expression on anti-Ig induced apoptosis and anti-CD40 mediated rescue in WEHI 231 cells 126
3.3.21 PKC α CAT and KR expression provide protection from anti-Ig induced dissipation of the MMP 126
3.3.22 Effect of PKC δ expression and activation on anti-Ig induced growth arrest and apoptosis in WEHI 231 cells 128
3.3.23 PKCδ CAT and KR WEHI 231 cells are rescued from anti-Ig induced dissipation of the MMP 129

3.3.24 Effect of PKCε CAT and KR expression on anti-Ig mediated growth arrest and apoptosis in WEHI 231 cells 130
3.3.25 Effect of PKC ζ CAT and KR expression on anti-Ig mediated growth arrest and apoptosis in WEHI 231 131
3.3.26 Differential expression and activation of PKCs leads to altered expression of pro-apoptotic Bcl-2 family members 132
3.4 Discussion 134
3.4.1 $BclX_L$ mediates WEHI 231 rescue from BCR-stimulated PLA_2 mediated apoptosis and dissipation of the MMP 134
3.4.2 Calcium signalling may be used to induce PLA_2 activation during BCR-mediated apoptosis and is downregulated following $BclX_L$ overexpression 136
3.4.3 Ligation of the BCR induces the expression of pro-apoptotic Bcl-2 family members whereas CD40 engagement induces the expression of anti-apoptotic Bcl-2 family members and sequestration of pro-apoptotic Bcl-2 family members 138
3.4.4 Constitutive activation of the RasERKMAPK pathway can provide protection from BCR-induced growth arrest and apoptosis at 24 h 139
3.4.5 Constitutive activation of the RasERKMAPK pathway can enhance BCR-induced growth arrest and apoptosis at 48 h 141
3.4.6 Potential roles for the PKC family in both BCR-induced growth arrest and apoptosis and CD40-mediated rescue in WEHI 231 cells 143
3.4.6.1 PKC α 143
3.4.6.2 PKC δ 146
3.4.6.3 PKC ε 146
3.4.6.4 PKC ζ 147
3.4.7 Concluding Remarks 149

Chapter 4: Signalling mechanisms underlying FcγRIIb mediated growth arrest and apoptosis during negative feedback inhibition of B cell activation

4.1 Introduction 205
4.1.1 FcγRIIb signalling negatively regulates BCR signalling in mature B lymphocytes 205

4.1.2 FcγRIIb antagonises the action of PI-3 kinase 206
4.1.3 FcγRIIb can reduce BCR-stimulated calcium mobilization 207
4.1.4 FcγRIIb downmodulates the activation of the RasERKMAPK pathway 208
4.1.5 FcγRIIb can induce apoptosis 208
4.2 Aims and Objectives 209
4.3 Results 211
4.3.1 Ligation of the BCR results in proliferation whereas coligation of FcγRIIb mediates growth arrest 211
4.3.2 Coligation of the BCR and FcγRIIb results in apoptosis 212
4.3.3 Simultaneous coligation of the BCR and FcγRIIb results in mitochondrial-dependent apoptosis 212
4.3.4 BCR-mediated proliferative signalling is mediated by the ERKMAP kinase cascade and can be abrogated by the coligation of FcγRIIb 214
4.3.5 FcγRIIb-mediated apoptosis requires abrogation of the PI-3 kinase signal 215
4.3.6 Neither JNK nor p38 MAPK are involved in BCR-mediated proliferative or FcγRIIb-mediated apoptotic signalling 217
4.3.7 FcγRIIb-mediated apoptosis is not likely to be caspase 3-dependent 218
4.3.8 Simultaneous cathepsin B, calpain and caspase inhibition rescues mature B cells from FcγRIIb-mediated apoptosis 219
4.3.9 A potential role for caspase 8 in FcγRIIb-mediated apoptosis 221
4.3.10 The murine SLE model is unable to undergo FcγRIIb-mediated growth arrest or apoptosis 223
4.3.11 The pro-apoptotic Bcl-2 family members Bid and Bad are upregulated during FcγRIIb-mediated apoptosis 223
4.3.12 Inhibition of the PI-3 kinase and MAP kinase cascades inhibits Bad activation 225
4.3.13 Coligation of the BCR and FcγRIIb upregulates the activation of p53 225
4.3.14 Coligation of the BCR and FcγRIIb upregulates the activation of NF-κB 226

4.4 Discussion 228

4.4.1 BCR ligation results in ERKMAPK/PI-3 kinase dependent-proliferation 228

4.4.2 FcγRIIb-mediated growth arrest can be mimicked by abrogation of both the BCR-stimulated ERKMAPK and PI-3 kinase signals 229

4.4.3 FcγRIIb-mediated apoptosis can be mimicked by the abrogation of PI-3 kinase signalling 229

4.4.4 FcγRIIb-mediated apoptosis is caspase 8-dependent and may involve multiple executioner protease families 230

4.4.5 FcγRIIb-induced apoptosis is mediated by pro-apoptotic members of the Bcl-2 family 232

4.4.6 FcγRIIb-mediated apoptosis involves the upregulation of p53 233

4.4.7 FcγRIIb-mediated apoptosis involves the differential upregulation of NF-κB subunits 233

4.4.8 Concluding Remarks 235

Chapter 5: General Discussion

5.1 Immature B cell signalling 264

5.2 Mature B cell signalling 267

5.3 Concluding Remarks 268

Bibliography 270

Publications 314

Figures **Page**

Figure 1.1: Summary of the Development of conventional B2 cells 46
Figure 1.2: B cell activation and selection in germinal centres 47
Figure 1.3: The structure of the B cell receptor (BCR) 48
Figure 1.4: Ligation of the BCR results in the activation of PTKs 49
Figure 1.5: Syk is able to recruit adaptor proteins that can activate the three major cell signalling cascades 50
Figure 1.6: The PI-3 kinase superfamily 51
Figure 1.7: The phosphorylation status of Bad is critical for differentiating between a pro-apoptotic and anti-apoptotic signal 52
Figure 1.8: Mitogen-activated protein kinase (MAP kinase) signalling pathways 53
Figure 1.9: The BCR is able to activate the RasMAPKinase pathway via SOS 54
Figure 1.10: Protein structure of the PKC family members 55
Figure 1.11: Activation of p53 results in a variety of cellular responses 56
Figure 1.12: The transcription factor, NF-κB can direct a variety of cellular responses depending on the subunits that are utilised 57
Figure 1.13: The cell cycle 58
Figure 1.14: Caspase 8 can be activated by TNFR1 type receptors to initiate apoptosis. 59
Figure 1.15: The Bcl-2 family of apoptosis regulators 60
Figure 1.16: Apoptosis in under the control of a diverse family of BH domain containing Bcl-2 proteins 61
Figure 1.17: The roles of calpain and caspase in protein degradation and apoptosis 62
Figure 1.18: FcγRIIb coligation inhibits BCR-mediated proliferative cell signalling 63
Figure 1.19: Coligation and BCR and FcγRIIb by cognate Ag-Ab complexes induces cell cycle arrest whereas homo-aggregation of FcγRIIb by non-cognate Ab induces apoptotic signalling 64
Figure 1.20: Simultaneous coligation of the BCR and FcγRIIb recruits Gab1 which can inhibit the PI-3 kinase pathway 65
Figure 2.1: FACS histogram of DNA content analysis 87

Figure 2.2: Analysis of the mitochondrial membrane potential of cells using $DiOC_6$ stain 88
Figure 2.3: Flow diagram to show how cytoslic, mitochondrial and nuclear fractions were generated from mature B cells 89
Figure 2.4: Measurement of Ca^{2+} levels in WEHI 231 cells 90
Figure 3.1: BCR mediated apoptosis correlates with arachidonic acid mediated loss of mitochondrial membrane integrity 151
Figure 3.2: CD40 structure and signalling 152
Figure 3.3: Schematic view of Ras regulatory factors 153
Figure 3.4: In fibroblasts, Ras follows a biphasic pattern of activation following stimulation with mitogen, each phase corresponding to activation of different effector molecules 154
Figure 3.5: Use of the RasV12, RasV12 S35 and RasV12 C40 mutants allows for dissection of the Ras signals important in proliferation and apoptosis in WEHI 231 cells 155
Figure 3.6: Dominant negative SHIP and Dok mutations allow for furtherdissection of the contributions of the MAP kinase and PI-3 kinase pathways 156
Figure 3.7: In WEHI 231 cells ligation of the BCR with anti-Ig leads to growth arrest whereas coligation of both the BCR and CD40 results in proliferation 157
Figure 3.8: Ligation of the BCR induces apoptosis whereas engagement of CD40 drives cells to enter the mitogenic phases of the cell cycle in WEHI 231 cells 158
Figure 3.9: Ligation of the BCR results in dissipation of MMP whereas coligation of CD40 prevents the loss of mitochondrial membrane integrity 159
Figure 3.10: Ligation of the BCR induces the expression of the pro-apoptotic Bcl-2 family members Bad, Bak and Bax in WEHI 231 cells 160
Figure 3.11: Ligation of the BCR downregulates expression of Bcl-2, $BclX_L$ and Mcl-1 whereas coligation of CD40 alone rescues the expression of $BclX_L$ only 161
Figure 3.12: Potential complexing of $BclX_L$ and Bak and under conditions of CD40-mediated rescue of BCR-coupled apoptosis 162

Figure 3.13: Overexpression of $BclX_L$ provides protection from both anti-Ig and arachidonic acid induced apoptosis 163
Figure 3.14: Overexpression of $BclX_L$ does not provide protection from either arachidonic acid or anti-Ig induced growth arrest 164
Figure 3.15: Treatment with anti-CD40 can rescue cells from arachidonic acid mediated growth arrest 165
Figure 3.16: The PLA_2 inhibitors used were non-metabolisable forms of arachidonic acid 166
Figure 3.17: Treatment with PLA_2 inhibitors induces apoptosis 167
Figure 3.18: COX and LOX are responsible for the generation of prostaglandins and leukotrienes, respectively, during arachidonic acid metabolism 168
Figure 3.19: Treatment with COX2 or pan-LOX inhibitors alone or in combination enhances anti-Ig-induced growth arrest and apoptosis 169
Figure 3.20: $BclX_L$ overexpression antagonises BCR mediated disruption of the MMP however it cannot overcome anti-Ig induced growth arrest 170
Figure 3.21: BCR-induced calcium release is reduced in $BclX_L$ WEHI 231 cells as compared to Neo WEHI 231 cells 171
Figure 3.22: Addition of anti-Ig results in a calcium oscillation in WEHI 231 cells 172
Figure 3.23: WEHI 231 cells undergo sustained, cyclical ERK activation when unstimulated or treated with anti-CD40, whereas ligation of the BCR abrogates this sustained ERK activation. WEHI 231 cells expressing the RasV12 construct have enhanced ERK activation compared to empty vector cells 173
Figure 3.24: Expression of the RasV12 construct enhances sustained, cycling ERK activation which provides protection from BCR-induced growth arrest at 24 h but not at 48 h in WEHI 231 cells 174
Figure 3.25: The RasV12 mutation does not significantly alter cell division at 72 h 175
Figure 3.26: Both RasV12 S35 and Ras V12 C40 mutations provide protection from BCR-mediated growth arrest 176
Figure 3.27: Constitutive activation of Ras provides protection from anti-Ig induced dissipation of the MMP 177
Figure 3.28: Constitutive activation of Ras provides protection from anti-Ig induced dissipation of the MMP at 24 and 48 hours 178

Figure 3.29: Expression of the MEKK3 construct rescues cells from BCR-induced dissipation of the MMP and apoptosis 179
Figure 3.30: Expression of the MEKK3 construct reduces cell division in response to all stimuli 180
Figure 3.31: Expression of constitutively active MEKK3 reinstates ERK activation in BCR-treated cells to the level observed following coligation of CD40 181
Figure 3.32: Treatment with anti-Ig results in the reduction of AKT activation in empty vector WEHI 231 cells but not RasV12 and MEKK3 mutants 182
Figure 3.33: SHIP SH2, SHIP CI and Dok PH/PTB mutants do not provide any protection from anti-Ig mediated growth arrest 183
Figure 3.34: SHIP SH2, SHIP CI and Dok PH/PTB mutants do not affect anti-CD40 mediated rescue of anti-Ig stimulated growth arrest 184
Figure 3.35: SHIP SH2 and SHIP CI mutants display a biphasic caspase 3 activation profile whereas Empty Vector and Dok PH/PTB mutants do not 185
Figure 3.36: Constructs utilised to generate PKC mutants 186
Figure 3.37: Effect of expression of PKCα constructs on anti-Ig induced growth arrest in WEHI 231 cells 187
Figure 3.38: Effect of expression of PKCα constructs on anti-Ig induced apoptosis and CD40-mediated rescue in WEHI 231 cells 188
Figure 3.39: The effect expression PKCα constructs in WEHI 231 cells on cellular division at 72 h 189
Figure 3.40: Effects of PKC mutations on the MMP following BCR ligation 190
Figure 3.41: PKCα expression and activity protects from BCR-stimulated dissipation of the MMP 191
Figure 3.42: Effects of expression of PKCδ constructs on anti-Ig induced growth arrest in WEHI 231 cells 192
Figure 3.43: Effects of expression of PKCδ constructs on anti-Ig induced apoptosis and CD40-mediated rescue in WEHI 231 cells 193
Figure 3.44: Expression and activity of PKCδ protects from BCR-stimulated dissipation of the MMP 194
Figure 3.45: Effects of expression of PKCε constructs on anti-Ig induced growth arrest in WEHI 231 cells 195

Figure 3.46: The effect expression PKCε CAT construct in WEHI 231 cells on cellular division at 72 h 196
Figure 3.47: Effects of expression of PKCε mutants on anti-Ig induced apoptosis and CD40-mediated rescue in WEHI 231 cells 197
Figure 3.48: Expression of PKCε constructs may partially rescue WEHI 231 cells from BCR-stimulated dissipation of the MMP 198
Figure 3.49: Effects of expression of PKCζ constructs on anti-Ig induced growth arrest in WEHI 231 cells 199
Figure 3.50: The effect of expression of PKCζ CAT construct in WEHI 231 cells on cellular division at 72 h 200
Figure 3.51: Effects of expression of PKCζ CAT construct on anti-Ig induced apoptosis and CD40-mediated rescue in WEHI 231 cells 201
Figure 3.52: Expression of PKC ζconstructs protects from BCR-stimulated dissipation of the MMP 202
Figure 3.53: Pro-apoptotic Bcl-2 family members are differentially regulated in PKC mutants 203
Figure 3.54: Dynamic switch model for conversion of BCR stimulated arachidonic acid apoptosis signal to a CD40 stimulated PGE_2 mitogenic signal 204
Figure 4.1: Inhibition of BCR signalling by FcγRIIb 236
Figure 4.2: Ligation of the BCR results in proliferation whereas simultaneous coligation of the BCR and FcγRIIb results in growth arrest 237
Figure 4.3: Coligation of the BCR and FcγRIIb induces apoptosis 238
Figure 4.4: Simultaneous coligation of BCR and FcγRIIb results in chromatin condensation, a hallmark of apoptosis 239
Figure 4.5: Simultaneous coligation of the BCR and FcγRIIb results in dissipation of MMP 240
Figure 4.6: Simultaneous coligation of the BCR and FcγRIIb induces mitochondrial-dependent apoptosis 241
Figure 4.7: Ligation of the BCR produces a strong phospho-ERK signal whereas coligation of the BCR and FcγRIIb abrogates this signal. 242
Figure 4.8: Inhibitors of the MAP kinase pathway can inhibit BCR-mediated proliferation 243
Figure 4.9: PI-3 kinase inhibition results in growth arrest and apoptosis 244

Figure 4.10: Ligation of the BCR induces a strong phospho-AKT signal which can be abrogated by simultaneous coligation of FcγRIIb 245
Figure 4.11: Inhibition of the p38 pathway does not have any effect on either BCR- induced proliferation or FcγRIIb- induced apoptosis 246
Figure 4.12: Ligation of the BCR or coligation of the BCR and FcγRIIb does not stimulate either JNK or p38 activation 247
Figure 4.13: FcγRIIb-mediated apoptosis is caspase 3 –independent 248
Figure 4.14: Executioner protease inhibitors do not prevent FcγRIIb-mediated growth arrest 249
Figure 4.15: Executioner protease inhibitors used in combination can provide partial rescue from FcγRIIb-mediated apoptosis 250
Figure 4.16: Executioner protease inhibitors used in combination can increase the proportion of FcγRIIb-treated cells in mitogenic phases of the cell cycle 251
Figure 4.17: Treatment with executioner protease inhibitors does not prevent FcγRIIb mediated-dissipation of the MMP 252
Figure 4.18: Caspase 8 inhibition does not prevent FcγRIIb-mediated growth arrest 253
Figure 4.19: Caspase 8 inhibition prevents FcγRIIb-mediated apoptosis 254
Figure 4.20: Caspase 8 inhibition provides a partial rescue from FcγRIIb-mediated dissipation of the MMP 255
Figure 4.21: Coligation of BCR and FcγRIIb in mature splenic B cells derived from lpr mice does not induce growth arrest 256
Figure 4.22: Ligation of the BCR and FcγRIIb induces the expression of pro-apoptotic Bcl-2 family members, Bid and Bad 257
Figure 4.23: Bad activation is downregulated by both MAP kinase and PI-3 kinase inhibition 258
Figure 4.24: Coligation of the BCR and FcγRIIb upregulates the activation of p53 259
Figure 4.25: Coligation of the BCR and FcγRIIb differentially modulates individual members of the NF-KB family: cRel , p52 and Rel B have upregulated activation levels at 24 h but not 48 h 260

Figure 4.26: Coligation of the BCR and FcγRIIb differentially modulates the activation of individual members of the NF-κB family: Both p50 and p65 have upregulated activation levels at 48 h but not 24 h 261
Figure 4.27: Current working model for the signals involved in FcγRIIb-mediated growth arrest 262
Figure 4.28: Current working model for FcγRIIb-mediated apoptosis 263

Tables

		Page
Table 2.1	Antibodies used in WEHI 231 and mature B cell experiments	84
Table 2.2	Constructs used in transfection of WEHI 231 cells.	87

Abbreviations

Ag	antigen
AKT	protein kinase B (PKB)
aPKC	atypical PKC
BAFF	B cell activating factor
BAFF-R	B cell activating factor receptor
BCR	B cell antigen receptor
BH	Bcl-2 homology
BLNK	B cell linker protein
BSA	bovine serum albumin
Btk	Bruton's tyrosine kinase
cAMP	cyclic adenosine monophosphate
CARD	caspase activation and recruitment domain
CD40-L	CD40 ligand
Cdk	cyclin dependent kinase
COX	cyclooxygenase
cPKC	conventional PKC
$cPLA_2$	cytosolic phospholipase A_2
cpm	counts per minute
DAG	diacylglycerol
DED	death effector domain
ERK	extracellular signal regulated kinase
FADD	Fas-associated death domain
FcR	Fc portion Receptor
FcγRIIb	Fc Receptor γIIb
Gab-1	Grb-2-associated binder-1
GFP	green fluorescence protein
H	hour
HRP	horse radish peroxidase
IAP	inhibitor of apoptosis proteins
Ig	immunoglobulin
IL	interleukin
INK	inhibitor of Cdk4
IP_3	inositol-1, 4, 5-trisphosphate

IP_4	inositol-1, 3, 4, 5-tetraphosphate
ITAM	immunoreceptor tyrosine-based activation motif
ITIM	immunoreceptor tyrosine-based inhibitory motif
JNK	c-Jun N-terminal kinase
LAB	linker for activation of B cells
LOX	lipoxygenase
mAb	monoclonal antibody
MAPK	mitogen-activated protein kinase
MEF2	myocyte enhancer factor 2
Min	minute
MKK	MAP kinase kinase
MKKK	MAP kinase kinase kinase
MMP	Mitochondrial membrane potential
NF-AT	nuclear factor for activated T cells
nPKC	novel PKC
NS-398	N-[2-(Cyclohexyloxy)-4-nitrophenyl]methanesulfonamide
PARP	poly(ADP-ribose) polymerase
PBS	phosphate buffered saline
PDK	phosphoinositide-dependent kinase
pERK	phospho-Erk
PGE_2	prostaglandin E_2
PH	pleckstrin homology
PI	propidium iodide
PI-3 kinase	phosphatidylinositol-3-kinase
PIP_2	phosphatidyiinositoi-4, 5-bisphosphate
PIP_3	phosphatidylinositol-3, 4, 5-trisphosphate
PKC	protein kinase C
PLC	phospholipase C
PLD	phospholipase D
pMEK	phospho-MEK
PP2A	protein phosphatase 2A
pSAkt	phospho-serine^{473} Akt
pTAkt	phospho-threonine^{308} Akt
PTB	phospho-tyrosine binding

PTEN	phosphatase and tensin homologue
RACK	receptor for activated C kinase
RasGAP	Ras GTPase activating protein
Rb	retinoblastoma protein
S	seconds
SD	standard deviation
sem	standard error of the mean
SH2	Src homology 2
SH3	Src homology 3
SHIP	SH2 domain-containing inositol 5-phosphatase
SHP-1	SH2 domain-containing protein tyrosine phosphatase-1
SHP-2	SH2 domain-containing protein tyrosine phosphatase-2
sIg	surface immunoglobulin
SOS	Son of Sevenless
tBid	truncated Bid
TBS	Tris buffered saline
TCR	T cell antigen receptor
TdT	terminal deoxynucleotide transferase
TNF	tumor necrosis factor
TRAF	TNF-receptor-associated factor
Z-VAD-FMK	N-benzyloxycarbonyl-Val-Ala-Asp-fluoromethylketone

Chapter 1: Introduction

1.1 The Humoral Immune System

The immune system has evolved to protect the host from pathogens such as parasites, bacteria or viruses. The cells and molecules that comprise the immune system, through a finely balanced network of interactions, enable the host to detect the presence of a foreign agent, co-ordinate a specific attack, and finally, once the agent has been successfully removed, quench that specific response. The innate immune response is the first line of defence a host has against infection, and as such is non-specific in nature as it functions regardless of the foreign substance or pathogen. The innate response is mainly driven by phagocytes, cells that engulf microorganisms before exposing them to an array of killing mechanisms. In contrast, adaptive immunity relies upon the ability of lymphocytes to recognise antigens (Ag) and respond in a highly specific manner, as each lymphocyte recognises a unique Ag. Moreover, the adaptive immune system also has memory for agents that have been successfully cleared in the past, allowing a more rapid and effective response upon subsequent encounter.

B cells generate and secrete antibodies (Ab), molecules that are specific for each unique Ag, and are important for combating infection by extracellular pathogens. These Abs circulate in the bloodstream and permeate other body fluids. When an Ab molecule encounters its Ag and binds to it, it protects the host via one of three key processes, neutralisation, opsonisation or complement activation. Neutralisation is the process by which Ag-Ab complexes prevent antigen binding to receptors on host cells and causing pathology, for instance by preventing entry of viral particles or bacterial toxins into cells. Opsonisation is the process by which the Ab coating allows the antigen to be recognised as foreign by phagocytic cells, leading to its ingestion and destruction. The third mechanism involves the recruitment of a system of plasma proteins known as complement by Ag-Ab complexes, particularly when Abs coat a bacterial cell. The Abs form a receptor for the C1 component of complement, leading to activation of the system, which enhances opsonisation of the Ag, or can even lead to direct lysis of some bacteria.

These Ab are secreted by mature B cells following ligation of the BCR and therefore the development and function of mature B cells has become a major research topic. One area that has received much interest, yet has still to yield much more information, is the elucidation of the molecular and biochemical mechanisms underlying B cell development and differentiation, and the differential responses that depend on maturation status. The B cell Ag receptor (BCR) is responsible for the transduction of Ag encounter throughout B cell development, yet the biological response varies depending on the developmental stage. For example, at the immature stage ligation of the BCR leads to growth arrest and apoptosis whereas at the mature B cell stage ligation of the BCR mediates proliferation and enhanced Ab production. The study of these differential responses will further our understanding not only of normal B cell development, but also the role of B lymphocyte dysfunction in a number of disease states. Prevention of dysregulated proliferation may help provide treatments for leukaemia as well as autoimmune disorders such as SLE and arthritis. Furthermore, a proper and complete understanding of B cell development will provide information for the production of better vaccines.

1.2 B Cell Development

1.2.1 B cell development

As stated above, B cells are the principal cellular mediators of the specific humoral response to infection by bacteria, viruses and parasites as they produce antigen-specific antibodies. The processes controlling development of B cells are tightly regulated to ensure a constant supply of B cells expressing antigen receptors of distinct specificity, enabling identification of any encountered antigen, yet at the same time avoiding generation of autoreactive B cells that recognise 'self' antigens. This complex process involves the integration of numerous signals at a number of stages, including antigen, soluble mediators and accessory cells.

In mammals, B cell development begins with the commitment of haematopoietic stem cells (HSCs) to the B cell lineage, a process that occurs in the foetal liver, then after birth and into adult life in the bone marrow (Figure 1.1). Commitment of

HSCs to the B cell lineage is dependent on the expression of the paired box transcription factor Pax5 (1). Pax5 acts to promote the expression of B cell lineage genes whilst suppressing those genes responsible for T cell, erythroid or myeloid cell development. Once committed, the precursor B cells pass through a number of developmental stages marked by a series of changes in location and in the expression of genes, intracellular signalling proteins and cell surface markers. The stages of B cell development can be broadly divided into two quite distinct phases; antigen-independent and antigen-dependent (2). The antigen-independent phase is completed in the bone marrow, and involves the production of a repertoire of immature B cells bearing functional Ag receptors. Encounter with Ag in the bone marrow during the process of receptor editing, however, leads to death by apoptosis, or anergy, a process by which the B cell becomes unresponsive to future encounters with its particular antigen. The B cells that emerge into the periphery are termed immature B cells, and these migrate to the secondary lymphoid organs, such as the spleen and lymph nodes. It is here, in association with specialised antigen-presenting cells and stromal cells, that B cell recognition of antigen can lead to one of several developmental pathways in the production of mature B cells from transitional B cells: (1) anergy and/or apoptosis, (2) activation, proliferation and differentiation into high rate antibody secreting plasma cells, or (3) differentiation into memory B cells (3).

1.2.2 Pro-B and Pre-B cells

The production of a functional BCR relies on the completion of a complex pattern of immunoglobulin gene rearrangements to produce one functional heavy chain, followed by one functional light chain (4). This rearrangement is under the control of the protein products of the recombination-activating genes, RAG-1 and RAG-2, which are highly expressed at the pro- and pre-B cell stages of differentiation and are essential for rearrangement (5). The immunoglobulin heavy chain variable region is encoded by V (variable) and J (joining) gene segments, with additional diversity provided by the D (diversity) gene segment. Rearrangement of the heavy chain gene begins in the early pro-B stage with the joining of D_H to J_H. Cells are allowed to progress to the next stage provided a productive rearrangement is achieved. Progression to the late pro-B cell stage is accompanied by the joining of

a V_H gene to the pre-formed DJ_H complex. Although no functional immunoglobulin is expressed in late pro-B cells, recent studies have shown the expression of components of the mature BCR on their surface, namely the accessory Ig-α/Ig-β heterodimers in association with calnexin (6). These accessory molecules have been shown to be essential for the continuing development of the pro-B cells to the pre-B cell stage (7, 8). Indeed, it has been shown that mice deficient in Ig-β exhibit a complete block in B cell development before V_H to D_HJ_H rearrangement. It has therefore been suggested that signalling through the Ig-α/Ig-β-calnexin receptor on pro-B cells may be required for successful initiation of V_H to D_HJ_H gene rearrangement (6). However, it has recently been shown that V_H to D_HJ_H recombination can still take place in pro-B cells from mice lacking either Igα or Igβ (9).

A successful first rearrangement of $V_HD_HJ_H$ genes results in the production and transient expression of intact μ heavy chains in an immunoglobulin-like "pre-BCR" complex with the surrogate light chains, λ5 and VpreB (10). λ5 bears close similarity to the known constant (C) λ light-chain domains, whilst VpreB resembles a variable (V) domain but bears an extra N-terminal protein sequence. If this first $V_HD_HJ_H$ rearrangement is unsuccessful, a second rearrangement is undertaken. Pro-B cells in which both rearrangements of $V_HD_HJ_H$ genes are unsuccessful are unable to produce a pre-B cell receptor. Surface expression of a pre-BCR is known to be important for instructing the cell to stop further V_H gene rearrangements (11) by inhibiting recombination at the heavy chain locus, a process described as allelic exclusion (12). Pre-B cell receptor expression also drives the transition to the large pre-B cell stage and induces proliferation in addition to signalling to the cell that gene rearrangements of the immunoglobulin light chain should begin.

1.2.3 Immature B cells

Maturation of pre-B cells to immature B cells involves the rearrangement of immunoglobulin light chain genes to generate a conventional light chain (κ or λ),

with appropriate constant and variable regions. Once a light chain gene has been rearranged successfully, a BCR consisting of μ heavy chain, conventional light chains and accessory Ig-α/Ig-β molecules is expressed by the immature B cells. This intact surface IgM is the first BCR to exhibit antigen specificity (13) and thus the B cell enters the antigen-dependent stage of development. It has been estimated that about 10^8 B lineage precursors are generated every day in the murine bone marrow, which in turn give rise to about 2×10^7 BCR-expressing immature B cells (14). Thus, it is clear that the majority of B cells (80%) maturing in the bone marrow undergo a process of negative selection. Indeed, ligation of the antigen receptors on the vast majority of immature B cells leads ultimately to anergy, a state of non-responsiveness to antigen (15) or deletion via apoptosis (programmed cell death) (16, 17, 18). The inactivation of self-reactive B cell clones by deletion or inactivation (anergy) is important for the maintenance of self-tolerance by the immune system. Immature B cells that are capable of recognising self-antigens are eliminated or inactivated, preventing them from developing further and secreting antibodies that bind to host cells or tissues.

Self-reactive immature B cells may be rescued from deletion by undergoing receptor editing, where the autoreactive receptor is replaced with the product of a further rearrangement event (19). Immature B cells isolated from the bone marrow undergo apoptosis when cultured *in vitro* in the presence of anti-Ig antibodies. It is important to note that these cells are purified, and therefore not in their physiological context (20). In contrast, when immature B cells are cocultured with whole syngeneic bone marrow they respond to anti-Ig by re-expressing *RAG-2*, permitting receptor editing (21). These studies suggest that the consequences of an immature B cell recognising its Ag are dictated by the site of Ag encounter, with the bone marrow microenvironment providing signals that promote receptor editing. By contrast, if the immature B cell first encounters its Ag in the periphery, the absence of these signals results in commitment to apoptosis.

By maintaining high-level expression of IgM BCR, transitional-immature (T1) B cells entering the periphery remain sensitive to antigen deletion for a number of days (22). This is especially important for the development of tolerance, since not

all self-antigens are expressed within the bone marrow (21, 23). To promote their survival and migration to the spleen, these cells require T cell-dependent help. Typically, of the 2 x 10^7 BCR^+ B cells that develop daily in murine bone marrow only 10% will reach the spleen and only 1 to 3% will survive and develop to the next stage of maturation (22) The development into a transitional (T2) B cell is accompanied by the surface expression of IgD and requires constant BCR-derived signals for progression, resulting in a IgM^{hi} IgD^{hi} phenotype (11, 23, 24). In addition, stimulation via cytokines or co-receptor ligation is thought to help shape the BCR repertoire and signalling thresholds (25). As the B cells migrate into the primary follicles of the spleen they are finally regarded as "mature" IgM^{lo} IgD^{hi} B2 follicular cells.

1.2.4 Mature B cells

In stark contrast to the immature B cell, Ag-receptor ligation leads to the activation of mature B cells. The activated mature B cell can then further develop into an IgM antibody-secreting plasma cell. Alternatively, the mature B cell can undergo isotype switching and V region somatic mutation to become a memory B cell, in the presence of the correct T cell-derived cytokines and cell-cell contacts (26). Following re-exposure to the same Ag and affinity maturation, whereby the affinity of the cell for its particular Ag improves by a process of somatic hypermutation, the memory B cell can evolve into an IgG secreting plasma cell. The formation of memory is critical for mounting a rapid, specific secondary immune response. Moreover, the ability of the immune system to generate these memory B cells forms the basis of effective vaccination.

The generation of memory B cells occurs in germinal centres (GCs), which are formed during primary immune responses to T cell-dependent antigens in lymphoid follicles (Figure 1.2). B cells activated by T cell-dependent antigens enter the primary lymphoid follicles where they undergo proliferation in areas rich in follicular dendritic cells (FDCs), which fix unprocessed antigen on their surface for presentation to newly formed B cells. Following their expansion, the B cell blast population migrates from the centre of the follicle to form the dark zone of the GC,

where they continue to proliferate and lose sIgM expression, becoming centroblasts. Centroblasts undergo somatic mutation of the immunoglobulin variable region genes and subsequently migrate to the light zone of the GC, which is rich in FDCs, and are now termed centrocytes, which express the mutated antigen receptors. In the light zone, centrocytes with the highest affinity antigen receptors are selected and return to the dark zone for further rounds of mutation and selection, whilst those with lower affinities undergo apoptosis. As centrocytes are intrinsically programmed to undergo apoptosis unless they are actively rescued, the level of B cell apoptosis in the light zone is very high. Rescue of centrocytes from apoptosis is driven by two signals. The first is generated by FDC-displayed antigen resulting in ligation of the high-affinity surface immunoglobulin, the second by CD40 ligation on the surface of centrocytes, suggesting a role for helper T cell interactions in promoting centrocyte survival (25). This process results in the selection of high affinity B cell clones whilst low affinity receptors are selected against by neglect. Positively selected centrocytes then go on to establish the memory B cell pool in the apical light zone, providing the precursors for plasma cells that will produce antibodies of high affinity.

1.3 B Cell Signalling

1.3.1 Initiation of BCR Signalling

The BCR has a complex structure and is a member of the immunoglobulin (Ig) superfamily (Figure 1.3). The membrane bound BCR is associated with two other polypeptides on the B cell, Igα and Igβ that act as signal transducing molecules. Their intracellular tails contain immunoreceptor tyrosine based activation motifs (ITAMS.) Tyrosine residues of the ITAM sequence become reversibly phosphorylated following crosslinking, and hence aggregation, of the BCR. The BCR has no intrinsic kinase activity and it is the recruitment and activation of cytosolic PTKs that is responsible for the initiation of intracellular signalling.

The Src-family of non-receptor tyrosine kinases are the primary effectors of BCR-ITAM phosphorylation (27, 28). These kinases are associated with the BCR in an

inactive conformation and become activated following BCR ligation. Thus during BCR signalling, CD45, a transmembrane tyrosine phosphatase, mediates the dephosphorylation of the C-terminal inhibitory tyrosine residue of the Src family kinases leading to the activation of one such PTK, Lyn (29). Once activated Lyn is recruited to the ITAMS of the Igα/β chains where it phosphorylates the tyrosine residues (30). This enables the ITAM sequences to bind SH2 domain containing proteins including additional Lyn molecules and other Src-family kinases. Syk, a related non-receptor tyrosine kinase, can then act to further phosphorylate the tyrosine residues of ITAMs leading to further recruitment and activation of Syk and other tyrosine kinases like the Tec-family kinase Btk. (Figure 1.4) (31) (32). It has been demonstrated that all three types of PTKs (Src family kinases, Syk and Tec family kinases) are necessary for functional BCR signalling (33).

Ligation of the BCR complex and recruitment and activation of multiple PTKs provides docking sites for essential adaptor SH2 domain containing proteins. These adaptor proteins are critical for stimulating downstream signalling pathways. For example BLNK (also known as SLP-65) is phosphorylated by Syk, which creates multiple phospho-tyrosine residues that can recruit other signalling molecules via their SH2 domains. These include Btk and PLCγ allowing for Btk to phosphorylate, and therefore activate, PLCγ (34). Moreover, bringing PLCγ close to the plasma membrane increases the proximity of PLCγ to its substrate PI-(4,5)-P_2. The phospho-tyrosine residues on BLNK also act to recruit signalling molecules such as Vav (a guanine nucleotide exchange factor of Rho-family G proteins) which is required for the activation of both the p38 and JNK kinase systems (35). BLNK is also capable of activating the ERKMAPKinase pathway by recruiting the adaptor protein Grb2 that in turn recruits SOS to the membrane complex to activate Ras and eventually ERK (reviewed in (36)). The PLCγ and PI-3 kinase signalling cascades can also be activated by parallel activatory mechanisms (Figure 1.5). Thus, ligation of the BCR can lead to amplification of the signal and the activation of multiple cell signalling pathways through a complicated series of recruitment of both non-receptor tyrosine kinases and adaptor proteins.

1.3.2 Cell signalling cascades activated by the BCR

BCR signalling can activate multiple signalling cascades which allows B cells to respond to BCR stimulation in many disparate ways. The appropriate response to BCR ligation may be differentiation, proliferation, anergy apoptosis or survival depending on the maturation stage of the B cell and other signals received. The early events in BCR signalling such as activation of PTKs, Phospholipase C γ (PLCγ), phosphoinositide-3-kinase (PI-3 kinase), protein kinase C (PKC) and the RasMAPK (mitogen activating protein kinase) cascades are observed throughout B cell maturation. However there are differences in the functional responses initiated by BCR-mediated signals during B cell maturation. The mechanistic reasons for these differential responses have not all been fully resolved however they are dependent on parameters including signal strength and duration, maturation-specific expression of effector molecules, subcellular localization of the signal and modulation of the signal by co-receptors (reviewed in (37).

In mature B cells the 3 major signalling pathways activated by BCR signalling are the PI-3 kinase, PLCγ and MAP kinase pathways (26).

1.3.2.1 The PI-3 kinase Pathway

PI-3 kinases phosphorylate inositol phospholipids on the 3 position of the inositol ring (38-40). This results in the production of phospholipids that are present at very low levels prior to receptor engagement. The major substrate of PI-3 kinase is PI-(4,5)-P_2 which is phosphorylated to produce PI-(3,4,5)-P_3. Both of these molecules can act as second messengers by acting as ligands for pleckstrin homology (PH) domains found in a large number of cytosolic proteins. This enables the co-localisation of PH domain containing proteins as well as recruitment to the plasma membrane. PI-3 kinase is also known to produce the phosphoinositides PI-(3)-P and PI-(3,4)-P_2 which along with PI(3,4,5)-P_3 are known to govern events such as cell survival, growth, cytoskeletal remodelling and the trafficking of intracellular organelles (41).

The PI-3 kinase family is made up of four different classes of protein: IA, IB, II and III on the basis of structural characteristics and substrate specificity (40) (Figure

1.6). Each protein contains a C2 domain, which acts to bind phospholipids in a calcium-dependent manner, and a catalytic domain. Classes II and I also contain a Ras binding domain (RBD) at the N terminal (42). Class IA family members are heterodimers consisting of a regulatory subunit, encoded by at least 3 genes: p85α, p55α and p50α, and a catalytic subunit, encoded by 3 genes p110α, p110β, p110δ (38). Among distinct regulatory subunits, p85α is the most abundantly expressed subunit in a wide range of cell types (43). By contrast, Class IB has only one catalytic member p110γ that interacts with a p101 regulatory subunit. This family is generally activated via G protein coupled receptors where the Gβγ subunit activates p110γ (42). Class II has three members, PI-3 kinases C2α and C2β, which are ubiquitously expressed, and C2γ that is found exclusively in hepatocytes. This family is primarily activated downstream of polypeptide growth factor receptors, chemokine receptors and integrins (39). Finally class III has only one member and is a mammalian ortholog of a *Saccharomyces cerevisae* protein Vsp34p. This PI-3 kinase has not been well characterised but exclusively generates PIP and is involved in the localisation of proteins to the lysosome (39).

PI-3 kinase has been shown to be essential for normal B cell function. Impaired PI-3 kinase signalling leads to immunodeficiency whereas unrestrained PI-3 kinase signalling leads to autoimmunity and leukaemia (44). Activation of PI-3 kinase is one of the earliest events following BCR ligation (45, 46) and it acts as a crucial signal for initiating the recruitment of PH domain containing molecules, such as Btk and AKT, to the membrane via the generation of PI-(3,4)-P_2 and PI-(3,4,5)-P_3 (47-52). PI-3 kinase is thus also required for the full activation of PLCγ (34, 53, 54).

A major downstream target of the PI-3 kinase pathway that can modulate cell fate decisions such as survival, apoptosis and proliferation is AKT (PKB). The AKT protein family consists of three isoforms AKT1, AKT2 and AKT3 which are all regulated by similar PI-3 kinase and phosphorylation dependent-mechanisms. AKT enzymes contain a PH domain (with a higher affinity for PI-(3,4)-P_2 than PI-(3,4,5)-P_3) that acts to recruit AKT to the plasma membrane where it undergoes dimerisation and a consequent conformational change. This conformational

change allows AKT to be phosphorylated by serine/threonine kinases such as PDK1. PDK1, 3-Phosphoinositide-dependent protein kinase 1, plays an important role in activating the AGC family of kinases. In particular, PDK1 plays a central role in the regulation of AKT by phosphorylating AKT on threonine 308. For example, human AKT is phosphorylated on threonine 308 by PDK1 and serine 473 by an as yet unidentified kinase (55). Once AKT has been phosphorylated, it translocates to the cytosol and nucleus where it has multiple pro-survival actions targeting both mitochondrial and caspase-dependent apoptotic events (56). For example, AKT acts to neutralise the pro-apoptotic function of the Bcl-2 family member Bad. Under some apoptotic conditions, Bad interacts with the pro-survival Bcl-2 family member $BclX_L$ via its BH3 domain. This prevents $BclX_L$ from protecting the mitochondrial membrane integrity and hence stimulates apoptosis. However, phosphorylation of Bad by AKT leads to the dissociation of Bad from $BclX_L$ and its sequestration by cytoplasmic 14-3-3 proteins (57). Sequestration protects Bad from dephosphorylation and prevents Bad from interacting with pro-survival mitochondrial targets (Figure 1.7) In addition, AKT can also phosphorylate caspase 9 and hence prevent its cytochrome c-dependent proteolytic activation which is required for the subsequent activation of the canonical effector caspase 3 cascade (58). Moreover, AKT1 and 2 can disrupt death receptor signalling by translocating to the nucleus where they suppress Fas ligand expression by phosphorylating forkhead transcription factors and causing them to exit the nucleus (59). Furthermore, in addition to promoting growth, AKT promotes proliferation by activating NF-κB via E2F, a transcription factor necessary for G1 to S phase transition (60, 61). Therefore PI-3 kinase activation of AKT can be both a pro-survival and pro-proliferative signal.

The first evidence for a role for PI-3 kinases in the immune system came from studies in which rats were exposed to wortmannin *in vivo*. Wortmannin, and the structurally unrelated inhibitor LY294002, have high selectivity for PI-3 kinases (62, 63). These studies indicated that wortmannin might act as a potent immune suppressor. However, wortmanin was found to be highly toxic (64), possibly because neither wortmannin nor LY294002 discriminate between the different isoforms of PI-3 kinase. Nevertheless, there has recently been some genetic

analysis using mice and cell lines that are deficient in different class I subunits that have suggested specific roles for particular PI-3 kinases in the immune system. For instance, consistent with the wortmannin data, knock out mice generated lacking p110α or p110β die *in utero* whereas mice with the genotypes $p85\alpha^{-/-}$,$p55\alpha^{-/-}$ or $p50\alpha^{-/-}$ all die after birth (65, 66). This suggests that all these subunits play an essential role in development. Indeed, both $p85\alpha^{+/-}$ and $p110\delta^{-/-}$ lymphocytes have impaired B cell development at the pro to pre-B cell transition (65-68). In addition, proliferation of mature B cells *ex vivo* in response to either LPS or crosslinking of the BCR is also impaired in these cells. This data suggests that p110 or p85 are required for normal B cell development and function. Consistent with this, in $p110\delta^{-/-}$ mice, marginal zone B cell development and germinal centre formation is blocked and aberrant mature B cells that are unable to produce normal amounts of Ab are produced (69). It was also noted that mice lacking class IA δ PI-3 kinases had the same phenotype as mice lacking BLK, Btk, PKCβ, PLCγ2 and Vav1/2 (67). It has therefore been postulated that all of these proteins function within the same signalling cascade or may act together in a signalosome. In contrast to this, class IB deficiency did not affect the B cell compartment suggesting that class IB PI-3 kinases are of less importance in B cells than class 1A PI-3 kinases.

1.3.2.2 The RasMAPKinase pathway

The mitogen-activated protein (MAP) kinases are a family of serine-threonine protein kinases that have been widely conserved throughout the evolution of eukaryotic cells. They are activated by a wide range of extracellular stimuli and are able to mediate a wide range of cellular functions ranging from proliferation and activation to growth arrest and cell death. The MAP kinase family is subdivided into three groups; the classical extracellular signal-regulated kinases (ERKMAPKinase), the c-Jun N-terminal kinases, also known as the stress activated protein kinases (JNK/SAPK) and the p38 MAPKinases (reviewed in (70)). Activation of each group is determined by distinct upstream MAP kinase kinases (MEKs) and MAP kinase kinase kinases (MEKK) (Figure 1.8). MAPKs are activated by dual phosphorylation on tyrosine and threonine residues, located in a T-X-Y motif, where X is different in each sub-class of kinase. Following MAP

kinase activation, activation of a number of downstream transcription factors occurs: for example, ERKMAPKinase activates Elk-1 and c-myc, JNK activates c-Jun and ATF-2 and p38 MAPKinase activates ATF-2 and MAX. The phosphorylation and activation of these transcriptional regulators enables the MAP kinase families to regulate gene expression and hence, cellular responses.

1.3.2.3 The ERK 1/2 Module

This signalling system can operate via the MAPKKKs, A Raf, B Raf and Raf 1, the MAPKKs MEK1 and MEK 2 and the MAP kinases ERK 1 and 2. (Figure 1.8). The MAPKKK, Raf is activated by the small GTPase Ras. The activation of Ras is achieved by recruitment of SOS, a Ras activating guanine nucleotide exchange factor. SOS stimulates the conversion of RasGDP to RasGTP and allows interaction with downstream effector proteins including Raf (71) (Figure 1.9). Activated Ras functions as an adapter that binds to Raf kinases with high affinity and causes their translocation to the cell membrane, where full activation of Raf takes place. The exact mechanism for this is not known however it requires Ras binding and multiple phosphorylations including autophosphorylation at threonine 372 in the conserved region 2 domain (72). Activated Raf then binds and phosphorylates the dual specificity kinases, MEK1/2 which in turn phosphorylate ERK 1/2 on the conserved TEY motif in their activation loop.

Amplification in this system is very efficient as evidenced by estimates that activation of just 5% of Ras leads to full activation of ERK 1/2 (73). ERK 1/2 can target cytoplasmic proteins, membrane proteins, cytoskeletal proteins and nuclear proteins (74). One subset of ERK 1/2 targets are protein kinases including Rsk 1-3, Mnk1 and Mnk2 which have been implicated in the promotion of protein synthesis (75-78). In addition to enhancing gene expression by intermediary kinases, ERK 1/2 can also directly phosphorylate transcription factors, such as Elk-1, cFos and cJun, and hence increase transcription of pro-proliferative genes (79-81). ERK 1/2 can also phosphorylate membrane protein substrates such as phospholipase A_2 (PLA_2) and the epidermal growth factor receptor (82, 83). Differential utilisation of these pathways by the ERK module is implicated in many

diverse downstream cellular responses including proliferation, survival and apoptosis.

1.3.2.4 The p38 Module

This signalling system operates via the MAPKKKs, MEKK 1,2 3,4 (amongst many others), the MAPKKs MEK 3 and MEK 6 and the p38 MAP kinase isoforms α, β, γ and δ (Figure 1.8). MEK 3 and 6 have a high degree of specificity for p38α and p38β and MEK 6 is able to activate all the p38 isoforms (reviewed in (84)). All of the isoforms of p38 are activated by phosphorylation of a conserved TGY motif.

The role of p38 seems to be cell and context specific, as with the other MAP kinases. Similarly to ERK 1/2, p38 can activate many cellular substrates including cytoskeletal and cytosolic proteins, for example the microtubule associated protein (tau) at physiologically relevant sites (85). p38 has also been implicated in the early phosphorylation of PLA_2 in platelets (86). In addition, the p38 module has been associated with signalling for apoptosis via the classical executioners of apoptosis, the caspases. It is thought that p38 can activate both the caspase 8 and canonical effector caspase 9 cascades (87). Nuclear targets of p38 include p53 and by mediating N terminal phosphorylation of p53, p38 can transduce p53-dependent apoptosis in response to UV radiation (88). In contrast, p38 has also been implicated in promotion of cell proliferation as p38 activation is necessary for progression through G1 (89) and G2/M phases of the cell cycle (90) under certain circumstances. Consistent with this, there are also a number of pro-proliferative nuclear targets of p38 including AP-1, ATF-1 and NF-κB (91).

1.3.2.5 The JNK Module

The MAP kinases JNK 1, 2 and 3 exist in 10 or more differentially spliced forms that are ubiquitously expressed (reviewed in (84) (Figure 5.3D) and require dual phosphorylation of tyrosine and threonine residues in a conserved TPY motif. This signalling system operates via the MAPKKKs, MEKK 1, 2,3 and 4, MLK 2 and 3 and Tpl 2, the MAPKKs MEK4 and MEK 7 (Figure 1.8). Following activation, JNK is also relocalised from the cytosol to the nucleus, like p38 and ERK 1/2 (92). The

major substrate of the JNK pathway is c-Jun which is phosphorylated on serine 63 and serine 73 to increase c-Jun transcription (93). However JNK can also affect other transcription factors including ATF-2, NF-ATc1, HSF-1 and STAT3. The JNK pathway is well known to be a stress activated pathway and has been reported to activate genes that increase caspase-mediated apoptosis including Apaf 1 and caspase 9 (94).

1.3.2.6 The PLC pathway

1.3.2.6.1 PLC generates the second messengers DAG and IP_3

PLC acts to generate the second messengers diacylglycerol (DAG) and inositol-1,4,5-trisphosphate, (IP_3) from the hydrolysis of the membrane phospholipid PI-(4,5)-P_2. DAG can act to activate both novel and conventional PKC isoforms and IP_3 binds to IP_3 R in the endoplasmic reticulum (ER) to stimulate intracellular calcium release. The PLC family contains 3 homologous groups of enzymes (PLC β, γ and δ) all containing PH domains. The PLCγ1 isoform is expressed in all tissues whereas the PLCγ2 isoform is expressed exclusively in cells of a haematopoietic origin (95). Genetic evidence suggests that the functions of these 2 isoenzymes may not overlap. Targeted disruption of PKCγ1 results in embryonic death in mice (96). However PLCγ2-deficient mice develop B cell abnormalities with severe immunodeficiency and dysfunction of the platelets and mast cells (97). PLCγ2 has been particularly well studied as a component of the BCR signalosome and can be phosphorylated by all 3 PTK families, Src, Syk and Tec *in vitro*, although it is not clear which PTK is utilised *in vivo* (98). In addition to the PH domain, which allows docking to the inner plasma membrane, PLCγ2 also contains two SH2 domains, which allow for recruitment by Btk and Syk and a SH3 domain (27).

1.3.2.6.2 The Protein Kinase C (PKC) Family

DAG, one product of PLC, is a known activator of both novel and conventional PKC isoforms. In B cells PKCs can mediate a plethora of functional responses which are discussed further in chapter 3. PKC was initially identified and

characterised as a proteolytically activated kinase and named protein kinase M in the late 1970s (99, 100). In fact PKC activity comprises of a family of 11 mammalian isoenzymes of serine/ threonine kinases which exhibit a wide tissue distribution and differential cellular localization (101). All members contain conserved structural features including a kinase domain, a regulatory domain and a basic pseudosubstrate prototype. PKCs can be further grouped into 3 categories according to the presence or absence of motifs that dictate cofactor requirements for optimal catalytic activity (Figure 1.10). The conventional (sometimes known as classical) PKCs (cPKCs; α, β_I, β_{II}, γ) are Ca^{2+}-dependent and are activated by diacylglycerol (DAG); the novel PKCs (nPKCs; δ, ε, η, θ) are Ca^{2+}-independent but are also activated by DAG and the atypical PKCs (aPKCs; ζ, λ/ι – λ being the murine isoform, ι the human isoform) are calcium-independent and are not activated by DAG.

1.3.2.6.3 Isoform specific activators of PKC

The current model for activation of PKC isoforms has been established using fibroblasts as a model system (reviewed in (102)). PKC enzymes first undergo auto-phosphorylation which renders them competent for activation. In the case of conventional and novel PKCs these primed enzymes bind, via their C1 domain, to DAG at the plasma membrane and this induces a conformational change that allows phosphorylation at two additional sites in the activation loop and C terminal hydrophobic site.

Whilst, activation of cPKCs depends primarily on activation of the phospholipase C (PLC) pathway, and the consequent generation of DAG and IP_3- dependent increases in cytoplasmic Ca^{2+} concentrations, the nPKCs can also be activated by PLC-dependent DAG. However, PKCs can also be activated by other pathways that produce DAG including phosphatidylcholine-specific PLD hydrolysis and the dephosphorylation of phosphatidic acid to DAG. Nevertheless, the full activation of nPKC isoforms however also requires phosphorylation by other kinases such as PDK1 and PKCζ which are downstream targets of PI-3 kinase. Likewise, aPKCs are downstream targets of PI-3 kinase signalling, therefore, as BCR ligation leads

to the activation of both the PLC and PI-3 kinase pathway, it seems highly likely that multiple PKC isoforms participate in BCR signalling (27).

1.3.2.6.4 The Generation of Calcium

As stated above, PLC also generates IP_3 which acts to open IP_3R Ca^{2+} channels and hence stimulate Ca^{2+} release from intracellular stores. Ca^{2+} represents another cell signalling molecule that may be important in both apoptotic and proliferative signalling. IP_3 evoked Ca^{2+} release produces localized rises in Ca^{2+} and under some conditions these localized responses can summate to produce a global increase in Ca^{2+} (103). The mechanism involved in the switch between local and global signalling is not clear. However, the Ca^{2+} puff represents a quantal release of Ca^{2+} by a small autonomous cluster, probably a few tens, of IP_3 receptors in the ER. Puffs stimulate a localized, transient and asynchronous rise in Ca^{2+} (104). As the IP_3 levels are increased the puffs become synchronous in multiple clusters and the Ca^{2+} rise occurs successively to produce a wave. Following this IP_3 mediated release of calcium from intracellular stores, there is a lower but sustained rise in intracellular calcium by influx of extracellular calcium via L type channels (105). Localised Ca^{2+} responses can affect the localisation of molecules such as Bcl-2 family members (106) as well the activation of signalling proteins such as PLA_2 (107) and calpain (108, 109). By contrast, globalised Ca^{2+} responses are associated with changes in transcription factor activation such as NF-AT (110) and a prolonged global Ca^{2+} increase is associated with the commitment of the cell to apoptosis (111).

IP_3R are important in BCR-Induced Ca^{2+} mobilization as mice deficient in all 3 IP_3R isoforms abolish BCR-induced Ca^{2+} mobilization (112). However BCR-driven Ca^{2+} mobilization can be maintained in mice in which individual IP_3R isoforms are knocked out (112), albeit that the detailed signalling patterns differ among the 3 IP_3R knock outs. For example, DT40 B cells lacking type 2 iP_3R have a regular and robust BCR induced Ca^{2+} oscillation whereas mice deficient in either type 1 or 3 IP_3R respond to BCR ligation with a monophasic Ca^{2+} transient or rapidly dampened Ca^{2+} oscillations. However the functional outcomes of altering IP_3R prolfiles have not yet been elucidated (113). Ca^{2+} rises result in the activation of

calmodulin dependent protein kinase II and the calmodulin activated serine/ threonine phosphatase calcineurin (114). The transcription factor NF-ATc is translocated to the nucleus following dephosphorylation by calcineurin (115, 116). In addition, BCR induced apoptosis in WEHI 231 cells and proliferation in splenic B cells is inhibited by cyclosporin A indicating the importance of calcineurin for these responses (115, 117).

1.3.2.7 p53

p53 is a tumour suppressor with a crucial role in preventing the onset of cancer. The best evidence for this comes from a naturally occurring p53 mutation in humans which causes Li-Fraumeni syndrome. Individuals with this syndrome have a lower than normal level of p53 expression which renders individuals highly prone to diverse cancers at a young age (118). The transcription factor p53, forms a homo-tetramer than can act to transcribe p53-regulated genes which can be divided into five categories depending on the process that they regulate; apoptosis, cell cycle arrest, genome stability, cellular senescence and angiogenesis (Figure 1.11) (119). p53 levels are generally low in normal cells due to rapid turnover controlled by a negative feedback loop involving interaction with MDM2 and consequent ubiquitination and degradation (Figure 1.11). p53 has been demonstrated to be of particular importance in thymocyte biology as T cells that are deficient in p53 are resistant to both DNA damaging drugs and γ radiation suggesting p53 plays an important role in induction of apoptosis in thymocytes (120-122).

The best-studied target of p53 is the cyclin dependent kinase inhibitor, p21 which has been shown to be critical for cell cycle arrest function (123). However, another important cell cycle regulator, PTEN is also upregulated by p53. This protein can antagonise both the PI-3 kinase (124) and RasMAPKinase cascades (125) and hence inhibit uncontrolled proliferation. There are also multiple apoptotic genes that are under the control of p53 that are involved in both the intrinsic and extrinsic pathways to cell death. For example, members of the classical caspase-dependent extrinsic pathway, Apaf 1 and caspase 9 are both upregulated by p53 (126). Furthermore, components of the mitochondrial pathway to apoptosis including pro-

apoptotic BH3 only Bcl-2 proteins can be upregulated by p53 action including Bax, Bid, PUMA and NOXA (127, 128). In addition to this, p53 has recently been demonstrated to have a transcription-independent, pro-apoptotic function. It has been postulated that p53 translocates to the mitochondria following exposure to apoptosis-inducing stimuli where it can interact directly with Bax and open the mitochondrial transition pore and hence stimulate apoptosis (129, 130).

1.3.2.8 NF-κB Signalling

The NF-κB family of transcription factors, also known as the Rel family, comprise either homo or heterodimers of the following five NF-κB subunits: RelA (p65), RelB, cRel, p50 and p52 (131). All of these subunits are related with a sequence of approximately 300 amino acids at the N terminal known as the Rel homology domain. This domain is required for DNA binding, dimerisation, nuclear localisation and inhibitor (IKB) binding. However the C terminal transactivation domains are not highly conserved suggesting diverse systems of NF-κB regulation have evolved.

The primary level of regulation of NF-κB is by IκB, which binds to the NF-κB dimer complex and sequesters it in the cytoplasm. This prevents NF-κB from accessing the nucleus and hence inhibits DNA binding. However activators, such as the MAP kinase cascade, stimulate IκB kinase complex (IKK) which phosphorylates IκB. This phosphorylated form of IκB is preferentially ubiquitinated and hence degraded in the proteosome, allowing free NF-κB to translocate to the nucleus and bind to DNA (132).

NF-κB transcription factors are highly constitutively activated in most cell types however in B cells this family appears to be under much tighter regulation (133). In fact amplification of NF-κB genes is very common in a number of B cell lymphomas including diffuse large B cell lymphoma, Follicular B cell lymphoma and Hodgkin's lymphoma (133, 134). Consistent with this, NF-κB is known to control the regulation of genes that signal for diverse cellular responses including growth, proliferation and survival depending on the subunits utilised (Figure 1.12).

For example, NF-κB signalling is known to upregulate anti-apoptotic genes including Bcl-2 family members Bcl-2 and $BclX_L$ as well as cell cycle proteins such as cyclin D2, E2F3a and IL-1β (135-139) in order to promote cell survival and proliferation.

1.4 Cell Cycle and apoptosis

1.4.1 The cell cycle

The cell cycle ensures DNA is replicated and the cellular mass is doubled prior to cell division. There are four basic stages to the cell cycle (Figure 1.13 A). Initially cells undergo a period of growth (G1 phase) before replicating their DNA (S phase). DNA replication is followed by a second growth phase (G2) that generally passes more quickly than the G1 phase, since by G2 phase the cell has more ribosomes allowing faster protein synthesis. The final stage of the cell cycle is mitosis (M phase) in which the cell divides to form two daughter cells.

The cell cycle is a very tightly regulated process with two major checkpoints (Figure 1.13 B). Firstly at the G1-S boundary where cells commit to DNA synthesis and secondly at the G2-M transition where cells commit to mitotic cell division. Progression through these checkpoints is dependent upon the activity of cyclin-dependent kinases (Cdks) and their regulators, the cyclins (Figure 1.13 B). Progression through the early stages of the G1 phase of the cell cycle requires the activation of Cdk4 and Cdk6. These are cyclin D-dependant kinases and are activated by cyclin D1, D2 or D3. Cdk2 and its activator cyclin E are required during the late stages of G1 and for progression into S phase. The Cdk-cyclin complexes of G1 phase promote cell cycle progression by phosphorylating the retinoblastoma (Rb) pocket domain protein (140). Hypophosphorylated Rb binds to transcription factor III B and to an upstream binding factor and hence prevents transcription mediated by RNA polymerase III. RNA polymerase III activation is required for the generation of transfer RNA and the small ribosomal subunit and hence, protein synthesis and cell growth. Phosphorylation of Rb allows RNA polymerase III-mediated transcription and hence cellular growth. Hypophosphorylated Rb also binds to the transcription factor E2F and prevents it

from forming dimers with DP transcription factors. Dimerisation with a DP family member is essential for E2F to activate transcription therefore Rb prevents E2F-dependent transcription. Phosphorylation of Rb by Cdks causes Rb to dissociate from E2F, allowing transcription to proceed. Activation of E2F is necessary for the G1-S phase transition since it regulates the expression of genes required for DNA synthesis and cell cycle progression including DNA polymerase alpha, thymidine synthetase, cyclin D3, cyclin E and cyclin A (140-142).

DNA is replicated during S phase of the cell cycle and this phase is sustained by the activation of cyclins A and E and Cdk2 which enter the nucleus and facilitate DNA replication. On completion of DNA synthesis the cells enter the second period of growth, the G2 phase. During G2 the Cdk2-cyclin B complex accumulates (143) and Cdc25, a protein phosphatase that is only expressed once DNA replication is complete, can activate this complex. Phosphorylation of various target proteins by the active Cdk2-cyclin B complex then allows cells to enter mitosis. Cdk2-cyclin B can also phosphorylate and inhibit itself thus forming a negative feedback loop.

The ability of Cdk-cyclin complexes to allow cell cycle progression is regulated by two structurally distinct families of Cdk inhibitors (Figure 1.13 B): firstly the WAF1 family of proteins (p21, p27 and p57) and secondly the INK4 (inhibitor of Cdk4) family (p15, p16, p18 and p19). The inhibitors p15 and p16 are specific for cyclin D-dependent kinases therefore they are particularly important regulators of Rb and hence can suppress progression through G1 phase and entry into S phase of the cell cycle. The inhibitor p27 suppresses Cdk2-cyclin E and hence prevents completion of S phase (144). Several Cdk-cyclin complexes can be inhibited by p21 including Cdk4-cyclin D1, Cdk2-cyclin E, Cdk2-cyclin A and Cdc2-cyclin A (141). Thus, the activation of p21 can inhibit DNA synthesis and induce cell cycle arrest at both G1 and G2 phases (145). As stated above, expression of the gene encoding p21 can be stimulated by p53 (146) levels of which within a cell are increased during cellular stress or damage and can be further enhanced by $p19^{INK4}$, which stimulates the degradation of MDM2, an inhibitor of p53 (147, 148). By stopping DNA synthesis and cell cycle progression, p53 is able to prevent the replication of faulty DNA or a damaged cell. Following the activation of p53 and

cell cycle arrest, proteins involved in DNA-repair are induced and minor damage to DNA is repaired. The expression of MDM2 is regulated by p53, creating a negative feedback loop that enables cell cycle progression to proceed once DNA damage has been repaired.

1.4.2 Apoptosis: There are many routes to cell death

During the development of B cells, apoptosis plays an essential role in preventing autoimmunity. Earnshaw, Martins and Kaufmann (1999) defined Apoptosis as a "genetically programmed morphologically distinct form of cell death triggered by a variety of stimuli" (149). This process is widely used in development and normal organismal function, for example to delete interdigital webs during mammalian limb development. It is a complex process with a very characteristic morphology. Thus, cells undergoing apoptosis have their DNA fragmented into 200bp sections (and multiples thereof), condensed chromatin, dynamic plasma membrane blebbing, phosphatidlyserine exposure on the plasma membrane and cleavage of enzymes such as Poly (ADP ribose) Polymerase (PARP) (reviewed in (149)). Exposure of phosphatidylserine on the cell surface acts to label the dying cells for phagocytosis by macrophages. It has even been suggested that macrophages may act to simulate apoptosis in "healthy cells" such as initiating apoptosis in vascular endothelial cells during capillary regression (150).

The molecular mechanisms of apoptosis were first studied in the nematode worm *C. elegans* with the discovery of the CED 3 gene that is a homologue of the mammalian caspase proteins (151). The caspases are defined by the MEROPS database (a protease classification system) as cysteine nucleophiles with their catalytic residues in the order His, Cys that cleave proteins after aspartic acid residues. Generally caspases are present in the cytosol as inactive zymogens often referred to as the pro-caspase form. Apoptotic stimuli mediate the processing of these pro-caspases into active caspases. The caspases are divided into two main groups- the initiator (caspases 2, 8, 9 and 10),which are processed first, and effector caspases (caspases 3, 6, 7), which can be activated by initiator caspases.

There are 2 major pathways known to activate caspase-dependent apoptosis, the classical caspase and the mitochondrial pathways. The classical caspase, or extrinsic pathway, is initiated by the ligation of death receptors such as Fas/ CD95 and Tumour necrosis factor receptor (TNFR) which in turn can recruit Fas associated protein with a death domain (FADD). FADD can activate procaspase 8 to become caspase 8, which in turn activates the effector caspase, caspase 3. In contrast the mitochondrial, or intrinsic pathway, involves both the opening of the mitochondrial transition pore and thus loss of mitochondrial membrane potential (MMP) and signalling by the Bcl-2 family of pro and anti-apoptotic proteins. Loss of mitochondrial membrane integrity allows the release of cytochrome c from the mitochondria via the opening of large protein channels sometimes referred to as the mitochondrial megachannel. Cytochrome c then binds to Apaf 1 which stimulates oligomerisation of Apaf 1 and recruits procaspase 9. Cytochrome c, Apaf 1 and procaspase 9 together are sometimes referred to as the apoptosome. This causes autoprocessing of procaspase 9 to caspase 9 which can then activate caspase 3 which acts as an effector caspase. There are a large number of Bcl-2 family members that can either inhibit or aid signalling via the intrinsic pathway. For example, $Bcl X_L$ prevents cytochrome c release from the mitochondria by maintaining mitochondrial membrane integrity whereas Bax and Bak act to induce cytochrome c release by opening mitochondrial channels.

Both pathways are well described however the complex crosstalk between the two is not. Indeed, recent publications describe these two pathways as two aspects of an all-encompassing apoptotic pathway rather than 2 distinct mechanisms for signalling apoptosis (150, 152, 153). Green and Kroemer (1998) thus describe apoptosis as comprising of two major decisions, each decision being mediated by temporally distinct signalling mechanisms. The first is the life/death decision i.e. the decision to commit the cell to apoptosis that is "taken" by the mitochondrial pathway. That is to say that once the mitochondrial permeability pore has opened, the cell has committed itself to die. The second is the apoptosis/necrosis decision i.e. the decision as to whether active death or passive swelling and bursting of the cell will occur that is "taken" by the classical caspase pathway. Therefore the default position, following commitment to cell death, is to die by necrosis unless

this is prevented through initiation of the caspase cascades. However it is not just the caspase cascades that can govern apoptosis as many recent studies have demonstrated that there are more executioner protease systems that are involved in apoptosis. Novel death inducing systems including lysozomal aspartic acid and cysteine proteases such as cathepsin B (154-156), the ubiquitin/ proteosome pathway (157) and a specialized granzyme B pathway in T helper (Th) cells (158). Therefore, we would modify the Green and Kroemer (1998) hypothesis to the apoptosis/ necrosis decision being "taken" by a superfamily of executioner proteases rather than just the caspase cascade.

1.4.2.1 Caspase-mediated apoptosis

Caspases are proteases that share a stringent specificity for cleaving their substrate after aspartic acid residues in target proteins. All caspases contain the active site pentapeptide QACXG where X is R, Q or G. In mammals at least 10 members of the caspase family have been identified. Seven are involved in apoptosis, three in pro-inflammatory cytokine production and one in keratinocyte differentiation. Initiator caspases are identified by their ability to process executioner caspases via either a homeotypic caspase recruitment domain (CARD) or a death effector domain (DED) interaction at the N termini. There are two possible initiation pathways, one via death receptors which process pro-caspase 8 to the active caspase 8 which results in the activation of the executioner caspase, caspase 3. The second is via the release of cytochrome c from mitochondria which leads to the formation of the apoptosome and hence generates active caspase 9. Additionally, it is possible that both the caspase 8 and caspase 9 initiation pathways are activated at the same time as both converge on the activation of caspase 3. Executioner, or effector, caspases are simply defined by the absence of recognizable recruitment domains e.g. caspase 3 and 7. Once activated from their pro-enzyme form they cleave critical cellular substrates including poly (ADP-ribose) (PARP), polymerases and lamins. The caspases are the best-studied family of executioner proteases and have a well-documented role in apoptosis and other forms of programmed cell death

1.4.2.2. Caspase 8

Caspase 8 (MACH/FLICE) is the prototypical apoptosis initiator caspase downstream of the TNF superfamily of death receptors. Substrates for caspase 8 include apoptosis-related effector caspases and pro-apoptotic Bcl-2 family members (159). For example, active caspase 8 cleaves Bid to produce the active pro-apoptotic form tBid (160) which then translocates to the mitochondrial membrane where it acts to trigger cytochrome c release and initiate the mitochondrial apoptotic pathway (Figure 1.14). Caspase 8 is recruited to Fas (Apo1) though the association of a duplicated N terminal motif death effector domain with a homologous motif in an adaptor protein MORT1/FADD. These two proteins form the DISC, or death inducing signalling complex, which can recruit many pro-caspase 8 molecules resulting in self-processing and formation of active caspase 8 enzymes (161). Consequently caspase 8 can induce apoptosis by the activation of downstream caspases 2, 3, 6 and 7.

Consistent with this, caspase $8^{-/-}$ cells are resistant to death receptor mediated apoptosis both *in vitro* and *in vivo* (162). Interestingly, caspase $8^{-/-}$ B and T cells are not capable of repopulating lymphoid organs from sub-lethally irradiated mice suggesting an additional important non-apoptotic role for caspase 8 in immune cell function (163). Consistent with this, the Cre/LoxP system was used to create mice that are both viable and have a caspase 8 deficiency specific to the T cell lineage. These mice display deficiencies in T cell expansion and activation suggesting that caspase 8 is necessary for proper T cell function, homeostasis and preventing immunodeficiencies (164).

1.4.2.3 Caspase 9

Caspase 9 is synthesized as 46 kDa precursor protein containing an inactivating pro-domain. Caspase 9 becomes active after association with Apaf 1 (a homologue of another *C. elegans* death protein CED 4) through its N-terminal pro-domain (165). The amino terminal sequences of Caspase 9 and Apaf 1 both contain a caspase recruitment domain (CARD) motif which is indispensable for their interaction (166). After association, Caspase 9 is thought to be auto-processed and become an active p20/p20/p10//p10 tetramer (167). Human

Caspase 9 activation is negatively regulated by phosphorylation by AKT, a serine–threonine kinase previously implicated in suppressing apoptosis. AKT phosphorylates caspase 9 on serine 96 and inhibits its cleavage and hence protease activity (168).

Apoptotic stimuli such as hypoxic stress, growth factor withdrawal, chemotherapeutic agents or irradiation induce the loss of mitochondrial membrane integrity and facilitate release of cytochrome c to the cytosol. Cytochrome c binds to Apaf 1 and results in a change of conformation of Apaf 1. Subsequently caspase 9 is recruited to this complex and activated by auto-processing that facilitates the cleavage of downstream caspases including caspase 3. Thus, cytochrome c-mediated caspase activation through caspase 9 serves as an amplification mechanism during apoptosis as one apoptosome can mediate the processing of many pro-caspase 3 molecules (169).

The physiological function of caspase 9 has been investigated by analysis of knockout mice. Casapse 9 homozygous knock out mice generally die perinatally with a markedly enlarged cerebrum caused by a reduction of apoptosis at an earlier stage of brain development (170). In contrast, the loss of caspase 9 does not affect morphological developments of the spinal cord and other non-neural tissues. Interestingly, despite normal development of the thymus, isolated thymocytes are nevertheless resistant to a subset of apoptotic stimuli (etoposide, dexamethasone, radiation and treatment with anti-CD3 and CD28 Abs) and exhibit delayed DNA fragmentation (171). However Fas-mediated apoptosis is not affected in caspase 9-deficient thymocytes demonstrating that such apoptosis can occur in a completely caspase 9-independent fashion via the extrinsic pathway (171).

1.4.3. The Bcl-2 family

The Bcl-2 proteins comprise of a family of small proteins between 18 kDa and 26kDa in size. Individual members can be sub-divided into 3 categories as shown in Figure 1.15. The anti-apoptotic family members, such as Bcl-2, and Mcl 1, contain 4 Bcl-2 homology (BH) regions. The pro-apoptotic members e.g. Bak and

Bax are structurally very similar to the anti-apoptotic proteins but do not contain a BH4 domain. Finally, there are the BH3 only proteins such as Bim, Bad, and Bid, which are pro-apoptotic. All of the Bcl-2 family members appear to be able to bind to membranes both in the ER and the mitochondria as well as being present in the cytosol (172). The original doctrine was that the pro-survival Bcl-2 proteins act by binding to the mitochondrial membrane and preventing the release of cytochrome c and hence inhibiting the activation of caspase 9. By contrast, the pro-apoptotic Bcl-2 family members, such as Bax, were proposed to sequester Bcl-2 and hence stimulate apoptosis. However the actions and interactions of Bcl-2 family members appear to be far more complicated than first anticipated (173, 174). A recent review by Christoph Borner (2003) suggested that there are at least 4 possible modes of action for Bcl-2 family members. Furthermore he suggested that it is likely that different Bcl-2 family members use combinations of these methods and the precise method employed may be signal and cell type specific (172).

1.4.3.1 Bcl-2 family members can form channels in intracellular membranes

Protein crystallography has revealed that many Bcl-2, family members, such as Bax and $BclX_L$, have strong homology to bacterial pore-forming toxins (175). Therefore it was suggested that the pro-apoptotic Bcl-2 proteins could insert into the mitochondrial membrane and hence stimulate release of Smac, a pro-apoptotic mitochondrial protein, and cytochrome c (176). It has been demonstrated that purified, recombinant Bax can induce channels that allow for cytochrome c release. Indeed, it is possible that such channels are formed by interaction with existing mitochondrial channels such as the voltage dependent anion channel (VDAC) rather than direct insertion into the mitochondrial membrane (177). In contrast, it has been proposed that anti-apoptotic Bcl-2 family members, such as $BclX_L$, can oppose this by binding to VDAC and stimulating closure of the pore (178). There is still much controversy over which method of Bcl-2-induced channel formation is employed *in vivo*.

1.4.3.2. Bcl-2 family members can interact and sequester other Bcl-2 family members

As would be predicted by the nature of their closely related structures Bcl-2 proteins can interact closely and bind to each other. The functional outcome of these interactions depends on the specific Bcl-2 family members involved. For example, homodimerisation of $BclX_L$ molecules has anti-apoptotic functions in protecting mitochondrial membrane integrity (179) whereas sequestration of $BclX_L$ by dimerisation with Bad prevents such protective functions and allows for opening of the permeability transition pore (180). Similarly, Fluorescence Resonance Energy Transfer (FRET) demonstrated that Bax can interact with many other Bax molecules (181) and such Bax oligomerisation results in loss of MMP and commitment of the cell to apoptosis (182).

1.4.3.3 Bcl-2 family members may interact with other cell signalling proteins

The yeast 2-hybrid system demonstrated potential interactions between Bcl-2 and $BclX_L$ and many other signalling proteins such as Bap 31, 53BP-2, ANT, R-Ras and calcineurin (reviewed in (183)). However, these signalling elements did not interact with Bak or Bax and it was therefore postulated that the binding of Bcl-2 and $BclX_L$ to these proteins had a cytoprotective function. For example, pro-survival Bcl-2 family proteins might prevent the induction of p53, and hence pro-apoptotic genes, by sequestering the p53-binding protein 53BP-2. Similarly, pro-survival Bcl-2 family proteins might prevent exposure to mitochondrial poisons by binding to the mitochondrial channel ANT. However there is little causal evidence to support a cytoprotective function of Bcl-2/ $BclX_L$ in binding to non-Bcl-2 family members.

1.4.3.4. Bcl-2 family members have anti-oxidant properties

Production of reactive oxygen species (ROS) by damaged mitochondria has been shown to induce apoptosis and has been implicated as the major apoptotic signal in some disease states, such as cell death following cardiac ischemia (184). Hockenberry et al showed that the anti-apoptotic Bcl-2 protein could counteract the damage done by some reactive oxygen species (185) and postulated that the molecular structure of Bcl-2 allows for quenching of ROS. Furthermore, Bcl-2 can also promote maintenance of mitochondrial membrane integrity and thus prevent the amplification of the apoptotic signal by inhibiting the further release of

cytochrome c (186, 187). There is no formal evidence to confirm that anti-apoptotic Bcl-2 family members do have this ROS quenching capacity.

Consistent with the idea that more than one of these mechanisms may be required for apoptosis, recent reviews have suggested that there are three "ingredients" necessary to produce a dissipation of the MMP during apoptosis mediated by Bcl-2 family members. These are the simultaneous presence of: (i) truncated Bid (cleaved by caspase 8) (ii) oligomerised Bax or oligomerised Bax and Bak complexes (<200Kda) (iii) a specific lipid environment including cardiolipin which is localised at the inner membrane/ outer membrane (im/om) contact sites.

1.4.3.5 Activation of Bax and Bak

Treatment of chronic lymphocytic leukaemia B cells with chemotherapeutic drugs, such as dexamethasone, has been found to increase the number of cells undergoing Bax/Bak dependent apoptosis and this activation of Bax and Bak is independent of upstream caspase activation (188). However, use of the pan-caspase inhibitor Z-VAD-FMK could rescue the cells from apoptosis and prevent some of the hallmarks of apoptosis including caspase 3 activation, exposure of cell surface phosphatidylserine residues and even partially reverse the dissipation of the MMP. However, there is no change in the conformation of Bax or Bak and both remained active. This indicates that activation of the Bax/Bak is an early apoptotic event occurring prior to caspase activation and thus, induction of apoptotic morphology.

To investigate the mode of Bak/Bax action, Capano and Crompton (2002) used a Bax-GFP fusion protein which was transfected into cultures of cardiomyocytes (182). These cells were treated with staurosporine to induce apoptosis and Bax-GFP action imaged using a confocal microscope. At early time points, and also in the control cells, there is a dispersed distribution of Bax throughout the cytosol and this pattern can be seen for up to 3 hours after drug treatment. However, after 4 hours there is a punctate distribution of Bax, which is found in large aggregates in close proximity to the mitochondria. They termed these two phases the pre and post-Bax aggregation phases and suggested that the start of the post-Bax

aggregation phase signals the time point of initiation of the apoptotic process resulting in dissipation of the MMP and cytochrome c release. Previous work (189, 190) had suggested that the VDAC could provide the structure that makes the mitochondria permeable to cytochrome c. Moreover, it had been postulated that Bax would act to open the pore whilst $BclX_L$ could protect MMP by promoting closure of the VDAC pore (189, 190). Capano and Crompton have now extended this theory by suggesting that, during the pre-Bax aggregation phase, the VDAC interacts with Bax and leads to the formation of large Bax aggregates and the release of cytochrome c. Moreover, it was suggested that during the post-Bax aggregation phase Bax interacts with the adenine dependent anion channel (ANT) to further increase mitochondrial permeability (182). It is still not clear if Bax is the only pro-apoptotic Bcl-2 family member responsible for this. However, it has recently been suggested that the Bcl-2 family members can actually change the physical structures within the mitochondria. For example, in wild type mice apoptosis is associated with an increase in mitochondrial contact sites, where the inner and outer mitochondrial membranes meet and pro-apoptotic Bcl-2 family members are postulated to act (191). However, in $BclX_L$ overexpressing mice, mitochondria maintain a normal appearance in the presence of apoptosis inducing stimuli (191). This study showed that the presence of $BclX_L$ stops the increase in mitochondrial contact sites and implies that Bcl-2 family members are capable of making a permanent change to subcellular morphology of the mitochondria.

1.4.3.6. The BH3-only members of the Bcl-2 family modulate apoptosis

The BH3-only proteins had originally been considered to be "messengers" of apoptosis by acting to trigger Bax/Bak oligomerisation. However this now seems to be an over-simplification of the actions of this family of proteins. Indeed, the BH3-only proteins represent a set of proteins that have distinct and diverse cellular functions. Consistent with this, whilst all the BH3-only proteins share the BH3 domain, they otherwise appear structurally unrelated. The BH3 domain functions as an important death domain for these proteins that is essential for both pro-apoptotic activity and ability to bind to the multi-domain Bcl-2 family members. However, the BH3-only family can now be further subdivided into two groups:

"activators" e.g. Bid which can act to directly bind and activate mitochondrially localised Bax and Bak and the "enablers" e.g. Bad which sensitise cells to apoptosis by binding anti-apoptotic Bcl-2 family members (Figure 1.16). (192).

1.4.3.6.1. The BH3 only activator Bid

Although Bid is often described as being activated by the caspase 8 family it can in fact be cleaved by multiple protease systems including granzyme B, lysozomal enzymes and calpains. It is a 195 residue, 22 KDa protein which has been demonstrated, by NMR, to have remarkably similar structural elements to both Bcl-2 and $BclX_L$ (2 central hydrophobic α helices surrounded by 6 amphipathic helices) which may suggest an anti-apoptotic function (reviewed in (176)). By contrast, truncated Bid is an important activator of the caspase 9 cascade as tBid induces Bax/Bak oligomerisation and hence stimulates their activation of the VDAC and ANT. This opens the mitochondrial permeability pore and results in dissipation of the MMP, release of cytochrome c and hence caspase 9 activation (193). After cleavage tBid remains associated with the amino terminal fragment of Bid, nBid. Only after dissociation from nBid can tBid translocate to the mitochondria where it can induce the oligomerisation of Bax/Bak (194). It is thought that this dissociation is mediated by cardiolipin, a mitochondrial-specific phospholipid, which has a higher affinity for tBid than nBid (195). It has been shown that the presence of cardiolipin or monolysocardiolpin (a metabolite of cardiolipin that increases during apoptosis) are sufficient for the dissociation of nBid from tBid (194). Kuwana et al also demonstrated that cardiolipin is essential for the formation of the supra-molecular complex that contains tBid and Bax (196). Cardiolipin is found in high concentrations in the inner mitochondrial membrane, including the contact sites where the inner and outer mitochondrial membranes interact following induction of apoptotic signalling. Truncated Bid has been shown to be associated with these contact sites where it can induce a conformational change in the N terminal domain of Bax (193). This change in Bax combined with a change in mitochondrial cristae structure is thought to activate the release of cytochrome c (197).

The exact mechanism by which Bid is able to trigger cytochrome c release is still under debate. Bid is thought to have some intrinsic activity as a protein channel

due to its structural homology to bacterial porin molecules, however this activity has not been demonstrated *in vivo* (198). In addition to this, tBid is able to trigger integration of Bax into the mitochondrial membrane (199). This may allow Bax to act as a protein channel itself or may stimulate opening of the permeability transition pore through interaction with the voltage dependent anion channel (177). Regardless of the mechanism, this would lead to swelling of the mitochondria, rupture of the mitochondrial membrane and release of cytochrome c. However to add a further layer of complexity, some forms of apoptosis, where the mitochondrial pathway has been implicated, have reported shrinkage of the mitochondria suggesting there may be other factors involved in the opening of the permeability transition pore (200-202). Finally, Bid can act to sensitize the cells to apoptosis by binding to, and sequestering, anti-apoptotic Bcl-2 family member $BclX_L$ (203).

1.4.3.6.2. The BH3 only enabler Bad

Bad is the best-characterised pro-apoptotic BH3-only family member. Indeed, it was the first BH3 only molecule that was shown to be connected to proximal signal transduction through a phosphorylation response (204, 205). Thus, when Bad is in its non-phosphorylated state it is able to bind, and sequester, the anti-apoptotic Bcl-2 family members Bcl-2 and $BclX_L$. This prevents Bcl-2 and $BclX_L$ from protecting the mitochondrial membrane integrity and hence allows for mitochondrial permeability pore transition and initiation of apoptosis. However if Bad is phosphorylated, for example by AKT, this allows for binding of Bad with the cytosolic 14-3-3 proteins. This prevents Bad from being translocated to the mitochondria and therefore such sequestration of Bad acts as a pro-survival signal (206, 207) (Figure 1.7). Interestingly, Bad is unable to directly interact with either Bak or Bax and so is not thought to directly stimulate their oligomerisation, and opening of the permeability transition pore (208).

As indicated above, protein- protein interactions between Bcl-2 family members constitutes an important regulatory mechanism governing cell fate as the ratio between pro-apoptotic and anti-apoptotic Bcl-2 family dimers can be the primary

determining factor in the commitment to life or death. For example, Bad has been demonstrated to be able to bind both Bcl-2 and $BclX_L$ via its BH3 domain. However Bad can bind $BclX_L$ far more strongly than Bcl-2 can bind $BclX_L$ suggesting that Bad can displace $BclX_L$ from $BclX_L$ –Bcl-2 dimers (204, 209). In addition to this, Bad can interact more strongly with $BclX_L$ than either Bak or Bax and would therefore displace $BclX_L$ from Bax/ Bak complexes. This increase in free Bax and Bak would promote Bax/Bax oligomerisation and therefore apoptosis (210). Moreover, overexpression of Bad in the absence of $BclX_L$ has also be shown to produce an acceleration of the apoptotic response suggesting that Bad may also be able to mediate apoptosis by other mechanisms (211).

Surprisingly, Bad has also been shown to act as a pro-survival factor in some cell types. In fact it has been suggested that pro-apoptotic Bcl-2 family members are not only latent death factors but may also carry out important functions in healthy cells. For example, Bax and Bak have been postulated to function as anti-death factors in some neurones and mouse models however the mechanisms involved remain elusive (212, 213). By contrast, Bad has been shown to regulate cellular metabolism and facilitate the utilisation of the glycolytic pathway. Glucose can actually induce the phosphorylation of Bad and such phosphorylated Bad was found in a large mitochondrial complex including glucokinase, a member of the hexokinase family where it is thought to enhance glucose production (214). Consistent with this, knock out mice that are deficient in Bad exhibit characteristics of diabetes (214). This suggests that Bad can act as a sentinel to monitor glycolysis such that if there are abnormalities in glucose metabolism, Bad can trigger apoptosis in pancreatic and liver cells and hence integrate the apoptotic and metabolic pathways.

One possible mechanism for distinguishing the pro and anti-apoptotic effects of Bad is presented by a report suggesting that full length Bad had a solely anti-apoptotic function in neurones, and protected against apoptosis in response to non-viral death stimuli (215). The exact mechanism for this protection is not known. By contrast, the cleavage product of Bad (N terminally truncated, Bad_S) is generated by members of the caspase family. Indeed, Bad was shown to act as a

potent inhibitor of cell death in this system prior to conversion to the pro-death stimulus Bad_S by cleavage at aspartate 61 by recombinant casapse 3.

Further evidence for pro and anti-apoptotic functions of Bad have been provided by mice deficient in Bad, which were viable with a reduced lifespan (216). Investigation of the B and T lymphocytes subsets in such mice found them to be present and normal. Moreover, the Bad-deficient thymocytes apoptosed normally in response to serum withdrawal although they exhibited a modest, but consistent, delay in apoptosis following γ irradiation suggesting apoptosis can be Bad-independent in these cells. Interestingly, Bad-deficient B cells were found to exhibit a reduced proliferative response to anti-IgM and anti-CD40 (but demonstrated a normal response to LPS). Consistent with this, whilst Bad $^{-/-}$ B cells also displayed a normal production of IgM, they showed a decreased production of IgG. Further characterisation of such lymphocytes revealed that these differences were not due to cell death or subset differentiation suggesting that Bad may be essential for anti-CD40 and anti-IgM induced proliferation and differentiation of mature B cells. Nevertheless, the decreased lifespan resulted from the Bad $^{-/-}$ mice developing a large B cell type lymphoma in both the spleen and lymph nodes which was found to be of a B220 positive mature B cell phenotype of germinal centre origin (216). This also therefore implicates Bad in normal mature B cell apoptosis. Therefore Bad has been implicated in both proliferative and apoptotic responses in mature B cells.

1.5 Alternative executioner proteases

1.5.1 Cathepsins

In addition to the canonical caspase cascades described above, there are other executioner protease systems that can be induced by pro-apoptotic stimuli to mediate apoptosis. The cathepsins are another family of cysteine proteases that are lysosomal thiol proteases. The murine cathepsin family has 15 known members that are involved in bulk protein turnover, protein processing, Ag presentation, tumour formation and apoptosis. Cathepsins B, H and L are expressed ubiquitously however the other cathepsins have tissue specific

expression (217). They are active during acidic conditions, such as within the lysosome, however they are unstable in neutral or alkaline conditions. These proteases are regulated by the binding of endogenous protein inhibitors called cystatins.

Lysosomes have traditionally been seen as "suicide bags" due to their ability to degrade proteins, carbohydrates and lipids. However many forms of apoptosis have now been shown to involve moderate rupture of the lysosomes referred to as small scale lysosomal leakage (ssLL) (218, 219). This allows release of cathepsins into the cytosol and hence degradation of cellular proteins. Enzymes termed lysoapoptases, which can convert inactive pro-caspase zymogens into their active forms, are also released which have been demonstrated to activate pro-caspase 3 (220). However there is no evidence for direct activation of caspases by cathepsins. The molecular identity of many of the mediators of cathepsin-activated apoptosis have yet to be identified. However there in strong evidence for the involvement of cathepsins in both caspase-dependent and independent apoptosis (221).

There has been resistance to the idea that apoptosis can be mediated by cathepsins due to two lines of evidence. Firstly, as has already been mentioned, cathepsins have optimal activity in acidic conditions and so were thought to act only within the lysosomes. Secondly cathepsin $B^{-/-}$ mice were generated which were found to have an overtly normal phenotype (222). However it is important to note that knock out animals defective in Bid, Bax, Caspases 1, 2, 6, 11 and 12 also had overtly normal phenotypes. Animals defective in caspase 3, 7 and 9 also had phenotypes of differing severity depending on the strain used to produce the animals suggesting that defects are tissue and strain specific (reviewed (223)). New evidence has now shown specific phenotypes in cathepsin $B^{-/-}$ animals. For example, treatment of hepatocytes from these animals with TNFα did not result in apoptosis, cytochrome c release and caspase 3 and 9 activation as is observed in wild type animals suggesting that cathepsins are activated in a stimulus and cell type specific manner (224).

In some systems cathepsins can act in a caspase-independent manner to induce apoptosis. For example, astrocytes, cultured from rat cerebral cortices, undergo apoptosis in response to H_2O_2 exposure in a caspase-independent manner and the death-inducing properties were found to be regulated by cathepsins B and D (225). Furthermore, anti-thymocyte globulins induce a rapid, dose-dependent T cell depletion in peripheral lymphoid tissues which is caspase-independent and associated with the activation of cathepsin B (226). Moreover, work conducted in our own laboratory has also implicated cathepsins in the caspase-independent apoptosis of the immature B cell line WEHI 231 (156). Such apoptosis, triggered by ligation of the BCR, results in translocation of PLA_2 from the cytosol to the mitochondria, reduction in ATP levels and disruption of the MMP. However, there are none of the hallmarks of classical caspase-mediated cell death such as cytochrome c release, PARP cleavage or activation of caspase 3. By contrast, there was a strong increase in the activation of cathepsin B. Perhaps consistent with all of the above, there is also evidence to suggest that cathepsin B can cleave the pro-apoptotic Bcl-2 family member Bid to the active form tBid (218).

1.5.2 Calpains

The calpains represent another family of cysteine thiol proteases that have been implicated in cellular responses as diverse as cell death and proliferation. They are expressed in ubiquitous forms (calpains m and μ) and tissue specific forms (n calpains). Calpain n1 is found exclusively in skeletal muscle whereas calpains n2 and n2' are found in the stomach (reviewed in (227)). Calpains are regulated by calcium flux, intracellular inhibitors and membrane targeting and are under tight regulation as calpain is abundant in the cytosol and is thus capable of cleaving many intracellular signalling and structural proteins. Calpains have been implicated in the regulation of proliferation and normal cellular function. For example, in the immature B cell line WEHI 231, calpain is implicated in the degradation of IκB and hence activation of NF-κB resulting in cell growth. Moreover, knock out mice that lack the large calpain regulatory subunit die during embryonic development due to defects in vascular development (228). Furthermore, one form of human muscular dystrophy is associated with defects in the muscle-specific calpain 3 gene (229).

Collectively these data suggest that correct expression and regulation of calpains is necessary for normal cell function.

Consistent with reports that calpains have been implicated in cell death there is evidence that the cellular targets for calpain and caspase proteolysis are very similar. For example, caspase 3 and calpain share many substrates including Tau, keratins, PLC, PKCα, β, γ, Bcl-2 and Bax and indeed, many of the resulting fragments produced by cleavage are similar or identical regardless of which of these executioner proteases are utilised (230). As calpains are regulated by calcium influx they tend to become activated in extreme pathological conditions, for example necrosis and apoptosis are associated with a sustained rise in intracellular calcium levels. The exact mechanism of calpain involvement and integration with the caspase pathway has not yet been elucidated. It has, however, been demonstrated that activated caspase 3 cleaves cytoskeletal proteins which can increase membrane permeability and hence, calcium influx resulting in activation of calpain. Additionally, caspases are able to degrade the endogenous inhibitor of calpain, calpastatin, and so activate calpains suggesting calpains may act downstream of caspases. However, calpains can act to cleave caspase 3. The consequence of this is unknown, however some groups report that this may inhibit caspase 3 activation by producing a fragment that is resistant to subsequent activation (reviewed in (230))(Figure 1.17). Further research in this area will hopefully resolve this issue soon

Another important question still remains as to whether calpains act to initiate and effect apoptosis on their own, without utilising caspase cascades. For example, it is known in UV treated cortical neurones that both caspase 3 and calpains are activated. Furthermore, it has been demonstrated that it is the calpains that act to produce the hallmarks of apoptosis, as apoptosis occurs in this system even when all initiator and effector caspases are inhibited (231). Similarly, it has also been shown that in human breast cancer cells, the active form of vitamin D3 acts to increase intracellular calcium levels and induce μ calpain-dependent apoptosis. This also occurs in the absence of any effector caspase activation (109). However, investigation of other systems reveals that the type of calpain-dependent apoptosis

induced appears to be stimulus specific. For example, using a neuronal cell line, addition of either staurosporine or a neurotoxin produces calpain activation which is either caspase-dependent or independent in the same cells depending on the stimuli (232). Taken together these data suggest that caspase-independent and calpain-dependent apoptosis can occur, however the phenotype of apoptosis is both cell type and stimuli specific. Nevertheless, calpain-dependent and caspase-independent apoptosis has now been demonstrated in many systems including dexamethasone treated thymocytes, (108), staurosporine treated neuroblastoma cells, growth factor derived PC12 cells and UV treated rat neurones (233).

Interestingly, it has been demonstrated that in chronic lymphocytic leukaemia a decrease in apoptosis and prolonged survival of B cells is associated with impaired calpain function. Indeed, the ubiquitously expressed μ calpain is found to be transcriptionally downregulated three fold in this system (234). Consistent with a key role in B cell apoptosis calpain was found to specifically trigger the activation and processing of caspase 7 following ligation of the BCR, a pro-apoptotic signal in the immature B cell line WEHI 231. Interestingly, CD40 ligation, which is a pro-survival signal in these cells was associated with an increase in the expression of the calpain inhibitor calpastatin (235). Taken together this suggests that calpain may be critical for B cell deletion during lymphocyte development and function.

1.6. Negative Feedback Inhibition in mature B cells

1.6.1 Negative Feedback Inhibition is mediated by FcRs

Once an infection has been cleared it is important that the B cell response is properly switched off. This involves a homeostatic process called negative feedback inhibition (236). This restores B cell numbers to their original pre-infection levels by preventing further proliferation and hence prevents the aberrant overproduction of Abs. This process is mediated by coligation of both the BCR and FcγRIIb by Ag-Ab immune complexes (Figure 1.18).

Fc receptors (FcRs) provide a critical link between the humoral and cellular arms of the immune system by binding the Fc domain of antibodies. Separate FcRs

exist for each of the five classes of immunoglobulin: FcαR (IgA), FcδR (IgD), FcεR (IgE), FcγR (IgG), and FcμR (IgM) (236). The FcγRs are specific for the Fc domain of IgG, and comprise a family of structurally homologous, yet distinct, receptors that were first discovered over 35 years ago. Four classes of FcγR exist, FcγRI, FcγRII, FcγRIII and FcγRIV. These 4 classes are defined by their cellular distribution, structure and affinity for the IgG subclasses (237). For example, FcγRI is a high affinity receptor, which is capable of binding monomeric IgG at physiological concentration (238). In contrast, FcγRII and FcγRIII are low affinity receptors that can only bind IgG that is complexed to multivalent soluble antigen as immune complexes (237). The binding properties of IgG Abs was found to be independent of the $F(Ab)_2$' fragment and only the Fc portion was required for interaction with the receptor.

The only FcγR found on B cells is the FcγRIIb receptor (CD32), and as stated above, this receptor inhibits signalling through the BCR upon coligation of the BCR and FcγRIIb by IgG containing immune complexes. FcγRIIb is a single chain glycoprotein that binds to IgG with a low affinity. Signalling is initiated courtesy of a 13 amino acid inhibitory immuno-tyrosine inhibitory motif (ITIM) motif on the cytoplasmic domain of FcγRIIb (239). The ITIM sequence has been shown to be necessary and sufficient to inhibit BCR generated calcium mobilisation and cellular proliferation (240). Phosphorylation of the tyrosine residue of the ITIM by the PTK Lyn occurs upon coligation of the BCR with FcγRIIb. This generates a SH2 recognition domain that can bind the SH2-containing inositol phosphatase SHIP and possibly the tyrosine phosphatases SHP1 and SHP2 (241, 242).

FcγRIIb signalling is proposed to have different functions depending on the context of the signal. Thus, homo-aggregation of FcγRIIb by non-cognate immune complexes, i.e. without coligation of the BCR, is thought to provide a pro-apoptotic signal (Figure 1.19) (243). Although the exact nature and function of this signal has not been elucidated it is thought to maintain peripheral tolerance to potentially cross-reactive auto antigens (244). The main evidence for this proposal comes from FcγRIIb deficient mice that die at 8 months due to the development of auto-antibodies and an autoimmune glomerulonephritis which closely models the

human autoimmune disease Goodpasture's Syndrome. Furthermore, such FcγRIIb $^{-/-}$ mice develop autoimmune diseases, such as arthritis, with increased severity compared to wild type mice. In contrast, coligation of the BCR and FcRIIb leads to inhibition of the extracellular Ca^{2+} influx (245), reduction of cell proliferation (246) and blockage of blastogenesis (247).

1.6.2 Signalling mechanisms underlying FcRIIb-mediated growth arrest and apoptosis

1.6.2.1 SHP1/2

As stated above, once the ITIM of FcγRIIb has been phosphorylated it is has the potential to recruit a number of SH2 domain containing phosphatases. Early studies had implicated key roles for the tyrosine phosphatases SHP1 and SHP2, which are capable of dephosphorylating ITAMs and other signalling molecules and hence antagonising the action of tyrosine kinases (248). SHP1 is a 64-kDa protein, which is expressed predominantly in haematopoietic cells. Whereas the 68-kDa, SHP2 protein is ubiquitously expressed. Both phosphatases have been functionally implicated in the regulation of signaling in haematopoietic cells using transgenic mice (249). The overall structure of these 2 phosphatases is similar, with two SH2 domains in their amino terminal half, a phosphatase domain in the carboxy-terminal half of the protein and a C-terminal tail region, important for regulation of phosphatase activity.

A naturally occurring strain of mice, *Motheaten*, does not express SHP1 and a variant, *motheaten viable*, expresses catalytically inactive SHP1. Both of these mutations cause premature death of the mice reflecting the phenotype of these mice which includes systemic autoimmunity, severe inflammation and dysregulation of multiple immune cell lineages including B and T cells, macrophages and natural killer cells. Evidence for a role for this signalling element in negative regulation of B cells came from the exaggerated signalling via the BCR in *motheaten* mice and the resultant hyper-reactive B cells which produced auto-Abs. This hyperactivity of such B cells reflected increased tyrosine phosphorylation, calcium mobilisation, and proliferation and decreased threshold

for BCR signalling (249, 250). Likewise, SHP2 has been implicated in the regulation of similar pathways including the dephosphorylation of Grb2 associated binder (Gab1) adaptor protein. SHP2 disrupts the PI-3 kinase/ Gab1 interaction and inhibits PI-3 kinase-mediated downstream signals which would downmodulate proliferation (Figure 1.20) (251).

However more recent studies have been unable to find physical interactions between FcγRIIb and SHP1. Indeed work in this laboratory has been able to show a physical interaction between FcγRIIb and SHP2 and SHIP but not SHP1 (124). Studies in human B cell lines have also yielded similar results demonstrating a physical link between FcγRIIb and Lyn, PKC, SHIP and SHP2 but not SHP1 (252). Furthermore, FcγRIIb-mediated inhibitory signalling has been shown to be normal in *motheaten* mast cells (253) and BCR-induced calcium flux can still be inhibited by FcγRIIb signalling in SHP1$^{-/-}$ deficient DT40 cells (254). Taken together this data suggests that SHP1 is dispensable for FcγRIIb-mediated negative feedback. By contrast, numerous studies have suggested that 5' inositol phosphatase SHIP selectively binds to phosphorylated FcγRIIb *in vivo* and is responsible for the FcγRIIb mediated negative regulation of B cell activation (255, 256).

1.6.2.2. SH2 domain-containing Inositol-5-Phosphatase (SHIP)

SHIP1 is a 145KDa protein with an N terminal SH2 domain and a C terminal phosphatase domain (257, 258). SHIP is able to negatively regulate calcium flux, activation of the ERK signalling cascade and activation of AKT (259). There are three splice variants of SHIP, all of which are found only in the leukocyte lineage. In contrast, SHIP2, the product of a distinct gene from SHIP, is ubiquitously expressed (260).

SHIP knock out mice have been generated and they are viable but show a markedly decreased life span reflecting splenomegaly, increased B cell numbers, and an increase in both basal serum Ab levels and elevated Ab production upon challenge. SHIP$^{-/-}$ B cells are hypersensitive to both constitutive and Ag induced signals and show increased survival and activation suggesting that SHIP$^{-/-}$ B cells

have abrogated FcγRIIb-mediated negative feedback inhibition (261). Furthermore, crossing SHIP$^{-/-}$ and FcγRIIb$^{-/-}$ mice on a B57B1/6 background produces animals that spontaneously develop a lupus like autoimmunity. This suggests a pivotal role for both FcγRIIb and SHIP in regulation of peripheral tolerance (262).

SHIP has been suggested to negatively regulate BCR-mediated B cell activation by 3 distinct mechanisms. Firstly, SHIP can act to reduce calcium flux by converting PI-(3,4,5)-P_3 to PI-(3,4)-P_2 and thus reducing the docking sites for PH domain proteins including Btk and PLCγ. By impairing the membrane translocation of these proteins SHIP inhibits the production of second messengers (IP_3 and DAG) that mediate both calcium mobilisation and PKC activation (263). Secondly, reduction of PI-(3,4,5)-P_3 levels has been demonstrated to suppress the recruitment of the anti-apoptotic element AKT (264). However there is some controversy in this field as the product of SHIP, PI-(3,4)P_2 has also been postulated to recruit and activate AKT (265). However, some of the confusion relating to the roles of SHIP-derived PI-(3,4)-P_2 may be resolved by the recent finding that the 3' inositol phosphatase PTEN is also recruited by FcγRIIb to antagonise the action of PI-3 kinase (124). Inhibition of the PI-3 kinase pathway also potentially inhibits the ERKMAPKinase cascade and suppresses cell proliferation (266). PTEN activation is slower than SHIP activation and may therefore sequentially terminate ongoing PI-3 kinase activity. This would ensure a strong desensitization of AKT and hence induce both growth arrest and apoptosis (124). Finally, SHIP is able to act as an adaptor binding to both Shc and p62Dok and hence inhibiting the RasMAPKinase pathway. For example, SHIP is thought to be able to displace the Grb:SOS complex from Shc and so inhibit BCR-mediated recruitment of Ras and its downstream effectors (267, 268). Moreover, SHIP can bind to, and recruit, p62Dok via its PTB domain resulting in the phosphorylation of Dok which in turn recruits RasGAP (269). RasGAP stimulates the conversion of RasGTP to RasGDP and hence inhibits both Ras and ERK activation. Consistent with this, recruitment of SHIP to FcγRIIb is known to prevent cells from entering the cell cycle by abrogation of cyclin induction (270).

Finally, previous work in this laboratory has demonstrated that ligation of FcγRIIb also leads to a rapid association of ERK and the ERKMAP kinase phosphatase Pac1 (124). Pac1 is a dual specificity tyrosine/threonine phosphatase that is expressed predominantly in haematopoietic cells was discovered by virtue of its specific inactivation of ERK in T cells (271, 272). Pac1 acts to dephosphorylate the activatory motif of ERK directly and hence allows for rapid and direct termination of the ongoing ERK signals. Indeed, the induction of Pac1 seems to represent a universal mechanism for inhibition of ongoing ERK signals leading to proliferation in B cells (271, 273, 274).

1.7 Aims and Objectives of the thesis

The nature of the signal produced by the BCR is both context and maturation stage specific. Thus, BCR signalling displays a dichotomy in as much as ligation of the BCR at the immature B cell stage generates an apoptotic signal that can be rescued by co-engagement of CD40, whereas in mature B cells, BCR ligation results in survival, proliferation and Ab production. However, in mature B cells, simultaneous coligation of the BCR with FcγRIIb results in cell cycle arrest and apoptosis. This project aimed to characterise the role of the differential signals involved in such proliferative and apoptotic pathways in immature and mature B cells

For this study, the lymphoma cell line WEHI 231 has been utilised as a model for the immature B cell stage. In these cells it has been previously shown in this laboratory that ligation of the BCR induces an early, strong and transient peak in phospho-ERK activity which is associated with the induction of apoptosis (275). A key feature of this form of apoptosis is the ERK-dependent mitochondrial translocation and activation of PLA_2 (156) which results in the loss of mitochondrial membrane integrity, depletion of ATP and activation of the executioner protease, cathepsin B (156). By contrast, there is an essential role for sustained yet cyclic ERKMAP kinase signalling in CD40-mediated rescue from BCR-mediated apoptosis in WEHI 231 cells (275). Moreover, this increased cell survival has been shown to be associated with an increase in the expression of $BclX_L$ which is known to act to maintain mitochondrial integrity (191, 276, 277).

The specific objectives were therefore to further delineate the precise molecular mechanisms regulating the ERK-dependent, $cPLA_2$-mediated apoptotic pathway of immature B cell deletion and its rescue by CD40 signals involving sustained, yet cycling ERK activation, and $BclX_L$ upregulation (see 3.2 Aims and Objectives).

By contrast and as stated above, previous work in our laboratory and others has demonstrated that ligation of the BCR in mature B cells results in ERKMAPK-

dependent proliferation and Ab production (124, 275, 278-280).However, negative feedback inhibition of B cell activation by Ag-Ig immune complexes induces simultaneous coligation of the BCR and FcγRIIb and results in inhibition of growth and a reduction in antibody production (124, 281-283). We have also recently demonstrated that such coligation of BCR and FcγRIIb eventually results in apoptosis. The specific aims of the present study were therefore to fully characterise the phenotype of growth arrest and apoptosis resulting from coligation of the BCR and FcγRIIb in mature B cells and to define the signalling elements involved (see 4.2 Aims and Objectives).

Figure 1.1: Summary of the Development of conventional B2 cells

The various stages of B cell development are marked by a series of changes in location and in the expression of immunoglobulin heavy and light genes, intracellular proteins, and surface markers. B cell development starts in the bone marrow (or foetal liver) with the commitment of haematopoietic stem cells (HSCs) to the B cell lineage. Rearrangement of the heavy chain locus genes begins in the early pro-B stage. Cells are allowed to progress to the next stage if a productive rearrangement has been achieved. Although no functional immunoglobulin is expressed in late pro-B cells there is surface expression of accessory Igα/Igβ heterodimers. Ag-independent development continues within the bone marrow, where pre-B cells express a pre-BCR consisting of cytoplasmic μ chain in combination with a surrogate light chain, V_{preB} and $\lambda 5$. Successful light-chain gene rearrangements result in the surface expression of a functional IgM molecule at the immature B cell stage. Immature B cells then undergo the Ag-dependent stage of B cell development where recognition of self-Ag can lead to clonal deletion (apoptosis), receptor editing or clonal inactivation (anergy). Once in the periphery, the mature B cells migrate to the lymphoid follicles and following further selection stages, enter the mature B cell pool until they encounter antigen. Upon interacting with their specific antigen in conjunction with co-stimulatory signals from T_H cells, the B cell is activated. Depending on the nature of the signals, the mature B cell gives rise to antibody generating plasma cells or long-lived memory cells which contribute to lasting protective immunity (Adapted from Alt, 1997).

	B cells		Heavy-chain genes	Light-chain genes	Intra-cellular proteins	Surface Marker proteins	
ANTIGEN INDEPENDENT	Stem cell	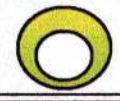	Germline	Germline		CD34 CD45	BONE MARROW
	Early pro-B cell		D-J rearranged	Germline	RAG-1 RAG-2 TdT λ5, VpreB	CD34, CD45 MHCII CD10, CD19 CD38	
	Late pro-B cell		V-DJ rearranged	Germline	TdT λ5, VpreB	CD45R, CD40 MHCII, CD10, CD19 CD38, CD20	
	Large pre-B cell		VDJ rearranged	Germline	RAG-1 RAG-2 μ λ5, VpreB	CD45R, CD40 MHCII, preBCR CD10, CD19 CD38, CD20	
	Small pre-B cell		VDJ rearranged	V-J rearranged		CD45R MHCII, preBCR CD19, CD38, CD20, CD40	
	Immature B cell		VDJ rearranged μ heavy chain	V-J rearranged		CD45R, MHCII IgM, CD19 CD20, CD40	
ANTIGEN DEPENDENT	T1 B cell		VDJ rearranged μ heavy chain	V-J rearranged		CD45R MHCII IgM, CD19, CD20,CD40	
	T2 B cell	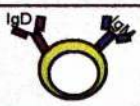	VDJ rearranged μ heavy chain	V-J rearranged		CD45R MHCII IgM, IgD CD19, CD20, CD21, CD40	
	Mature naive B cell	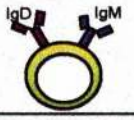	VDJ rearranged μ heavy chain	V-J rearranged		CD45R, MHCII IgM, IgD CD19, CD20, CD21, CD40	PERIPHERY
	Lympho-blast		VDJ rearranged secreted μ chains	V-J rearranged	IgM	CD45R MHCII CD19, CD20, CD21, CD40	
	Memory B cell		Isotype Switch to Cγ, Cα or Cε hypermut^n	V-J rearranged Somatic hypermut^n		CD45R, MHCII IgG, IgA CD19, CD20, CD21, CD40	
	Plasma cell	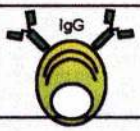	Secreted γ, α or ε chains	V-J rearranged	Ig	Plasma cell antigen -1 CD38	

Figure 1.2: B cell activation and selection in germinal centres

Following T cell dependent activation (1) B cells migrate from the follicular mantle into the primary lymphoid follicles and form germinal centres. Here, B cells undergo proliferation (2) and differentiate into centroblasts (3) where they form the dark zone of the germinal centre. The rapidly dividing centroblasts undergo somatic hypermutation of their immunoglobulin variable-domain genes before differentiating into centrocytes (4). Within the light zone of the germinal centre, the small, non-dividing centrocytes are programmed to die unless they interact with follicular dendritic cells (FDC) that display complexed antigen on their cell surface. Positive selection of centrocytes is dependent on the affinity of their mutated antigen receptors. Centrocytes with low affinity or autoreactive antigen receptors undergo spontaneous apoptosis. The positively selected centrocytes move to the outer edge of the light zone and interact with CD40 ligand expressing T cells (5). Here the centrocytes may undergo CD40-mediated isotype switching, become protected from Fas-induced apoptosis and finally differentiate into either memory B cells (6) or plasma cells (7).

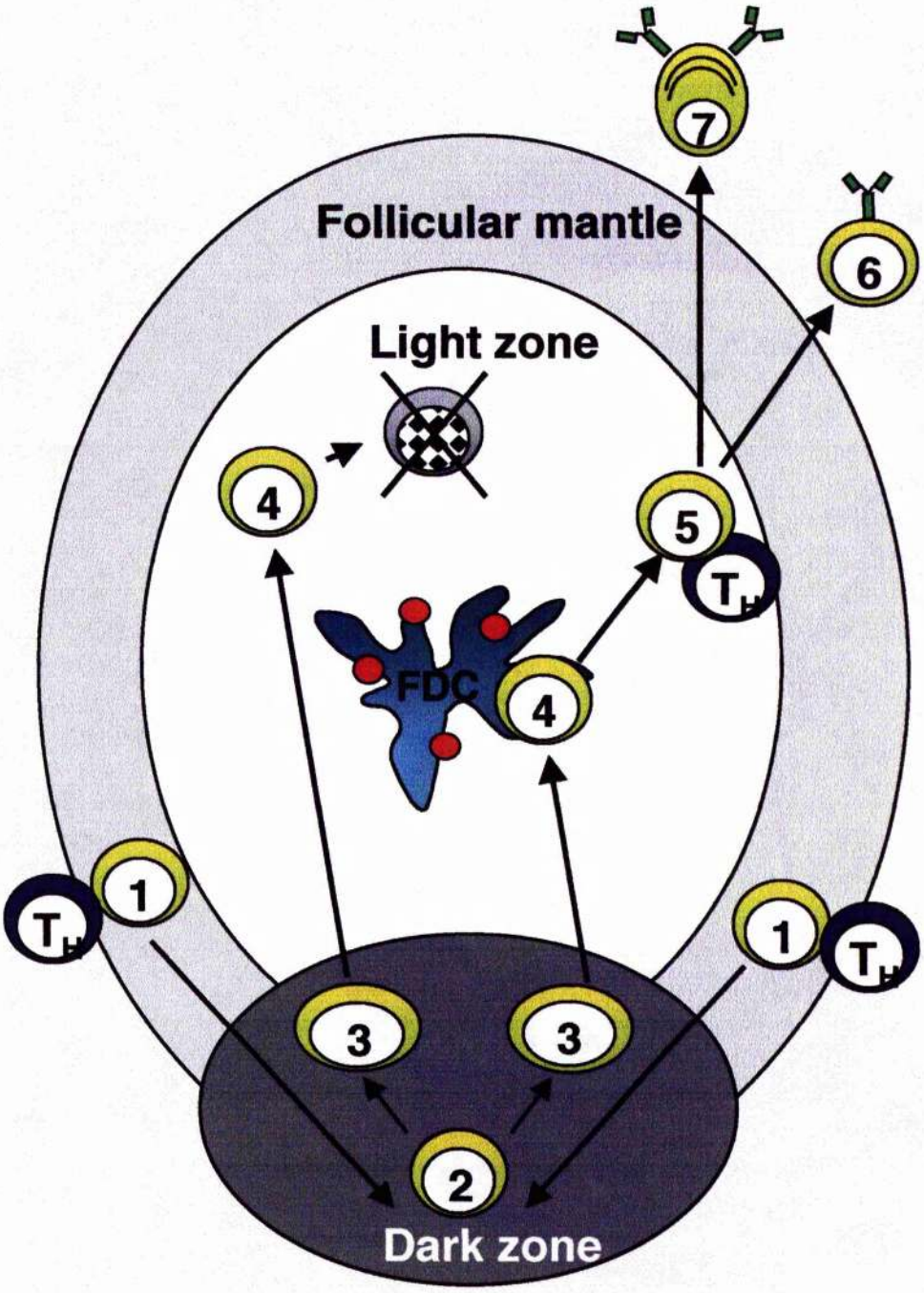
7
Follicular mantle
6
Light zone
4
5
T_H
FDC
4
1
T_H
1
T_H
3
3
2
Dark zone

Figure 1.3: The structure of the B cell receptor (BCR)

The B cell receptor for antigen (BCR) is functionally divided into the immunoglobulin molecule (sIg), which is responsible for ligand binding, and the Igα (CD79a) and Igβ (CD79b) accessory molecule heterodimers, which are responsible for signal transduction. Conserved immunoreceptor tyrosine-based activation motifs (ITAMs), present in the cytoplasmic domains of the accessory molecules are tyrosine phosphorylated following BCR engagement and essential for the signal transducing capacity of the receptor.

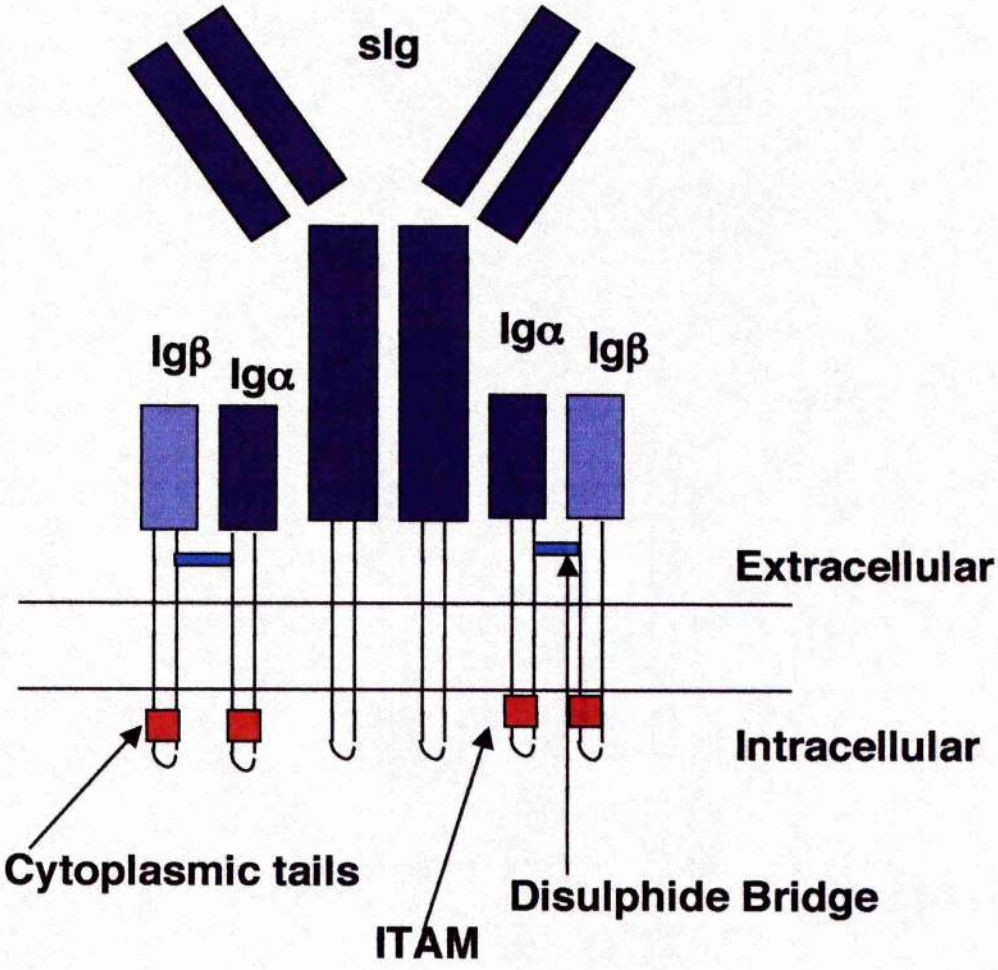
sIg
Igβ
Igα
Igα
Igβ
Extracellular
Intracellular
Cytoplasmic tails
ITAM
Disulphide Bridge

Figure 1.4: Ligation of the BCR results in the activation of PTKs

Binding of Ag to the BCR promotes the activation of several protein tyrosine kinases (PTK) that alter the homeostasis of reversible tyrosine phosphorylation in the resting B cell. The effect is a transient increase in protein tyrosine phosphorylation that facilitates the phosphotyrosine-dependent formation of a scaffold of effector protein complexes. Studies have demonstrated that Src family PTKs, particularly Lyn, are activated initially and serve to phosphorylate the ITAMs of Igα and Igβ thereby creating phosphotyrosine motifs that recruit downstream signalling proteins. In particular, phosphorylation of the BCR complex leads to the recruitment and activation of the PTK Syk, which in turn promotes the recruitment and phosphorylation of downstream effectors such as PLCγ, Shc and Vav (see Figure 1.5).

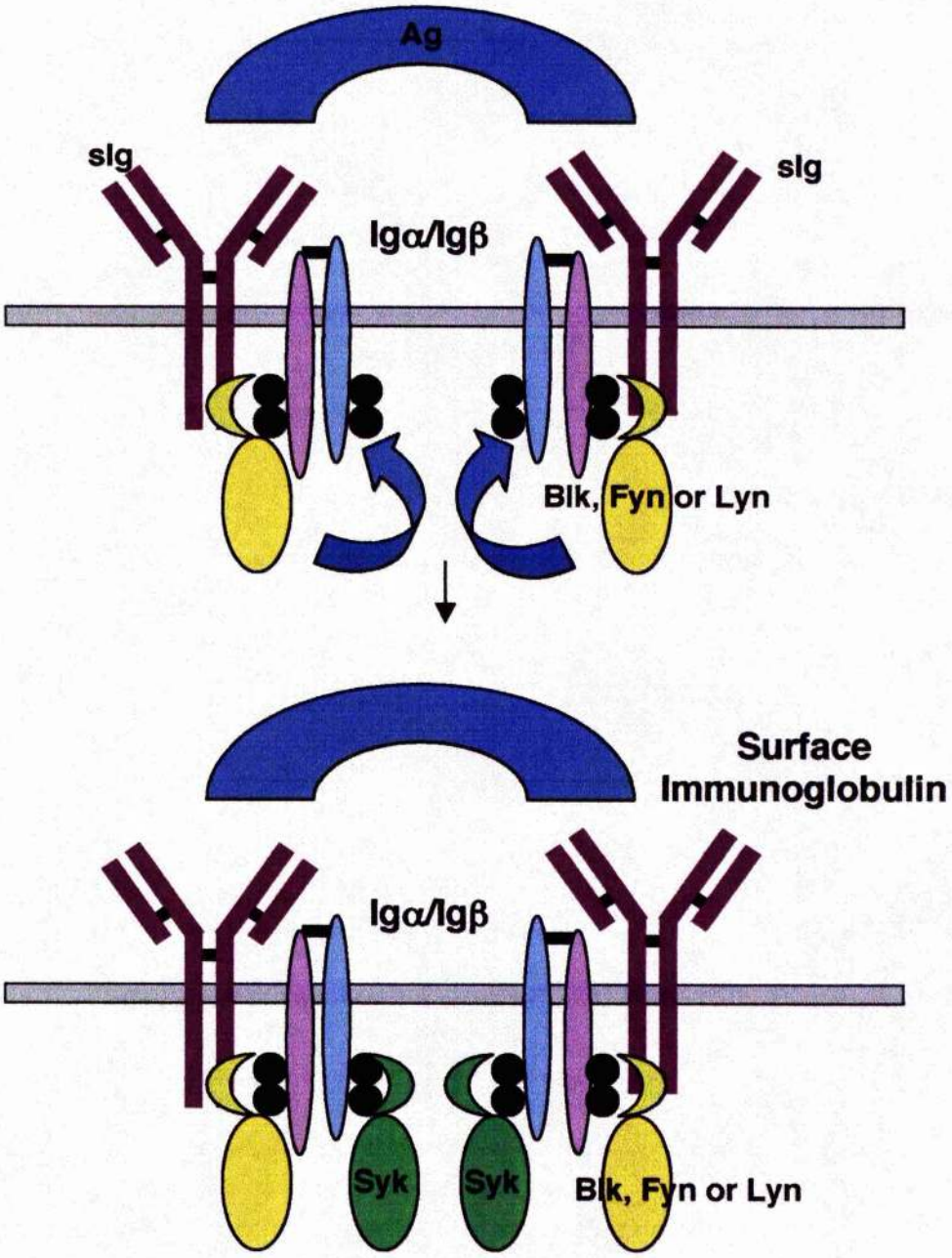
Ag
sIg
sIg
Igα/Igβ
Blk, Fyn or Lyn
Surface
Immunoglobulin
Igα/Igβ
Syk
Syk
Blk, Fyn or Lyn

Figure 1.5: Syk is able to recruit adaptor proteins that can activate the three major cell signalling cascades

A schematic representation of the parallel, yet interacting, cascades initiated following ligation of the B cell receptor (BCR) on mature B cells. The tyrosine phosphorylation of conserved ITAMs, present in the cytoplasmic domains of the BCR accessory molecules Igα and Igβ, results in the recruitment of BCR associated PTKs. These include the Src-PTK family (Blk, Fyn, Lck, and Lyn), Syk, and the Tec-kinase Btk. Following activation of these kinases, three parallel, but potentially cross-regulatory, pathways are recruited to the activated BCR complex. The phospholipase C γ (PLCγ) pathway results in the hydrolysis of phosphatidylinositol 4,5 bisphosphate (PIP_2), to produce diacylglycerol (DAG) and inositol 1,4,5-triphosphate (IP_3). The phosphatidylinositol 3-kinase (PI-3 kinase) pathway generates phosphatidylinositol 3,4,5 triphosphate (PIP_3) whilst the classical RasMAPKinase cascade leads to the activation of ERKMAPKinase. These pathways converge on the level of the nucleus to initiate gene expression resulting in a cellular response.

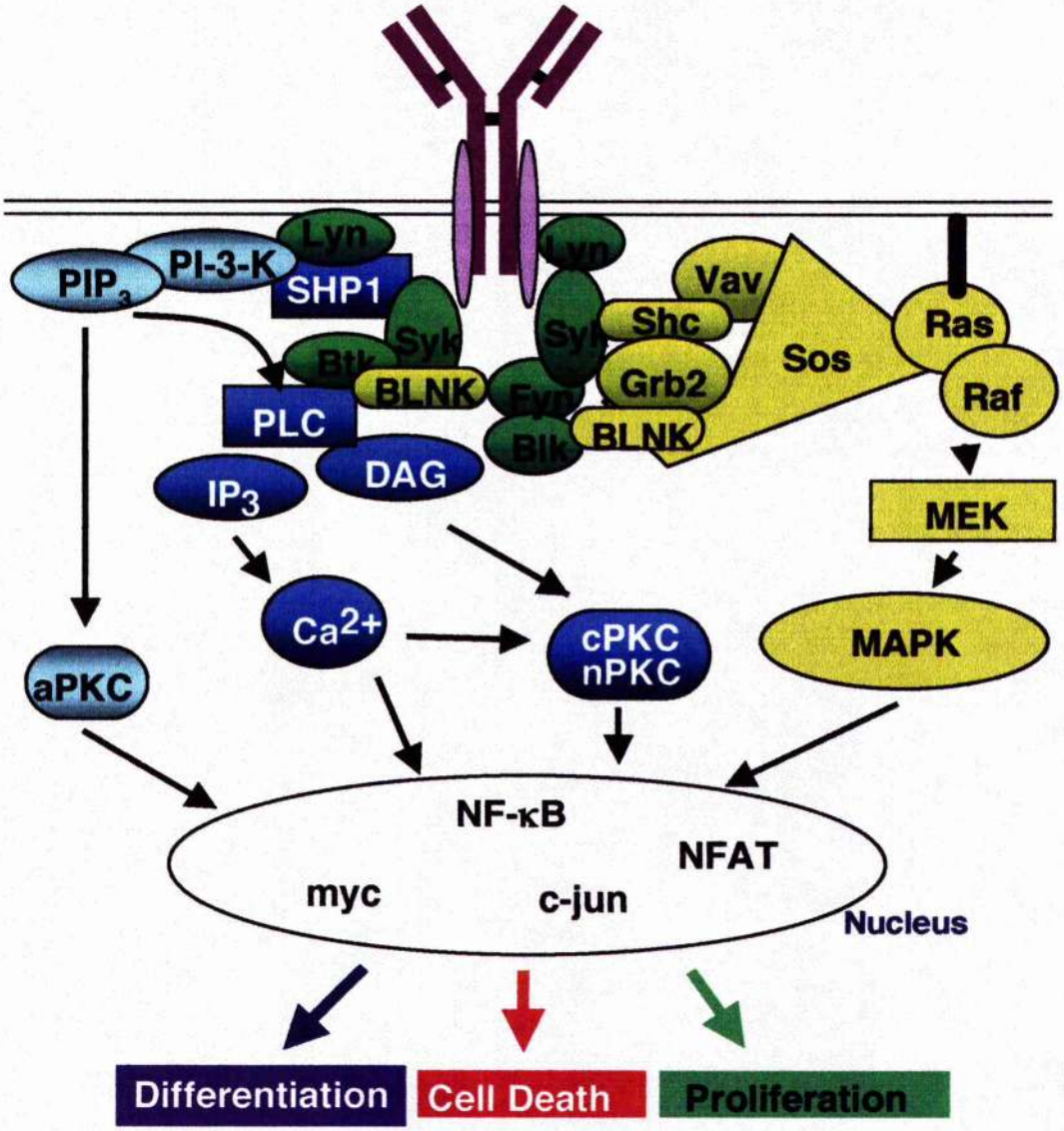
Lyn
PIP3
PI-3-K
SHP1
Syk
Btk
BLNK
PLC
DAG
IP3
Ca2+
aPKC
Lyn
Syk
Fyn
Blk
Vav
Shc
Grb2
BLNK
Sos
Ras
Raf
MEK
MAPK
cPKC
nPKC
NF-κB
NFAT
myc
c-jun
Nucleus
Differentiation
Cell Death
Proliferation

Figure 1.6: The PI-3 kinase superfamily

PI-3 kinase comprises of a family of structurally related enzymes, with differing PI substrate requirements and modes of regulation allowing for the reported diversity of function. PCR cloning strategies and data mining of genome sequencing projects have identified 8 distinct PI-3 kinase catalytic subunits that are capable of phosphorylating inositol lipids. These eight isoforms have been divided into three functional classes on the basis of their protein domain structure, lipid substrate specificity and associated regulatory subunits: namely, the class I enzymes, p110α, p110β and p110δ; the class II enzymes, PI3K C2α, PI3K C2β and PI3K C2β; and the sole class III enzyme, Vps34. All PI-3 kinase classes contain the C2 domain which acts to mediate interactions with lipids or other proteins in either a calcium-dependent or independent manner, a helical domain and a catalytic domain that mediates the kinase action of the enzyme. Further to this, class I and II PI-3 kinases contain a putative Ras binding domain (RBD).

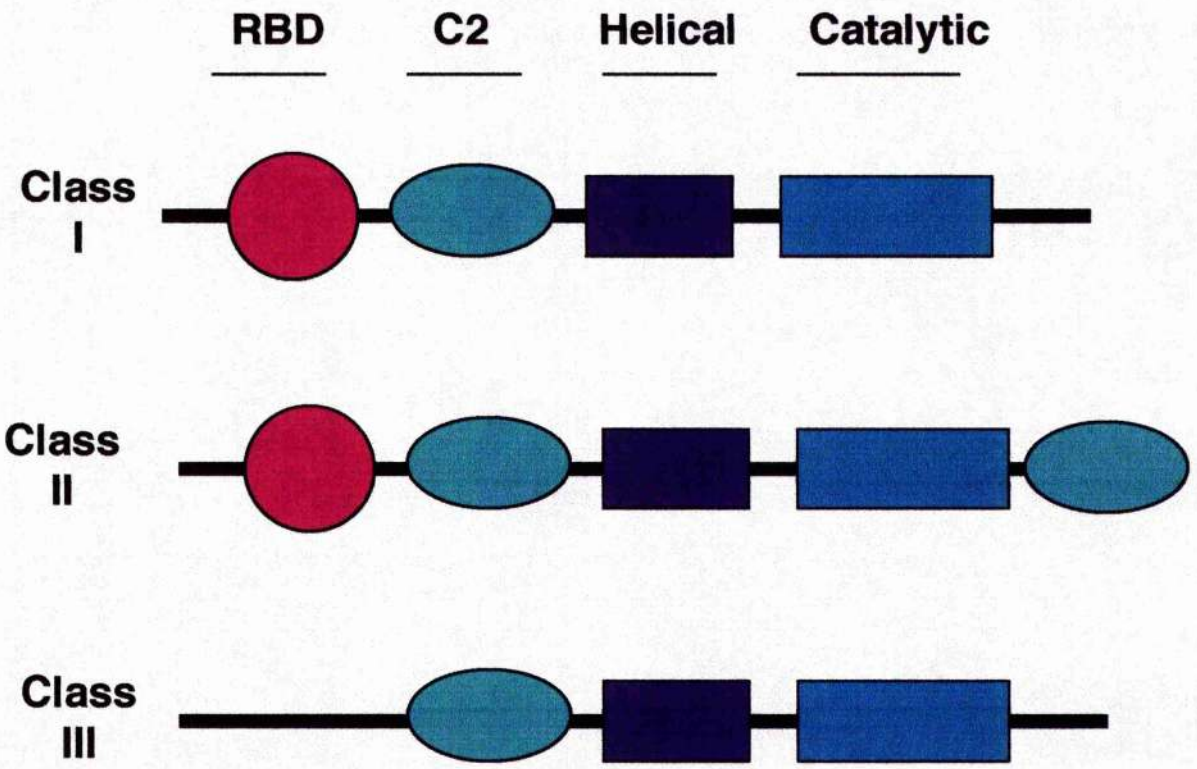
RBD
C2
Helical
Catalytic
Class I
Class II
Class III

Figure 1.7: The phosphorylation status of Bad is critical for differentiating between a pro-apoptotic and anti-apoptotic signal

The phosphorylation status of Bad is under the control of AKT and hence the PI-3 kinase pathway. AKT mediates the phosphorylation of Bad upon which it binds to the cytoskeletal scaffold proteins 14-3-3 and is therefore sequestered in the cytoplasm and unable to deliver pro-apoptotic signals at the mitochondrial membrane. In contrast, when Bad is not phosphorylated it is able to bind the anti-apoptotic Bcl-2 family member $BclX_L$, preventing $BclX_L$ from having a protective effect on the maintenance of mitochondrial membrane integrity.

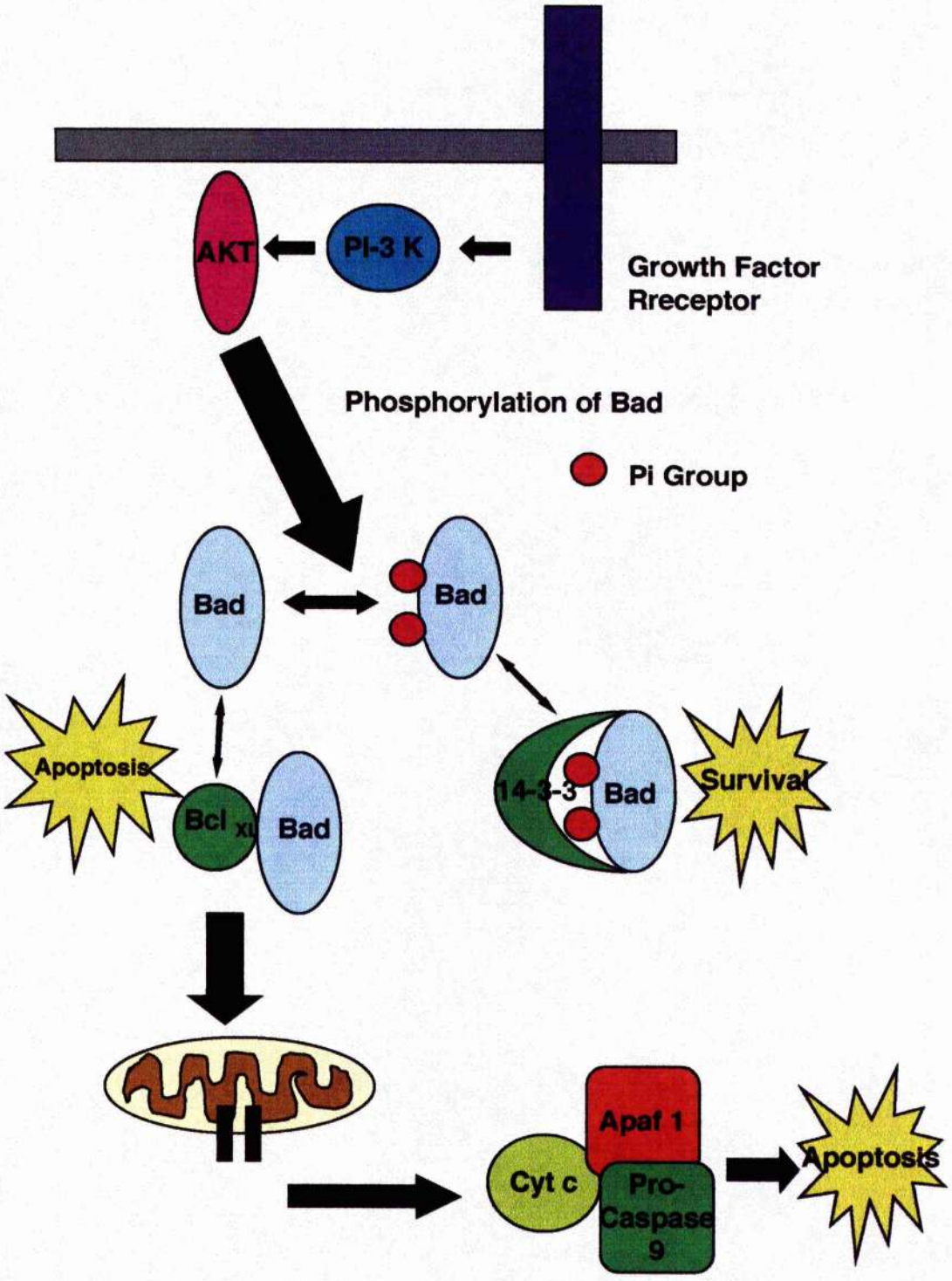
AKT
PI-3 K
Growth Factor
Rreceptor
Phosphorylation of Bad
Pi Group
Bad
Bad
Apoptosis
Bcl xL
Bad
14-3-3
Bad
Survival
Apaf 1
Cyt c
Pro-
Caspase
9
Apoptosis

Figure 1.8: Mitogen-activated protein kinase (MAP kinase) signalling pathways

The mitogen-activated protein (MAP) kinases are a family of serine-threonine protein kinases that have been widely conserved throughout evolution. They are activated by a wide range of extracellular stimuli and are able to mediate a wide range of cellular functions ranging from proliferation and activation to growth arrest and cell death. The MAP kinase family is subdivided into three groups; the classical extracellular signal-regulated kinases (ERKMAPKinase), the c-Jun N-terminal kinases, also known as the stress activated protein kinases (JNK/SAPK) and the p38 MAP kinases. Activation of each group is determined by distinct upstream MAP kinase kinases (MEKs) and MAP kinase kinase kinases (MEKK). MAP kinases are activated by dual phosphorylation on tyrosine and threonine residues, located in a T-X-Y motif, where X is different in each group. Following MAP kinase activation, activation of a number of downstream transcription factors occurs; ERKMAPKinase activates Elk-1 and c-myc, JNK activates c-Jun and ATF-2 and p38 MAP kinase activates ATF-2 and MAX. The phosphorylation and activation of these transcriptional regulators enables the MAP kinase families to regulate gene expression and hence, cellular responses.

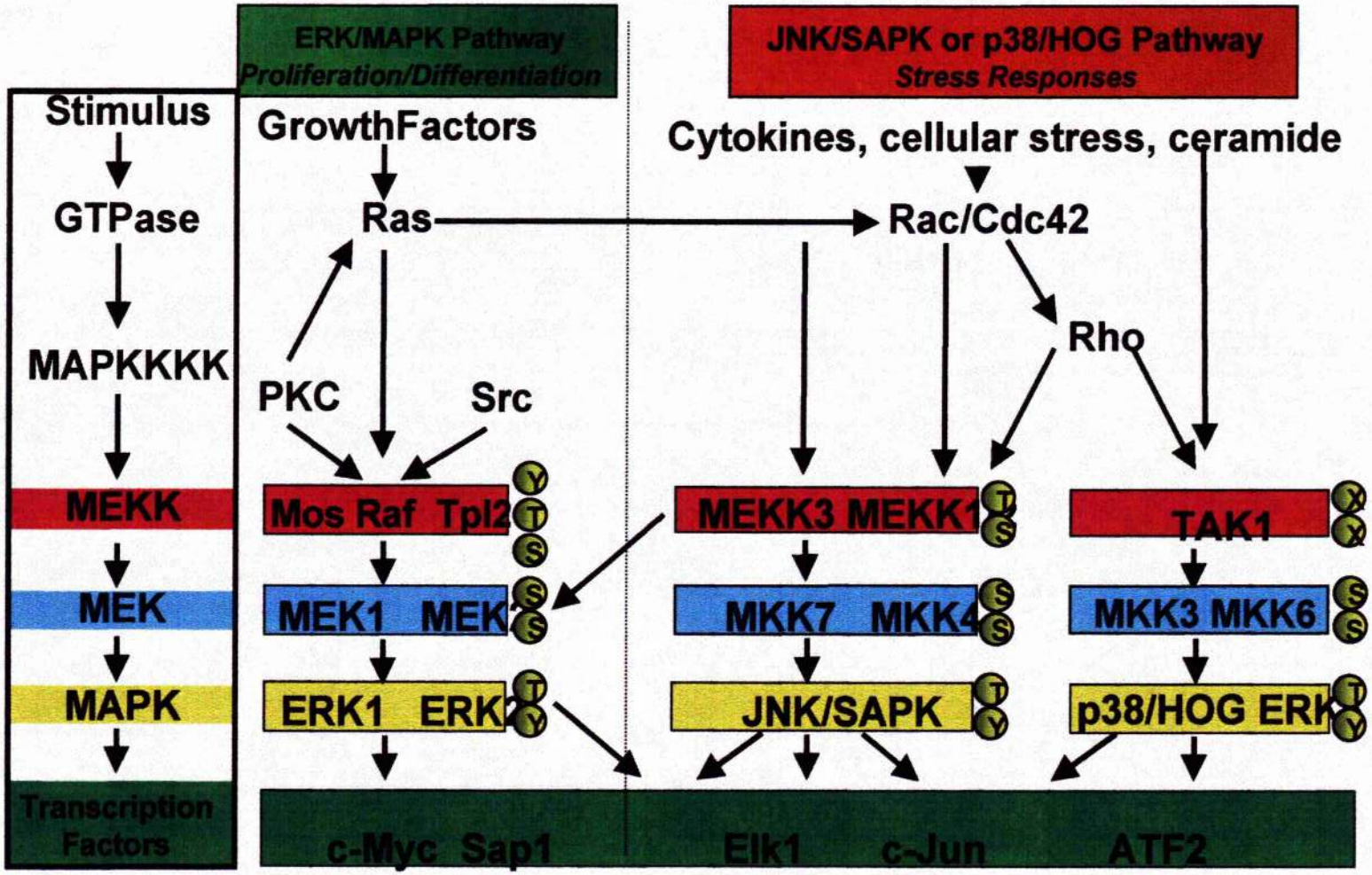
ERK/MAPK Pathway
Proliferation/Differentiation
JNK/SAPK or p38/HOG Pathway
Stress Responses
Stimulus
GTPase
MAPKKKK
MEKK
MEK
MAPK
Transcription Factors
GrowthFactors
Ras
PKC
Src
Mos Raf Tpl2
MEK1 MEK2
ERK1 ERK2
Cytokines, cellular stress, ceramide
Rac/Cdc42
Rho
MEKK3 MEKK1
MKK7 MKK4
JNK/SAPK
TAK1
MKK3 MKK6
p38/HOG ERK
c-Myc Sap1
Elk1
c-Jun
ATF2

Figure 1.9: The BCR is able to activate the RasMAPKinase pathway via SOS

Phosphorylation of ITAMS on Igα and Igβ create binding sites for proteins with SH2 (phosphotyrosine binding) domains such as the adaptor proteins Grb2 and BLNK. Recruitment of Grb2 or BLNK allows binding and activation of SOS which catalyses the exchange of GDP for GTP on Ras and hence causes a change in Ras conformation. Activated Ras binds Raf1 and recruits it from the cytosol to the cell membrane, where Raf activation takes place. Raf1 is then activated by a multistep process involving dephosphorylation of inhibitory sites by protein phosphatase 2A (PP2A), phosphorylation of activating sites by p21 activated kinase (PAK), Src family kinases and the PKC family. Activated Raf1 phosphorylates and activates MEK which in turn activates the ERK cascade.

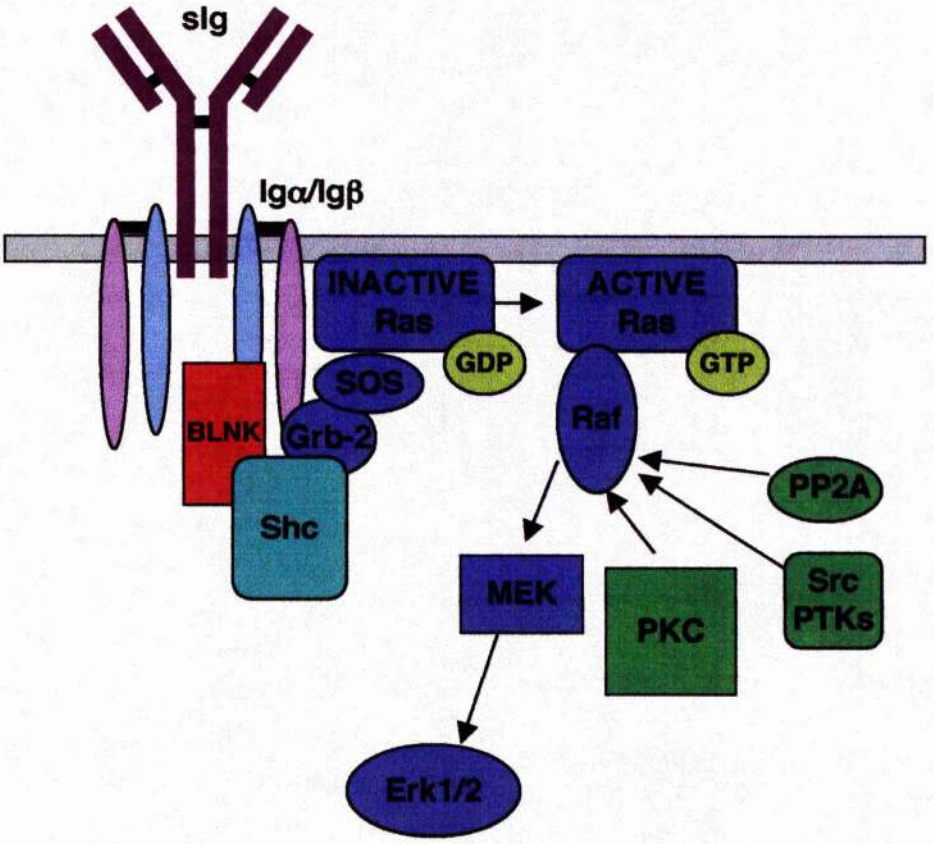
sIg
Igα/Igβ
INACTIVE Ras
GDP
ACTIVE Ras
GTP
SOS
Grb-2
BLNK
Shc
Raf
PP2A
MEK
PKC
Src PTKs
Erk1/2

Figure 1.10: Protein structure of the PKC family members

PKC proteins have two well-defined domains: an amino terminal regulatory domain and a carboxy terminal catalytic domain. All isoforms contain highly conserved regions (regions C1 to C4) as well as variable regions unique to the specific enzyme. The C1 region contains an auto inhibitory pseudosubstrate domain that binds to the catalytic domain and maintains the enzyme in an inactive state in the absence of activators. The C1 domain also contains a cysteine rich domain that is a binding site for the second messenger DAG (or phorbol esters) in cPKCs and nPKCs. In addition cPKCs also contain a conserved C2 region involved in calcium binding.

CLASSICAL/ CONVENTIONAL PKCs α, β and γ

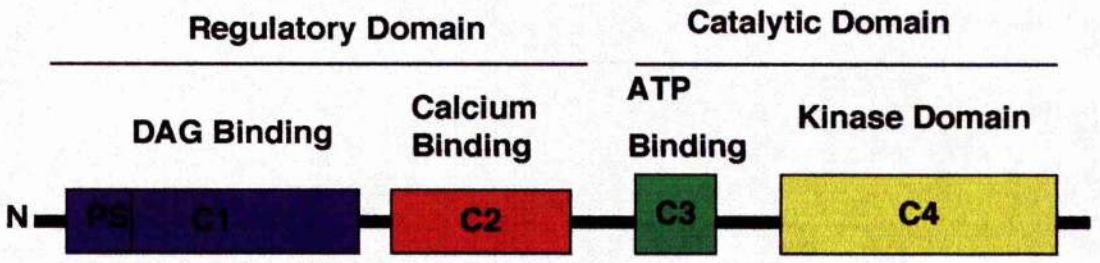

NOVEL PKCs δ, ε, η and θ

ATYPICAL PKCs ζ and λ/τ

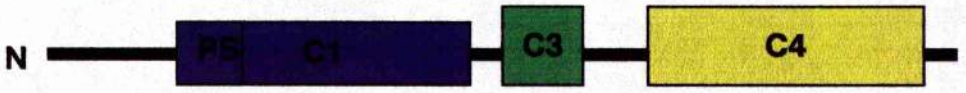

Figure 1.11: Activation of p53 results in a variety of cellular responses

In response to certain stress signals p53 is activated through a number of post-translational modifications, such as phosphorylation and acetylation, which increase that stability of the p53 protein. In healthy cells, MDM2 is bound to p53 and this stimulates p53 ubiquitination and hence degradation. By contrast, when cells are stressed, MDM2-p53 associations are downregulated resulting in an increase in free p53. Once p53 is activated, it can bind to response elements in p53 target genes, and increase or repress, their expression. The products of these genes carry out various p53 effector functions, including apoptosis, cell cycle arrest, cellular senescence and differentiation. MDM2 is itself encoded by a p53 target gene.

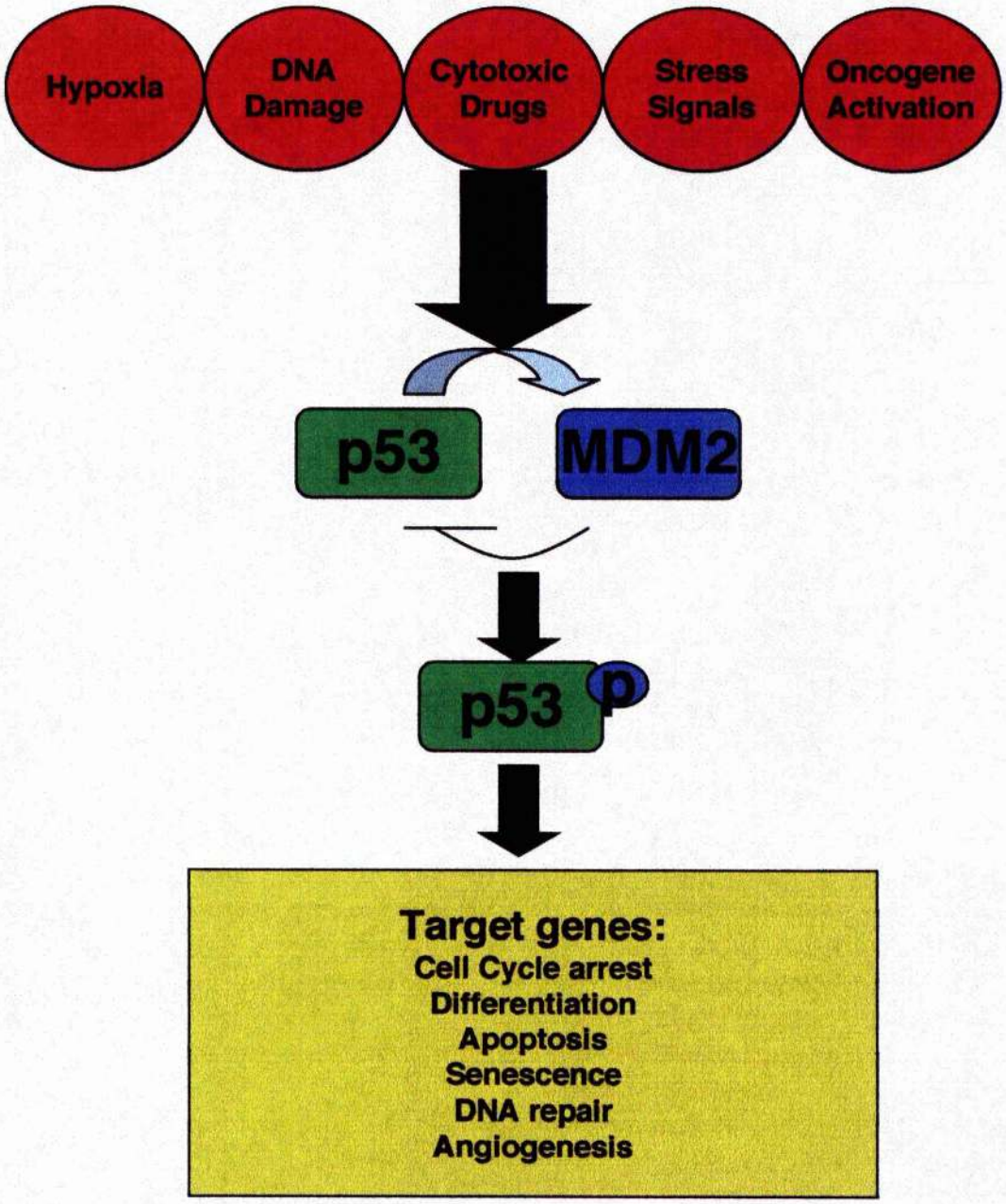
Hypoxia
DNA Damage
Cytotoxic Drugs
Stress Signals
Oncogene Activation
p53
MDM2
p53
P
Target genes:
Cell Cycle arrest
Differentiation
Apoptosis
Senescence
DNA repair
Angiogenesis

Figure 1.12: The transcription factor, NF-κB can direct a variety of cellular responses depending on the subunits that are utilised

In mature, resting B cells NF-κB complexes are predominantly held inactive in the cytoplasm until the receipt of extracellular signals such as Ag through the BCR, CD40 ligand via CD40, bacterial cell wall products through the Toll Like Receptors or apoptosis-inducing stimuli through death receptor 6 (DR6). The NF-κB family of transcription factors are involved mainly in stress-induced, immune, and inflammatory responses. In addition, these molecules play important roles during the development of certain hematopoietic cells, keratinocytes, and lymphoid organ structures. NF-κB is also an important regulator in cell fate decisions, such as programmed cell death and proliferation control, and is critical in tumorigenesis. NF-κB is composed of homo- and heterodimers of five members of the Rel family including p50, p52, RelA (p65), RelB, and c-Rel (Rel). Hetero and Homo-dimerisation of NF-κB proteins which exhibit differential binding specificities include; p50/RelA, p50/c-Rel, p52/c-Rel, p65/c-Rel, RelA/RelA, p50/p50, p52/p52, RelB/p50 and RelB/p52. The specific NF-κB dimers formed determine the genes which are transcribed.

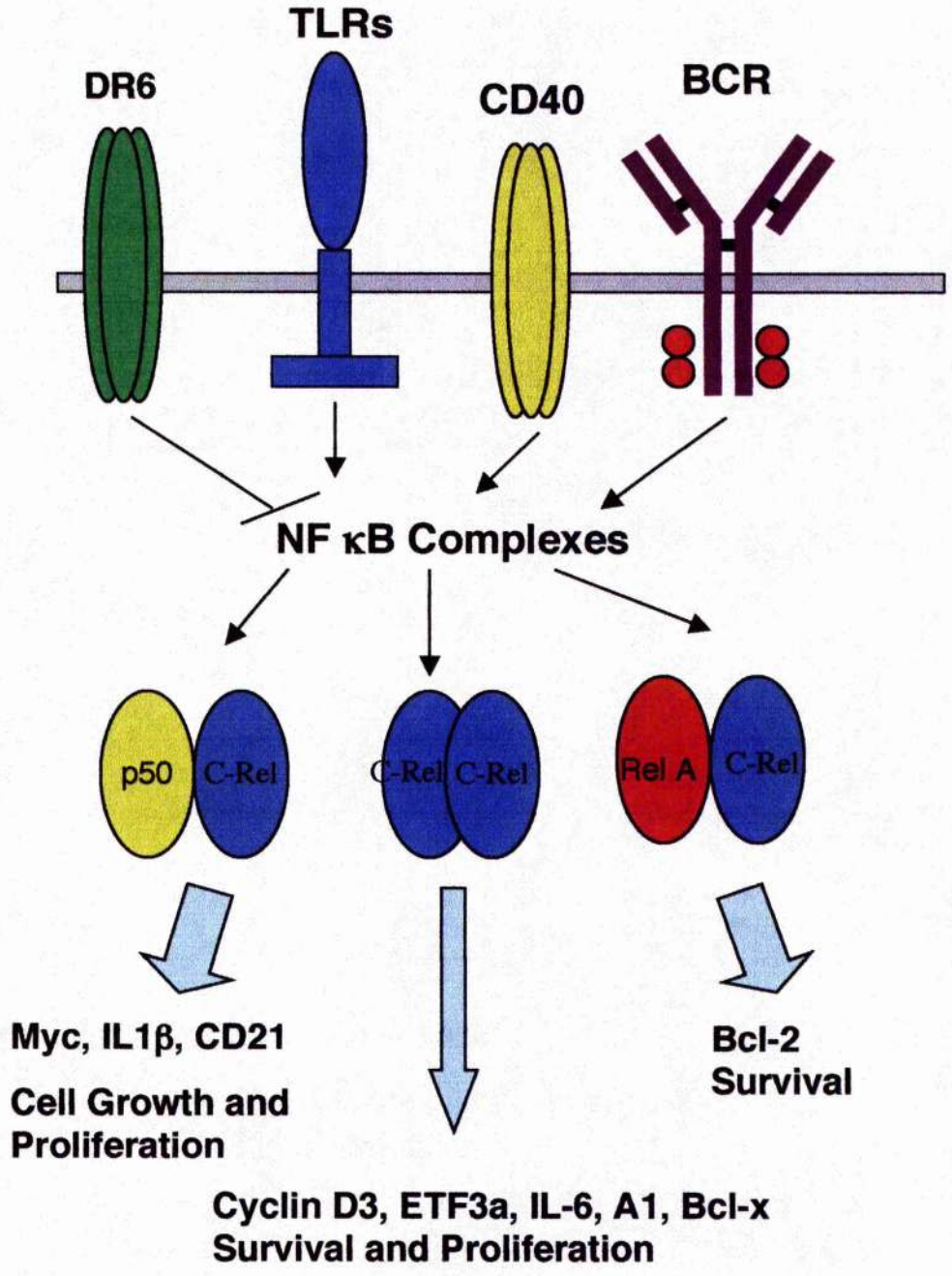
TLRs
DR6
CD40
BCR
NF κB Complexes
p50
C-Rel
C-Rel
C-Rel
Rel A
C-Rel
Myc, IL1β, CD21
Cell Growth and Proliferation
Bcl-2
Survival
Cyclin D3, ETF3a, IL-6, A1, Bcl-x
Survival and Proliferation

Figure 1.13: The cell cycle

(A) The cell cycle represents a co-ordinated series of events required for cell growth and division. There are four main stages of the cycle, during which a cell must duplicate its contents and divide. G1 is characterised by gene expression and protein synthesis, resulting in an increase in cell size and production of all the proteins required for DNA synthesis. DNA duplication occurs in the S phase (synthesis). After chromosome replication a second growth period, G2, allows the cell to monitor DNA integrity and cell growth prior to M phase (mitosis) when the cell finally divides. The resulting daughter cells either immediately enter G1 to go through the full cycle again, or alternatively stop cycling temporarily and enter the G0 phase (quiescence).

(B) The cell cycle is carefully regulated with distinct checkpoints at the end of each growth phase. Progression through the cell cycle is regulated as indicated by the appropriate cyclin-Cdk complexes and by regulators of these complexes including Rb, p15, p16, p21, p27, p53 and p19.

A

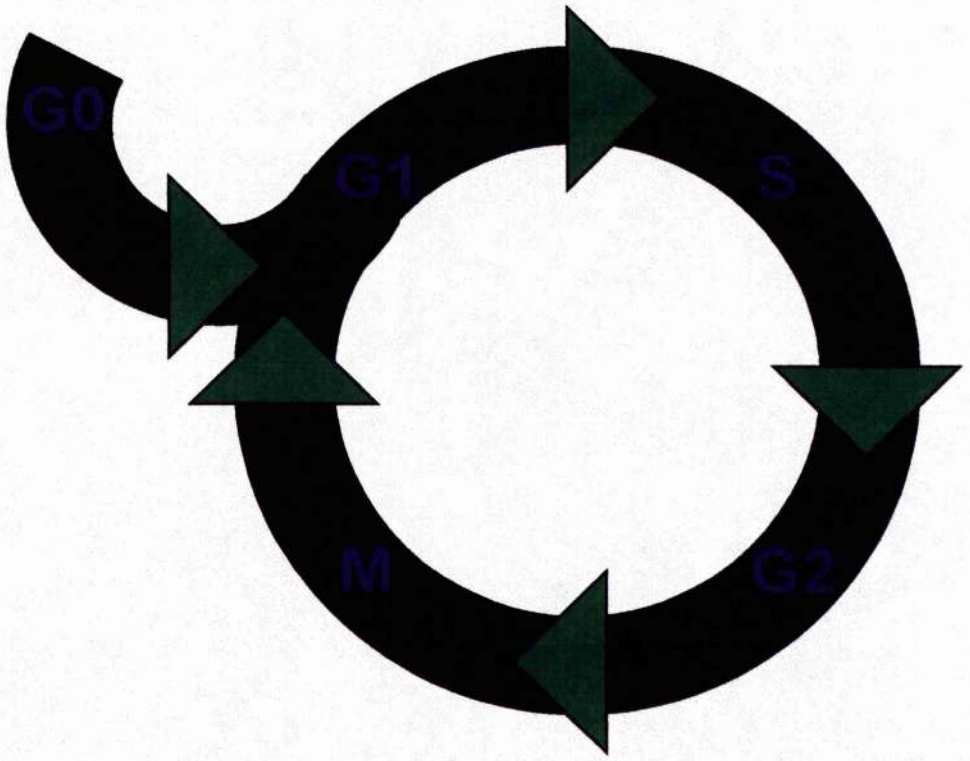
G0
G1
S
M
G2

B

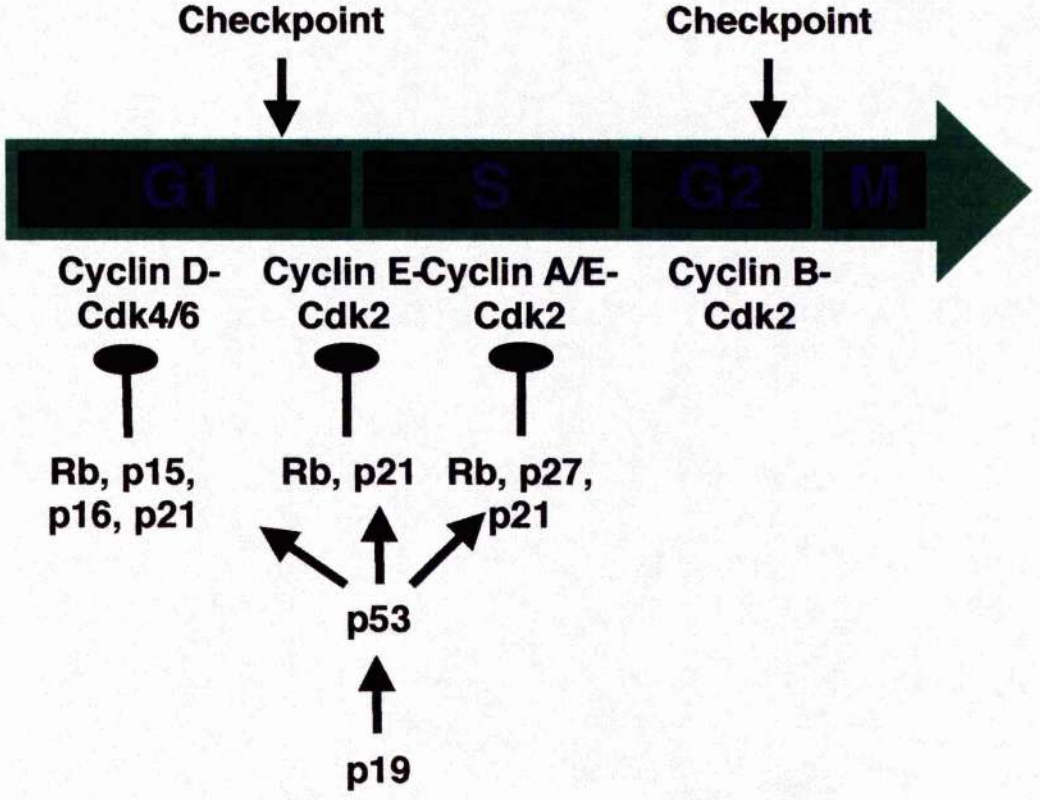
Checkpoint
Checkpoint
G1
S
G2
M
Cyclin D-Cdk4/6
Cyclin E-Cdk2
Cyclin A/E-Cdk2
Cyclin B-Cdk2
Rb, p15, p16, p21
Rb, p21
Rb, p27, p21
p53
p19

Figure 1.14: Caspase 8 can be activated by TNFR1 type receptors to initiate apoptosis.

Binding of ligands such as CD95L/FasL and TNF leads to the recruitment of the adaptor molecules FADD and TRADD, which can process pro-caspase 8 into the active caspase 8. This in turn activates the effector caspase, caspase 7. In some cases this occurs in a mitochondrial-independent fashion, however the cleavage of Bid to tBid by caspase 8 can act to induce mitochondrial-dependent/ intrinsic apoptosis. Truncated Bid stimulates the opening of the permeability transition pore and hence mediates cytochrome c release. This is a component of the apoptosome and leads to caspase 3 activation and hence apoptosis.

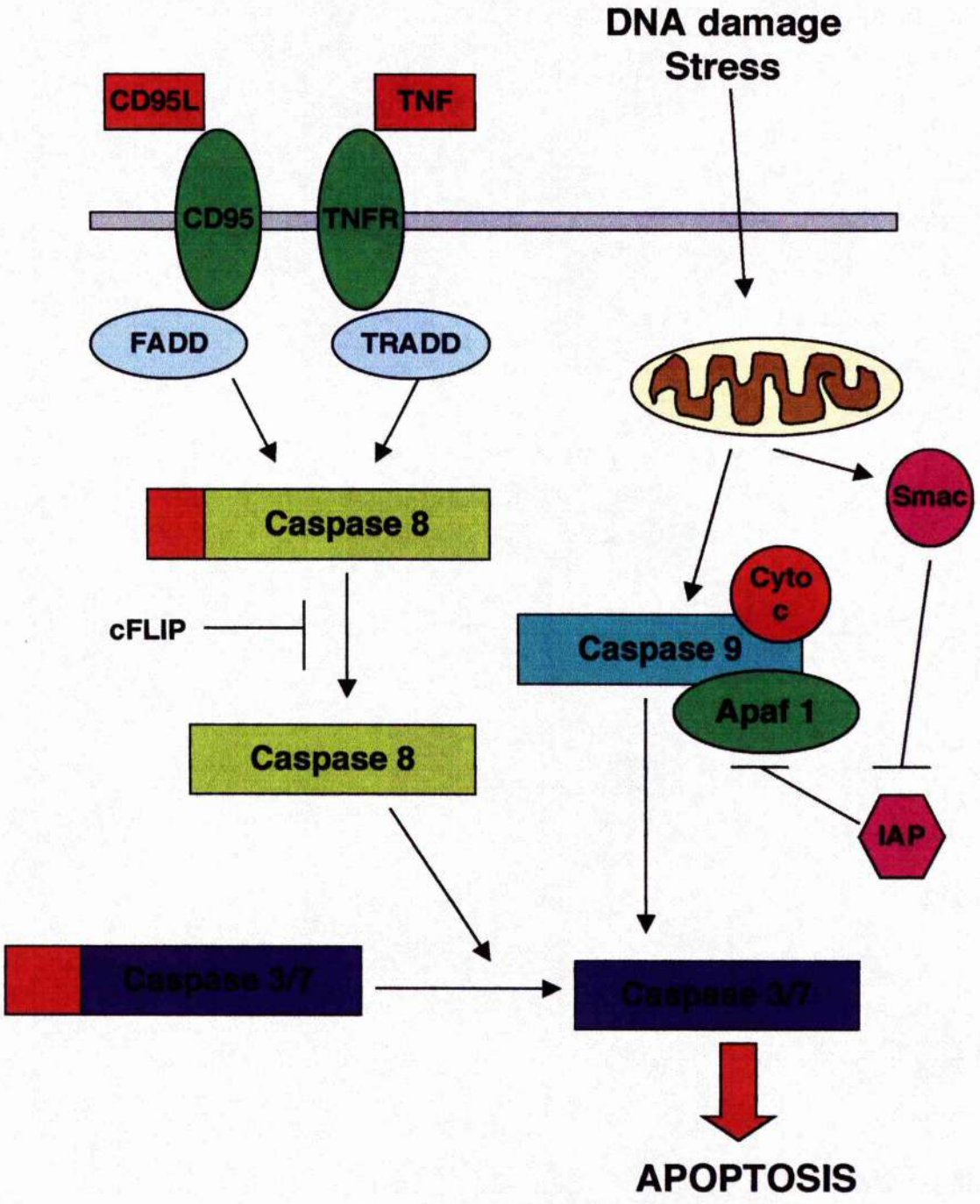
DNA damage
Stress
CD95L
TNF
CD95
TNFR
FADD
TRADD
Caspase 8
cFLIP
Caspase 8
Caspase 3/7
Smac
Cyto
c
Caspase 9
Apaf 1
IAP
Caspase 3/7
APOPTOSIS

Figure 1.15: The Bcl-2 family of apoptosis regulators

The Bcl-2 family of apoptosis regulators is comprised of over a dozen proteins, which have been classified into three functional groups. Bcl-2 family members are recognised due to the presence of one or more conserved Bcl-2 homology (BH) domains. Group I members all possess anti-apoptotic activity, thus protect cells from death, and contain all 4 BH domains, as well as a transmembrane domain allowing their insertion into the mitochondrial membrane. Members of group II and III promote cell death, hence are known as pro-apoptotic Bcl-2 family members. Pro-apoptotic Bcl-2 family members have fewer BH domains, indeed some contain only a single BH3 domain. Many family members can homodimerise, but more importantly, pro- and anti-apoptotic members can form heterodimers to either promote or inhibit apoptosis. For example, pro-apoptotic Bax can heterodimerise with the anti-apoptotic protein, Bcl-2, which blocks the anti-apoptotic capabilities of Bcl-2.

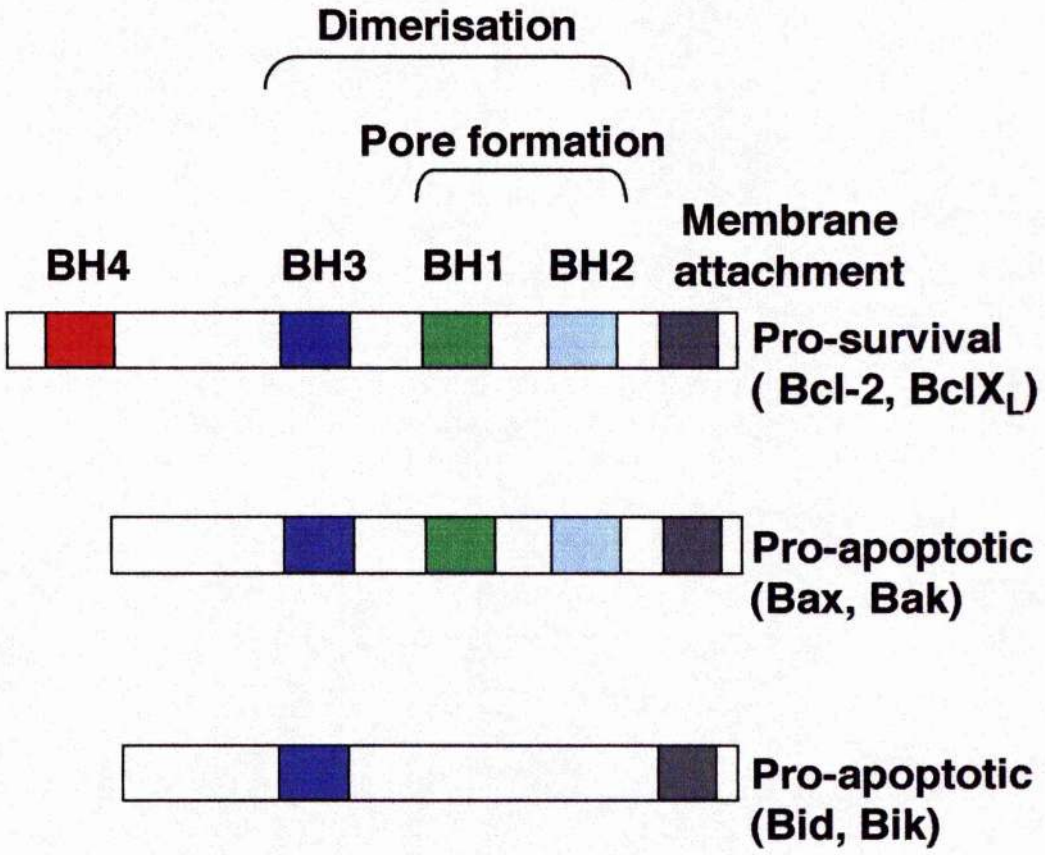
Dimerisation
Pore formation
BH4
BH3
BH1
BH2
Membrane attachment
Pro-survival (Bcl-2, BclX$_L$)
Pro-apoptotic (Bax, Bak)
Pro-apoptotic (Bid, Bik)

Figure 1.16: Apoptosis in under the control of a diverse family of BH domain containing Bcl-2 proteins

Cell death signals can engage two distinct classes of BH3-only proteins termed the activators, (e.g. Bid and Bim) and the enablers (e.g. Bad and Bik). In the absence of either enabler or activator BH3-only proteins Bax/Bak are not stimulated to oligomerise and hence apoptosis is not stimulated (i). Activators can directly bind and activate mitochondrially localised Bak and Bax triggering oligomerization of Bax/Bak and hence initiating apoptosis (ii). Anti-apoptotic regulators, such as Bcl-2, can sequester BH3-only activators preventing their interaction with Bax/Bak and hence inhibiting apoptosis (iii). By contrast, enablers can sensitize cells to apoptosis by binding anti-apoptotic Bcl-2 regulators and thus preventing the Bcl-2/ $BclX_L$-mediated sequestration of BH3-only activators such as Bid (iv). It is therefore the ratio and complex status of Bcl-2 family proteins, rather than expression of any one member, that is likely to regulate apoptosis. Consistent with this proposal, overexpression of Bcl-2 proteins in cancer cells results in the sequestration both classes of BH3-only proteins by mutli-domain regulators such as Bcl-2 which inhibits the pro-apoptotic effects of the Bcl-2 family members and hence blocks apoptosis (v).

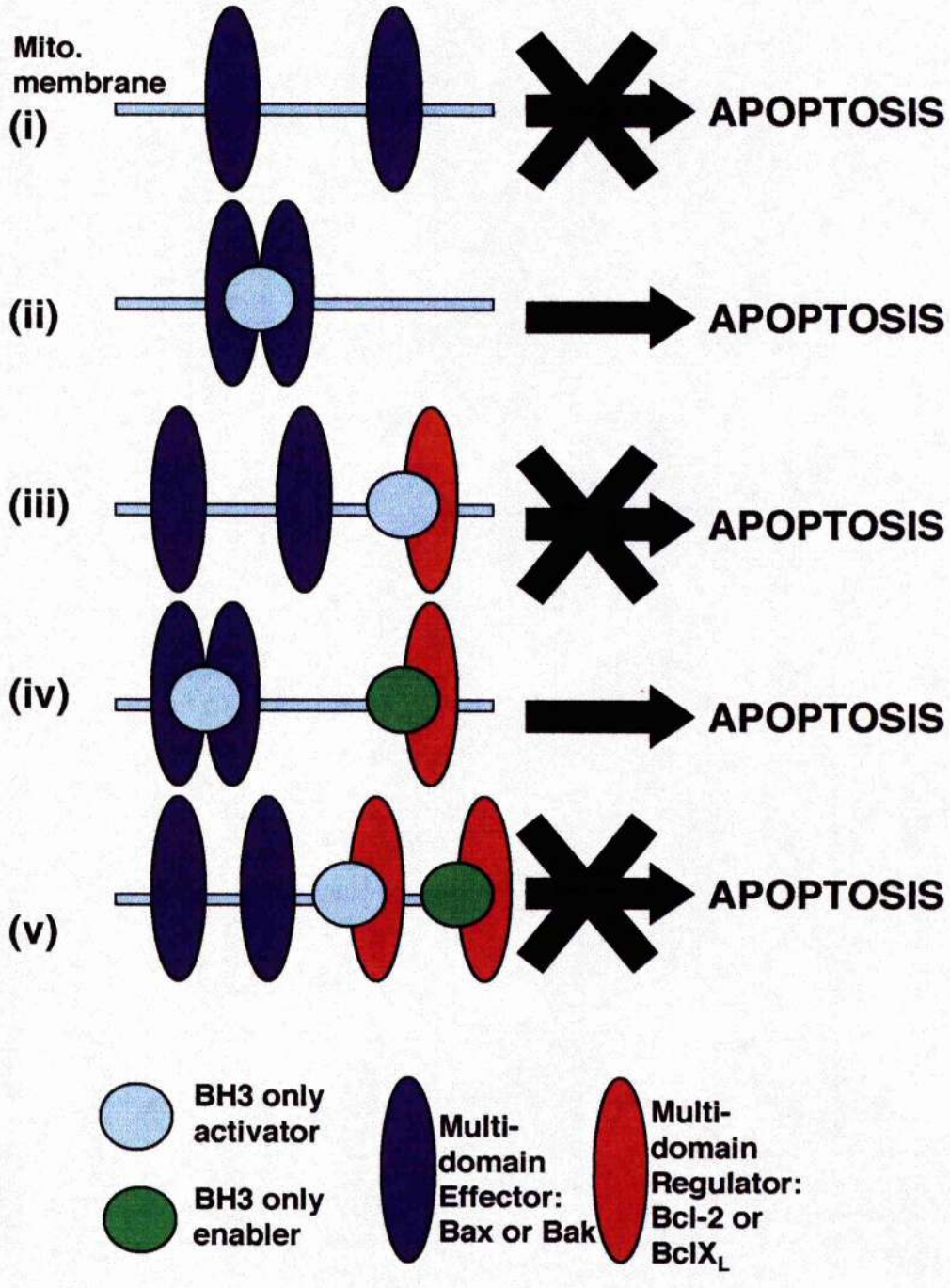
Mito.
membrane
(i)
APOPTOSIS
(ii)
APOPTOSIS
(iii)
APOPTOSIS
(iv)
APOPTOSIS
(v)
APOPTOSIS
BH3 only
activator
BH3 only
enabler
Multi-
domain
Effector:
Bax or Bak
Multi-
domain
Regulator:
Bcl-2 or
BclX$_L$

Figure 1.17: The roles of calpain and caspase in protein degradation and apoptosis

Pro-apoptotic signalling, via the either the extrinsic or extrinsic pathways, can lead to processing and activation of caspase 3. The action of caspase 3 on cytoskeletal or plasma membrane integral proteins compromises the membrane permeability to calcium, leading to elevated intracellular calcium. Caspase 3 also degrades calpastatin which facilitates calpain activation. Activated caspase 3 and calpains can degrade important cytosolic, cytoskeletal and nuclear substrates resulting in functional and structural destruction of the cell and hence apoptosis.

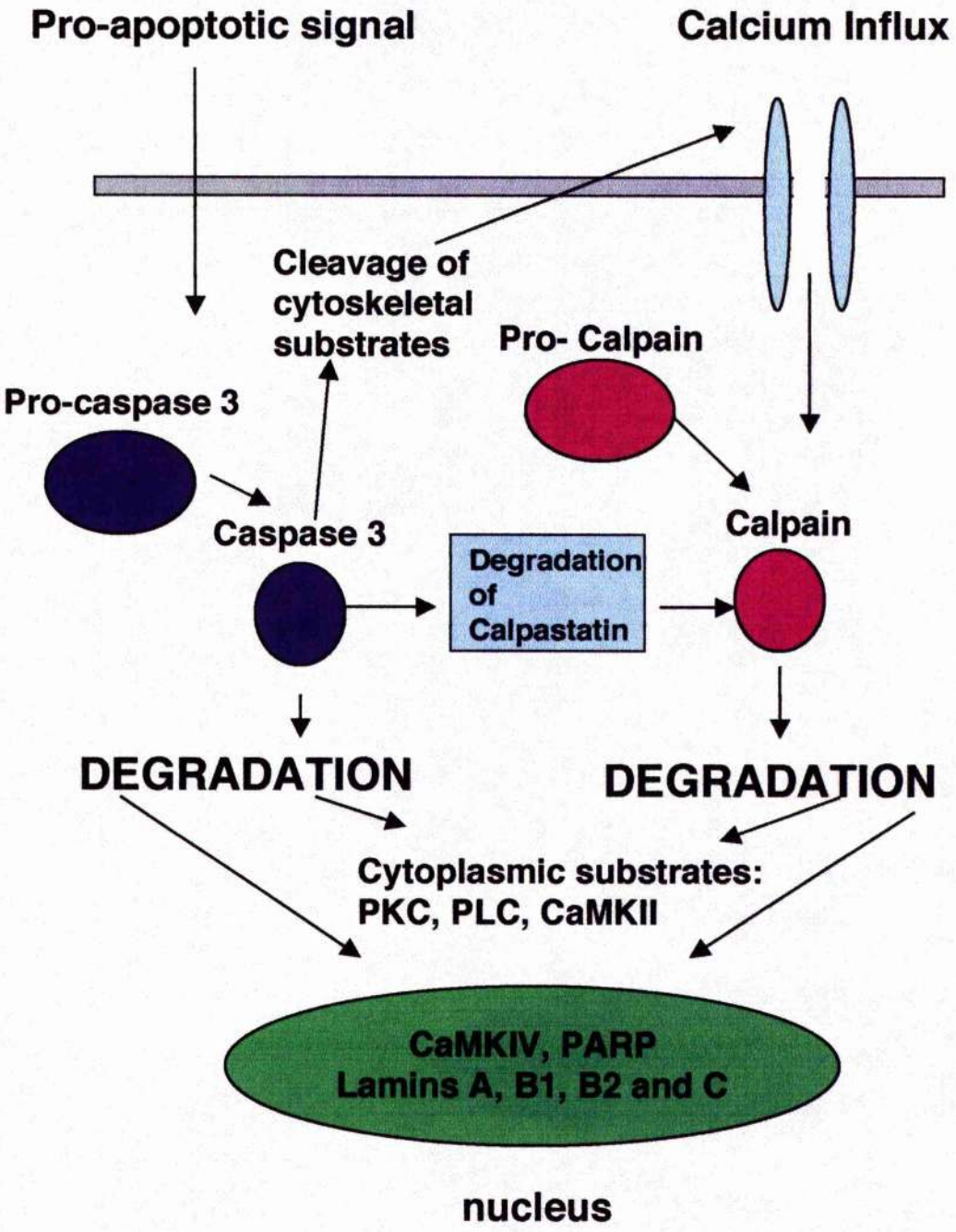
Pro-apoptotic signal
Calcium Influx
Cleavage of cytoskeletal substrates
Pro- Calpain
Pro-caspase 3
Caspase 3
Calpain
Degradation of Calpastatin
DEGRADATION
DEGRADATION
Cytoplasmic substrates: PKC, PLC, CaMKII
CaMKIV, PARP
Lamins A, B1, B2 and C
nucleus

Figure 1.18: FcγRIIb coligation inhibits BCR-mediated proliferative cell signalling

FcγRIIb (CD32) is a single chain, low affinity receptor for the Fc domain of IgG molecules, and as such can only interact with IgG in the form of immune complexes. It is the only Fcγ receptor found on B cells, and contains a 13 amino acid inhibitory ITIM motif in its cytoplasmic domain that is responsible for its inhibitory effects on BCR signalling. Coligation of the BCR and FcγRIIb by cognate antigen-antibody complexes leads to tyrosine phosphorylation of the ITIM by the Src-family kinase Lyn, and subsequent recruitment of the protein phosphatases SHP-1, SHP-2 and the inositol phosphatase SHIP. The overall outcome of the recruitment of these molecules is the abrogation of the 3 key signalling pathways activated upon BCR ligation, the ERKMAPK, PI-3 kinase and PKC pathways.

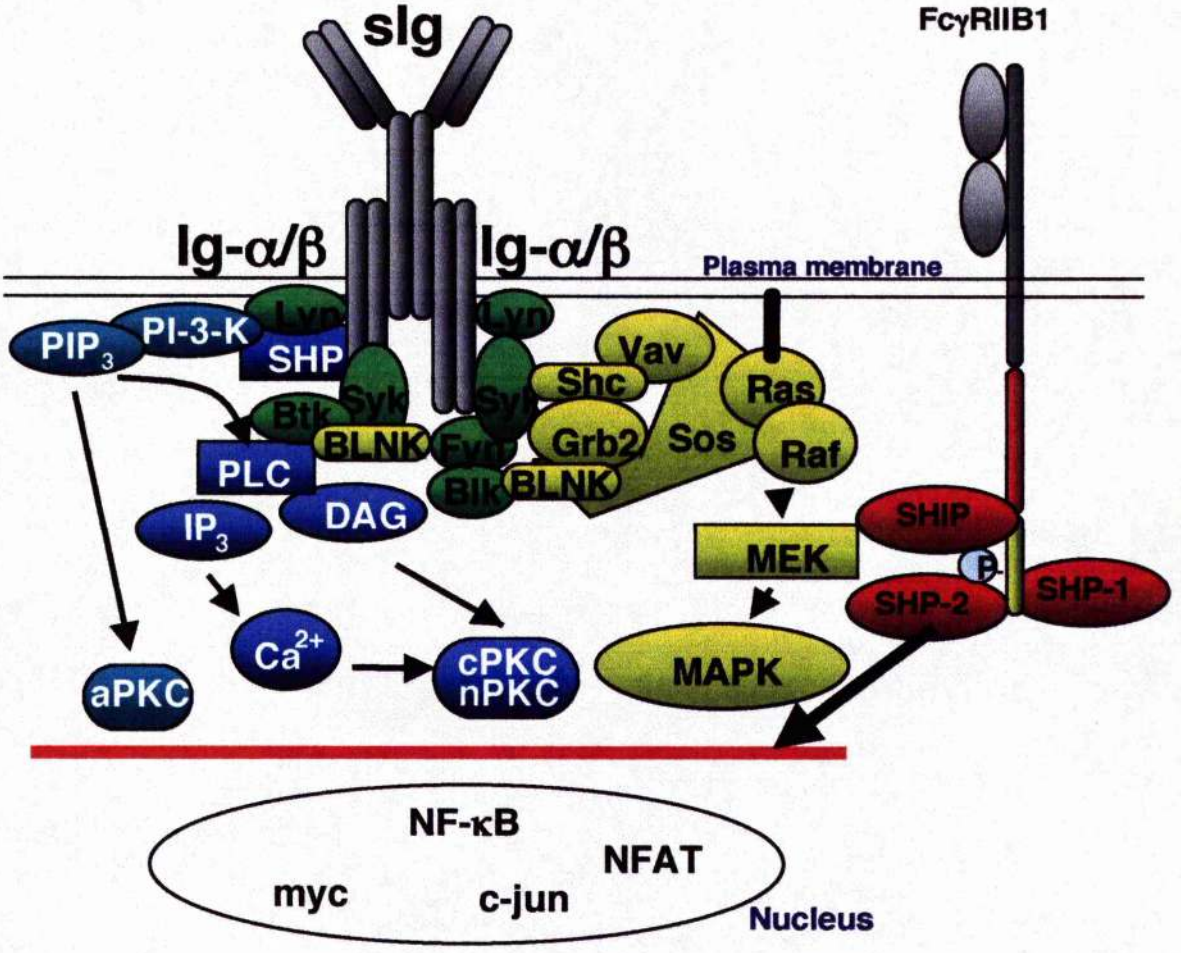
sIg
FcγRIIB1
Ig-α/β
Ig-α/β
Plasma membrane
PIP3
PI-3-K
Lyn
SHP
Lyn
Vav
Shc
Ras
Syk
Syk
Btk
BLNK
Fyn
Grb2
Sos
Raf
PLC
Blk
BLNK
IP3
DAG
SHIP
MEK
P
SHP-2
SHP-1
Ca2+
cPKC
nPKC
MAPK
aPKC
NF-κB
NFAT
myc
c-jun
Nucleus

Figure 1.19: Coligation and BCR and FcγRIIb by cognate Ag-Ab complexes induces cell cycle arrest whereas homo-aggregation of FcγRIIb by non-cognate Ab induces apoptotic signalling

As stated in figure 1.18, coligation of the BCR and FcγRIIb results in the inhibition of both the MAP kinase and PI-3 kinase pathways and hence cell cycle arrest. This coligation occurs via the binding of localised BCR and FcγRIIb within the same lipid raft by cognate Ag-Ab complexes. In contrast, FcγRIIb can be homo-aggregated by non-cognate Ab complexes. This results in an apoptotic signal however the mechanism for this has yet to be elucidated.

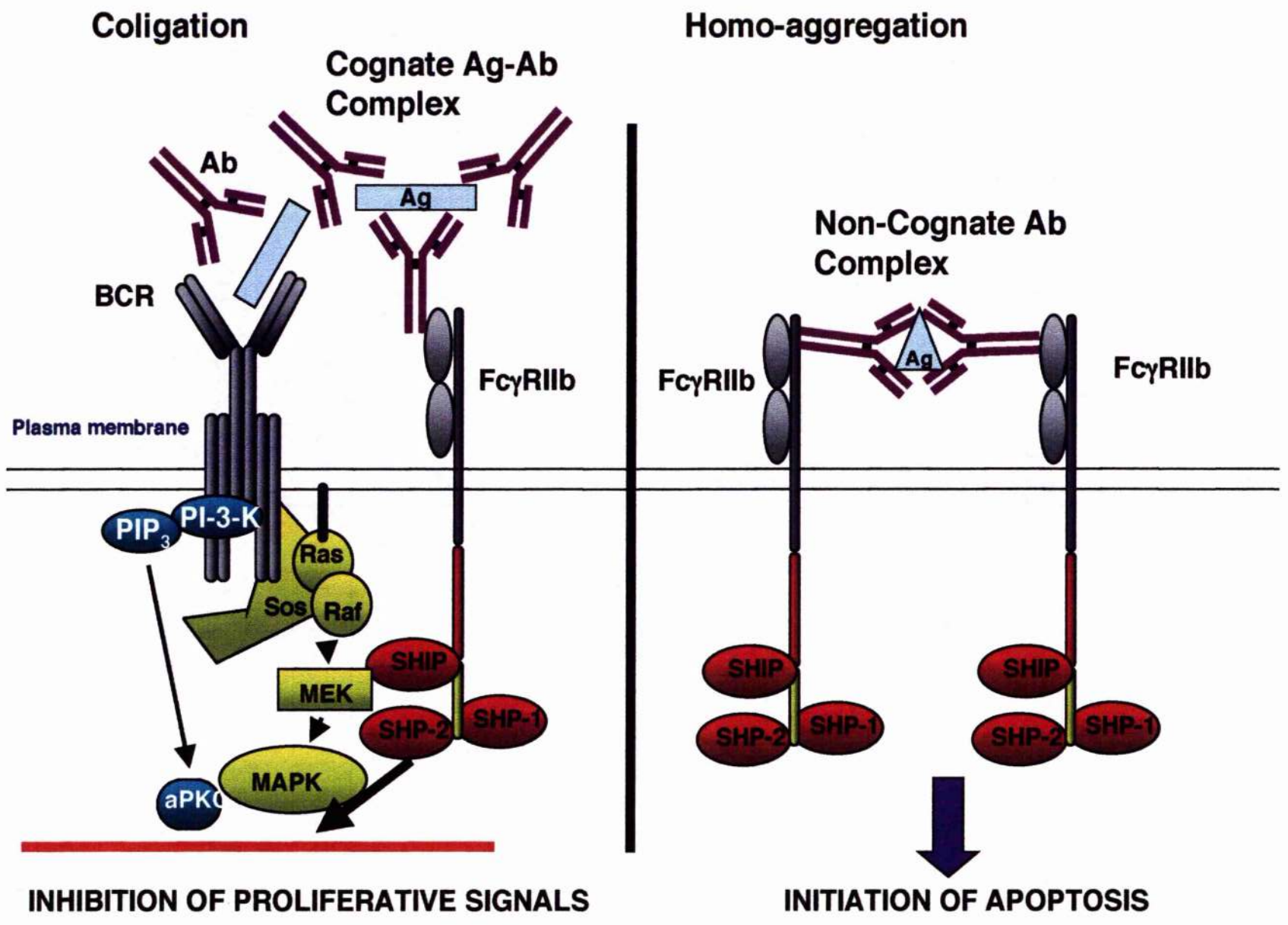
Coligation
Cognate Ag-Ab Complex
Ab
Ag
BCR
FcγRIIb
Plasma membrane
PIP3
PI-3-K
Ras
Sos
Raf
MEK
SHIP
SHP-2
SHP-1
MAPK
aPKC
INHIBITION OF PROLIFERATIVE SIGNALS
Homo-aggregation
Non-Cognate Ab Complex
FcγRIIb
Ag
FcγRIIb
SHIP
SHP-2
SHP-1
SHIP
SHP-2
SHP-1
INITIATION OF APOPTOSIS

Figure 1.20: Simultaneous coligation of the BCR and FcγRIIb recruits Gab1 which can inhibit the PI-3 kinase pathway

Grb2-associated binder 1 docking protein (Gab1) is a docking protein that forms part of the multi-protein complex assembled by the BCR upon ligation. Gab1 is predominantly found in the membrane enriched fractions of activated B cells and contains a plekstrin homology domain (PH domain), tyrosine phosphorylation sites and proline rich sequences. Once tyrosine phosphorylated it recruits other SH2 domain containing proteins, such as the p85 subunit of PI-3 kinase and Shc, to the cell membrane where their substrates reside. On co-clustering with FcγRIIb Gab1 becomes dephosphorylated by SHP2 which leads to disruption of the PI-3 kinase mediated downstream pathway.

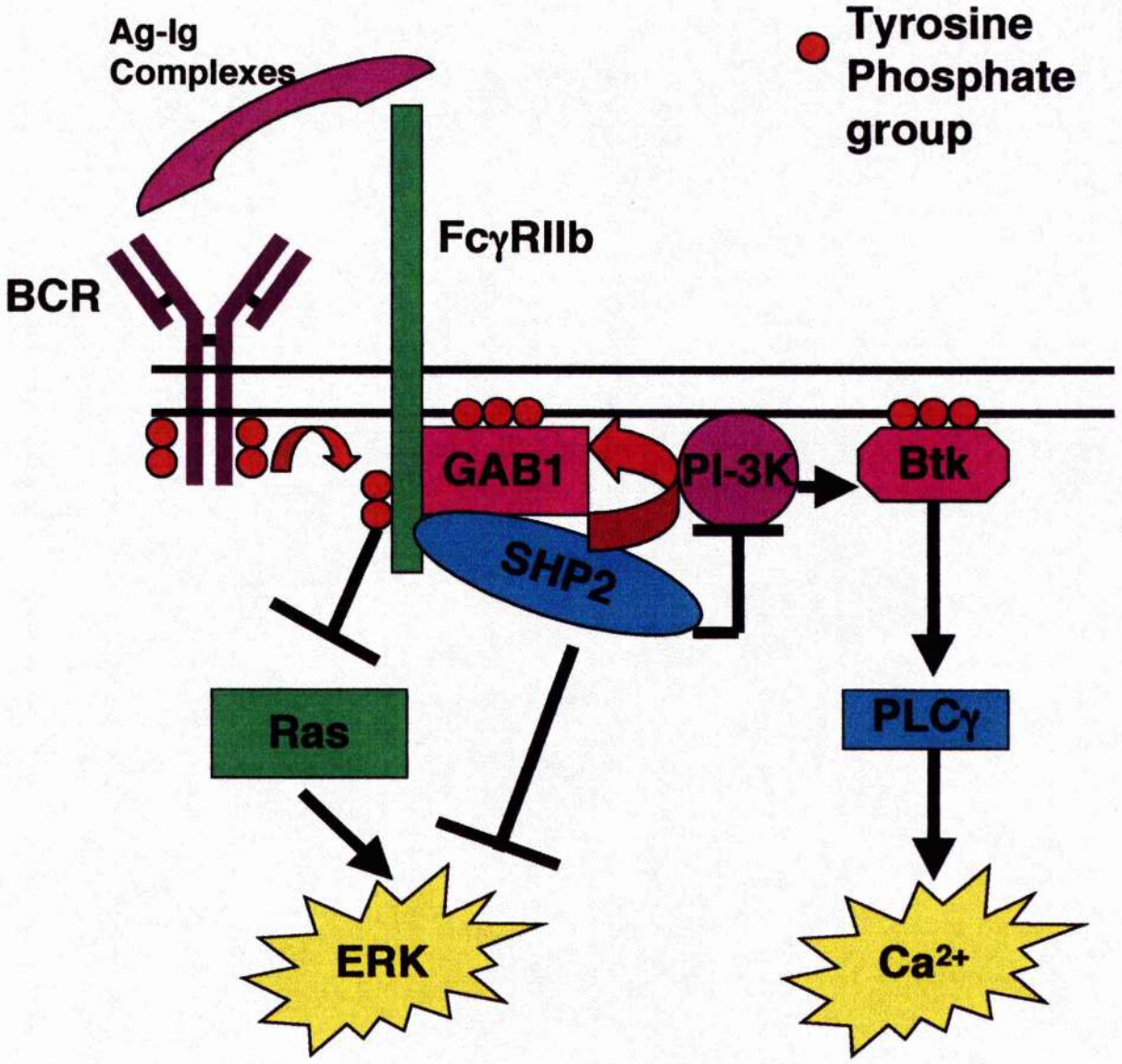
Ag-Ig
Complexes
Tyrosine
Phosphate
group
FcγRIIb
BCR
GAB1
PI-3K
Btk
SHP2
Ras
PLCγ
ERK
Ca2+

Chapter 2: Materials and Methods

2.1 Cell culture, Antibodies and Inhibitors

All cell culture reagents were purchased from Invitrogen Life Technologies. All other reagents were obtained from Sigma-Aldrich unless otherwise stated (see 2.17 for supplier's addresses). For experiments using WEHI 231 cells, monoclonal Ab (mAb) B7.6. anti-IgM and mAb anti-CD40 were used at a final concentration of 10 μg/ml. For FACS experiments and proliferation assays with mature B cells, $F(Ab')_2$ fragments of goat anti-mouse IgM Abs (Jackson Immunoresearch laboratories) were used at 50 μg/ml to ligate the BCR. Intact rabbit anti-mouse anti-IgM at 75 μg/ml (Jackson Immunoresearch laboratories) was used to coligate the BCR with FcγRIIb. However for Western Blotting, FACE and TransAM assays using mature B cells the following antibodies were used: B7.6 anti-IgM to ligate the BCR (50 μg/ml), 24G.2 IgG to ligate FcγRIIb (50 μg/ml) and 75 μg/ml Donkey anti-Rat IgG (Jackson Immunoresearch laboratories) to crosslink the B7.6 and 24G.2 Abs and hence coligate the BCR and FcγRIIb. For a full list of antibodies used, see table 2.2. Unless specified, cell signalling inhibitors were used at the following concentrations 10 μM PD98059 (Calbiochem), 1 μM LY294002 (Promega), 5 μM SB203500 (Alexis biochemicals) and 1 μM U0126 (Promega). N-benzyloxycarbonyl-Val-Ala-Asp(Ome)- fluoromethylketone (Z-VAD-FMK), (25,35) *trans*-epoxysuccinyl-L-leucylamido-3-methylbutane ethyl ester (EST) and Mu-Val-HPh-FMK (Calpain Inhibitor V) were used at 10 μM (all supplied by Calbiochem). The panlipoxygenase inhibitor ethyl 3,4- dihydroxybenzlidenecyanoacetate (EDBC, Alexis Biochemicals) was used at 10 μM and the Cox2 inhibitor N-(2-Cyclohexyloxy-4-nitrophenyl)methanesulphonamide (NS 398 Alexis Biochemicals) was used at 10 μM. Two different PLA_2 inhibitors were used; Arachidonyltrifluoromethyl Ketone (AACOCF3) and Methyl Arachidonyl Fluorophosphonate (MAFP) both at 20 μM. These inhibitors are non-hydrolysable forms of arachidonic acid and were supplied by Calbiochem.

2.2 Animals

Male Balb/c mice aged between 6 and 10 weeks were used to isolate primary splenic B cells. These mice were maintained at the Central Research Facility (CRF), University of Glasgow. All mice were purchased from Harlan UK Ltd and were quarantined for at least 7 days prior to starting an experiment. Lpr-/- mice (SLE model mice) were kept at the Animal Research Facility at the Royal Infirmary, Glasgow, UK. The model was administered by Dr. A. Gracie (University of Glasgow).

2.3 Purification of murine splenic B cells

Primary B cells were prepared from murine spleens using the CD43-magnetic bead negative-selection method of Miltenyi Biotec (274). The CD43 antigen is expressed on nearly all leukocytes, except for immature and mature naive B cells. By using anti-CD43 coated MicroBeads, all CD43 expressing cells are magnetically labeled and removed by negative selection column, whereas the naive B cell subset can be collected in the column elutant. All procedures were performed at 4 °C. Briefly; a single cell suspension was prepared by mashing the spleens through wire mesh, in RPMI-1640 media. The resultant suspension was centrifuged (450 g, 7 min, 4 °C) and the pellet resuspended in 9 ml of red blood cell removal buffer (0.168 M NH_4Cl, pH 7.2). The suspension was carefully layered over 1 ml heat-inactivated foetal calf serum (FCS) and incubated on ice for 7 min to permit red blood cell lysis and lipid precipitation. The supernatant was removed, carefully layered over 1 ml FCS in a fresh tube and centrifuged again (450 g, 7 min, 4 °C). The resulting cell pellet was resuspended in 9 ml dead cell removal buffer (HEPES-buffered, mouse tonicity, balanced salt solution (BSS) supplemented with 0.12 M Sorbitol and 20 mM Glucose) (284, 285). The suspension was immediately filtered through two prepared dead cell removal columns (absorbent cotton wool plugged, short-form, glass pipettes, wetted with 1 ml RPMI/5% FCS). Cells were recovered from the column into 1 ml RPMI/5% FCS. The cells were centrifuged (450 g, 7 min, 4 °C) and resuspended in 50 ml ice-cold MACS buffer (phosphate buffered saline (PBS), 0.5% BSA, 2 mM EDTA) counted by Trypan blue exclusion, and pelleted by centrifugation (450 g, 7 min, 4

°C). The cells were then resuspended in ice-cold MACS buffer (2 x 10^8 cells/ml) and passed through gauze, to produce a single cell suspension for labelling. Cells were incubated for 25 min at 4 °C with anti-CD43 (Ly-48) beads (100 µl anti-CD43+ beads/ 2 x 10^8 cells). Labelled cells were passed through gauze again and applied to a CS-type negative selection magnetic column (Miltenyi Biotec) in a strong magnetic field. Purified mature B cells (CD43-) were eluted from the column by washing with 50 ml ice-cold MACS buffer. The cells were centrifuged (400 X g, 7 min, 4 °C), resuspended in RPMI-1640 medium supplemented with 5% FCS, 100 U/ml penicillin, 100 µg/ml streptomycin, and 2 mM glutamine, and live B cells counted by trypan blue exclusion.

2.4 Cell Lines

2.4.1 WEHI 231 Immature B cell line

The murine B cell lymphoma, WEHI 231 (obtained from ECACC) was cultured in RPMI-1640 medium supplemented with 5% FCS, 100 U/ml penicillin, 100 µg/ml streptomycin, 50 µM mercaptoethanol and 2 mM Glutamine at 37°C in a 5% (v/v) CO_2 atmosphere at 95% humidity. All cell culture reagents were of the highest quality available.

2.4.2 BclX_L WEHI 231 cells

WEHI 231.7 JM cells were transfected by electroporation with the pSFFV-Neo plasmid containing either the human *bcl-x_L* gene (BclX_L WEHI 231) or no insert as control (Neo WEHI 231). Stable transfectants were selected for the acquisition of neomycin resistance by growth in the presence of the antibiotic G418 (500 µg/ml) (286, 287) and were a kind gift from Dr. C. B. Thompson (University of Pennsylvania). Overexpression of BclX_L was confirmed by Western Blotting using an anti-Bcl$X_{L/S}$ antibody. Stable transfectants were cultured in RPMI 1640 media supplemented with 5% FCS, 100 U/ml penicillin, 100 µg/ml streptomycin, 50 µM mercaptoethanol, 2 mM Glutamine and 500 µg/ml G418 at 37°C in a 5% (v/v) CO_2 atmosphere at 95% humidity.

2.4.3 Retroviral transfection of WEHI 231 cells with SHIP and Dok constructs

Retroviral constructs were generated by subcloning the gene of interest into the retroviral vector pMXI-egfp, 5' to the internal ribosomal entry site and green fluorescence protein (GFP) was encoded 3' to this site. Amphotropic phoenix cells were used as packaging cells for the retroviral transfection system. Pheonix cells were transfected using the effectine transfection reagent as per manufacturers instructions (Qiagen) with pMXI-egfp vectors containing no construct (empty vector control, pMXI-egfp), SHIP CI construct, SHIP SH2 construct or Dok PH/PTB construct (see Table 2.2 for details of constructs). Two days after transfection, the supernatants were collected, filtered (0.22 µm) and polybrene was added to a final concentration of 4 µg/ml. WEHI 231 B cells (5 x 10^5 cells/ml) were centrifuged in 12 well plates to promote adherence. Viral supernatants were added to adherent cells followed by centrifugation at 1,000 g for 2 h at 32°C. Cells were then incubated at 32°C overnight before transferring them into 25 cm^3 flasks for expansion. Following expansion, cells were sorted for GFP-expression (Mo-Flo, Cytomation, Fort Collins, CO). Successful transfectants were a kind gift from Dr. S. B. Gauld (National Jewish Medical and Research Center, Denver, CO).

2.4.4 Generation of PKC, Ras and ΔMEKK 3 WEHI 231 mutant cells

WEHI 231 cells (5 x 10^6 cells) undergoing logarithmic growth were washed and resuspended (2 x 10^7 cells/ml) in electroporation media (RPMI-1640 with 20% FCS). Linearised DNA (5 µg), recovered from an agarose gel, was chilled on ice for 5 min in an electroporation cuvette. WEHI 231 cells (5 x 10^6) were added to the cuvette, gently mixed and chilled for 10 min on ice. Cells were electroporated at 960 µFarads at 220 Volts and were then chilled on ice for a further 10 min. Cells were then removed from the cuvette and were grown in RPMI complete medium for 48 h at 37°C in 5% (v/v) CO_2 atmosphere at 95% humidity before selecting for successful transfectants using the antibiotic G418 (500 µg/ml). Electroporation of WEHI 231 B cells was used to generate several mutant WEHI 231 cell types including an empty vector control, pcDNA3.1. Transfection of WEHI 231 cells by electroporation was performed by Derek Blair in this laboratory. Stable transfectants were cultured in RPMI 1640 media supplemented with 5% FCS, 100 U/ml penicillin, 100 µg/ml streptomycin, 50 µM mercaptoethanol, 2 mM Glutamine

and 500 μg/ml G418 at 37°C in a 5% (v/v) CO_2 atmosphere at 95% humidity.

2.5 Purification of antibodies from hybridoma cell lines

Anti-CD40 was purified from the FGK 45 hybridoma, anti-IgM from the B7.6 hybridoma and anti-FcγRII from 2.4G2 hybridoma as has previously been described (288, 289). Cells were cultured in RPMI complete medium and the antibody-rich tissue culture supernatant was collected. Ab was purified using a protein G-sepharose column. The column of 1 ml protein G-sepharose beads (immunoglobulin capacity >20 μg/ml) was washed with binding buffer (0.2 M $NaH_2PO_4.2H_2O$, 0.2 M $Na_2HPO_4.2H_2O$, pH 7.0) then tissue culture supernatant was run through the column at 4°C. The column was washed with binding buffer then the immunoglobulin was eluted in 1 ml fractions using elution buffer (0.1 M glycine, pH 2.7). The protein concentration of each 1 ml fraction was determined using spectrophotometry to measure the absorbance at 280 nm (an optical density of 1.4 was approximately equivalent to 1 mg/ml of protein). The most protein-rich fractions were pooled and dialysed exhaustively in PBS. The resultant purified Abs were filter sterilised and stored at -20°C.

2.6. DNA Synthesis Assay

For measurement of DNA synthesis, cells (WEHI 231 cells: 10^4 cells/ well, Mature B cells: 5 x 10^5 cells/ well) were cultured in triplicate in round bottom microtitre plates in RPMI 1640 media supplemented with 2 mM glutamine, 1 mM sodium pyruvate, 1% nonessential amino acids, 50 μM 2 mercaptoethanol, 100 U/ml penicillin, 100 μg/ml streptomycin, 5% FCS (and G418 If appropriate) in the presence of the appropriate agonist in a total volume of 200 μl. For WEHI 231 cells, B7.6. anti-IgM and anti-CD40 Abs were used at 10 μg/ml unless otherwise stated. For mature B cells, $F(Ab')_2$ fragments of Anti-IgM Abs were used at 50 μg/ml and Intact Rabbit Anti-mouse anti-IgM at 75 μg/ml. Cells were cultured at 37°C in a 5% (v/v) CO_2 atmosphere at 95% humidity for 48 h. [^{3}H] Thymidine (0.5 μCi/ well, Amersham) was added 4 h before cell harvesting with an automated cell harvester (Molecular Devices) (288, 289). Incorporated label was estimated by liquid scintillation counting and is represented as cpm +/- SEM.

2.7 Flow Cytometry

2.7.1 Flow Cytometric Analysis of cell cycle stage by DNA content

Cells (5 x 10^5 cells/well for WEHI 231 and 1 x 10^6 cells/well for mature B cells) were cultured in RPMI complete medium in the presence of appropriate stimuli. Cells were cultured at 37°C in a 5% (v/v) CO_2 atmosphere with 95% humidity for up to 120 h. Cells were harvested and washed twice in ice-cold FACS buffer (PBS with 1% BSA and 0.1% sodium azide). Cells were then resuspended in 200 µl propidium iodide (PI) stain (0.1% (w/v) sodium (tri) citrate, 0.1% (v/v) triton-X-100, 50 µg/ml propidium iodide and 200 µg/ml RNase A) for 45 min on ice (288). After addition of a further 200 µl of FACS buffer, cells were passed through nitex and analysed for PI fluorescence on a FACScalibur™ (Becton Dickinson) (156) using CELLQuest™ software (Becton Dickinson).

Cell cycle analysis was used to determine the percentage of cells in the different phases of the cell cycle: sub-diploid (apoptotic), G0/G1, S phase or G2/M (figure 1.6). PI is able to intercalate DNA in a stochiometric fashion and so enables assessment of the DNA content of cells. PI fluorescence was measured using both FL3 (linear scale) and FL2 (logarithmic scale) channels. Cell counts for either 5 or 10 seconds, depending on cell density, were also recorded. When using FL3, the voltage was adjusted until the large G0/G1 peak was at 200-300 units. This voltage was kept constant whilst the data from any one experiment was acquired. Data was analysed by setting gates (Figure 2.1). The G0/G1 peak represents 2N DNA. The centre of this peak was identified and a gate was set to include all cells in this peak. The 2N DNA peak was doubled (representing 4N DNA) and markers were set either side of this point to form the G2/M gate. The S phase gate represents the cells between G0/G1 and G2/M phases. Cells located at lower fluorescence than the G0/G1 peak are the sub-diploid (apoptotic) cells.

2.7.2 Cell Cytometric analysis of mitochondrial membrane potential (MMP)

2.7.2.1. $DiOC_6$

Cells (5 x 10^5 cells/well for WEHI 231 and 1 x 10^6 cells/well for mature B cells) were cultured in RPMI complete medium in the presence of appropriate stimuli.

Cells were cultured at 37°C in a 5% (v/v) CO_2 atmosphere with 95% humidity for up to 120 h. Cells were harvested and washed in ice-cold FACS buffer (PBS with 1% BSA and 0.1% sodium azide). Cells were then resuspended in 1 ml of $DiOC_6$ stain (2.5 μM $DiOC_6$ in FACS buffer) for 30 min at room temperature. Cells were then washed twice in 3 ml FACS buffer, resuspended in 200 μl of FACS buffer and passed through nitex. At least 10^4 cells were collected and analysed for FL1 fluorescence on a FACScalibur™ (Becton Dickinson) using CELLQuest™ software (Becton Dickinson) (156).

Incorporation of cationic lipophilic dye $DiOC_6$ (Molecular Probes) into mitochondria is proportional to the mitochondrial transmembrane potential, $\Delta\Psi_m$ (156). The histogram produced can be divided into cells with high or low MMP (Figure 2.2) depending on their $DiOC_6$ fluorescence on the FL1 axis relative to fresh unstimulated cells.

2.7.2.2. JC 1

Cells (5 x 10^5 cells/well for WEHI 231 and 1 x 10^6 cells/ well for mature B cells) were cultured in RPMI complete medium in the presence of appropriate stimuli. Cells were cultured at 37°C in a 5% (v/v) CO_2 atmosphere with 95% humidity for up to 120 h. Cells were harvested and washed twice in ice-cold FACS buffer (PBS with 1% BSA and 0.1% sodium azide). Cells were then resuspended in 200μl of JC 1 stain (1 μM 5,5',6,6'-tetrachloro-1,1',3,3'-tetraethylbenzaidazolylcarbocyanine iodide in FACS buffer, Molecular Probes) for 15 min at room temperature (290). Cells were then washed twice in FACS buffer and resuspended in 200 μl of FACS buffer cells. Cells were then passed through nitex and analysed for FL1 and FL2 fluorescence on a FACScalibur™ (Becton Dickinson) using CELLQuest™ software (Becton Dickinson). The cationic dye JC 1 is used to signal the loss of MMP. In healthy cells the mitochondria are stained red (FL2) however when MMP is dissipated JC 1 is visualised as a green fluorescent, monomeric dye that can be monitored in FL1 (290).

2.7.3. Cell Cytometric analysis of Caspase Activation

Cells were plated out at 1 x 10^6 cells/well with the appropriate treatments and incubated for up to 48 h. CaspACE™ FITC-VAD-FMK in situ marker (Promega) was added to a final concentration per well of 10 μM. The plates were incubated for 20 mins at 37°C in the dark and then washed twice with PBS. At least 10^4 cells/ sample were used for FACS analysis (Becton Dickson FACScan™). CaspACE™ FITC-VAD-FMK is a FITC conjugated version of the cell permeable, irreversible pan caspase inhibitor Z-VAD-FMK. As it binds to cleaved caspases, it can be used to monitor the amount of activated caspases present in the cell by measuring fluorescence in the FL1 channel.

2.7.4 Flow Cytometric Analysis of cell proliferation by CFSE staining

The number of cell divisions was determined according to procedures previously described (291). Briefly cells (1 x 10^6 cells/well mature B cells and 5 x 10^5 cells/well WEHI 231 cells) were suspended in FACS buffer and incubated with 1 μM CFSE (Promega) for 1 min at 5°C in the dark followed by 2 washes. These cells were then plated out and cultured at 37°C in a 5% (v/v) CO_2 atmosphere at 95% humidity for the appropriate time period. The cells were then washed twice in FACS buffer and resuspended in 200 μl of FACS buffer. At least 10^4 cells/ sample were analysed (Becton Dickson FACScan™) (292).

CFSE is a dye that fluoresces in the FL1 channel and binds to proteins within the cell. As the cells divide each daughter population has half the original amount of CFSE present. Therefore it is possible to monitor cell division by the shift in FL1 brightness.

2.8 Western Blotting

2.8.1.Cell Stimulation and Whole Cell Lysate Preparation

Either Mature B cells or WEHI-231 cells (10^7 cells/ stimulation) were stimulated as indicated. The cells were then washed in PBS and the reactions were terminated by the addition of 100 μl of ice-cold modified RIPA lysis buffer (50 mM Tris buffer, pH 7.4 containing 150 mM sodium chloride, 2% (v/v) NP 40, 0.25% (w/v) sodium deoxycholate, 1 mM EGTA, 10 mM sodium orthovanadate, 0.5 mM

phenylmethylsulfonylfluoride, chymostatin (10 μg/ml), leupeptin (10 μg/ml), antipain (10 μg/ml), and pepstatin A (10 μg/ml)). After vortexing the cells were solubilised for 30 minutes on ice before centrifugation of lysates at 450 g for 15 minutes. The resulting supernatants (whole cell lysate) were stored at -20°C before being used for Western Blot analysis.

2.8.2 Immunoprecipitation

Whole cell lysates were pre-cleared with 10 μl of protein G bead slurry and incubated for 1 hour at 4 °C on orbital rotator. Samples were centrifuged to remove beads (19,800 g, 30 min, at 4 °C) and the supernatant was decanted. Samples were diluted to 1 mg/ml with lysis buffer and incubated with Ab (1.5 μg per 10^6 cells) overnight at 4 °C on an orbital rotator. Protein G slurry (25 μl) was added and incubated for 4 hours at 4 °C. The bead pellet contains the immune complexes. The beads are washed four times, at 19,800 g for 30 min at 4 °C, with 1 ml of ice cold lysis buffer and 2 X loading buffer (60 μl) was added. Before use, the samples were boiled for 5 min to separate immune complexes from the beads. The samples were centrifuged for 2 min at 13,000 g and the supernatant used for gel electrophoresis and Western Blotting.

2.8.3 Gel Electrophoresis

Equal protein loadings of whole cell lysates (30 μg protein per lane) determined by BSA protein assay (Pierce) or cell equivalents of immunoprecipitated samples were resolved on the XCell *SureLock* Mini-Cell kit with NuPAGE Novex high-performance pre-cast Bis-Tris gels and NuPAGE buffers and reagents (all supplied by Invitrogen). Lysates were diluted in lysis buffer to a constant final volume and the appropriate volume of 4 x NuPAGE LDS sample buffer and 10 x NuPAGE reducing agent were added prior to heating samples to 70°C for 10 min. Samples were resolved using NuPAGE Bis-Tris gels (10%) with NuPAGE MOPS running buffer (supplemented with NuPAGE antioxidant) at 200 V for 50 min following the manufacturers instructions. The gel was then transferred onto nitrocellulose

membrane (Amersham) using NuPAGE transfer buffer with 20% (v/v) methanol at 30V for at least 1 h.

2.8.4 Western blot analysis

Following transfer, nitrocellulose membranes were washed once in Tris buffered saline (TBS) (0.5 M NaCl and 20 mM Tris pH7.5) with 0.1% (v/v) Tween-20 (TBS/Tween) and blocked for 1 h in TBS/Tween with 5% non-fat milk when antibodies generated in rabbit or mouse were being used. Alternatively, blots that were to be probed with an antibody generated in a goat were blocked for 1 h in a 1 in 4 dilution of a non-animal blocking reagent, Chemiblocker (Chemicon International). Membranes were then incubated with the appropriate primary detection antibody overnight at 4°C. All antibodies were diluted in TBS/Tween with either 5% non-fat milk or 1 in 4 dilution of ChemiBlocker. Following incubation with primary antibody nitrocellulose membranes were washed (6 x 5 min) with TBS/Tween and incubated in the appropriate horse radish peroxidase (HRP)-conjugated secondary antibody for 1 h at room temperature. Nitrocellulose membranes were then washed (10 x 10 min) with TBS/Tween and protein bands were visualised using the ECL detection system. Nitrocellulose membranes were incubated in a mixture of equal volumes of ECL solution A (2.5 mM luminol, 0.4 mM p-coumaric acid and 100 mM Tris pH8.5) and ECL solution B (0.002% hydrogen peroxide and 100 mM Tris pH8.5) for 1 min before exposing membranes to Kodak X-Ray film.

2.8.5 Stripping Western Blots

Nitrocellulose membranes were sometimes stripped and re-probed with an alternative primary antibody. Membranes were stripped at room temperature for 1 h in stripping buffer (100 mM 2-mercaptoethanol, 2% SDS and 62.5 mM Tris pH6.7). Nitrocellulose membranes were washed thoroughly in TBS/Tween and checked for residual signal before re-starting the Western Blotting protocol.

2.9 DNA analysis of cells using DAPI staining

Mature B cells were plated out at 1 x 10^6 cells/well with appropriate stimulations and incubated at 37°C in a 5% (v/v) CO_2 atmosphere at 95% humidity for 48 h.

Cells were then washed once in FACS buffer and resuspended in 200 μl of FACS buffer which was dropped onto a microscope slide and then allowed to air dry for 1 hour. Slides were then treated with 8% formaldehyde for 10 min then tapped and allowed to air dry again. After this a drop of Vectashield containing DAPI (Vector Labs) was dropped onto the slide and a cover placed on top. The cover was attached using clear nail varnish and the slides were stored in the dark until needed for image analysis.

2.10 Fast Activated Cell Based ELISA (FACE)

2.10.1 Plating out for the cell based assay

FACE was developed to provide a fast and easy way to identify the phosphorylation and expression levels of intracellular proteins. The cells are permeablised and then treated with a protocol very like an ELISA to provide information on the status of cell signalling proteins. The kits we used were purchased from Active Motif, Rixensart, Belgium and developed using a protocol from Versteeg et al (293). Firstly, 200 μl of Poly-L-lysine 0.01% (w/v) in sterile water is added per well to allow for cell attachment to the plate as B cells are non adherent. The Poly-L-lysine solution is incubated at 37°C for 30 min. The wells are then washed 3 times for 5 min with sterile PBS. Cells are added (5×10^5 cells/well for mature B cells and 2×10^4 cells/well for WEHI 231 cells) with the appropriate stimulations and cultured at 37°C in a 5% (v/v) CO_2 atmosphere at 95% humidity for the time period desired. For FACE assays of AKT, cells were cultured in the presence and absence of 1 μM microcystin (Biomol). Microcystin is a protein phosphatase inhibitor that allows for assessment of AKT phosphorylation accumulated over a given period. Following culture, 200 μl of 8% formaldehyde was added to each well. This could either be incubated for 20 min or the plate could be sealed and stored in the fridge for up to 2 weeks before further analysis.

2.10.2 Addition of Primary and Secondary Antibodies

Following fixation, wells were washed (3 x 5 min) with 200 μl TBS/Tween and then treated with 100 μl of quenching buffer (1% H_2O_2, 0.1% Sodium Azide in TBS/Tween) for 20 min. Wells were washed twice more followed by addition of

100 μl of blocking buffer (TBS/Tween with 5% non-fat milk) for 1 . Following 2 further washes wells were treated with 40 μl of primary antibody (1 in 1000 dilution in TBS/Tween with 5% non-fat milk) and the plate sealed and left overnight in the fridge. Wells were then washed twice and treated with 100 μl of HRP conjugated secondary antibody (1 in 1000 dilution in TBS/Tween with 5% non-fat milk) for 1 h. The wells were the washed twice with wash buffer and a further 3 times with PBS.

2.10.3 Colorimetric reaction

After drying the plate on a paper towel, 100 μl of 3,3',5,5' tetramethylbenzidine (TMB, Pierce) was added and allowed to develop until there was a medium dark blue colour (2 to 20 min). TMB is a chromagen that yields a blue color when oxidized with hydrogen peroxide (catalyzed by HRP). 100 μl of 0.1% HCl was then added, to stop the reaction, and the plate absorbance read at 450 nm followed by statistical analysis.

2.11 TransAM Nuclear Transcription Factor ELISAs

These assays were purchased from Active Motif and 2 different kits were used: the p53 TransAM and the NF κB TransAM.

2.11.1 Nuclear Extraction

Cells were plated out at 1 x 10^7 cells/well and incubated with appropriate stimulations at 37°C in a 5% (v/v) CO_2 atmosphere at 95% humidity. An Active Motif nuclear extraction kit was used to produce nuclear and cytosolic fractions as per the manufacturers instructions. Briefly, samples were washed with 5 ml of PBS containing phosphatase inhibitors which terminate any cellular reactions, and then centrifuged for 5 min at 400 X g. The pellets were resuspended in 500 μl of hypotonic buffer by pipetting and then incubated on ice for 15 min. Following this, 25 μl of detergent was added and the samples were vortexed on the highest setting for 10 s. Samples were then centrifuged at 14,000g for 30 s and the supernatant removed. This supernatant is the cytosolic fraction and can be stored at –80 °C for further use. The pellet was then resuspended in 50 μl of complete lysis buffer (containing DTT and protease inhibitor cocktail) and vortexed for 10 s.

The samples were then left on ice for 30 min and after a further vortexing centrifuged at 14,000 g for 10 min. The resultant supernatant is the nuclear fraction and is stored at –80 °C.

2.11.2 TransAM ELISA assay

The TransAM ELISA kit provides 96 well plates on which oligonucleotides containing the transcription factor consensus binding site have been immobilised. The transcription factor in the nuclear extract then binds to this and can then be detected using an antibody which recognises the transcription factor in its DNA-bound conformation. Manufacturers instructions were followed. Briefly, 40 μl of complete binding buffer (containing DTT and Poly [d(I-C)]) was added to each well. For each sample well 2 μg of nuclear extract, as determined by Bradford assay, was added to each well diluted in 10 μl of complete lysis buffer. For the "positive control", 5 μg of provided sample was added diluted in 10 μl of complete lysis buffer and for the "blank" wells 10 μl of complete lysis buffer alone was added. All wells were plated out in duplicate unless otherwise stated. Samples were then incubated at room temperature for 1 h with mild agitation, washed 3 times with 200 μl of wash buffer followed by a 1 h incubation with 100 μl of primary antibody. After an additional 3 washes, the wells were incubated with 100 μl of HRP conjugated secondary antibody. The plate was then washed 4 times and allowed to dry for 5 min on a paper towel. After drying the plate 100 μl of developing solution was added and allowed to develop until there was a medium dark blue colour (2 to 20 min). 100 μl of stop solution was then added and the plate absorbance read at 450nm within 5 min of the reaction being stopped. The mean values of the duplicates were then calculated.

2.12 Cytochrome C Function ELISA

2.12.1 Preparation of cytosolic and mitochondrial fractions

The mitochondrial extraction kit was obtained from Active Motif and was completed as per the manufacturers instructions but with the modifications listed below (Figure 2.3). Cells were cultured (5×10^7 cells/sample) at 37°C in a 5% (v/v) CO_2 atmosphere at 95% humidity for the time period desired. Cells were then taken

from the well and washed with 2ml of ice cold PBS. The pellet was resuspended in 1 ml of ice cold cytosolic buffer and transferred to microtubes on ice for 15 min. The samples were then transferred to homogenising pestles on ice and treated with 50 strokes before being transferred to a fresh tube. Samples were then centrifuged at 400 g for 20 min, the supernatant transferred to a fresh tube and the centrifuged pellet discarded. The supernatant contained the cells that had been broken following homogenisation whereas the pellet contained residual intact cells. This supernatant was centrifuged again at 800 g for 10 min and the resulting supernatant transferred to a fresh tube. The pellet, which contained intact nuclei, was treated with 100 µl of complete mitochondrial lysis buffer on ice for 15 min to produce the nuclear fraction, whereas the supernatant which contained the cytosol and mitochondria was centrifuged again at 10,000 g for 20 min. The resulting supernatant was transferred to a fresh tube, this being the cytosolic fraction. The pellet, which contained the mitochondria, was treated with 100 µl of complete mitochondrial lysis buffer on ice for 15 min to produce the mitochondrial fraction. All fractions were stored at –80 °C.

2.12.2 Cytochrome c ELISA Procedure

This kit was supplied by Active Motif and completed as suggested in the manufacturers instructions. Briefly, cell equivalents of mitochondrial and cytosolic fractions were prepared in the manufacturer's blocking buffer (total 100 µl). The blank wells contained only 100 µl of blocking buffer. The wells were then left for 2 h at room temperature. Wells were then washed 3 times with 250 µl of wash buffer and incubated with 100 µl of anti cytochrome c Ab (1 in 1000 dilution in blocking buffer) for 1 h. The wells were then washed again 3 times and 100 µl of HRP conjugated secondary antibody added (1 in 1000 dilution in blocking buffer) for 1 h. Wells were washed 4 times and the plate allowed to air dry for 1 min before the addition of 100 µl of developing solution. This was allowed to develop until there was a medium dark blue colour (2 to 20 min). 50 µl of stop solution was then added and the plate absorbance read at 450nm within 5 min of the reaction being stopped. The mean values of the triplicates were then calculated.

2.13 Calcium Imaging and Measurements

2.13.1 Ca^{2+} Measurements of single WEHI 231 cells using Real Time Image Recording

WEHI 231 cells (1 x 10^6) in 0.5 ml of S-MEM medium lacking Ca^{2+} were placed in a 2 ml glass vial. The vial was then covered with aluminium foil and 5 μM Fluo 3 (Molecular Probes) added and incubated for 30 min. Cells were observed using a microscope (Nikon) with an oil immersion lens and a wide field digital imaging system. The cells were illuminated at 488 nm and the emitted light from Fluo 3 (535 nm) was transferred to a CCD camera operating in virtual chip mode. Full frame images (160 x 160 pixels), with a pixel size of 532 nm at the cell, were acquired at 100 frames $^{-1}$. A puffer pipette was placed adjacent to the cell using a Micromanipulator (Burleigh) and a Picospritzer (General Valve Corporation) used to apply anti-IgM (10 μg/ml) directly to the cell to stimulate a Ca^{2+} signal. Data was recorded on a PC and synchronised with the timing of anti-IgM application using Clampex 8.0 software and an analogue output from a CCD camera reporting its readout status (294). The real time recordings were analysed using Metamorph Imaging software (Figure 2.4).

2.13.2 Measurement of Cytosolic Calcium in WEHI 231 populations

Cytosolic calcium was measured in cell populations at 37 °C using a Cairn Research Spectrophotometer as described previously (295). Cells were loaded with Fura2 (Molecular Probes) in Ca^{2+} free HBS. After dilution and centrifugation to remove excess dye, the cells were resuspended in a small volume of HBS containing 1 mM Ca^{2+} to give a final density of 10^6 cells/100 μl. From this, cells were added to stirred cuvettes containing 1.4 ml of nominally Ca^{2+} -free HBS (at 37 °C) in a Cairn Spectrophotometer system (Cairn Research Ltd.). Excitation wavelengths of 340, 360, and 380 nm were provided by a filter wheel rotating at 35 Hz in the light path. Emitted light was filtered by a 485-nm-long pass filter, and samples were averaged to give a data point every 500 ms. The background-corrected 340/380 ratio was calibrated using the method of Grynkiewicz *et* al (296). Following each experiment, cells were lysed by the addition of 50 μM digitonin in the presence of external 2 mM Ca^{2+} to give an *R*max value. *R*min was subsequently determined by the addition of 20 mM EGTA (pH 7.4) in the presence

of an equimolar concentration of Tris base. Thapsigargin, a cell-permeable tumor promoter that promotes the discharge of Ca^{2+} from intracellular stores by specifically inhibiting endoplasmic reticulum (E.R) Ca^{2+} ATPase, was also added to cell samples to determine whether cell types have equivalent amounts of E.R stored Ca^{2+}.

2.14 Suppliers addresses

Active Motif
104 Avenue Franklin Roosevelt
Box 25
B-1330 Rixensart
Belgium

Alexis Biochemicals
c/o AXXORA (UK) Ltd.
P.O. Box 6757 Bingham
Nottingham NG13 8LS

Amersham Pharmacia Biotech
Amersham Place
Little Chalfont
Buckinghamshire HP7 9NA

BD Biosciences
21 Between Towns Road
Cowley
Oxford OX4 3LY

Burleigh
C/o EXFO Europe s.a.r.l.
Le Dynasteur 10-12, rue Andras Beck
92366 Meudon La Forêt Cedex
FRANCE

Calbiochem
c/o CN Biosciences
Boulevard Industrial Park
Padge Road
Beeston
Nottingham NG9 2JR

Cell Signalling Technology
New England Biolabs (UK) Ltd
73 Knowl Piece, Wilbury Way
Hitchin
Hertfordshire SG4 0TY

CHEMICON Europe, Ltd.
The Science Centre
Eagle Close
Chandlers Ford
Hampshire SO53 4NF

Harlan UK Ltd
Shaw's Farm, Blackthorne
Bicester
Oxon OX25 1TP

Invitrogen Life Technologies
3 Fountain Drive
Inchinnan Business Park
Paisley

Jackson Immunoresearch Laboratories
c/o Stratech Scientific
61-63 Dudley Street
Luton
Bedfordshire LU2 0NP

Kodak Ltd
Kodak House
Station Road
Hemel Hempstead
Hertfordshire HP1 1JU

Miltenyi Biotec
Almac House
Church Lane
Bisley
Surrey GU24 9DR

Molecular Devices Ltd
135 Wharfedale Road
Winnersh Triangle
Winnersh, Wokingham
RG41 5RB

Molecular Probes
c/o Cambridge Bioscience
24-25 Signet Court
Newmarket Road
Cambridge CB5 8LA

Nikon UK Limited
Nikon House
380 Richmond Road
Kingston upon Thames
Surrey KT2 5PR

Pierce
C/o Perbio Science UK Ltd.
Unit 9, Atley Way
North Nelson Industrial Estate
Cramlington, Northumberland
NE231WA

Promega
Delta House
Chilworth Science Park
Southampton SO16 7NS

Sigma-Aldrich Company Ltd
Fancy Road
Poole
Dorset BH12 4QH

Vector Laboratories Ltd
3 Accent Park
Bakewell Road
Orton Southgate
Peterborough PE2 6XS

Table 2.1 Antibodies

Specificity of Antibody	Host	Use	Manufacturer
A1	Goat	Western Blot	Santa Cruz
AKT	Rabbit	FACE	Active Motif
Bad	Rabbit	FACE	Active Motif
Bad C20	Goat	Western Blot	Santa Cruz
Bad pSer112	Rabbit	IP and western Blot	New England Biolabs
Bad pSer136	Rabbit	IP and western Blot	New England Biolabs
Bak	Mouse	IP and western Blot	Pharmigen
Bcl-2	Mouse	Western Blot	Pharmigen
BclX	Rabbit	IP and western Blot	Transduction Laboratories
$BclX_L$	Rabbit	IP and western Blot	Santa Cruz
Bid D19	Goat	Western Blot	Santa Cruz
Bim/ BOD	Rabbit	Western Blot	Bioquote Ltd
CD40	FGK 45 Hybridoma	Stimulation	In house
CD43 on magnetic beads	Rat	Purification	Miltenyi Biotech
Cytochrome C	Rabbit	ELISA	Active Motif
Fas	Mouse	Stimulation	Transduction Laboratories
FcγRIIb	24G.2 Hybridoma	Stimulation	In house
Goat IgG HRP	Various	Western Blot	Jackson Immunoresearch

			Labs
Intact Rabbit anti mouse IgM	Rabbit	Stimulation	Jackson Immunoresearch Labs
JNK	Rabbit	FACE	Active Motif
Mcl-1	Mouse	IP and western Blot	Transduction Laboratories
Mouse IgM (μ chain) $F(Ab)_2$'	Goat	Stimulation	Jackson Immunoresearch Labs
NF-KB subunits	Rabbit	TransAM assay	Active Motif
P44/42 ERKMAPK	Rabbit	Western Blot FACE	Cell signalling Technology
p38	Rabbit	FACE	Active Motif
p53	Rabbit	TransAM assay	Active Motif
Phospho Akt	Rabbit	FACE	Active Motif
Phospho Bad	Rabbit	FACE	Active Motif
Phospho JNK	Rabbit	FACE	Active Motif
Phospho p38	Rabbit	FACE	Active Motif
Phospho p44/42 ErkMAPK	Rabbit	Western Blot FACE	Cell signalling Technology
Rabbit IgG HRP	Various	Western Blot	Cell Signalling Technology

A Constructs used in retroviral transfection of WEHI-231 cells

	Activity	**Mutation/ Coding Sequence**
SHIP-CI	phosphatase inactive	$D^{675}A$
SHIP-SH2	prevents SHIP-pITIM association	residues 1-114
Dok-PH/PTB	lacks pro/tyr-rich region	residues 1-258

B Constructs used in transfection by electroporation of WEHI-231 cells

	Activity	**Mutation/ Coding Sequence**
PKC αKR	kinase inactive	residues 2-672 ($K^{368}R$)
PKC αCAT	constitutively active	residues 326-674
PKC δKR	kinase inactive	residues 2-674 ($K^{376}R$)
PKC δCAT	constitutively active	residues 334-674
PKC εKR	kinase inactive	residues 2-732 ($K^{437}R$)
PKC εCAT	constitutively active	residues 395-737
PKC ξKR	kinase inactive	residues 2-592 ($K^{281}M$)
PKC ξCAT	constitutively active	residues 239-592
$RasV^{12}$	constitutively active, interacts with all Ras effectors	V^{12}
$RasV^{12}S^{35}$	constitutively active, only interacts with Raf-1	$V^{12}S^{35}$
$RasV^{12}C^{40}$	constitutively active, only interacts with PI-3-K	$V^{12}C^{40}$
ΔMEKK3	constitutively active	residues 340-626

Figure 2.1: FACS histogram of DNA content analysis

Histogram markers determine the percentage of cells in each stage of the cell cycle. The G1 peak (2N DNA) is set around 300 fluorescence units on the FL-3 x-axis, here around 340, and the G2/M peak (4N DNA) calculated accordingly (680). Cells exhibiting subdiploid DNA content (representing apoptotic cells) are marked as those below the 2N peak, whilst cells in S phase are determined as those between the 2N and 4N peaks.

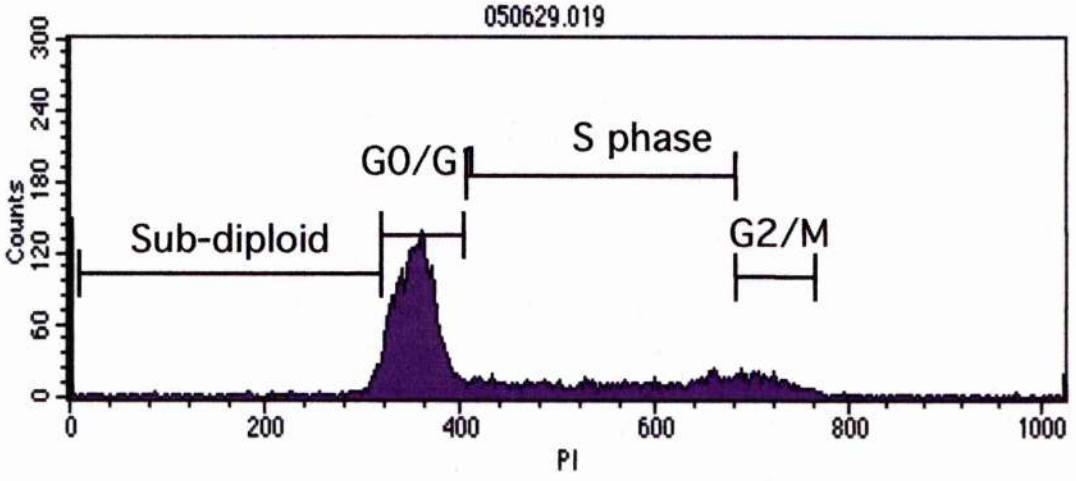

Histogram Statistics

File: 050629.019
Sample ID: WEHI 231 BclXL 48hrs PI
Acquisition Date: 29-Jun-05
X Parameter: FL3-H PI (Linear)

Log Data Units: Linear Values
Patient ID: No Inhibs No Stim
Total Events: 10000

Marker	Left, Right	Events	% Gated	% Total	Mean	CV
All	0, 1023	10000	100.00	100.00	422.36	39.57
G0/G1	321, 406	5845	58.45	58.45	356.00	5.17
S phase	409, 686	2357	23.57	23.57	556.67	15.56
G2/M	686, 769	815	8.15	8.15	716.46	2.92
Sub-diploid	10, 321	475	4.75	4.75	260.00	33.25

Figure 2.2: Analysis of the mitochondrial membrane potential of cells using $DiOC_6$ stain

Histograms show cells stained with the cationic lipophilic dye $DiOC_6$ (2.5 μM) for analysis of mitochondrial membrane potential. Histogram markers determine the proportion of cells with low or high $DiOC_6$ fluorescence on the FL-1 x-axis. Cells with low $DiOC_6$ fluorescence are adjudged to represent the population that are committed to apoptosis, having dissipated their mitochondrial membrane potential (MMP). The untreated cells show the majority of cells with a high, healthy MMP, whereas coligation of both the BCR and FcγRIIb induces apoptosis in mature B cells, therefore the histogram displays a far greater proportion of cells with low mitochondrial membrane potential.

Unstimulated

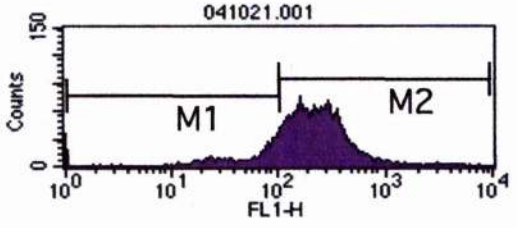

File: 041021.001
Sample ID: No Inhib No Stim
Patient ID: DiOC6 48 hrs Mature b cells
Gate: No Gate
Gated Events: 10000
X Parameter: FL1-H (Log)

Marker	Left, Right	Events	% Gated	Mean	SD
All	1, 9910	10000	100.00	244.05	272.42
M1	1, 102	1598	15.98	65.65	28.02
M2	102, 9390	8401	84.01	278.43	284.23

BCR and FcγRIIb

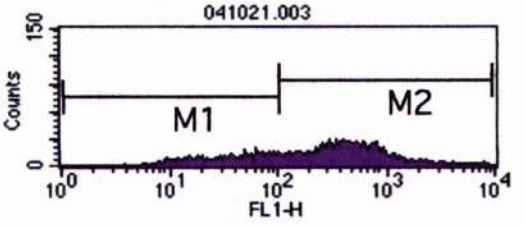

File: 041021.003
Sample ID: No Inhib F(Ab)2' & i
Patient ID: DiOC6 48 hrs Mature b cells
Gate: No Gate
Gated Events: 5640
X Parameter: FL1-H (Log)

Marker	Left, Right	Events	% Gated	Mean	SD
All	1, 9910	5640	100.00	425.16	623.59
M1	1, 102	1633	28.95	45.03	27.23
M2	102, 9390	4016	71.21	579.01	680.90

Figure 2.3: Flow diagram to show how cytoslic, mitochondrial and nuclear fractions were generated from mature B cells

Mature B cells (5×10^7 cells/sample) were homogenised and then transferred to a fresh tube. Samples were then centrifuged at 400 g for 20 min, the supernatant transferred to a fresh tube and the centrifuged pellet discarded. The supernatant contained the cells that had been broken following homogenisation whereas the pellet contained intact cells. This supernatant was centrifuged again at 800 g for 10 min and the resulting supernatant transferred to a fresh tube. The pellet, which contained intact nuclei, was treated with 100 µl of complete mitochondrial lysis buffer on ice for 15 min to produce the nuclear fraction. By contrast the supernatant, which contained the cytosol and mitochondria, was centrifuged again at 10,000 g for 20 min. The resulting supernatant was transferred to a fresh tube, this being the cytosolic fraction. The pellet, which contained the mitochondria, was treated with 100 µl of complete mitochondrial lysis buffer on ice for 15 min to produce the mitochondrial fraction.

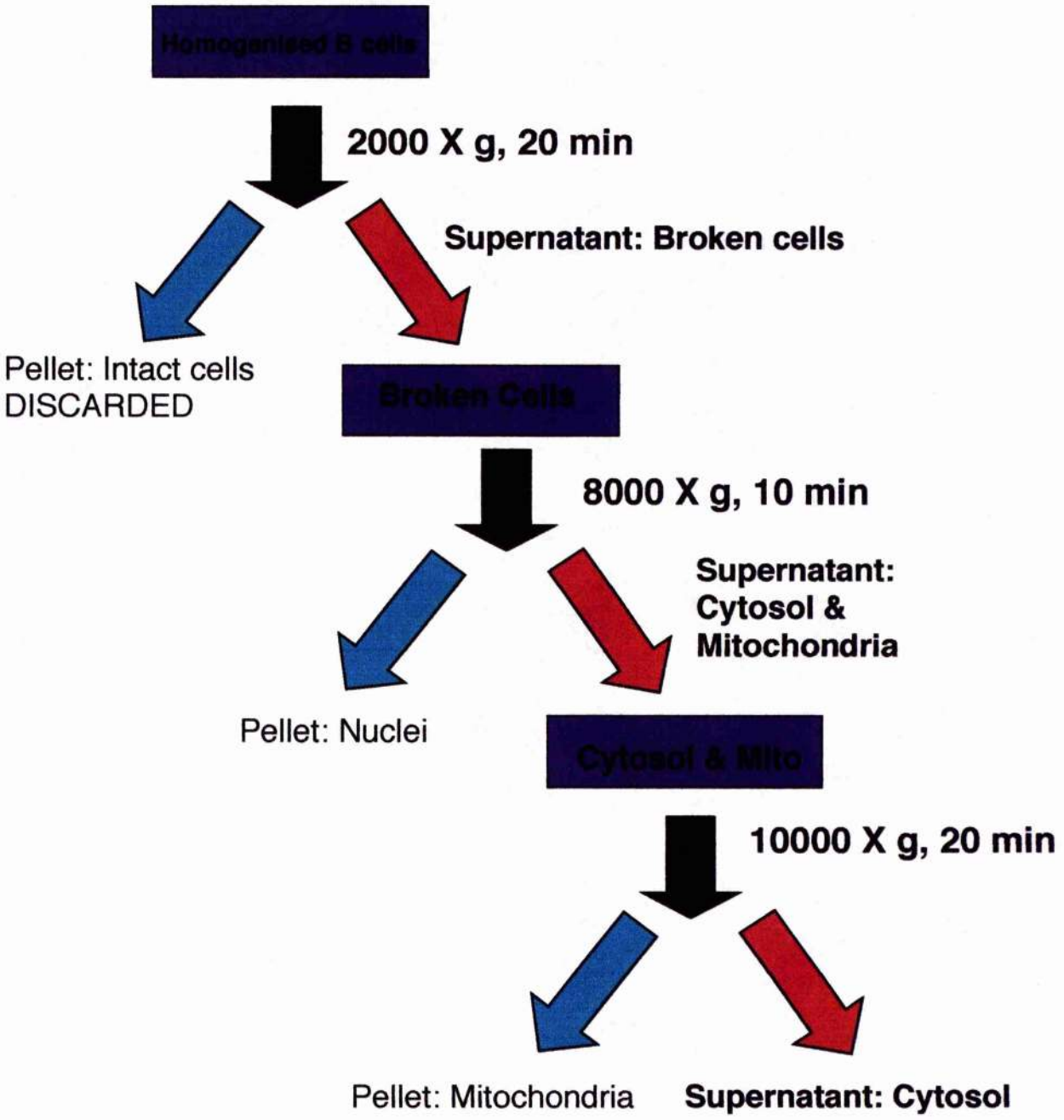
Homogenised B cells
2000 X g, 20 min
Supernatant: Broken cells
Pellet: Intact cells
DISCARDED
Broken Cells
8000 X g, 10 min
Supernatant:
Cytosol &
Mitochondria
Pellet: Nuclei
Cytosol & Mito
10000 X g, 20 min
Pellet: Mitochondria
Supernatant: Cytosol

Figure 2.4: Measurement of Ca^{2+} levels in WEHI 231 cells

(A) Bright field image to show multiple WEHI 231 cells within the field of vision of the microscope.

(B) We then used metamorph software colour the image according to the relative Ca^{2+} levels. Furthermore, we could identify three separate regions of interest (ROI) within the cells where Ca^{2+} levels could be individually monitored. The 3 distinct ROI were decided arbitrarily by 3 equidistant measurements across the cell. A puffer pipette was used to apply 10 μg/ml of anti-IgM directly onto the cell and a recording of 25 seconds was made.

A

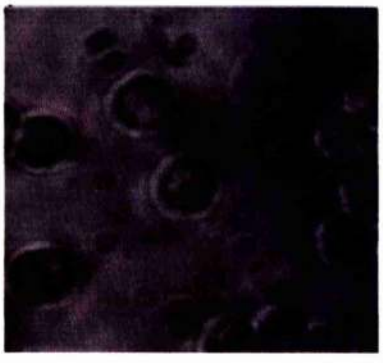

B

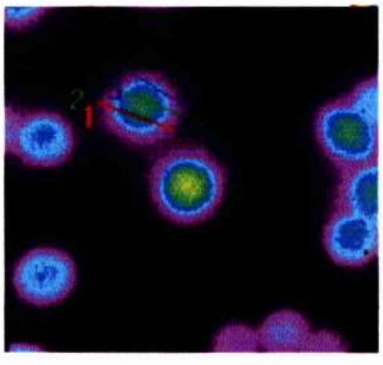

Chapter 3: Dissection of the signailing mechanisms involved in BCR induced growth arrest and apoptosis and CD40 mediated rescue in the immature B cell line WEHI 231

3.1 Introduction

3.1.1 WEHI 231: a model for immature B cells

WEHI 231 is a murine B cell lymphoma cell line that has been used extensively as a model for the induction of tolerance following ligation of the BCR at the immature B cell stage. This cell line has the phenotype of immature B cells and expresses sIgM, CD5, and FcR gamma, but lacks the B cell-specific isoform of CD45 (B220), Fas and sIgD. Crosslinking of the BCR with anti-Ig results in growth arrest and apoptosis which models anergy and clonal deletion of immature B cells following ligation of the BCR with self-Ag during clonal selection (17, 297). In addition LPS, which drives immature B cells to a more mature phenotype, can overcome this BCR mediated growth arrest in WEHI 231 cells (298-301). Furthermore, co-engagement of CD40 also results in both survival and proliferation and has hence been used as a model for T cell derived help which rescues immature B cells from apoptosis (276, 302, 303). Unlike mature B cells, immature B lymphocytes usually undergo anergy and/or apoptosis rather than proliferation upon triggering of the BCR (304, 305). This response is the foundation of negative selection, a process that ensures the generation of a self tolerant repertoire during lymphocyte development (306).

3.1.2 ERKMAP kinase acts as an essential regulator of both proliferation and apoptosis in the WEHI 231 cell line

Previous work in this laboratory has investigated the role of ERKMAP kinase in both BCR-mediated apoptosis and CD40-mediated rescue in WEHI 231 cells. Ligation of the BCR couples to an early ERKMAP kinase signal (less than 2 hours post stimulation) which activates a PLA_2 apoptotic pathway (275). This results in an upregulation of PLA_2 expression and translocation to the mitochondrial membrane (156) and the consequent generation of arachidonic acid by PLA_2 correlates with the dissipation of the MMP and loss of ATP (156). All the classical hallmarks of apoptosis are seen such as mitochondrial

dysfunction, Annexin V staining, induction of a subdiploid population and DNA fragmentation (156). However there is no evidence of activation of the canonical effector caspase cascade although there was activation of the executioner protease, cathepsin B (156) (Figure 3.1).

The ability of CD40 to rescue both immature B lymphocytes from BCR-mediated apoptosis and prevent the spontaneous death of mature B cells is well documented (23, 276). Indeed, loss of MMP, depletion of ATP and apoptosis can be prevented by rescue signals via CD40 (156). However, the signalling mechanisms utilised by CD40 to achieve these outcomes are only just coming to light, particularly the downstream events. The initial signalling mechanisms, however, have been partially elucidated in recent years. For example, it has been shown that CD40 ligation results in the activation of the ERK, JNK, and p38 MAP kinases. However the precise complement of signals depends on the maturation stage of the cell, making dissection of the signalling mechanisms downstream of CD40 complicated (307, 308).

The CD40 receptor is a 48-kDa transmembrane glycoprotein (309) (Figure 3.2) comprising of a 193 amino-acid extracellular domain, a 22 amino-acid transmembrane domain and a 62 amino-acid cytoplasmic domain. The extracellular domain consists of four homologous, repeating, cysteine-rich extracellular domains characteristic of TNFR family motifs (310). It has been shown that murine CD40 shares approximately 60% homology to human CD40, with the greatest homology (78%) to the human form in the cytoplasmic domain (311). This cytoplasmic domain contains no sequence of known protein tyrosine kinase activity. Indeed, the cytoplasmic tail of human CD40 contains no tyrosine residues, whilst only one exists in the murine form. Nevertheless, the cytoplasmic domain of CD40 is constitutively phosphorylated and threonine 234 has been shown to be crucial for signal transduction (311). Like both the p55 and p70 isoforms of the TNF receptor, CD40 has no intracellular kinase domain and no consensus sequence for binding kinases (309). However, CD40 ligation is known to rapidly activate the protein tyrosine kinases Lyn and Syk (312), whilst also inducing the tyrosine phosphorylation of PI-3 kinase and PLCγ2 (313) and activating serine/threonine kinases (314). However, like all signalling mechanisms, it is important to be careful when comparing data from different

cell types. Consequently, studies highlight quite distinct differences in proximal CD40 signalling events in B cells depending on whether the cells used were resting, activated or EBV-transformed (312). In addition, some studies suggest that instead of phosphorylating and activating a number of protein tyrosine kinases, CD40 engagement dephosphorylates the Src family PTKs or Syk (25). CD40 is expressed on B cells and can modulate BCR signalling (309, 315).

CD40 acts to block BCR stimulated apoptosis in both normal B cells and the WEHI 231 cell line (316-318). CD40 ligand (CD40L) is expressed on activated T cells and therefore Ag stimulated B cells require interaction with T helper cells for survival and activation. Self reactive B cells are suggested to be unable to achieve this requirement and so undergo apoptosis, resulting in the maintenance of self tolerance (316, 319). Nevertheless, we have previously shown that engagement of CD40 results in desensitization of the early ERK signal in WEHI 231 cells resulting in the uncoupling of the BCR from PLA_2 mediated apoptosis (156, 320). CD40 has also been demonstrated to induce the anti-apoptotic Bcl-2 family members A1 and $BclX_L$ (277, 321, 322), which correlate with maintenance of the mitochondrial membrane integrity and survival. Furthermore, both proliferating and anti-CD40 treated WEHI 231 cells exhibit a sustained and cycling pattern of ERK activation which correlates with cell cycle progression, growth and proliferation (320) suggesting that CD40 mediates rescue from BCR-induced growth arrest by restoring the sustained ERK activation.

3.1.3 Ras acts to modulate both the ERKMAP kinase and PI-3 kinase pathways

Ras proteins provide critical regulatory crossroads in cellular signalling pathways. The *ras* genes code for 4 different 21 KDa proteins: H-Ras, N-Ras, K-Ras4A and K-Ras4B. These proteins function as GDP/GTP regulatory switches for cellular proliferation. Ras possesses an intrinsic GTPase activity however this is too low to account for the rapid, transient GDP/GTP cycling which is seen. A complete model for Ras activation/ deactivation includes 2 other families of proteins: Guanine nucleotide exchange factors (GEFs) e.g.

SOS that acts to activate Ras and GTPase activating proteins (GAPs) e.g. p120 GAP that acts to deactivate Ras (Figure 3.3) (reviewed in (323)).

The best characterised Ras effector is Raf which is a serine/ threonine kinase (324). Ras/ Raf association leads to translocation of Raf to the plasma membrane that results in the activation of its kinase function. The phosphorylation of Raf leads to activation of MEKK1/2 and hence the ERKMAP kinase cascade. In addition, Ras can act to stimulate PI-3 kinase activity as the p110 subunit of PI-3 kinase (through amino acids 133 to 314) interacts with RasGTP (325). Ras acts to regulate cell growth in all eukaryotic cells through modulation of these 2 pathways. Thus, when serum-starved NIH-3T3 (fibroblast) cells that are arrested in G0/G1 are exposed to serum, they undergo a period of intense signalling lasting 30-60 minutes, and this starts to decline as receptors are internalised and degraded. Serum or growth factors are then required for a further 8-10 hours if the cells are to enter the cell cycle (326, 327). In cells continuously exposed to such growth factors Ras signalling is required in at least two phases of the G0 to S phase transition (328-330). This biphasic pattern of Ras activation appears to elicit different efffector molecules (Figure 3.4). Thus, ERK is activated in the early stages of Ras activation, but its activity is not detected at later stages of G1 progression, even though Ras is still active. By contrast, PI-3 kinase is active during the G0/G1 transition and in mid to late G1 phase and is associated with phosphorylation of AKT and the induction of cyclin D1 expression (331).

Whilst an early strong burst of ERK activation is associated with apoptosis, the sustained, yet cycling, activation of ERK appears to be essential for proliferation in WEHI 231 cells. By contrast, short-term inhibition of PI-3 kinase activity in WEHI 231 cells had no effect on spontaneous proliferation, anti-Ig induced growth arrest or apoptosis or CD40-mediated rescue. However, prolonged inhibition (up to 30 hours) of PI-3 kinase results in growth inhibition of unstimulated cells, suggesting that PI-3 kinase activity may be important for the basal proliferation of WEHI 231 cells. Prolonged inhibition also abrogated CD40-mediated rescue of anti-Ig induced growth arrest, but this may be due to the fact that PI-3 kinase inhibition blocks basal proliferation of these cells (320).

In order to dissect the role of Ras signalling via the ERKMAP kinase and PI-3 kinase pathways several constitutively active Ras mutants have been generated. RasV12 is a constitutively active form of Ras, the consequence of a point mutation that results in the substitution of valine for glycine at position 12. This mutation disables the intrinsic GTPase activity of Ras, therefore once Ras binds GTP and becomes active it is unable to deactivate itself by hydrolysing GTP to GDP. RasV12 S35 contains a further point mutation in the effector domain of the protein, resulting in the substitution of serine for threonine. This mutation prevents Ras from binding the p110α subunit of PI-3 kinase, an interaction that is known to lead to the activation of PI-3 kinase (325, 332, 333). By contrast, RasV12 C40 contains a point mutation in the effector domain resulting in the substitution of cysteine for tyrosine. This mutation abrogates the interaction between Ras and Raf, preventing Ras from activating the ERKMAP kinase pathway. Figure 3.5 summarises the action of these Ras mutants.

3.1.4 Dok

The Dok proteins are a family of adaptor proteins that are phosphoryiated by a wide range of protein tyrosine kinases. The first Dok protein to be isolated was p62 Dok, originally identified as a 62 kDa tyrosine-phosphorylated protein associated with the negative regulator of Ras, Ras-GAP (334-336). p62 Dok is rapidly tyrosine phosphorylated in response to a wide range of stimuli, including ligation of the BCR (337) and FcγRIIb1 ligation (338), and once phosphorylated interacts with a number of signalling molecules including Ras-GAP (334, 335), Nck (339), and Csk (338) via their SH2 domains. In addition to SH2 domain-binding sites, p62 Dok also contains a pleckstrin homology (PH) domain, a phosphotyrosine binding (PTB) domain, and potential SH3 domain-binding sites.

Initially, p62 Dok was suspected of playing a positive role in mitogenic signalling as it was first identified as a substrate for the p210 bcr/Abl oncoprotein (334), as well as a target of v-Abl in v-Abl transformed B cells (335). However, evidence has accumulated to suggest that p62 Dok actually plays a negative role in ERKMAPkinase activation and proliferation. For example, cells from mice deficient in p62 Dok demonstrate increased proliferation in response to growth factors, and these cells exhibit prolonged Ras and ERKMAPkinase activation in

response to growth factors (340). Moreover, inactivation of p62 Dok also enhances the transforming ability of p210 bcr/Abl, accelerating the onset of the chronic myelogenous leukaemia (CML)-like disease triggered by expression of the chimeric protein (340). Reintroduction of p62 Dok into mouse embryo fibroblast (MEF) cells from p62 Dok deficient mice results in a return to a normal level of proliferation in response to PDGF, rather than the enhanced proliferative response normally seen in p62 Dok deficient MEFs (341). Indeed, p62 Dok has been shown to negatively regulate ERKMAP kinase activation and cell proliferation mediated by the BCR, by abrogating Ras activation (342).

In addition, p62 Dok and is phosphorylated in response to BCR and FcγRIIb coligation, enhancing its binding of Ras-GAP and implicating p62 Dok as a key mediator of FcγRIIb inhibition of BCR-mediated Ras activation (269). The phosphorylation of p62 Dok, and subsequent association with Ras-GAP, is dependent on phosphorylation of the ITIM of FcγRIIb, and the concomitant recruitment of SHIP to the ITIM, as p62 Dok does not interact directly with the ITIM but rather has been shown to interact with FcγRIIb via SHIP (269). This brings p62 Dok into close proximity with tyrosine kinases and the C-terminal region of p62 Dok becomes phosphorylated. Phosphorylation of p62 Dok increases its association with RasGAP and p62 Dok can then regulate the activity of RasGAP. RasGAP enhances the intrinsic GTPase activity of Ras leading to the inhibition of Ras and the downstream effectors of Ras including ERK and PI-3 kinase (269) (Figure 3.6).

3.1.5 SHIP

SHIP is a highly conserved cytosolic phosphatase that can be activated downstream of FcγRIIb in mature B lymphocytes where it functions as a negative regulator of BCR signalling (343, 344). More recently SHIP has also been shown to be an important mediator of negative signalling via FcγRIIb on B cells (345). SHIP can remove the 5' phosphate from PIP_3 resulting in the depletion of lipids that serve as anchors for PH domain-containing proteins. SHIP therefore antagonises the function of PI-3 kinase and can suppress the activation of AKT (282, 346) (Figure 3.6).

SHIP is also a regulator of the ERKMAP kinase pathway. For example, SHIP binds to Shc using the same phospho-tyrosine residues as are required for the formation of the Grb2-Shc complexes and hence prevents the recruitment and activation of SOS and the classical MAP kinase cascade (346) (Figure 3.6). However, this mechanism is controversial as more recent reports have also suggested that tyrosine phosphorylation of Shc downstream of the BCR is SHIP-dependent and the formation of SHIP-Shc-Grb-2 complexes are necessary for mitogenic BCR signalling (347). Nevertheless, SHIP can negatively influence the ERKMAPK cascade as tyrosine phosphorylated SHIP can bind to the adaptor protein p62 Dok via the phospho-tyrosine-binding domain of p62 Dok as has been discussed previously.

3.1.6 The Protein Kinase C (PKC) family

3.1.6.1 The Importance of the PKC family in B lymphocyte development and function

PKC α, β, δ, ε, ζ, η and θ isoforms are all expressed in mature B lymphocytes (348, 349) and PKCs are proposed to mediate many cellular responses as diverse as proliferation and apoptosis in B lymphocytes. BCR ligation leads to an increase in PKC activity (350, 351) resulting from activation of Btk/ Tec, Syk and Src-family PTKs, molecules which activate PLC to generate both DAG and cytoplasmic Ca^{2+} second messengers that can act to activate certain members of the PKC family. In B lymphocytes PKCs have been implicated in NF κB, AP1, ERKMAPkinase, JNK, p38 and $p70^{s6}$ activation (352-356). In addition, PKCs have been reported to mediate chemokine driven B cell migration (357), induce proteins that protect from Fas-dependent apoptosis (358) and regulate integrin-mediated adhesion (359). Recent knock out studies, which will be discussed below highlight non-redundant roles for PKC isoforms in B lymphocytes. Previous studies within our laboratory have shown that both BCR and CD40 signalling in immature B cells can regulate the expression of multiple PKC isoforms. In particular, PKC α, PKC δ, PKC ε and PKC ζ were identified as potential regulators of CD40-dependent rescue from BCR-induced growth arrest (Harnett, unpublished).

3.1.6.2 PKC α

PKC α was the first member of the PKC family to be identified and cloned, being isolated from a brain cDNA library over 15 years ago (360). It has since been found to have a wide tissue distribution, and as such has been implicated in the control of a number of major cellular functions, including proliferation, differentiation, apoptosis and cellular mobility. Indeed, in some cell types, overexpression of PKC α is sufficient to induce proliferation, and it has recently been shown that expression of constitutively active PKC α in NIH-3T3 cells results in increased expression of cyclins D1 and E which are required for cell cycle progression, and increased proliferation rates (361). As well as promoting proliferation, accumulating evidence suggests a role for PKC α in the inhibition of apoptosis. Thus, reducing the level of PKC α results in apoptosis in a number of cell types, including U937 cells (362) and glioma cells (363). Moreover, PKC α has also been shown to phosphorylate the survival promoting protein Bcl-2 on a site that enhances the anti-apoptotic properties of Bcl-2 (364, 365). Furthermore, the induction of apoptosis by ceramide appears to involve the inhibition of PKC α (366).

However there is very little known about the role of PKC α in B lymphocyte functional responses. Nevertheless, it has been demonstrated that selective inhibitors of classical PKCs (α, β and γ) induce both growth arrest and apoptosis in a dose dependent manner in the human cell line Ramos-BL (367). This cell line has the surface phenotype of germinal centre B cells and responds to ligation of the BCR with cell death in a similar fashion to WEHI 231 cells. Reduction in levels of PKC α in Ramos-BL cells using antisense DNA, produced levels of cell death similar to that induced by ligation of the BCR (367). Moreover, prolonged treatment with anti-IgM results in a reduction in expression levels of PKC α (367). This suggests that PKC α is essential for B cell survival and expression of PKC α is reduced by ligation of the BCR in these cells.

3.1.6.3 PKC β

PKC β has been implicated as an important mediator of mature B cell activation since PKC $\beta^{-/-}$ mice have reduced humoral immune responses and their B

lymphocytes display impaired activation downstream of the BCR (368). More specifically, mature B lymphocytes from PKCβ$^{-/-}$ mice are less able to activate $BclX_L$ and Bcl-2 and hence are prone to apoptosis (54, 368). Indeed, treatment of primary splenic immature B cells or WEHI 231 cells with phorbol ester can prevent BCR-driven apoptosis suggesting the diminished BCR-coupled activation of cPKC and nPKC isoforms in immature B cells contributes to their cell death (369, 370). Consistent with this, activation of PKC further promotes survival of mature B cells by inducing NF-κB since NF-κB can regulate the transcription of c-Myc, and the anti-apoptotic Bcl-2 family members $BclX_L$ and Bcl-2 (54, 352, 371). Thus, the inability of BCR signalling in immature B cells to sustain NF-κB activation may due to the defective stimulation of PKC in these cells. Such ablation of NF-κB signalling is likely to contribute to cell death since NF-κB signalling is enhanced under conditions that favour cell survival, including CD40 co-stimulation (372, 373).

3.1.6.4. PKC δ

PKC δ has also been demonstrated to be a direct target of BCR signalling (374, 375). PKC δ has the unusual property of being tyrosine phosphorylated after BCR engagement and in the WEHI 231 immature cell line it is tyrosine phosphorylated very rapidly after ligation of the BCR (375). Furthermore, there is translocation of PKC from soluble to membrane fractions after treatment with anti-IgM (375), a process which brings PKC δ into direct contact both with its substrates and its activators. Indeed, it has been shown that in order for PKC δ to be properly activated both membrane translocation and phosphorylation events must occur (375). PKC δ is phosphorylated on Tyr^{52} and Tyr^{187} in the amino terminal of the protein (376, 377) and it has been postulated that the tyrosine kinase responsible for this may be Lyn or Btk. The role of this tyrosine phosphorylation is still under some debate but some groups report that it can reduce phorbol ester dependent catalytic activity whilst others show that activity can be increased in some cell types (376, 378-380). This phosphorylation event is thought to alter substrate specificity and may act to create a binding domain for SH2 containing proteins.

PKC δ has been reputed to have diverse roles depending of the cell type and maturation stage used. For example in fibroblasts, PKC δ activates the Raf1/

MEK/ ERK pathway which leads to the activation of the AP1 transcription factor that is normally associated with proliferation (381). However, in other cell types PKC δ activation can suppress proliferation and in fact in human U937 cells, caspases cleave PKC δ creating a constitutively active form of PKC δ which is associated with the induction of apoptosis (382). This, combined with other data, has lead to the hypothesis that cleaved PKC δ products can induce apoptosis (reviewed in (383)). However, in murine splenic B lymphocytes induction of apoptosis by various agents has been shown to induce translocation of either full length PKC δ (PKC δFL) or the caspase 3 mediated cleavage product (PKC δ-CF) to the nucleus (384). In addition, caspase inhibitors could not prevent nuclear translocation and there were no significant differences in the resulting induction of pro/ anti- apoptotic molecules suggesting caspases are not essential for PKC δ induced apoptosis. Potentially PKC δ may modulate a novel apoptotic cell signalling mechanism in B lymphocytes which may involve the phosphorylation of histone H2B at serine 14 by PKC δ (384).

PKC $\delta^{-/-}$ knock out mice were created simultaneously by two separate laboratories (385, 386). The gross phenotypes of the PKC $\delta^{-/-}$ mice were reported to be the same by both groups. Thus, these mice had both splenomegaly and lymphadenopathy with a massive increase in peripheral B lymphocytes, reflecting both increased numbers of naïve and activated follicular mature B cells and increased numbers of germinal centres as a result of increased proliferation. However, PKC $\delta^{-/-}$ knock out mice were viable up to 12 months with no pre-disposition to cancer. By contrast, mice developed severe lupus like autoimmune disease, produced auto-Abs to their own DNA and died from glomerulonephritis. This points to PKC δ having an important role in maintenance of B cell tolerance to self-Ag.

Consistent with this, Mecklenbrauker et al found that mature B cells produced abnormal responses to anti-IgM and hence suggested that loss of PKC δ results in a defect in the induction of anergy (385). However, Miyamoto et al found both an increase in response to mitogenic stimuli including LPS and anti-CD40 and an increase in the expression of IL6, which stimulates B cell maturation and

proliferation. Miyamoto et al therefore suggested that loss of PKC δ results in increased and unchecked proliferation in B cells (386).

3.1.6.5. PKC ε

PKC ε is generally considered to be a positive regulator of cell survival and proliferation. For example, PKC ε has been shown to activate the Raf-1/ERK pathway (387), thus promoting the activation of the two key survival factors NF κB and AKT (388). Indeed, expression of a catalytically inactive form of PKC ε has been shown to inhibit the activation of AKT by insulin (389).

Indeed, PKC ε also can be activated in response to a variety of mitogens (390, 391) and in certain cell types, overexpression of PKC ε results in transformation as a consequence of PKCε inducing the phosphorylation of Raf1 and resulting in sustained activation of the ERKMAPK signalling pathway (392-394). More recently, it has also been shown that expression of a constitutively active form of PKC ε in NIH3T3 cells activates the cyclin D1 promoter resulting in entry into the proliferative phases of the cell cycle (361). However in contrast to this, overexpression of PKC ε in NIH3T3 cells increases radiation-induced cell death, also as a result of increased ERK1/2 activation (395). Whilst such overexpression of a constitutively active PKC ε caused an even greater increase in radiation-induced cell death, overexpression of a dominant negative PKC ε returned cell death to control levels. Interestingly, strong early ERK signals are also associated with the apoptosis induced by BCR ligation in WEHI 231 cells (275).

The role of PKC ε in BCR signalling remains to be elucidated, however, as stated above in other cell types activation of PKCε has been strongly linked to cell survival and proliferation. PKCε activation inhibits both TNF- and TRAIL-induced apoptosis in the monocytic cell line U937 and fibroblast COS cells (388, 396), so it would seem likely that PKCε activation might contribute to survival signals. The CD40-induced survival signal is thought to involve, at least in part, NF-κB, and it has been shown that PKCε promotes the activation of NF-κB in fibroblasts (388). PKC ε is highly expressed in mature B lineage cells, and

ligation of the BCR in A20 murine B cells induces PKC ε translocation from the cytoplasm to cellular membranes. Additionally, this translocation coincides with PI-3 kinase-dependent phosphorylation of PKC ε which is required for maximal activation of PKC (397). Further support for the idea that PKC ε activation could be involved in B cell proliferation comes from the fact that PKC ε was found to be constitutively phosphorylated in a number of B lymphoma cell lines. However, such phosphorylation was only induced in mature splenic B cells by BCR ligation (397).

3.1.6.6. PKC ζ

PKC ζ also plays an important role in B lymphocytes. PKC $\zeta^{-/-}$ knock out mice have been produced with a generally well preserved splenic structure and normal percentages of B cell populations. However these mice have reduced absolute numbers of B cells due to severely increased spontaneous apoptosis. Additionally, PKC $\zeta^{-/-}$ transgenic mice display impaired segregation between B and T cell zones and a temporal delay in the development of secondary lymphoid organs such as the Peyer's patches (398). PKC $\zeta^{-/-}$ cells have impaired activation of the ERKMAPkinase pathway following ligation of the BCR even though JNK and p38 activation appears to be normal. There is also a severe inhibition of IκB transcription and decrease in both IL6 and $BclX_L$ transcription following BCR ligation in PKC $\zeta^{-/-}$ B lymphocytes (399). The fact that the PKC $\zeta^{-/-}$ mutation does not cause embryonic lethality may be due to compensation by the other atypical, and ubiquitously expressed, PKC λ.

In addition PKC ζ has also be implicated as playing an important role in the transduction of survival signals. Nerve Growth Factor (NGF) is a well characterised neurotropic protein that has been demonstrated to act as a survival factor for memory B cells and enhance mature B cell proliferation (400, 401). It has also been shown to share structural homology to CD40 (402, 403) and can inhibit IgM mediated apoptosis in the Ramos cell line in a PKCζ dependent manner (404). After induction of apoptosis PKCζ is translocated from the cytosol to the nucleus this is prevented by treatment with NGF (404). Taken

together this data implicates PKC ζ as an important regulator of rescue signals in B cells.

3.2 Aims and Objectives

Previous work in this laboratory has highlighted an essential role for sustained yet cyclic ERKMAP kinase signalling in WEHI 231 immature B cell survival, growth and proliferation (275). By contrast, ligation of the BCR, resulting in growth arrest and apoptosis, induces an early, strong peak in ERK activity and abrogation of the sustained phospho-ERK signal. Recent data has suggested that $BclX_L$ overexpression can overcome such BCR-mediated apoptosis. Investigation of signalling in $BclX_L$ overexpressing WEHI 231 cells reveals that that $BclX_L$ overexpression is not capable of rescuing the sustained cyclic ERK activation, suggesting that whilst $BclX_L$ is essential for survival, the ERK signal may be necessary for proliferation in WEHI 231 cells (405). Moreover, it suggests that CD40 signalling provides signals other than $BclX_L$ that rescue BCR- mediated growth arrest.

It was therefore the aim of this chapter to further characterise the role of the BCR-$cPLA_2$ pathway in regulating immature B cell fate. In particular it was planned to investigate the mechanism(s) underlying $BclX_L$- mediated rescue of cell survival and to identify the signals involved in CD40-mediated restoration of cell growth.

In particular it was planned to address:

- Whether the product of PLA_2 activation, arachidonic acid, or an eicosanoid metabolite, played a direct role in determining immature B cell fate
- Whether, by use of a $BclX_L$ expressing WEHI 231 mutant cell line, $BclX_L$ is sufficient for CD40-mediated rescue from BCR-mediated apoptosis and growth arrest or if additional signals are required
- Whether $BclX_L$ expression stabilises mitochondrial integrity by blocking PLA_2-mediated MMP dissipation
- Whether expressing constitutively active mutants of Ras in WEHI 231 cells blocked BCR-mediated growth arrest and apoptosis

- Which the potential upstream signals e.g. PI-3 kinase or PKC (by use of mutant WEHI 231 cells lines), lead to the ERK activation which is uncoupled in BCR stimulated cells and restored following signalling via CD40

3.3 Results

3. 3. 1 Crosslinking of the BCR on WEHI 231 cells leads to growth arrest and apoptosis

Unlike mature B cells, immature B lymphocytes usually undergo apoptosis, rather than proliferation, upon strong triggering of the BCR (304, 305). This response is the foundation of negative selection, a process that ensures the generation of a self tolerant repertoire during lymphocyte development (306). The murine WEHI 231 immature B lymphoma cell line has been widely used as an *in vitro* model system to study both negative signalling and BCR induced apoptosis (406, 407). Treatment of WEHI 231 cells with anti-IgM induces growth arrest followed by cell death by apoptosis which occurs in a mitochondrial-dependent but effector caspase-independent manner (156, 408).

Ligation of the BCR by anti-Ig leads to growth arrest as indicated by both a profound reduction in DNA synthesis (Figure 3.7 A) and a reduction in the number of cell divisions undertaken (Figure 3.7 B). Indeed, there was a complete cessation in proliferation in a large number of cells, as 24% of cells did not undergo cell division (Figure 3.7 B). By contrast, the mode number of cell divisions was 3 for unstimulated groups and 6 for CD40-rescued cells (Figure 3.7 B).

Following this identification of growth arrest in BCR-ligated WEHI 231 cells it was necessary to investigate whether this reflected growth arrest and/or apoptosis. Thus, cell cycle status and apoptosis was assessed by the Propidium Iodide (PI) that fluoresces on intercalating DNA and thus indicates the amount of DNA within a cell. Following treatment of WEHI 231 cells, with anti-Ig there is decrease in the number of live cells entering mitogenic phases of the cell cycle from 51% in unstimulated cells to 30% in anti-Ig treated cells (Figure 3.8). This is associated with a concomitant large increase in the subdiploid population from 20% in unstimulated cells to 76% in anti-Ig treated cells (Figure 3.8 A). Collectively, these data indicate that BCR signalling induces reduced proliferation both by growth arrest and apoptosis.

Furthermore, we investigated whether loss of MMP was involved in this form of apoptosis using the FACS dye $DiOC_6$ which binds to cells proportionally to their MMP (156, 409). It is well documented that cells undergoing apoptosis enter the "mitochondrial permeability transition" which leads to a breakdown of mitochondrial membrane integrity, dissipation of the MMP and the cytosolic translocation of pro-apoptotic molecules such as Smac and cytochrome c (152, 173, 410-415). Importantly, dissipation of the MMP is known to be one of the earliest steps in commitment of the cell to the apoptotic programme (410). Therefore by using $DiOC_6$ we can probe the MMP of cells and assess the percentage of cells with a high, and therefore healthy, MMP and the percentage with a low, dissipated MMP. Ligation of the BCR using anti-Ig lead to a dissipation of the MMP with only 17% of cells maintaining a high, healthy MMP after 48 hours as compared to 69% in unstimulated cells (Figure 3.9). This demonstrates that loss of mitochondrial membrane integrity is a good marker of commitment of WEHI 231 cells to apoptosis.

3.3.2 Ligation of the BCR and CD40 simultaneously leads to increased survival and proliferation

It is well established that CD40 signalling acts as a rescue signal to promote survival of BCR-stimulated WEHI 231 cells (316-318). Consistent with this mitochondrial membrane integrity is protected and the number of cells with a high MMP in anti-CD40 treated groups is maintained at 65%, as compared with 17% in the anti-Ig treatment group (Figure 3.9). The number of subdiploid cells is also vastly reduced from 76% in anti-Ig treated groups to 14% in anti-Ig and anti-CD40 treated groups (Figure 3.8). In addition to reduction in apoptosis, there is also a release from the growth arrest induced by anti-Ig treatment. DNA synthesis is increased by 400% in anti-Ig and anti-CD40 treated cells as compared to cells treated with anti-Ig alone (Figure 3.7 A). Furthermore, anti-CD40 treatment stimulates proliferation with the mode generation number at 6 as compared to generation number 3 in the unstimulated cells (Figure 3.7 B).

3.3.3 Bcl-2 family members are essential regulators of both anti-Ig-induced apoptosis and anti-CD40-mediated rescue

There have been recent reports that the anti-apoptotic Bcl-2 family members such as A1 and Mcl-1 may play a role in anti-CD40 mediated rescue of BCR-mediated apoptosis (322, 416-420). Therefore I investigated the expression of Bcl-2 family members both following ligation of the BCR and during anti-CD40 mediated rescue. Ligation of the BCR with anti-Ig induces expression of the pro-apoptotic Bcl-2 family members Bad, Bak and Bax however, expression of Bid was not detected (Figure 3.10 and data not shown). Both Bad and Bak expression is induced 8 h following BCR ligation and maintained up to 48 h (Figure 3.10 A and B). Interestingly, ligation of both the BCR and CD40 also induced Bad and Bak expression between 8 and 48 h, however ligation of CD40 alone does not induce either of these pro-apoptotic family members. Bax expression follows a different pattern with an increase 8 h post CD40 engagement (Figure 3.10 C). However, at 24 hours there is a strong induction of Bax following ligation of the BCR or addition of endogenous arachidonic acid, according to data shown previously this would correlate with the loss of MMP. Surprisingly at 48 h, Bax expression is maintained at this high level only when both the BCR and CD40 are ligated.

By contrast, ligation of the BCR using anti-Ig induced a downregulation of the anti-apoptotic family members Bcl-2, $BclX_L$ and Mcl-1 within 24 hours (Figure 3.11 A). However, $BclX_L$ was upregulated in response to treatment with both anti-Ig and anti-CD40 (Figure 3.11 A and B) and this suggests that $BclX_L$ has a pivotal role in mediating CD40-maintenance of the MMP and rescuing cells from BCR-stimulated apoptosis. Furthermore, it may imply that sequestration of Bax by CD40-mediated induction of expression of $BclX_L$ may provide a mechanism for preventing BCR-mediated apoptosis in CD40 rescued cells.

Nevertheless, the mere presence of Bcl-2 family members is not definitive proof that they are integral to the induction of either survival or apoptosis. All Bcl-2 family members are characterised by the presence of a conserved sequence motif called the Bcl-2 homology (BH) domain. The BH domains 1 to 3 in anti-apoptotic proteins such as Bcl-2 and $BclX_L$ form an elongated hydrophobic groove which acts as a docking site for the BH3 domains of pro-apoptotic

binding partners such as Bax and Bad (175, 421). Binding of pro and anti-apoptotic members in dimers prevents pro-apoptotic effects. In addition to these heterodimers, members can also form homodimers. For example Bax-Bax homodimers are thought to be sufficient and essential for induction of apoptosis (188, 193, 422, 423) and $BclX_L$- $BclX_L$ homodimers bind to the mitochondrial membrane to maintain integrity and inhibit the release of pro-apoptotic molecules such as Smac, Omi and cytochrome c (191, 424). Therefore it is the ratio of promoters and inhibitors of apoptosis that determines the cell response to diverse signals. With this in mind I investigated the binding partners of various Bcl-2 family members.

Firstly, the binding partners for the anti-apoptotic Bcl-2 family member $BclX_L$ as indicated by the Bcl-2 family members that were found in $BclX_L$-containing immune complexes were investigated. I first investigated the association of Mcl-1 with $BclX_L$ but was unable to find any association of Mcl-1 with $BclX_L$ over 48 hours regardless of the stimulation used (Figure 3.12 B). By contrast, when the association of $BclX_L$ with Bak, a potent inducer of apoptosis, was investigated. An increased association of $BclX_L$ with Bak in groups treated with both anti-Ig and anti-CD40 at all time points was found (Figure 3.12 C). This may suggest that $BclX_L$ can sequester Bak following CD40 engagement in order to prevent loss of mitochondrial membrane integrity and induction of apoptosis. This corroborates the previous Western Blot data that implicates Bak as important in anti-Ig mediated apoptosis. Interestingly, there is no induction of $BclX_L$ associated Bak following treatment with anti-CD40 alone (Figure 3.12 C). This suggests that $BclX_L$ association with Bak is an anti-apoptotic rather than pro-survival signal and in addition supports that Bak expression may be specifically upregulated in response to anti-Ig.

To corroborate the potential for $BclX_L$-Bak complexes Bak immunoprecipitates were probed for BclX expression. These studies demonstrated that Bak associated BclX is greatly upregulated by treatment with both anti-Ig and anti-CD40 at 48 h (Figure 3.12 D). This suggests that upregulated Bak is sequestered by BclX to prevent dissipation of the MMP and hence inhibit the pro-apoptotic signal. Furthermore, I looked for an association between Bak and Mcl-1. There seems to be equal expression of Bak associated Mcl-1 at all time

points regardless of the stimulation (Figure 3.12 E), suggesting that Mcl-1 interactions with Bak are not important in anti-CD40 mediated rescue from anti-Ig induced apoptosis.

Finally, the role of Bad in WEHI 231 cells was investigated. Bad is known to function in both pro and anti-apoptotic signalling depending on its cleavage and phosphorylation status. When unphosphorylated, Bad sequesters $BclX_L$ and acts as a pro-apoptotic signal. However, once Bad is phosphorylated on either, or a combination of, serines 112, 115 or 136 it is sequestered by 14-3-3 proteins. This prevents Bad from interacting with other Bcl-2 family members and hence is a pro-survival signal. Furthermore, whereas the cleavage product of Bad, Bad_s, is a potent inducer of apoptosis, some groups have reported that full length Bad has an anti-apoptotic function (215). These data reveal an upregulation of total Bad associations following both treatment with anti-Ig or the combination of anti-Ig and anti-CD40 (Figure 3.12 F). Interestingly, the majority of Bad present seems to be in the cleaved, and hence pro-apoptotic form. By contrast, there is a downregulation of total Bad expression following treatment with anti-CD40, as would be expected as CD40 ligation provides a pro-survival signal. Interpretation of the Bad phospho-Bad status is more difficult. Nevertheless, consideration of the anti-Ig and arachidonic acid treated cells demonstrates that there is a reduction in both phospho-serine136-Bad and phospho-serine112-Bad compared to the control cells, cultured in media alone (Figure 3.12 G and H). It is initially puzzling to see that the phospho-Bad complexed with Bad is reduced in anti-CD40 treated cells as compared to anti-Ig or arachidonic acid treated cells. However, taken together with the fact that there is far less Bad expression in anti-CD40 treated groups these data actually demonstrate that Bad is highly phosphorylated on serine 136 following anti-CD40 treatment. This suggests that whilst cleaved and non-phosphorylated, and thus pro-apoptotic, Bad is upregulated following anti-Ig and arachidonic acid treatment in WEHI 231 cells there is a reduction in Bad expression following CD40-mediated rescue. Furthermore, the Bad found in CD40-rescued cells is highly phosphorylated on serine 136 and hence active in pro-survival signalling.

3. 3. 4 Overexpression of $BclX_L$ can protect from either anti-Ig or arachidonic acid induced apoptosis however it cannot overcome growth arrest induced by these stimuli

Previous work in this laboratory and others has indicated that CD40-mediated upregulation of the anti-apoptotic Bcl-2 family member $BclX_L$ plays a key role in the prevention of BCR induced apoptosis (210, 276, 321). In addition, figures 3.11 and 12 indicate that $BclX_L$ is pivotal to CD40-mediated rescue of WEHI 231 cells. Therefore it was decided to utilise the WEHI 231 $BclX_L$ cell line, which expresses $BclX_L$ to levels seen post CD40 engagement (Figure 3.11 B), in order to dissect the specific role of this protein in CD40-mediated rescue of BCR-driven apoptosis. Apoptosis can be induced in WEHI 231 Neo (empty vector control WEHI 231 cells) following either anti-Ig treatment or the addition of exogenous arachidonic acid, as indicated by the subdiploid population being increased from 20% when cells are left unstimulated to 45% and 34% of WEHI 231 Neo cells following addition of anti-Ig or arachidonic acid respectively (Figure 3.13). By contrast, in WEHI 231 $BclX_L$ cells neither of these stimuli can increase the apoptotic population above 25% suggesting that $BclX_L$ provides protection from anti-Ig/ arachidonic acid mediated apoptosis (Figure 3.13). However, anti-CD40 treatment can further reduce apoptosis following either anti-Ig/ arachidonic acid treatment in $BclX_L$ cells perhaps suggesting CD40 ligation provides survival signals over and above those generated by overexpression of $BclX_L$ alone (Figure 3.13).

Induction of growth arrest post anti-Ig and arachidonic acid treatment in WEHI 231 cells can also be clearly seen in Figure 3.14 A which shows that incorporation of ^{3}[H] thymidine is reduced from 120,000 cpm in unstimulated cells to essentially zero after addition of 50 μM of arachidonic acid. Interestingly, arachidonic acid and BCR-induced growth arrest are both observed in WEHI 231 Neo (empty vector control WEHI 231 cells) and $BclX_L$ cells (Figure 3.14 A and B), suggesting that whilst expression of $BclX_L$ can overcome anti-Ig or arachidonic acid induced apoptosis, it cannot prevent the growth arrest response to either stimulus. By contrast, anti-CD40 treatment prevents, at least partially, both apoptosis and growth arrest resulting from culture with either anti-Ig or arachidonic acid (Figure 3.14 and 3.15). Therefore ligation of CD40 not only promotes survival by the induction of $BclX_L$ expression but also must

provide additional signals which stimulate proliferation. For example, previous work in our laboratory has demonstrated that CD40 engagement is associated with a sustained cycling ERK signal which is responsible for maintenance of proliferation in WEHI 231 cells (275).

3.3.5 Is BCR-stimulated apoptosis in WEHI 231 cells dependent on the activation of PLA_2?

The finding that exogenous arachidonic acid induces apoptosis, together with previous work in this laboratory that demonstrated that anti-Ig induced mitochondrial translocation and activation of PLA_2, led us to postulate that activation of PLA_2 and hence generation of arachidonic acid may be responsible for the loss of mitochondrial membrane integrity and consequential loss of MMP. In order to investigate a possible causal role for PLA_2 in BCR stimulated apoptosis 2 different classes of PLA_2 inhibitor: Methyl Arachidonyl Fluorophosphonate (MAFP) and Arachidonyltrifluoromethyl Ketone ($AACOCF_3$) were used. Both of these inhibitors are non-metabolisable analogues of arachidonic acid which bind to PLA_2 and prevent enzymatic activity (Figure 3.16).

Rather suprisingly, these PLA_2 inhibitors increased the subdiploid population from 11% in untreated cells to 25% and 38% by treatment with MAPF and AACOCF3 respectively (Figure 3.17 A). Moreover, addition of anti-CD40 failed to reduce apoptosis in AACOCF3 treated cells (Data not shown). Consistent with this, CD40 ligation also failed to reinstate proliferation in AACOCF3 treated cells with the percentage of cells in mitogenic phases of the cell cycle less than 5% with or without anti-CD40 treatment (Figure 3.14 B and results not shown). Furthermore, treatment with AACOCF3 induces a profound dissipation of the MMP with less than 2% of cells exhibiting a high MMP even in the absence of anti-Ig treatment (Figure 3.17 C). This suggests that AACOCF3 is a potent inducer of apoptosis and this is associated with a profound loss of MMP and cell cycle arrest that cannot be reinstated by anti-CD40 treatment.

As has been discussed previously PLA_2 is upregulated by anti-Ig treatment and translocated to the mitochondria. Therefore one would expect that activation of PLA_2 is a crucial stage in the activation of the apoptotic programme and that

inhibition of PLA_2 would act to inhibit apoptosis. However consideration of the effects of these inhibitors in fact suggests that they enhance apoptosis. Given that addition of arachidonic acid to WEHI 231 cells produces a dose dependent profound growth arrest, loss of the MMP and apoptosis ((Figures 3.13 to 15) and (156)), these results are likely to simply reflect that such non-metabolisable arachidonic acid analogues have a similar effect to addition of arachidonic acid, and therefore induce apoptosis. However this makes it impossible to demonstrate the role of PLA_2 directly by using specific PLA_2 inhibitors.

3.3.6 Anti-Ig stimulated growth arrest and apoptosis in WEHI 231 cells is dependent on the generation of arachidonic acid

It was decided therefore to investigate the role of PLA_2-derived arachidonic acid by assessing whether endogenously produced arachidonic acid can act as the active metabolite. In order to do this, inhibitors of enzymes that metabolise arachidonic acid to ecosinoids were utilised. Cycloxygenase 2 (COX2) and lipoxygenase (LOX) are enzymes that act to convert arachidonic acid to prostaglandins and leukotrienes respectively (Figure 3.18). Use of these specific inhibitors results in an accumulation of the product of PLA_2, arachidonic acid, within cells.

Use of either the COX2 inhibitor N- (2- Cyclohexloxyl- 4- nitrophenyl) methansulfonamide (NS398), the pan- LOX inhibitor EDBC or culture with both inhibitors induces growth arrest in a dose dependent manner (Figure 3.19 A and B). Furthermore, treatment of cells with these inhibitors reduces the threshold for BCR-mediated growth arrest and apoptosis and also actually results in a superinduction of BCR-mediated apoptosis (Figure 3.18 A to D and results not shown). In agreement with this, treatment with these inhibitors alone or in combination enhances the dissipation of the MMP causes by ligation of the BCR (Figure 3.18 D). Indeed, the percentage of cells with a low MMP is increased from 40% in cells treated with anti-Ig alone to 80% in cells treated with anti-Ig in combination with EDBC and NS398 (Figure 3.18 D). These results suggest that BCR-coupled generation of arachidonic acid has a causal role in the engagement of the apoptotic pathway. Interestingly, simply expressing $BclX_L$ in WEHI 231 cells appears to be sufficient to prevent such arachidonic acid-induced apoptosis (Figure 3.18 C).

3.3.7 Overexpression of $BclX_L$ protects the cells from arachidonic acid-induced dissipation of the MMP and resultant apoptosis

To determine how $BclX_L$ was acting, I decided to investigate whether the overexpression of $BclX_L$, a known mitochondrial membrane stabilising protein, could prevent the dissipation of the MMP induced by PLA_2. In order to do this I used the $BclX_L$ WEHI 231 cell line that expresses $BclX_L$ at levels equivalent to those following ligation of CD40. As stated above, anti-Ig induced growth arrest is observed in both Neo and $BclX_L$ WEHI 231 cells and consistent with a role for arachidonic acid in BCR-mediated growth arrest and apoptosis, DNA synthesis was reduced by addition either NS398 or EDBC alone or combination in both cell types (Figure 3.20 A and B). Treatment with anti-CD40 rescues both the Neo and $BclX_L$ expressing cells from BCR-induced growth arrest, however the growth arrest induced by treatment with NS298 and EDBC can only be partially rescued (Figure 3.20 A and B). By contrast, apoptosis in response to anti-Ig and its superinduction by NS398/ EDBC is reduced in $BclX_L$ WEHI 231 cells (Figure 3.19 C) and consideration of the MMP shows that $BclX_L$ cells are also protected from dissipation of the MMP (Figure 3.20 B). Addition of anti-Ig reduces the population with a high MMP to 14% in wild type cells whereas, MMP is maintained in the $BclX_L$ cells with 60% of the population exhibiting a high MMP (Figure 3.20 B). Similarly, addition of NS398 or EDBC alone or in combination induces loss of MMP in wild type cells, with the percentage of cells exhibiting a high MMP decreasing to between 47% and 13% depending on inhibitor treatment (Figure 3.20 B). However the $BclX_L$ expressing cells do not demonstrate this loss of MMP in response to inhibitor treatments (Figure 3.20 B). Indeed, $BclX_L$ cells even maintain mitochondrial membrane integrity following treatment with anti-Ig in the presence of the inhibitors (Figure 3.20 B).

3.3.8 BCR-induced Ca^{2+} release is decreased in WEHI 231 $BclX_L$ cells as compared to wild type WEHI 231 cells

CD40 signalling can overcome PLA_2/ arachidonic acid induced apoptosis and $BclX_L$ is a key molecule in protecting WEHI 231 from induction of apoptosis and the consequent arachidonic acid-induced disruption of mitochondrial membrane integrity. It was therefore decided to investigate the effect of $BclX_L$ and CD40 on the key signals that activate PLA_2. Indeed, we have previously shown that CD40 and $BclX_L$ signalling inhibit BCR coupling to the mitochondrial $cPLA_2$-

arachidonic acid pathway. For example, both ERK phosphorylation and Ca^{2+} regulate PLA_2 activation and I have previously shown that CD40 acts to downmodulate the ERK signals responsible for PLA_2 activation, however this is not mimicked by the overexpression of $BclX_L$ (320, 425). Therefore it was now decided to investigate how Ca^{2+} flux is affected by $BclX_L$ overexpression. Ligation of the BCR using anti-Ig in WEHI 231 Neo cells increased Ca^{2+} levels from approximately 100 nM to 400 nM (Figure 3.21). This is not surprising as Ca^{2+} flux is a well-known regulator of apoptosis. Ca^{2+} can act to activate the caspase 8 pathway as well as modulate the localisation of Bcl-2 family members (180, 426, 427). Furthermore, Ca^{2+} activates PLA_2 and this may be responsible for the translocation and activation of PLA_2 followed by arachidonic acid generation and apoptosis. Indeed, there is a recent precedent for apoptosis in epithelial cells lines that is Ca^{2+}-dependent, mitochondrial pathway-activated and triggered by arachidonic acid released by PLA_2 (428). Interestingly, BCR-mediated Ca^{2+} levels after CD40 engagement also resulted in a Ca^{2+} increase which peaked at a slightly higher level (450 nM, Figure 3.21). We have established that CD40 engagement results in a decrease in PLA_2 activation. The fact that Ca^{2+} levels are unaffected by anti-CD40 treatment suggests that the early Ca^{2+} signal is not modulated by CD40 to suppress PLA_2 activation.

However, when the calcium fluxes following anti-Ig and anti-CD40 treatment in $BclX_L$ cells were investigated it was clear that in WEHI 231 $BclX_L$ cells there is a massive reduction in the Ca^{2+} release stimulated by either of these treatments relative to that observed with Neo WEHI 231 cells (Figures 3.21 B). Thus, $BclX_L$ WEHI 231 cells exhibit just 27% of the Ca^{2+} increase observed in Neo WEHI 231 cells after anti-Ig treatment (Figure 3.21). There is an even greater difference in Ca^{2+} release levels after treatment with both anti-Ig and anti-CD40, with $BclX_L$ cells exhibiting only 21% of the Ca^{2+} release observed with Neo WEHI 231 cells (Figure 3.21 A). Interestingly, when the cells are treated with thapsigargin to induce complete release of all Ca^{2+} from E.R stores there is an essentially equal amount of Ca^{2+} release from both cells types (Figure 3.21 B). This suggests that there are no fundamental differences between the two cell types in their ability to take up and store Ca^{2+} and hence, that the reduction in anti Ig-mediated Ca^{2+} release is related to the overexpression of $BclX_L$. There is some evidence to suggest that Bcl-2 can prevent Ca^{2+} release from the E.R and

arachidonic acid pathway. For example, both ERK phosphorylation and Ca^{2+} regulate PLA_2 activation and I have previously shown that CD40 acts to downmodulate the ERK signals responsible for PLA_2 activation, however this is not mimicked by the overexpression of $BclX_L$ (320, 425). Therefore it was now decided to investigate how Ca^{2+} flux is affected by $BclX_L$ overexpression. Ligation of the BCR using anti-Ig in WEHI 231 Neo cells increased Ca^{2+} levels from approximately 100 nM to 400 nM (Figure 3.21). This is not surprising as Ca^{2+} flux is a well-known regulator of apoptosis. Ca^{2+} can act to activate the caspase 8 pathway as well as modulate the localisation of Bcl-2 family members (180, 426, 427). Furthermore, Ca^{2+} activates PLA_2 and this may be responsible for the translocation and activation of PLA_2 followed by arachidonic acid generation and apoptosis. Indeed, there is a recent precedent for apoptosis in epithelial cells lines that is Ca^{2+} -dependent, mitochondrial pathway-activated and triggered by arachidonic acid released by PLA_2 (428). Interestingly, BCR-mediated Ca^{2+} levels after CD40 engagement also resulted in a Ca^{2+} increase which peaked at a slightly higher level (450 nM, Figure 3.21). We have established that CD40 engagement results in a decrease in PLA_2 activation. The fact that Ca^{2+} levels are unaffected by anti-CD40 treatment suggests that the early Ca^{2+} signal is not modulated by CD40 to suppress PLA_2 activation.

However, when the calcium fluxes following anti-Ig and anti-CD40 treatment in $BclX_L$ cells were investigated it was clear that in WEHI 231 $BclX_L$ cells there is a massive reduction in the Ca^{2+} release stimulated by either of these treatments relative to that observed with Neo WEHI 231 cells (Figures 3.21 B). Thus, $BclX_L$ WEHI 231 cells exhibit just 27% of the Ca^{2+} increase observed in Neo WEHI 231 cells after anti-Ig treatment (Figure 3.21). There is an even greater difference in Ca^{2+} release levels after treatment with both anti-Ig and anti-CD40, with $BclX_L$ cells exhibiting only 21% of the Ca^{2+} release observed with Neo WEHI 231 cells (Figure 3.21 A). Interestingly, when the cells are treated with thapsigargin to induce complete release of all Ca^{2+} from E.R stores there is an essentially equal amount of Ca^{2+} release from both cells types (Figure 3.21 B). This suggests that there are no fundamental differences between the two cell types in their ability to take up and store Ca^{2+} and hence, that the reduction in anti Ig-mediated Ca^{2+} release is related to the overexpression of $BclX_L$. There is some evidence to suggest that Bcl-2 can prevent Ca^{2+} release from the E.R and

hence protect against apoptosis (reviewed in (426)) and it is possible that $BclX_L$ may play a similar role in preventing the initiation of cell death. These data may therefore go some way to explaining the ability of $BclX_L$ WEHI 231 cells to reduce BCR-coupled $mPLA_2$ activation. However the above data did not provide any information relating to the localisation of the Ca^{2+} signal as it simply measured total intracellular Ca^{2+}. It was therefore decided to investigate the localisation of this Ca^{2+} signal in single WEHI 231 cells.

3.3.9 Ligation of the BCR on WEHI 231 cells induces cellular calcium oscillation

Further to investigating Ca^{2+} signals in populations of WEHI 231 cells, I decided to investigate the subcellular Ca^{2+} signals in individual WEHI 231 cells in response to ligation of the BCR. In order visualise the Ca^{2+} signals single WEHI 231 cells were imaged in real time and the Ca^{2+} signals measured using the fluorescent dye Fluo 3. During analysis each cell was divided into 3 roughly equidistant regions of interest (ROI, Figure 3.22 B) and Ca^{2+} levels were separately analysed in each ROI to identify whether the Ca^{2+} signals were generated globally or followed individual patterns in localised areas. After the initial addition of anti-Ig, there is a spike of increased Ca^{2+} which then seems to return to near basal Ca^{2+} levels. A smaller and slower Ca^{2+} peak then follows this (Figure 3.22 C). In each responsive cell observed there was an increase in Ca^{2+} signal following ligation of the BCR. The most dominant pattern observed is a Ca^{2+} oscillation pattern in all ROI, as has been described (Figure 3.22 a). This pattern is found in all ROI within each individual cell. Ca^{2+} cycling has been postulated, along with dissipation of the MMP, to be a hallmark of apoptosis following cellular ATP depletion (111).

However this approach did not provide us with definitive information as to where the Ca^{2+} signal was being produced. The microscope used for these experiments was only capable of identifying the WEHI 231 nucleus with a small layer of cytoplasm surrounding it suggesting that peak Ca^{2+} signals were located in the nuclear/ perinuclear region. Attempts to use differential dye loadings to identify Ca^{2+} signalling in the nucleus, mitochondria and E.R unfortunately proved unsuccessful.

3.3.10 Expression of constitutively active Ras mutations rescue cells from growth arrest at 24 hours

The cyclic phospho-ERK signal has already been discussed as being important in the maintenance of survival and proliferation. The suppression of this ERK signalling by ligation of the BCR stimulates both growth arrest and apoptosis (275). Although overexpression of $BclX_L$ is able to provide relief from anti-Ig mediated apoptosis, engagement of CD40 is required to reinstate this cycling ERK signal and hence restore proliferation (425).

As shown previously, proliferating wild type WEHI 231 cells display cyclic ERK activation as indicated by an increase in dually phosphorylated ERK 1 and ERK 2 (Figure 3.23 A). This can be quantified by FACE assay which allows determination of the ratio of phospho-ERK to total ERK expression. In wild type WEHI 231 cells after 48 h there are typically phospho-ERK/ERK ratios of around 0.5 (Figure 3.23 B), the ratio being at its lowest when the cells are treated with anti-Ig, as would be predicted, and at its highest when the cells were treated with anti-CD40, as would also be predicted (Figures 3.22 B). By contrast, cells expressing RasV12 have an extremely large phospho-ERK/ERK ratio in untreated cells, 105 as compared to just 0.4 in wild type cells (Figure 3.23 B). However, BCR signalling is incredibly effective at shutting off this ERK signal as even though in RasV12 cells there is massively increased ERK signalling (phospho-ERK/ERK ratio = 105) it induces a 24-fold decrease in activated ERK (Figure 3.23 B).

To determine whether constitutively activated Ras, and hence sustained cycling ERK, is sufficient to restore growth, I investigated DNA synthesis post BCR engagement in WEHI 231 cells stably expressing various Ras constructs. Consideration of WEHI 231 RasV12 cells 24 hours post anti-Ig treatment demonstrates that expression of the RasV12 construct results in the rescue of WEHI 231 cells from anti-Ig induced growth arrest (Figure 3.24 A). This is most effective after addition of 10 μg/ml anti-Ig when RasV12 cells have 2.5 times greater [^{3}H] thymidine incorporation than empty vector cells (Figure 3.24 A). Consistent with this, whilst treatment of wild type WEHI 231 cells with anti-Ig leads to a reduction in the cycling phospho-ERK signal proposed to promote proliferation in these cells (275), in WEHI 231 RasV12 cells this late phospho-

ERK signal is maintained regardless of anti-Ig signal (Figure 3.24 B). This suggests that the late cycling ERK signal may be sufficient for rescue from growth arrest and that the Ras pathway is the important apical activator of ERK signalling in WEHI 231 cells. Moreover, it suggests that sustained deactivation of the RasMAPKinase pathway is pivotal to BCR induced growth arrest. Interestingly, consideration of ERK activation over a 48 h time course demonstrates that the RasV12 mediated activation of ERK is still cyclical in nature in contrast to anti-Ig induced cells (Figures 3.23 and 3.24 B). This suggests that even though ERK activation is upregulated the regulatory elements that control ERK phosphorylation are still fully functional. For example, the ERKMAP kinase phosphatase Pac1 has already been demonstrated to be important in the dephosphorylation of ERK in immature B cells (320).

In addition to signalling via Raf, MEK and ERK, Ras has a number of effector pathways involved in an array of biological outcomes including the PI-3 kinase pathway. To address the relative roles of the PI-3 kinase and Raf/MEK/ERK pathways in the regulation of proliferation versus growth arrest, stable WEHI 231 cell lines expressing the RasV12 S35 and RasV12 C40 mutant constructs were utilised.

To determine the effect that Raf/MEK/ERK signalling (RasV12 S35) has on the response of WEHI 231 cells to anti-Ig and anti-CD40 stimulation, transfected cells were stimulated as before and their biological responses assessed. As with the previous RasV12 WEHI 231 expressing cells, RasV12 S35 cells have a reduced growth arrest response to anti-Ig as compared to empty vector WEHI 231 cells (Figure 3.25 A). CD40-mediated rescue from anti-Ig induced growth arrest is slightly enhanced by RasV12 S35, as these cells exhibit a more robust proliferative response upon stimulation by anti-Ig and anti-CD40 (Figure 3.25 A). However, this enhancement is not significantly different to the advantage afforded by the RasV12 WEHI 231 cells.

Cells that have been transfected with the RasV12 C40 construct behaved similarly and demonstrated a low level of growth arrest in response to a wide range of concentrations of anti-Ig, from 0.1 to 10 μg/ml (Figure 3.25 B). This strongly suggests that RasV12 C40 also affords some level of protection

against anti-Ig induced growth arrest in WEHI 231 cells, as cells expressing RasV12 C40 display around 80% of the proliferation of untreated cells when stimulated with 10 μg/ml anti-Ig. Cells transfected with the empty vector alone on the other hand, display only around 40% of the proliferation of untreated cells when stimulated with anti-Ig, ruling out the vector as a possible explanation for this observation (Figure 3.25 B). Costimulation of cells expressing RasV12 C40 with anti-Ig and anti-CD40 results in proliferation levels higher than untreated cells, but as the growth arrest was much less in response to anti-Ig, this is a less than surprising observation (Figure 3.25 B). Indeed, the levels of proliferation of RasV12 C40 expressing cells appear to be greater than those of cells containing the empty vector by a consistent amount when cells are stimulated with anti-Ig alone or in combination with anti-CD40. This strongly implicates the abrogation of PI-3 kinase pathway may also be pivotal to BCR mediated growth arrest.

3.3.11 The RasV12 mutation increases apoptosis 48 h post BCR ligation

Further studies revealed that at time points subsequent to 24 hours (48 and 72 h) there was no rescue from BCR-induced growth arrest associated with the expression of RasV12 (Figure 3.24 C and 26). In order to investigate this further, the number of cellular divisions undergone was assessed. In agreement with this, CFSE analysis of empty vector (pcDNA3.1) and RasV12 cells post anti-Ig treatment shows a cessation of proliferation by 72 h (Figure 3.26). This would suggest that the huge increase in ERK activation at early time points benefits the WEHI 231 cells as they are protected from BCR-induced growth arrest. However, at the beginning of this chapter I demonstrated that 24 h following BCR ligation WEHI 231 cells dissipate their MMP and hence become committed to apoptosis. In terms of ERK signalling, apoptosis is associated with a strong, early ERK signal. The massive ERK signal generated in RasV12 WEHI 231 cells may protect from BCR-induced growth arrest before 24 h, however it also seems to superinduce apoptosis after 48 h. The percentage of subdiploid cells following BCR ligation is increased from 26% in pcDNA3.1 WEHI 231 cells to 46% in RasV12 WEHI 231 cells (Figure 3.24 C).

3.3.12 Constitutively active Ras mutants have a protective effect on BCR-induced dissipation of the MMP in WEHI 231 cells

To investigate the mechanism utilised by RasV12 mutants, to rescue WEHI 231 cells from BCR-induced growth arrest and apoptosis prior to 24 h I monitored MMP over 48 h. At 0 h of culture, as would be expected, the expression of constitutively active Ras constructs had very little effect on the MMP of the cells (Figure 3.27). Even after 24 h of culture, there were no major differences between the mutant cell lines when left unstimulated (Figure 3.28 A). By contrast, anti-Ig treatment for 24 h induced a reduction in the number of empty vector (pcDNA3.1) cells with a high MMP to 81%, whereas those expressing Ras constructs maintained mitochondrial integrity with between 93% and 96% of the cells exhibiting a high MMP (Figure 3. 28 A). This suggests that the constitutively active Ras mutants offer some protection from anti-Ig induced dissipation of the MMP after 24 h of culture. By 48 h, the empty vector cells are following the pattern of wild type WEHI 231 cells with the number of cells with a high MMP following anti-Ig treatment falling to 58% (Figures 3.27 and 28). Moreover, treatment with the combination of anti-Ig and anti-CD40 provides rescue with 91% of the cells maintaining a high MMP. As with the 24 h time point, expression of any of the Ras mutation constructs seems to provide some protection from the dissipation of the MMP. Thus, the RasV12 and the RasV12 S35 mutations increase the number of cells with a high MMP to 68% as compared to 58% in empty vector cells (Figure 3.28 A). The RasV12 C40 mutation seems to provide even more protection with 73% of cells maintaining a high MMP (Figure 3.28 B). There are also an increased number of cells expressing Ras constructs with a high MMP in the combination treatment group (Ras V12 98%, Ras V12 S35 98%, Ras V12 C40 77%) as compared to the empty vector cells, 67% (Figure 3.28 A). Taken together this data suggests that constitutively active Ras signalling either through the MAP kinase pathway or the PI-3 Kinase pathway can provide some protection from the dissipation of the MMP in response to ligation of the BCR. Interestingly, this maintenance of MMP is not reflected by a commensurate reduction in either BCR-induced growth arrest or apoptosis after 48 hours in culture.

3.3.13 The MEKK3 mutant increases growth arrest in response to anti-Ig

Previous work undertaken in this laboratory has demonstrated that normal proliferating or anti-CD40-treated WEHI 231 cells exhibited strong cycling dual phosphorylation of ERK, but not JNK or p38, between 8 and 48 h, whereas protein levels of ERK, JNK, and p38 expression remained constant (275). Furthermore, anti-Ig treatment did not affect the JNK or p38 levels whereas it led to a strong, early induction of phospho-ERK (275). In order to further investigate the roles of JNK and p38 and their crosstalk in ERKMAPK signalling I utilized the MEKK3 mutant which can activate several different types of MAP kinase simultaneously. MEKK3 can stimulate p38 via MKK3/6, JNK via MKK4/7 as well as ERK via MEK1/2.

Expression of the MEKK3 construct causes a decrease in the number of subdiploid cells after anti-Ig treatment, 8% compared to 41% in wild type cells (Figure 3.29 A). This construct may provide protection from apoptosis however it does not provide release from growth arrest. The number of cells in G0/G1 increases from 10% in empty vector cells to 41% in MEKK3 cells (Figure 3.29 A) suggesting that although cells are rescued from apoptosis there are arrested in G0/G1. Interestingly this rescue from BCR-induced apoptosis is reflected by the maintenance of MMP following ligation of the BCR (Figures 3.29 B). MEKK3 mutants also have a defective proliferative response to combined anti-Ig and anti-CD40 treatment. The G0/G1 population is increased to 41% as compared to 29% in empty vector cells (Figure 3.29 A). In agreement with the cell cycle data, CFSE data collected for WEHI 231 cells expressing the MEKK3 construct show that these cells have a reduced proliferation rate regardless of the stimulation used. The vast majority of the cells have not divided even after treatment with anti-CD40 (Figure 3.30). In fact there does not seem to be any proliferation, except in the unstimulated cells where there appears to be a small peak of cells in generation 5 (Figure 3.30). This suggests that constitutive signalling by all MAP kinase pathways simultaneously can prevent normal proliferation.

In order to investigate the impact of activation of JNK, p38 and ERK on BCR-mediated suppression of ERK we investigated both ERK expression and phosphorylation status in the MEKK3 expressing cells using the FACE ELISA

method. Interestingly in the MEKK3 expressing cells there is only a modest increase in phospho-ERK/ERK ratio in response to anti-Ig treatment, from 0.4 to 0.705 (Figure 3.31) as compared to that seen in RasV12 expressing cells (Figure 3.23 B). This modest increase in ERK may explain the fact that although MEKK3 expressing WEHI 231 cells are rescued from BCR-mediated apoptosis there is very little rescue of proliferation. Indeed, when the cells are left unstimulated the ratio in the MEKK3 expressing cells is actually lower than in the wild type cells (Data not shown). Moreover, ERK activation does not appear to be increased in MEKK3 cells as compared to empty vector WEHI 231 cells following anti-CD40 treatment (Figure 3.31).

3.3.14 The mechanism of RasV12 and MEKK3 rescue from BCR-induced apoptosis may involve AKT activation

As has already been demonstrated earlier in this chapter, the RasV12 and MEKK3 expressing cells can provide some protection from BCR-mediated dissipation of the MMP at 24 and 48 h (Figures 3.28 to 29). Furthermore, expression of the RasV12 constructs provides protection from anti-Ig induced growth arrest and apoptosis at 24 h (Figure 3.24 A). I have also demonstrated that expression of either the RasV12 or MEKK3 construct can mediate these effects, at least in part, via restoration of ERK signalling in BCR ligated cells. In order to further investigate some of the downstream targets that mediate these pro-survival and pro-proliferation signals, I decided to investigate the role of AKT in the generation of survival signals, particularly the phosphorylation of AKT that leads to phosphorylation of Bad. When non-phosphorylated, Bad can form Bad-BclX_L dimers which remove BclX_L from its mitochondrial membrane position and hence enhance the opening of the permeability transition pore stimulating apoptosis (207, 429). However, when phosphorylated by AKT, Bad is sequestered by cytoplasmic 14-3-3 proteins leading to maintenance of the mitochondrial membrane integrity. The phospho-AKT/AKT ratios observed in both the MEKK3 and RasV12 cells are comparable to the levels observed in the empty vector cells when unstimulated (Figure 3.32). Interestingly, whilst addition of anti-Ig to empty vector WEHI 231 cells induces a decrease in the phospho-AKT/AKT ratio from 0.6 to 0.2 at 24 hours (Figure 3.32) there is no reduction observed in RasV12 or MEKK3 expressing cells. These data suggest that such reduction in AKT levels, mediated by a BCR-induced switching off of the PI-3

kinase cascade, may play an important role in the mechanism utilised to induce mitochondrial dependent apoptosis via the pro-apoptotic Bcl-2 family member Bad in anti-Ig treated wild type WEHI 231 cells. This corroborates previous data that has demonstrated BCR-mediated upregulation of pro-apoptotic Bcl-2 family members including Bad (Figure 3.10). Moreover, it suggests that in the RasV12 and MEKK3 expressing cells the abrogation of the PI-3 kinase cascade does not occur and this contributes to the maintenance of survival of these cells following BCR ligation.

3.3.15 Expression of the Dok PH/PTB domain does not protect WEHI 231 cells from anti-Ig-induced growth arrest

To complement the above studies, I decided to use WEHI 231 cells expressing the amino terminal portion of Dok, which contains pleckstrin homology (PH) and phosphotyrosine binding domains (PTB). This protein also contained a GFP tag that was utilised to select for Dok PH/PTB positive mutants using flow cytometry. These portions of the protein should not be able to abrogate Ras, and concomitant ERKMAPKinase activation, as these domains are not involved in Ras-GAP binding and therefore will not be able to induce the GTPase activity of Ras. These first 258 amino acids of Dok (Dok-PH/PTB) therefore act as a dominant negative mutant and were used to determine the role Dok plays, if any, in the anti-Ig mediated suppression of ERK and PI-3 kinase leading to growth arrest and apoptosis in WEHI 231 cells.

To investigate the effects of this Dok construct on anti-Ig induced growth arrest, cells expressing this domain were stimulated with anti-Ig and proliferation assessed after 24, 48 and 72 h by the [^{3}H] thymidine incorporation assay. WEHI 231 cells expressing high levels of Dok PH/PTB exhibit no significant difference in growth arrest induced by anti-Ig, or in anti-CD40-mediated rescue when compared to cells transfected with the empty vector alone (Figures 3.33). Initially, this is not what was anticipated, as cells lacking Dok have been reported to exhibit sustained Ras activation (340). However, recent studies in our laboratory have suggested that rather than abrogating Ras activity, BCR ligation in WEHI 231 cells increases the association of the ERKMAP kinase specific phosphatase, Pac1, with ERKMAPKinase (320) to terminate ERK activation downstream from Ras and MEK. Therefore this mutant cell line

provides further support for this mode of action of BCR-mediated suppression of cycling ERK.

3.3.16 Expression of the catalytically inactive SHIP (SHIP CI) or the SHIP SH2 construct does not rescue WEHI 231 cells from anti-Ig mediated growth arrest

A parallel study in this laboratory has recently shown that the RasV12 C40 construct which activates PI-3 kinase, but not Raf signalling, actually led to ERK activation in WEHI 231 cells at analogous levels to that seen in cells expressing either the RasV12 or RasV12 S35 constructs which activate MAP kinase signalling directly via Raf (405). Therefore to further investigate the role of PI-3 kinase signalling independently of ERK activation, we decided to use cells expressing mutant versions of the 5' inositol phosphatase SHIP, a negative regulator of PI-3 kinase signalling. SHIP antagonises the functions of PI-3 kinase by dephosphorylating the 5' position of PIP_3, a product of PI-3 kinase that is important for the membrane localisation of many PH domain-containing proteins. WEHI 231 cells retrovirally infected to overexpress either a catalytically inactive mutant of SHIP (SHIP CI) or the SH2 domain alone (SHIP SH2) were used to determine the role SHIP plays in the anti-Ig mediated growth arrest in WEHI 231 cells. Overexpression of these mutant constructs should elicit a dominant negative effect, by antagonising endogenous SHIP activity and preventing endogenous SHIP interacting with its target proteins respectively. To investigate the effects of expression of these SHIP mutant constructs on anti-Ig induced growth arrest in WEHI 231 cells, WEHI 231 SHIP CI and WEHI 231 SHIP SH2 cells were stimulated with anti-Ig, either alone or in combination with anti-CD40, and their proliferation relative to empty vector controls assessed after 24, 48 and 72 h by the [^{3}H] thymidine incorporation assay.

WEHI 231 cells expressing these SHIP mutant constructs do not appear to exhibit any significant difference in anti-Ig induced growth arrest when compared to cells containing the empty vector (Figures 3.33). CD40-mediated rescue does not appear to be affected by expression of either of these SHIP mutants either, as cells transfected with these mutants display similar levels of proliferation in response to anti-Ig and anti-CD40 as cells containing the empty vector (Figure 3.34). These data suggest that BCR signalling does not use

SHIP to modulate the activation of the PI-3 kinase pathway during induction of growth arrest and apoptosis.

3.3.17 Downregulation of active SHIP results in alteration of the caspase 3 activation profiles

Following our data showing that BCR-signalling acts to downregulate AKT and Bad phosphorylation, we also investigated caspase 3 activation as another pro-apoptotic signal that may be a mediator of BCR-induced apoptosis. Moreover, I decided to utilise the SHIP and Dok expressing cells to investigate the relative contribution of the PI-3 kinase and Ras pathways respectively. Rather surprisingly, there was a high level of caspase 3 activation at 48 h in empty vector cells in the absence of any stimulus (Figures 3.35). This presumably reflects the role of this effector caspase in normal apoptosis in this cell line. The caspase 8 activating anti-Fas Ab and mitochondrial pathway activator Bax both produced caspase 3 activation profiles very similar to the unstimulated cells in empty vector WEHI 231cells (Data not shown). This suggests that caspase 3 is not increased above basal levels either by engagement of the mitochondrial pathway or Fas engagement in these cells . However, stimulation with anti-Ig, anti-CD40 or both also resulted in a very similar caspase 3 activation profile to unstimulated cells (Figure 3.35). This is unsurprising as anti-Ig stimulated apoptosis in WEHI 231 cells is thought to occur in the absence of caspase 3 activation (156), hence we would not expect elevated caspase 3 activation.

Consideration of WEHI 231 cells expressing Dok PH/PTB caspase 3 activation profiles show that they are very similar to empty vector WEHI 231 profiles for each given stimulation (Figures 3.35). This suggests that caspase 3 activation is not altered in these cells which reflects the fact that the Dok mutant does not seem to display altered growth or apoptotic responses. However the SHIP CI and SHIP SH2 expressing cells do display significantly different caspase 3 activation profiles as compared to the empty vector WEHI 231 cells (Figure 3.35). For every stimulus the SHIP mutants have a biphasic caspase 3 profile with a higher level of caspase 3 activation than either empty vector or Dok PH/PTB WEHI 231 cells (Figure 3.35). The exact role of caspase 3 in WEHI 231 mediated growth arrest, apoptosis and proliferation is not yet known. These data are very interesting as they imply that switching off SHIP provides a pro-

apoptotic signal. Although this may appear contradictory to what might have been expected, this fits in with data which describe a positive role for SHIP in promoting the tyrosine phosphorylation of Shc and therefore enhancing the Grb-2 mediated binding of Shc to Sos and SHIP resulting in enhanced RasERKMAPK signalling (347). The dominant negative SHIP mutants may prevent this signalling via RasERKMAPK and hence stimulate caspase 3-dependent apoptosis.

3.3.18 Transfection of WEHI 231 cells with PKC mutants

PKC α, β, δ, ε, ζ, η and θ isoforms are all expressed in mature B lymphocytes (348, 349). However immature B cells have diminished PKC signalling compared to mature B lymphocytes suggesting PKC may contribute to the differential response of distinct developmental stages of B cells to ligation of the BCR. For example, ligation of the BCR on mature B cells leads to PIP_2 hydrolysis, Ca^{2+} mobilisation and stimulation of PKC. In contrast, ligation of the BCR on immature B cells can mobilise calcium but PIP_2 hydrolysis and subsequent PKC activation are significantly reduced. Previous work in this laboratory has demonstrated that PKCs α, δ, ε and ζ are all expressed in the immature B cell line WEHI 231. Considering that previous studies have suggested a non-redundant role for PKC isoforms in B lymphocytes we decided to investigate the role of PKCs α, δ, ε and ζ in proliferation, growth arrest and apoptosis in WEHI 231 cells.

To investigate the roles of the four PKC family members PKCα, PKCδ, PKCε, and PKCζ, two mutant constructs of each were expressed in WEHI 231 cells using the pcDNA 3.1 vector (Figure 3.36 A). The mutant forms used were either constitutively active catalytic domain (CAT) or full-length kinase dead (as the result of a lysine – arginine substitution, KR) constructs (Figure 3.36 B). All 8 mutants were transfected into WEHI 231 cells by electroporation (as described in Materials and Methods) to generate stably expressing PKC CAT or PKC KR WEHI 231 lines.

3.3.19 Effect of PKCα expression and activation on anti-Ig mediated growth arrest in WEHI 231 cells

Wild type WEHI 231 cells exhibit a pronounced growth arrest in G1 phase of the cell cycle in response to anti-Ig, as shown in Figure 3.7. To investigate the effects of expression of a constitutively active PKCα (PKCα CAT) or a kinase dead form of PKCα (PKCα KR) on anti-Ig mediated growth arrest in WEHI 231 cells, transfected cells were stimulated with various concentrations of anti-Ig, and DNA synthesis assessed by the [^{3}H] thymidine uptake assay at 24 and 48 h (Figure 3.37). Cells transfected with the empty vector were used as a control.

Even at 24 hours, WEHI 231 cells transfected with the empty pc DNA3.1 vector exhibit a pronounced growth arrest in response to anti-Ig, with [^{3}H] thymidine uptake levels approximately only 60% of those of unstimulated cells in response to 1 μg/ml anti-Ig, and only about 50% in response to 10 μg/ml anti-Ig (Figure 3.37 A). By 48 hours, both concentrations of anti-Ig have reduced levels of thymidine uptake to around 40% of those of the unstimulated cells (Figure 3.37 B). In contrast to this, cells transfected with the PKCα mutant constructs do not show signs of growth inhibition even in response to 10 μg/ml anti-Ig at 24 h (Figure 3.37 A). If anything, PKCα KR cells actually exhibit slightly increased levels of proliferation after 24 h stimulation with anti-Ig, particularly 0.1 μg/ml and 10 μg/ml (Figure 3.37 A). After 48 h treatment, cells expressing either PKCα mutant construct demonstrate growth arrest in response to anti-Ig at 1 or 10 μg/ml, but not to the same extent as cells containing the empty vector alone (Figure 3.37 B). Surprisingly, both mutants confer the same properties upon WEHI 231 cells, despite the fact that whilst PKCα CAT is constitutively active, PKCα KR would be predicted to act as a dominant negative enzyme and hence antagonise the actions of endogenous PKCα.

3.3.20 Effect of PKCα CAT and KR expression on anti-Ig mediated apoptosis and CD40-mediated rescue in WEHI 231 cells

Although not statistically significant, unstimulated PKCα CAT and PKCα KR WEHI 231 cells demonstrate an increase in the percentage of cells in the mitogenic phases of the cell cycle as compared to empty vector WEHI 231 cells (38 and 32% respectively as compared to 23%, Figure 3.38). This is

complimented by a decrease in the percentage of subdiploid and therefore apoptotic cells from 9% in empty vector cells to 3% in both PKCα CAT and PKCα KR cell lines (Figure 3.38). This suggests that both PKCα CAT and PKCα KR expression provides a release from the basal level of apoptosis by stimulating entry into the cell cycle. Interestingly, consideration of the CFSE data demonstrates that in the unstimulated cells there is only a very slight enhancement of proliferation in either PKCα CAT or PKCα KR mutants which may suggest that whilst cells enter both S and G2/M phases of the cell cycle they may be arrested in these stages (Figure 3.39).

In agreement with figure 3.37 B that shows enhanced DNA synthesis in both PKCα CAT and PKCα KR mutants at 48 h in response to anti-Ig treatment, cell cycle analysis indicates a decrease in the number of subdiploid cells at 48 h following anti-Ig treatment (Figure 3.38). Although the results are not statistically significant, in the empty vector cells 67% of cells are in the subdiploid population following anti-Ig treatment whereas in PKCα CAT cells this is reduced to 31% and in PKCα KR cells it is reduced to 40%. This reduction in the subdiploid popuiation is accompanied by slight increases in cells in all other phases of the cell cycle as compared to empty vector cells. Conversely, assessment of the CFSE data suggests that anti-Ig induced growth arrest is actually increased by 72 h following stimulation. In empty vector cells anti-Ig treatment results in an average of 3 daughter generations whereas both PKCα CAT and PKCα KR WEHI 231 cells do not appear to undergo cell divisions (Figure 3.39). This suggests that although such cells are rescued from anti-Ig induced apoptosis, cessation of DNA synthesis and can enter later mitogenic phases of the cell cycle there is still a block on cellular proliferation. It is surprising that both constructs would have the same effect in rescuing WEHI 231 cells from anti-Ig induced apoptosis. Collectively this data strongly suggests that PKCα expression and activity can rescue BCR-stimulated apoptosis but not fully rescue growth arrest.

When empty vector cells were treated with a combination of both anti-Ig and anti-CD40 there was a decrease in the number of subdiploid cells to 6% and a corresponding increase to 37% in the number of cells arrested in G0/G1 (Figure

3.38). Neither PKCα CAT nor PKCα KR WEHI 231 cells showed a statistically significant difference in cell cycle profile in response to anti-Ig and anti-CD40 treatment (Figure 3.38). However, CFSE data suggests that even though there may have been no inhibition of entry to later phases of the cell cycle there was actually a decrease in proliferation of these cells in response to anti-Ig and anti-CD40 (Figure 3.39). For example, the average number of daughter populations following combined anti-Ig and anti-CD40 treatment in empty vector cells is 6 however this is reduced to 4 in both PKCα CAT and PKCα KR cell lines (Figure 3.39).

3.3.21 PKCα CAT and PKCα KR expression provides protection from anti-Ig induced dissipation of the MMP

As the data suggested that either PKCα CAT or PKCα KR expression provides protection from anti-Ig induced apoptosis, we investigated whether this mechanism was initiated up or downstream of the opening of the mitochondrial permeability pore. As shown extensively above, treatment with anti-Ig decreases the number of cells with a high MMP (to 52% in empty vector cells in this experiment), however in both PKCα CAT and PKCα KR cell lines this high MMP is maintained in 80% of cells (Figure 3.40 and 41). However at 96 h the MMP in BCR-stimulated empty vector, PKCα CAT and PKCα KR WEHI 231 cells is reduced (Figure 3.41 B), suggesting that dissipation of the MMP still occurs in both PKCα CAT and PKCα KR mutants although the kinetics of the opening of the permeability transition pore is delayed. There are generally little or no differences in MMP when cells are left unstimulated, treated with anti-CD40 or given combination treatment amongst the 3 cell lines (Figure 3.40 and 41).

3.3.22 Effect of PKCδ CAT and KR expression on anti-Ig mediated growth arrest and apoptosis in WEHI 231 cells

As described for the PKCα expressing WEHI 231 cells, after 24 h of stimulation with anti-Ig, WEHI 231 cells expressing either PKCδ CAT or PKCδ KR show no growth arrest, even at the maximum concentration of anti-Ig, whereas cells containing the empty vector exhibit only 50% of the [^{3}H] thymidine uptake of control cells (Figure 3.42 A). However, by 48 h in both PKCδ CAT and PKCδ KR

WEHI 231 cells, 10 μg/ml of anti-Ig induced growth arrest of a similar magnitude to that assessed in WEHI 231 cells containing the empty vector (Figure 3.42 B).

Interestingly, given reports that cleaved PKCδ can transduce apoptosis in a number of cell types (382, 383, 430), PKCδ CAT cells have a higher basal rate of apoptosis than empty vector cells- 24% as compared to 16% in unstimulated cells (Figure 3.43). Moreover, PKCδ KR WEHI 231 cells exhibit a reduced basal rate of apoptosis- 11% as compared to 16% in empty vector containing cells (Figure 3.43). However, this pattern is not observed following anti-Ig treatment as whilst ligation of the BCR induces a large increase in the subdiploid population in empty vector cells (84%) there is a profound rescue of PKCδ CAT cells from anti-Ig induced apoptosis and a corresponding increase in cells in G0/G1 (Figure 3.43). The subdiploid population is reduced from 84% in empty vector WEHI 231 cells to 11% in PKCδ CAT WEHI 231 cells. Similarly, in PKCδ KR cells there is decrease in the subdiploid population from 84% in the empty vector WEHI 231 cells to 65% in the PKCδ KR WEHI 231 cells.

Surprisingly, when PKCδ CAT and KR expressing WEHI 231 cells are treated with a combination of both anti-CD40 and anti-Ig there was an increase in apoptotic populations with a corresponding decrease in the cells growth arrested in G0/G1 (Figure 3.43). In empty vector cells there are 49% of cells in G0/G1 however in PKCδ CAT cells there are only 36%, and in PKCδ KR cells this is further reduced to 30% (Figure 3.43). This suggests that PKCδ may be important for CD40-mediated rescue and cell cycle entry.

3.3.23 PKCδ CAT and PKCδ KR WEHI 231 cells are rescued from anti-Ig induced dissipation of the MMP

Following the assertion that PKCδ CAT and to a lesser extent PKCδ KR expression provides protection from anti-Ig induced apoptosis, it was investigated whether this mechanism was initiated up or downstream of the opening of the mitochondrial permeability pore. Treatment with anti-Ig decreases the number of cells with a high MMP to 48% in empty vector cells however in PKCδ CAT and PKCδ KR mutants this is maintained at 83% and 70% respectively (Figure 3.40 and 44). This increased MMP in response to anti-Ig treatment is effectively lost by 96 h, particularly in PKCδ KR cells (Data not

shown) indicating that dissipation of the MMP still occurs in both PKCδ CAT and PKCδ KR mutants albeit with a delay in the opening of the permeability transition pore. There are no alterations in MMP as compared to empty vector cells when cells are left unstimulated, treated with anti-CD40 or given combination treatment over this period (Figure 3.44 and Results not shown).

3.3.24 Effect of PKCε CAT and KR expression on anti-Ig mediated growth arrest and apoptosis in WEHI 231 cells

WEHI 231 PKCε CAT cells appear to increase their proliferation upon stimulation with anti-Ig for 24 h, in a dose–dependent manner, exhibiting 150% of the DNA synthesis seen In control cells after addition of 10 μg/ml anti-Ig (Figure 3.45 A). WEHI 231 PKCε KR cells do not undergo growth arrest in response to anti-Ig after 24 h, but nor do they increase their proliferation (Figure 3.45 A). In contrast, by 48 h, however, anti-Ig (1 and 10 μg/ml) has induced growth arrest in both these cell types, to the same level as the empty vector control (Figure 3.45 B). This is corroborated by CFSE data which shown similar number of cellular divisions undertaken in both empty vector and PKCε CAT cells following anti-Ig treatment at 72 h, both have a mode generation number of 4 (Figure 3.46). By contrast, when cells are left unstimulated there is increased cell division in PKCε CAT cells (mode generation = 6) as compared to empty vector WEHI 231 cells (mode generation = 5, Figure 3.46).

When PKCε CAT and PKCε KR cells are left unstimulated there is a slightly decreased level of basal apoptosis as compared to empty vector cells- 6 and 8% subdiploid respectively as compared to 16% subdiploid in empty vector cells (Figure 3.47). This is associated with an increase in the percentage of cells in G2/M phase, 4% in PKCε CAT cells and 16% in PKCε KR cells as compared to 1% in empty vector cells (Figure 3.47). However the DNA synthesis data does not demonstrate that either of these mutations provides a growth advantage after 24 h (Figure 3.45 B) therefore these cells may be growth arrested in G2/M phase of the cell cycle.

When cells are treated with anti-Ig to ligate the BCR there is a decreased level of apoptosis in both PKCε CAT and PKCε KR cells as compared to empty

vector cells at 48 h- just 35% and 42% subdiploid respectively as compared to 84% subdiploid in empty vector cells (Figure 3.47). Interestingly, this is not strongly associated with a decrease In cells with a dissipated MMP (Figure 3.40 and 3.48). In fact at 48 h both PKCε mutants have a slightly increased number of cells with a high MMP (PKCε CAT: 58% and PKCε KR: 63%) as compared to empty vector cells (48%, Figure 3.48).

By contrast, when PKCε CAT and PKCε KR cells were treated with both anti-Ig and anti-CD40 there was an increase in the percentage of cells entering the proliferative phases of the cell cycle (Figure 3.47). For example, there are 33% of PKCε CAT cells and 31% of PKCε KR cells in S phase following anti-Ig and anti-CD40 treatment as compared to 24% in empty vector WEHI 231 cells, this corresponds with a decrease in cells in G0/G1 in PKCε expressing cell lines. However the CFSE data, for 72 h post-stimulation, shows that there is no increase in proliferation in PKCε CAT following anti-Ig and anti-CD40 suggesting that although there may be an increase in cells entering mitogenic phases, they are blocked at this point and increased cellular division does not follow, at least by 72 h (Figure 3.46).

3.3.25 Effect of PKCζ CAT and KR expression on anti-Ig mediated growth arrest and apoptosis in WEHI 231 cells

After 24 h stimulation with 0.1 μg/ml anti-Ig, WEHI 231 cells expressing either PKCζ construct display a decrease in proliferation compared to the empty vector, but when stimulated with 1 or 10 μg/ml anti-Ig WEHI 231 cells expressing these constructs exhibit a minimal decrease in proliferation (Figure 3.49 A). In fact at 24 h post 10 μg/ml anti-Ig, PKCζ CAT and PKCζ KR WEHI 231 cells exhibit 100% and 90% of the DNA synthesis observed in control cells, as compared to just 50% in empty vector WEHI 231 cells. By contrast, after 48 h stimulation, there is no great difference in the growth arrest induced by 10 μg/ml anti-Ig upon WEHI 231 cells expressing either PKCζ mutant construct compared to cells containing the empty vector (Figure 3.49 B). Puzzlingly, CFSE data demonstrate that PKCζ CAT WEHI 231 cells have reduced proliferation, in response to all stimuli, at 72 h (Figure 3.50).

At 48 h there are only negligible differences between PKCζ CAT and empty vector cells when left unstimulated or treated with a combination of anti-Ig and anti-CD40 in terms of cell cycle status (Figure 3.51). However when PKCζ CAT cells are treated with anti-Ig there is a decreased level of apoptosis (48% subdiploid) as compared to empty vector cells (84% subdiploid, Figure 3.51). Furthermore, there is a concomitant increase in cells entering the mitogenic phases of the cell cycle. However, as stated above, this is not associated with increase cellular proliferation which suggests that cells are growth arrested in mitogenic phases of the cell cycle. Moreover, this is not associated with the maintenance of the MMP as empty vector, PKCζ CAT and PKCζ KR cells have similar levels of cells with a high MMP over 96 h (Figure 3.40 and 52). This would suggest that any protective effects that PKCζ may mediated are induced downstream of the opening of the mitochondrial transition pore.

3.3.26 Differential expression and activation of PKCs leads to altered expression of pro-apoptotic Bcl-2 family members

As PKCδ CAT and PKCδ KR cell lines exhibited differential sensitivity to induction of apoptosis relative to empty vector WEHI 231 cells, we investigated whether there had been any alteration in expression of pro-apoptotic Bcl-2 family members in response to PKCδ expression. Firstly we assessed Bad expression in empty vector cells. Bad is upregulated from 5 min post stimulation by anti-Ig and this is partially reversed by coligation with anti-CD40 (Figure 3.53). By contrast, there is an upregulation of Bad in unstimulated cells commensurate with induction of spontaneous apoptosis due to media exhaustion (Figure 3.53). Interestingly, in PKCδ CAT cells Bad is downregulated under all conditions tested apart from a strong induction of Bad expression 48 h following anti-Ig (Figure 3.53). This suggests although pro-apoptotic Bcl-2 family members are induced, there is a substantial delay in their expression which provides a rationale for previous data that demonstrated that PKCδ CAT WEHI 231 cells are rescued from anti-Ig induced apoptosis (Figure 3.43). Similarly, this also corroborates the MMP data which also suggested that PKCδ CAT induced an increased lag time between BCR ligation and the induction of apoptosis (Figure 3.44). Additionally, the pro-apoptotic Bcl-2 family member Bad is also upregulated at 48 h in PKCζ KR cells by all stimulations as

compared to the empty vector WEHI 231 cells (Figure 3.53). The greatest expression of Bad occurs 48 h post anti-Ig stimulation (Figure 3.53).

The empty vector WEHI 231 cells have virtually no visible expression of the pro-apoptotic Bcl-2 family member Bid (Figure 3.53). Even though the expression shown in PKC ζCAT cells does not look very impressive it does represent a real upregulation of Bid expression relative to wild type cells (Figure 3.53). Added to this, Bid may only need to be present in very small amounts in order to exert its pro-apoptotic action, as seen in mature B cells. There is no visible Bid present in the PKC ζCAT lysates prepared 5 min post stimulation regardless of the stimulation used (Figure 3.53). However in both unstimulated and anti-Ig treated groups there is an upregulation of Bid both at 24 and 48 h. The greatest expression of Bid can been seen in the anti-Ig treated groups at 48 h suggesting that not only is Bid expression increased by ligation of the BCR but also increases over time in these cells (Figure 3.53). Moreover, the pro-apoptotic Bcl-2 family member Bid is upregulated with all stimulations in PKCζ KR cells as compared to the empty vector WEHI 231 cells (Figure 3.53). There is an increase in Bid expression over time with the greatest Bid expression at 48 h post anti-Ig stimulation (Figure 3.53).

3.4 Discussion

The data presented in this chapter has provided information on the signalling mechanisms employed during BCR-mediated apoptosis. I have demonstrated that BCR ligation results in the generation of apoptosis-inducing arachidonic acid by PLA_2, consequent loss of mitochondrial membrane integrity and induction of the pro-apoptotic Bcl-2 family members Bak, Bax and Bad. Moreover, coligation of CD40 antagonises all of these effects by reinstating sustained, cyclical ERK activation and expression $BclX_L$. $BclX_L$ has dual effects as it can form homo-dimers which may protect from arachidonic acid-induced loss of mitochondrial membrane integrity. In addition, it may form hetero-dimers with Bak and hence inhibit Bak/Bax oligomer-induced apoptosis.

3.4.1 $BclX_L$ mediates WEHI 231 rescue from BCR-stimulated PLA_2-mediated apoptosis and dissipation of the MMP

Immature B cells generally respond to self Ag by induction of anergy or apoptosis however *in vivo* the presence of other extrinsic signals can lead to alternative fates. For example engagement of CD40 by T cells can prevent apoptosis and reinstate proliferation. Previous work in our laboratory and others has established that CD40 ligation acts to rescue BCR-mediated apoptosis and growth arrest by upregulation of anti-apoptotic Bcl-2 family members such as $BclX_L$ and also maintenance of sustained cycling ERK signals associated with proliferation (156, 210, 275, 276, 308, 321, 322, 416, 431). To assess the role of $BclX_L$ in CD40-mediated rescue from BCR induced-growth arrest, dissipation of the MMP and apoptosis WEHI 231 cells expressing elevated levels of $BclX_L$ were utilised. It has now been demonstrated that anti-Ig induced apoptosis and dissipation of the MMP can both be prevented in WEHI 231 cells by overexpression of $BclX_L$ (Figures 3.13 to 15, 3.19 C and D and 3.20). These findings corroborate data that suggest $BclX_L$ protects from BCR-mediated apoptosis by protecting the mitochondrial membrane integrity (179, 209, 276, 321, 432, 433).

Previous work in this laboratory has implicated PLA_2 as an important signalling molecule in anti-Ig mediated apoptosis. For example, cytosolic PLA_2 was found to translocate to both the nucleus and mitochondria within 3 hours of anti-Ig treatment and in addition, levels of PLA_2 mRNA and protein were both upregulated by such treatment (156). Moreover, treatment with anti-CD40 could prevent this upregulation of PLA_2 activity and expression (156). Furthermore, addition of exogenous arachidonic acid resulted in dose dependent growth arrest and apoptosis mimicking ligation of the BCR by anti-Ig (289). Arachidonic acid has been previously implicated in the loss of integrity of the inner mitochondrial membrane (434-436) an event which can result in both the dissipation of MMP and loss of ATP seen in anti-Ig treated immature B cells (156). Taken together these data suggest a key role for PLA_2 in the induction of BCR-mediated apoptosis and collapse of the MMP. Therefore, it was decided to further investigate the role of PLA_2 by using specific inhibitors of this enzyme that are non-metabolisable analogues of arachidonic acid (Figure 3.16). However it was not possible to demonstrate a causal role for PLA_2 using these

inhibitors as they mimicked arachidonic acid and so induced both a dissipation of the MMP and apoptosis in WEHI 231 cells (Figures 3.17). To resolve this problem inhibitors of cycloxygenase 2 (COX2) and lipoxygenase (LOX) were utilised. These enzymes convert arachidonic acid to prostaglandins and leukotrienes respectively (Figure 3.18), resulting in a cellular decrease in arachidonic acid. Therefore, COX and LOX inhibitors induce an intracellular accumulation of arachidonic acid that allows investigation of the action of PLA_2 without using specific inhibitors of this enzyme. As predicted, inhibitors of both COX2 (NS398) and LOX (EDBC) resulted in dissipation of the MMP, growth arrest and apoptosis and when used in conjunction with anti-Ig resulted in a superinduction of apoptosis (Figures 3.19). This apoptosis is most potent when both inhibitors are used in combination (Figure 3.19 C) but can be partially reversed by coligation of CD40 (Figure 3.20 A). Interestingly, overexpression of $BclX_L$ could prevent COX2/LOX mediated disruption of the MMP, superinduction of anti-Ig induced apoptosis and growth arrest (Figures 3.20 A and B).

Taken together these data suggest that $BclX_L$ is sufficient to overcome the effects of BCR-induced dissipation of the MMP and induction of apoptosis. However parallel studies in this laboratory have demonstrated that $BclX_L$ is unable to reverse the anti-Ig mediated desensitization of ERK activation and reverse growth arrest (405) suggesting that CD40 engagement provides additional signals that can restore ERK cycling and therefore reinstate proliferation. Since anti-CD40, but not $BclX_L$, can convert arachidonic acid to prostaglandin E_2 (425), one candidate for the additional signal required for ERK activation is the conversion of arachidonic acid to prostaglandins/leukotrienes by COX2/LOX action. Indeed, parallel studies have demonstrated that culture with these inhibitors blocks the sustained, cycling ERK activation that is necessary for proliferation (425). This would suggest that COX2/LOX metabolites such as prostaglandin E_2 (PGE_2) are able to act as anti-apoptotic/ pro-mitogenic signals and hence these enzymes provide a dynamic switch mechanism for the regulating the commitment and rescue of a cell from apoptosis. PGE_2 is a product of arachidonic acid and its action is antagonistic to arachidonic acid and so the balance of these 2 signals regulates the functional outcome. For example arachidonic acid down regulates the ERK signal and

induces apoptosis whereas conversion to PGE_2 removes apoptotic arachidonic acid and promotes mitogenic ERK signalling (Figure 3.54).

3.4.2 Ca^{2+} signalling may be used to induce PLA_2 activation during BCR-mediated apoptosis and is downregulated following $BclX_L$ expression

It was found that simply overexpressing $BclX_L$ in WEHI 231 cells is sufficient to antagonise BCR-coupled mitochondrial PLA_2 activation. The mechanisms underlying this have not yet been delineated but it is clear that such $BclX_L$ expression does not suppress the early BCR-coupled ERK activation that is necessary for $cPLA_2$ activation (275). However, it is well established that $cPLA_2$ translocation and activation is also dependent on rises in intracellular Ca^{2+} (107). Furthermore, since Bcl-2 family members have been implicated in Ca^{2+} homeostasis (111, 426, 437-441) it was decided to investigate whether $BclX_L$ mediated its effects, at least in part, via suppression of BCR-elicited Ca^{2+} mobilisation. As widely established, treatment with anti-Ig resulted in a increase in calcium release by a population of wild type WEHI 231 cells (Figure 3.21). Simultaneous coligation of CD40 did not prevent the induction of this intracellular Ca^{2+} rise. However these Ca^{2+} measurements did not provide any information on the specific Ca^{2+} levels in each individual cell or indeed in each organelle/localised subcellular area of the cell and thus, it is possible that CD40 engagement may stimulate the formation of specific "micro-domains" of low Ca^{2+} concentration, for example close to the mitochondrial membranes. Interestingly and, by contrast, in $BclX_L$ WEHI 231 cells the BCR-mediated Ca^{2+} release is severely reduced as compared to Neo WEHI 231 cells (Figure 3.21). Previous work in this laboratory has demonstrated that translocation of $cPLA_2$ to either the nucleus or mitochondria occurs 3 h post BCR ligation (156) and expression of $BclX_L$ is fully upregulated within 4 h post CD40 ligation (425). Therefore, $BclX_L$ may mediate longer-term inhibition of Ca^{2+} release and hence prevent induction of apoptosis, however it is not likely to prevent $cPLA_2$ activation immediately after BCR ligation.

Further to identifying global BCR-mediated Ca^{2+} rise in WEHI 231 populations, I decided to try to identify the localised Ca^{2+} patterns in single WEHI 231 cells. Although no definitive answers to the spatial pattern of these Ca^{2+} increases following BCR ligation were obtained, the dominant pattern appeared to be Ca^{2+}

oscillations (Figure 3.22). Each of the cells viewed appeared to have an individual profile of Ca^{2+} increase following ligation of the BCR, with differing intensities of Ca^{2+} signal with some cells even being unresponsive to anti-Ig treatment. However, it is important to note that I did not synchronise the cells and so the strength of Ca^{2+} signal produced may be related to the cell cycle stage of the cells. In order to assess whether the oscillation is the predominant Ca^{2+} signature it would be necessary to use a different system where the anti-Ig is perfused into the media and many synchronised cells can be imaged at one time.

In addition, it may be necessary to further change the experimental design as poly-L-lysine was used to adhere the cells to the slides. This may have produced signalling via additional receptors and hence potentially depleting the Ca^{2+} stores prior to ligation of the BCR. Furthermore, although we failed to detect differential pools of Ca^{2+} by imaging, it would be extremely interesting to further investigate the subcellular localisation of these Ca^{2+} fluxes using differential dye loading of organelles or specifically localising calcium by monitoring GFP-FRET pairs in specific localisations.

Interestingly, it is possible that the calcium release observed following anti-Ig treatment may be transduced and modulated by expression of Bcl-2 family members (442). For example, and consistent with our data in $BclX_L$ cells, it has been demonstrated that overexpression of the anti-apoptotic protein Bcl-2 decreases the ER Ca^{2+} load and protects cells from death (440, 443). Conversely, Bax /Bak overexpression favours the transfer of Ca^{2+} from E.R to mitochondria and induces cell death (437, 441). How Bax, Bak, and Bcl-2 interfere with the E.R Ca^{2+} load is uncertain, but clearly this interference depends on the movement of Ca^{2+} from the E.R to the mitochondria. Interestingly, whilst Bcl-2 is known to protect from death when targeted to the E.R, it is found to induce apoptosis when directed to mitochondria (444). Furthermore, such E.R-targeted Bcl-2 can protect from death induced by mitochondria-targeted Bax (445), suggesting that the E.R exerts a dominant role in its coupling to mitochondria. This data suggests that identification of Ca^{2+} concentrations in the subcellular organelles and visualisation of Bcl-2 family member localisation would be essential to assess how these molecules

modulate apoptosis. This approach may also resolve much of the confusion surrounding the lack of correlation between Bcl-2 family member expression and functional outcome.

3.4.3 Ligation of the BCR induces the expression of pro-apoptotic Bcl-2 family members whereas CD40 engagement induces the expression of anti-apoptotic Bcl-2 family members and sequestration of pro-apoptotic Bcl-2 family members

As a first approach to addressing this problem, I investigated the binding partners of $BclX_L$ as it was clear from previous work (276, 321, 425) and the results of this thesis that $BclX_L$ played a key role in the regulation of BCR-mediated apoptosis. Indeed, it is already well documented that Bcl-2 family members can form hetero/homo dimers or oligomers (446) and that these Bcl-2 complexes can either act in a pro-apoptotic or pro-survival manner. For example, Bak/Bax oligomers promote apoptosis (177, 182, 193, 422, 423, 447) whereas Bad/BclX dimers prevent pro-apoptotic actions (204). Therefore it was decided to look not only at the absolute levels of Bcl-2 family member expression but also investigate possible binding associations.

Consistent with BCR-signalling inducing apoptosis, it was found that anti-Ig treatment suppresses Bcl-2 and $BclX_L$ expression but generally acted to maintain Bad, Bak and Bax expression, although Bax expression was decreased below the levels seen in unstimulated cells at 8 h (Figure 3.10 and 11). By contrast, anti-CD40 treatment was found to maintain or increase the expression of all anti-apoptotic Bcl-2 family members (Bcl-2, $BclX_L$, A1, Mcl-1, Figure 3.10) tested whereas although this also occurred for Bak (8 and 24 h) and Bax (8 h) expression at the early time points, by 48 h their expression was suppressed (Figure 3.10). Bad expression was profoundly reduced by anti-CD40 treatment at all time points examined (Figure 3.10). Interestingly, under conditions of CD40-mediated rescue of BCR-driven apoptosis, $BclX_L$ (but not Bcl-2, A1 and Mcl-1) expression was restored and Bad, Bak and Bax suppressed suggesting these elements played a role in regulating BCR-mediated apoptosis and CD40-rescue (Figure 3.10 and 11). Moreover, following CD40 engagement there is an increase in $BclX_L$/Bak (Figure 3.12 C) as well as BclX/Bak complexes (Figure 3.12 D). This suggests that the pro-apoptotic

molecule Bak may be sequestered by $BclX_L$ and hence prevents the formation of pro-apoptotic Bax/Bak oligomers following coligation of CD40.

3.4.4. Constitutive activation of the Ras pathway can provide protection from BCR-induced growth arrest and apoptosis at 24 h

A pivotal role for the sustained, cycling ERK signal in the control of both proliferation and apoptosis in WEHI 231 cells has been reported by this laboratory (275). One of the key upstream regulators of ERK activity is the small GTPase, Ras, which regulates growth in all eukaryotic cells. The mechanisms involved in regulating such sustained ERK activity and its role in proliferating WEHI 231 cells was further explored utilising WEHI 231 cells expressing constitutively active Ras mutant constructs (Figure 3.5). Figure 3.23 A shows the large increase in basal ERK activation resulting in WEHI 231 cells expressing the RasV12 mutant as compared to that observed in wild type WEHI 231 cells and this demonstrates successful functional expression of Ras in this mutant cell line. The effect of such Ras activation on anti-Ig induced apoptosis and growth arrest was investigated. At 24 h there is no growth arrest or apoptosis in the RasV12 WEHI 231 cells in response to anti-Ig treatment (Figure 3.24 A). This ability of the expression of RasV12 to overcome anti-Ig mediated apoptosis and growth arrest in not surprising as this mutation has been shown to result in transformation in a number of cell types and Ras has been shown to be important in positive proliferative signalling (323). Perhaps more surprisingly however, expression of RasV12 does not reflect constitutive ERK activation. Rather expression of RasV12 construct maintains the late cycling activation of ERK regardless of anti-Ig treatment providing an explanation for the lack of growth arrest (Figure 3.24 B). This demonstrates that regulatory elements capable of dephosphorylating and inactivating ERK, such as Pac1, are still induced in this mutant cell line and perhaps act to limit proliferation. Indeed this data suggests that Pac1 is likely to be induced in a ERK-dependent manner. Interestingly, the RasV12 C40 cells, which direct Ras signals via the PI-3 kinase pathway, affords an enhanced level of protection against anti-Ig induced growth arrest over and above the protection seen in RasV12 cells (Figure 3.26 B). Costimulation of cells expressing RasV12 C40 with anti-Ig and anti-CD40 results in proliferation levels higher than untreated

cells. However, RasV12 S35 cells, in which Ras transduces signals only via the MAP kinase pathway, does not have significantly different BCR or CD40-mediated responses when compared to the RasV12 mutant cell line (Figure 3.26 A). Interestingly, parallel studies in this laboratory have shown that expression of RasV12 C40 also results in cycling ERK activation suggesting that PI-3 kinase activation can result in ERK signalling possibly via AKT or PKC intermediates (405).

Further to this rescue from growth arrest, there is also protection from dissipation of the MMP 24 h following anti-Ig treatment (Figures 3.27 and 28). All RasV12 expressing cells, as well as MEKK3 expressing cells, provided some protection from anti-Ig induced dissipation of the MMP (Figures 3.27, 28 and 29 C). The mechanism for maintenance of the MMP, at least in RasV12, RasV12 C40 and MEKK3 mutants, may involve the activation of AKT, which when activated (phosphorylated) acts to phosphorylate Bad and hence prevent pro-apoptotic Bad signalling. In wild type cells anti-Ig treatment is associated with reduction in active AKT levels (Figure 3.32) however both the RasV12 and MEKK3 mutants do not display reduced AKT signalling at 24 h (Figure 3.32) suggesting that AKT regulation of Bad may, at least in part, act to prevent the dissipation of the MMP.

To further investigate the role of PI-3 kinase, we utilised mutant forms of an antagonist of PI-3 kinase activity, SHIP (Figure 3.6). SHIP antagonises the functions of PI-3 kinase by dephosphorylating the 5' position of PIP_3, a product of PI-3 kinase that is important for the membrane localisation of many PH domain containing proteins. However, our results using two distinct mutant forms of SHIP which interfere with SHIP activity, by either competing for SH2 domain interactions (SHIP SH2) or competing for SH2 interactions as well as substrate binding (SHIP CI), suggest that SHIP does not play a significant role in the regulation of anti-Ig induced growth arrest or apoptosis in WEHI 231 cells (Figure 3.23). By contrast, in mature B cells SHIP has been shown to play a major role in the FcγRIIb mediated inhibition of BCR induced proliferative signalling (256). A role for the 3'-inositol phosphatase, PTEN, in FcγRIIb mediated inhibition of BCR induced proliferative signalling has recently been demonstrated in this laboratory, suggesting that B cells are capable of

antagonising PI-3 kinase activity via the recruitment of both 3'- and 5'-inositol phosphatases (124). Therefore, perhaps in WEHI 231 cells, inhibition of SHIP by the overexpression of a catalytically inactive mutant or its SH2 domain does not lead to an observable effect as the levels of PIP_3 can still be reduced by the 3'-inositol phosphatase activity of PTEN. It would be very interesting to assess the activity of PTEN in WEHI 231 cells under different conditions, by expressing various mutant constructs, to determine whether or not it plays a role in regulating responses in WEHI 231 cells. An alternative possibility is that the action of SHIP may be compensated for by SHIP2, therefore it would be interesting to produce double SHIP/SHIP2 knock outs to assess the relative contribution of both of these proteins to BCR-induced growth arrest and apoptosis of WEHI 231 cells.

3.4.5. Constitutive activation of the RasERKMAPK pathway can enhance BCR-induced growth arrest and/or apoptosis at 48 hours

Although expression of all 3 RasV12 constructs protected against BCR-mediated growth arrest at 24 h there is no longer any protection from anti-Ig induced growth arrest and apoptosis, in fact there is enhanced apoptosis in response to ligation of the BCR in RasV12 cells by 48 h (Figure 3.23). Furthermore, at 72 h the RasV12 mutant does not display any enhanced proliferation as compared to empty vector cells regardless of the stimulation used (Figure 3.24 C). This is very surprising, as ERK activation has been demonstrated to be a pivotal consideration in the maintenance of survival and proliferation in WEHI 231 cells and Ras activation would, in turn, activate ERK. Consistent with this, at 48 h the MMP is maintained in RasV12, RasV12 S35, RasV12 C40 and MEKK 3 cells following BCR ligation (Figures 3.27, 28 and 29 C). Additionally, when the cells are left unstimulated the basal levels of apoptosis in both the RasV12 and MEKK3 cells are lower than empty vector cells (Figure 3.24 C and 3.29 A).

However, under conditions of anti-Ig stimulation increased levels of ERK would also be capable of activation of PLA_2 and there have been recent reports that PLA_2 can downregulate c-Myc expression by interacting with the nuclear transcription factor B-Myb (448). The interaction of $cPLA_2$ and B-Myb in the

cytoplasm facilitates translocation and activation of PLA_2 in the nucleus and these nuclear complexes inhibit B-Myb- dependent transcriptional upregulation of c-Myc (448). Furthermore, ATP-depletion, as seen in WEHI 231 cells following BCR- mediated apoptosis (156), can actually facilitate nuclear translocation of PLA_2 (449) and Tip60, an acteyltransferase which forms complexes with $cPLA_2$ that has been demonstrated to induce apoptosis (450). Taken together with the fact that we have demonstrated $cPLA_2$ translocation to the nucleus 3 h post BCR stimulation in WEHI 231 cells (156) this suggests that nuclear PLA_2 downmodulation of c-Myc may contribute to BCR-mediated growth arrest and apoptosis. Constitutively active Ras signalling may enhance anti-Ig mediated ERK and thus PLA_2 signalling resulting in strong inhibition of c-Myc transcription. This may result in the superinduction of BCR-driven apoptosis seen in RasV12 cells and the rescue of growth arrest at 24 h may simply reflect the induction of apoptosis in WEHI 231 cells is slow, requiring 24-48 h to take effect.

Furthermore, we have not ruled out the possibility that Ras activation may activate pro-apoptotic signalling systems at later time points. Ras activation has been implicated in induction of apoptosis in both the phaechromocytoma cell line PC12 and in T cells following IL-2 deprivation depending on the context of the Ras signalling (451-453). Interestingly, although apoptosis is increased at 48 hours there is still protection of the MMP. This suggests that anti-Ig mediated apoptosis in RasV12 mutants may be occurring via a different apoptotic pathway to that of wild type cells or that expression of the RasV12 construct slows the kinetics of the loss of mitochondrial integrity. Therefore it would be very interesting to investigate the caspase activation profile as well as effects of caspase, calpain and cathepsin inhibitors on these mutants.

Having ascertained that the constitutive activation of Ras does not necessarily lead to the constitutive activation of the downstream signalling components, such as ERK, Dok was investigated as a possible important regulator of Ras signalling in BCR-stimulated WEHI 231 cells. Dok is a well characterised negative regulator of Ras and in B cells has been shown to negatively regulate ERK activation by the BCR by abrogating Ras activation (342) (Figure 3.6). It might therefore be predicted that WEHI 231 cells expressing the Dok PH/PTB

dominant negative mutant construct could respond in much the same way as those expressing the RasV12 mutant construct due to a sustained activation of Ras. However there was no evidence for a release from anti-Ig induced growth arrest at 24 h (Figure 3.33) and also no observable differences anti-CD40 mediated rescue (Figure 3.34). This would suggest that signalling events downstream of Ras/Dok signalling are key to mediating ERK-driven growth and proliferation in WEHI 231 cells.

Similarly, WEHI 231 cells expressing the MEKK3 mutant are also susceptible to anti-Ig induced growth arrest at 48 h, although unlike the RasV12 WEHI 231 cells these cells are protected from anti-Ig induced apoptosis (Figure 3.29 A). However, there is greatly reduced proliferation in MEKK3 WEHI 231 cells following anti-Ig treatment relative to the RasV12 WEHI 231 cells (Figure 3.29 A) even when cells are left unstimulated or treated with anti-CD40 (Figure 3.30). This suggests that the enhancement of the p38, JNK and ERK pathways simultaneously does not result in enhanced proliferation or survival. Indeed, both JNK and p38 are generally implicated as pro-apoptotic signalling cascades however all of the MAP kinases have been reported to be activated following BCR and/ or CD40 ligation in immature B cells (307, 454, 455). Nevertheless, although ERK activation has been associated with both survival and proliferation in WEHI 231 cells (275) there was no evidence from this laboratory to suggest activation of either JNK or p38 pathways (320). However recent reports have suggested that BCR and CD40 ligation may lead to different patterns of the type or kinetics of MAP kinase family activation depending on the maturation state of the cell (307, 454). Therefore this suggests that it is the overall balance of MAP kinase activation that determines B cells fate and the aberrant activation of all the MAP kinase pathways in the MEKK3 mutant cell line, perhaps not surprisingly, appears to prevent normal proliferative responses.

3.4.6. Potential roles for the PKC family in both BCR-induced growth arrest and apoptosis and CD40-mediated rescue

3.4.6.1 PKC α

PKC α is a classical PKC that has been implicated in maintenance of cell survival and proliferation. Both PKCα CAT and PKCα KR mutants resulted in

the partial rescue from both BCR mediated-growth arrest (Figures 3.37). Moreover, cell cycle analysis at 48 h revealed a reduction in apoptosis in both PKCα CAT and PKCα KR cells associated with an increase in the percentage of cells in mitogenic phases of the cell cycle (Figures 3.38). Additionally both PKCα CAT and PKCα KR expressing WEHI 231 cells provided protection from dissipation of the MMP in response to BCR ligation (Figures 3.41). Interestingly, WEHI 231 cells expressing PKCα mutant constructs appear to be growth arrested in G2/M phase rather than proliferating, as there is no increased cell division induced by BCR ligation (Figure 3.39). WEHI 231 cells expressing PKCα mutant constructs also exhibited decreased proliferation in response to anti-CD40 suggesting a role for PKC α in the regulation of anti-CD40 mediated rescue (Figure 3.39).

Surprisingly, PKCα CAT and PKCα KR WEHI 231 cells demonstrated very similar effects. These results were initially surprising as PKC α has been implicated as an essential factor for Ramos-BL B cell survival (367). Therefore it may have expected that, whilst use of the PKC αCAT construct may have been protective, use of the kinase dead PKC α mutant would have stimulated both growth arrest and apoptosis. Whilst a reduction in proliferation was observed at 72 h (Figure 3.39), there was a decrease in apoptosis at 48 h (Figure 3.38). Moreover, in a similar fashion to PKC αCAT, PKC αKR WEHI 231 cells displayed enhanced proliferation following BCR ligation at 24 h relative to wild type controls (Figures 3.37 A) although they were unable to rescue at later time points (Figures 3.37 to 39).

Nevertheless, although the Ramos-BL cell line seems to use PKCα signalling to maintain survival, it is clear that PKCα produces cell type specific effects. For example the activation of PKCα can induce apoptosis of cells by inhibiting AKT in LNCaP prostate cancer cells. Indeed, induction of PKCα leads to the activation of PP2A, which can dephosphorylate and inhibit AKT (430). By contrast, PKCα can also mediate its effects by promoting the activation of Ras. For example, in mast cells, ligation of FcεRI leads to the induction of Syk, which can phosphorylate Tyr^{658} of PKCα and Tyr^{662} of PKCβ1. The resultant phospho-tyrosine residues can interact with the SH2 domain of Grb-2 and hence promote

the formation of the Grb-2/SOS complex, leading to the induction of Ras and downstream effectors including ERKMAPK which can promote proliferation (456). Therefore PKCα may produce different effects depending on the period of stimulation and cell type used.

However, more puzzling is the fact that both constitutively active and kinase dead forms of PKC α seems to have the same effects on WEHI 231 cells. The PKCα CAT mutant consists of a constitutively active catalytic domain whereas the PKCα KR mutant is the full length PKC enzyme with a point mutation inactivating the kinase domain. The observation that both mutants produce the same biological outcome suggests that in WEHI 231 cells the catalytic activity of PKCα may not always be essential for PKCα mediated functions. This is not an isolated example of PKCα signalling that is independent of kinase activity. For example, in IFNγ-primed U937 cells, PKCα assists the activation of PLD1 following ligation of FcγRI by directly binding to PLD1 in a PKCα kinase-independent manner. Indeed, inhibition of PKCα kinase activity does not prevent FcγRI-mediated induction of PLD1 whereas downregulation of PKC α levels does impair PLD1 activation. FcγRI-dependent induction of PLD1 thus requires the recruitment of PKCα but PKCα kinase activity is not necessary indicating PKCα can perform important signalling functions independently of its kinase activity (457).

Interestingly, although the biological responses are similar in both the PKCα CAT and PKCα KR expressing cells it has recently emerged that there are differences in the mechanisms used to produce these responses suggesting that not all PKCα effects are independent of the PKCα kinase domain. For example, parallel studies in this laboratory revealed that the PKCα CAT WEHI 231 cells were able to maintain sustained, cycling ERK activity following BCR ligation whilst the PKCα KR WEHI 231 cells were not (405) and this correlates with the data displaying enhanced DNA synthesis following BCR ligation (Figure 3.37). By contrast, there was enhanced $BclX_L$ expression in cells expressing either PKCα mutant construct (405) which may explain the decreased levels of subdiploid populations following BCR ligation.

3.4.6.2 PKC δ

Similar effects were found in WEHI 231 cells expressing constitutively active and kinase dead forms of PKC δ. In WEHI 231 cells, PKCδ CAT acts to protect cells from apoptosis in response to ligation of the BCR and prevent BCR-mediated growth arrest (Figures 3.42 and 43) and dissipation of the MMP (Figure 3.44). In addition, PKCδ CAT expression delays the expression of the pro-apoptotic Bcl-2 family member Bad (Figure 3.53). This suggests that PKC δ is involved in the maintenance of cell survival. Puzzlingly, PKCδ KR expressing cells also display reduced growth arrest at 24 h, reduction in anti-Ig induced apoptosis (although this is much less impressive than the rescue observed in PKCδ CAT WEHI 231 cells) and a delay in dissipation of the MMP in response to BCR ligation (Figures 3.42 to 44).

PKCδ$^{-/-}$ knock out mice have both increased numbers of naïve and activated B lymphocytes and increased B cell expansion (385, 386). In addition these mice exhibit a severe lupus like autoimmune disease. This suggests, that in mature B cells, PKC δ is essential for keeping B lymphocyte proliferation within normal levels and regulating B cell tolerance. However these data for WEHI 231 cells suggest that PKC δ can have an anti-apoptotic, positive regulatory rather than anti-proliferative, negative regulatory role in immature B cells. In agreement with this, parallel studies in this laboratory demonstrated that the PKCδ CAT expressing cells exhibited enhanced expression of BclX_L and maintained a sustained cycling ERK signal following BCR ligation (405) which would be associated with both increased survival and proliferation. Consistent with this, PKCδ CAT cells also failed to induce p27 is response to BCR ligation (458) a response which is opposite to the response seen in empty vector WEHI 231 cells. Such an increase in p27, a cyclin dependent kinase inhibitor, is associated with growth arrest and this loss of p27 induction may represent one mechanism used to rescue PKCδ CAT cells from apoptosis and growth arrest.

3.4.6.3 PKC ε

WEHI 231 PKCε CAT and PKC ε KR cells were similarly found to be rescued from apoptosis and growth arrest induced by BCR ligation prior to 48 h (Figures

3.45-47) and this was also associated with maintenance of the MMP following ligation of the BCR (Figure 3.48).

The current literature suggests that PKCε generally acts as a positive regulator of cell survival and proliferation. For example, PKCε has been shown to activate the Raf-1/ERK pathway (387), thus promoting the activation of the key survival factor NF-κB (388). PKCε may also promote cell survival by contributing to the activation of AKT, a protein kinase that mediates PI-3-kinase survival signals (389). PKCε appears to play a role in cell proliferation also, as it is activated in response to a variety of mitogens (390, 391). This would suggest that PKCε is an essential molecule for the transduction of cell survival and proliferative signals in WEHI 231 cells. In agreement with this a parallel study in this laboratory found that PKCε CAT, but not PKCε KR, cells maintained their sustained cycling ERK activation following ligation of the BCR (405). However this is at odds with my data that demonstrates enhanced survival but not proliferation in PKCε CAT WEHI 231 cells at 48 and 72 h.

3.4.6.4 PKC ζ

PKCζ has been implicated in BCR signalling and B cells derived from mice defective in PKCζ have decreased activation of both ERK and NF-κB resulting in defective activation, reduced proliferation and spontaneous apoptosis (368, 398, 399). However the data from the WEHI 231 cells expressing PKCζ CAT and PKCζ KR are confusing. For example, constitutive activation of PKCζ results in both a partial protection from BCR-induced apoptosis and a reduction CD40-stimulated proliferation (Figures 4.49 to 51). Moreover, the pro-apoptotic Bcl-2 family member Bid is also expressed suggesting that PKCζ can mediate pro-apoptotic signals (Figure 4.53). Again the kinase dead mutant PKCζ KR induces similar effects to those of PKCζ CAT expressing cells suggesting that catalytic activity may not be essential for some PKCξ mediated functions. Indeed, PKCζ KR also results in protection from BCR-induced growth arrest at 24 h (Figure 3.49). These latter data seem to partially agree with the current literature, as it might have been predicted that both apoptosis and a reduction in proliferation would result from use of the kinase dead mutant. We do see a

reduction in proliferation in response to anti-CD40 and an increase in pro-apoptotic Bcl-2 family members. However, BCR ligation results in a reduction in apoptosis in both PKCζ CAT and PKCζ KR expressing cells.

Collectively, these data using CAT and KR forms of PKC isoforms suggests that PKCs α, δ, ε and ζ may have some activities which are independent of their catalytic action. However, although the functional responses of cells expressing the CAT and KR constructs are similar, in parallel studies we have obtained some evidence to suggest that the CAT and KR mutants have differential effects on downstream effector molecules such as ERK. Another possible explanation comes from the structure of these mutants in relation to the structure of native PKCs. For example, the regulatory domains of PKCs are responsible for the binding of receptors for activated C kinases (RACKs), a family of anchoring proteins that determine the ultimate sub-cellular locations of PKCs after activation (459). The CAT mutants used in this study lack their regulatory domains, therefore it is possible that they are not targeted to their correct sub-cellular locations. This could result in lack of phosphorylation of the appropriate targets, or even phosphorylation of inappropriate targets, as the constructs are not able to interact with the correct substrates, or are not targeted to the same area within the cell as their intended substrates. If the appropriate substrates are not phosphorylated, this may go some way to explaining the surprising similarity of the effects of both PKC CAT and KR mutant constructs.

This study has highlighted an unexpected problem associated with the investigation of the action of a given protein by simply overexpressing mutant forms of the signalling element. In order to elucidate fully the actions of different PKC isoforms we could use specific inhibitors of PKC isoforms however this would still provide problems as there are not specific inhibitors available for most isoforms. Perhaps in future studies we could utilise anti-sense DNA technology to reduce PKC activity without the attendant problems of overexpression of the proteins. In addition this study has also emphasised the importance of time courses to investigate cellular functions. Some of the effects seen in this study were only occurring at defined time points and simple experiments only investigating responses at 24 or 48 h would have missed

these effects completely. I set out to use both CAT and KR PKC isoform constructs to corroborate each other, as we expected one form to be a stimulant and the other to antagonise cellular function. However, this study has ultimately provided more questions than answers to the role of PKC isoforms in BCR-mediated growth arrest and apoptosis in WEHI 231 cells and its rescue by CD40 signalling.

3.4.7 Concluding Remarks

In conclusion, the key findings of this chapter are that BCR-mediated apoptosis is dependent on the generation of arachidonic acid, abrogation of the sustained ERK signal and induction of Bcl-2 pro-apoptotic family members. Moreover, CD40-mediated rescue of BCR-induced apoptosis and growth arrest can reverse each of these processes.

The results in this chapter demonstrate that anti-Ig initiated apoptosis is mediated by the generation of arachidonic acid by PLA_2. In addition, the CD40-mediated generation of prostaglandins/leukotreines by COX2 and LOX, and hence degradation of arachidonic acid, provides a dynamic switch mechanism for switching on/off the cycling ERK signal that mediates proliferation in WEHI 231 cells (Figure 3.54). Moreover, there is a BCR-driven upregulation of pro-apoptotic Bcl-2 family members such as Bak and Bax and a downregulation of anti-apoptotic Bcl-2 family members such as Bcl-2 and $BclX_L$. Rescue by CD40 engagement involves the upregulation of $BclX_L$, which has a two-fold protective mechanism. Firstly it acts to protect from arachidonic acid-mediated loss of mitochondrial membrane integrity presumably by forming homo-dimers at the mitochondrial membrane, and secondly by sequestering Bak and hence, preventing Bak from stimulating the opening of the mitochondrial transition pore.

Consistent with the proposal that sustained, cycling ERK is required for proliferation, constitutive activation of Ras, and hence ERK, can provide relief from both anti-Ig induced growth arrest and apoptosis within the first 24 h. Further investigation has revealed that neither SHIP nor Dok appear to affect such Ras-dependent BCR signalling in a non-redundant manner. However after 24 hours there is a superinduction of apoptosis in cells expressing the RasV12 mutant construct. This may reflect that ERK signalling may result in induction of

nuclear translocation of both Tip60 and PLA_2 which form pro-apoptotic complexes (450).

Finally, studies involving mutant forms of PKC constructs have not provided any definitive answers as to which PKCs are involved in BCR-mediated apoptosis or CD40-mediated rescue. However, they do suggest that PKCs α, δ, ε and ζ merit further investigation.

Figure 3.1: BCR mediated apoptosis correlates with arachidonic acid mediated loss of mitochondrial membrane integrity.

In WEHI 231 cells ligation of the BCR leads to a strong, early ERK signal which mediates activation and translocation of PLA_2 to the mitochondria and nucleus. PLA_2 generates arachidonic acid that correlates with dissipation of the MMP, depletion of ATP and activation of the executioner protease cathepsin B. Coligation of the BCR and CD40 leads to the upregulation of $BclX_L$ expression which can protect the mitochondrial membrane integrity and prevent apoptosis.

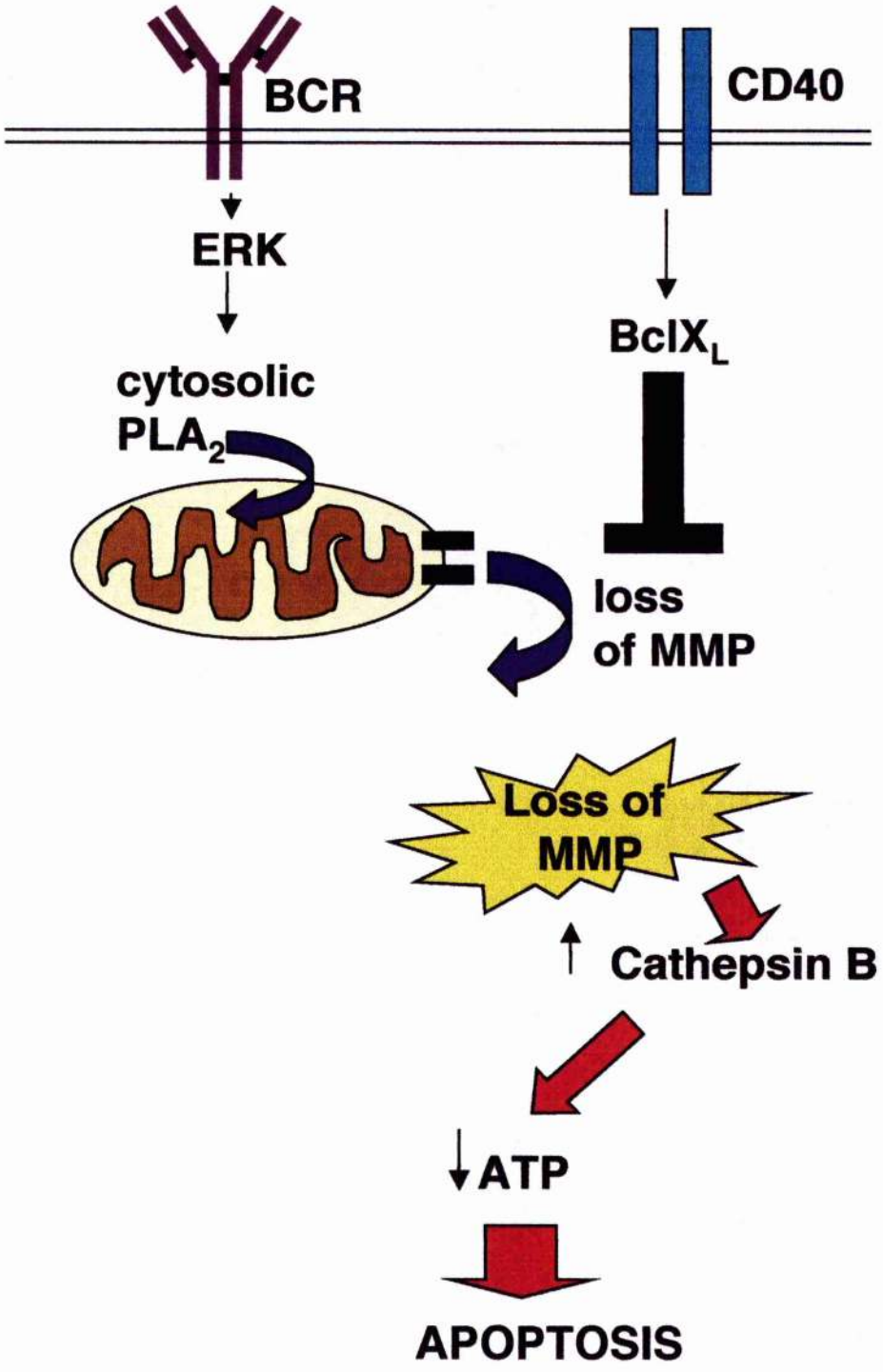
BCR
CD40
ERK
BclX$_L$
cytosolic
PLA$_2$
loss
of MMP
Loss of
MMP
Cathepsin B
ATP
APOPTOSIS

Figure 3.2: CD40 structure and signalling

The CD40 receptor is a 48-kDa transmembrane glycoprotein which is a member of the TNF receptor (TNFR) superfamily. CD40 consists of a 193 amino-acid extracellular domain, a 22 amino-acid transmembrane domain and a 62 amino-acid cytoplasmic domain. The extracellular domain consists of four homologous, repeating, cysteine-rich extracellular domains characteristic of TNFR family motifs. CD40 is known to associate with intracellular proteins termed TNF receptor-associated proteins (TRAFs). TRAF2, TRAF3 and TRAF 5 are known to associate with a specific region in the cytoplasmic domain of CD40 and stimulate transcription factors such as NF-κB to initiate transcription of pro-survival and pro-proliferation genes.

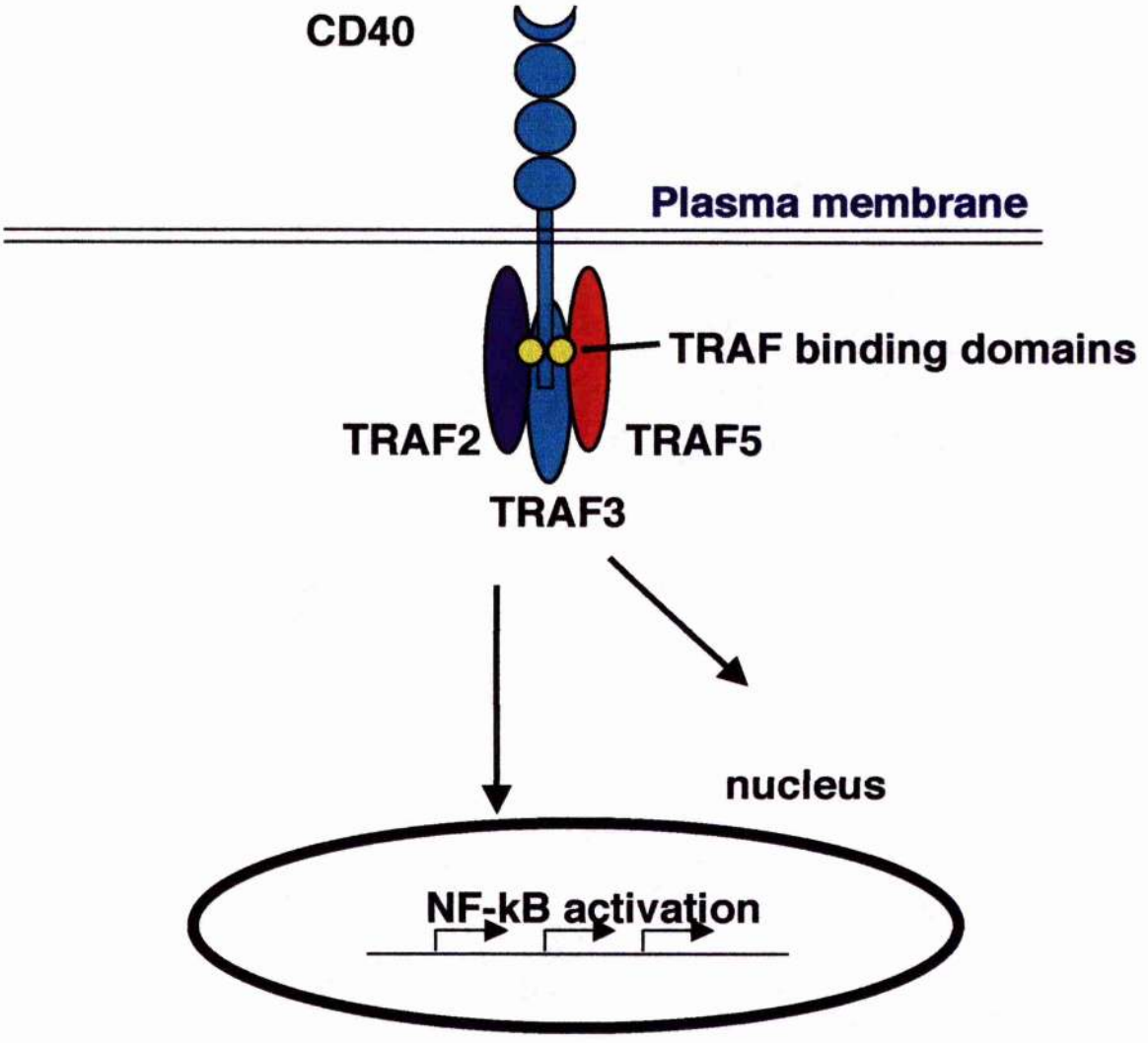
CD40
Plasma membrane
TRAF binding domains
TRAF2
TRAF5
TRAF3
nucleus
NF-kB activation

Figure 3.3: Schematic view of Ras regulatory factors

Ras proteins cycle between the active GTP- bound form and the inactive GDP-bound state. Guanine exchange factors (GEFs) such as GRF and SOS catalyse Ras activation by facilitating the dissociation of bound GDP. Free radicals such as nitric oxide can also promote Ras-GTP formation. Ras then remains active until it hydrolyses bound GTP to GDP. This process is accelerated by GTPase activating proteins such as p120 GAP.

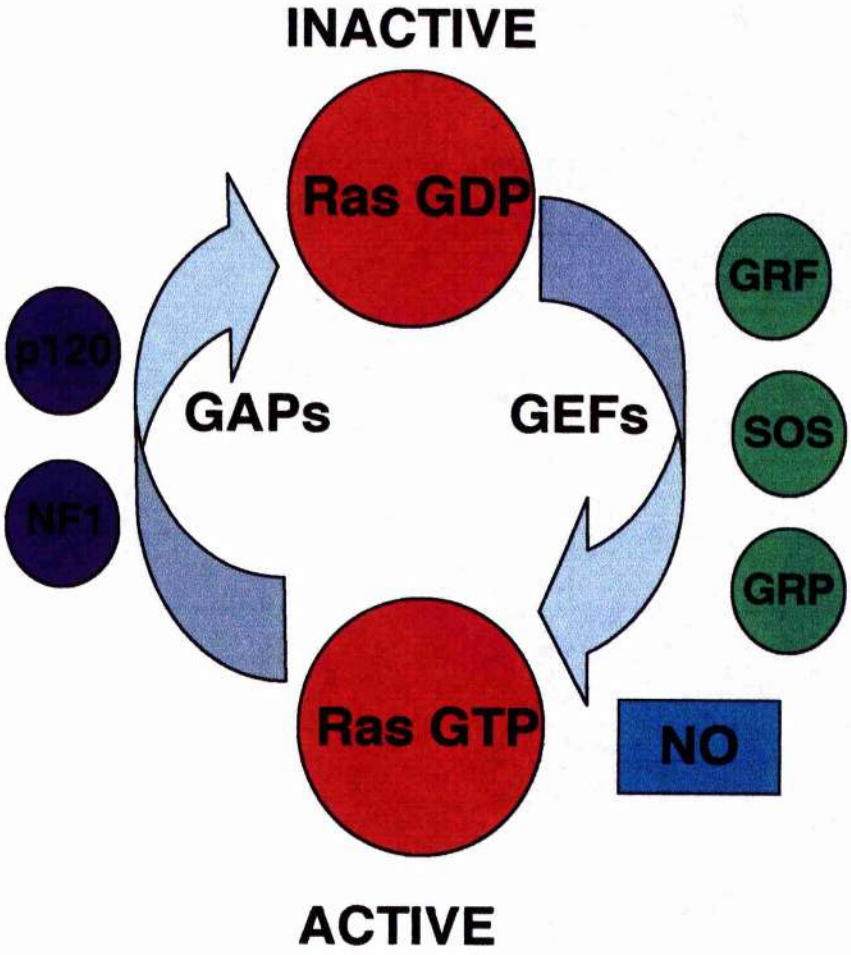
INACTIVE
Ras GDP
GRF
p120
GAPs
GEFs
SOS
NF1
GRP
Ras GTP
NO
ACTIVE

Figure 3.4: In fibroblasts, Ras follows a biphasic pattern of activation following stimulation with mitogen, each phase corresponding to activation of different effector molecules

Ras is required for both G1 entry and progression. Upon mitogen stimulation of quiescent cells there are 2 peaks of Ras activation. The first occurs immediately on entry into G1 and is associated with the activation of the Raf/MEK/ERK pathway. The second occurs at mid-G1 and corresponds to the activation of the PI-3 kinase/ AKT effector pathway. Ras activation is essential for mitogen stimulated upregulation of cyclin D1 and $p21^{Cip1}$ and downregulation of $p27^{Kip1}$ protein expression.

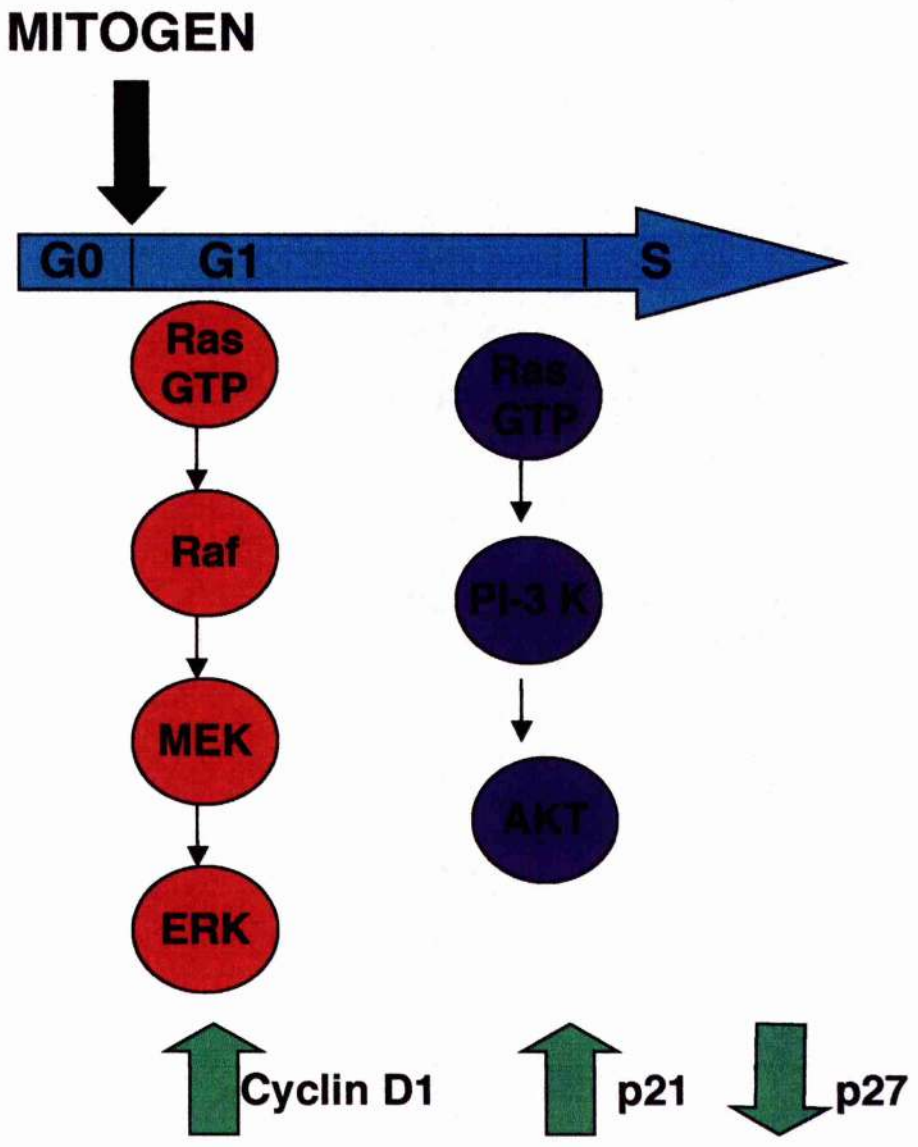
MITOGEN
G0
G1
S
Ras GTP
Raf
MEK
ERK
Ras GTP
PI-3 K
AKT
Cyclin D1
p21
p27

Figure 3.5: Use of the RasV12, RasV12 S35 and RasV12 C40 mutants allows for dissection of the Ras signals important in proliferation and apoptosis in WEHI 231 cells

In order to dissect the role of Ras signalling via the ERKMAP kinase and PI-3 kinase pathways we utilised several constitutively active Ras mutants. RasV12 is a constitutively active form of Ras, the consequence of a point mutation that results in the substitution of valine for glycine at position 12. This mutation disables the intrinsic GTPase activity of Ras, therefore once Ras binds GTP and becomes active it is unable to deactivate itself by hydrolysing GTP to GDP. RasV12 S35 contains a further point mutation in the effector domain of the protein, resulting in the substitution of serine for threonine. This mutation prevents Ras from binding the p110α subunit of PI-3 kinase, an interaction that is known to lead to the activation of PI-3 kinase. By contrast, RasV12 C40 contains a point mutation in the effector domain resulting in the substitution of cysteine for tyrosine. This mutation abrogates the interaction between Ras and Raf, preventing Ras from activating the ERKMAP kinase pathway.

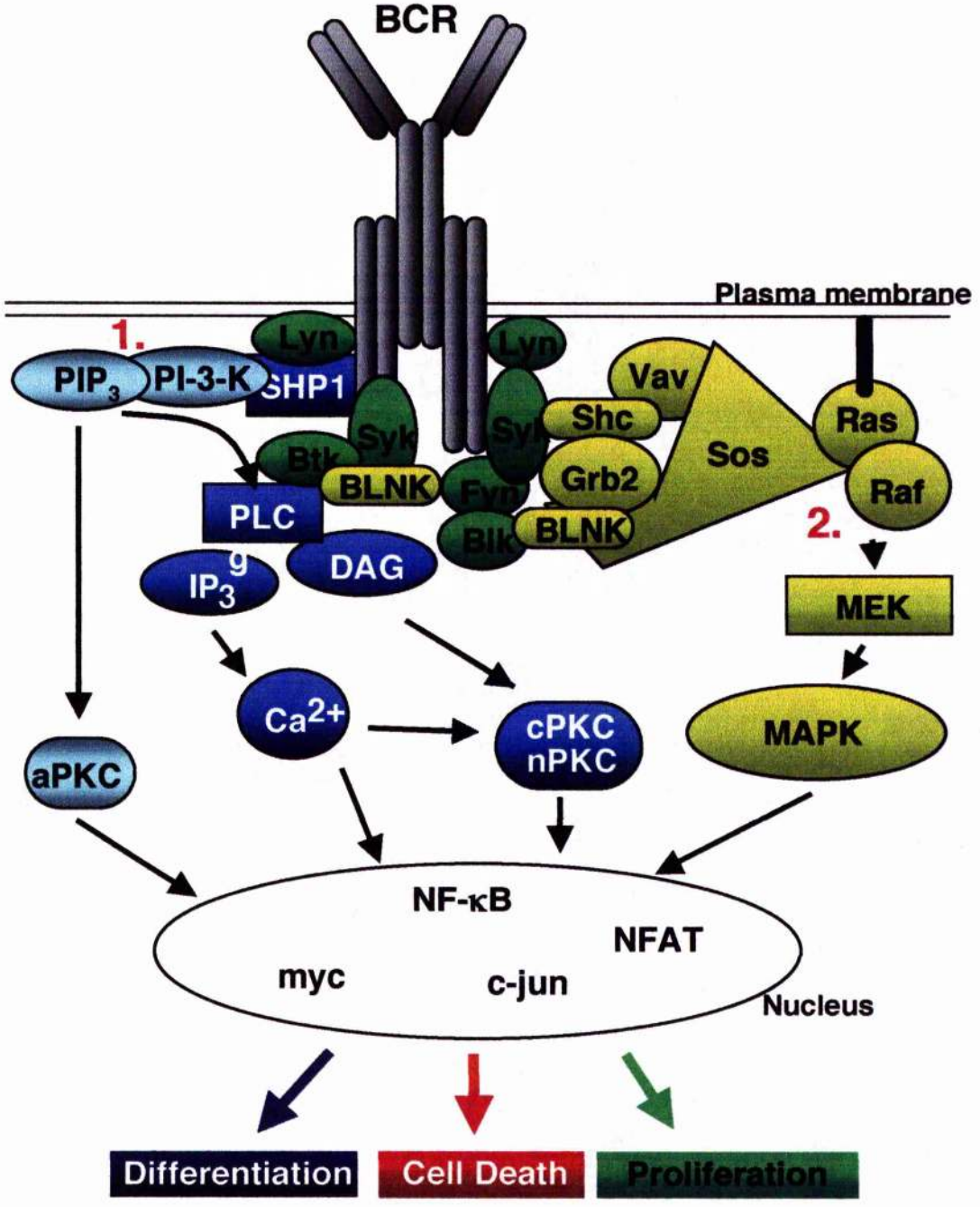

1. RasV12 S35
2. RasV12 C40

Figure 3.6: Dominant negative SHIP and Dok mutations allow for further dissection of the contributions of the MAP kinase and PI-3 kinase pathways

Dok acts to negatively regulate Ras in WEHI 231 cells. The Dok PH/PTB mutant lacks the proline rich regions of Dok and hence prevents normal protein interactions allowing us to assess the contribution of Ras in BCR mediated apoptosis and CD40 mediated rescue. SHIP has multiple actions including antagonizing the action of PI-3 kinase by degradation of PIP_3 and downregulation of the RasMAP kinase pathway by inhibition of SOS action. We utilised 2 SHIP mutants a catalytically inactive form of SHIP, SHIP CI, and a dominant negative form of SHIP, SHIP SH2, to assess the contribution of PI-3 kinase in BCR mediated apoptosis and CD40 mediated rescue.

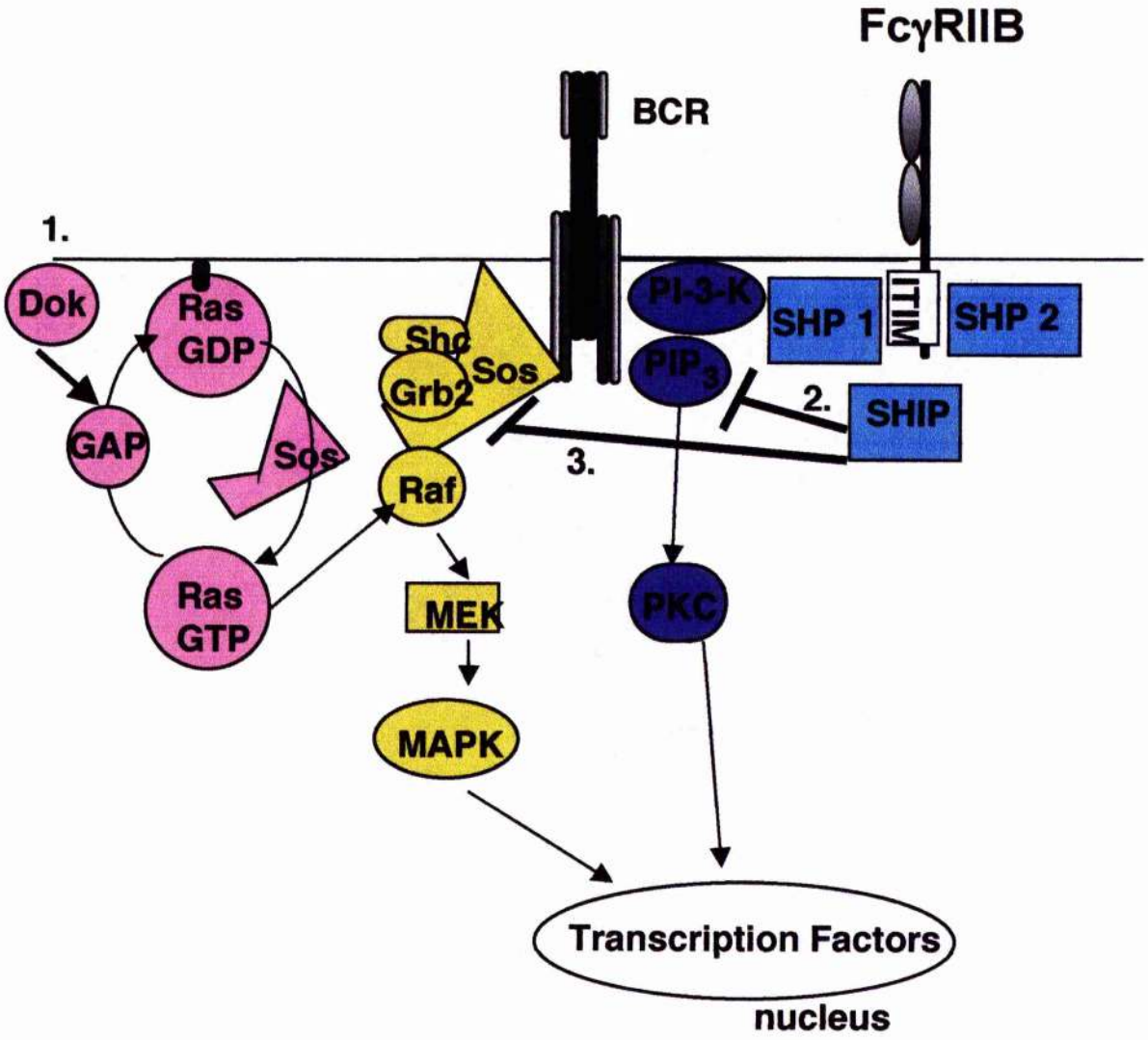

1. Dok PH/PTB
2. SHIP CI
3. SHIP SH2

Figure 3.7: In WEHI 231 cells ligation of the BCR with anti-Ig leads to growth arrest whereas coligation of both the BCR and CD40 results in proliferation

(A) All cells were cultured for 48 h and then DNA synthesis was assessed by [^{3}H] thymidine uptake. Cells were either treated with media alone (unstimulated), 10 μg/ml anti-Ig (aIg), or 10 μg/ml anti-Ig in combination with anti-CD40 (aIg & aCD40). These data are the mean of three separate wells ± SD. These data are from a single experiment, representative of five separate experiments.

(B) All cells were stained with 1 μM CFSE and then left in culture for 72 h with appropriate stimulations. Cells were either treated with media alone (No stimulation), 10 μg/ml anti-Ig (aIg), 10 μg/ml anti-CD40 (aCD40) or 10 μg/ml anti-Ig in combination with anti-CD40 (aIg & aCD40). Proliferation was assessed by an estimate of the percentage of cells in each cell generation. This calculation was done with the FlowJo proliferation data analysis programme. The data was then displayed as the mode generation for each stimulation i.e. the generation number containing the highest percentage of cells. The percentage of cells in the mode generation is displayed above the column. These data are from a single experiment, representative of three separate experiments.

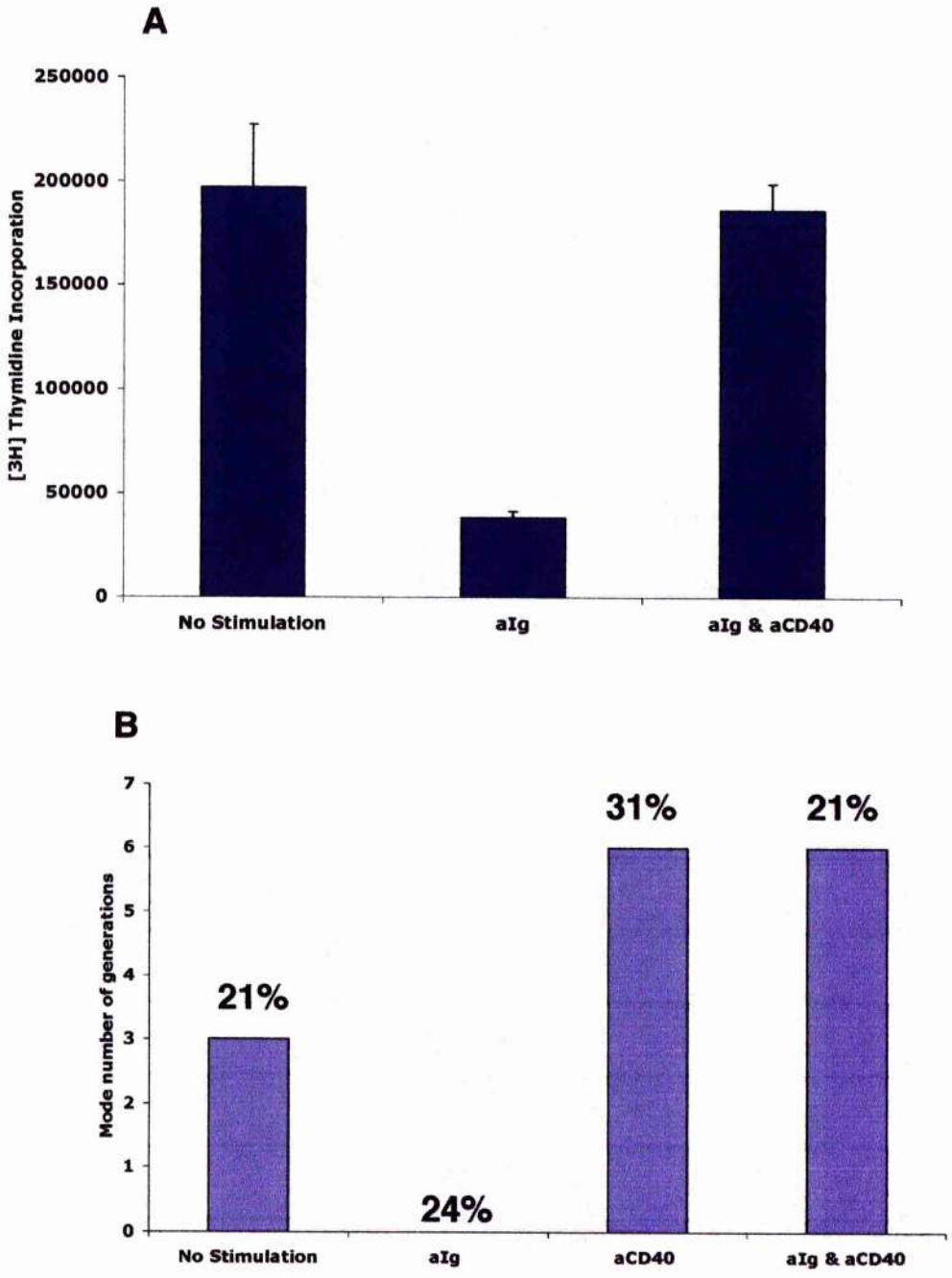
A
250000
200000
150000
100000
50000
0
[3H] Thymidine Incorporation
No Stimulation
aIg
aIg & aCD40
B
7
6
5
4
3
2
1
0
Mode number of generations
21%
24%
31%
21%
No Stimulation
aIg
aCD40
aIg & aCD40

Figure 3.8: Ligation of the BCR induces apoptosis whereas engagement of CD40 drives cells to enter the mitogenic phases of the cell cycle in WEHI 231 cells

(A) All cells were stained with 50 μg/ml PI after being in culture for 48 h with appropriate stimulations. Cells were either treated with media alone (None), 10 μg/ml anti-Ig (aIg), 10 μg/ml anti-CD40 (aCD40) or 10 μg/ml anti-Ig in combination with anti-CD40 (aIg & aCD40). FACS analysis was used to calculate the number of cells in G0/G1, S phase, G2/M phase and subdiploid cells. The data is displayed as the percentage of living cells in each live phase of the cell cycle and the percentage of subdiploid cells. These data are from a single experiment which is representative of 11 experiments.
(B) Cells were treated as described above. The data is displayed as a histogram of PI fluorescence (FL2). This data set is separate from the data shown in panel A.

A

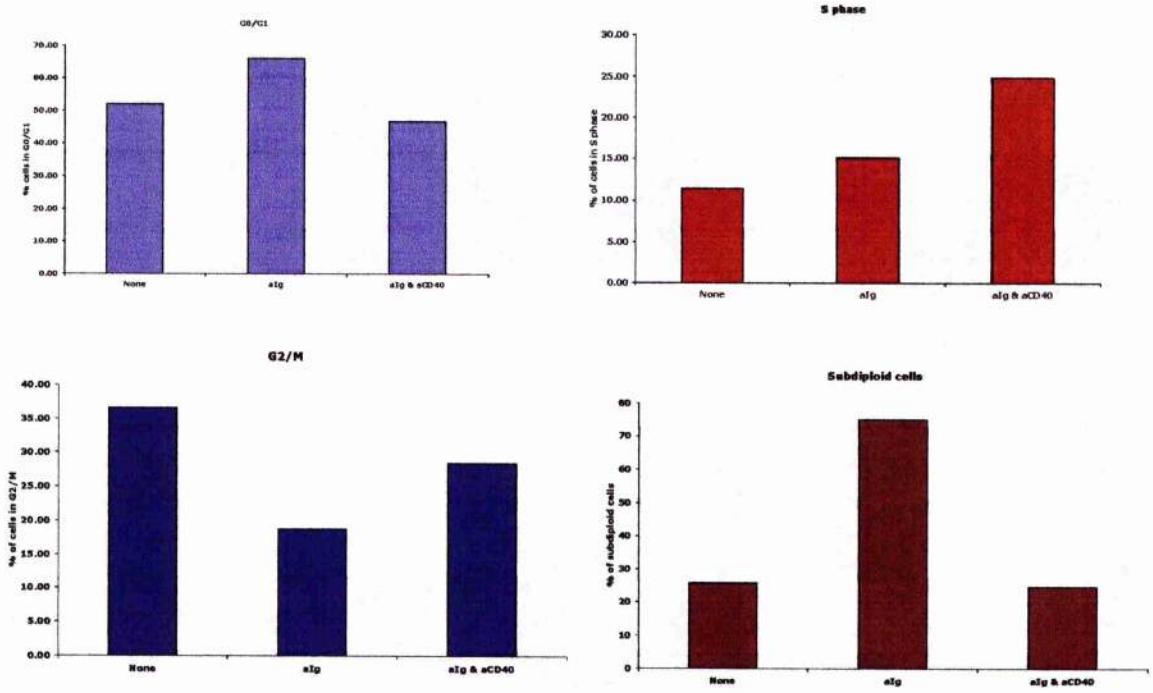

B

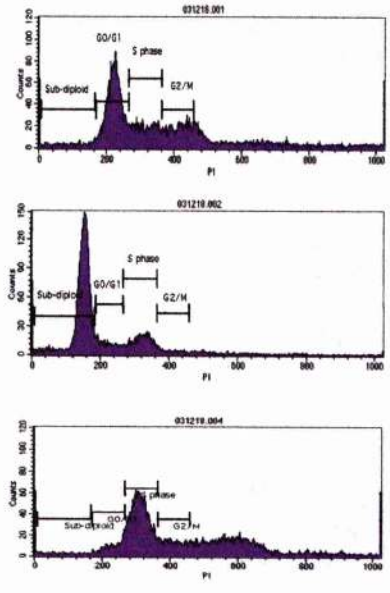

No Stimulation

BCR

BCR & CD40

Figure 3.9: Ligation of the BCR results in dissipation of MMP whereas coligation of CD40 prevents the loss of mitochondrial membrane integrity

(A) Cells were left in culture for 48 h with appropriate stimulations and then stained with 2.5 μM $DiOC_6$. Cells were either treated with media alone (None), 10 μg/ml anti-Ig (aIg), 10 μg/ml anti-CD40 (aCD40) or 10 μg/ml anti-Ig in combination with anti-CD40 (aIg & aCD40). Dissipation of MMP can been seen as a reduction in $DiOC_6$ brightness (FL1 fluorescence). Dissipation of the MMP was assessed by dividing the cells into two populations. The right hand peak having a high healthy MMP and the second having a low apoptotic MMP. The data was then displayed as the percentage of cells with a high MMP. These data are from a single experiment, representative of 4 experiments.
(B) Cells were treated as described above. The data is displayed as a histogram of $DiOC_6$ fluorescence (FL1). This data set is separate from the data shown in panel A.

A

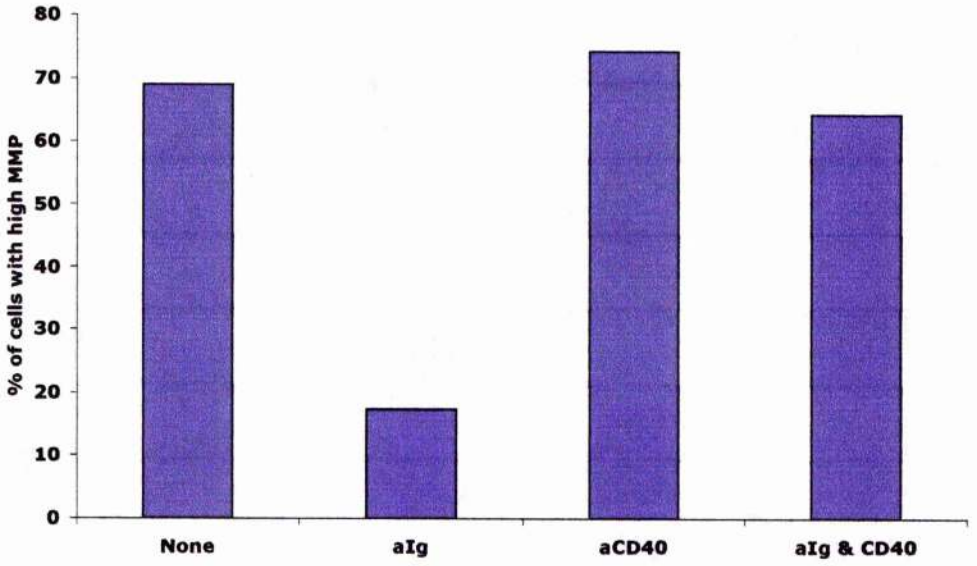
% of cells with high MMP
80
70
60
50
40
30
20
10
0
None
aIg
aCD40
aIg & CD40

B

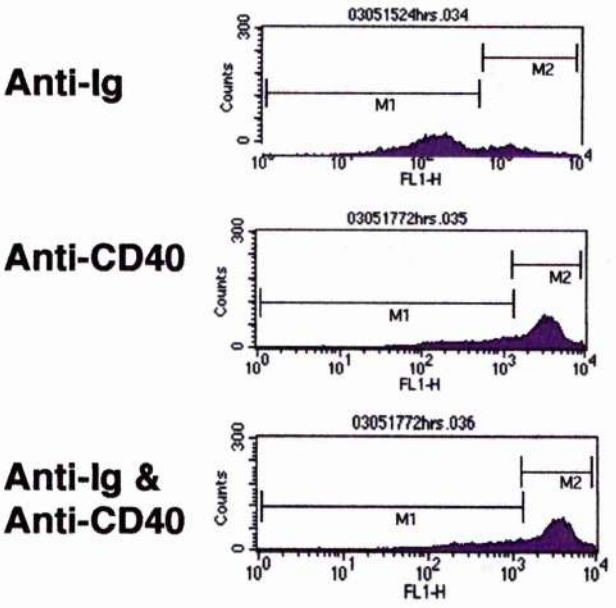
Anti-Ig
03051524hrs.034
M2
M1
Counts
FL1-H
Anti-CD40
03051772hrs.035
M2
M1
Counts
FL1-H
Anti-Ig &
Anti-CD40
03051772hrs.036
M2
M1
Counts
FL1-H

Figure 3.10: Ligation of the BCR induces the expression of the pro-apoptotic Bcl-2 family members Bad, Bak and Bax in WEHI 231 cells

Wild type WEHI 231 cells (10^7 cells/lane) were cultured with medium alone, anti-Ig 10 μg/ml, anti-CD40 10 μg/ml, a combination of anti-Ig 10 μg/ml and anti-CD40 10 μg/ml or arachidonic acid 100 μM for up to 48 h. Cell lysates were then prepared and analysed using gel electrophoresis and western blotting using Bad **(A)**, Bak **(B)** and Bax **(C)** specific Abs. Experimental conditions were as follows: lane 1, medium 0 h, lane 2, anti-Ig 8 h, lane 3, anti-CD40 8 h, lane 4, anti-Ig plus anti-CD40 8 h, lane 5, arachidonic acid 8 h, lane 6, anti-Ig 24 h, lane 7, anti-CD40 24 h, lane 8 anti-Ig plus anti-CD40 24 h, lane 9, arachidonic acid 24 h, lane 10, anti-Ig 48 h, lane 11, anti-CD40 48 h, lane 12, anti-Ig plus anti-CD40 48 h, lane 13, arachidonic acid 48 h and lane 14, medium 48 h .

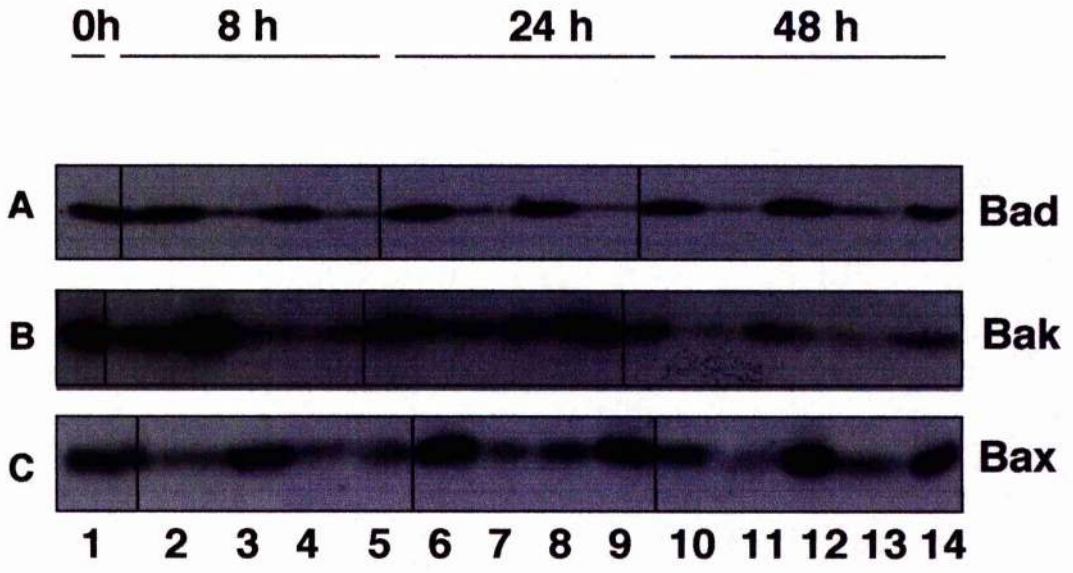
0h
8 h
24 h
48 h
A
Bad
B
Bak
C
Bax
1 2 3 4 5 6 7 8 9 10 11 12 13 14

Figure 3.11: Ligation of the BCR downregulates expression of Bcl-2, $BclX_L$ and Mcl-1 whereas coligation of CD40 alone rescues the expression of $BclX_L$ only

(A) Wild type WEHI 231 cells (10^7 cells/lane) were cultured with medium, anti-Ig 5 μg/ml or a combination of anti-Ig 5 μg/ml and anti-CD40 10 μg/ml for up to 48 h. Cell lysates were then prepared and analysed using gel electrophoresis and western blotting using A1, Bcl-2, $BclX_L$ and Mcl-1 Abs. Experimental conditions were as follows: lane 1, medium 0 h (C0), lane 2, anti-Ig 8 h, lane 3, anti-CD40 8 h, lane 4, anti-Ig plus anti-CD40 8 h, lane 5, anti-Ig 24 h, lane 6, anti-CD40 24 h, lane 7, anti-Ig plus anti-CD40 24 h, lane 8, anti-Ig 48 h, lane 9, anti-CD40 48 h, lane 10, anti-Ig plus anti-CD40 48 h, lane 11, medium 48 h (C48). Data are representative of a least 3 independent experiments.

(B) Wild type WEHI 231 cells were stimulated with anti-CD40 (10 μg/ml) for up to 48 h, cell lysates were prepared and western blotting of $BclX_L$ expression performed. Expression of $BclX_L$ in anti-CD40 treated wild type WEHI 231 cells was compared with that of unstimulated Neo cells or $BclX_L$ cells. The blot was stripped and probed fro ERK1/2 expression as a loading control. Data are representative of a least 3 independent experiments.

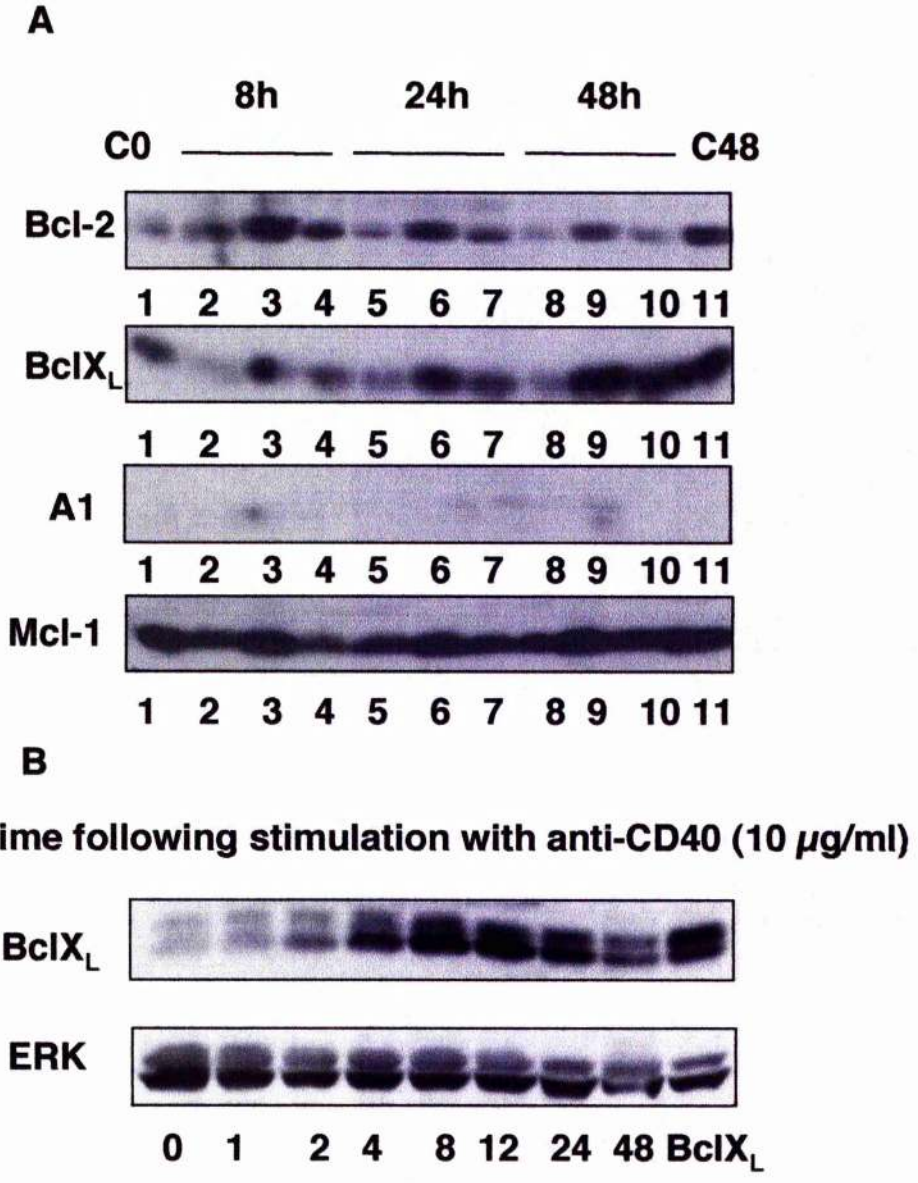
A
8h
24h
48h
C0
C48
Bcl-2
1 2 3 4 5 6 7 8 9 10 11
BclX$_L$
1 2 3 4 5 6 7 8 9 10 11
A1
1 2 3 4 5 6 7 8 9 10 11
Mcl-1
1 2 3 4 5 6 7 8 9 10 11
B
Time following stimulation with anti-CD40 (10 μg/ml)
BclX$_L$
ERK
0 1 2 4 8 12 24 48 BclX$_L$

Figure 3.12: Potential complexing of $BclX_L$ and Bak and under conditions of CD40-mediated rescue of BCR-coupled apoptosis

Wild type WEHI 231 cells (10^7 cells/lane) were cultured with medium, anti-Ig 10 μg/ml, anti-CD40 10 μg/ml, a combination of anti-Ig 10 μg/ml and anti-CD40 10 μg/ml, arachidonic acid or arachidonic acid and 10 μg/ml anti-CD40 for up to 48 h. Cell lysates were then prepared and used to make immunoprecipitates (IPs) with $BclX_L$ **(A)**, Bak **(B)** and Bad **(C)** specific Abs. These IPs were then used for gel electrophoresis and western blotting using BclX, Mcl-1, Bak, Bad, phospho-serine112-Bad or phospho-serine136-Bad specific Abs. The experimental conditions for $BclX_L$ **(A)** and Bak **(B)** IPs were as follows: lane 1, medium 0 h, lane 2, anti-Ig 8 h, lane 3, anti-CD40 8 h, lane 4, anti-Ig plus anti-CD40 8 h, lane 5, anti-Ig 48 h, lane 6, anti-CD40 48 h, lane 7, anti-Ig plus anti-CD40 48 h and lane 8, medium 48 h. The experimental conditions for Bad **(C)** IPs were as follows: lane 1, medium alone 48 h, lane 2, anti-CD40 48 h, lane 3, anti-Ig 48 h, lane 4, arachidonic acid 48 h, lane 5, anti-Ig and anti-CD40 48 h and lane 6, arachidonic acid and anti-CD40 48 h.

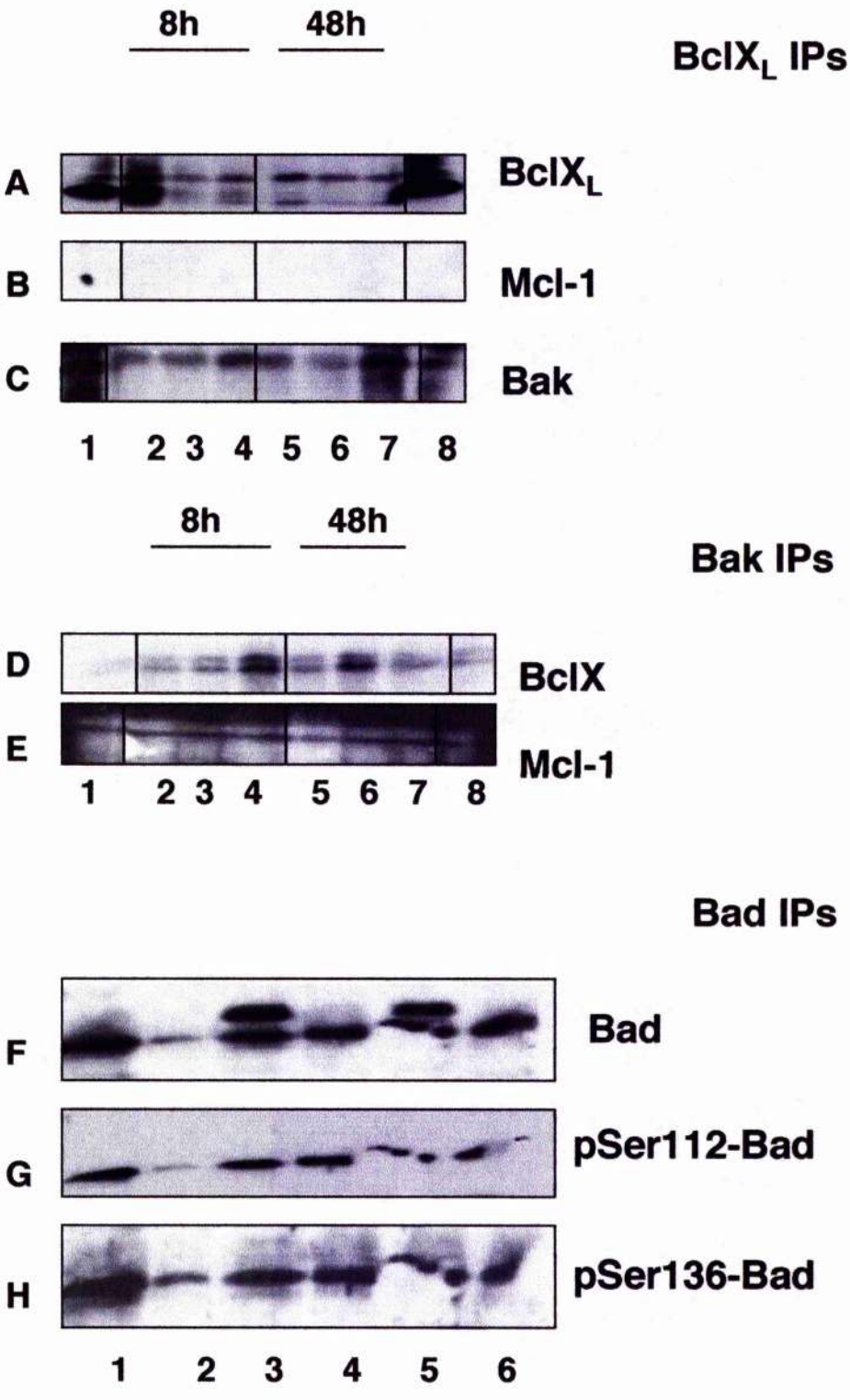
8h
48h
BclX$_L$ IPs
A
BclX$_L$
B
Mcl-1
C
Bak
1 2 3 4 5 6 7 8
8h
48h
Bak IPs
D
BclX
E
Mcl-1
1 2 3 4 5 6 7 8
Bad IPs
F
Bad
G
pSer112-Bad
H
pSer136-Bad
1 2 3 4 5 6

Figure 3.13: Overexpression of $BclX_L$ provides protection from both anti-Ig and arachidonic acid induced apoptosis

Neo and $BclX_L$ WEHI 231 cells were stained with 50 μg/ml PI after being in culture for 48 h with appropriate stimulations. Cells were either treated with media alone (unstimulated), 10 μg/ml anti-Ig (aIg), 10 μg/ml anti-CD40 (aCD40), 10 μg/ml anti-Ig in combination with anti-CD40 (aIg & aCD40), 100 μM arachidonic acid (AA) or 100 μM arachidonic acid in combination with 10 μg/ml anti-CD40 (AA & aCD40). FACS analysis was used to calculate the percentage of subdiploid cells. The data is displayed as the mean percentage of subdiploid cells from 13 independent experiments ± SEM.

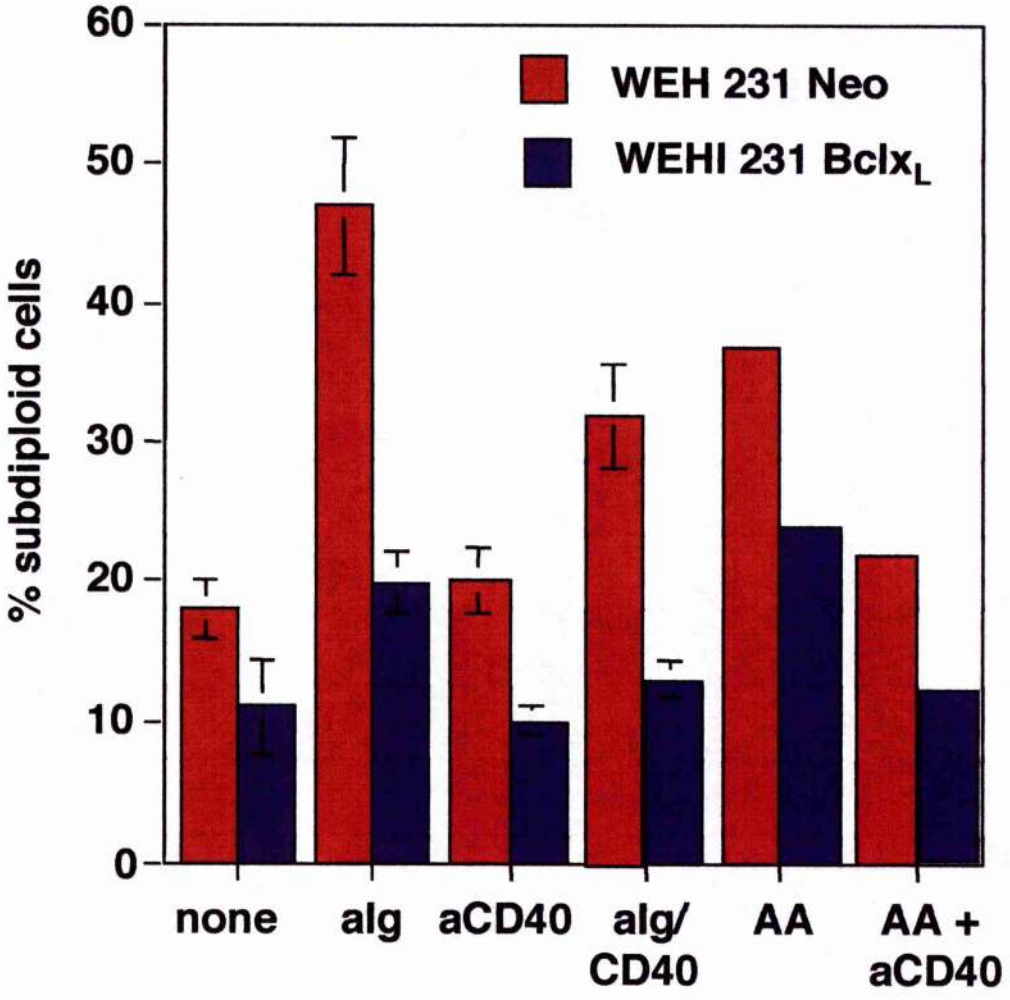
60
50
40
30
20
10
0
% subdiploid cells
WEH 231 Neo
WEHI 231 Bclx$_L$
none
alg
aCD40
alg/
CD40
AA
AA +
aCD40

Figure 3.14: Overexpression of $BclX_L$ does not provide protection from either arachidonic acid or anti-Ig induced growth arrest

Neo and $BclX_L$ WEHI 231 cells were cultured for 48 h and then DNA synthesis was assessed by [^{3}H] thymidine uptake. In panel A, cells were treated with arachidonic acid (0 to 100 μM) or 10 μg/ml anti-Ig (aIg). In panel B cells were treated with anti-Ig (0 to 100 μg/ml) or 10 μg/ml anti-Ig in combination with 10 μg/ml aCD40 (aIg & aCD40). Data are expressed as means ± SD (n=3). These data are from single experiments, representative of at least three separate, independent experiments.

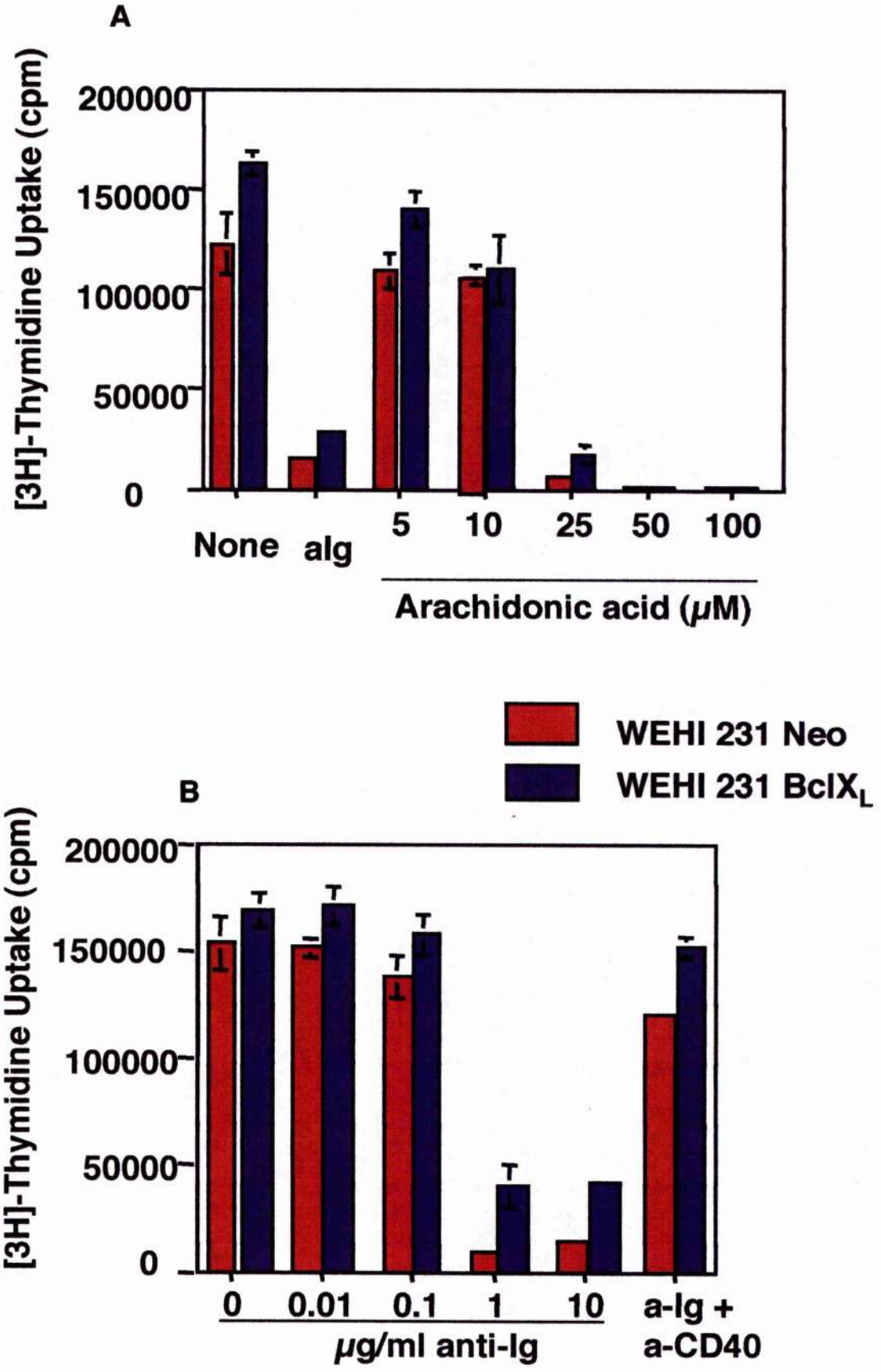
A
[3H]-Thymidine Uptake (cpm)
200000
150000
100000
50000
0
None
alg
5
10
25
50
100
Arachidonic acid (μM)
WEHI 231 Neo
WEHI 231 BclX$_L$
B
[3H]-Thymidine Uptake (cpm)
200000
150000
100000
50000
0
0
0.01
0.1
1
10
μg/ml anti-Ig
a-Ig +
a-CD40

Figure 3.15: Treatment with anti-CD40 can rescue cells from arachidonic acid mediated growth arrest

WEHI 231 cells were cultured for 48 h and then DNA synthesis was assessed by [^{3}H] thymidine uptake. Cells were treated with arachidonic acid (0 to 100 μM) either alone, in combination with 1 μg/ml anti-CD40 or 10 μg/ml aCD40. Data are expressed as means ± SD (n=3). These data are from a single experiment, representative of three separate experiments.

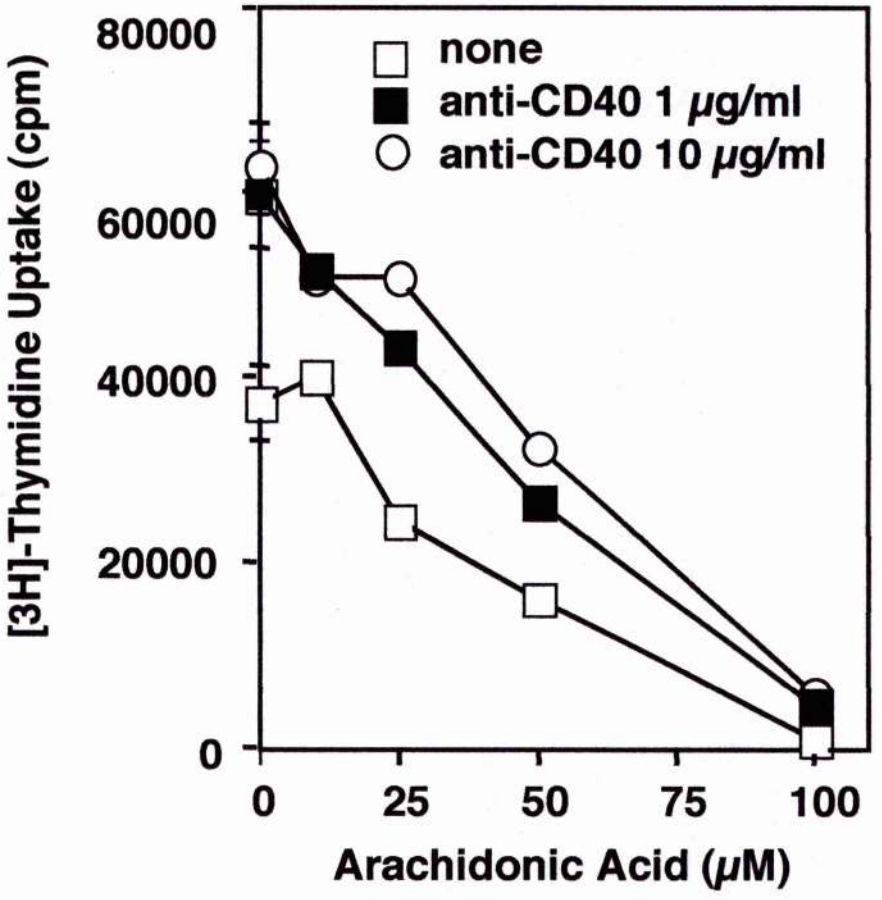
80000
60000
40000
20000
0
[3H]-Thymidine Uptake (cpm)
none
anti-CD40 1 μg/ml
anti-CD40 10 μg/ml
0
25
50
75
100
Arachidonic Acid (μM)

Figure 3.16: The PLA_2 inhibitors used were non-metabolisable forms of arachidonic acid

Arachidonyltrifluoromethyl Ketone (AACOCF3) is a cell-permeable trifluoromethyl ketone analog of arachidonic acid. It is both a potent and selective slow-binding inhibitor of $cPLA_2$. Methyl Arachidonyl Fluorophosphonate (MAFP) is a selective, active site-directed, irreversible inhibitor of both calcium-dependent and calcium-independent $cPLA_2$ but not of secretory PLA_2.

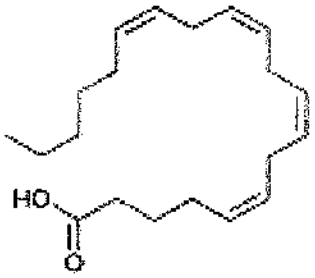

Arachidonic Acid

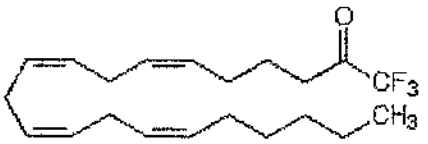

AACOCF3

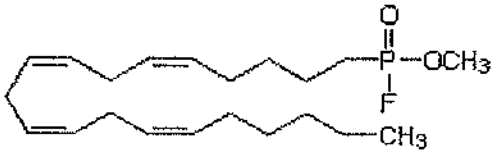

MAFP

Figure 3.17: Treatment with PLA_2 inhibitors induces apoptosis

(A) WEHI 231 cells were stained with 50 μg/ml PI after being in culture for 48 h with media alone. PLA_2 inhibitors were used at the following concentrations: MAFP 20 μM and AACOCF3 20 μM. FACS analysis was used to calculate the number of cells in each phase of the cell cycle. The data is displayed as the percentage of subdiploid cells.

(B) WEHI 231 cells were stained with 50 μg/ml PI after being in culture for 48 h with either media alone (No Stimulation) or 10 μg/ml anti-Ig in combination with 10 μg/ml anti-CD40 (aIg & aCD40). The PLA_2 inhibitor AACOCF3 was used at 20 μM. FACS analysis was used to calculate the number of cells in each phase of the cell cycle. The data is displayed as the percentage of cells in S and G2/M phases combined i.e. mitogenic phases of the cell cycle.

(C) Cells were cultured for 48 h with either media alone (None) or 20 μM AACOCF3 and then stained with 2.5 μM $DiOC_6$. Dissipation of MMP can been seen as a reduction in $DiOC_6$ brightness (FL1 fluorescence). Dissipation of the MMP was assessed by dividing the cells into two populations. The right hand peak having a high healthy MMP and the second having a low apoptotic MMP. The data was then displayed as the percentage of cells with a high MMP.

A

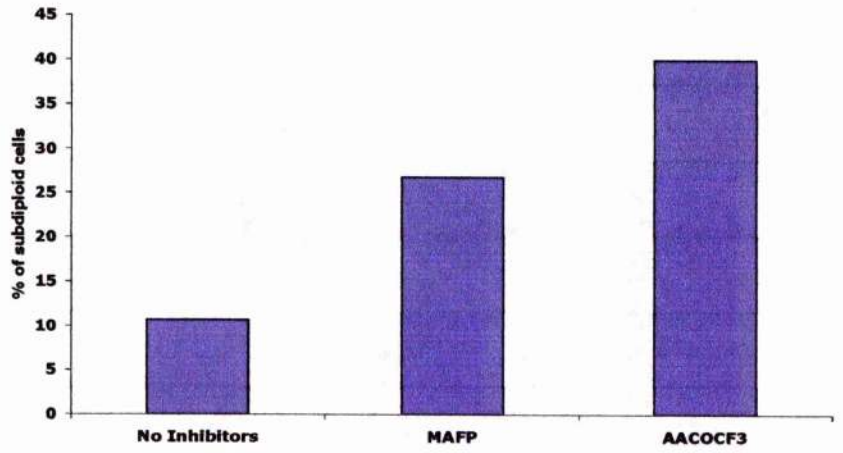
% of subdiploid cells
45
40
35
30
25
20
15
10
5
0
No Inhibitors
MAFP
AACOCF3

B

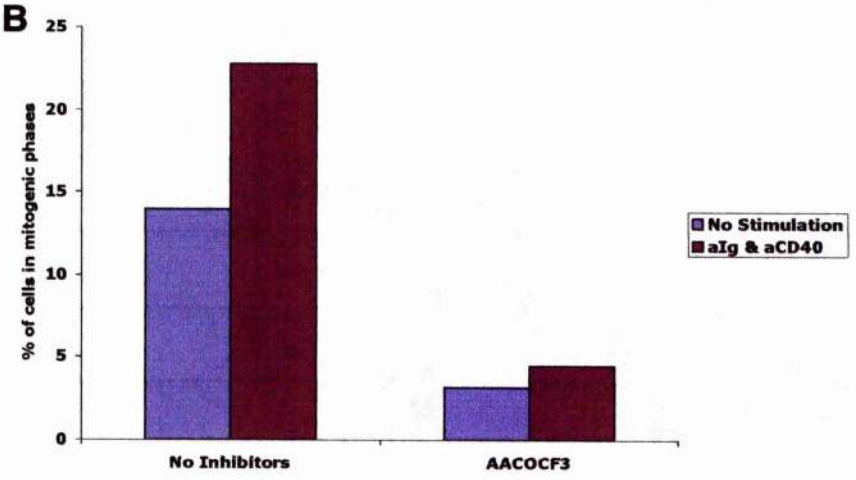
% of cells in mitogenic phases
25
20
15
10
5
0
No Inhibitors
AACOCF3
No Stimulation
aIg & aCD40

C

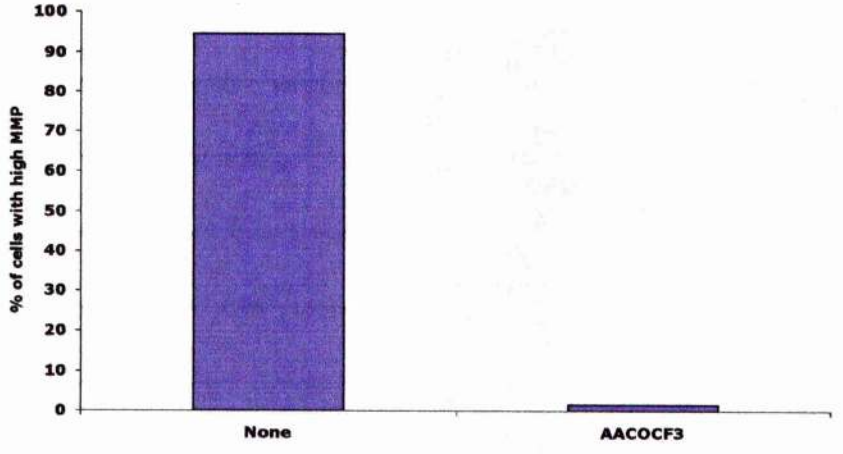
% of cells with high MMP
100
90
80
70
60
50
40
30
20
10
0
None
AACOCF3

Figure 3.18: COX and LOX are responsible for the generation of prostaglandins and leukotrienes, respectively, during arachidonic acid metabolism

Arachidonic acid, a 20-carbon polyunsaturated fatty acid is liberated from cellular membrane phospholipids, phosphatidylcholine and phosphatidyl inositol, in response to enzymatic signaling from a phospholipase. Once liberated into the cytoplasm, cyclooxygenase (COX) or lipoxygenase (LOX) catalyzes the formation of downstream metabolites as prostaglandins and leukotrienes, respectively. The hydroperoxy fatty acids (e.g 5-HPETE) act as pro-inflammatory molecules as well as autocrine regulators. Conversion of HPETE by leukotriene synthesizing enzymes results in leukotriene molecules which are extremely bronchoconstrictive, vasodilatory or chemotactic. Prostaglandin (PG) molecules are formed in similar fashion by the action of COX on arachidonic acid. This results in the parent PGG_2 which, when acted upon by a peroxidase, generates PGH_2, from which all other PGs result. These PG molecules have many physiological actions such as vasodilation, inhibition of platelet aggregation, stimulation of renin secretion and induction of calcium release from bones.

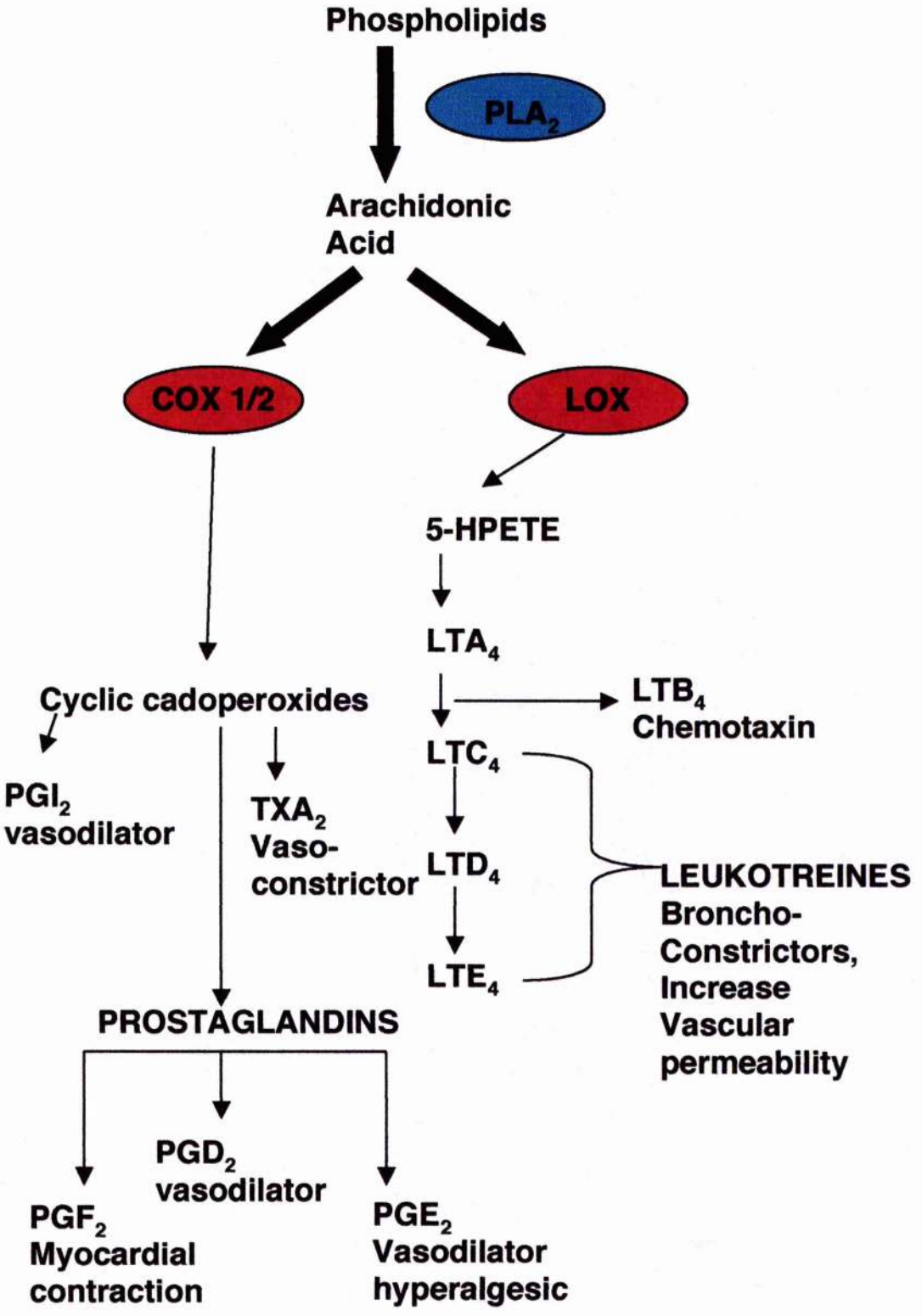
Phospholipids
PLA2
Arachidonic Acid
COX 1/2
LOX
5-HPETE
LTA4
Cyclic cadoperoxides
LTB4 Chemotaxin
LTC4
PGI2 vasodilator
TXA2 Vaso-constrictor
LTD4
LEUKOTREINES Broncho-Constrictors, Increase Vascular permeability
LTE4
PROSTAGLANDINS
PGD2 vasodilator
PGF2 Myocardial contraction
PGE2 Vasodilator hyperalgesic

Figure 3.19: Treatment with COX2 or pan-LOX inhibitors alone or in combination enhances anti-Ig-induced growth arrest and apoptosis

(A) WEHI 231 cells were stimulated with anti-Ig (0 to 10 μg/ml) in the absence or presence of 4 μM or 10 μM NS398 (COX2 inhibitor) for 48 h. DNA synthesis was then assessed by [^{3}H] thymidine uptake. Data are expressed as means ± SD (n=3). These data are from a single experiment, representative of three separate experiments.

(B) WEHI 231 cells were stimulated with anti-Ig (0 to 10 μg/ml) in the absence or presence of 1 μM or 10 μM EDBC (pan-LOX inhibitor) for 48 h. DNA synthesis was then assessed by [^{3}H] thymidine uptake. Data are expressed as means ± SD (n=3). These data are from a single experiment, representative of three separate experiments.

(C) Neo and BclX_L WEHI 231 cells were stimulated with 10 μg/ml anti-Ig in the presence and absence of 10 μM NS398 plus 10 μM EDBC for 48 h. Cells were then stained with 50 μg/ml PI and FACS analysis was used to calculate the number of cells in each phase of the cell cycle. The data is displayed as the percentage of subdiploid and therefore apoptotic cells. These data are from a single experiment, representative of 3 experiments.

(D) Cells were cultured for 48 h with 10 μg/ml anti-Ig and in the presence or absence of 10 μM NS398 and 10 μM EDBC and then stained with 2.5 μM $DiOC_6$. Dissipation of MMP can been seen as a reduction in DiOC6 brightness (FL1 fluorescence). Dissipation of the MMP was assessed by dividing the cells into two populations. The right hand peak having a high healthy MMP and the second having a low apoptotic MMP. The data was then displayed as the percentage of cells with a low MMP. These data are from a single experiment, representative of 3 experiments.

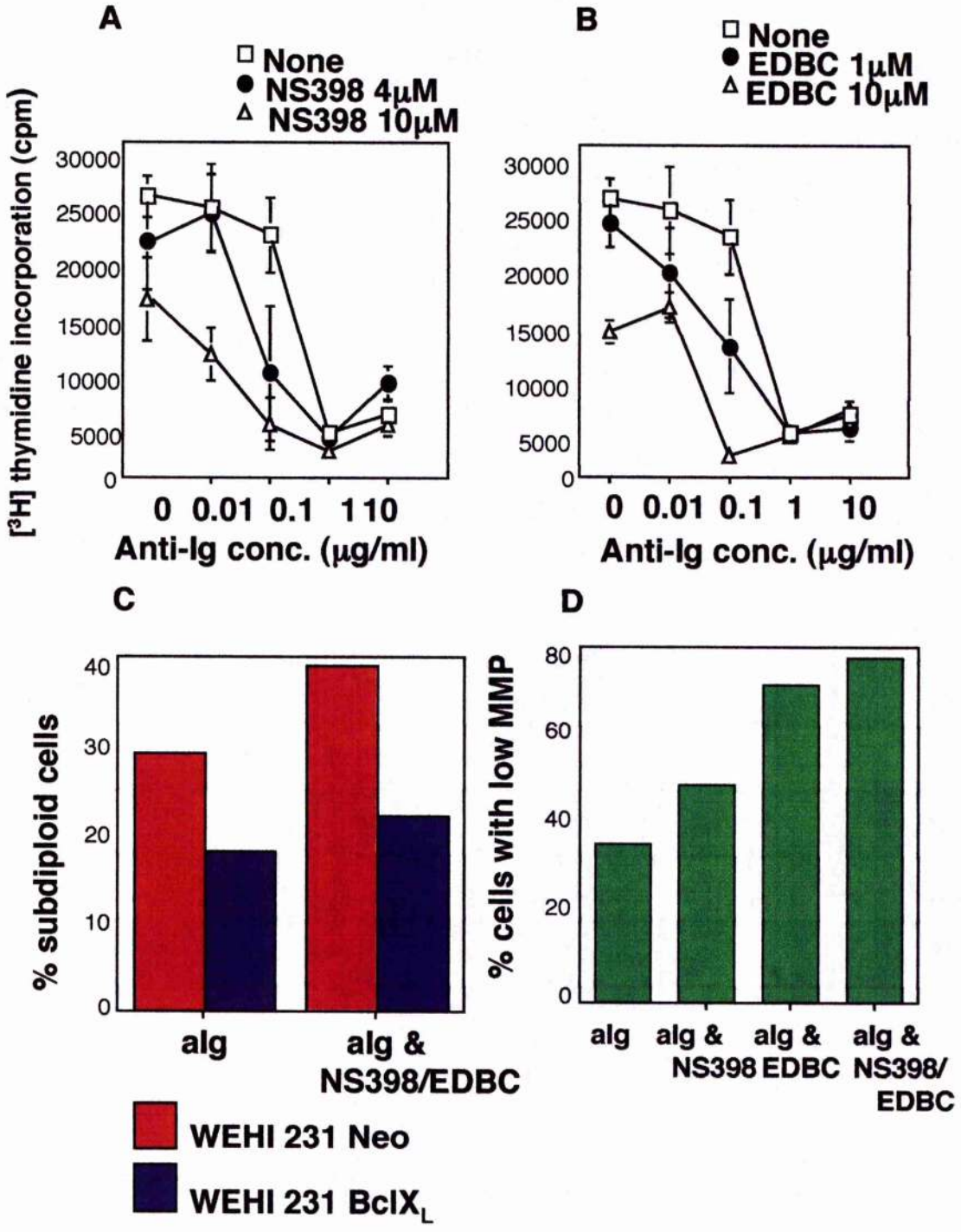
A
None
NS398 4μM
NS398 10μM
[3H] thymidine incorporation (cpm)
30000
25000
20000
15000
10000
5000
0
0 0.01 0.1 1 10
Anti-Ig conc. (μg/ml)
B
None
EDBC 1μM
EDBC 10μM
30000
25000
20000
15000
10000
5000
0
0 0.01 0.1 1 10
Anti-Ig conc. (μg/ml)
C
% subdiploid cells
40
30
20
10
0
alg
alg & NS398/EDBC
WEHI 231 Neo
WEHI 231 BclX$_L$
D
% cells with low MMP
80
60
40
20
0
alg
alg & NS398
alg & EDBC
alg & NS398/ EDBC

Figure 3.20: $BclX_L$ overexpression antagonises BCR mediated disruption of the MMP however it cannot overcome anti-Ig induced growth arrest

(A) Neo and $BclX_L$ WEHI 231 cells were stimulated with media alone (none), 10 μg/ml anti-Ig (aIg), 10 μg/ml anti-CD40 (aCD40) or a combination of 10 μg/ml anti-Ig and 10 μg/ml anti-CD40 (aIg & aCD40) in the absence or presence 10 μM NS398 plus 10 μM EDBC for 48 h. DNA synthesis was then assessed by [^{3}H] thymidine uptake. Data are expressed as means ± SD (n=3). These data are from a single experiment, representative of three separate experiments. **(B)** Wild type and $BclX_L$ WEHI 231 cells were cultured for 48 h with anti-Ig (10 μg/ml) and in the presence or absence of 10 μM NS398 and 10 μM EDBC and then stained with 2.5 μM $DIOC_6$. Dissipation of MMP can been seen as a reduction in $DiOC_6$ brightness (FL1 fluorescence). Dissipation of the MMP was assessed by dividing the cells into two populations. The right hand peak having a high healthy MMP and the second having a low apoptotic MMP. The data was then displayed as the percentage of cells with a high MMP.

A

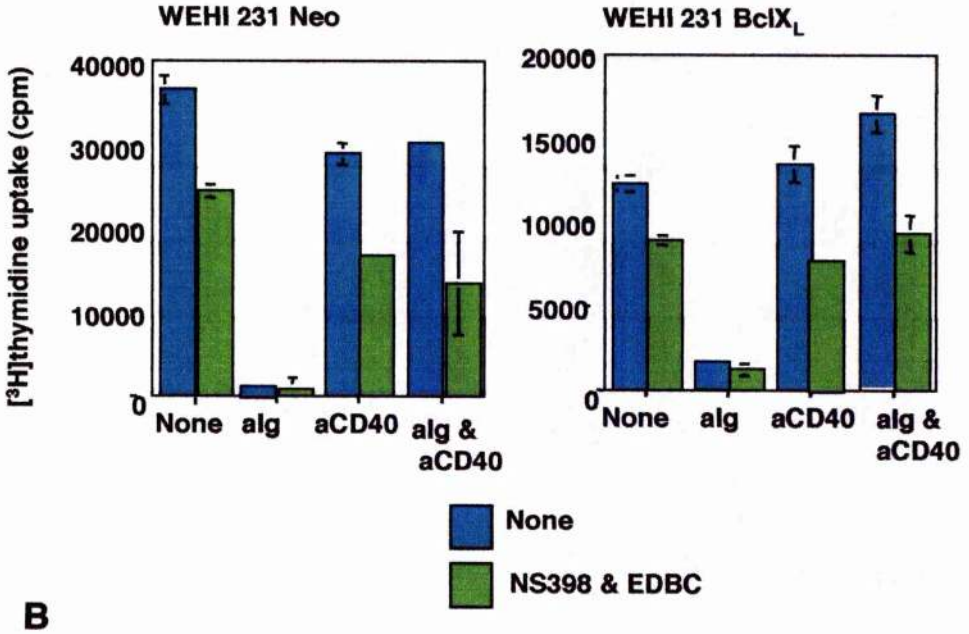
WEHI 231 Neo
WEHI 231 BclX$_L$
[^{3}H]thymidine uptake (cpm)
40000
30000
20000
10000
0
20000
15000
10000
5000
0
None
aIg
aCD40
aIg & aCD40
None
NS398 & EDBC

B

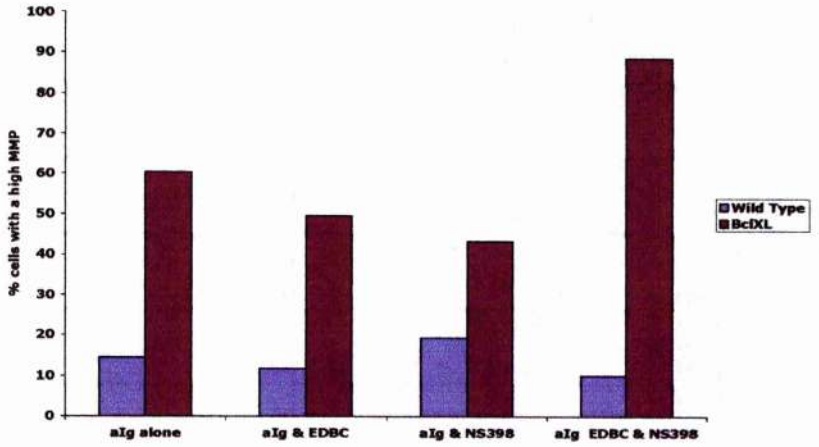
% cells with a high MMP
100
90
80
70
60
50
40
30
20
10
0
aIg alone
aIg & EDBC
aIg & NS398
aIg EDBC & NS398
Wild Type
BcDXL

Figure 3.21: BCR-induced calcium release is reduced in $BclX_L$ WEHI 231 cells as compared to Neo WEHI 231 cells

(A) Neo and $BclX_L$ WEHI 231 cells were loaded with FURA2 and placed in stirred cuvettes. Cytosolic calcium was measured in cell populations using a spectrophotometer following addition of 10 μg/ml of anti-Ig or 10 μg/ml of anti-CD40. The data is displayed as Ca^{2+} rise (nM). The data is representative of cellular Ca^{2+} rise in 5 different cuvettes.

(B) Neo and $BclX_L$ WEHI 231 cells were loaded with FURA2 and placed in stirred cuvettes. Cytosolic calcium was measured in cell populations using a spectrophotometer following addition of either 10 μg/ml of anti-Ig, 10 μg/ml of anti-CD40 or 50 μM thapsigargin. The data is displayed as mean peak Ca^{2+} rise (nM) and expressed as the mean value ± SD. The data is representative of cellular Ca^{2+} rise in 5 different cuvettes.

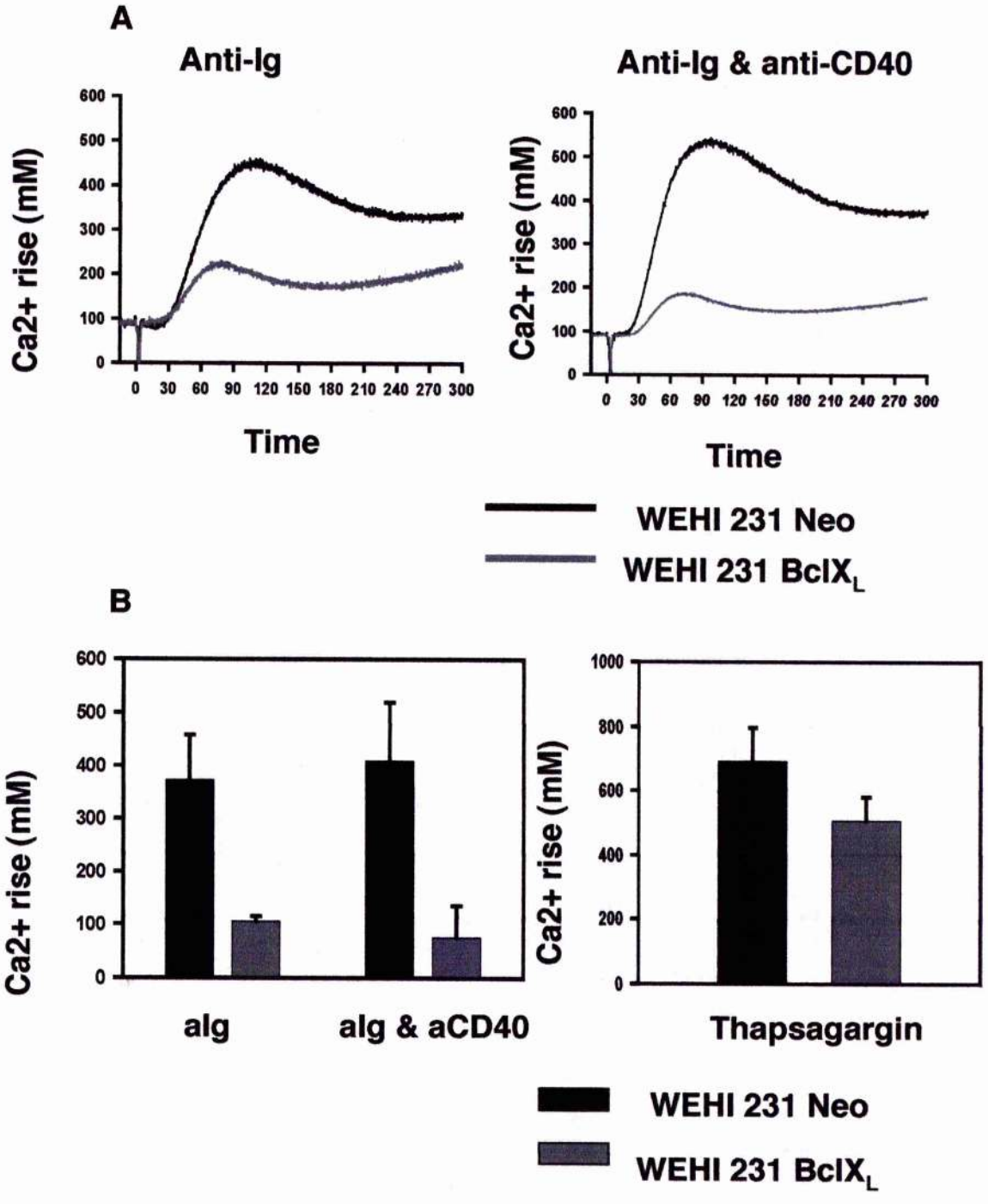
A
Anti-Ig
Anti-Ig & anti-CD40
Ca2+ rise (mM)
Time
WEHI 231 Neo
WEHI 231 BclX$_L$
B
alg
alg & aCD40
Thapsagargin
WEHI 231 Neo
WEHI 231 BclX$_L$

Figure 3.22: Addition of anti-Ig results in a calcium oscillation in WEHI 231 cells

(A) Wild type WEHI 231 cells were loaded with 5μM Fluo3 and illuminated at 488nm to visualise cellular calcium levels. A puffer pipette was placed adjacent to the cell and used to apply anti-Ig 10 μg/ml directly to stimulate a Ca^{2+} signal. The real time recordings were analysed using Metamorph Imaging software. The images shown here are for one frame every 5 sec of a 20 sec recording. The images are representative of 6 different fields.
(B) Fluorescence image to demonstrate that each cell was divided into 3 roughly equidistant regions of interest (ROI).
(C) The real time recordings were analysed using Metamorph Imaging software to assess the calcium levels in each region of interest over 20 sec. The data is displayed as the calcium rise measured against time (sec) for each of 3 ROI. The data is representative of 4 cells.

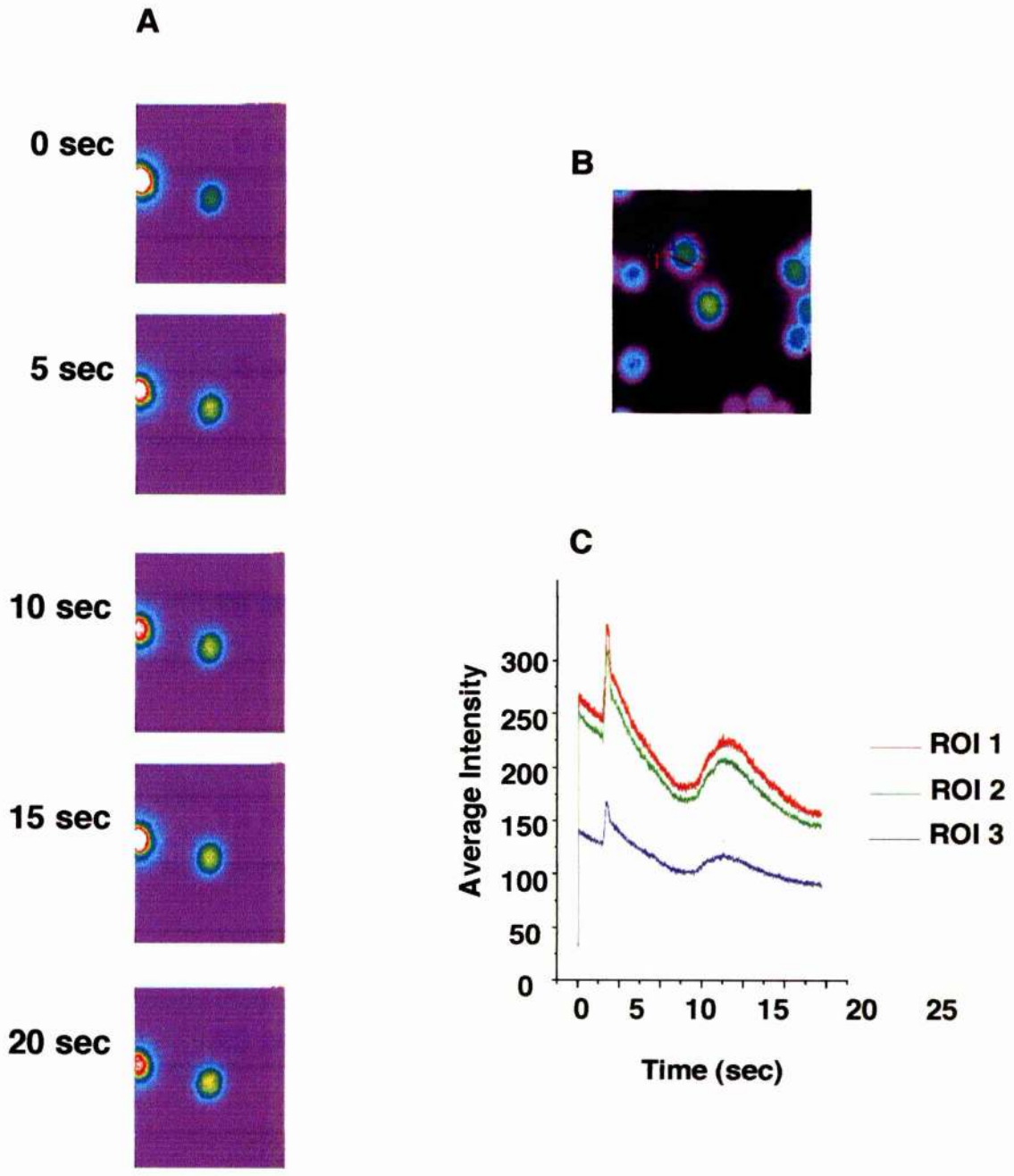
A
0 sec
5 sec
10 sec
15 sec
20 sec
B
C
Average Intensity
300
250
200
150
100
50
0
0
5
10
15
20
25
Time (sec)
ROI 1
ROI 2
ROI 3

Figure 3.23: WEHI 231 cells undergo sustained, cyclical ERK activation when unstimulated or treated with anti-CD40, whereas ligation of the BCR abrogates this sustained ERK activation. WEHI 231 cells expressing the RasV12 construct have enhanced ERK activation compared to empty vector cells

(A) Neo (empty vector) WEHI 231 cells (10^7 cells/lane) were cultured with medium alone (None), anti-Ig 10 μg/ml (aIg) or a combination of anti-Ig 10 μg/ml and anti-CD40 10 μg/ml (aIg & aCD40) for up to 48 h. Cell lysates were then prepared and analysed using gel electrophoresis and western blotting using total ERK 1/2 (wERK1/2) or phospho-ERK 1/2 (pERK1/2). Data are representative of a least 13 independent experiments.

(B) RasV12 and wild type WEHI 231 cells were incubated for 24 h with appropriate stimulations prior to fixation, permeablisation and assessment of ERK levels. Cells were either cultured with media alone (No Stimulation), 10 μg/ml anti-Ig (aIg) or a combination of 10 μg/ml anti-Ig and 10 μg/ml anti-CD40 (aIg & aCD40). The modified ELISA method- FACE- was used to assess the levels of ERK and phospho-ERK. Results are displayed as the ratio of the phospho-ERK signal to ERK signals. All ERK levels were calculated as the mean of three wells ± SD.

A

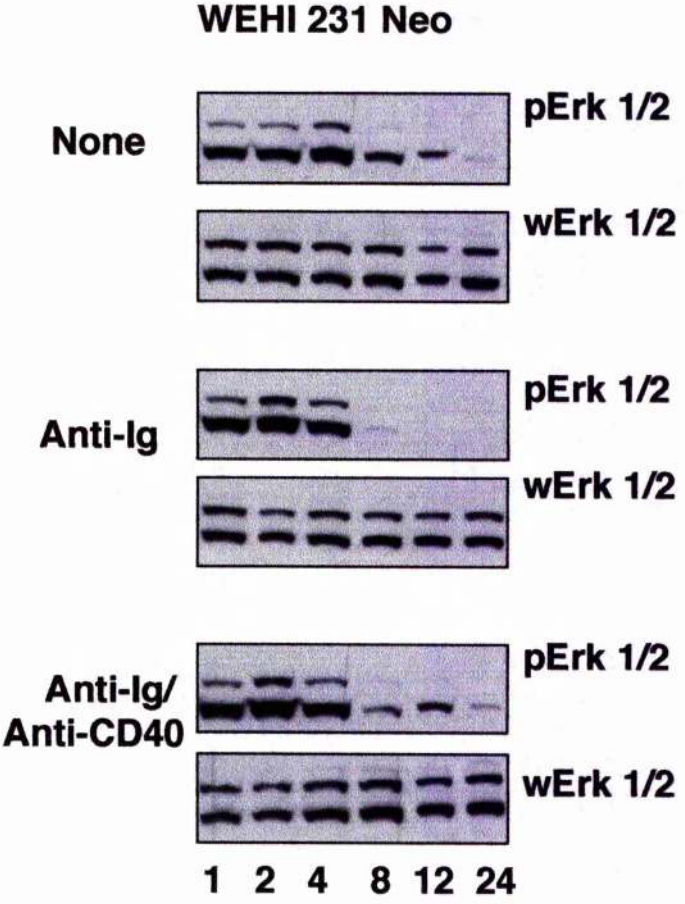
WEHI 231 Neo
None
pErk 1/2
wErk 1/2
Anti-Ig
pErk 1/2
wErk 1/2
Anti-Ig/
Anti-CD40
pErk 1/2
wErk 1/2
1 2 4 8 12 24

B

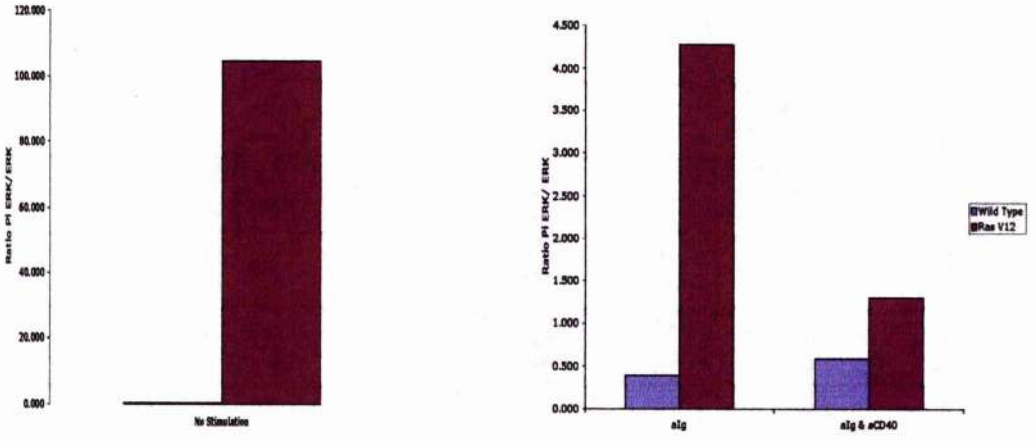
120.000
100.000
80.000
60.000
40.000
20.000
0.000
Ratio PI ERK/ ERK
No Stimulation
4.500
4.000
3.500
3.000
2.500
2.000
1.500
1.000
0.500
0.000
Ratio PI ERK/ ERK
aIg
aIg & aCD40
Wild Type
Ras V12

Figure 3.24: Expression of the RasV12 construct enhances sustained, cycling ERK activation which provides protection from BCR-induced growth arrest at 24 h but not at 48 h in WEHI 231 cells

(A) Empty Vector and RasV12 WEHI 231 cells were cultured with anti-Ig (0 to 10 μg/ml) for 24 h and then DNA synthesis was assessed by [^{3}H] thymidine uptake. These data are the mean of three separate wells ± the SEM. These data are from a single experiment, representative of five separate experiments. **(B)** RasV12 WEHI 231 cells (10^7 cells/lane) were cultured with either medium alone (None) or anti-Ig 10 μg/ml (anti-Ig) for the time periods shown. Cell lysates were then prepared and analysed using gel electrophoresis and western blotting using total p42/44 ERK or dual phosphorylated p42/44 ERK. This was compared to a total p42/44 ERK positive control (w) and dual phosphorylated p42/44 ERK positive control (p).
(C) Empty vector (pcDNA3.1) and RasV12 WEHI 231 cells were stained with 50 μg/ml PI after being in culture for 48 h with appropriate stimulations. Cells were either treated with media alone (none), 10 μg/ml anti-Ig (aIg) or 10 μg/ml anti-Ig in combination with anti-CD40 (aIg & aCD40). FACS analysis was used to calculate the percentage of subdiploid cells. The data is displayed as the mean percentage of subdiploid cells from 5 independent experiments ± SEM.

A

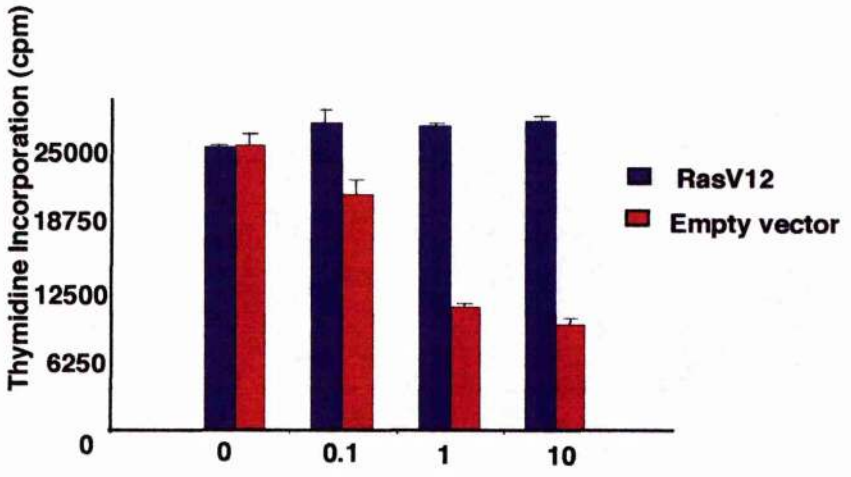
Thymidine Incorporation (cpm)
25000
18750
12500
6250
0
0
0.1
1
10
RasV12
Empty vector

B

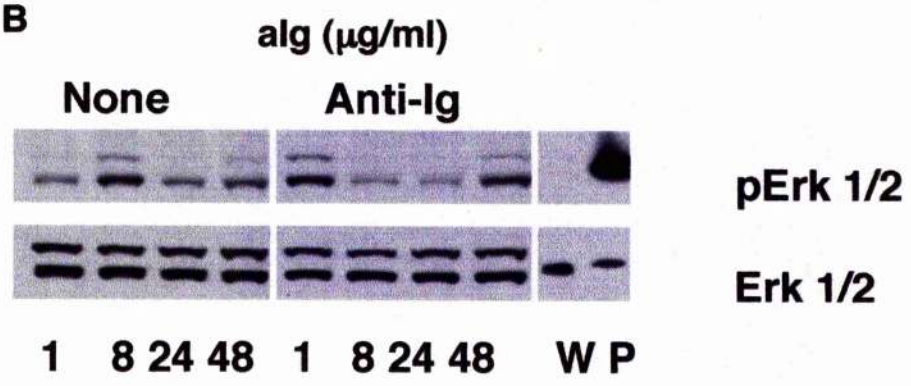
alg (μg/ml)
None
Anti-Ig
pErk 1/2
Erk 1/2
1 8 24 48 1 8 24 48 W P

C

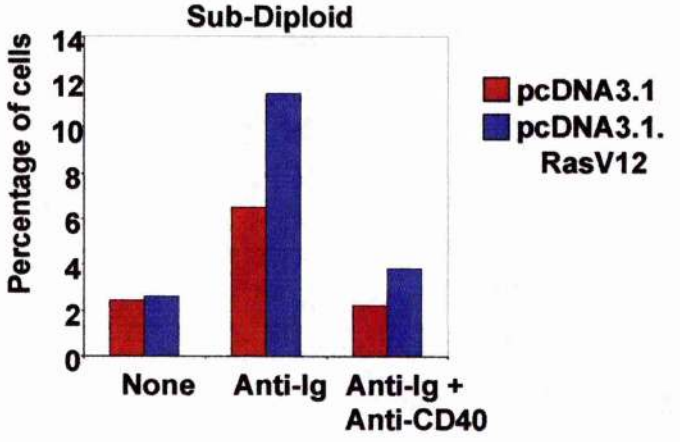
Sub-Diploid
Percentage of cells
14
12
10
8
6
4
2
0
None
Anti-Ig
Anti-Ig + Anti-CD40
pcDNA3.1
pcDNA3.1. RasV12

Figure 3.25: Both RasV12 S35 and Ras V12 C40 mutations provide protection from BCR-mediated growth arrest

(A) WEHI 231 cells (1 x 10^4 cells/well) containing the empty pcDNA3.1 vector, RasV12, or RasV12 S35 vectors were cultured, in triplicate, in the presence of increasing concentrations of anti-Ig (0, 0.01, 0.1, 1, 10 μg/ml), or a combination of anti-Ig (10 μg/ml) and anti-CD40 (10 μg/ml), for 24 h. Culture wells were pulsed with [^{3}H] thymidine (0.5 μCi/well) 4 hours prior to harvesting and [^{3}H] incorporation was assessed by liquid scintillation counting. Data from individual experiments were normalised by expressing the mean [^{3}H] thymidine uptake values of anti-Ig treated cells as a percentage of those obtained with control, unstimulated cell cultures for each cell line. The normalised values from 4 independent experiments were then pooled and expressed as means ± SEM. **(B)** WEHI 231 cells (1 x 10^4 cells/well) containing the empty pcDNA3.1 vector, RasV12, or RasV12C40 vectors were cultured and proliferation assessed as in **(A)**. Data from individual experiments were normalised by expressing the mean [^{3}H] thymidine uptake values of treated cells as a percentage of those obtained with control cell cultures as described below. The normalised values from 4 independent experiments were then pooled and expressed as means ± SEM.

A

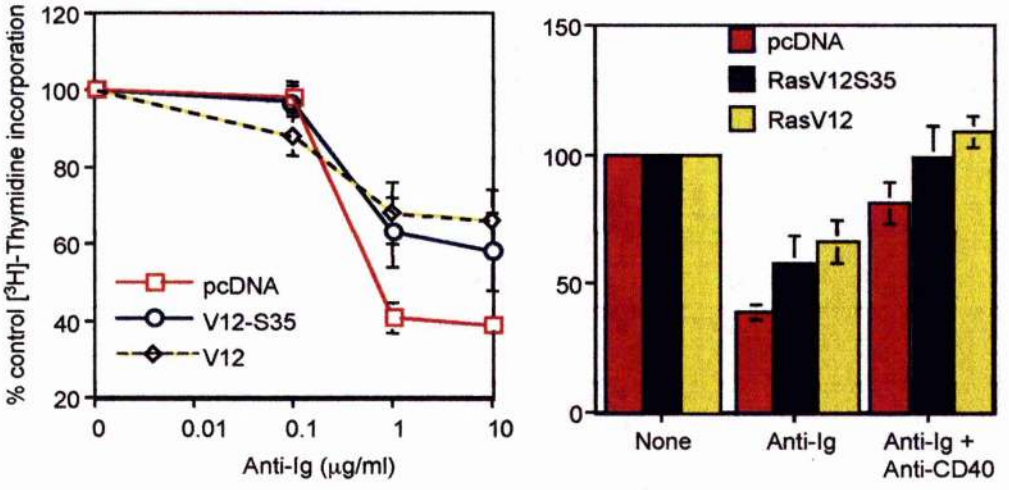
% control [3H]-Thymidine incorporation
120
100
80
60
40
20
0
0.01
0.1
1
10
Anti-Ig (μg/ml)
pcDNA
V12-S35
V12
150
100
50
0
pcDNA
RasV12S35
RasV12
None
Anti-Ig
Anti-Ig +
Anti-CD40

B

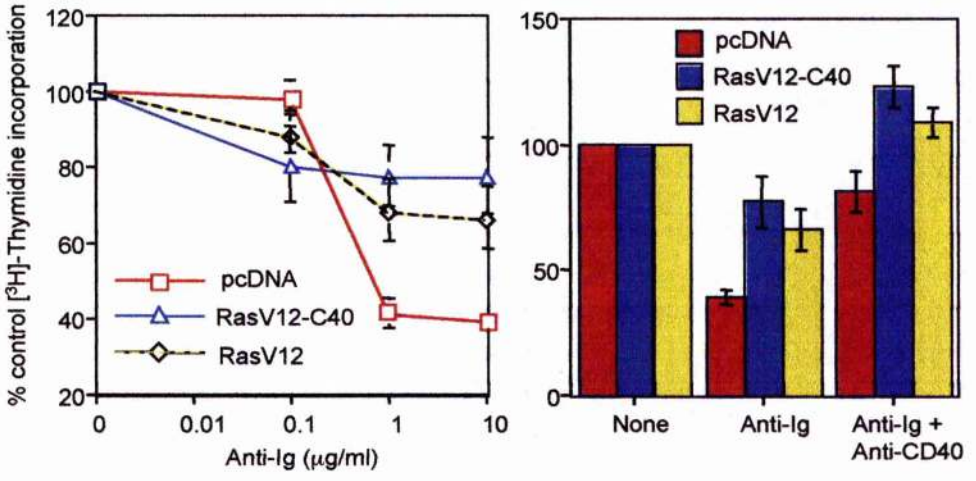
% control [3H]-Thymidine incorporation
120
100
80
60
40
20
0
0.01
0.1
1
10
Anti-Ig (μg/ml)
pcDNA
RasV12-C40
RasV12
150
100
50
0
pcDNA
RasV12-C40
RasV12
None
Anti-Ig
Anti-Ig +
Anti-CD40

Figure 3.26: RasV12 does not significantly alter cell division in response to anti-Ig at 72 h

Empty Vector (pcDNA3.1) and RasV12 WEHI 231 cells were stained with 1 μM CFSE and then left in culture for 72 hours with media alone (No Stimulation), 10 μg/ml anti-Ig (aIg), 10 μg/ml anti-CD40 (aCD40) or a combination of 10 μg/ml anti-Ig and 10 μg/ml anti-CD40 (aIg & aCD40). Proliferation was assessed by an estimate of the percentage of cells in each generation. This calculation was done with the FlowJo proliferation data analysis programme. These data are from a single experiment, representative of 2 separate experiments.

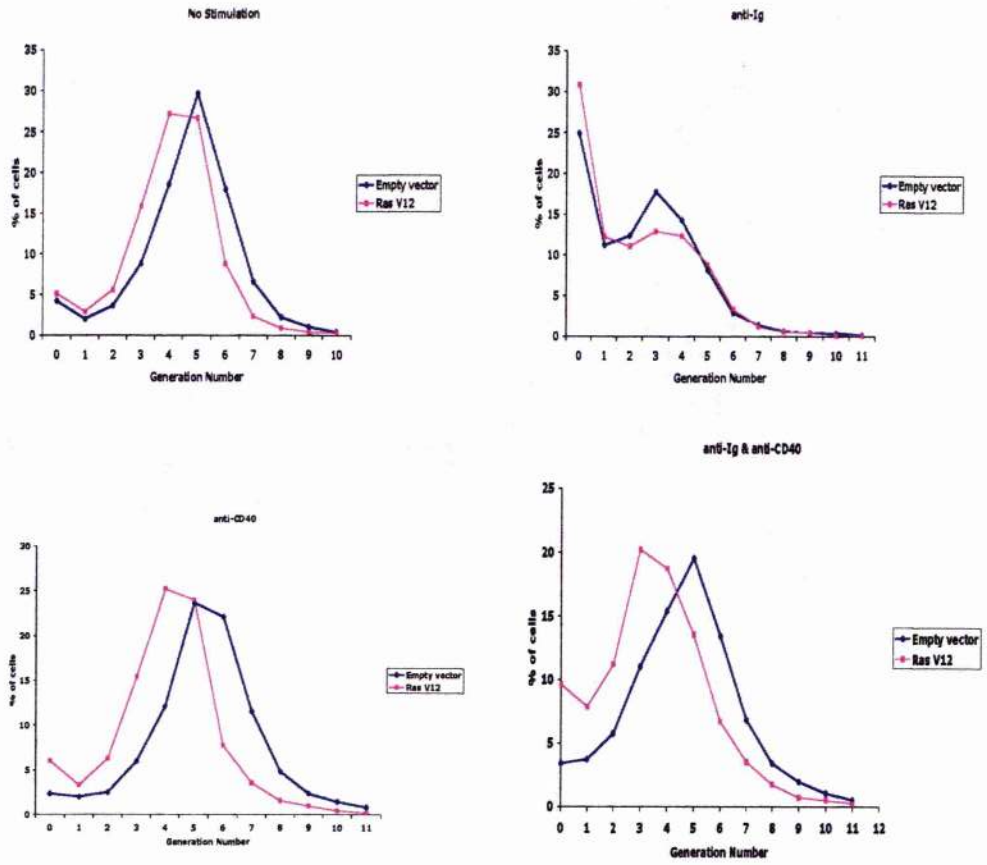
No Stimulation
% of cells
Generation Number
Empty vector
Ras V12
anti-Ig
% of cells
Generation Number
Empty vector
Ras V12
anti-CD40
% of cells
Generation Number
Empty vector
Ras V12
anti-Ig & anti-CD40
% of cells
Generation Number
Empty vector
Ras V12

Figure 3.27: Constitutive activation of Ras provides protection from anti-Ig induced dissipation of the MMP

Empty Vector (pcDNA3.1), RasV12, RasV12 S35 and RasV12 C40 WEHI 231 cells were left in culture for either 0 h with media alone (control), 48 h with 10 μg/ml anti-Ig (aIg) or 48 h with 10 μg/ml anti-Ig in combination with 10 μg/ml anti-CD40 (aIg & aCD40). Cells were then stained with 2.5 μM $DiOC_6$ and used for FACS analysis. Dissipation of MMP can been seen as a reduction in $DiOC_6$ brightness (FL1 fluorescence). These plots are from a single experiment, representative of 4 experiments.

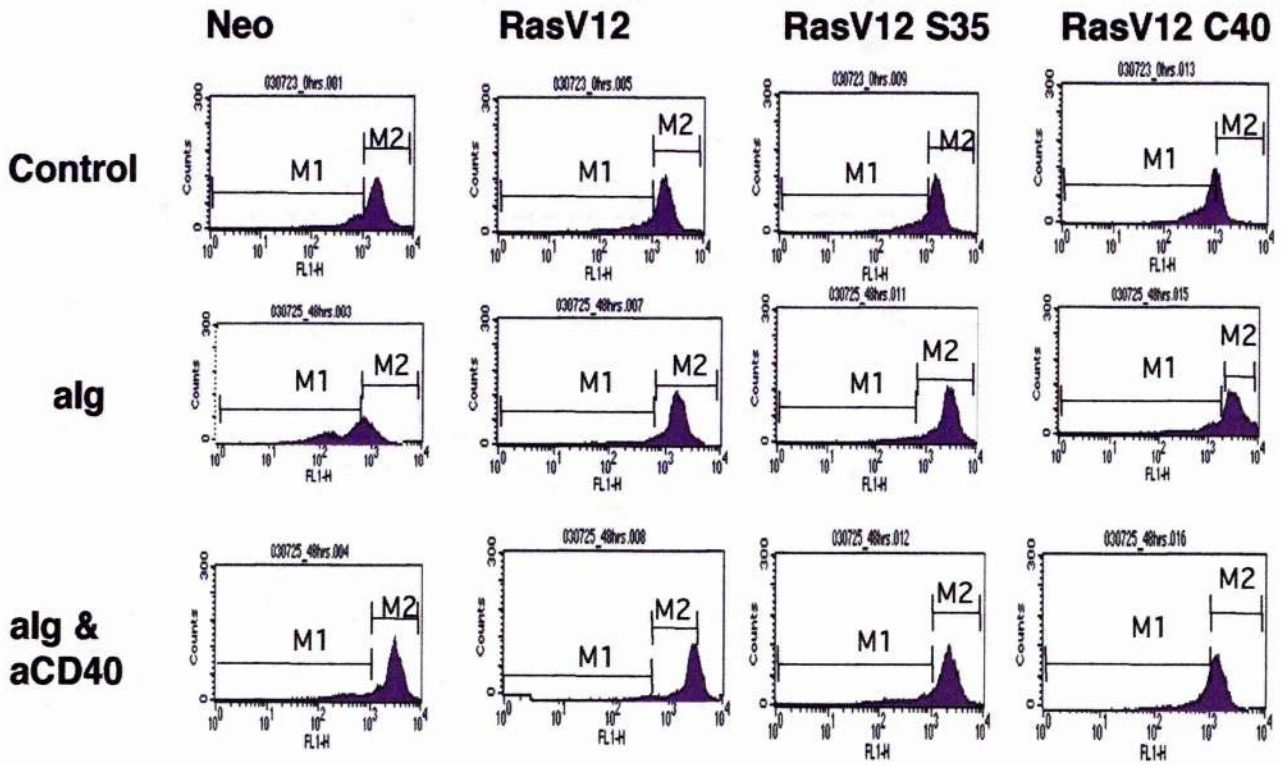
Neo
RasV12
RasV12 S35
RasV12 C40
Control
alg
alg &
aCD40
M1
M2
Counts
FL1-H

Figure 3.28: Constitutive activation of Ras provides protection from anti-Ig induced dissipation of the MMP at 24 and 48 hours

(A) Empty Vector (pcDNA3.1), RasV12, RasV12 S35 and RasV12 C40 WEHI 231 cells were cultured with either media alone (No Stimulation), 10 μg/ml anti-Ig (aIg) or 10 μg/ml anti-Ig in combination with 10 μg/ml anti-CD40 (aIg & aCD40) for 24 h. Cells were then stained with 2.5 μM $DiOC_6$ and used for FACS analysis. Dissipation of MMP can been seen as a reduction in $DiOC_6$ brightness (FL1 fluorescence). Dissipation of the MMP was assessed by dividing the cells into two populations. The right hand peak having a high healthy MMP and the second having a low apoptotic MMP. The data was then displayed as the percentage of cells with a high MMP. These data are from a single experiment, representative of 3 experiments. The data set shown here is separate from figure 3.27.

(B) Empty Vector (pcDNA3.1), RasV12, RasV12 S35 and RasV12 C40 WEHI 231 cells were cultured with either media alone (No Stimulation), 10 μg/ml anti-Ig (aIg) or 10 μg/ml anti-Ig in combination with 10 μg/ml anti-CD40 (aIg & aCD40) for 48 h. Cells were then stained with 2.5 μM $DiOC_6$ and used for FACS analysis. Dissipation of MMP can been seen as a reduction in $DiOC_6$ brightness (FL1 fluorescence). Dissipation of the MMP was assessed by dividing the cells into two populations. The right hand peak having a high healthy MMP and the second having a low apoptotic MMP. The data was then displayed as the percentage of cells with a high MMP. These data are from a single experiment, representative of 3 experiments. The data set shown here is separate from figure 3.27.

A

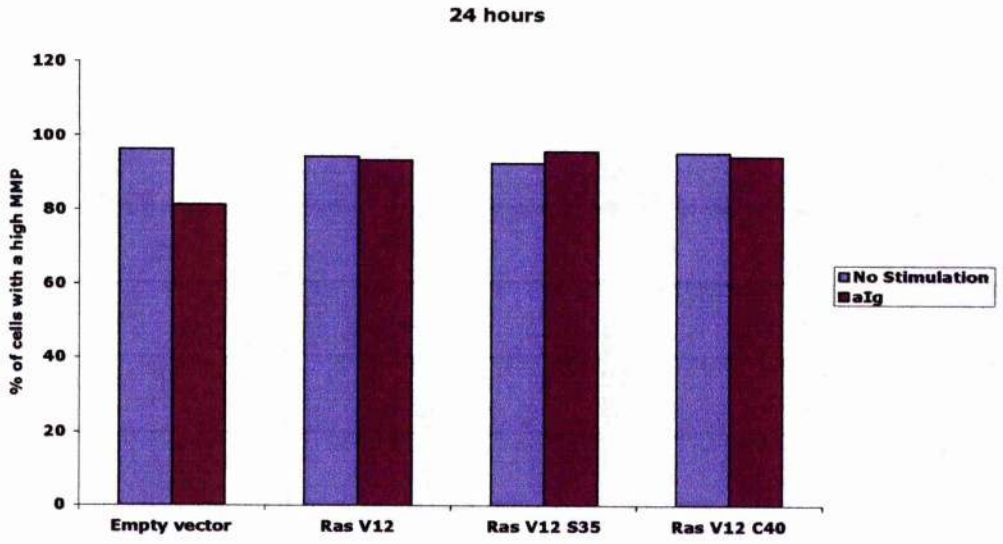
24 hours
% of cells with a high MMP
120
100
80
60
40
20
0
Empty vector
Ras V12
Ras V12 S35
Ras V12 C40
No Stimulation
aIg

B

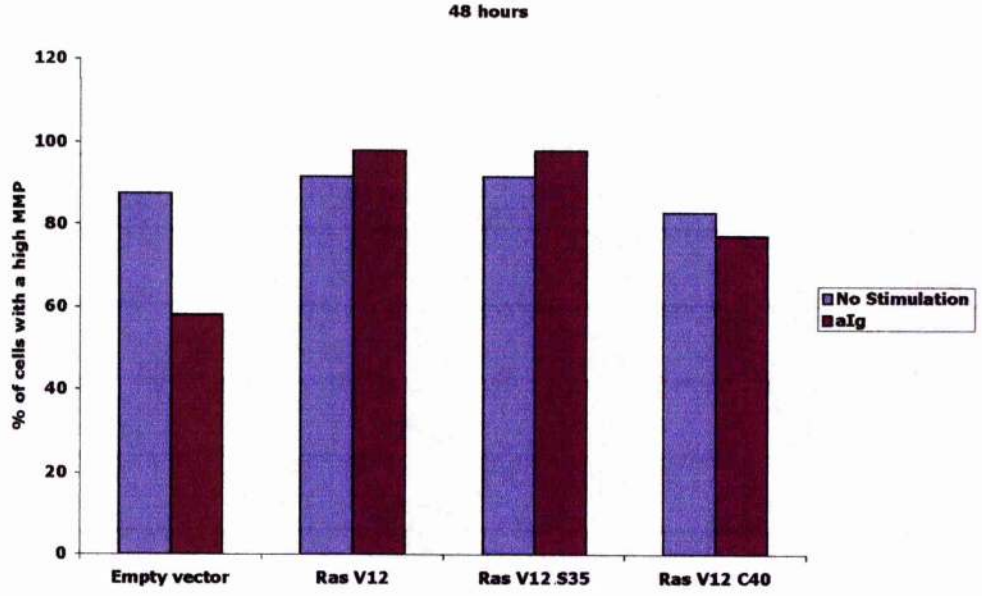
48 hours
% of cells with a high MMP
120
100
80
60
40
20
0
Empty vector
Ras V12
Ras V12 S35
Ras V12 C40
No Stimulation
aIg

Figure 3.29: Expression of the MEKK3 construct rescues cells from BCR-induced dissipation of the MMP and apoptosis

(A) Empty Vector (pcDNA3.1) and MEKK3 WEHI 231 cells were cultured with media alone (No Stimulation), 10 μg/ml anti-Ig (aIg), 10 μg/ml anti-CD40 (aCD40) or a combination of 10 μg/ml anti-Ig and 10 μg/ml anti-CD40 (aIg & aCD40) for 48 h and then stained with 50 μg/ml PI. FACS analysis was used to calculate the number of cells in each phase of the cell cycle. The data is displayed as the percentage of cells in each phase. These data are from a single experiment, representative of 4 experiments.

(B) Empty Vector (pcDNA3.1) and MEKK3 WEHI 231 cells were cultured with 10 μg/ml anti-Ig for 48 h. Cells were then stained with 2.5 μM $DiOC_6$ and used for FACS analysis. Dissipation of MMP can been seen as a reduction in $DiOC_6$ brightness (FL1 fluorescence). Dissipation of the MMP was assessed by dividing the cells into two populations. The right hand peak having a high healthy MMP and the second having a low apoptotic MMP. The data was then displayed as the percentage of cells with a high MMP. These data are from a single experiment, representative of 3 experiments.

A

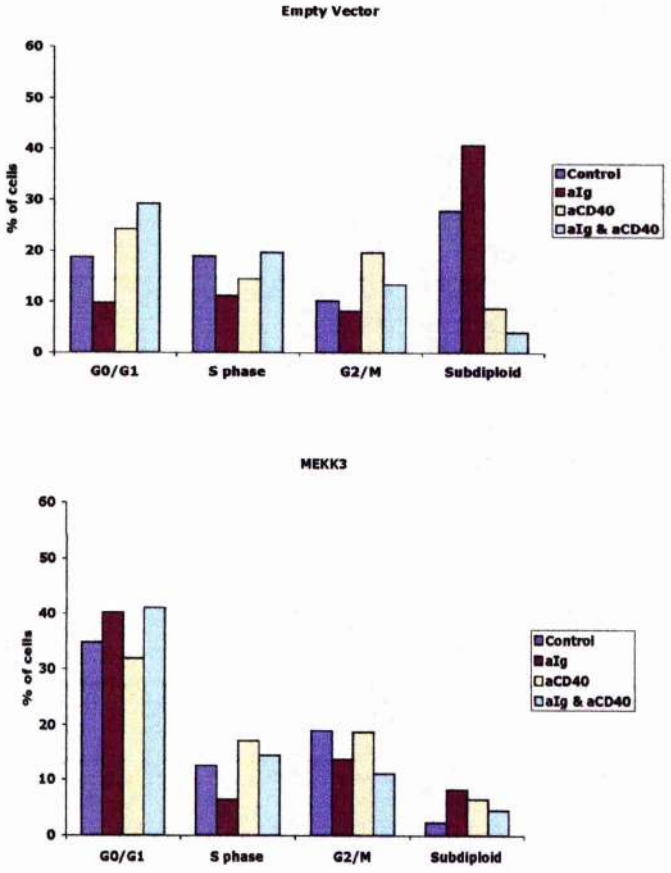
Empty Vector
% of cells
60
50
40
30
20
10
0
G0/G1
S phase
G2/M
Subdiploid
Control
aIg
aCD40
aIg & aCD40
MEKK3
% of cells
60
50
40
30
20
10
0
G0/G1
S phase
G2/M
Subdiploid
Control
aIg
aCD40
aIg & aCD40

B

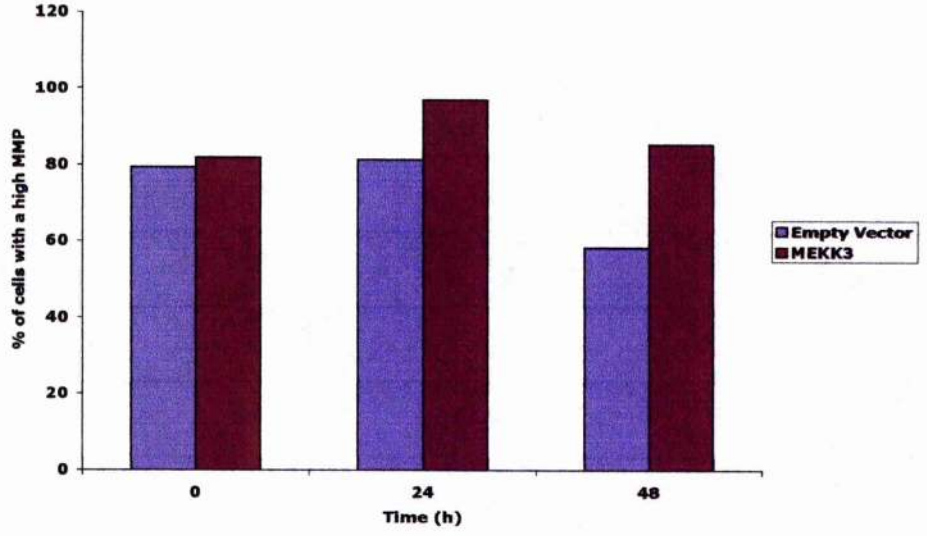
% of cells with a high MMP
120
100
80
60
40
20
0
0
24
48
Time (h)
Empty Vector
MEKK3

Figure 3.30: Expression of the MEKK3 construct reduces cell division in response to all stimuli

Empty Vector (pcDNA3.1) and MEKK3 WEHI 231 cells were stained with 1 μM CFSE and then left in culture for 72 h with media alone (No Stimulation), 10 μg/ml anti-Ig (aIg), 10 μg/ml anti-CD40 (aCD40) or a combination of 10 μg/ml anti-Ig and 10 μg/ml anti-CD40 (aIg & aCD40). Proliferation was assessed by an estimate of the percentage of cells in each generation. This calculation was done with the FlowJo proliferation data analysis programme. These data are from a single experiment, representative of 2 separate experiments.

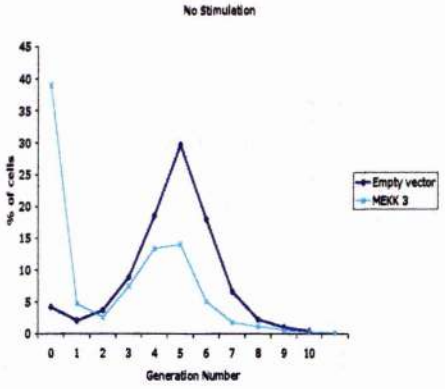
No Stimulation
% of cells
Generation Number
Empty vector
MEKK 3

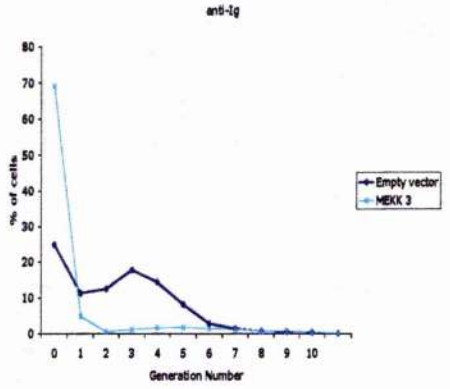
anti-Ig
% of cells
Generation Number
Empty vector
MEKK 3

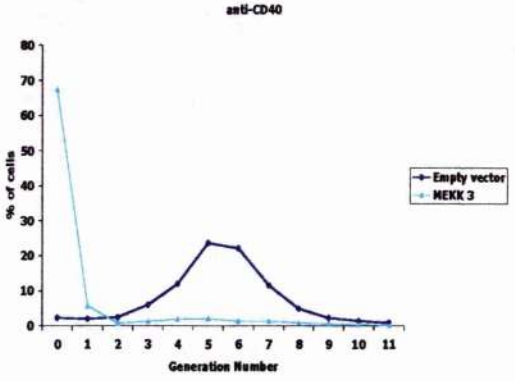
anti-CD40
% of cells
Generation Number
Empty vector
MEKK 3

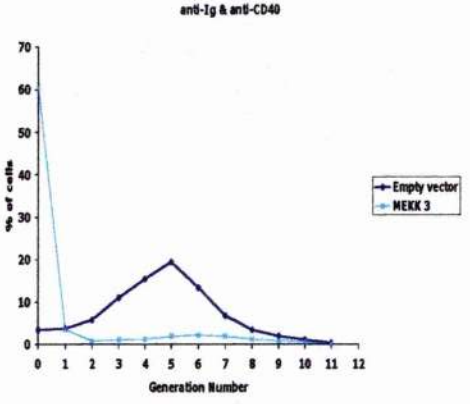
anti-Ig & anti-CD40
% of cells
Generation Number
Empty vector
MEKK 3

Figure 3.31: Expression of constitutively active MEKK3 induces ERK activation that is elevated compared to wild type WEHI 231 cells following BCR ligation

MEKK3 and wild type WEHI 231 cells were incubated for 48 h with appropriate stimulations prior to fixation, permeablisation and assessment of ERK levels. Cells were either cultured with 10 μg/ml anti-Ig (aIg) or a combination of 10 μg/ml anti-Ig and 10 μg/ml anti-CD40 (aIg & aCD40). The modified ELISA method- FACE- was used to assess the levels of ERK and phospho-ERK. Results are displayed as the ratio of the phospho-ERK signal to ERK signals. All ERK levels were calculated as the mean of triplicate cultures ± SEM.

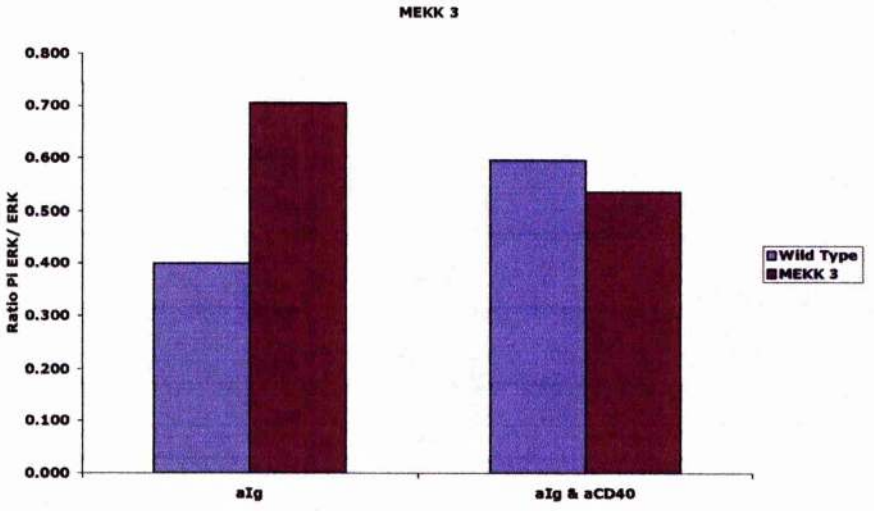
MEKK 3
0.800
0.700
0.600
0.500
0.400
0.300
0.200
0.100
0.000
Ratio PI ERK/ ERK
aIg
aIg & aCD40
Wild Type
MEKK 3

Figure 3.32: Treatment with anti-Ig results in the reduction of AKT activation in empty vector WEHI 231 cells but not RasV12 and MEKK3 mutant cell lines

Empty vector, RasV12 and MEKK3 WEHI 231 cells were incubated for 1 or 24 h with appropriate stimulations prior to fixation, permeablisation and assessment of phospho-AKT levels. Cells were either cultured with media alone (None) or 50 μg/ml anti-Ig. The modified ELISA method- FACE- was used to assess the levels of AKT and phospho-AKT. Results are displayed as the ratio of the phospho-AKT signal to AKT signals. All AKT levels were calculated as the mean of triplicate values and results are for a single, representative experiment.

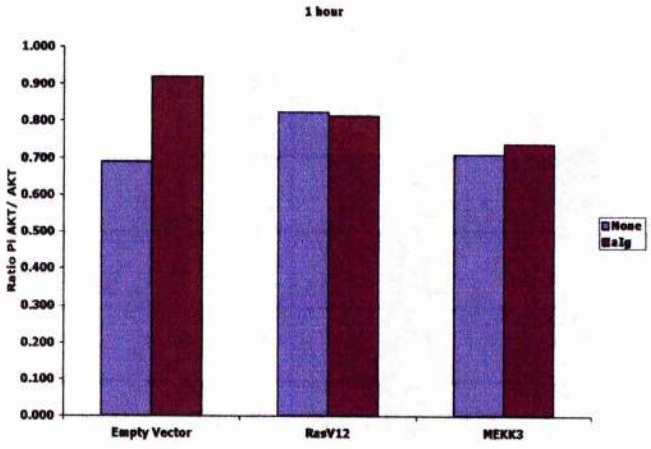
1 hour
Ratio Pi AKT/ AKT
1.000
0.900
0.800
0.700
0.600
0.500
0.400
0.300
0.200
0.100
0.000
Empty Vector
RasV12
MEKK3
None
aIg

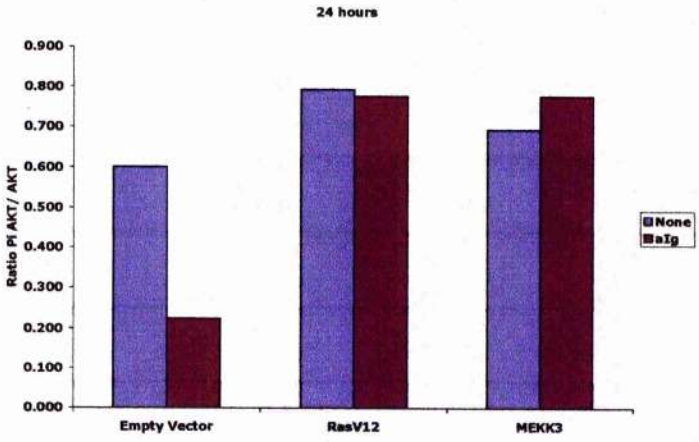
24 hours
Ratio Pi AKT/ AKT
0.900
0.800
0.700
0.600
0.500
0.400
0.300
0.200
0.100
0.000
Empty Vector
RasV12
MEKK3
None
aIg

Figure 3.33: SHIP SH2, SHIP CI and Dok PH/PTB mutants do not provide any protection from anti-Ig mediated growth arrest

Empty Vector, SHIP SH2, SHIP CI and Dok PH/PB WEHI 231 cells were cultured as indicated for 24, 48 or 72 h and then DNA synthesis was assessed by [^{3}H] thymidine uptake. Cells were treated with anti-Ig (0 to 10 μg/ml). Data from individual experiments were normalised by expressing the mean [^{3}H] thymidine uptake values of anti-Ig treated cells as a percentage of those obtained with control, unstimulated cell cultures. These data are the mean of 5 separate experiments ± SEM.

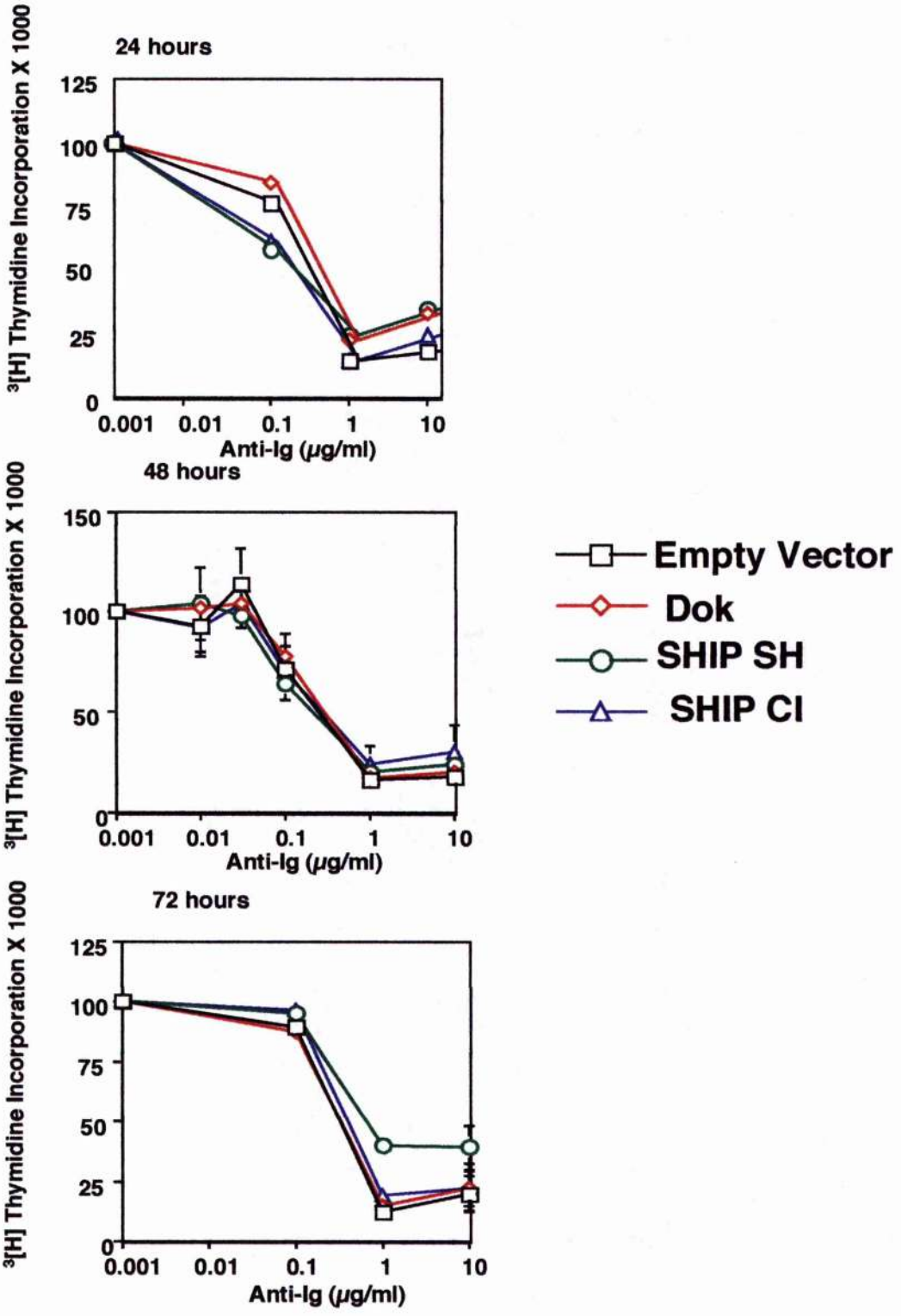
24 hours
3[H] Thymidine Incorporation X 1000
125
100
75
50
25
0
0.001
0.01
0.1
1
10
Anti-Ig (μg/ml)
48 hours
3[H] Thymidine Incorporation X 1000
150
100
50
0
0.001
0.01
0.1
1
10
Anti-Ig (μg/ml)
72 hours
3[H] Thymidine Incorporation X 1000
125
100
75
50
25
0
0.001
0.01
0.1
1
10
Anti-Ig (μg/ml)
Empty Vector
Dok
SHIP SH
SHIP CI

Figure 3.34: SHIP SH2, SHIP CI and Dok PH/PTB mutants do not affect anti-CD40 mediated rescue of anti-Ig stimulated growth arrest

Empty Vector, SHIP SH2, SHIP CI and Dok PH/PB WEHI 231 cells were cultured for 48 h with appropriate stimulations and then DNA synthesis was assessed by [^{3}H] thymidine uptake. Cells were treated with either media alone (None), 10 μg/ml anti-Ig (aIg) or a combination of 10 μg/ml anti-Ig plus 10 μg/ml anti-CD40 (aIg & aCD40). Data from individual experiments were normalised by expressing the mean [^{3}H] thymidine uptake values of each treatment group as a percentage of those obtained with the control, unstimulated cell cultures. These data are the mean of 5 separate experiments ± SEM.

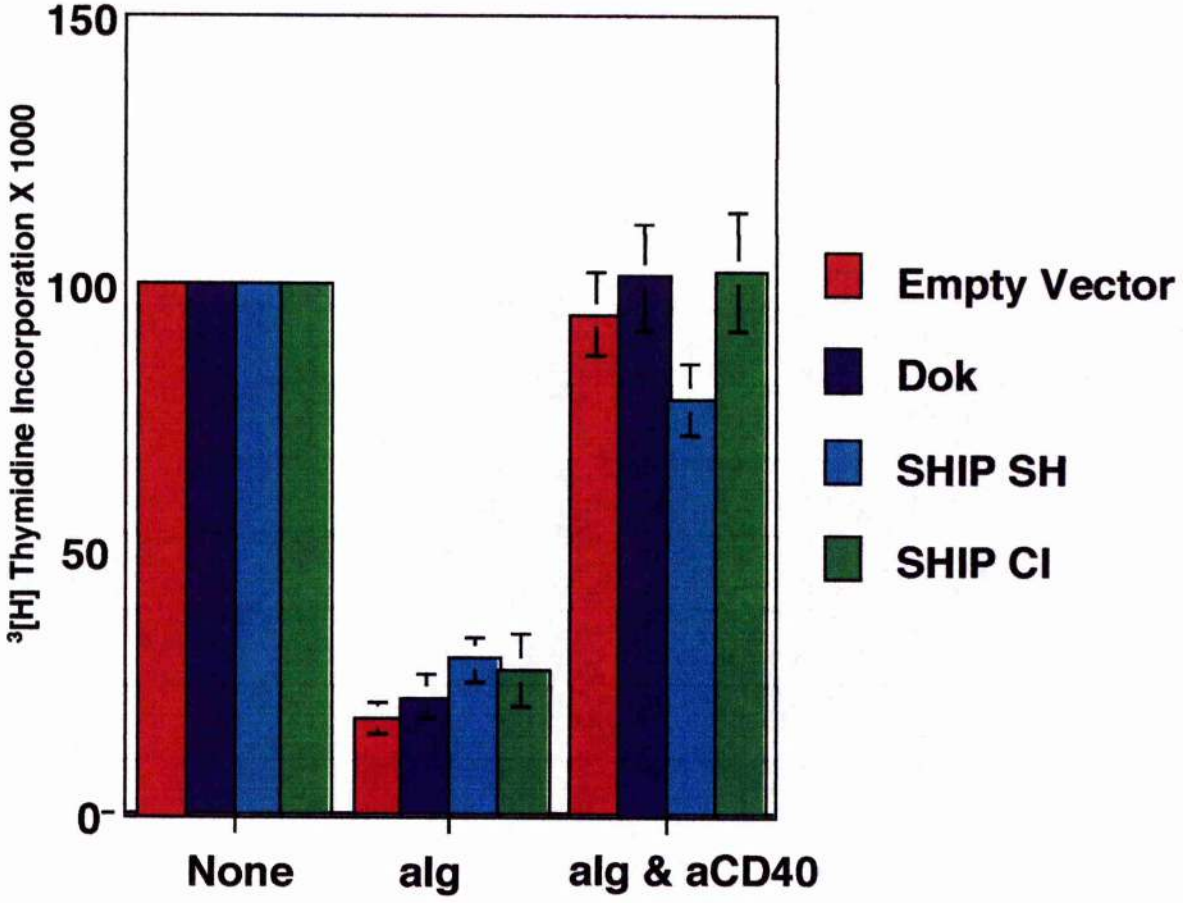
150
100
50
0
^{3}[H] Thymidine Incorporation X 1000
None
alg
alg & aCD40
Empty Vector
Dok
SHIP SH
SHIP CI

Figure 3.35: SHIP SH2 and SHIP CI mutants display a biphasic caspase 3 activation profile whereas Empty Vector and Dok PH/PTB mutants do not

Empty Vector, SHIP SH2, SHIP CI and Dok PH/PTB cells were cultured for 48 h, with appropriate stimulations, and then stained with 10 μM CaspACE™ FITC-VAD-FMK. This acts as a FITC conjugated version of the cell permeable, irreversible pan caspase inhibitor Z-VAD-FMK. Therefore it can be used to monitor the amount of activated caspase 3 present in the cell by measuring fluorescence in the FL1 channel. Stimulations used were: media alone (No Stim), 10 μg/ml anti-Ig (aIg), 10 μg/ml anti-CD40 (aCD40) and 10 μg/ml anti-Ig plus 10 μg/ml anti-CD40 (aIg & aCD40). The results are displayed as histograms of the amount of caspase 3 activation (FL1 fluorescence).

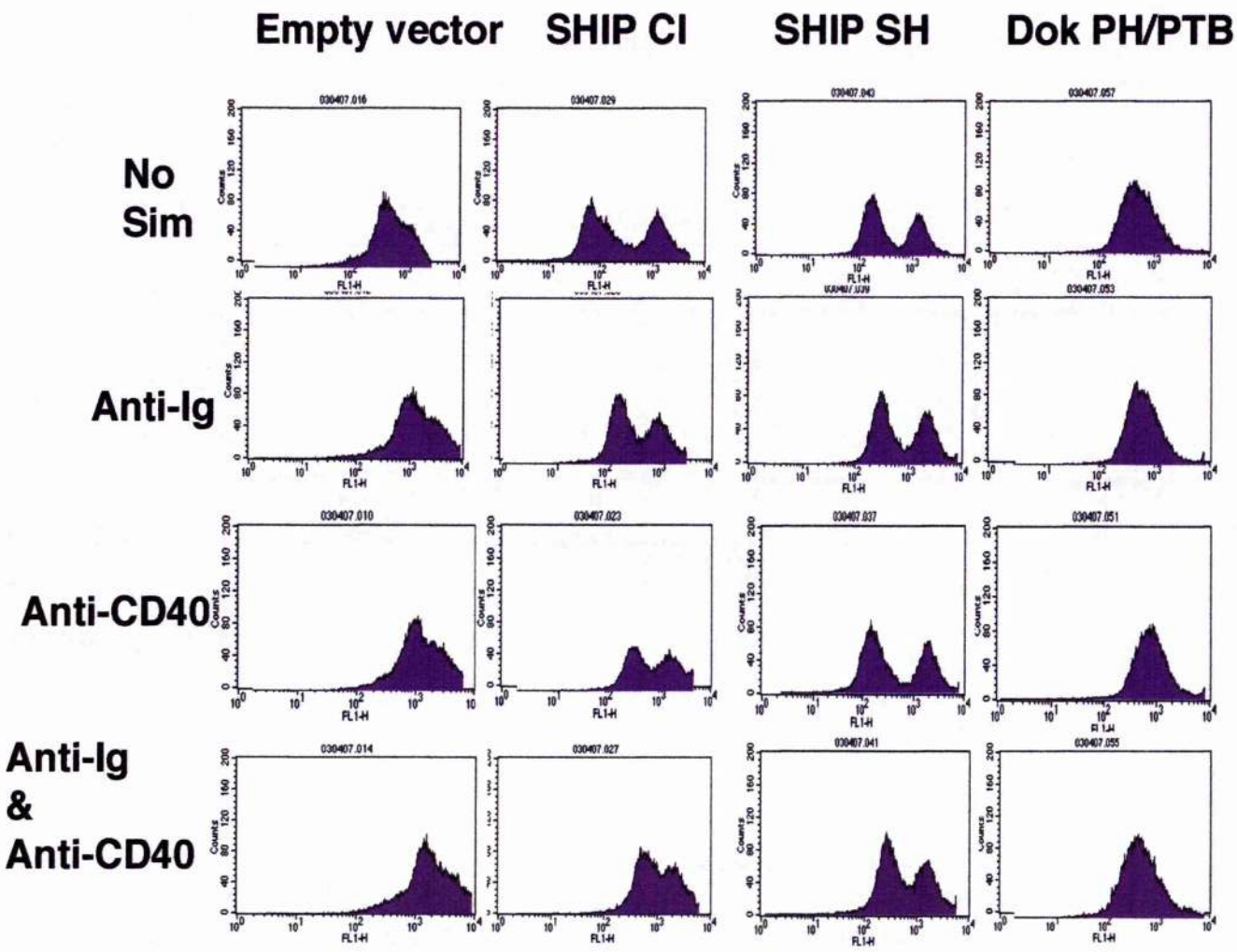
Empty vector
SHIP CI
SHIP SH
Dok PH/PTB
No Sim
Anti-Ig
Anti-CD40
Anti-Ig & Anti-CD40
Counts
FL1-H

Figure 3.36: Constructs utilised to generate PKC mutants

(A) Map of the pcDNA3.1 vector. The pcDNA3.1 (+) vector (Invitrogen Life Technologies) was used to introduce a variety of mutant PKC isotypes into the WEHI231 cell line.

Ampicillin: ampicillin resistance gene (*bla*)

P_{CMV}: cytomegalovirus promoter

BGH pA: BGH polyadenylation sequence

f1 ori: origin of replication from the f1 phage

SV40 ori: SV40 early promoter and origin

Neomycin: neomycin resistance gene

SV40 pA: SV40 polyadenylation sequence

pUC ori: pUC origin

(B) Schematic diagrams of structures of PKC mutants. PKC CAT constructs encode a truncated protein in which the catalytic domain is expressed but the entire regulatory domain has been deleted. PKC KR constructs encode a full-length PKC with a point mutation that abolishes ATP binding ability.

A

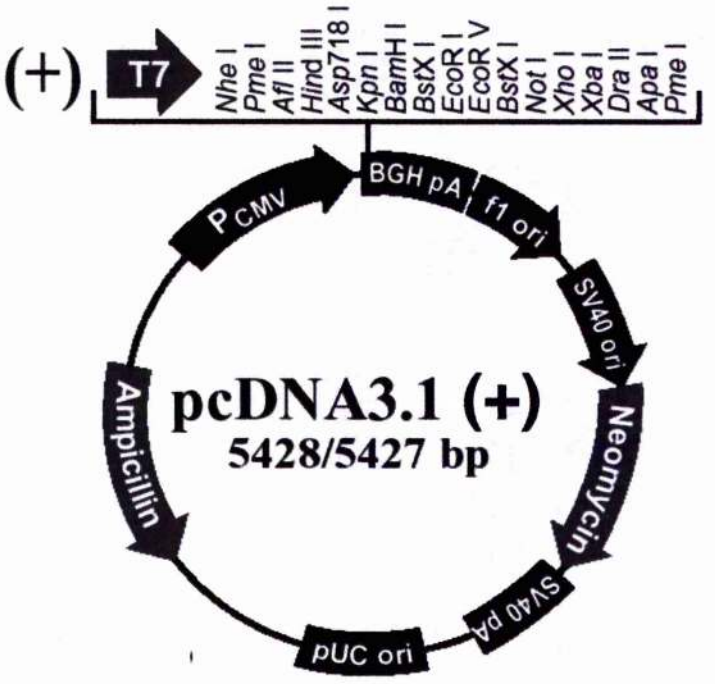
(+)
T7
Nhe I
Pme I
Afl II
Hind III
Asp718 I
Kpn I
BamH I
BstX I
EcoR I
EcoR V
BstX I
Not I
Xho I
Xba I
Dra II
Apa I
Pme I
P CMV
BGH pA
f1 ori
SV40 ori
Neomycin
SV40 pA
pUC ori
Ampicillin
pcDNA3.1 (+)
5428/5427 bp

B

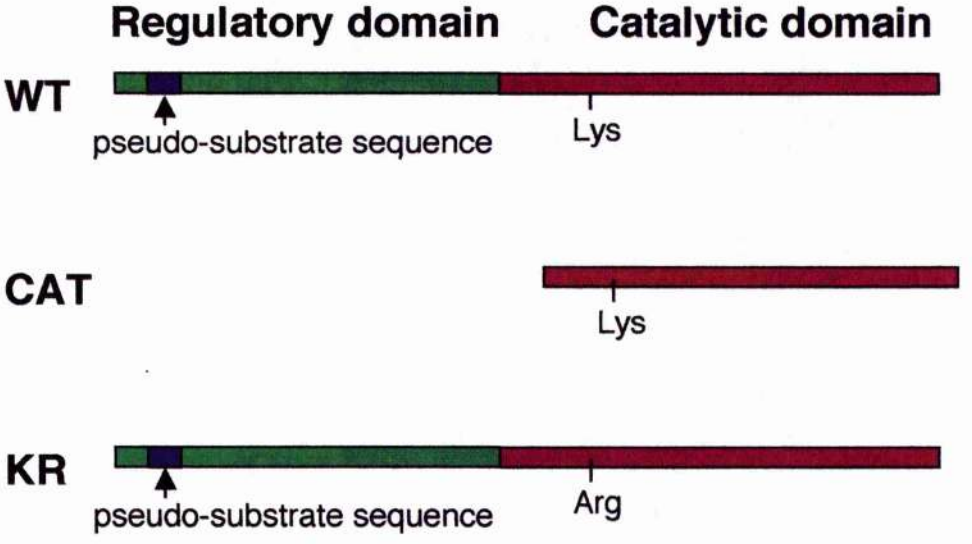
Regulatory domain
Catalytic domain
WT
pseudo-substrate sequence
Lys
CAT
Lys
KR
pseudo-substrate sequence
Arg

Figure 3.37: Effect of expression of PKCα constructs on anti-Ig induced growth arrest in WEHI 231 cells

(A) WEHI 231 cells (1 x 10^4 cells/well) containing the pcDNA3.1 vector (empty vector), PKCα CAT or PKCα KR were cultured, in triplicate, in the presence of increasing concentrations of anti-Ig antibodies (0, 0.1, 1, 10 μg/ml). Culture wells were pulsed with [^{3}H] thymidine (0.5 μCi/well) for 4 h prior to harvesting at 24 h and [^{3}H] incorporation was assessed by liquid scintillation counting. Data from individual experiments were normalised by expressing the mean [^{3}H] thymidine uptake values of anti-Ig treated cells as a percentage of those obtained with control, unstimulated cell cultures. The normalised values from 3 independent experiments were then pooled and expressed as means ± SEM.
(B) Cells were treated as described above in **(A)**, except that cells were cultured for 48 h.

A

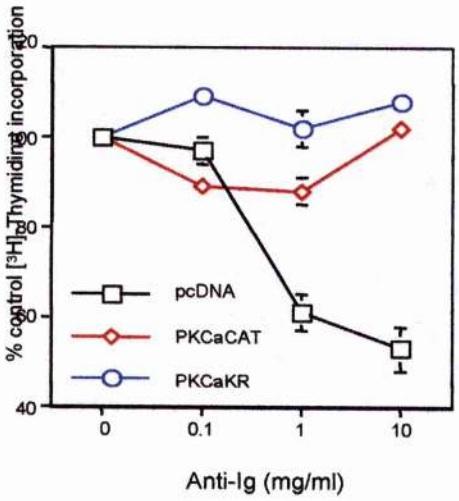
% control [3H]-Thymidine incorporation
120
100
80
60
40
pcDNA
PKCaCAT
PKCaKR
0
0.1
1
10
Anti-Ig (mg/ml)

B

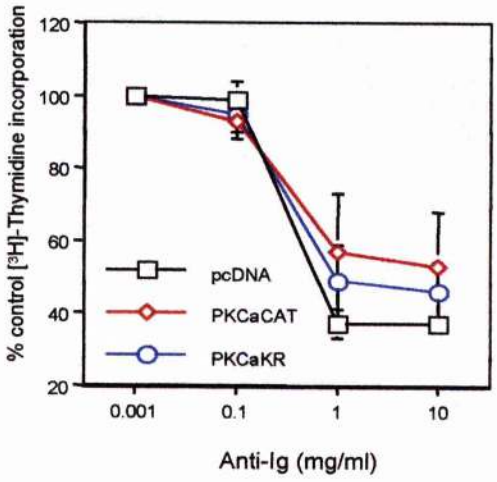
% control [3H]-Thymidine incorporation
120
100
80
60
40
20
pcDNA
PKCaCAT
PKCaKR
0.001
0.1
1
10
Anti-Ig (mg/ml)

Figure 3.38: Effect of expression of PKCα constructs on anti-Ig induced apoptosis and CD40-mediated rescue in WEHI 231 cells

WEHI 231 cells (5 x 10^5 cells/ml) containing the pcDNA3.1 vector (empty vector) or expressing PKCα CAT or PKCα KR were cultured in the presence of media alone (No stimulation), 10 μg/ml anti-Ig (anti-Ig) or a combination of 10 μg/ml anti-Ig and 10 μg/ml anti-CD40 (anti-Ig & anti-CD40) for 48 h. Levels of apoptosis and the proportion of cells in each cell cycle phase were determined by staining with 50 μg/ml PI staining followed by FACS analysis to assess DNA content as described in Materials and Methods. Data are displayed as the percentage of cells in each phase of the cell cycle. These data are the mean of 3 independent experiments ± SEM.

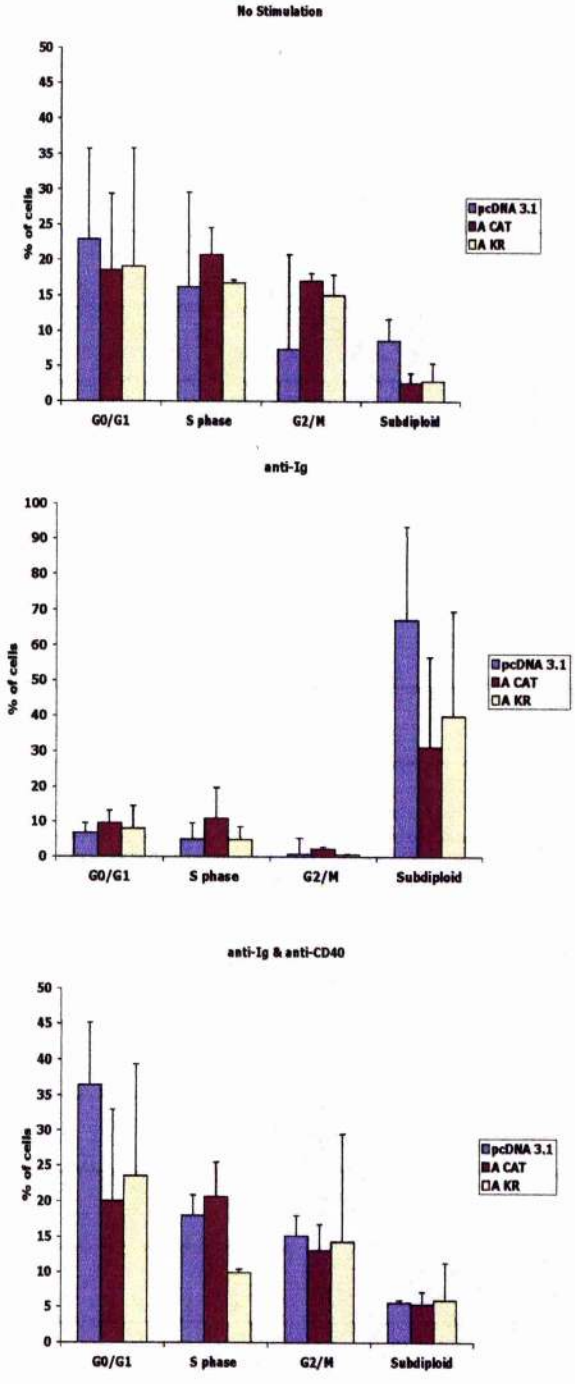
No Stimulation
% of cells
50
45
40
35
30
25
20
15
10
5
0
G0/G1
S phase
G2/M
Subdiploid
pcDNA 3.1
A CAT
A KR
anti-Ig
% of cells
100
90
80
70
60
50
40
30
20
10
0
G0/G1
S phase
G2/M
Subdiploid
pcDNA 3.1
A CAT
A KR
anti-Ig & anti-CD40
% of cells
50
45
40
35
30
25
20
15
10
5
0
G0/G1
S phase
G2/M
Subdiploid
pcDNA 3.1
A CAT
A KR

Figure 3.39: The effect of expression of PKCα constructs in WEHI 231 cells on cellular division at 72 h

WEHI 231 pcDNA3.1 (empty vector) or cells expressing PKCα CAT or PKCα KR were stained with 1 μM CFSE and then left in culture for 72 h with appropriate stimulations. Cells were either treated with media alone (control), 10 μg/ml anti-Ig (aIg), 10 μg/ml anti-CD40 (aCD40) or 10 μg/ml anti-Ig in combination with anti-CD40 (aIg & aCD40). Proliferation was assessed by an estimate of the percentage of cells in each generation. This calculation was done with the FlowJo proliferation data analysis programme. These data are from a single experiment, representative of 2 separate experiments.

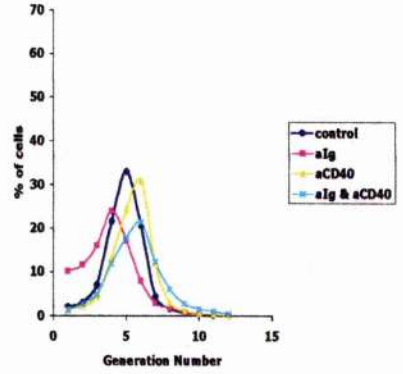

pcDNA 3.1

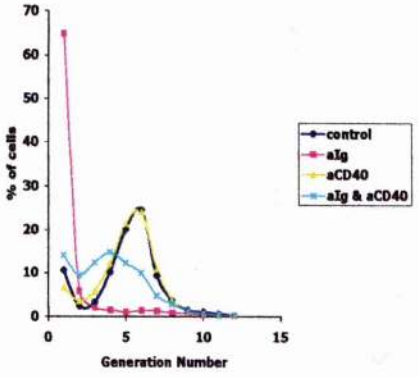

PKC α CAT

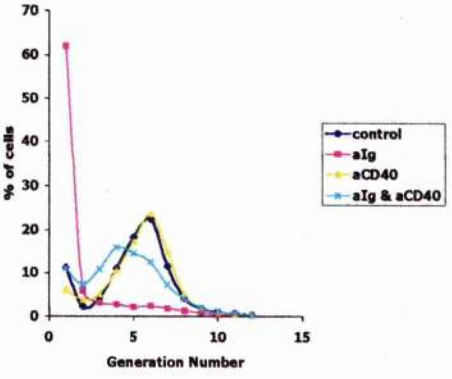

PKC α KR

Figure 3.40: Effects of PKC isoform expression on the MMP following BCR ligation

WEHI 231 pcDNA3.1 (empty vector), PKCα CAT, PKCα KR, PKCδ CAT, PKCδ KR, PKCε CAT, PKCε KR, PKCζ CAT and PKCζ KR cells (5×10^5 cells/ml) were cultured in the presence of 10 μg/ml anti-Ig (anti-Ig) or a combination of 10 μg/ml anti-Ig and 10 μg/ml anti-CD40 (anti-Ig & anti-CD40) for 48 h prior to staining with 2.5 μM $DiOC_6$. Dissipation of the MMP can been seen as a reduction in $DiOC_6$ brightness (FL1 fluorescence). The data are displayed as histograms of $DiOC_6$ brightness (FL1 fluorescence). These data are from a single experiment, representative of 3 experiments.

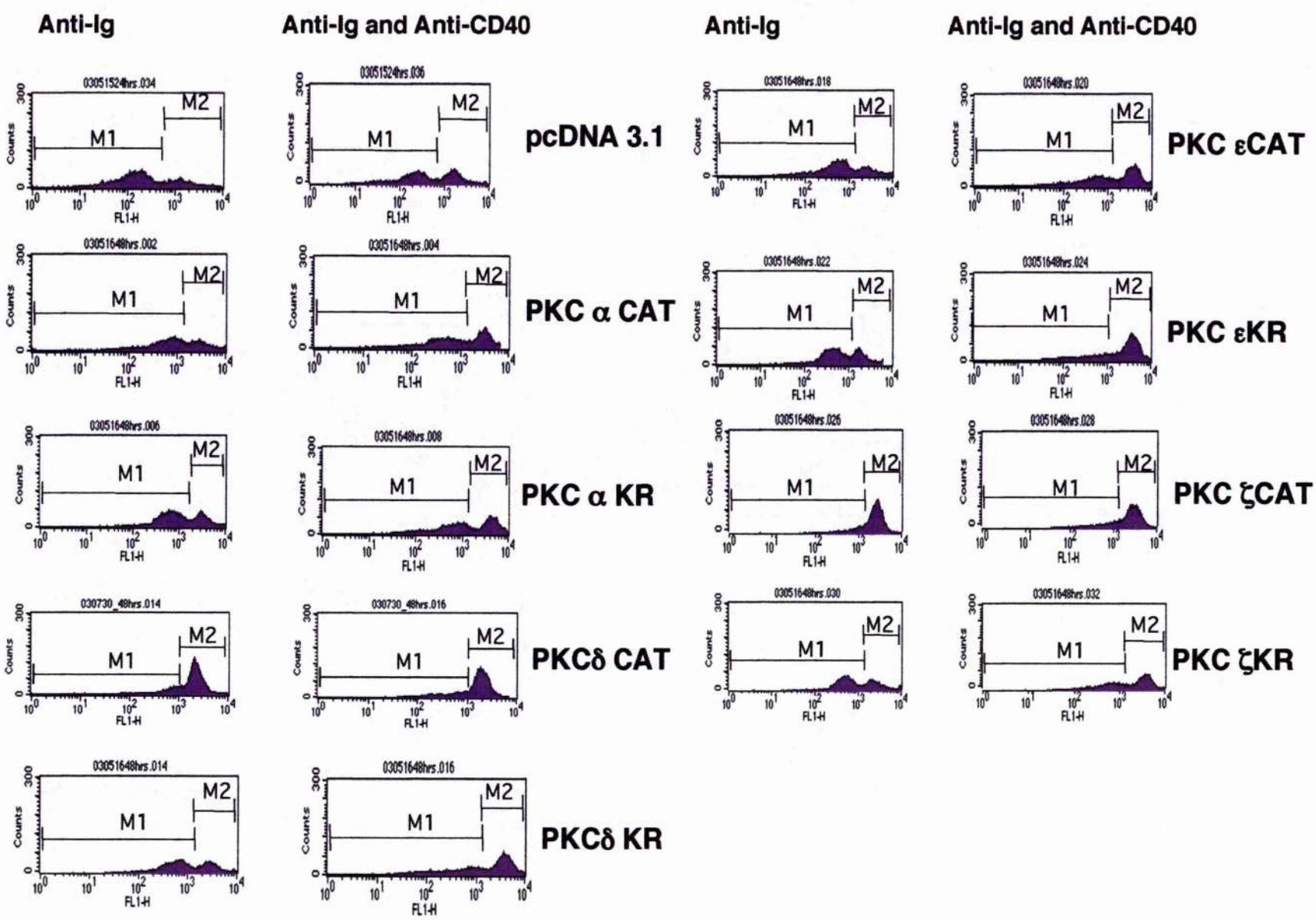
Anti-Ig
Anti-Ig and Anti-CD40
Anti-Ig
Anti-Ig and Anti-CD40
pcDNA 3.1
PKC α CAT
PKC α KR
PKCδ CAT
PKCδ KR
PKC εCAT
PKC εKR
PKC ζCAT
PKC ζKR
M1
M2
Counts
FL1-H

Figure 3.41: PKCα expression and activity protects from BCR-stimulated dissipation of the MMP

(A) WEHI 231 cells (5 x 10^5 cells/ml) containing the pcDNA3.1 vector (empty vector) or expressing PKCα CAT or PKCα KR were cultured in the presence of media alone (No stimulation), 10 μg/ml anti-Ig (aIg), 10 μg/ml anti-CD40 (aCD40) or a combination of 10 μg/ml anti-Ig and 10 μg/ml anti-CD40 (aIg & aCD40) for 48 h prior to staining with 2.5 μM $DiOC_6$. Dissipation of the MMP can been seen as a reduction in $DiOC_6$ brightness (FL1 fluorescence and was assessed by dividing the cells into two populations, high MMP (M2) and low apoptotic MMP (M1). The data was then displayed as the percentage of cells with a high MMP. These data are the mean values of 3 experiments ± SEM. **(B)** Cells were treated as described as above and cultured for 0 to 96 hours prior to DiOC6 staining and FACS analysis. The data is from one, representative experiment.

A

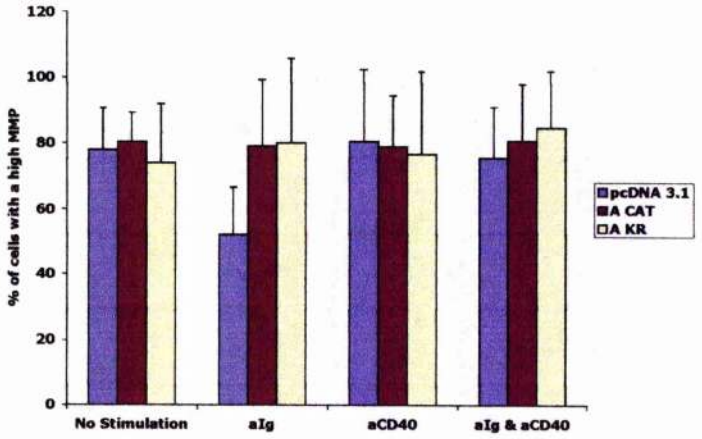
% of cells with a high MMP
120
100
80
60
40
20
0
No Stimulation
aIg
aCD40
aIg & aCD40
pcDNA 3.1
A CAT
A KR

B

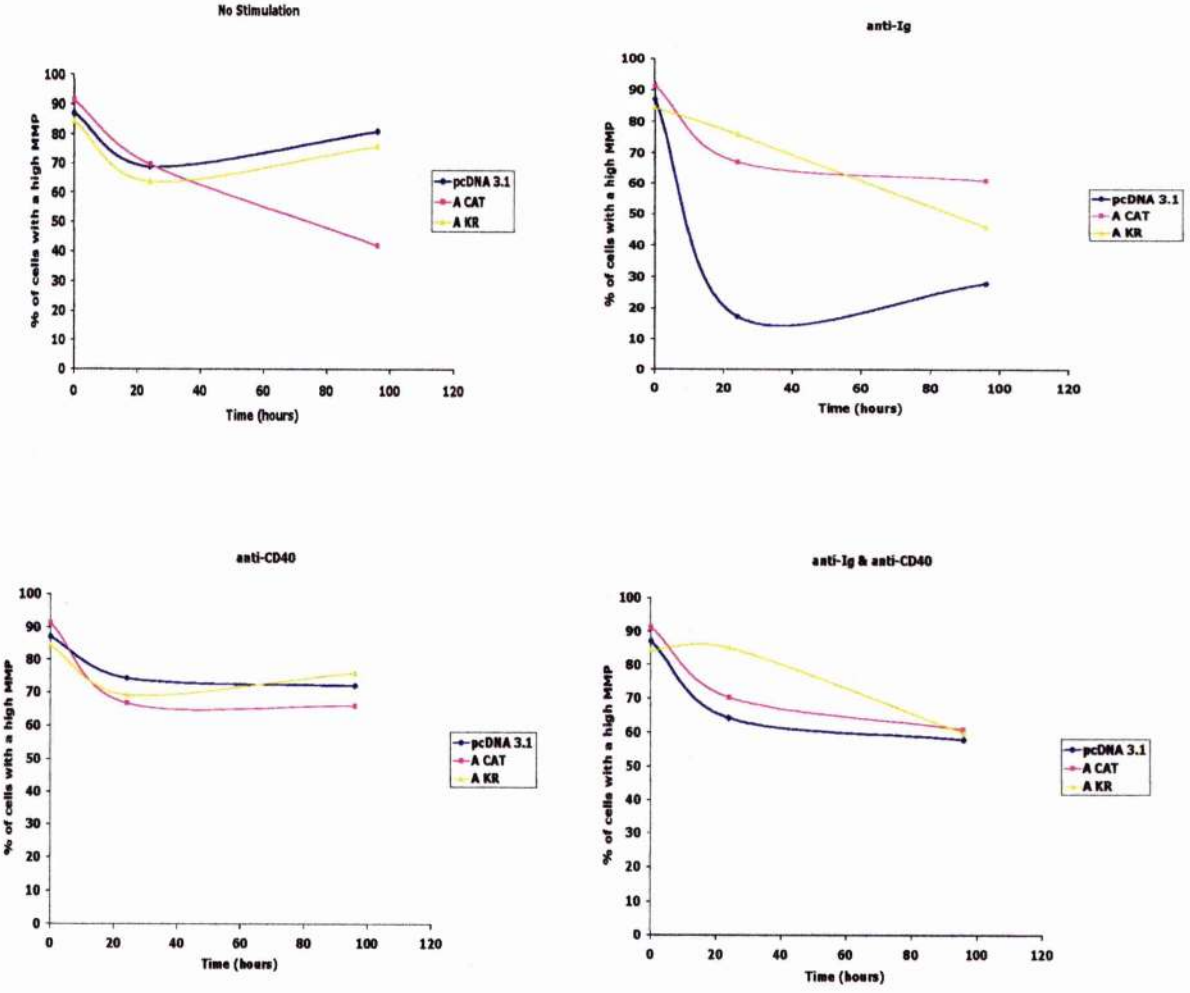
No Stimulation
anti-Ig
anti-CD40
anti-Ig & anti-CD40
% of cells with a high MMP
Time (hours)
pcDNA 3.1
A CAT
A KR

Figure 3.42: Effects of expression of PKCδ constructs on anti-Ig induced growth arrest in WEHI 231 cells

(A) WEHI 231 cells (1 x 10^4 cells/well) containing the pcDNA3.1 vector (empty vector) or expressing PKCδ CAT or PKCδ KR were cultured, in triplicate, in the presence of increasing concentrations of anti-Ig antibodies (0, 0.1, 1, 10 μg/ml). Culture wells were pulsed with [^{3}H] thymidine (0.5 μCi/well) for 4 h prior to harvesting at 24 h and [^{3}H] incorporation was assessed by liquid scintillation counting. Data from individual experiments were normalised by expressing the mean [^{3}H] thymidine uptake values of anti-Ig treated cells as a percentage of those obtained with control, unstimulated cell cultures. The normalised values from 3 independent experiments were then pooled and expressed as means ± SEM.

(B) Cells were treated as described above, except cultured for 48 h prior to harvesting.

A

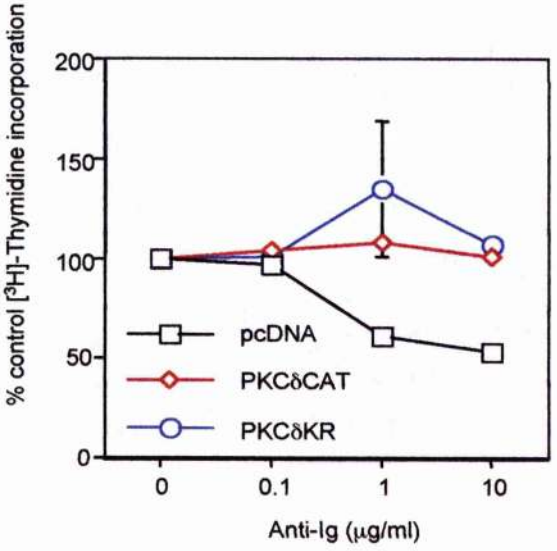
% control [3H]-Thymidine incorporation
200
150
100
50
0
pcDNA
PKCδCAT
PKCδKR
0
0.1
1
10
Anti-Ig (μg/ml)

B

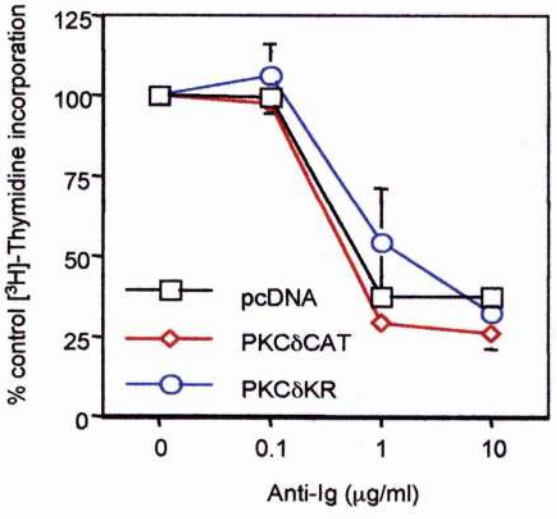
% control [3H]-Thymidine incorporation
125
100
75
50
25
0
pcDNA
PKCδCAT
PKCδKR
0
0.1
1
10
Anti-Ig (μg/ml)

Figure 3.43: Effects of expression of PKCδ constructs on anti-Ig induced apoptosis and CD40-mediated rescue in WEHI 231 cells

WEHI 231 cells (5 x 10^5 cells/ml) containing the pcDNA3.1 vector (empty vector) or expressing PKCδ CAT or PKCδ KR were cultured in the presence of media alone (No stimulation), 10 μg/ml anti-Ig (anti-Ig) or a combination of 10 μg/ml anti-Ig and 10 μg/ml anti-CD40 (anti-Ig & anti-CD40) for 48 h. Levels of apoptosis and the proportion of cells in each cell cycle phase were determined by staining with 50 μg/ml PI staining followed by FACS analysis to assess DNA content as described in Materials and Methods. Data are displayed as the percentage of cells in each phase of the cell cycle. These data are the mean of 3 independent experiments ± SEM.

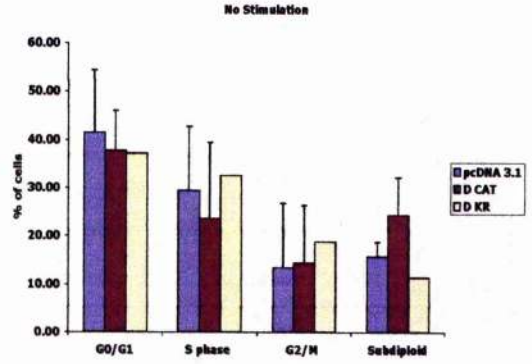
No Stimulation
60.00
50.00
40.00
30.00
20.00
10.00
0.00
% of cells
G0/G1
S phase
G2/M
Subdiploid
pcDNA 3.1
D CAT
D KR

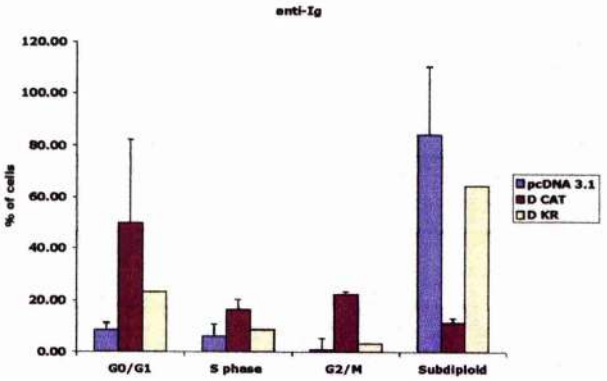
anti-Ig
120.00
100.00
80.00
60.00
40.00
20.00
0.00
% of cells
G0/G1
S phase
G2/M
Subdiploid
pcDNA 3.1
D CAT
D KR

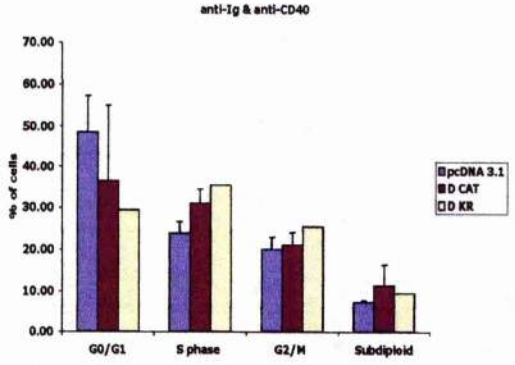
anti-Ig & anti-CD40
70.00
60.00
50.00
40.00
30.00
20.00
10.00
0.00
% of cells
G0/G1
S phase
G2/M
Subdiploid
pcDNA 3.1
D CAT
D KR

Figure 3.44: Expression and activity of PKCδ protects from BCR-stimulated dissipation of the MMP

WEHI 231 cells (5 x 10^5 cells/ml) containing the pcDNA3.1 vector (empty vector) or expressing PKCδ CAT or PKCδ KR were cultured in the presence of media alone (No stimulation), 10 μg/ml anti-Ig (alg), 10 μg/ml anti-CD40 (aCD40) or a combination of 10 μg/ml anti-Ig and 10 μg/ml anti-CD40 (alg & aCD40) for 48 h prior to staining with 2.5 μM $DiOC_6$. Dissipation of the MMP can been seen as a reduction in $DiOC_6$ brightness (FL1 fluorescence). Dissipation of the MMP was assessed by dividing the cells into two populations. The right hand peak having a high healthy MMP and the second having a low apoptotic MMP. The data was then displayed as the percentage of cells with a high MMP. These data are the mean of 3 independent experiments ± SEM.

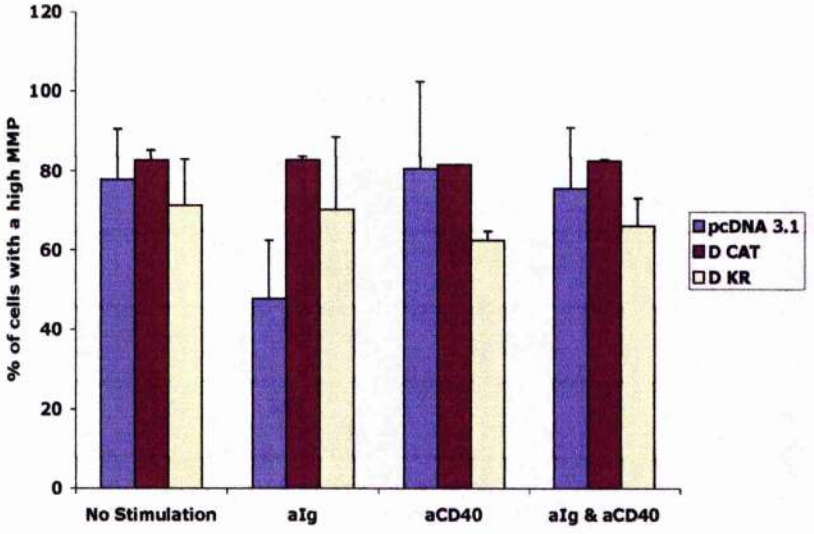
120
100
80
60
40
20
0
% of cells with a high MMP
No Stimulation
aIg
aCD40
aIg & aCD40
pcDNA 3.1
D CAT
D KR

Figure 3.45: Effects of expression of PKCε constructs on anti-Ig induced growth arrest in WEHI 231 cells

(A) WEHI 231 cells (1 x 10^4 cells/well) containing the pcDNA3.1 vector (empty vector) or expressing PKCε CAT or PKCε KR were cultured, in triplicate, in the presence of increasing concentrations of anti-Ig antibodies (0, 0.1, 1, 10 μg/ml). Culture wells were pulsed with [^{3}H] thymidine (0.5 μCi/well) for 4 h prior to harvesting at 24 h and [^{3}H] incorporation was assessed by liquid scintillation counting. Data from individual experiments were normalised by expressing the mean [^{3}H] thymidine uptake values of anti-Ig treated cells as a percentage of those obtained with control cell cultures. The normalised values from 3 independent experiments were then pooled and expressed as means ± SEM. **(B)** Cells were treated as described above, except cells were cultured for 48 h prior to harvesting.

A

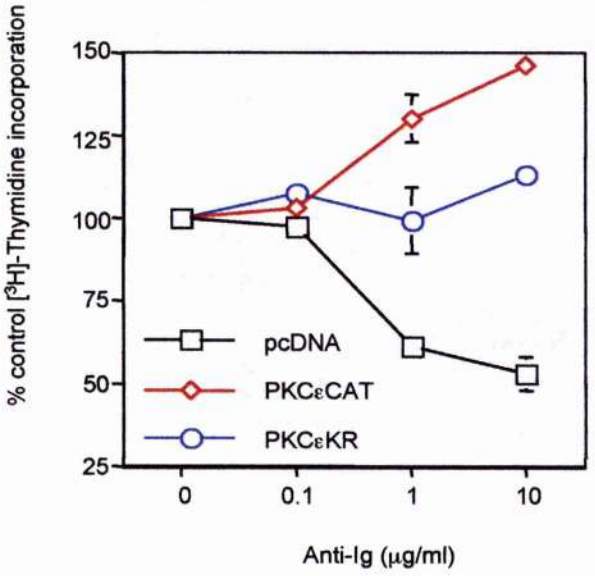
% control [3H]-Thymidine incorporation
150
125
100
75
50
25
0
0.1
1
10
Anti-Ig (μg/ml)
pcDNA
PKCεCAT
PKCεKR

B

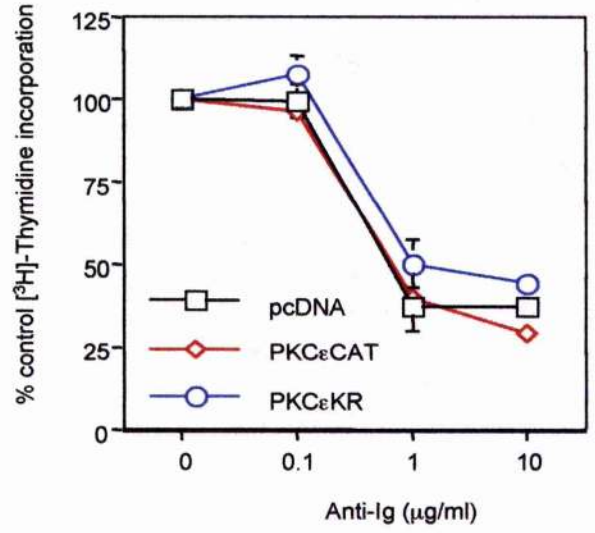
% control [3H]-Thymidine incorporation
125
100
75
50
25
0
0
0.1
1
10
Anti-Ig (μg/ml)
pcDNA
PKCεCAT
PKCεKR

Figure 3.46: The effect of expression of PKCε CAT construct in WEHI 231 cells on cellular division at 72 h

WEHI 231 pcDNA3.1 (empty vector) or cells expressing PKCε CAT were stained with 1 μM CFSE and then left in culture for 72 h with appropriate stimulations. Cells were either treated with media alone (control), 10 μg/ml anti-Ig (aIg), 10 μg/ml anti-CD40 (aCD40) or 10 μg/ml anti-Ig in combination with anti-CD40 (aIg & aCD40). Proliferation was assessed by an estimate of the percentage of cells in each generation. This calculation was done with the FlowJo proliferation data analysis programme. These data are from a single experiment, representative of 2 separate experiments.

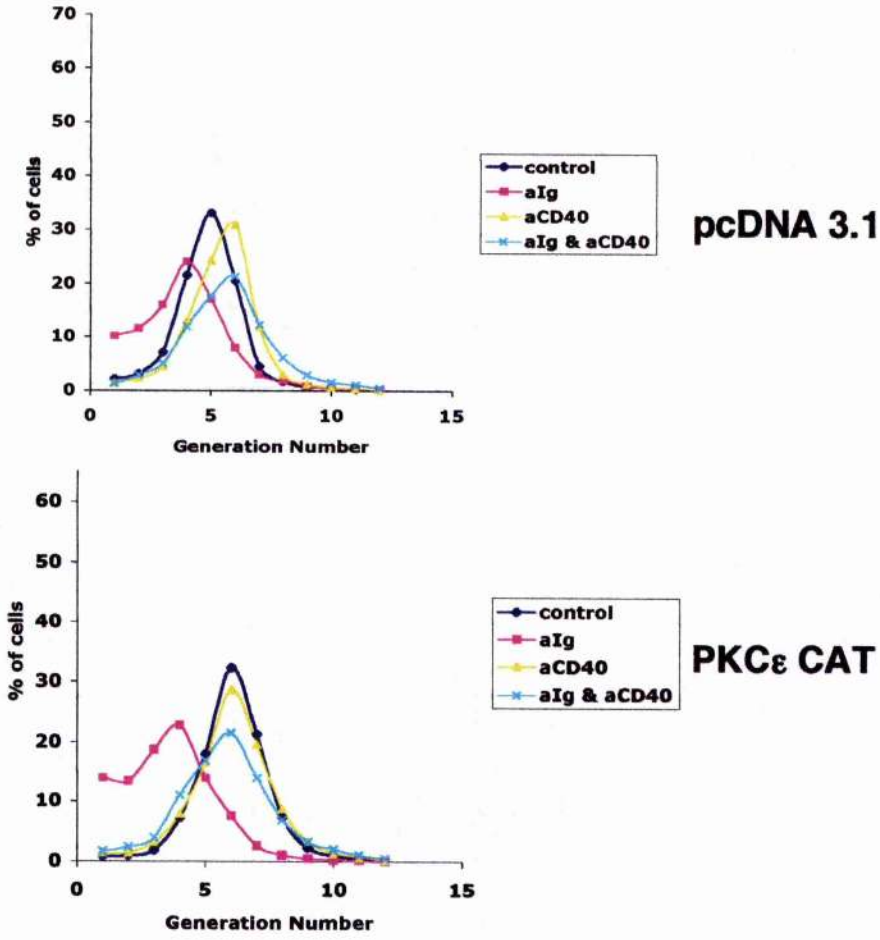
70
60
50
40
30
20
10
0
% of cells
0
5
10
15
Generation Number
control
aIg
aCD40
aIg & aCD40
pcDNA 3.1
60
50
40
30
20
10
0
% of cells
0
5
10
15
Generation Number
control
aIg
aCD40
aIg & aCD40
PKCε CAT

Figure 3.47: Effects of expression of PKCε mutants on anti-Ig induced apoptosis and CD40-mediated rescue in WEHI 231 cells

WEHI 231 cells (5 x 10^5 cells/ml) containing the pcDNA3.1 vector (empty vector) or expressing PKCε CAT or PKCε KR were cultured in the presence of media alone (No stimulation), 10 μg/ml anti-Ig (anti-Ig) or a combination of 10 μg/ml anti-Ig and 10 μg/ml anti-CD40 (anti-Ig & anti-CD40) for 48 h. Levels of apoptosis and the proportion of cells in each cell cycle phase were determined by staining with 50 μg/ml PI staining followed by FACS analysis to assess DNA content as described in Materials and Methods. Data are displayed as the percentage of cells in each phase of the cell cycle. These data are the mean values of 3 independent experiments ± SEM.

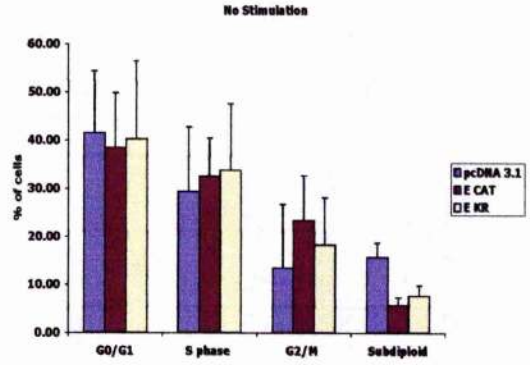
No Stimulation
60.00
50.00
40.00
30.00
20.00
10.00
0.00
% of cells
G0/G1
S phase
G2/M
Subdiploid
pcDNA 3.1
E CAT
E KR

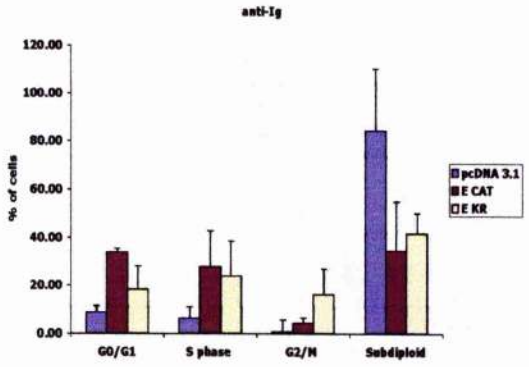
anti-Ig
120.00
100.00
80.00
60.00
40.00
20.00
0.00
% of cells
G0/G1
S phase
G2/M
Subdiploid
pcDNA 3.1
E CAT
E KR

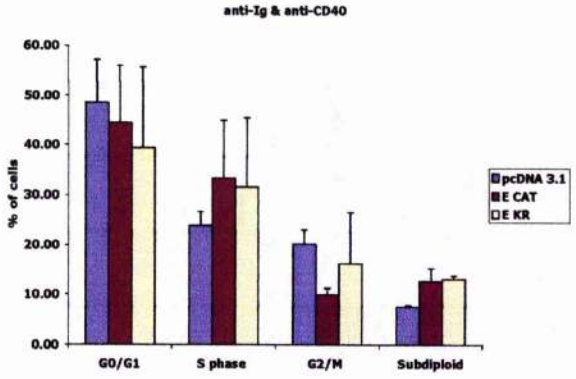
anti-Ig & anti-CD40
60.00
50.00
40.00
30.00
20.00
10.00
0.00
% of cells
G0/G1
S phase
G2/M
Subdiploid
pcDNA 3.1
E CAT
E KR

Figure 3.48: Expression of PKCε constructs may only partially rescue WEHI 231 cells from BCR-stimulated dissipation of the MMP

(A) WEHI 231 cells (5 x 10^5 cells/ml) containing the pcDNA3.1 vector (empty vector) or expressing PKCε CAT or PKCε KR were cultured in the presence of media alone (No stimulation), 10 μg/ml anti-Ig (alg), 10 μg/ml anti-CD40 (aCD40) or a combination of 10 μg/ml anti-Ig and 10 μg/ml anti-CD40 (alg & aCD40) for 48 h prior to staining with 2.5 μM $DiOC_6$. Dissipation of the MMP can been seen as a reduction in $DiOC_6$ brightness (FL1 fluorescence) and was assessed by dividing the cells into two populations having a high MMP (M2) or a low apoptotic MMP (M1). The data was then displayed as the percentage of cells with a high MMP. These data are the mean values of 3 independent experiments ± SEM.

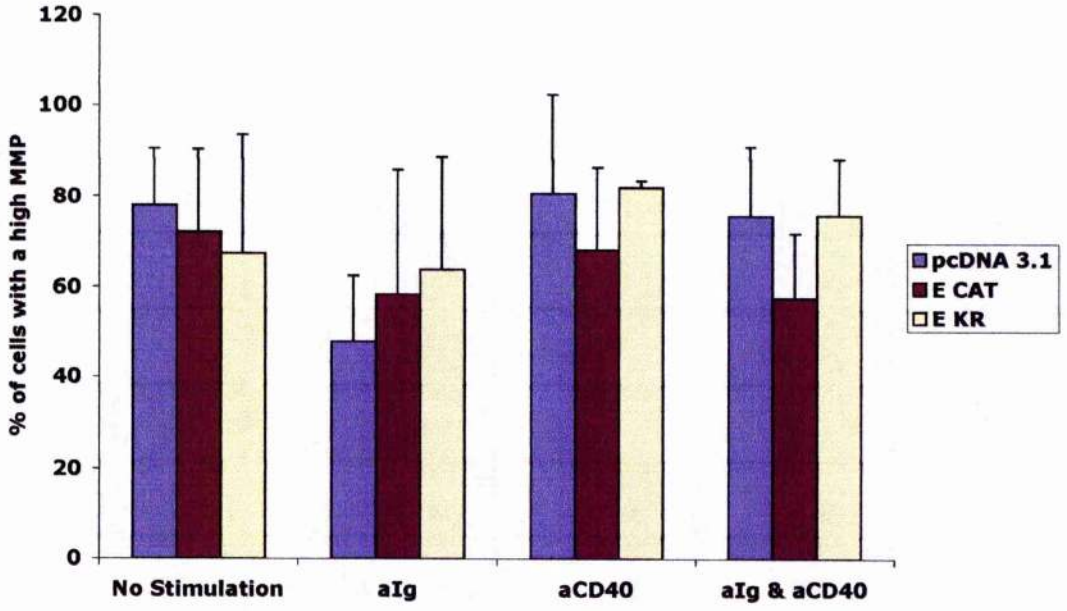
120
100
80
60
40
20
0
% of cells with a high MMP
No Stimulation
aIg
aCD40
aIg & aCD40
pcDNA 3.1
E CAT
E KR

Figure 3.49: Effects of expression of PKCζ constructs on anti-Ig induced growth arrest in WEHI 231 cells

(A) WEHI 231 cells (1 x 10^4 cells/well) containing the pcDNA3.1 vector (empty vector) or expressing PKCζ CAT or PKCζ KR were cultured, in triplicate, in the presence of increasing concentrations of anti-Ig antibodies (0, 0.1, 1, 10 μg/ml). Culture wells were pulsed with [^{3}H] thymidine (0.5 μCi/well) for 4 h prior to harvesting at 24 h and [^{3}H] incorporation was assessed by liquid scintillation counting. Data from individual experiments were normalised by expressing the mean [^{3}H] thymidine uptake values of anti-Ig treated cells as a percentage of those obtained with control cell cultures. The normalised values from 3 independent experiments were then pooled and expressed as means ± SEM. **(B)** Cells were treated as described above, except cultured for 48 h prior to harvesting.

A

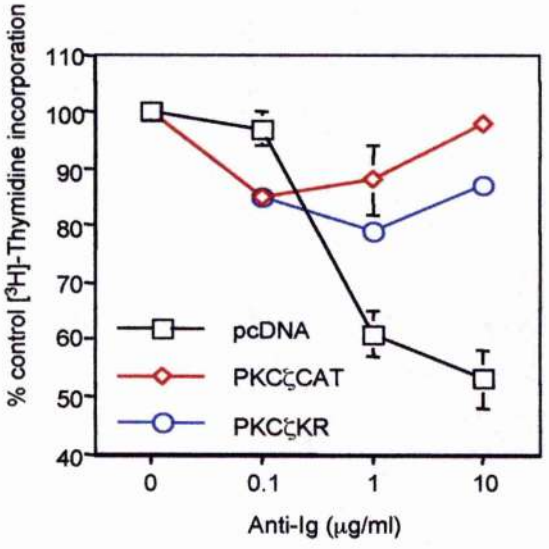
% control [3H]-Thymidine incorporation
110
100
90
80
70
60
50
40
0
0.1
1
10
Anti-Ig (μg/ml)
pcDNA
PKCζCAT
PKCζKR

B

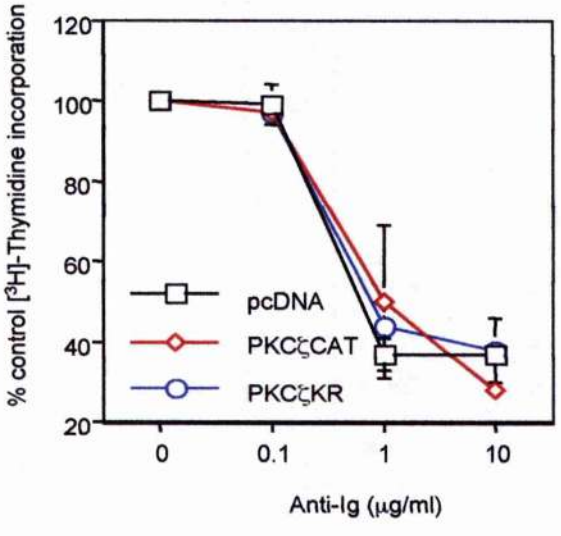
% control [3H]-Thymidine incorporation
120
100
80
60
40
20
0
0.1
1
10
Anti-Ig (μg/ml)
pcDNA
PKCζCAT
PKCζKR

Figure 3.50: The effect of expression of the PKCζ CAT construct in WEHI 231 cells on cellular division at 72 h

WEHI 231 pcDNA3.1 (empty vector) or cells expressing PKCζ CAT were stained with 1 μM CFSE and then left in culture for 72 h with appropriate stimulations. Cells were either treated with media alone (control), 10 μg/ml anti-Ig (aIg), 10 μg/ml anti-CD40 (aCD40) or 10 μg/ml anti-Ig in combination with anti-CD40 (aIg & aCD40). Proliferation was assessed by an estimate of the percentage of cells in each generation. This calculation was done with the FlowJo proliferation data analysis programme. These data are from a single experiment, representative of 2 separate experiments.

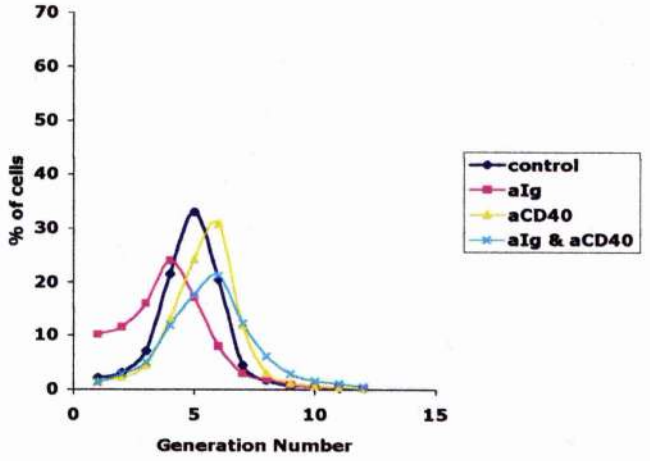

pcDNA 3.1

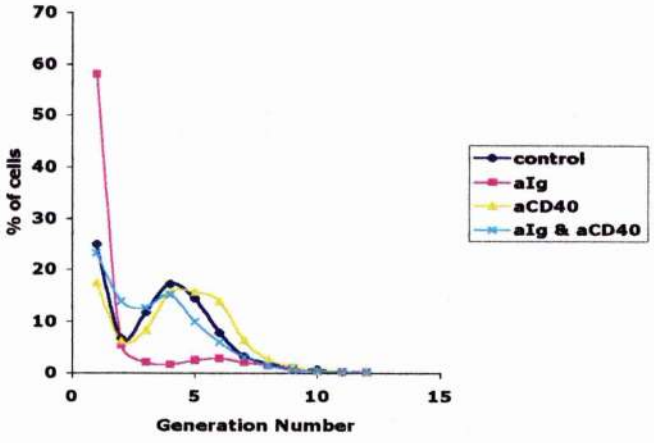

PKCζ CAT

Figure 3.51: Effects of expression of the PKCζ CAT construct on anti-Ig induced apoptosis and CD40-mediated rescue in WEHI 231 cells

WEHI 231 cells (5 x 10^5 cells/ml) containing the pcDNA3.1 vector (empty vector) or expressing PKCζ CAT or PKCζ KR were cultured in the presence of media alone (No stimulation), 10 μg/ml anti-Ig (anti-Ig) or a combination of 10 μg/ml anti-Ig and 10 μg/ml anti-CD40 (anti-Ig & anti-CD40) for 48 h. Levels of apoptosis and the proportion of cells in each cell cycle phase were determined by staining with 50 μg/ml PI staining followed by FACS analysis to assess DNA content as described in Materials and Methods. Data are displayed as the percentage of cells in each phase of the cell cycle. These data are the mean values of 3 independent experiments ± SEM.

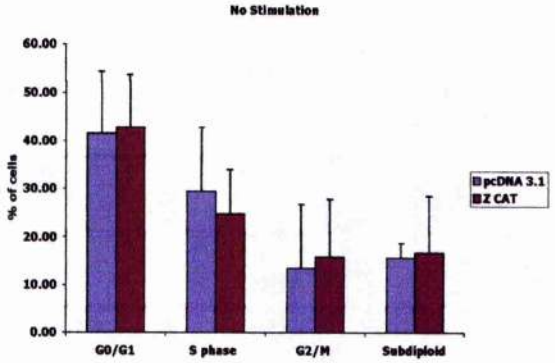
No Stimulation
60.00
50.00
40.00
30.00
20.00
10.00
0.00
% of cells
G0/G1
S phase
G2/M
Subdiploid
pcDNA 3.1
Z CAT

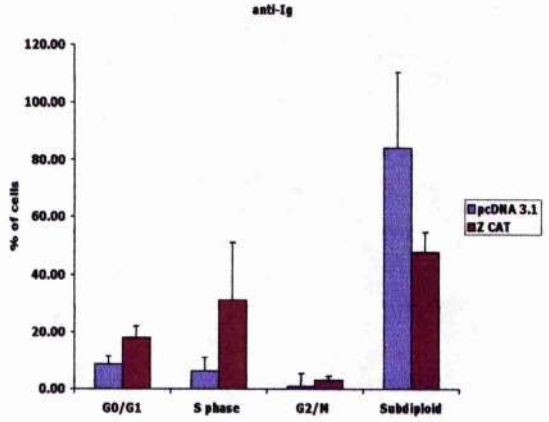
anti-Ig
120.00
100.00
80.00
60.00
40.00
20.00
0.00
% of cells
G0/G1
S phase
G2/M
Subdiploid
pcDNA 3.1
Z CAT

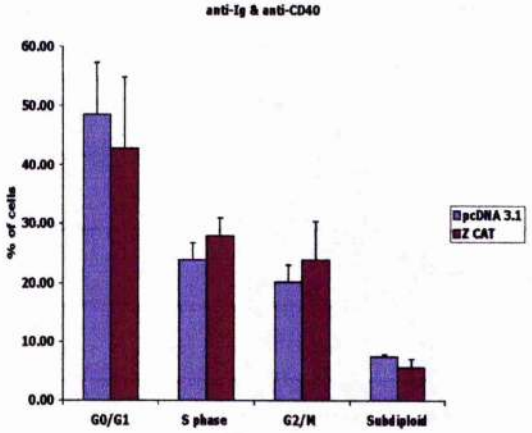
anti-Ig & anti-CD40
60.00
50.00
40.00
30.00
20.00
10.00
0.00
% of cells
G0/G1
S phase
G2/M
Subdiploid
pcDNA 3.1
Z CAT

Figure 3.52: Expression of PKCζ constructs protects from BCR-stimulated dissipation of the MMP

(A) WEHI 231 cells (5 x 10^5 cells/ml) containing the pcDNA3.1 vector (empty vector) or expressing PKCζ CAT or PKCζ KR were cultured in the presence of media alone (No stimulation), 10 μg/ml anti-Ig (alg), 10 μg/ml anti-CD40 (aCD40) or a combination of 10 μg/ml anti-Ig and 10 μg/ml anti-CD40 (alg & aCD40) for 48 h prior to staining with 2.5 μM $DiOC_6$. Dissipation of the MMP can been seen as a reduction in $DiOC_6$ brightness (FL1 fluorescence) and was assessed by dividing the cells into two populations having a high MMP (M2) or a low apoptotic MMP (M1). The data was then displayed as the percentage of cells with a high MMP. These data are the mean values of 3 independent experiments ± SEM.

(B) Cells were treated as described above but cultured for up to 96 h prior to $DiOC_6$ staining and FACS analysis.

A

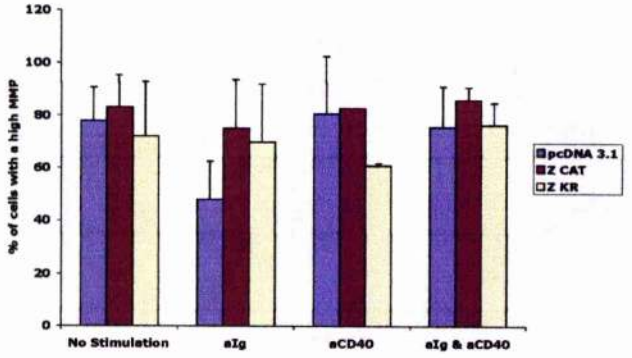
% of cells with a high MMP
120
100
80
60
40
20
0
No Stimulation
aIg
aCD40
aIg & aCD40
pcDNA 3.1
Z CAT
Z KR

B

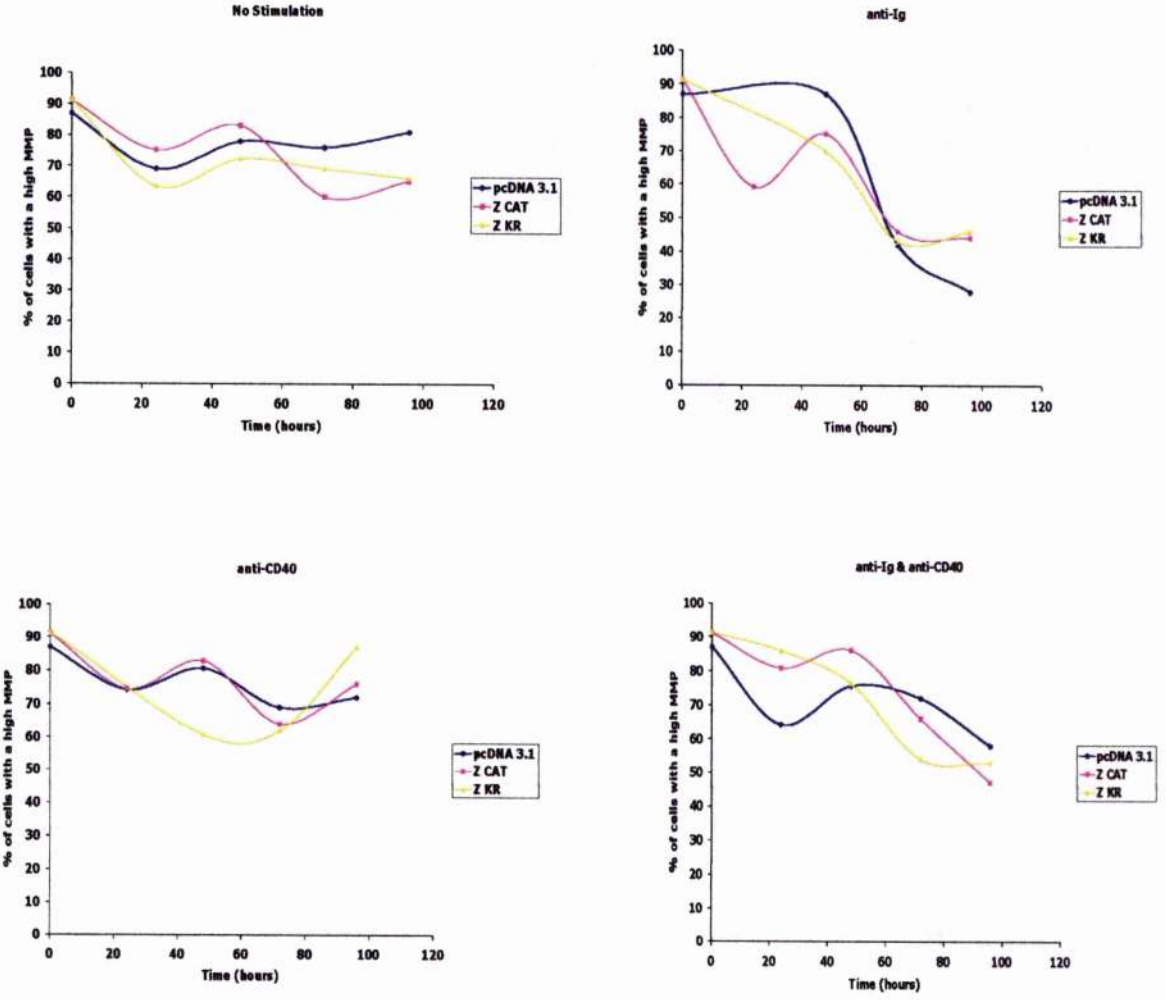
No Stimulation
anti-Ig
anti-CD40
anti-Ig & anti-CD40
% of cells with a high MMP
Time (hours)
pcDNA 3.1
Z CAT
Z KR

Figure 3.53: Pro-apoptotic Bcl-2 family members are differentially regulated in PKC mutants

WEHI 231 pcDNA3.1 (empty vector), PKCδ CAT, PKCζ CAT and PKCζ KR cells (10^7 cells/lane) were cultured for 5 minutes with (1) medium (no stimulation), (2) 10 μg/ml anti-Ig or (3) 10 μg/ml of anti-Ig and 10 μg/ml of anti-CD40 or 24 h with (4) medium (no stimulation), (5) 10 μg/ml anti-Ig or (6) 10 μg/ml of anti-Ig and 10 μg/ml of anti-CD40 μg/ml or 48 h with (7) medium (no stimulation), (8) 10 μg/ml anti-Ig or (9) 10 μg/ml of anti-Ig and 10 μg/ml of anti-CD40 before preparing whole cell lysates. Whole cell lysates (50 μg/lane) were analysed by Western blotting, using the NuPAGE system of gel electrophoresis. Levels of total Bad and Bid were determined by Western blotting.

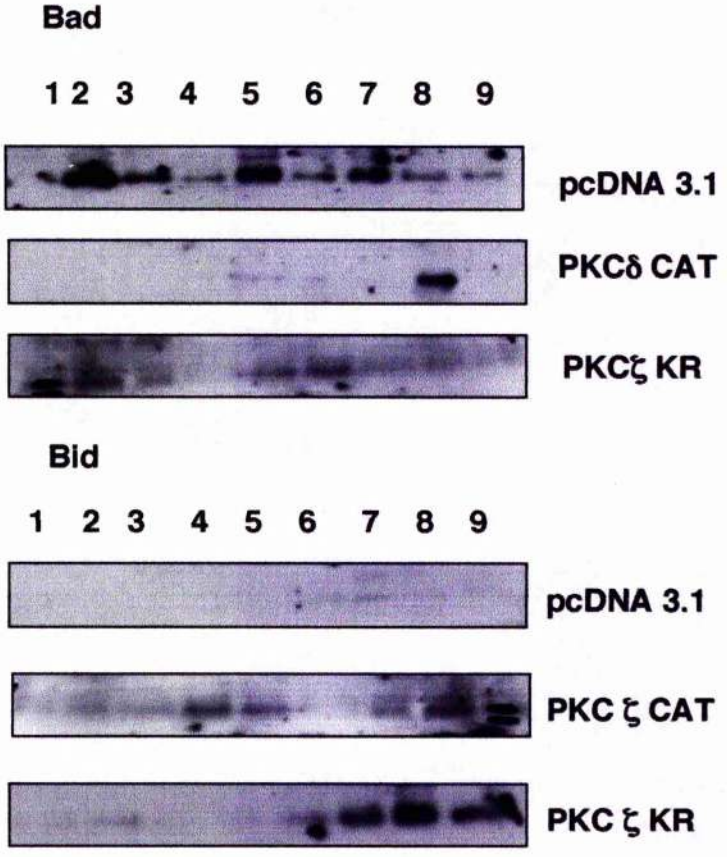
Bad
1 2 3 4 5 6 7 8 9
pcDNA 3.1
PKCδ CAT
PKCζ KR
Bid
1 2 3 4 5 6 7 8 9
pcDNA 3.1
PKC ζ CAT
PKC ζ KR

Figure 3.54: Dynamic switch model for conversion of BCR stimulated arachidonic acid apoptosis signal to a CD40 stimulated PGE_2 mitogenic signal

Ligation of the BCR induces early ERK signals that contribute to the activation of PLA_2 and arachidonic acid production. The accumulation of arachidonic acid leads to a loss of mitochondrial membrane potential and commitment of the cell to apoptosis. Ligation of CD40 prevents BCR-driven apoptosis via the induction of $BclX_L$. $BclX_L$ is a key mediator of CD40-dependent survival and it does so by protecting the mitochondria from arachidonic acid dependent disruption. The induction of $BclX_L$ by CD40 therefore impairs BCR driven activation of cathepsin B and subsequent apoptosis. However, expression of $BclX_L$ cannot protect WEHI 231 cells from consequent BCR-driven growth arrest. The precise mechanism of CD40 restoration of proliferation is incompletely understood but it involves the induction of sustained and cyclic ERK signals. The induction of COX2 and subsequent production of PGE_2 downstream of CD40 appears to contribute to the activation of sustained ERK signals and hence proliferation. However, CD40 may also induce the production of additional eicosanoids to further promote proliferation of WEHI 231 cells.

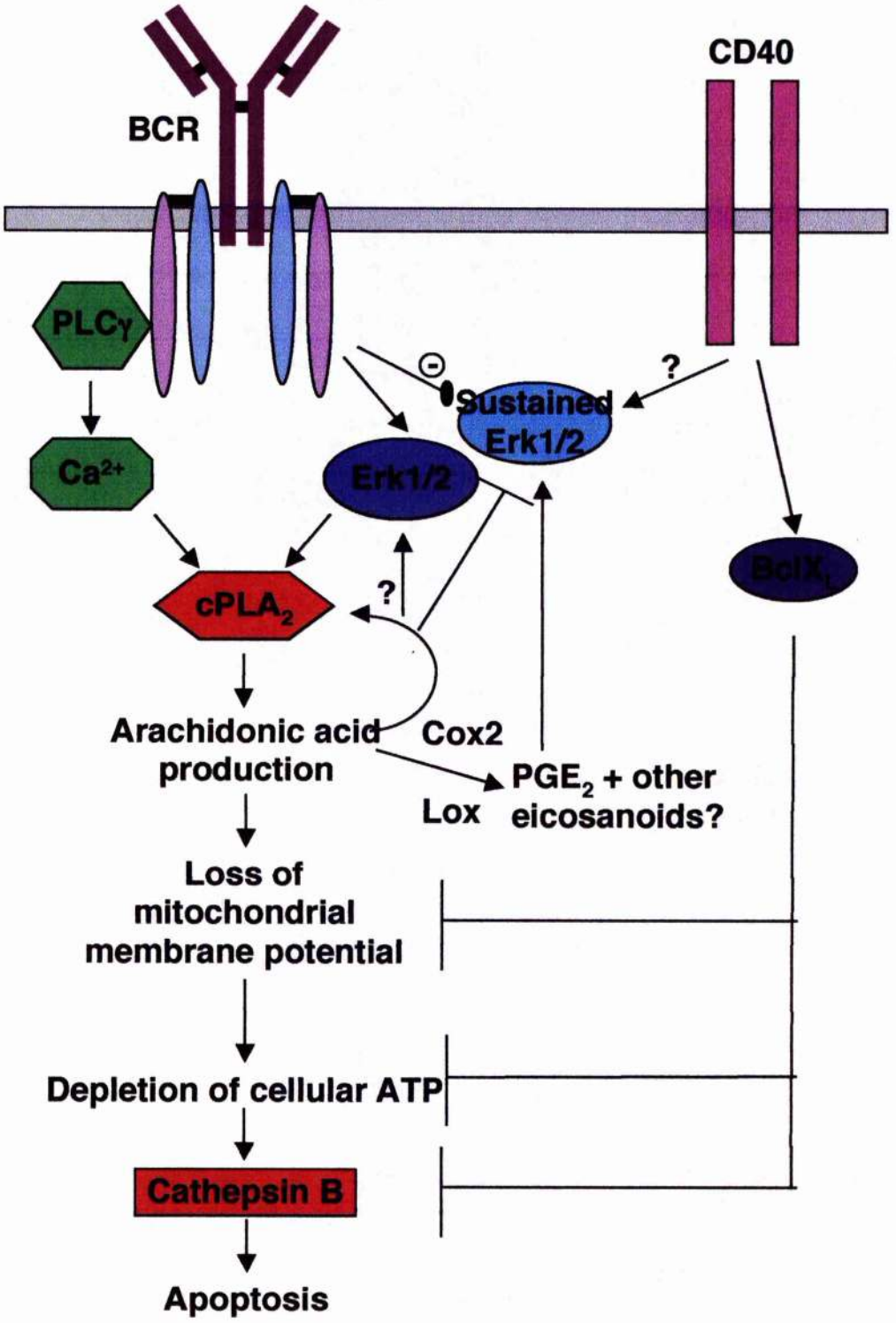
CD40
BCR
PLCγ
Sustained Erk1/2
?
Ca2+
Erk1/2
cPLA2
?
BclXL
Arachidonic acid production
Cox2
Lox
PGE2 + other eicosanoids?
Loss of mitochondrial membrane potential
Depletion of cellular ATP
Cathepsin B
Apoptosis

Chapter 4: Signalling mechanisms underlying FcγRIIb-mediated growth arrest and apoptosis during negative feedback inhibition of B cell activation

4.1 Introduction

4.1.1 FcγRIIb signalling negatively regulates BCR signalling in mature B lymphocytes

It is well documented that in splenic B cells with a mature phenotype (IgM^{lo}, IgD^{hi}, $CD5^-$) ligation of the BCR signals for survival, growth, proliferation and Ab production. Lipid rafts, which are one type of membrane microdomain enriched in glycosphingolipids and cholesterol, are important in transducing this positive BCR signalling. Upon BCR stimulation, lipid rafts build up spatially compartmentalised signalling clusters in which signalling molecules such as adaptor proteins and kinases/ phosphatases can be recruited to the BCR. In the later stages of the immune response, FcγRIIb, the low affinity receptor for the Fc portion of IgG, is recruited to BCR-containing lipid rafts enabling immune complexes to coligate the BCR and FcγRIIb. Coligation of FcγRIIb suppresses BCR-mediated signalling including calcium mobilisation, AKT and MAPK activation (Figure 1.20). FcγRIIb thus inhibits BCR-driven proliferation ensuring the activation of B lymphocytes is a carefully regulated process (346, 460).

The co-aggregation of the BCR and FcγRIIb within lipid rafts induces the tyrosine phosphorylation of a single ITIM located in the cytoplasmic tail of FcγRIIb (282, 461). Lyn is required for phosphorylation of FcγRIIb and B cells from Lyn-deficient mice display enhanced BCR-mediated induction of MAPK and proliferation reflecting the importance of Lyn in the negative regulation of BCR signalling (462). It has been demonstrated that the phosphorylated ITIM (p-ITIM) can bind the phosphatases SHIP, SHP1 and SHP2 however the functional substrates and mechanism of inhibition have not been fully resolved (248, 254, 255). The main protein to be recruited to the p-ITIM of FcγRIIb in mice, is the inositol phosphatase SHIP, which has been demonstrated to be indispensable for FcγRIIb mediated negative feedback inhibition (463, 464). As has been previously described, this inositol phosphatase can antagonise PI-3

kinase activation by degradation of PI-(3,4,5)-P_3. In the murine mast cell model, FcγRIIb signalling has been shown to both inhibit DNA synthesis and block cell cycle entry at G0/G1. This is done by the recruitment of SHIP which inhibits the activation of ERK, JNK, p38 and AKT and also by blocking the increase in expression of cyclins D2, D3 and A which is normally observed following stimulation of the Kit receptor (270). This suggests that FcγRIIb can inhibit multiple cell signalling cascades simultaneously. In contrast, in human B lymphocytes, both SHIP and SHP2 have been demonstrated to be important for negative signalling (465). Binding of SHP2 to FcγRIIb increases the phosphatase activity of SHP2 by 2 to 3 fold and acts to dissociate both SHIP and Shc from the multimeric protein complex suggesting that in SHP2 is the dominant phosphatase (465). Moreover, both Shc and SHIP are thought to be substrates for SHP2 and the dephosphorylation of Shc will result in inhibition of both the RasMAPkinase and PI-3 kinase pathways. The actions of SHP2 are now also thought to be of importance in the murine model (252).

Although SHIP, SHP2 and SHP1 are recruited to the p-ITIM of FcγRIIb following coligation of the BCR and FcγRIib on mature B lymphocytes, there is no definitive mechanistic pathway defined for how negative feedback inhibition converts the pro-proliferative BCR signal to a growth arrest signal. However there have been steps forward in defining some elements of this pathway.

4.1.2 FcγRIIb signalling antagonises the action of PI-3 kinase

Recruitment of SHIP acts to antagonise the action of PI-3 kinase, and hence BCR-mediated positive signalling, by the degradation of PI-(3,4,5)-P_3, the product of PI-3 kinase, to PI-(3,4)-P_2 (466). PI-(3,4)-P_2 has been shown to inhibit both AKT and Btk thus promoting apoptosis (346, 467). Indeed, the activity of AKT is enhanced in bone marrow-derived mast cells from *SHIP*$^{-/-}$ mice (344). However, AKT is known to bind both PI-(3,4,5)-P_3 and PI-(3,4)-P_2 via its PH domain and such binding acts to localise AKT to the cell membrane (468). Although activation of AKT requires phosphorylation by PDK1, membrane localisation appears to be the most potent factor in activation of AKT (59, 265). Thus in contrast to the proposal that to PI-(3,4)-P_2 can inhibit AKT, these translocation studies suggest that AKT can also be stimulated by PI-

(3,4)-P_2, the product of SHIP-mediated dephosphorylation of PI-(3,4,5)-P_3 and therefore SHIP could potentially activate AKT under conditions in which PI-(3,4)-P_2 is allowed to accumulate (282). One might predict that therefore FcγRIIb signalling could have an activatory effect on AKT. Nonetheless, FcγRIIb signalling is generally reported to be inhibitory of AKT (346, 467). Perhaps consistent with this, recent work in this laboratory has demonstrated that ligation of FcγRIIb in mature B cells can also induce PTEN resulting in a depletion of 3'-phosphorylated phosphatidylinositol lipids such as to PI-(3,4)-P_2 and hence an antagonism of PI-3 kinase and AKT signalling (124). Thus FcγRIIb signalling may alter membrane localisation of AKT. Indeed, GFP tagged AKT and time lapse confocal microscopy of live cells has shown that coligation of FcγRIIb abolishes membrane localisation of AKT (56).

4.1.3 FcγRIIb can reduce BCR-stimulated calcium mobilisation

Following ligation of the BCR there is an increase in intracellular calcium (112), which is attenuated by FcγRIIb coligation (469). However, the same experiment carried out in SHIP deficient cells resulted in sustained calcium mobilisation reflecting long lasting calcium oscillations (469). The precise pattern and localisation of calcium increases can affect the complement of proteins that are activated such that downstream effector molecules can decode the information contained in the duration and amplitude of the calcium signal providing a mechanism where calcium can achieve specificity in signalling to the nucleus. For example, NF-κB and JNK are activated by a large transient calcium rise whereas a low sustained calcium plateau activates NF-AT (470). Therefore, differential calcium signals may provide the transcriptional specificity used to modulate B cell activation states.

The exact mechanism for reduction in calcium levels is not known. However it has been demonstrated that in addition to removal of the 5' phosphate residue from PI-(3,4,5)-P_3, SHIP can also act to degrade inositol-1, 3, 4, 5-tetraphosphate (IP_4) to the inactive inositol- 1,3,4- triphosphate. IP_4 is an activator of an endothelial membrane Ca^{2+} channel therefore the degradation of IP_4 by SHIP may reduce the intracellular calcium flux using these channels (282, 346). The degradation of PI-(3,4,5)-P_3 by SHIP also impairs the ability of the BCR to recruit and activate PH domain-containing proteins. SHIP can thus

decrease the calcium flux further by impairing the recruitment of Btk and the activation of PLCγ that normally generates inositol- 1,4, 5-triphosphate and hence acts to increase intracellular calcium levels. (346).

4.1.4 FcγRIIb signalling downmodulates activation of the RasERKMAPkinase pathway

FcγRIIb signalling can also inhibit the ERKMAPK cascade since SHIP and Grb2 directly compete for the binding of phospho-tyrosine residues on Shc (Figure 4.1). Consequently, SHIP impairs the formation of Grb-2/SOS complexes, resulting in suppression of Ras and hence, the MAPK cascade (267, 268, 471). Furthermore, FcγRIIb and SHIP can suppress the MAPK cascade via the recruitment and activation of p62 Dok (62 kD protein downstream of tyrosine kinase, also known as Dok1). The N-terminal region of Dok1 has a PH domain to allow phospholipid/membrane-binding. Dok1 also has a phospho-tyrosine-binding (PTB) domain and a C-terminal proline/ tyrosine-rich region that regulates the repertoire of proteins that can associate with Dok1. Co-aggregation of FcγRIIb and the BCR increases the tyrosine phosphorylation of SHIP enabling Dok1 to bind to SHIP using its PTB domain. At the plasma membrane, Dok1 becomes tyrosine phosphorylated allowing it to interact with and activate RasGAP (Ras GTPase activating protein). RasGAP enhances the intrinsic GTPase activity of Ras leading to the inhibition of Ras and its downstream effectors including ERK (269) (Figure 4.1). In accordance with this, $Dok^{-/-}$ mice do not exhibit FcγRIIb-mediated suppression of B cell proliferation (342). FcγRIIb can also suppress BCR-mediated activation of ERK via the induction of the MAPK phosphatase Pac1 leading to dephosphorylation and inhibition of ongoing ERK activation (124).

4.1.5 FcγRIIb can induce apoptosis

FcγRIIb signalling is proposed to have different functions depending on the context of the signal. Homo-aggregation of FcγRIIb without coligation of the BCR is thought to provide a pro-apoptotic signal (243)(Figure 1.21). Although the exact nature and function of this signal has not been elucidated it is thought to maintain peripheral tolerance to potentially cross-reactive autoantigens (244).

The main evidence comes from FcγRIIb deficient mice that die at 8 months due to the development of autoantibodies and autoimmune glomerulonephritis that closely models the human autoimmune disease Goodpasture's Syndrome. In addition, these mice develop autoimmune diseases, such as arthritis, with increased severity as compared to wild type mice (244).

Simultaneous coligation of both the BCR and FcγRIIb is thought to be responsible for negative feedback inhibition of the BCR proliferative and Ab production response (236). This prevents B cells from overproducing Ab and switches off the immune response once the Ag has been cleared. This homeostatic mechanism restores the number of activated B cells to the levels seen pre-infection and prevents aberrant Ab production. Malfunction of negative feedback inhibition can cause pathology as seen in arthritis, SLE and Goodpasture's Syndrome. Previously groups have reported that coligation of FcγRIIb results in the prevention of DNA synthesis, reduction in cell proliferation and a block in the cell cycle at G0/G1. However, in this chapter, I will demonstrate that coligation of BCR and FcγRIIb can induce not only growth arrest but also apoptosis.

4.2 Aims and Objectives

Previous work in our laboratory and others has demonstrated that ligation of the BCR results in ERKMAPK-dependent proliferation in mature B cells (124, 275, 278-280). However, simultaneous coligation of the BCR and FcγRIIb results in inhibition of growth and a reduction in antibody production (124, 281-283). Work in this laboratory has recently demonstrated that coligation of BCR and FcγRIIb also results in apoptosis. This chapter aims to dissect the signalling mechanisms employed to mediate both BCR-stimulated proliferation and FcγRIIb-mediated growth arrest and apoptosis.

The specific aims of this chapter are to:

- Demonstrate that ligation of the BCR results in proliferation mediated by the ERKMAPK and PI-3 kinase pathways
- Demonstrate and that simultaneous coligation of the BCR and FcγRIIb results in both growth arrest and apoptosis

- Dissect whether FcγRIIb-mediated growth arrest and apoptosis are as a result of abrogation of the pro-proliferative signalling induced by BCR ligation (e.g. ERKMAPK and PI-3 kinase)
- Investigate whether coligation of FcγRIIb prevents proliferative signalling by downmodulating the expression and activation of pro-survival/ pro-proliferative NF-κB subunits
- Investigate whether loss of MMP and expression/ activation of the pro-apoptotic Bcl-2 family members Bid and Bad contribute to FcγRIIb-mediated apoptosis
- Identify which executioner proteases families are activated by FcγRIIb and whether this activation occurs up or downstream of the loss of mitochondrial membrane integrity. In particular it is planned to ascertain whether the canonical caspase 3 or the caspase 8 pathway are utilised to mediate the apoptotic phenotype
- Investigate whether FcγRIIb coligation can upregulate p53 and hence activate pro-apoptotic genes such as Apaf 1, Bid and Bax

4.3 Results

4.3.1 Ligation of the BCR results in proliferation whereas coligation of FcγRIIb mediates growth arrest

To investigate the key signals for growth, proliferation and apoptosis in negative feedback inhibition of mature splenic B cells we used 3 culture conditions throughout this chapter. Culture the B cells with media alone (No stimulation); addition of $F(Ab')_2$ fragments of anti-IgM were used mitogenically stimulate the BCR (BCR) and finally a combination of $F(Ab')_2$ fragments of anti-IgM and intact anti-IgM which act to simultaneously coligate both the BCR and FcγRIIb (BCR & FcγRIIb) to induce growth arrest and apoptosis (124).

Incubating the cells with media alone (No Stimulation) results in no DNA synthesis (Figure 4.2 A). Furthermore, cell counts show that after 48 hours there has been no significant increase in cell numbers (Figure 4.2 B), and CFSE staining shows that there has been no cell division (Figures 4.2 C and D).By contrast, ligation of the BCR results in an increase in DNA synthesis as measured by [^{3}H] Thymidine uptake (Figure 4.2 A). This is also corroborated by the CFSE data (Figure 4.2 C and D), the decrease in fluorescence demonstrating that cell division is occurring from 24 hours post BCR ligation. Moreover, the actual number of cells has increased by more than 2 fold within 48 h post-BCR ligation (Figure 4.2 B). Furthermore, statistical analysis of the CFSE data indicated that the mode number of divisions after ligation of the BCR was generation 2 (with 37% of cells) as compared to none (with 40%) of the cells when cells are unstimulated (Figure 4.2 D).

In contrast, treatment to coligate both the BCR and FcγRIIb resulted in a lack of proliferation as assessed by DNA synthesis assay (Figure 4.2 A). In corroboration, statistical analysis of CFSE data shows that the majority of cells have undergone one or less rounds of division, again reiterating that these cells are not proliferating (Figure 4.2 D). Furthermore, the number of cells recorded was actually slightly reduced over 48 hours following coligation of both the BCR and FcγRIIb (Figure 4.2 B) and this was corroborated by the finding that the

number of CFSE-stained cells recovered was reduced under conditions of coligation of the BCR and FcγRIIb (Figure 4.2 C).

4.3.2 Coligation of the BCR and FcγRiib results in apoptosis

The finding that there is a reduction in the number of cells recovered from culture in which the BCR and FcγRIIb are colligated suggested that such cells are dying. Indeed, coligation of the BCR and FcγRIIb results both in a block of cells in G0/GI and an increase in the number of subdiploid, and therefore apoptotic, cells as compared to unstimulated or BCR-ligated cells (Figures 4.3 A and B). The percentage of subdiploid cells increases from 11% in unstimulated cells to 28% in BCR and FcγRIIb coligated cells (Figure 4.3 B). There is a small decrease in the percentage of cells in G0/G1 after coligation of the BCR and FcγRIIb as compared to ligation of the BCR alone (Figure 4.3 B). However the greatest difference is in the shift from cells in the mitogenic phases of the cell cycle, 30% after ligation of the BCR compared to just 3% following coligation of the BCR and FcγRIIb (Figure 4.3 B). This demonstrates, again, that ligation of the BCR induces proliferation that can be inhibited by coligation of FcγRIIb. In fact there is a 15 fold increase in BCR ligated cells entering mitogenic phases of the cell cycle as compared to unstimulated cells (Figure 4.3 B).

To further confirm that cell death was occurring by apoptosis we investigated FcγRIIb-coligated cells using fluorescence microscopy to assess DNA condensation. By using the DAPI stain it possible to identify chromatin condensation, a distinct feature of apoptosis. When cells are left untreated the DNA staining is diffuse within the nuclei (Figure 4.4) however using dexamethasone to stimulate apoptosis you can observe brightly staining areas within the nuclei (Figure 4.4). This chromatin condensation is a classical hallmark of apoptosis. Consideration of FcγRIIb colligated cells reveals brightly staining nuclei (Figure 4.4) suggesting that an active process of apoptosis rather than necrosis is occurring.

4.3.3. Simultaneous coligation of the BCR and FcγRIIb results in mitochondrial-dependent apoptosis

To further analyse the mechanism utilised to mediate FcγRIIb-mediated apoptosis we investigated whether the mitochondrial apoptotic pathway was

involved. Coligation of the BCR and FcγRIIb resulted in the full loss of MMP by 120 h as indicated by the decrease in $DiOC_6$ staining (Figures 4.5 A and 4.6 A and B). By contrast, at 96 h BCR-stimulated cells have a normal MMP distribution and appear to be single population with a reasonably homogeneous MMP (Figure 4.5 A). However, at 120 h the cells fall into two populations: one with a high "healthy" MMP and one with a low, "apoptotic" MMP suggesting that only some of those cells may be beginning to die. Furthermore, the percentage of cells with a high MMP is decreased from 85% in cells treated to ligate the BCR alone to 51% following coligation of the BCR and FcγRIIb after 48 h (Figure 4.6 A) and the percentage of cells which have dissipated their MMP further increases over time following coligation of both the BCR and FcγRIIb (Figure 4.6 B). Figure 4.6 B shows that the percentage of cells with a high MMP following coligation of the BCR and FcγRIIb is reduced from 74% at 24 h to 36% at 96 h. Consideration of another marker of MMP, JC1, also demonstrates a reduction in the percentage of cells with a high MMP following coligation of FcγRIIb (Figure 4.5 B). Both types of analysis also indicate that unstimulated mature B cells die by apoptosis following disruption of their MMP between 48 and 120 h.

FcγRIIb-mediated loss of MMP is associated with another classical marker of apoptosis, translocation of cytochrome c from the mitochondria to the cytosol. Thus, following coligation of FcγRIIb the sub-cellular distribution of cytochrome c is altered, with an increase in the ratio of cytochrome c in the cytosol relative to the mitochondria. This increases from 0.4 following BCR to ligation to 5.4 following BCR and FcγRIIb coligation (Figure 4.6 C). Cytochrome c release from the mitochondria is a hallmark of apoptosis and in the cytosol it is known to induce both caspase-dependent and independent apoptosis. Furthermore, it is also an indication of mitochondrial permeability transition which allows molecules such as Smac to be released from the mitochondria, dissipates the MMP and irreversibly commits the cells to apoptosis (153, 173, 410, 412).

It is important to note, that the no stimulation treatment induces both a dissipation of the MMP (Figures 4.5 B and 4.6 B) and an increase in the subdiploid population (Figure 4.3) albeit at a much reduced rate to coligation of BCR and FcγRIIb or dexamethasone. However, this does mean that the no

stimulation condition does not provide a good survival control for coligation of BCR and FcγRIIb, as apoptosis is still occurring. Therefore in many of the experiments we have used murine IL4 which prevents apoptosis in mature B cells as a survival control. IL4 does indeed induce cell survival as demonstrated by the lack of apoptotic population (Figure 4.3) and can also act as a control for BCR-driven proliferation as it does not induce cell proliferation (Figure 4.2 D).

4.3.4. BCR-mediated proliferative signalling is mediated by the ERKMAPK cascade and can be abrogated by coligation of FcγRIIb

Previous work in this laboratory demonstrated a role for ERKMAPkinase signalling in proliferation following ligation of the BCR (124), however this focussed on early signalling events generated prior to 30 min post-BCR engagement (27, 124, 472). Therefore we decided to investigate the nature and kinetics of later ERK signals and the potential role in BCR-induced proliferation in mature B cells.

As is widely established, ligation of the BCR on mature B cells induces a strong phospho-ERK signal that is initiated within sec and peaks at 5 min and returns to basal levels within 30 to 60 min (Figure 4.7 A, and B (275)). Interestingly, this ERK signal may be cyclical in mature B cells, as ligation of the BCR induces a peak in phospho-ERK/ ERK ratio at 24 h and again after 48 h (Figure 4.7 B and Data not shown). Both the early and late phospho-ERK signals, stimulated by ligation of the BCR, are completely abrogated when both the BCR and FcγRIIb are coligated (Figure 4.7 A and B).

To determine the role of such ERK signalling we used a combination of 2 MEK inhibitors- PD98059 and U0126, to block MEK1/2 i.e. the upstream signalling pathway to ERK. This resulted in a reduction of the DNA synthesis response to ligation of the BCR, to 15% of the DNA synthesis observed following ligation of the BCR alone (Figure 4.8 A). Furthermore, analysis of cell cycle status reveals that the percentage of cells in both G0/G1 and subdiploid populations were increased by MEK inhibition combined with a concomitant decrease in cells in the mitogenic phases of the cell cycle from 52% without the inhibitor to 40% following MEK inhibition (Figure 4.8 B). Interestingly, MEK inhibition does not affect dissipation of the MMP following ligation of the BCR (Figure 4.8 C). This

suggests that the U0126-dependent increase in apoptotic cells is stimulated independently of or alternatively downstream of the opening of the mitochondrial permeability transition pore.

Taken together these data demonstrate that the RasERKMAPK pathway is required for proliferation following ligation of the BCR and abrogation of this signal, as seen by coligation of FcγRIIb, results in increased growth arrest and to a small extent, apoptosis. Moreover, they suggest that coligation of FcγRIIb can mediate the recruitment of signalling molecules which act to downmodulate the ERKMAPK pathway.

4.3.5. FcγRIIb-mediated apoptosis requires abrogation of the PI-3 kinase signal

The low level of apoptosis observed in the presence of MEK inhibitors suggested that suppression of ERK was sufficient to mimic apoptosis resulting from coligation of FcγRIIb. It was therefore decided to investigate the role of BCR-stimulated PI-3 kinase in BCR-mediated survival and proliferation as AKT transduces survival in B cells and FcγRIIb triggers PI-3 kinase-dependent pathways. We investigated the role of the PI-3 kinase pathway by using the specific inhibitor LY294002. The DNA synthesis response normally induced by ligation of the BCR was completely abrogated in cells treated with LY294002 at concentrations previously shown to be non-toxic in B cells (Figure 4.9 A and data not shown). To investigate whether this was due to growth arrest or apoptosis cell cycle status of this population was assessed. LY294002 treated cells were predominantly found in G0/G1 phase and there was also an increase in cell death relative to BCR control cells (Figure 4.8 B). Thus, the subdiploid population increases from just 10% in BCR-stimulated cells to 44% in such cells treated with LY294002 (Figure 4.8 B). That this is not simply a toxicity response to the PI-3 kinase inhibitor, is corroborated by the finding that cells unstimulated show only a small increase in subdiploid population in the presence of this inhibitor (Data not shown). Interestingly, consistent with an increase in apoptotic population there is also an enhanced loss of MMP (Figure 4.8 C). This suggests that LY294002-dependent apoptosis is stimulated upstream of the opening of the mitochondrial permeability transition pore.

One of the key downstream effectors of the PI-3 kinase survival pathway is the kinase AKT. This molecule is known to provide a mechanism whereby cells can modulate the activation and localisation of the pro-apoptotic Bcl-2 family member, Bad (Figure 1.7). Phosphorylation of AKT leads to phosphorylation of Bad and so sequestration of Bad by cytosolic 14-3-3 proteins, this prevents Bad from interacting with the mitochondria and hence prevents and pro-apoptotic action of Bad. However, when Bad remains unphosphorylated it can bind $BclX_L$ which sequesters $BclX_L$, preventing $BclX_L$ from protecting the mitochondrial membrane integrity. This allows opening of the mitochondrial permeability pore and initiates pro-apoptotic signalling. Therefore the implication is that PI-3 kinase has a pro-survival function by activating AKT and hence Bad. We would postulate that the PI-3 kinase inhibitor LY294002 might stimulate apoptosis by preventing AKT activation and hence initiating pro-apoptotic Bad signalling.

To further dissect such a role for PI-3 kinase in mature B cells we utilised the protein phosphatase inhibitor microcystin and the FACE method to analyse AKT activation. Microcystin, extracted from cyanobacteria, acts to inhibit both protein phosphatase 1 (PP1) and protein phosphatase 2A (PP2A) and hence can be used to monitor cumulative AKT phosphorylation over time. Cells not treated with microcystin provide a snapshot indication of AKT phosphorylation at a given point in time. In the absence of microcystin, BCR-stimulated cells demonstrate basal levels of AKT phosphorylation (Figure 4.10). In contrast in the presence of microcystin, indicates that BCR-stimulated cells show a strong yet dynamic phospho-AKT signal (Figure 4.10). Thus, the fact that the there are only small differences between the unstimulated and BCR ligated groups in the absence of microcystin treatment suggests that there is rapid cycling of AKT phosphorylation and dephosphorylation.

In the presence of microcystin, FcγRIIb coligation results in a phospho-AKT signal very similar to basal levels in unstimulated cells (Figure 4.10). Interestingly, in the absence of microcystin, we can observe that coligation of the BCR and FcγRIIb results in a phospho-AKT signal that is 8 times lower than the basal level in unstimulated cells (Figure 4.10). This suggests that coligation of FcγRIIb not only inhibits BCR-mediated activation of AKT but in addition enhances the dephosphorylation of AKT to below the basal levels presumably

via the activation of PP1 and/or PP2A. It is interesting to note that, in the absence of microcystin, BCR-stimulated and FcγRIIb-stimulated AKT signals appear to be the same. However, consideration of the dynamics of activation of AKT reveals that there is an alteration in the kinetics of AKT phosphorylation/ dephosphorylation. These data taken together suggest that coligation of FcγRIIb promotes apoptosis using mechanisms that result in both the inhibition of PI-3 kinase/AKT activation and also deactivation of ongoing AKT signals.

4.3.6. Neither JNK or p38 MAPK are involved in BCR-mediated proliferative signalling or FcγRIIb-mediated apoptotic signalling

Another MAP kinase, p38, has been implicated in both the initiation of apoptosis and in mediating proliferation depending on cell context (70, 91, 473). Therefore it was decided to investigate whether this kinase could be recruited by the BCR to mediate proliferation or by FcγRIIb to mediate apoptosis. In order to investigate the role of the p38 MAP kinase pathway, the p38 inhibitor SB203500, at concentrations previously found to be effective but not toxic in B cells (Data not shown), was tested for its effects on DNA synthesis, cell cycle and MMP status in response to BCR/ FcγRIIb signalling in mature B cells. The levels of BCR-mediated DNA synthesis, the distribution of such cells throughout the cell cycle and their MMP were not affected by SB203500 (Figures 4.11). In addition, inhibition of p38MAPK did not prevent FcγRIIb-mediated growth arrest and apoptosis. These data suggesting that p38 does not play a key role in either BCR or BCR/FcγRIIb-mediated responses is supported by the finding that p38 activity appears to be suppressed below basal levels at 48 h irrespective of B cell receiving survival (IL4), proliferative (BCR) or growth arrest/apoptotic (BCR/FcγRIIb) signals (Figure 4.12 A).

Similarly, the alternate SAPK, JNK which has also been associated with pro-apoptotic signalling (94, 474-476) and hence provided a good candidate for recruitment by FcγRIIb was also suppressed by all 3 types of signal (Figure 4.12 B). Collectively, these data therefore suggest that neither p38 or JNK MAP kinases play key roles in BCR-mediated proliferation or FcγRIIb- mediated apoptosis of mature B cells.

4.3.7 FcγRIIb-mediated apoptosis is not likely to be caspase 3-dependent

Having ascertained that during FcγRIIb-mediated apoptosis there is a dissipation of MMP we decided to investigate the role of the key effector molecules known to be involved in the mitochondrial apoptotic programme. Firstly, we investigated caspase 3, the canonical executioner protease that is associated with apoptotic morphology. The caspase 3 activating drugs, dexamethasone and ceramide, produced a caspase 3 activation profile with a large FL1 peak around 1500 units (Figure 4.13). This was used a positive control to demonstrate a high caspase activation profile. Unstimulated cells demonstrated a low caspase activation profile however there was some basal caspase 3 activation perhaps consistent with previous data that suggests that unstimulated cells undergo some degree of spontaneous apoptosis by 48 h (Figures 4.13). However, cells treated to ligate the BCR, which is both a pro-survival and pro-proliferative signal resulted in a caspase 3 activation profile which is reduced as compared to the unstimulated cells, as would be predicted (Figure 4.13). Interestingly, there is still a basal level of caspase 3 activation even in these proliferating cells. This may reflect evidence that caspase 3 has been implicated in the entry of B lymphocytes into the cell cycle (411, 477, 478). As an additional control we used a cell permeable Bax protein to stimulate mitochondrial dependent apoptosis (Figure 4.13 A). Interestingly, this did not induce a caspase 3 activation profile activation profile over basal levels. This suggests that apoptosis mediated by the mitochondrial pathway in mature B lymphocytes can be caspase-3 independent.

Interestingly, coligation of FcγRIIb produces a caspase activation profile that is only slightly enhanced above the basal level seen in unstimulated cells. These data suggest that FcγRIIb-mediated apoptosis may utilise alternative executioner proteins to induce an apoptotic morphology. Furthermore, it demonstrated that Bax activation of the mitochondrial pathway does not seem to activate caspase 3 in mature B cells. This might suggest that the mitochondrial pathway activated by FcγRIIb ligation may involve Bax and non-canonical executioner proteases.

4.3.8 Simultaneous caspase, cathepsin B and calpain inhibition rescues mature B cells from FcγRIIb-mediated apoptosis

Having ascertained that FcγRIIb-mediated apoptosis is unlikely to be caspase 3-dependent it was decided to identify other executioner proteases that may be involved in this form of apoptosis. Thus, inhibitors of alternative executioner proteases were assessed for their effects on the growth arrest, apoptosis and dissipation of the MMP induced by the coligation of the BCR and FcγRIIb. Dose-responses were completed to make sure I utilised a non-toxic, effective concentration of these inhibitors (Data not shown). Firstly we assessed DNA synthesis by [^{3}H] Thymidine assay which revealed that neither Z-VAD-FMK (inhibitor of caspases 1, 3, 4 and 7), EST (cathepsin B inhibitor) or the calpain inhibitor, either alone or in combination, provided rescue from FcγRIIb-mediated inhibition of DNA synthesis (Figure 4.14). However interestingly, these inhibitors did impact on BCR-mediated DNA synthesis (Figure 4.14). The pan-caspase inhibitor Z-VAD-FMK was inhibitory to BCR-mediated DNA synthesis (Figure 4.14). Use of some executioner proteases in combination also resulted in a reduction in BCR-mediated DNA synthesis and dose-response studies did not provide any relief from growth arrest (Figure 4.14 and Data not shown). However, this is not simply a toxicity effect as unstimulated cells treated with executioner proteases did not reduce their DNA synthesis levels (Figure 4.14). This points to a role of caspases and other executioner proteases in pro-proliferative signalling in mature B lymphocytes and is consistent with the finding that BCR-treated cells exhibit caspase 3 activation. (411, 477, 478).

Consistent with the finding that FcγRIIb did not substantially stimulate caspase 3 activity, use of the inhibitors singly did not block the FcγRIIb-mediated increase in apoptosis (Figure 4.15 A). However, used in combination these inhibitors reduce the number of subdiploid cells in response to coligation of the BCR and FcγRIIb, from 28% when no inhibitors are used, to around 12% when 2 inhibitors are used together or 14% when all 3 are used together (Figure 4.15 A). In addition to confirming that these reagents are not toxic, these data therefore suggest that these executioner protease systems are able to compensate for each other and only when multiple of the pathways are blocked can we observe inhibition of FcγRIIb-mediated apoptosis. Consistent with this,

cell counts reveal that recoveries following BCR and FcγRIIb coligation can be increased by 143% to 243% by treatment with any 2 executioner proteases in combination with each other (Figure 4.15 B). This would suggest that blocking multiple executioner protease families promotes survival of a larger population of mature B cells and may imply that blocking certain combinations of executioner pathways can not only reduce apoptosis but also reinstate proliferation. However, when all 3 inhibitors are used together the cell count drops to levels almost exactly the same as those when no inhibitors are used (Figure 4.15 B).

Analysis of the cell cycle status of cells after treatment to coligate both BCR and FcγRIIb shows that a high percentage of cells are in G0/G1(57%, Figure 4.16 A) presumably reflecting FcγRIIb-mediated growth arrest. This percentage of cells in G0/G1 stays at roughly the same level, between 54 and 57%, regardless of the use of caspase, cathepsin and calpain inhibitors on their own or in combination with each other (Figure 4.16 A). The exception is the use of the calpain inhibitor alone which decreases the cells in G0/G1 to 36% (Figure 4.16 A), this is due to a corresponding increase in the subdiploid population, as there is also a reduction in the number of cells in both S phase and G2/M phase (Figure 4.16 B). Consistent with the cell count data, the combination treatments resulted in an increase in the mitogenic population from 10% when the cells are not treated with inhibitors to between 26 and 28% depending on the combinations used (Figure 4.16 B). An increase in both the percentage of cells entering mitogenic phases of the cell cycle and number of cells following the addition of any 2 inhibitors in combination suggests that cell proliferation is occurring (Figures 4.15 B and 4.16 B). As there is no increase in DNA synthesis (Figure 4.14) this presumably reflects that the proteases may be targeting the S to G2/M transition or even mitosis itself.

Having established that inhibitors of executioner proteases used in combination can rescue cells from FcγRIIb-mediated apoptosis, we wanted to investigate if this rescue occurs up or downstream of the loss of mitochondrial membrane integrity. In order to do this we monitored whether use of the inhibitors could prevent dissipation of MMP induced by FcγRIIb. Use of Z-VAD-FMK (inhibitor of caspases 1, 3, 4 and 7), EST (cathepsin B inhibitor) or calpain inhibitor alone

did not prevent the dissipation of the MMP (Figures 4.17 A and B). This is consistent with the finding that none of these inhibitors used alone can prevent FcγRIIb-mediated apoptosis. Interestingly, consideration of the effect of Z-VAD-FMK on the MMP suggests that this inhibitor may actually be able to increase dissipation of the MMP resulting from coligation of the BCR and FcγRIIb (Figures 4.17 A and B). When cells are treated to coligate the BCR and FcγRIIb combined with Z-VAD-FMK there is a very large increase in the population with a low MMP. However this is not simply due to a toxic effect as Z-VAD-FMK treated cells left unstimulated or treated to crosslink the BCR do not display this heightened apoptotic population (Figure 4.17 B and data not shown). This finding may reflect that whilst Z-VAD-FMK did not increase the percentage of subdiploid cells, it resulted in the recovery of slightly less viable cell numbers (Figure 4.15).

Use of dual combinations of either Z-VAD-FMK, EST or the calpain inhibitor or all three inhibitors together was also unable to prevent the dissipation of the MMP in response to coligation of the BCR and FcγRIIb over 48 h (Figure 4.17 B). Indeed, treatment with all inhibitors alone (apart from Z-VAD-FMK) or in combination results in a percentage of cells with a high MMP ranging from 55% to 57%, only deviating slightly from cells not treated with any inhibitor (57%, Figure 4.17 B). Thus, none of the inhibitors, even when used in combination, can protect the cells from FcγRIIb-mediated dissipation of the MMP. This suggests that the caspase, calpain and cathepsin pathways do not act upstream of dissipation of the MMP resulting from coligation of the BCR and FcγRIIb.

4.2.9. A Potential role for caspase 8 in FcγRIIb-mediated apoptosis

Having ascertained that combinations of caspase, cathepsin B and calpain inhibitors could rescue cells from FcγRIIb-mediated apoptosis it was decided to investigate whether an apical, initiator apoptosis-signalling molecule, such as the non-canonical caspase, caspase 8, could activate all of these executioner protease families. The data presented so far has suggested that dissipation of the MMP is an important step in initiation and commitment of cells to FcγRIIb-mediated apoptosis. Given that the caspase 8 cascade is known to involve various proteins released from the mitochondria after the permeability pore

transition (162, 198, 479) it was decided to investigate the role of caspase 8 in this form of apoptosis. I utilised this inhibitor alone and in combination with other executioner protease inhibitors to investigate the impact of caspase 8 inhibition on DNA synthesis, cell cycle phase distribution, MMP and induction of apoptosis.

Consideration of the DNA synthesis data shows that coiigation of the BCR and FcγRIIb results in a profound growth arrest regardless of caspase 8 inhibitor treatment (Figure 4.18). This is not in agreement with cell cycle analysis data which demonstrates that caspase 8 inhibition appears to rescue cells from FcγRIIb-mediated growth arrest (Figure 4.19 A). In that it restores the levels of cells in both G0/G1 and mitogenic phases approximately to those seen following ligation of the BCR alone (Figure 4.19 A and B). The slight reduction in proliferation induced by caspase 8 inhibition following ligation of the BCR alone is however reflected by an increase in the percentage of those cells in G0/G1 (Figure 4.19 A). This suggests that caspase 8 inhibition may result in partial growth arrest following BCR-stimulation in mature B cells. As has been discussed previously, this may be due to caspase activation being necessary for cell cycle entry and progression (411, 477, 478). The discrepancy between the DNA synthesis response and cell cycle status of FcγRIIb ligated cells treated with caspase 8 inhibitors may therefore suggest that these cells are arrested in S phase.

As expected, treatment of the cells to coligate both the BCR and FcγRIIb increased the number of subdiploid cells from 23%, in unstimulated cells, to 45% (Figure 4.19 C). In the presence of the caspase 8 inhibitor however, this is decreased to 12%, a four-fold reduction compared to the no inhibitor treatment (Figure 4.19 C). As described above, the percentage of subdiploid cells can be reduced when multiple executioner protease pathways are inhibited together and consider with this, the greatest reduction in percentage of subdiploid cells is observed when the caspase 8 inhibitor, EST, Z-VAD-FMK and the calpain inhibitors are all used together, the subdiploid population being reduced to only 3% (Figure 4.19 C). Collectively these data suggest that caspase 8 is essential for FcγRIIb-mediated apoptosis.

To determine where caspase 8 may be acting, the effect of caspase 8 inhibition on FcγRIIb-mediated dissipation of the MMP was investigated. This demonstrated that addition of the caspase 8 inhibitor can protect MMP dissipation, 53% of cells treated with the caspase 8 inhibitor versus 35% exhibiting a high MMP (Figure 4.20). This corroborates the above data suggesting caspase 8 inhibition can prevent FcγRIIb-mediated apoptosis and furthermore suggests that caspase 8 can act upstream of the opening of the mitochondrial permeability transition pore and hence may occur upstream of caspase 3, 1/7, cathepsin B and calpain activation.

4.3.10 The murine SLE model is unable to undergo FcγRIIb-mediated growth arrest or apoptosis

Having established a role for caspase 8 in FcγRIIb-mediated apoptosis we wanted to investigate whether other well documented components of the caspase 8 cascade were involved. Fas is the best characterised membrane receptor that can activate apoptosis via the caspase 8 pathway. *Lpr*$^{-/-}$ mice model the human disease SLE and produce B cells that generate anti-self DNA Abs and a lupus like nephritis (480-482). *Lpr*$^{-/-}$ mice express Fas at only 2 to 4% of levels seen in wild type mice and this deficiency has been established as the cause for defective apoptosis of self reactive lymphocytes in this model. It was therefore decided to investigate whether deletion of Fas, a component of the caspase 8 cascade, could prevent FcγRIIb-mediated apoptosis in a similar manner to caspase 8 inhibition. Interestingly, mature B cells isolated from the *lpr*$^{-/-}$ mice with established disease do not undergo growth arrest in response to coligation of the BCR and FcγRIIb (Figure 4.21). Rather, the response is very similar to the that seen following mitogenic stimulation of the BCR. This would suggest that FcγRIIb signalling is defective or cannot occur and supports the idea of a pivotal role for the caspase 8 cascade in FcγRIIb-mediated apoptosis.

4.3.11 The pro-apoptotic Bcl-2 family members Bid and Bad are upregulated during FcγRIIb-mediated apoptosis

Having established an important role for both dissipation of the MMP and cytochrome c release in FcγRIIb-mediated apoptosis we decided to investigate

other proteins that act at the mitochondria. Considering that we have identified PI-3 kinase/ AKT inhibition and caspase 8 activation as features of FcγRIIb-mediated apoptosis, the Bcl-2 family members were good candidates for signalling molecules that may be recruited by FcγRIIb signalling. Firstly we investigated the expression of the pro-apoptotic family members Bid, Bad and Bim. When cells are left unstimulated there is no detection of Bim, Bid or Bad. However, ligation of the BCR or coligation BCR and FcγRIIb results in an upregulation of both Bid and Bad (Figure 4.22 A). However Bim is not expressed following either ligation of the BCR or coligation of FcγRIIb (Data not shown). Interestingly, although coligation of FcγRIIb induces a greater expression of Bid and Bad than that of ligation of the BCR alone mitogenic signalling via the BCR clearly upregulates substantial levels of Bid/Bad.

At first sight, this might suggest that ligation of the BCR produces an apoptotic signal as well as a proliferative signal. However as has been discussed, Bad expression does not necessarily signal for apoptosis (Figure 1.7). The phosphorylation status of Bad as well as absolute expression levels determines whether Bad induces apoptosis. The phosphorylation status of Bad was therefore assessed by using the modified ELISA technique- FACE (Figure 4.22 B). At 24 h the BCR ligated cells were found to have a higher phospho-Bad pro-survival signal relative to that observed in cells with the BCR and FcγRIIb coligated. Perhaps surprisingly, the phospho-Bad signal in FcγRIIb stimulated cells is well above those in unstimulated/ IL4 treated cells. However it is also important to note that FcγRIIb induces a massive increase in expression of Bad, with up to a 10 fold increase in Bad expression above basal levels in unstimulated cells (Figure 4.23 A and C). It is possible that with this large increase in Bad expression Bad can also act to bind to other pro-apoptotic Bcl-2 family members and induce oligomerization of Bak/ Bax. This may commit the cells to apoptosis and override the pro-survival phospho-Bad signal. Furthermore, addition of executioner protease inhibitors, either alone or in combination with each other, does not appear to have any effect on Bad expression (Figure 4.23 A). This corroborates previous data to suggest that these executioner proteases act downstream loss of MMP and hence the initiation of mitochondrial signalling.

4.3.12 Inhibition of the PI-3 kinase and MAP kinase cascades inhibits Bad activation

Inhibitors of the PI-3 Kinase pathway (LY294002) and the MAP kinase pathway (U0126) appear to reduce the phospho-Bad signal that is produced in response to either ligation of the BCR or coligation of FcγRIIb (Figure 4.23 B). This is most pronounced when the cells are treated to ligate the BCR. Ligation of the BCR alone results in a phospho-Bad: Bad ratio of 1.43 whereas treatment to inhibit PI-3 kinase or MAP kinase reduces this ratio to 0.54 and 0.46 respectively. This corroborates data previously described that implicated PI-3 kinase, AKT and ERKMAPK in BCR-mediated survival and proliferation (Figures 4.7 to 4.10). Interestingly, the changes in ratio of phospho-Bad to Bad ratio following cell signalling inhibitor treatments seem to target the phosphorylation status rather than expression of Bad. Firstly, it is clear that coligation of the BCR and FcγRIIb induces a large increase in Bad expression (Figure 4.23 C). However, there is a reduction in phospho-Bad following coligation of FcγRIIb combined with either PI-3 kinase or ERKMAPkinase inhibition as compared to no inhibitor treatment (Figure 4.23 B). These data suggest that the suppression of ERK and PI-3 kinase resulting from coligation of FcγRIIb results in an upregulation Bad in its unphosphorylated form which can sequester $BclX_L$. Furthermore, such inhibition of PI-3 kinase and MAP kinase pathways prevents the BCR-mediated upregulation of phospho-Bad which prevents the opening of the mitochondrial permeability transition pore and hence prevents apoptotic signalling. Therefore, this implicates PI-3 kinase and ERK-mediated upregulation of phospho-Bad as integral to BCR-mediated survival.

4.3.13. Coligation of the BCR and FcγRIIb upregulates the activation of p53

The transcription factor p53 acts to transcribe p53-regulated genes which can regulate many diverse processes including; apoptosis, cell cycle arrest, genome stability, cellular senescence and angiogenesis (Figure 1.11) (119). This transcription factor is important for the regulation of cell cycle related genes such as the cyclin dependent kinase inhibitor p21 which has been shown to be critical for cell cycle arrest function (123) and an important cell cycle regulator, PTEN (125). There are also multiple apoptotic genes that are under the control of p53 that are involved in both the intrinsic and extrinsic pathways to cell death

including Apaf 1 and caspase 9 (126) and numerous pro-apoptotic Bcl-2 family members (127, 128). In addition, p53 is thought to have a transcription-independent pro-apoptotic function and been postulated to function as a BH3-only protein (129, 130). Considering that both the recruitment of the PI-3 kinase antagonist PTEN (124) and the activation of the pro-apoptotic Bcl-2 family members have been implicated in FcγRIIb-mediated apoptosis of B cells this may suggest that activation of p53 may account for these cellular responses. It was therefore decided to investigate the potential activation of p53 in FcγRIIb-mediated negative feedback of mature B cells using the TransAM modified ELISA technique.

After 24 h there is little difference in p53 activation between cells mitogenically stimulated via the BCR and those undergoing FcγRIIb-mediated negative feedback. However, after 48 h there is a strong induction of p53 activity in the FcγRIIb coligated group that is not observed in other treatment groups (Figure 4.24 A). This may suggest that the mitochondrial apoptosis pathway is executed via FcγRIIb-driven p53-activated transcription of genes including Bid. There are many other p53-dependent pro-apoptotic genes that may be upregulated and p53 may even function to induce apoptosis in a transcription-independent manner. Interestingly, addition of EST or the calpain inhibitor appeared to reduce p53 activation following coligation of the BCR and FcγRIIb as compared to cells without inhibitor treatments (Figure 4.24 B). This suggests that even though biological readouts, like DNA synthesis, proliferation and MMP, are unaffected by addition of the inhibitors of executioner proteases when used singly, cell signalling events may still have been altered. Furthermore, whilst addition of the ERKMAPK Inhibitor increased BCR/FcγRIIb-driven p53 activation the PI-3 kinase inhibitor did not have a significant effect on p53 activation (Figure 4.24 C). These latter data suggest that whilst PI-3 kinase and ERK both modulate phospho-Bad status, only ERK regulates p53 activation.

4.3.14. Coligation of the BCR and FcγRIIb upregulates the activation of NF-κB

The NF-κB family of transcription factors, also known as the Rel family, comprise either homo or heterodimers of the following five NF-κB subunits:

RelA (p65), RelB, cRel, p50 and p52 (131). We were able to investigate the activation of each of these subunits separately using the TransAM modified ELISA technique. NF-κB is known to control the regulation of genes that signal for diverse cellular responses including growth, proliferation and survival depending on the subunits utilised (Figure 1.12). NF-κB is known to regulate anti-apoptotic genes including Bcl-2 family members Bcl-2 and $BclX_L$ as well as cell cycle regulators such as cyclin D2, E2F3a and IL-1 (135-139). Therefore, it was postulated that coligation of FcγRIIb may result in a modulation of activation levels of NF-κB subunits and it was therefore decided to investigate the relative activation levels of each of the NF-κB subunits in response to negative feedback inhibition signals via FcγRIIb.

The first subunit investigated was cRel which is upregulated at 24 h when the BCR and FcγRIIb are coligated however this increase appears to be downregulated again after 48 h (Figure 4.25 A). The same pattern is also followed by the p52 and RelB subunits (Figure 4.25 B and C). However, investigation of the p50 and p65 subunits revealed that the activation levels of all treatment groups were the same after 24 h (Figure 4.26). In contrast, after 48 h, coligation of the BCR and FcγRIIb strongly induced p50 and p65 activation (Figure 4.26).

4.4 Discussion

4.4.1 BCR ligation results in ERKMAPK/ PI-3 kinase dependent-proliferation

It has been well documented that ligation of the BCR results in survival and proliferation in mature B cells resulting in the differentiation to Ab secreting plasma cells (Figures 4.2 and 3), yet the exact mechanism of BCR-induced proliferation has not yet been elucidated. There is however evidence that both the PI-3 kinase and MAP kinase cascades are involved (124, 278, 483-485). In this chapter we have demonstrated that BCR-induced proliferation is ERKMAPK-dependent (Figures 4.7 and 8). For example, inhibition of MEK 1/2 and ERK 1/2 resulted in an increase in both cell cycle arrest and apoptosis (Figure 4.8). The mechanism for cell cycle arrest has not been fully elucidated however complementary evidence demonstrates that cyclin D2, which plays an essential role in G1 to S phase transition, is downregulated at both mRNA and protein levels by use of the MAP kinase inhibitor U0126 (483). Consistent with this, parallel studies in this laboratory have demonstrated that BCR ligation increases the expression of cyclin D2 (458). In addition, inhibition of the Raf1-dependent MEK1/2 cascade has been demonstrated to uncouple BCR signalling from proliferation (485) again suggesting that the ERKMAPK cascade is essential for proliferation.

Similarly, BCR-induced proliferation is also under the control of the PI-3 kinase pathway. Inhibition of the PI-3 kinase pathway using LY294002 resulted in increased growth arrest and apoptosis in mature B cells (Figures 4.9). Transgenic mice deficient in the p85α subunit of PI-3 kinase have a reduced number of mature B cells in the spleen, decreased Ab production and reduced proliferation in response to both LPS and anti-IgM demonstrating that the p85α subunit of PI-3 kinase plays an essential and non-redundant role in normal mature B cell function (68, 486). PI-3 kinase has also been demonstrated to have an obligatory role for Btk regulation after BCR ligation (487, 488). Involvement of this pathway is also corroborated by the fact that ligation of the BCR results in a strong induction of the major downstream effector of the PI-3

kinase pathway, AKT (Figure 4.10). Furthermore, there is a growing body of evidence to suggest that the activation of the PI-3 kinase cascade can act to phosphorylate and hence activate ERK1/2 (266, 489-491). This study has not addressed whether the activation of ERK is dependent on PI-3 kinase however this provides an attractive possible mechanism for fine tuning of the BCR-stimulated proliferative response.

4.4.2 FcγRIIb-mediated growth arrest can be mimicked by abrogation of both the BCR-stimulated ERKMAPK and PI-3 kinase signals

It is well documented that simultaneous coligation of the BCR and FcγRIIb results in growth arrest and this is corroborated by my data (Figures 4.2 and 4.3) (124, 252, 460). Consistent with a role for ERK in BCR-induced survival and proliferation there is a clear switching off of the ERK signal in response to co-ligation of FcγRIIb which occurs within 5 min and is still observable 48 h post FcγRIIb coligation (Figure 4.7). Parallel studies in this laboratory have demonstrated that abrogation of the BCR-ERK signal is maintained up to 96 h post FcγRIIb coligation (458). Similarly, previous studies in this, and other, laboratories suggest that PI-3 kinase is antagonised during FcγRIIb-mediated apoptosis (124). To corroborate this I have demonstrated downregulation of AKT activation, a major downstream effector of PI-3 kinase, following FcγRIIb ligation (Figure 4.10). Taken together these data suggest that whilst BCR engagement induces an upregulation of both PI-3 kinase and ERKMAPK signals which induce survival and proliferation, coligation of FcγRIIb abrogates these kinases and thus induces growth arrest. The mechanisms employed for switching off these pro-proliferative signals have not been addressed in this study but have been elucidated in parallel studies in this laboratory and hence, are summarised in figure 4.27.

4.4.3. FcγRIIb-mediated apoptosis can be mimicked by the abrogation PI-3 kinase signalling

There have been reports that homo-aggregation of FcγRIIb generates an apoptotic signal (243). However the data presented in this chapter also suggests that an apoptotic signal can be generated by coligation of both the BCR and FcγRIIb (Figures 4.3 to 6). Such apoptosis occurs between 48 and 96

h post FcγRIIb coligation. It is accompanied by translocation of cytochrome c from the mitochondria to the cytosol, dissipation of the MMP, an increase in numbers of subdiploid cells and chromatin condensation. Consistent with the downregulation of PI-3 kinase following FcγRIIb coligation, I have identified a mechanism whereby a reduction in phospho-AKT levels (Figure 4.10) contributes to the reduction in phospho-Bad levels as compared to ligation of the BCR (Figure 4.22 B). This may act to enhance the sequestration of $BclX_L$ from the mitochondria resulting in the loss of mitochondrial membrane integrity and commitment of the cell to apoptosis (Figure 1.7).

4.4.4. FcγRIIb-mediated apoptosis is caspase 8-dependent may involve multiple executioner protease families

Having identified an apoptotic phenotype, it was decided to investigate the effector molecules utilised by FcγRIIb in transducing such apoptosis during negative feedback inhibition of B cells. Initial consideration of the upregulation of the Bcl-2 pro-apoptotic BH3-only domain containing proteins, release of cytochrome c and dissipation of the MMP would suggest that the intrinsic, mitochondrial pathway would be the main execution programme utilised (Figures 4.6 and 4.22 B). However, although this pathway is described as culminating in the activation of the canonical caspase 3 cascade it was established that caspase 3 is barely activated above basal levels following coligation of FcγRIIb and the BCR (Figure 4.13). Therefore the role of other potential executioner proteases that could be activated by mitochondrial pathways was investigated. This demonstrated that any combination of caspase, cathepsin B or calpain inhibitors were all able to reduce FcγRIIb-mediated apoptosis (Figures 4.15 A). The most potent reduction of apoptosis was observed when all 3 of these inhibitors were used in combination (Figure 4.15 A). This suggests that there is a high level of redundancy in FcγRIIb-mediated apoptosis. In addition to this it is important to note that whilst addition of these executioner protease inhibitors was able to prevent apoptosis as assessed by the percentage of subdiploid cells, they were not able to prevent the dissipation of the MMP (Figure 4.17 B). Therefore these inhibitors act to suppress apoptosis downstream of the opening of the mitochondrial permeability transition pore.

Consistent with the above data providing evidence for non-canonical pathways, the pan-caspase inhibitor Z-VAD-FMK actually appears to potentate loss of MMP rather than suppressing it (Figures 4.17) Interestingly, other groups have found evidence for Z-VAD-FMK sensitizing for apoptosis rather than protecting against it when caspase-independent mechanisms are utilised in cell death (492). It has been suggested, that in these systems, caspases act as a surveillance system that can recognise and remove damaged mitochondria that are overproducing reactive oxygen species (ROS) (493, 494). It is thought that the caspase substrate PLA_2 may be essential for removal of damaged mitochondria within these cells. Therefore inhibition of caspases enhances ROS production and hence, apoptosis. Cawels et al (2003) demonstrated that Z-VAD-FMK sensitized cells to apoptosis, however this could be reversed by PLA_2 inhibition. In addition, they found that inhibition of caspase 8 had a specific protective role (492). This is extremely interesting as we have demonstrated that, in the immature WEHI 231 cell line, PLA_2 activation and loss of MMP are essential for BCR-mediated apoptosis (156). It would be interesting to investigate whether PLA_2 activation in mature germinal centre B cells contributes to the loss of MMP and commitment of the cells to apoptosis.

In line with this mechanism, my data demonstrates a specific role for caspase 8 in FcγRIIb-mediated apoptosis. In fact, caspase 8 inhibition can prevent FcγRIIb mediated apoptosis more potently than the cumulative action of inhibitors of either caspases 1, 2, 3, 7, cathepsin B and calpain (Figures 4.19). Interestingly, caspase 8 inhibition results in a partial rescue from the dissipation of the MMP in response to coligation of FcγRIIb (Figure 4.20). This suggests that caspase 8 is the initiator caspase activated upstream of the opening of the mitochondrial permeability pore and hence is apical to the executioner proteases involved. In agreement with a role for caspase 8 in FcγRIIb-mediated apoptosis we found that the *lpr* mouse, which lacks Fas, is unable to undergo FcγRIIb mediated-growth arrest (Figure 4.21). Fas is a receptor known to initiate caspase 8-dependent apoptosis and hence a defective FcγRIIb response in this animal reinforces the idea that caspase 8 is pivotal to FcγRIIb-mediated apoptosis.

4.4.5. FcγRIIb-mediated apoptosis is mediated by pro-apoptotic members of the Bcl-2 family

We have shown that both Bid and Bad, but not Bim, are upregulated by the coligation of the BCR and FcγRIIb on B cells (Figures 4.22). The truncated form of Bid is known to process and activate pro-caspase 8, however we have not provided evidence to suggest that tBid is the predominant form found in mature B cells undergoing FcγRIIb-mediated negative feedback inhibition. Bad is known to be able to induce the oligermerisation of Bax/Bak and hence open the permeability transition pore in mitochondria (160, 412). Expression of both Bid and Bad is upregulated within 5 min of coligation of the BCR and FcγRIIb (Figures 4.22 A). Given that dissipation of the MMP occurs between 24 and 48 h (Figure 4.6) these data suggest that upregulation of expression of both Bid and Bad precedes loss of mitochondrial membrane integrity.

Although it has not yet been established whether FcγRIIb signalling induces the truncated, pro-apoptotic form of Bid the phosphorylation status of Bad, and hence its functional outcome, has been assessed at various time points after FcγRIIb coligation. Ligation of the BCR produced a high ratio of phospho-Bad to Bad expression and this would be expected as the BCR transduces pro-survival signals (Figure 4.22 B). By contrast, coligation of the BCR and FcγRIIb produced a strongly reduced ratio of phospho-Bad/Bad expression, with a resultant increase in functionally pro-apoptotic Bad. It will be important to investigate the other Bcl-2 proteins that are expressed and their complex status over this time period as it has is well established that it is the ratio of pro-apoptotic and anti-apoptotic Bcl-2 family members that governs the decision to commit a cell to apoptosis rather than the absolute levels of any one protein (reviewed in (192)). Moreover, it is also known, for example, that Bad can bind the anti-apoptotic molecule $BclX_L$ (206, 207) and hence the particular combinations of Bcl-2 proteins are likely to have vastly different effects. Therefore it is also necessary to investigate the expression levels of other Bcl-2 family members and elucidate which BH domain containing proteins are capable of interaction with Bad.

4.4.6. FcγRIIb-mediated apoptosis involves the upregulation of p53

Interestingly, expression of active p53 is strongly upregulated within 48 h following co-ligation of FcγRIIb (Figure 4.24 A). This transcription factor controls genes involved in both the classical caspase and mitochondrial pathways of apoptosis (119, 495, 496). Interestingly, p53 is known to control the transcription of Bid which is upregulated by FcγRIIb signalling (127, 128). In addition, it has recently been proposed that p53 can itself act as a pro-apoptotic BH3 only Bcl-2 family member to directly initiate apoptosis by acting in concert with Bak and Bax (129, 130). It would be interesting to track the localisation of p53 before and after coligation of FcγRIIb, as translocation to the mitochondria rather than nucleus may suggest that p53 apoptotic signalling is transcription-independent. The effects of inhibitors of ERKMAP kinase and PI-3 kinase on p53 activation were tested and the results show that activation of p53 was increased by the ERKMAPK inhibitor in response to either ligation of the BCR or coligation of the BCR and FcγRIIb (Figure 4.24 C). These latter data corroborate the cell cycle analysis which demonstrates an increase growth arrest and in apoptosis is response to ERKMAP kinase inhibition further supporting a key role for this signal in BCR-mediated proliferation. By contrast, PI-3 kinase inhibitors did not enhance nuclear p53 activity suggesting that PI-3 kinase promotes survival and growth by alternative mediators.

4.4.7 FcγRIIb-mediated apoptosis involves the differential of upregulation of NF-κB subunits

NF-κB is known to control the regulation of genes that signal for diverse cellular responses including growth, proliferation and survival depending on the subunits utilised. NF-κB is known to regulate anti-apoptotic genes including Bcl-2 family members Bcl-2 and $BclX_L$ as well as cell cycle proteins such as cyclin D2, E2F3a and IL-1β 9 (135-139). It was found that following coligation of both the BCR and FcγRIIb there is increased activation of cRel, Rel B and p52 after 24 h which returns to basal levels by 48 h (Figure 4.43). However the p50 and Rel A subunits show increased activation at 48 h and no changes from basal levels at 24 hours (Figure 4.44). It is not surprising that the various NF-κB transcription factor family subunits are regulated differently as they have been documented to have essential, and non-overlapping functions in B lymphocytes.

NF-κB consists of dimeric proteins of any of the 5 NF-κB subunits, either as homo or heterodimers. Transgenic knock out studies in mice have revealed that NF-κB in involved in the inflammatory response, control of the cell cycle, apoptosis, growth, proliferation and lymphocyte maturation (497, 498).

Knock-out mice generated for each of the NF-κB subunits have individual phenotypes. For example, Rel A deficient mice are embryonic lethal dying before embryonic day 15 with massive hepatocyte apoptosis. Furthermore B cells defective in Rel A have reduced proliferative responses and impaired production of both IgA and IgG1 (138). Similarly, cRel deficient mice develop normally but show defects in lymphocyte proliferation and are unable to respond to most mitogenic stimuli (499). Likewise, mice deficient in p52 have impaired B cell functions and fail to produce Abs in response to T cell dependent Ag. In addition, $p52^{-/-}$ mice lack B cell follicles, follicular dendritic cell networks and have an inability to form germinal centres (500). Although mice deficient in p50 show no developmental abnormalities they also have defects in B lymphocyte function. Thus, mature $p50^{-/-}$ B lymphocytes do not proliferate in response to LPS and are defective in both basal and specific Ab production (501). By contrast, $Rel\text{-}B^{-/-}$ mice have myeloid hyperplasia and splenomegaly combined with mixed inflammatory cell infiltration of several organs and a dysregulated immune system (502). This suggests that Rel-B is necessary both peripheral tolerance and B cell apoptosis.

In these studies, negative feedback signalling mediated via FcγRIIb led to upregulated cRel, p52 and Rel B at 24 h. This was surprising as both cRel and p52 have been implicated in proliferation and Ab production. However Rel B has been suggested to be of importance in both apoptosis and the maintenance of tolerance and cRel and p52 may possibly be utilised as dimers with Rel B in order to fulfil this functional outcome. By 48 h cRel, p52 and Rel-B activation has returned to basal levels but p50 and RelA have become activated. Again this is surprising, as both subunits are also associated with B lymphocyte proliferation. However there has not been characterisation of all genes regulated by NF-κB and there may be many, as yet unidentified, apoptotic genes. In addition, we have not provided any information on the dimers formed and activated or the full kinetics of BCR and BCR/FcγRIIb signalling. In order to

investigate this fully it would be useful to use siRNA constructs to knock down multiple NF-κB subunits simultaneously to elucidate which dimers are essential and the level of redundancy in this system.

4.4.8 Concluding Remarks

In conclusion, it has been demonstrated that BCR ligation results in PI-3 kinase and ERKMAPK dependent proliferation (Figure 4.27) as abrogation of these signalling systems results in both growth arrest and apoptosis. Moreover, since these inhibitors mimic the effects of coligation of the BCR and FcγRIIb these studies further support the proposal that abrogation of these activities by FcγRIIb signalling plays a key role in negative feedback inhibition. Furthermore, this study has clearly demonstrated coligation of both the BCR and FcγRIIb results in not only growth arrest but also apoptosis. Such apoptosis utilises non-canonical executioner pathways to induce the apoptotic phenotype. Nevertheless, inhibition of the PI-3 kinase pathway results in the inhibition of AKT which in turn reduces the proportion of phospho-Bad. This presumably leads to the sequestration of $BclX_L$ and contributes to the loss of MMP. Furthermore, upregulation of pro-apoptotic elements such as Bid may be transduced by p53 which is suppressed by mitogenic BCR-signalling in an ERKMAPK-dependent manner and by contrast, upregulated by FcγRIIb signalling. Caspase 8 also acts upstream of the opening of the mitochondrial permeability pore and is apical to the activation of multiple executioner proteases. Thus, following loss of MMP, cytochrome c is released from the mitochondria and cathepsin B, caspases and calpains are activated. These executioner proteases appear to act in a redundant fashion to effect apoptosis. This model for FcγRIIb-mediated apoptosis is summarised in figure 4.28.

Figure 4.1: Inhibition of BCR signalling by FcγRIIb

FcγRIIb is a low affinity receptor for the Fc component of IgG therefore it can recognise immune complexes. Ligation of FcγRIIb causes Lyn to phosphorylate the single ITIM of the cytoplasmic region of FcγRIIb. The phospho-ITIM can recruit and activate the phosphatase SHIP. SHIP removes the 5' phosphate from PI-(3,4)-P_3 leading to impaired recruitment and activation of PH domain-containing proteins. Furthermore, SHIP suppresses the BCR mediated activation of MAPK by disrupting the association of Shc and Grb2 and by recruiting and activating RasGAP via Dok1. FcγRIIb can also impair the ongoing activation of ERK via the induction of Pac1. Moreover, FcγRIIb enhances the activity of the phosphatase PTEN to further impair PI-3 kinase signalling. PTEN acts to antagonize the activity of PI-3 kinase by dephosphorylation of PI-lipids at the 3' position. FcγRIIb therefore suppresses the PI-3 kinase pathway and the ERKMAPK cascade.

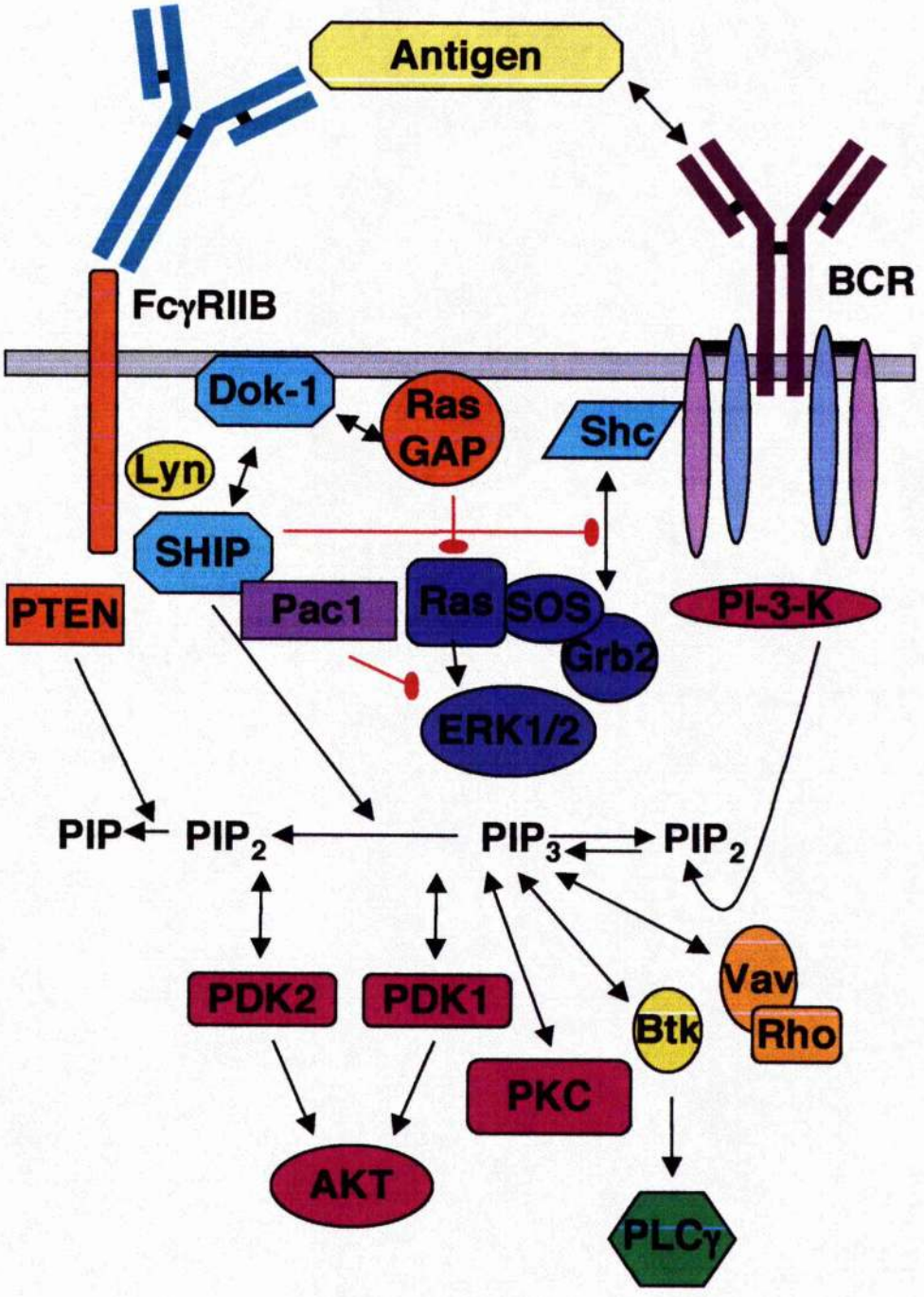
Antigen
BCR
FcγRIIB
Dok-1
Ras GAP
Shc
Lyn
SHIP
PTEN
Pac1
Ras
SOS
Grb2
PI-3-K
ERK1/2
PIP
PIP2
PIP3
PIP2
PDK2
PDK1
Vav
Rho
Btk
PKC
AKT
PLCγ

Figure 4.2: Ligation of the BCR results in proliferation whereas simultaneous coligation of the BCR and FcγRIIb results in growth arrest

(A) Cells were cultured for 48 h and then DNA synthesis was assessed by [^{3}H] thymidine uptake. Cells were either treated with media alone (No stimulation), 50 μg/ml $F(Ab)_2$' fragments of anti-IgM (BCR) or 50 μg/ml $F(Ab)_2$' fragments of anti-IgM combined with 75 μg/ml of intact anti-IgM (BCR & FcγRIIb). These data are the mean of triplicate determinations ± SEM. These data are from a single experiment, representative of 12 separate experiments.

(B) Cells were either treated with media alone (No stimulation), 56 pg/ml murine IL4 (IL4), 50 μg/ml $F(Ab)_2$' fragments of anti-IgM (BCR) or 50 μg/ml $F(Ab)_2$' fragments of anti-IgM combined with 75 μg/ml of intact anti-IgM (BCR & FcγRIIb) for 48 h. Additionally, a count of the number of cells per well at 0 h was taken for comparison. The number of cells counted in 5 s was recorded by flow cytometry. These data are from a single experiment, which is representative of 4 experiments.

(C) Cells were stained with 1 μM CFSE and then cultured for 72 h with appropriate stimulations. Cells were either treated with media alone (No stimulation), 50 μg/ml $F(Ab)_2$' fragments of anti-IgM (BCR) or 50 μg/ml $F(Ab)_2$' fragments of anti-IgM combined with 75 μg/ml of intact anti-IgM (BCR & FcγRIIb). Proliferation was assessed by a shift in CFSE brightness (FL1 fluorescence) from the right hand side to the left hand side of the FACS plots. These data are from a single experiment, representative of 3 separate experiments.

(D) Cells were treated as described for **(A)** for 72 h. Proliferation was assessed by an estimate of the percentage of cells in each generation. This calculation was done with the FlowJo proliferation data analysis programme. The data was then displayed as the percentage of cells in each generation. These data are from a single experiment, representative of 3 separate experiments. This is a different data set than shown in panel **(C)**.

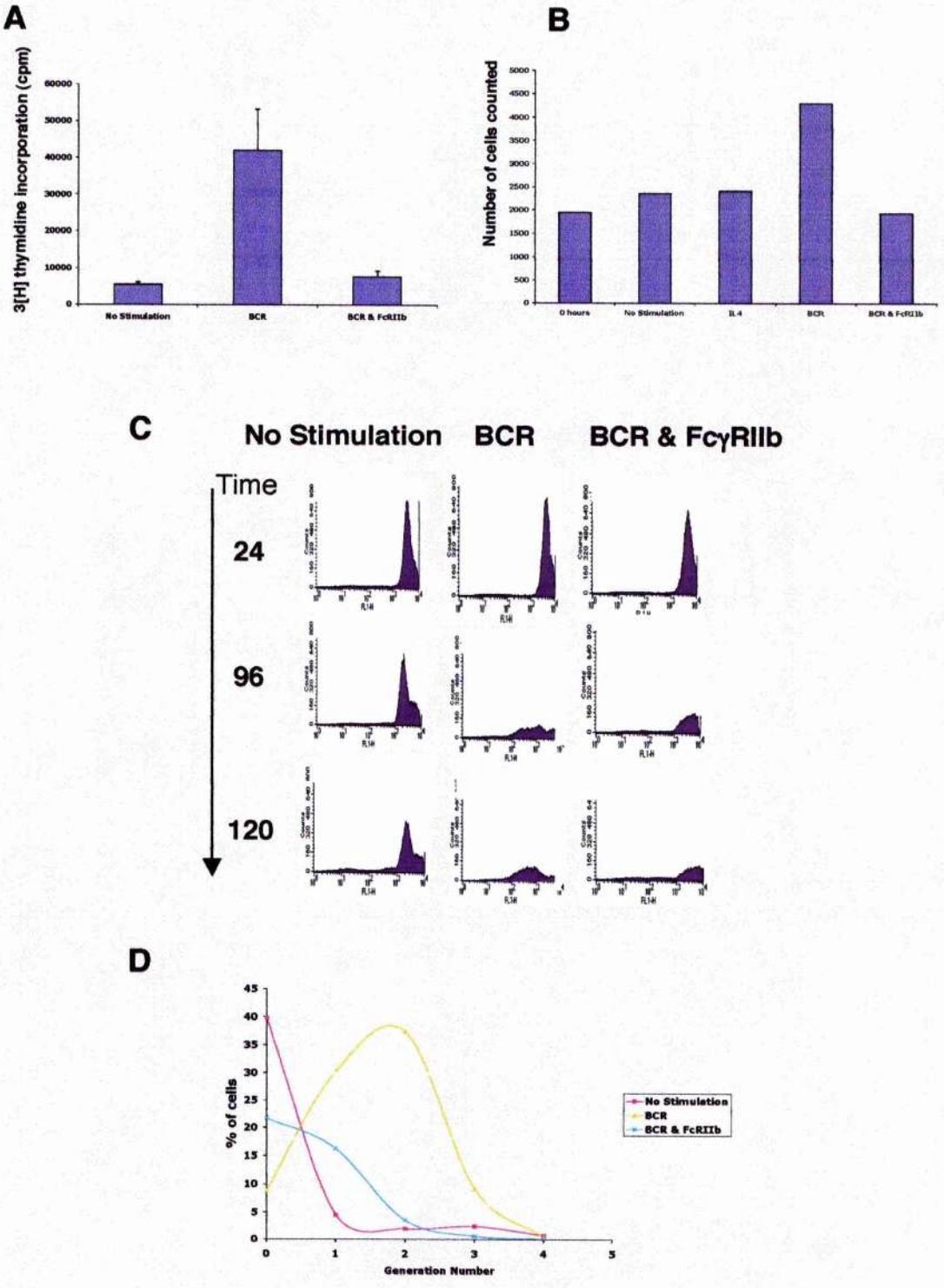
A
3[H] thymidine incorporation (cpm)
60000
50000
40000
30000
20000
10000
0
No Stimulation
BCR
BCR & FcRIIb
B
Number of cells counted
5000
4500
4000
3500
3000
2500
2000
1500
1000
500
0
0 hours
No Stimulation
IL-4
BCR
BCR & FcRIIb
C
No Stimulation
BCR
BCR & FcγRIIb
Time
24
96
120
D
% of cells
45
40
35
30
25
20
15
10
5
0
0
1
2
3
4
5
Generation Number
No Stimulation
BCR
BCR & FcRIIb

Figure 4.3: Coligation of the BCR and FcγRIIb induces apoptosis

(A) Cells were stained with 50 μg/ml PI after culture for 48 h with appropriate stimulations. Cells were either treated with media alone (No stimulation), 56 pg/ml murine IL4 (IL4), 50 μg/ml $F(Ab)_2'$ fragments of anti-IgM (BCR) or 50 μg/ml $F(Ab)_2'$ fragments of anti-IgM combined with 75 μg/ml of intact anti-IgM (BCR & FcγRIIb). FACS analysis was used to calculate the percentage of cells in G0/G1, S phase, G2/M phase and subdiploid cells. The data is displayed as a histogram of PI fluorescence (FL2). These data are from a single experiment, representative of 11 experiments.

(B) Cells were treated as described above. The data is displayed as the percentage of cells in each phase of the cell cycle. This data set is separate from the data shown in panel **(A)**. These data are from a single experiment, representative of 11 experiments.

A

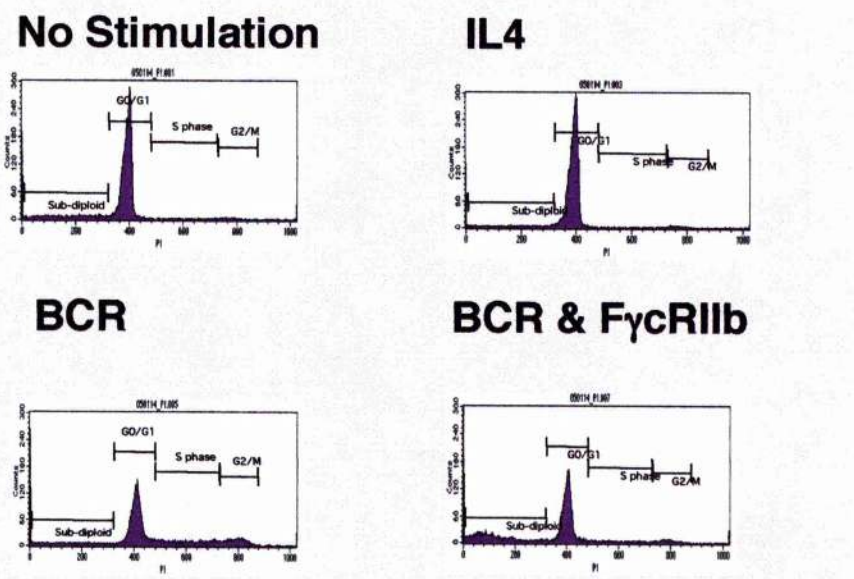
No Stimulation
IL4
BCR
BCR & FγcRIIb
G0/G1
S phase
G2/M
Sub-diploid

B

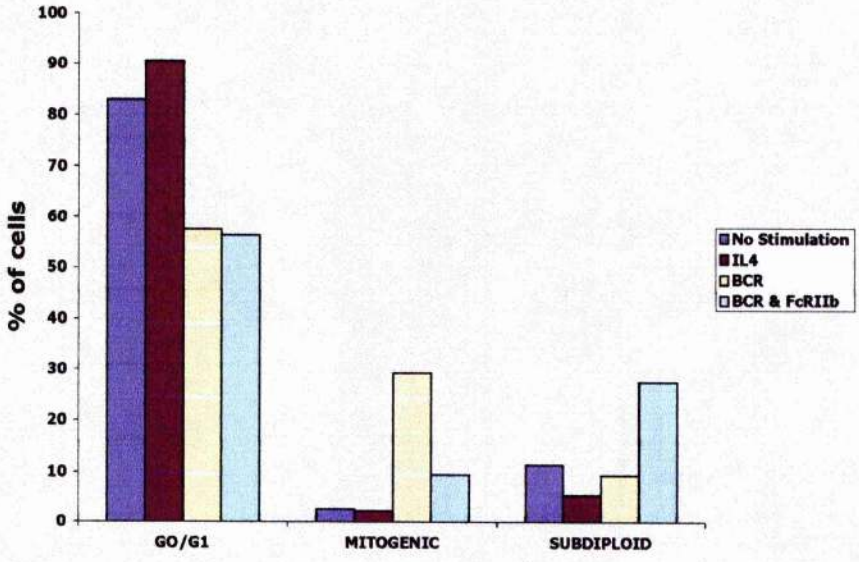
% of cells
100
90
80
70
60
50
40
30
20
10
0
GO/G1
MITOGENIC
SUBDIPLOID
No Stimulation
IL4
BCR
BCR & FcRIIb

Figure 4.4: Simultaneous coligation of BCR and FcγRIIb results in chromatin condensation, a hallmark of apoptosis

Cell were incubated with either media alone (No Stimulation), 100 nm dexamethasone, as a positive control for caspase-dependent apoptosis, or a combination of 50 μg/ml $F(Ab)_2$' fragments of anti-IgM and 75 μg/ml of intact anti-IgM (BCR & FcγRIIb) for 48 h. Culture was followed by fixation, DAPI staining and fluorescence microscope analysis. Brightly staining areas highlight areas of chromatin condensation which is a hallmark of apoptosis. Whereas cells with diffuse chromatin straining in their nuclei have healthy nuclei with a normal chromatin distribution.

Dexamethasone 100 nm

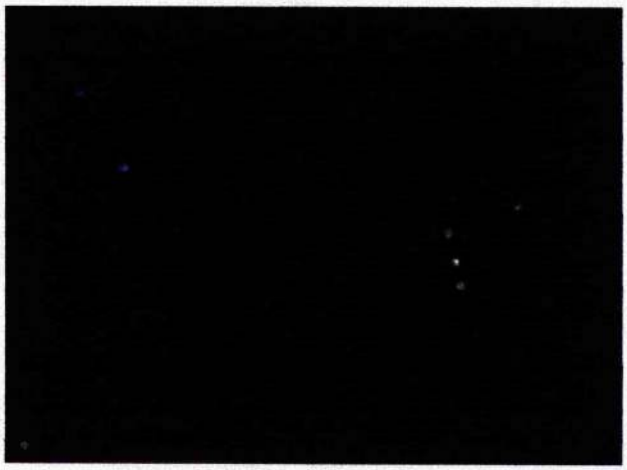

No Stimulation

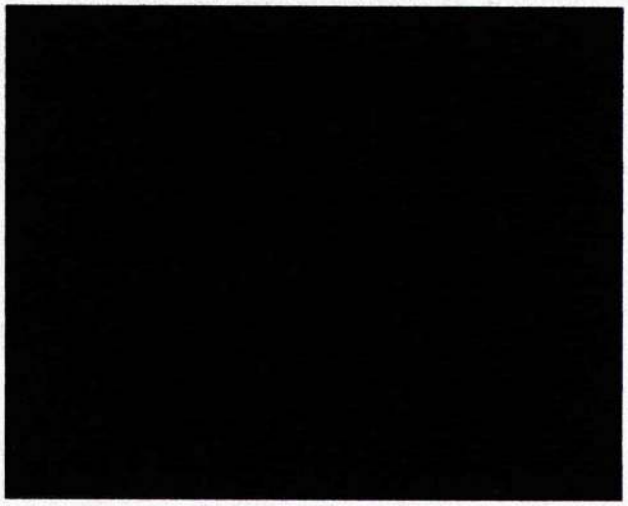

BCR & FcγRIIb

Figure 4.5: Simultaneous coligation of the BCR and FcγRIIb results in dissipation of MMP

(A) Cells were incubated with media alone (No stimulation), 50 μg/ml $F(Ab)_2$' fragments of anti-IgM (BCR) or 50 μg/ml $F(Ab)_2$' fragments of anti-IgM combined with 75 μg/ml of intact anti-IgM (BCR & FcγRIIb) for 96 or 120 h. Following this cells were stained with 2.5 μM $DiOC_6$. Dissipation of MMP can been seen as a reduction in $DiOC_6$ brightness (FL1 fluorescence). These data are from a single experiment, representative of 10 experiments.

(B) Cells were incubated as described in panel **(A)** for 48 h and then stained with JC1. JC1 acts by switching from a red aggregate when MMP is high (FL2 fluorescence) to a green monomer once MMP has been dissipated (FL1 fluorescence). The histograms show FL2 and so the monomeric, red, form of the dye which is present in healthy cells with a high MMP.

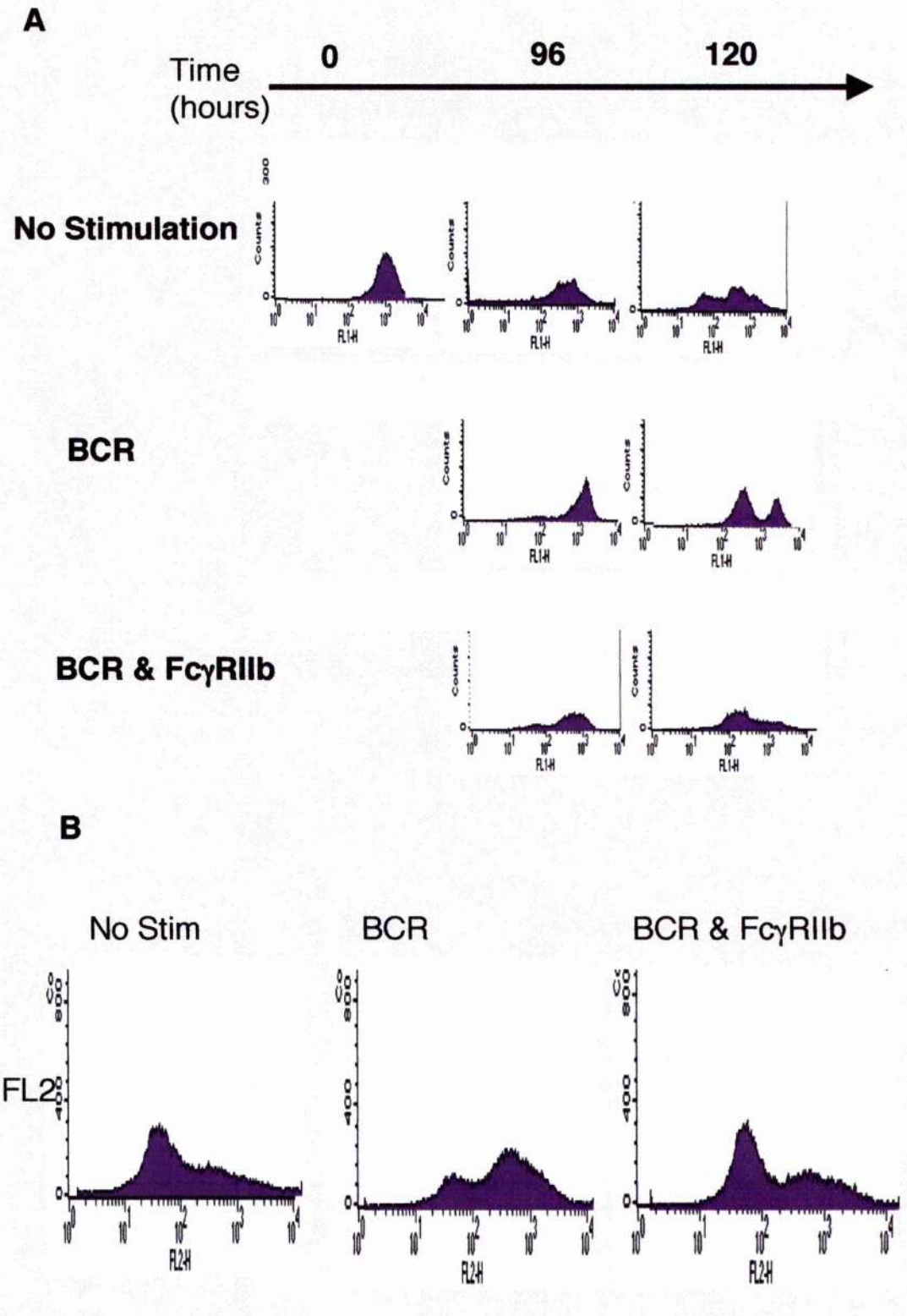
A
Time (hours)
0
96
120
No Stimulation
BCR
BCR & FcγRIIb
B
No Stim
BCR
BCR & FcγRIIb
FL2
FL1-H
FL2-H

Figure 4.6: Simultaneous coligation of the BCR and FcγRIIb induces mitochondrial- dependent apoptosis

(A) Cells were incubated with media alone (No stimulation), 50 μg/ml $F(Ab)_2'$ fragments of anti-IgM (BCR) or 50 μg/ml $F(Ab)_2'$ fragments of anti-IgM combined with 75 μg/ml of intact anti-IgM (BCR & FcγRIIb) for 48 h. Following this cells were stained with 2.5 μM $DiOC_6$. Dissipation of MMP can been seen as a reduction in $DiOC_6$ brightness (FL1 fluorescence) and can be assessed by dividing the cells into two populations. The right hand peak having a high, healthy MMP and the second having a low apoptotic MMP. The data was then displayed as the percentage of cells with a high MMP. These data are from a single experiment, representative of 10 experiments. The data set is different from that shown in figure 4.6.

(B) Cells were incubated as described in panel **(A)** and incubated for 24, 48 or 96 h prior to $DiOC_6$ staining. The data was then displayed as the percentage of cells with a high MMP for each time point. These data are from a single experiment, representative of 3 experiments. The data set is different from that shown in figure 4.6 and panel **(A)**.

(C) Cells were incubated as described in panel **(A)** for 48 h. Cells were then used to make both mitochondrial and cytosolic extracts which were assessed for their cytochrome c content by ELISA. The translocation of cytochrome c from the mitochondria to the cytosol is indicative of apoptosis and demonstrates that the cells have opened the mitochondrial permeability transition pore. Results are displayed as a ratio of cytochrome c levels (optical density at 450nm) in the cytosol as compared to the mitochondria. The data is a mean of three wells ± SD.

A

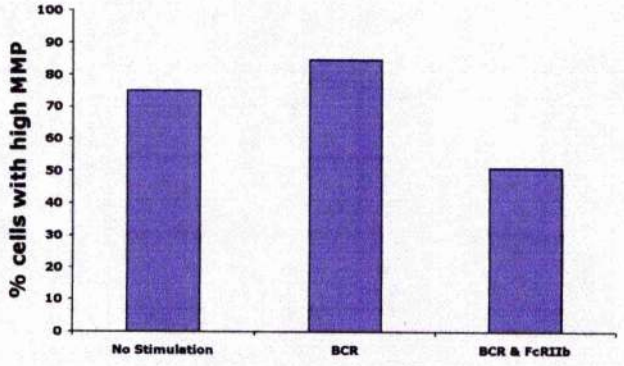
% cells with high MMP
100
90
80
70
60
50
40
30
20
10
0
No Stimulation
BCR
BCR & FcRIIb

B

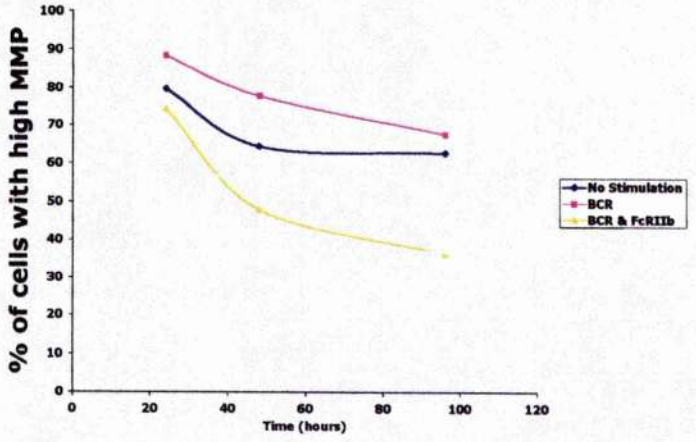
% of cells with high MMP
100
90
80
70
60
50
40
30
20
10
0
0
20
40
60
80
100
120
Time (hours)
No Stimulation
BCR
BCR & FcRIIb

C

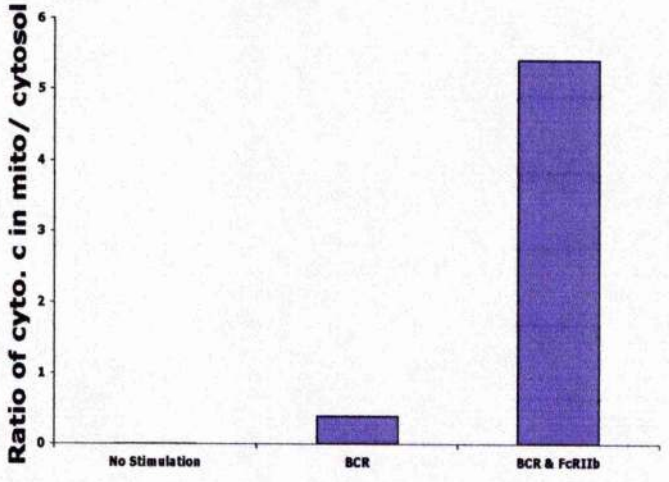
Ratio of cyto. c in mito/ cytosol
6
5
4
3
2
1
0
No Stimulation
BCR
BCR & FcRIIb

Figure 4.7: Ligation of the BCR produces a strong phospho-ERK signal whereas coligation of the BCR and FcγRIIb abrogates this signal.

(A) Cells were cultured with media alone (A), 50 μg/ml $F(Ab)_2$' fragments of anti-IgM (B) or 50 μg/ml $F(Ab)_2$' fragments of anti-IgM combined with 75 μg/ml of intact anti-IgM (C) for 5 min and used to make whole cell lysates. Lysates were then analysed by Western Blotting using the NuPAGE system with anti-phospho-ERK 1/2 antibodies. Lane (D) shows the positive control for this experiment, recombinant pERK2 protein. These data are from a single experiment, representative of 3 experiments.

(B) Cells were incubated for 48 h with appropriate stimulations prior to fixation, permeblisation and assessment of ERK and phospho-ERK levels by FACE assay. Cells were cultured with media alone (unstimulated), 56 pg/ml of murine IL4 (IL4), 50 μg/ml $F(Ab)_2$' fragments of anti-IgM (BCR) or 50 μg/ml $F(Ab)_2$' fragments of anti-IgM combined with 75 μg/ml of intact anti-IgM (BCR & FcγRIIb). The modified ELISA method- FACE- was used to assess ERK and phospho-ERK. Results are displayed as the ratio of the phospho-ERK signal to ERK signals. All ERK levels were calculated as the mean of three wells ± SD. These data are from a single experiment, representative of two experiments.

A

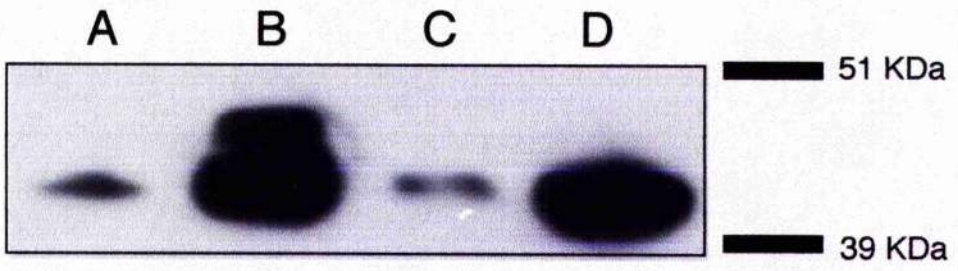
A
B
C
D
51 KDa
39 KDa

B

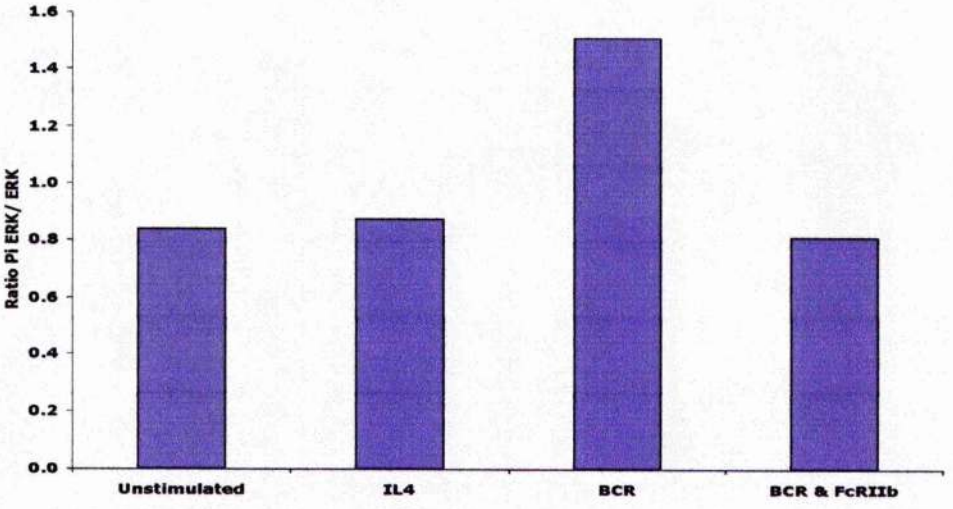
Ratio Pi ERK/ ERK
1.6
1.4
1.2
1.0
0.8
0.6
0.4
0.2
0.0
Unstimulated
IL4
BCR
BCR & FcRIIb

Figure 4.8: Inhibitors of the MAP kinase pathway can inhibit BCR-mediated proliferation

(A) Cells were cultured for 48 h and then DNA synthesis was assessed by [^{3}H] thymidine uptake. Cells were either treated with media alone (No stimulation), 50 μg/ml $F(Ab)_2$' fragments of anti-IgM (BCR) or 50 μg/ml $F(Ab)_2$' fragments of anti-IgM combined with 75 μg/ml of intact anti-IgM (BCR & FcγRIIb) in the presence or absence of 10 μM PD98059 and 1 μM U0126. These data are the mean of three replicate wells ± SD. These data are from a single experiment, representative of 4 experiments.

(B) Cells were stained with 50 μg/ml PI after culture for 48 h with 50 μg/ml $F(Ab)_2$' fragments of anti-IgM (BCR) in the presence or absence of 1 μM U0126. FACS analysis was used to calculate the number of cells in G0/G1, mitogenic and subdiploid phases of the cell cycle. Data was then displayed as the percentage of cells in each phase of the cell cycle. Data are from a single experiment, representative of 4 experiments.

(C) Cells were incubated as described in panel **(A)** for 48 h and then stained with 2.5 μM $DiOC_6$. Dissipation of the MMP was assessed by dividing the cells into two populations. The right hand peak having a high, healthy MMP and the second having a low, apoptotic MMP. The data was then displayed as the percentage of cells with a high MMP. Data are from a single experiment, representative of 4 experiments.

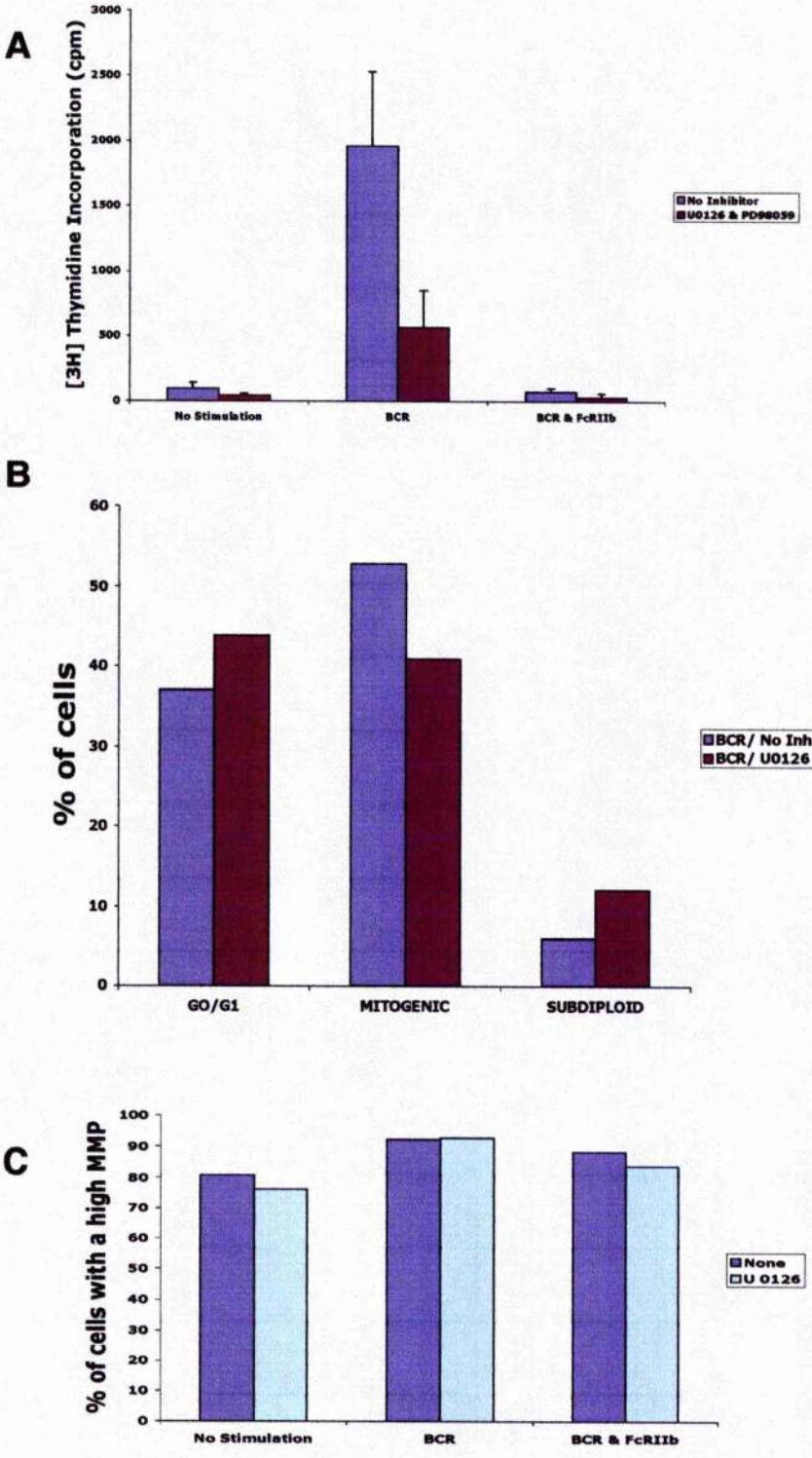
A
[3H] Thymidine Incorporation (cpm)
3000
2500
2000
1500
1000
500
0
No Stimulation
BCR
BCR & FcRIIb
No Inhibitor
U0126 & PD98059
B
% of cells
60
50
40
30
20
10
0
GO/G1
MITOGENIC
SUBDIPLOID
BCR/ No Inhibitor
BCR/ U0126
C
% of cells with a high MMP
100
90
80
70
60
50
40
30
20
10
0
No Stimulation
BCR
BCR & FcRIIb
None
U 0126

Figure 4.9: PI-3 kinase inhibition results in growth arrest and apoptosis

(A) Cells were cultured for 48 h and then DNA synthesis was assessed by [^{3}H] thymidine uptake. Cells were either treated with media alone (No stimulation), 50 μg/ml F(Ab)$_2$' fragments of anti-IgM (BCR) or 50 μg/ml F(Ab)$_2$' fragments of anti-IgM combined with 75 μg/ml of intact anti-IgM (BCR & FcγRIIb) in the presence or absence of 1 μM LY294002. These data are the mean of three separate wells ± SD. These data are from a single experiment, representative of 4 separate experiments.

(B) Cells were stained with 50 μg/ml PI after culture for 48 h with 50 μg/ml F(Ab)$_2$' fragments of anti-IgM (BCR) in the presence or absence of 1 μM LY294002. FACS analysis was used to calculate the number of cells in G0/G1, mitogenic and subdiploid phases of the cell cycle. Data was then displayed as the percentage of cells in each phase of the cell cycle. Data are from a single experiment, representative of 4 experiments.

(C) Cells were incubated as described in panel **(A)** for 48 h and then stained with 2.5 μM DiOC$_6$. Dissipation of the MMP was assessed by dividing the cells into two populations. The right hand peak having a high, healthy MMP and the second having a low, apoptotic MMP. The data were then displayed as the percentage of cells with a high MMP. Data are from a single experiment, representative of 4 experiments.

A

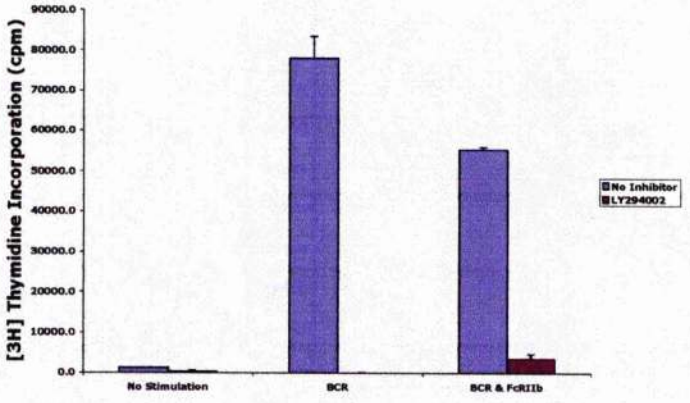
[3H] Thymidine Incorporation (cpm)
90000.0
80000.0
70000.0
60000.0
50000.0
40000.0
30000.0
20000.0
10000.0
0.0
No Stimulation
BCR
BCR & FcRIIb
No Inhibitor
LY294002

B

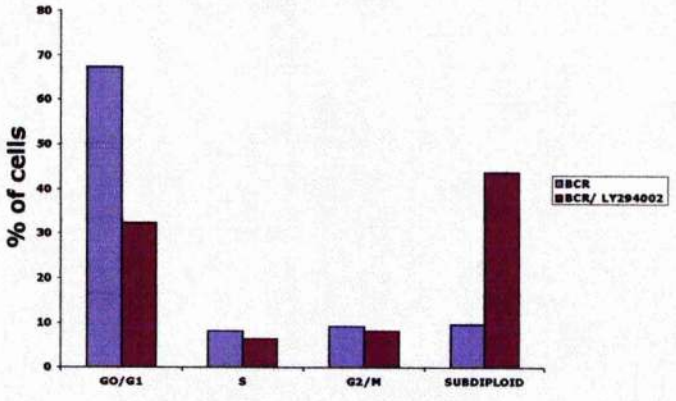
% of cells
80
70
60
50
40
30
20
10
0
GO/G1
S
G2/M
SUBDIPLOID
BCR
BCR/ LY294002

C

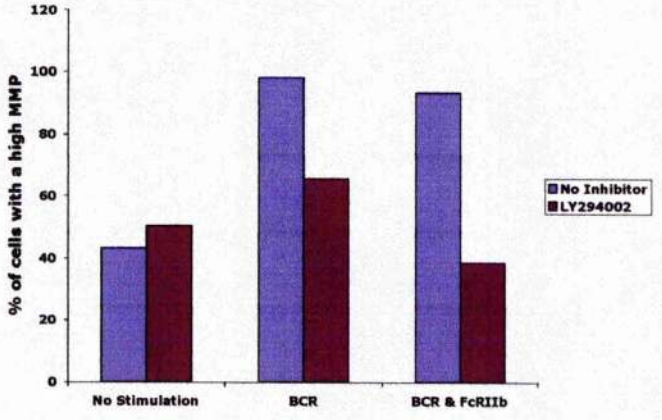
% of cells with a high MMP
120
100
80
60
40
20
0
No Stimulation
BCR
BCR & FcRIIb
No Inhibitor
LY294002

Figure 4.10: Ligation of the BCR induces a strong phospho-AKT signal which can be abrogated by simultaneous coligation of FcγRIIb

Cells were cultured for 48 h in the presence or absence of the protein phosphatase inhibitor microcystin and appropriate stimulations. Cells were cultured with media alone (No stimulation), 56 pg/ml of murine IL4 (IL4), 50 μg/ml $F(Ab)_2$' fragments of anti-IgM (BCR) or 50 μg/ml $F(Ab)_2$' fragments of anti-IgM combined with 75 μg/ml of intact anti-IgM (BCR & FcγRIIb). Cells treated with microcystin assessed the cumulative AKT phosphorylation over 48 h whereas cells without microcystin were used to assess the phospho-AKT levels at a single point in time. After 48 h AKT/ phospho-AKT was elucidated using the FACE ELISA method. Results were calculated as mean AKT signal (optical density at 450 nm) of three wells. The data is displayed as a ratio of the phospho-AKT to AKT signal.

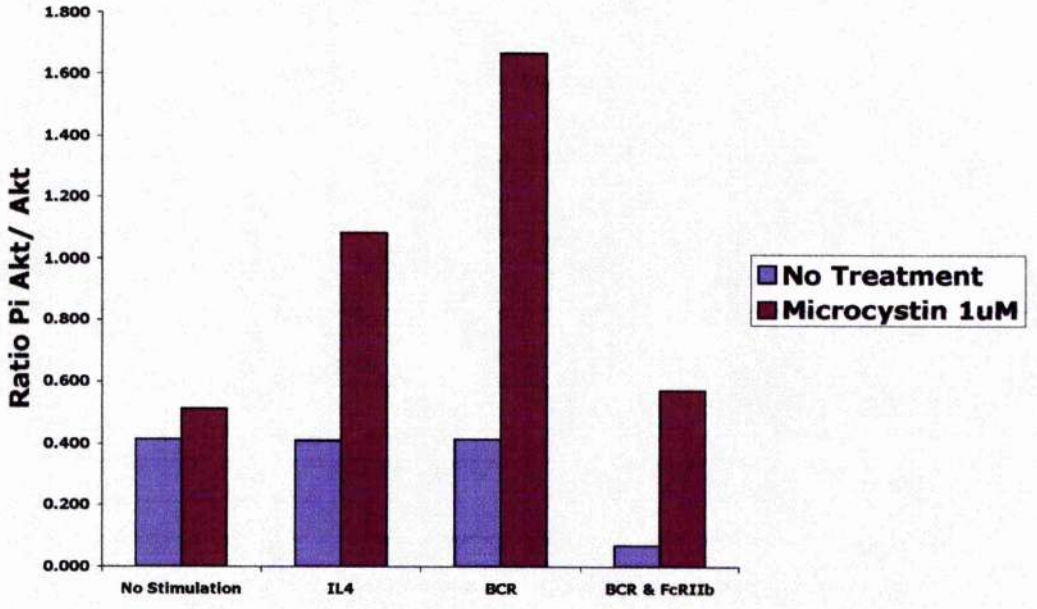
Ratio Pi Akt/ Akt
1.800
1.600
1.400
1.200
1.000
0.800
0.600
0.400
0.200
0.000
No Stimulation
IL4
BCR
BCR & FcRIIb
No Treatment
Microcystin 1uM

Figure 4.11: Inhibition of the p38 pathway does not have any effect on either BCR- induced proliferation or FcγRIIb- induced apoptosis

(A) Cells were cultured for 48 h and then DNA synthesis was assessed by [^{3}H] thymidine uptake. Cells were either treated with media alone (No stimulation), 50 μg/ml $F(Ab)_2$' fragments of anti-IgM (BCR) or 50 μg/ml $F(Ab)_2$' fragments of anti-IgM combined with 75 μg/ml of intact anti-IgM (BCR & FcγRIIb) in the presence or absence of 1 μM SB203500. These data are the mean of three separate wells ± SD. These data are from a single experiment, representative of 4 separate experiments.

(B) Cells were stained with 50 μg/ml PI after culture for 48 h with 50 μg/ml $F(Ab)_2$' fragments of anti-IgM (BCR) in the presence or absence of 1 μM SB203500. FACS analysis was used to calculate the number of cells in G0/G1, mitogenic and subdiploid phases of the cell cycle. Data was then displayed as the percentage of cells in each phase of the cell cycle. Data are from a single experiment, representative of 4 experiments.

(C) Cells were incubated as described in panel **(A)** for 48 h and then stained with 2.5 μM $DiOC_6$. Dissipation of the MMP was assessed by dividing the cells into two populations. The right hand peak having a high, healthy MMP and the second having a low, apoptotic MMP. The data were then displayed as the percentage of cells with a high MMP. Data are from a single experiment, representative of 4 experiments.

A

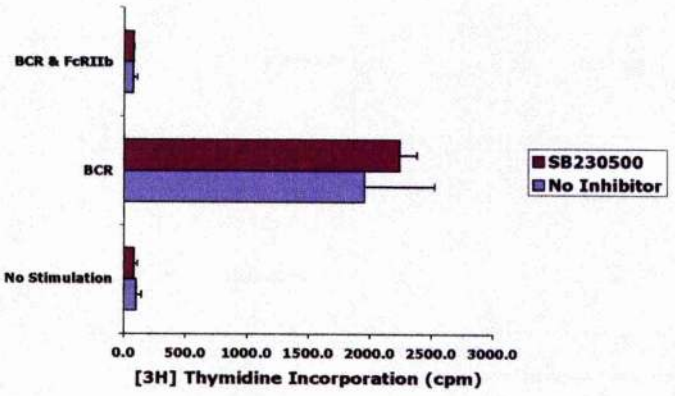
BCR & FcRIIb
BCR
No Stimulation
SB230500
No Inhibitor
0.0
500.0
1000.0
1500.0
2000.0
2500.0
3000.0
[3H] Thymidine Incorporation (cpm)

B

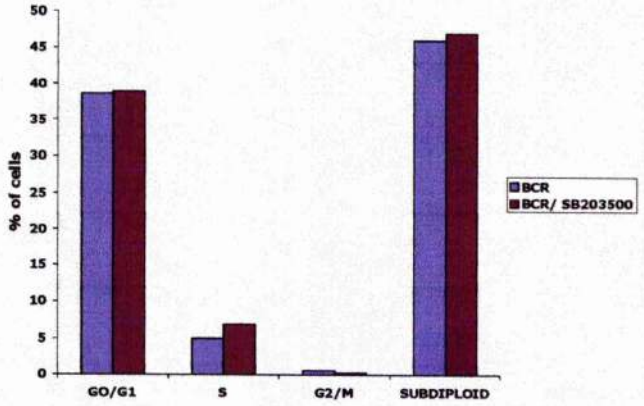
% of cells
50
45
40
35
30
25
20
15
10
5
0
GO/G1
S
G2/M
SUBDIPLOID
BCR
BCR/ SB203500

C

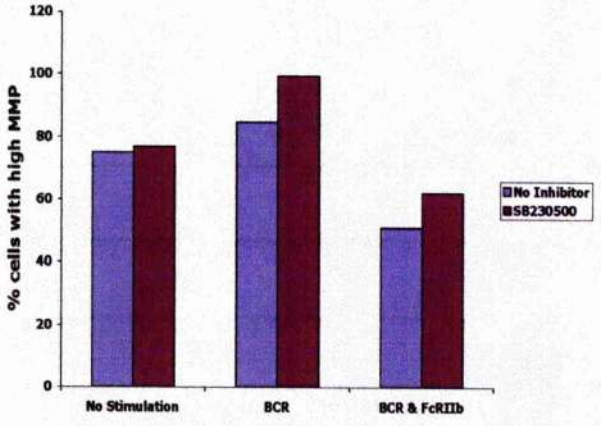
% cells with high MMP
120
100
80
60
40
20
0
No Stimulation
BCR
BCR & FcRIIb
No Inhibitor
SB230500

Figure 4.12: Ligation of the BCR or coligation of the BCR and FcγRIIb does not stimulate either JNK or p38 activation

(A) Cells were cultured for 24 h prior to fixation, permeblisation and assessment of p38 activation with media alone (No stimulation), 56 pg/ml murine IL4 (IL4), 50 μg/ml $F(Ab)_2$' fragments of anti-IgM (BCR) or 50 μg/ml $F(Ab)_2$' fragments of anti-IgM combined with 75 μg/ml of intact anti-IgM (BCR & FcγRIIb). After the stated time period phospho-p38/p38 levels were elucidated using the FACE ELISA method. Results were calculated as mean p38 signal (optical density at 450 nm) of three wells ± SD. These data are displayed as a ratio of the phospho-p38 to p38 signal.

(B) Cells were treated as described above and at the stated time period phospho-JNK/JNK levels were elucidated using the FACE ELISA method. Results were calculated as mean JNK signal (optical density at 450 nm) of three wells ± SD. These data are displayed as a ratio of the phospho-JNK to JNK signal.

A

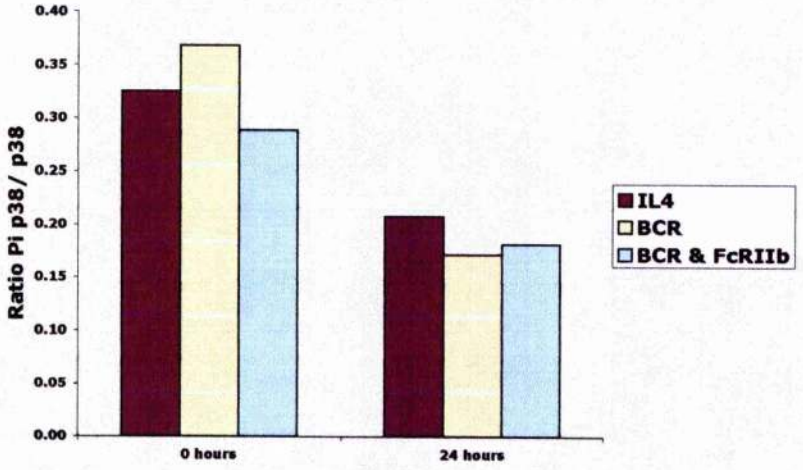
Ratio Pi p38/ p38
0.40
0.35
0.30
0.25
0.20
0.15
0.10
0.05
0.00
0 hours
24 hours
IL4
BCR
BCR & FcRIIb

B

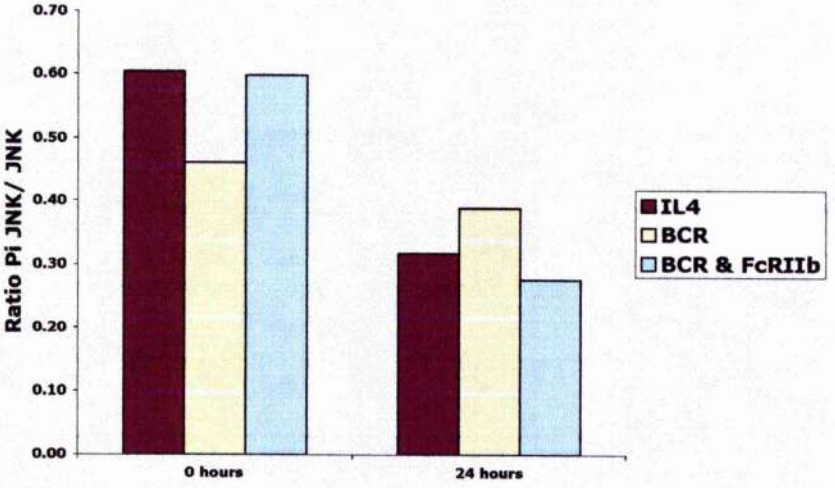
Ratio Pi JNK/ JNK
0.70
0.60
0.50
0.40
0.30
0.20
0.10
0.00
0 hours
24 hours
IL4
BCR
BCR & FcRIIb

Figure 4.13: FcγRIIb-mediated apoptosis is caspase 3 - independent

Cells were cultured for 48 h with media alone (No stimulation), 50 μg/ml $F(Ab)_2'$ fragments of anti-IgM (BCR) or 50 μg/ml $F(Ab)_2'$ fragments of anti-IgM combined with 75 μg/ml of intact anti-IgM (BCR & FcγRIIb) and then stained with 10 μM CaspACE™ FITC-VAD-FMK. This acts as a FITC conjugated version of the cell permeable, irreversible pan caspase inhibitor Z-VAD-FMK. Therefore it can be used to monitor the amount of activated caspase 3 present in the cell by measuring fluorescence in the FL1 channel. Ceramide (3 μM) and dexamethasone (100 nM) were used as positive controls for caspase 3 activation. Treatment with cell permeable Bax (50 μM) was used in an attempt to show caspase activation in response to initiation of the mitochondrial apoptotic cascade. The results are displayed as histograms of the amount of caspase activation (FL1 fluorescence).

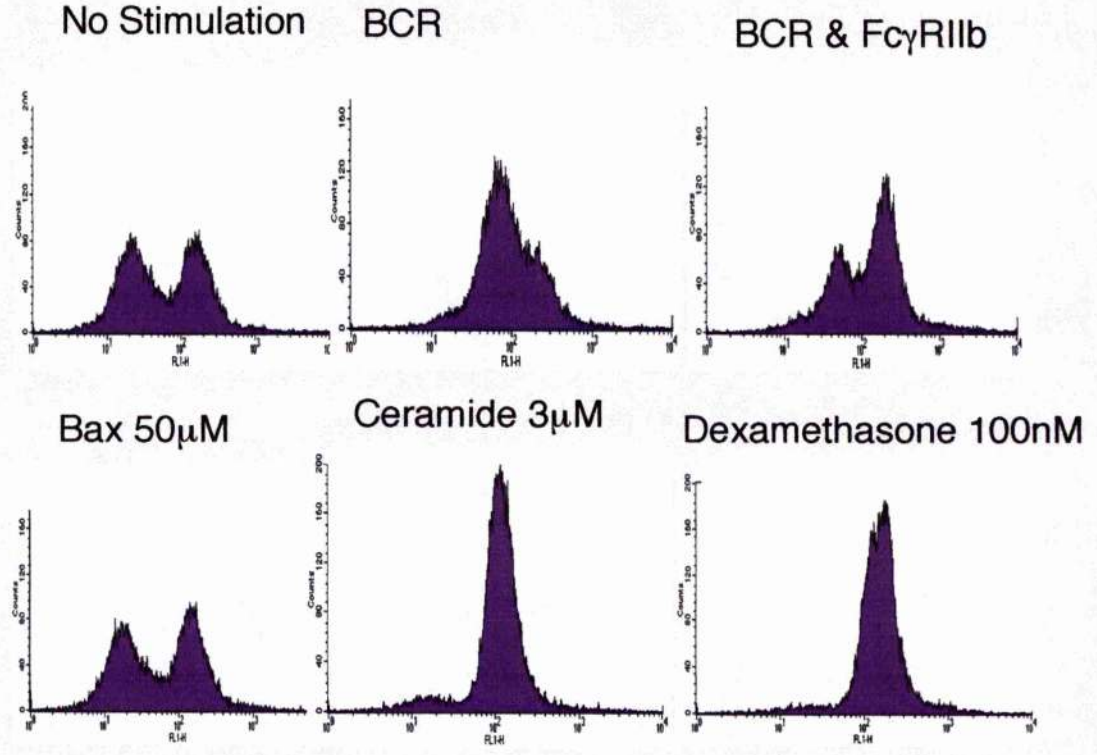
No Stimulation
BCR
BCR & FcγRIIb
Bax 50μM
Ceramide 3μM
Dexamethasone 100nM

Figure 4.14: Executioner protease inhibitors do not prevent FcγRIIb-mediated growth arrest

Cells (2 X 10^5 cells/ well) were incubated with either media alone (No stimulation), 50 μg/ml $F(Ab)_2$' fragments of anti-IgM (BCR) or 50 μg/ml $F(Ab)_2$' fragments of anti-IgM combined with 75 μg/ml of intact anti-IgM (BCR & FcγRIIb) in the presence or absence of executioner protease inhibitors (1 μM) for 48 h prior to assessment of DNA synthesis by [^{3}H] thymidine uptake. The data shown is the mean of three replicate wells ± SD. These data are from a single experiment, representative of three separate experiments.

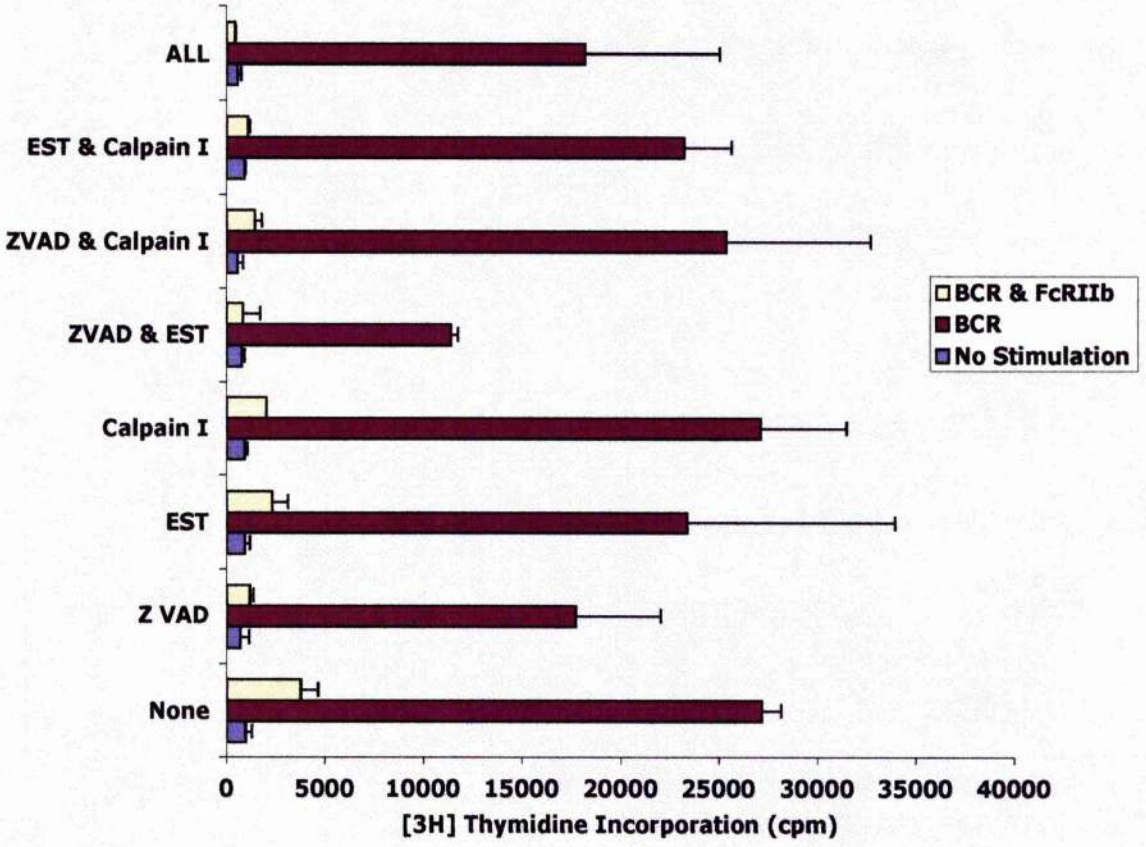
ALL
EST & Calpain I
ZVAD & Calpain I
ZVAD & EST
Calpain I
EST
Z VAD
None
BCR & FcRIIb
BCR
No Stimulation
0
5000
10000
15000
20000
25000
30000
35000
40000
[3H] Thymidine Incorporation (cpm)

Figure 4.15: Executioner protease inhibitors used in combination can provide partial rescue from FcγRIIb-mediated apoptosis

(A) Cells were incubated with 50 μg/ml $F(Ab)_2$' fragments of anti-IgM combined with 75 μg/ml of intact anti-IgM in the presence or absence of executioner protease inhibitors (1 μM) for 48 h. Following this, cells were stained with 50 μg/ml PI. Treatment with 56 pg/ml of murine IL4 was used as a control for cell survival. $F(Ab)_2$' fragments of anti-IgM (50 μg/ml), was used as a proliferation control. FACS analysis was used to calculate the percentage of cells in G0/G1, S phase, G2/M phase and apoptosis (subdiploid cells). Data are from a single experiment, representative of 3 experiments.

(B) Cells were treated as described above. Data displayed are the number of cells counted in 5 s from each sample. Data are from a single experiment, representative of 3 experiments.

A

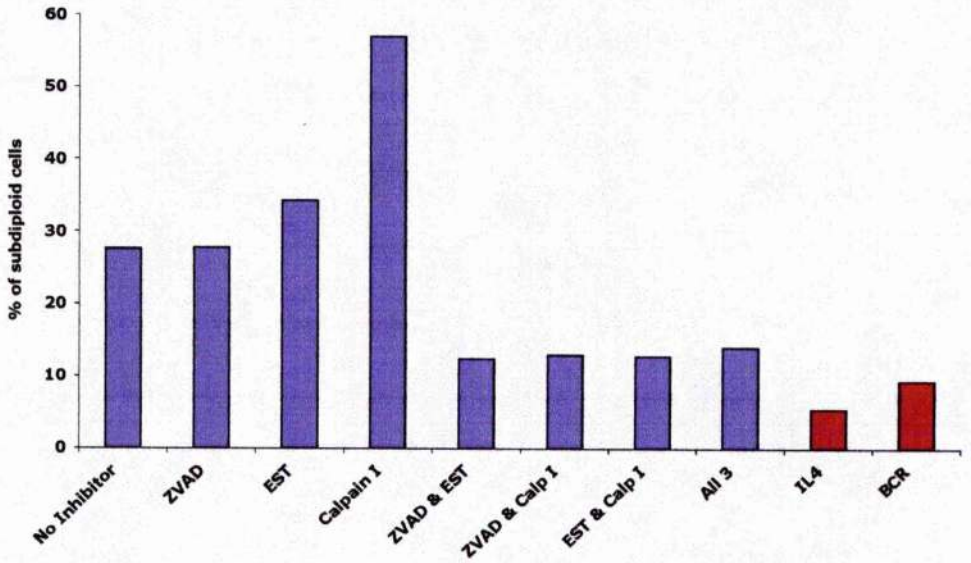
% of subdiploid cells
60
50
40
30
20
10
0
No Inhibitor
ZVAD
EST
Calpain I
ZVAD & EST
ZVAD & Calp I
EST & Calp I
All 3
IL4
BCR

B

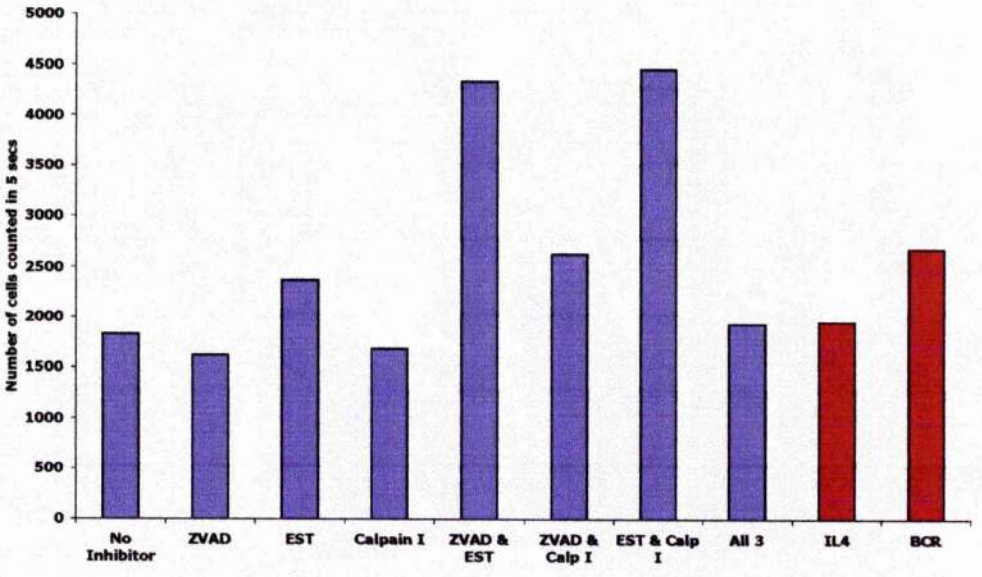
Number of cells counted in 5 secs
5000
4500
4000
3500
3000
2500
2000
1500
1000
500
0
No Inhibitor
ZVAD
EST
Calpain I
ZVAD & EST
ZVAD & Calp I
EST & Calp I
All 3
IL4
BCR

Figure 4.16: Executioner protease inhibitors used in combination can increase the proportion of FcγRIIb-treated cells in mitogenic phases of the cell cycle

Cells were incubated with 50 μg/ml $F(Ab)_2'$ fragments of anti-IgM combined with 75 μg/ml of intact anti-IgM in the presence or absence of executioner protease inhibitors (1 μM) for 48 hours. Following this, cells were stained with 50 μg/ml PI. Treatment with 56 pg/ml of murine IL4 was used as a survival control and 50 μg/ml $F(Ab)_2'$ fragments of anti-IgM was used as a proliferation control. FACS analysis was used to calculate the percentage of cells in G0/G1, S phase, G2/M phase and subdiploid cells. Data are displayed as the percentage of cells in G0/G1 phase (Panel A) or mitogenic phases of the cell cycle (Panel B). Data are from a single experiment, representative of 3 experiments.

A

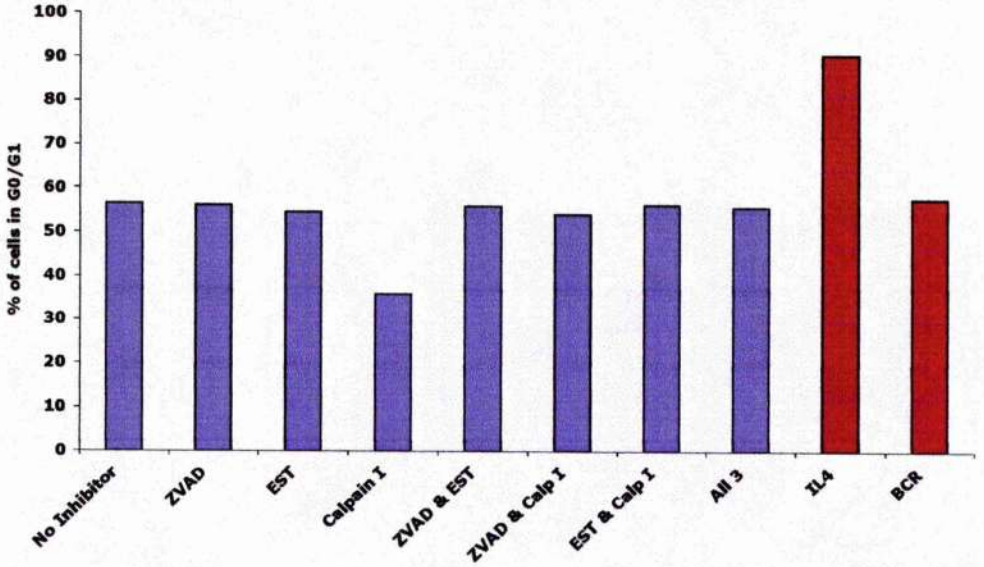
% of cells in G0/G1
100
90
80
70
60
50
40
30
20
10
0
No Inhibitor
ZVAD
EST
Calpain I
ZVAD & EST
ZVAD & Calp I
EST & Calp I
All 3
IL4
BCR

B

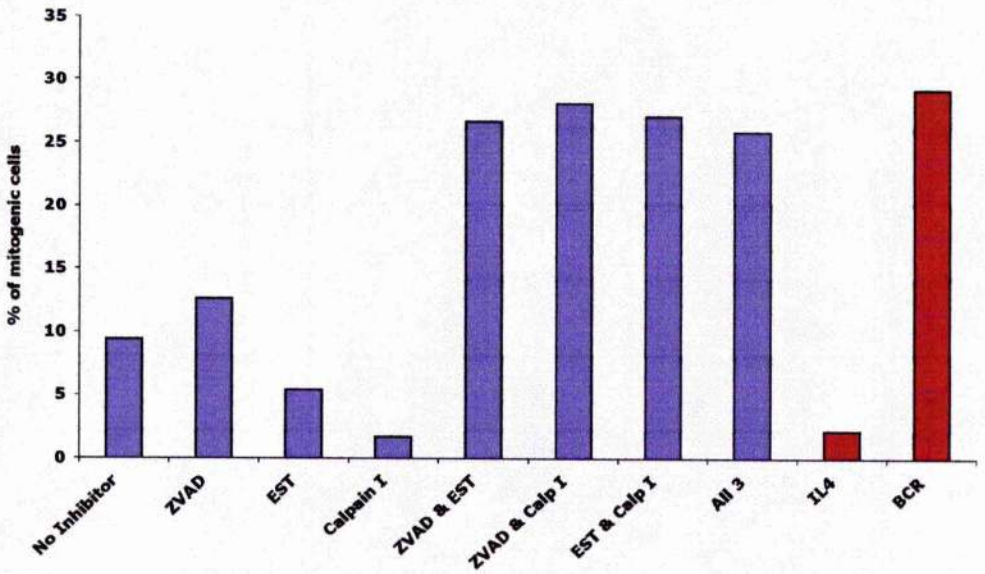
% of mitogenic cells
35
30
25
20
15
10
5
0
No Inhibitor
ZVAD
EST
Calpain I
ZVAD & EST
ZVAD & Calp I
EST & Calp I
All 3
IL4
BCR

Figure 4.17: Treatment with executioner protease inhibitors does not prevent FcγRIIb mediated-dissipation of the MMP

(A) Cells were incubated with 50 μg/ml $F(Ab)_2$' fragments of anti-IgM combined with 75 μg/ml of intact anti-IgM in the presence or absence of executioner protease inhibitors (1 μM) for 48 h. Following this cells were stained with 2.5 μM $DiOC_6$. Dissipation of MMP can been seen as a reduction in $DiOC_6$ brightness (FL1 fluorescence). Data are displayed as a histogram of $DiOC_6$ brightness (FL1 fluorescence). These data are from a single experiment, representative of 10 experiments.

(B) Cells were incubated with 50 μg/ml $F(Ab)_2$' fragments of anti-IgM (BCR) or 50 μg/ml $F(Ab)_2$' fragments of anti-IgM combined with 75 μg/ml of intact anti-IgM (BCR & FcγRIIb) in the presence or absence of executioner protease inhibitors (1 μM) for 48 h. Following this cells were stained with 2.5 μM $DiOC_6$. Dissipation of MMP can been seen as a reduction in $DiOC_6$ brightness (FL1 fluorescence) and can be assessed by dividing the cells into two populations. The right hand peak having a high, healthy MMP and the second having a low apoptotic MMP. The data was then displayed as the percentage of cells with a high MMP. These data are from a single experiment, representative of 10 experiments.

A

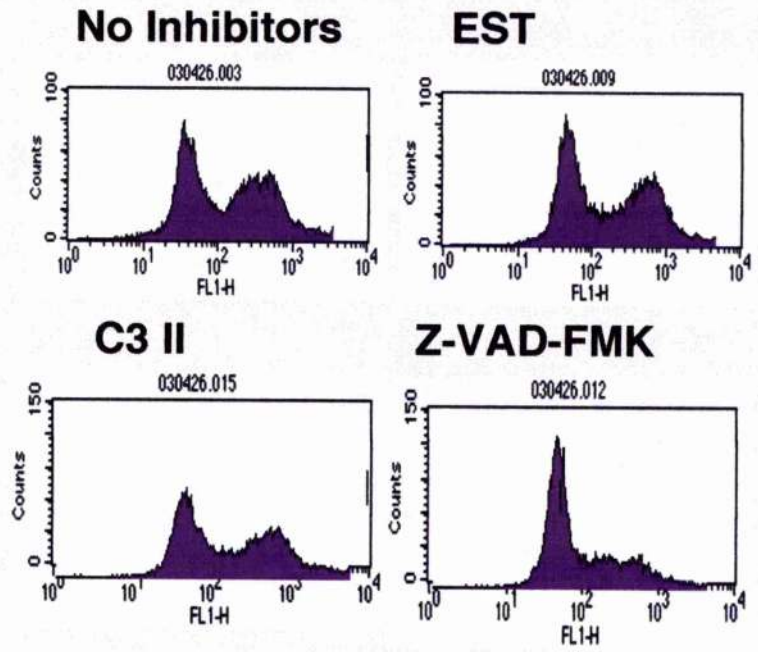
No Inhibitors
030426.003
EST
030426.009
C3 II
030426.015
Z-VAD-FMK
030426.012
Counts
FL1-H

B

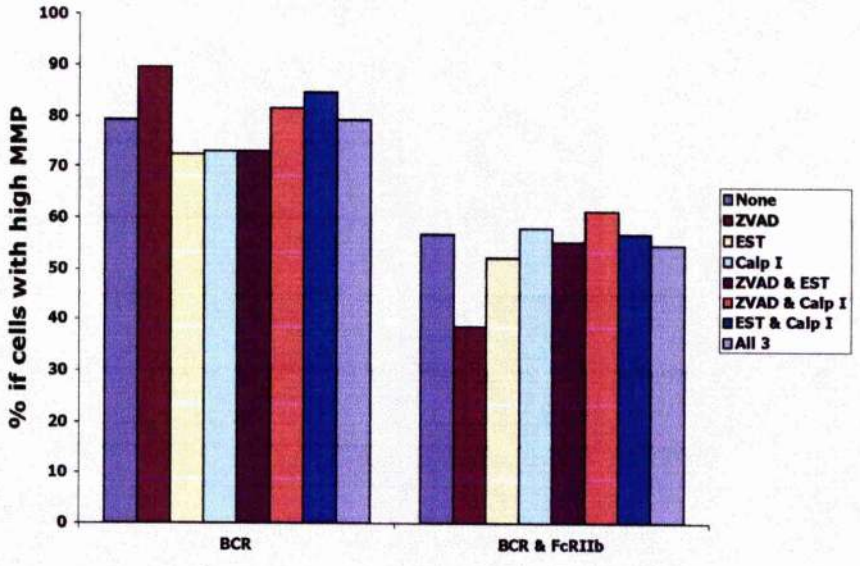
% if cells with high MMP
BCR
BCR & FcRIIb
None
ZVAD
EST
Calp I
ZVAD & EST
ZVAD & Calp I
EST & Calp I
All 3

Figure 4.18: Caspase 8 inhibition does not prevent FcγRIIb-mediated growth arrest

Cells (2 X 10^5 cells/ well) were incubated with either media alone (No Stimulation), 50 μg/ml $F(Ab)_2$' fragments of anti-IgM (BCR) or 50 μg/ml $F(Ab)_2$' fragments of anti-IgM combined with 75 μg/ml of intact anti-IgM (BCR & FcγRIIb) in the presence or absence of executioner protease inhibitors (1 μM) for 48 h prior to assessment of DNA synthesis by [^{3}H] thymidine uptake. The data shown are the mean values of three separate wells ± SD.

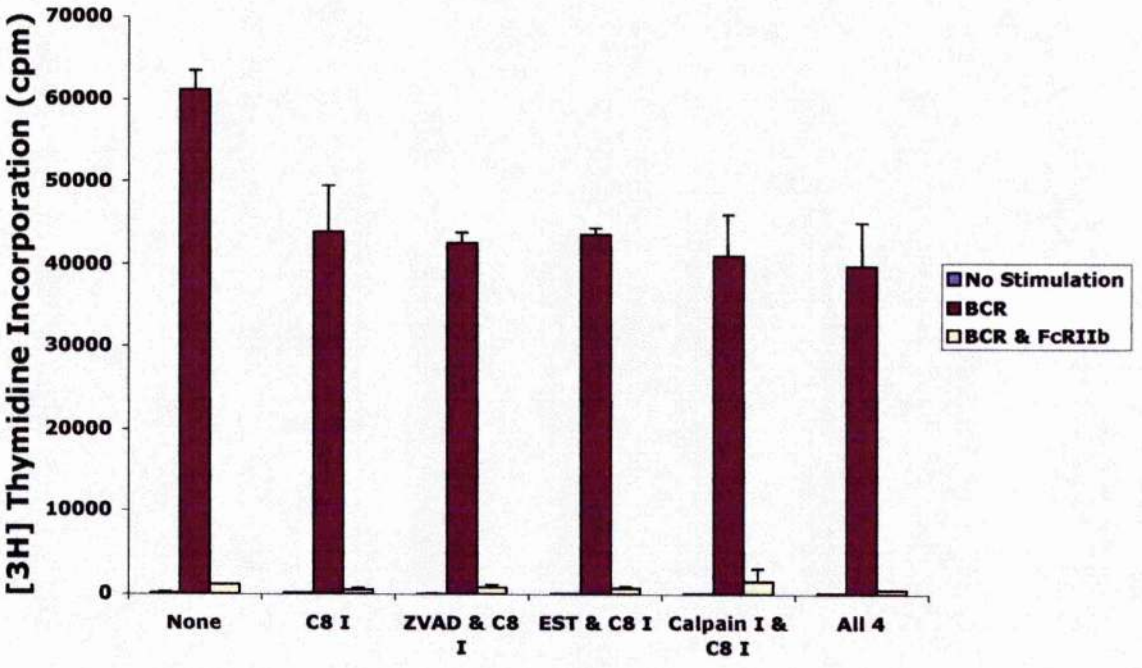
[3H] Thymidine Incorporation (cpm)
70000
60000
50000
40000
30000
20000
10000
0
None
C8 I
ZVAD & C8 I
EST & C8 I
Calpain I & C8 I
All 4
No Stimulation
BCR
BCR & FcRIIb

Figure 4.19: Caspase 8 inhibition prevents FcγRIIb-mediated apoptosis

Cells were incubated with media alone (No Stimulation), 50 μg/ml of $F(Ab)_2$' fragments of anti-IgM (BCR) or a combination of 50 μg/ml $F(Ab)_2$' fragments of anti-IgM and 75 μg/ml of intact anti-IgM (BCR & FcγRIIb) in the presence or absence of executioner protease inhibitors (1 μM) for 48 h. Following this cells were stained with 50 μg/ml PI and FACS analysis was used to calculate the number of cells in G0/G1 phase, S phase, G2/M phase and subdiploid cells.
(A) Data was then displayed as the percentage of cells in G0/G1 phase
(B) Data was then displayed as the percentage of cells in mitogenic phases.
(C) Data was then displayed as the percentage of cells in subdiploid cells.

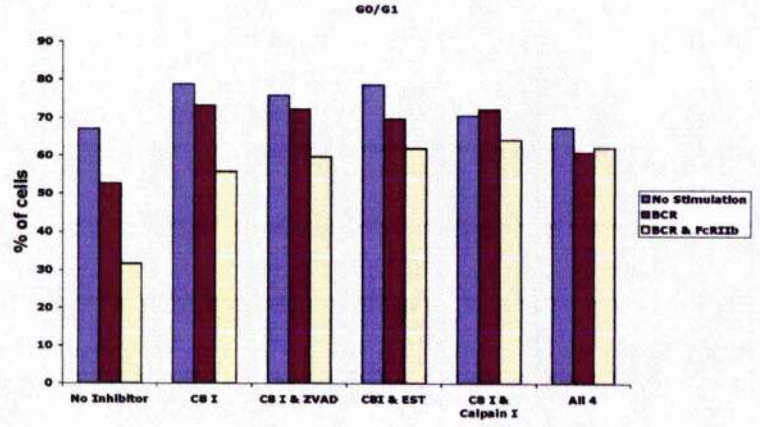
G0/G1
% of cells
90
80
70
60
50
40
30
20
10
0
No Inhibitor
CB I
CB I & ZVAD
CBI & EST
CB I & Calpain I
All 4
No Stimulation
BCR
BCR & FcRIIb

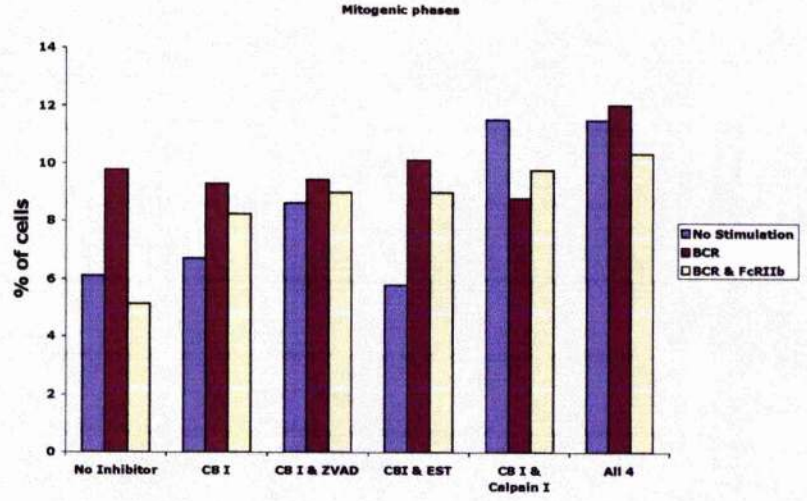
Mitogenic phases
% of cells
14
12
10
8
6
4
2
0
No Inhibitor
CB I
CB I & ZVAD
CBI & EST
CB I & Calpain I
All 4
No Stimulation
BCR
BCR & FcRIIb

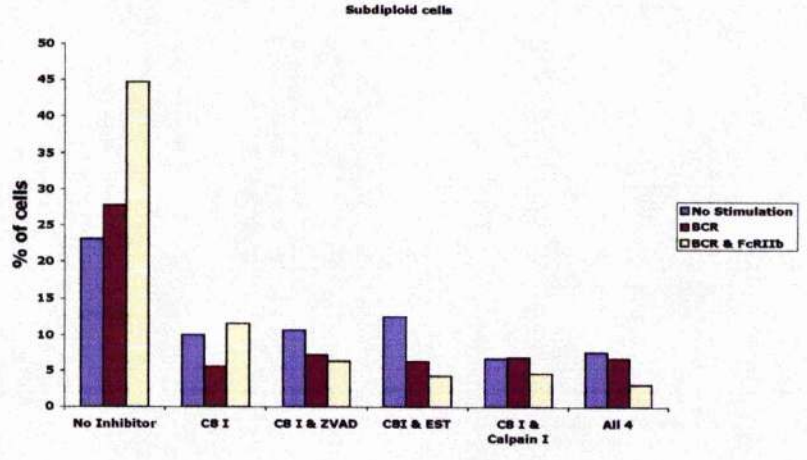
Subdiploid cells
% of cells
50
45
40
35
30
25
20
15
10
5
0
No Inhibitor
CB I
CB I & ZVAD
CBI & EST
CB I & Calpain I
All 4
No Stimulation
BCR
BCR & FcRIIb

Figure 4.20: Caspase 8 inhibition provides a partial rescue from FcγRIIb-mediated dissipation of the MMP

Cells were incubated with media alone (No Stimulation), 50 μg/ml $F(Ab)_2'$ fragments of anti-IgM (BCR) or 50 μg/ml $F(Ab)_2'$ fragments of anti-IgM combined with 75 μg/ml of intact anti-IgM (BCR & FcγRIIb) in the presence or absence of caspase 8 inhibitor (1 μM) for 48 h. Following this cells were stained with 2.5 μM $DiOC_6$. Dissipation of MMP can been seen as a reduction in $DiOC_6$ brightness (FL1 fluorescence) and can be assessed by dividing the cells into two populations. The right hand peak having a high, healthy MMP and the second having a low apoptotic MMP. The data was then displayed as the percentage of cells with a high MMP.

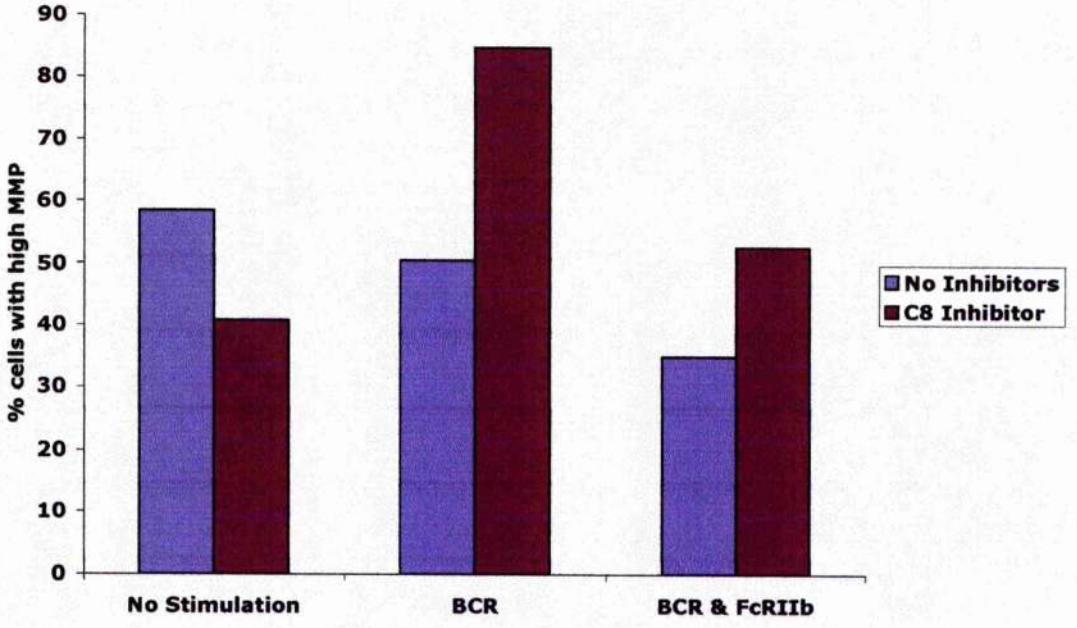
90
80
70
60
50
40
30
20
10
0
% cells with high MMP
No Stimulation
BCR
BCR & FcRIIb
No Inhibitors
C8 Inhibitor

Figure 4.21: Coligation of BCR and FcγRIIb in mature splenic B cells derived from *lpr* mice does not induce growth arrest

Mature B cells from *lpr/lpr*$^{-/-}$ mice (2 X 10^5 cells/ well) were incubated for 48 h with the appropriate stimulations prior to assessment of DNA synthesis by [^{3}H] thymidine uptake. Cells were cultured with either media alone (No Stimulation), 50 μg/ml $F(Ab)_2$' fragments of anti-IgM (BCR) or 50 μg/ml $F(Ab)_2$' fragments of anti-IgM and 75 μg/ml of intact IgM Ab (BCR & FcγRIIb). The data shown are the mean values of three separate wells ± SD.

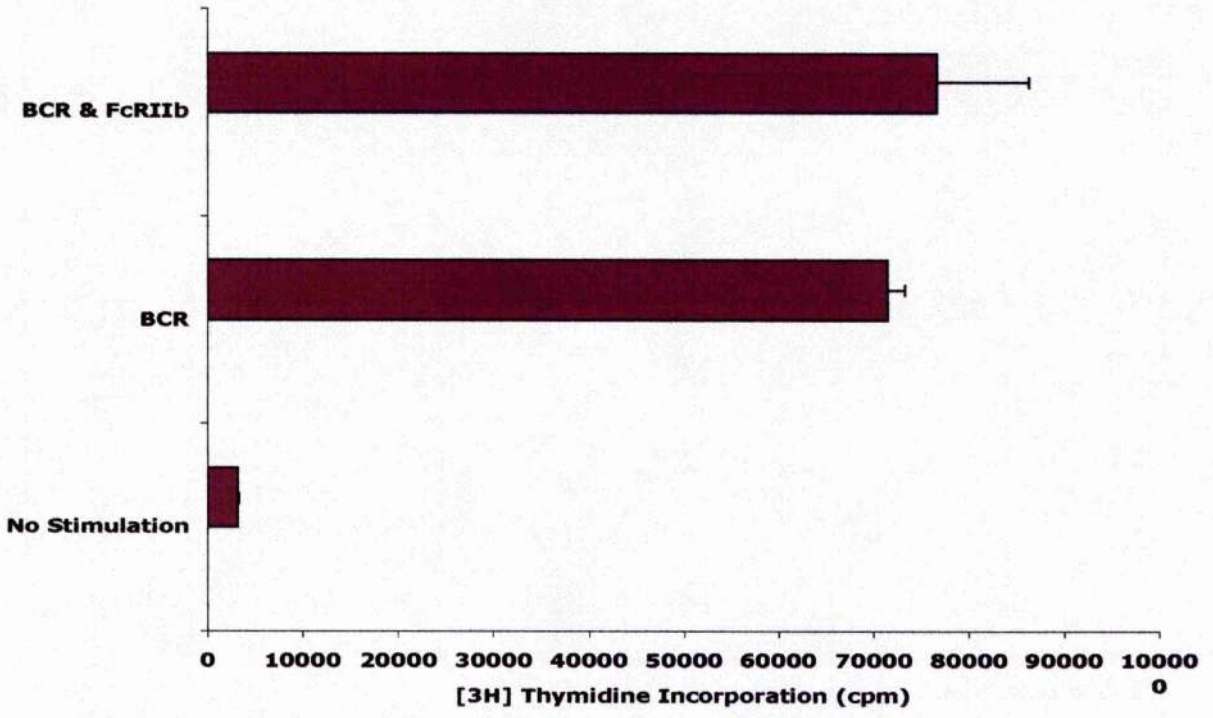
BCR & FcRIIb
BCR
No Stimulation
0
10000
20000
30000
40000
50000
60000
70000
80000
90000
100000
[3H] Thymidine Incorporation (cpm)

Figure 4.22: Ligation of the BCR and FcγRIIb induces the expression of pro-apoptotic Bcl-2 family members, Bid and Bad

(A) Mature B cells were cultured for 24 h with either 50 μg/ml $F(Ab)_2$' fragments of anti-IgM (BCR) or 50 μg/ml $F(Ab)_2$' fragments of anti-IgM and 75 μg/ml of intact anti-IgM (BCR & FcγRIIb) before making whole cell lysates. Lysates were then analysed by Western Blotting using the NuPAGE system with whole anti-Bad and whole anti-Bid antibodies

(B) Cells were cultured for 1 h or 24 h prior to fixation, permeablisation and assessment of Bad signal. Cells were incubated with either media alone (No Stimulation), 56 pg/ml murine IL4 (IL4), 50 μg/ml $F(Ab)_2$' fragments of anti-IgM (BCR) or 50 μg/ml $F(Ab)_2$' fragments of anti-IgM and 75 μg/ml of intact IgM Ab (BCR & FcγRIIb). The Bad/ phospho-Bad levels were elucidated using the FACE ELISA method. Results were calculated as mean Bad signal (optical density at 450 nm) of three wells. The data is displayed as a ratio of the phospho-Bad to Bad signal. These data are from a single experiment, representative of 2 experiments.

.

A

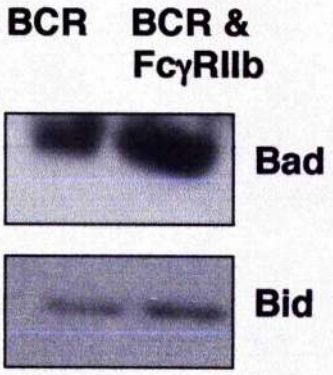
BCR
BCR &
FcγRIIb
Bad
Bid

B

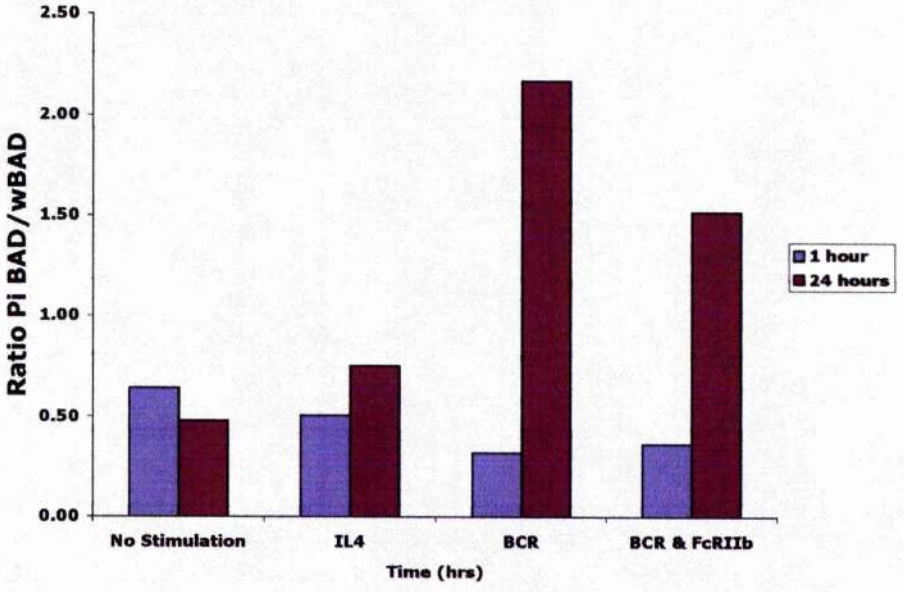
2.50
2.00
1.50
1.00
0.50
0.00
Ratio Pi BAD/wBAD
1 hour
24 hours
No Stimulation
IL4
BCR
BCR & FcRIIb
Time (hrs)

Figure 4.23: Bad activation is downregulated by both MAP kinase and PI-3 kinase inhibition

(A) Cells were cultured for 48 h prior to fixation, permeablisation and assessment of Bad signal. Cells were incubated with either media alone (No Stimulation), 50 μg/ml $F(Ab)_2$' fragments of anti-IgM (BCR) or 50 μg/ml $F(Ab)_2$' fragments of anti-IgM and 75 μg/ml of intact IgM Ab (BCR & FcγRIIb) in the presence and absence of executioner protease inhibitors (1 μM). The Bad levels were elucidated using the FACE ELISA method. Data is displayed as the mean Bad signal (optical density at 450 nm) of three wells ±SEM.

(B) Cells were cultured for 48 h prior to fixation, permeablisation and assessment of Bad signal. Cells were incubated with either media alone (No Stimulation), 50 μg/ml $F(Ab)_2$' fragments of anti-IgM (BCR) or 50 μg/ml $F(Ab)_2$' fragments of anti-IgM and 75 μg/ml of intact IgM Ab (BCR & FcγRIIb) in the presence and absence of 1 μM LY294002 and 1 μM U0126. The Bad/ phospho-Bad levels were elucidated using the FACE ELISA method. Results were calculated as mean Bad signal (optical density at 450 nm) of three wells ± SEM. The data is displayed as a ratio of the phospho-Bad to Bad signal.

(C) Cells were cultured for 48 h prior to fixation, permeablisation and assessment of Bad signal. Cells were incubated with either media alone (No Stimulation), 50 μg/ml $F(Ab)_2$' fragments of anti-IgM (BCR) or 50 μg/ml $F(Ab)_2$' fragments of anti-IgM and 75 μg/ml of intact IgM Ab (BCR & FcγRIIb) in the presence and absence of 1 μM LY294002 and 1 μM U0126. The Bad levels were elucidated using the FACE ELISA method. Data is displayed as the mean Bad signal (optical density at 450 nm) of three wells ±SEM.

A

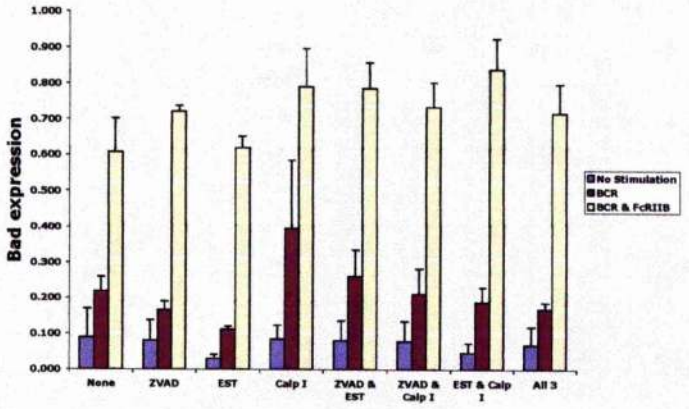
Bad expression
1.000
0.900
0.800
0.700
0.600
0.500
0.400
0.300
0.200
0.100
0.000
None
ZVAD
EST
Calp I
ZVAD & EST
ZVAD & Calp I
EST & Calp I
All 3
No Stimulation
BCR
BCR & FcRIIB

B

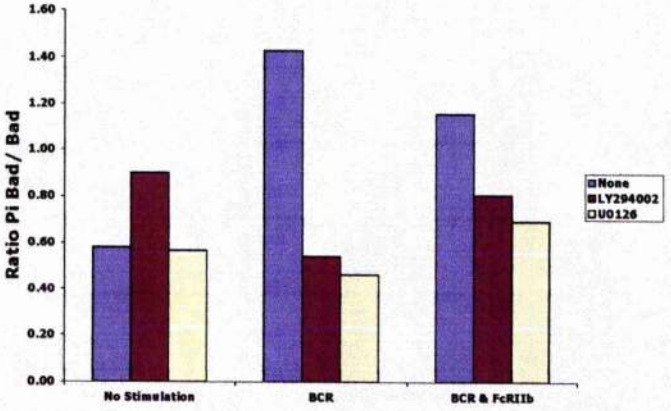
Ratio Pi Bad/ Bad
1.60
1.40
1.20
1.00
0.80
0.60
0.40
0.20
0.00
No Stimulation
BCR
BCR & FcRIIb
None
LY294002
U0126

C

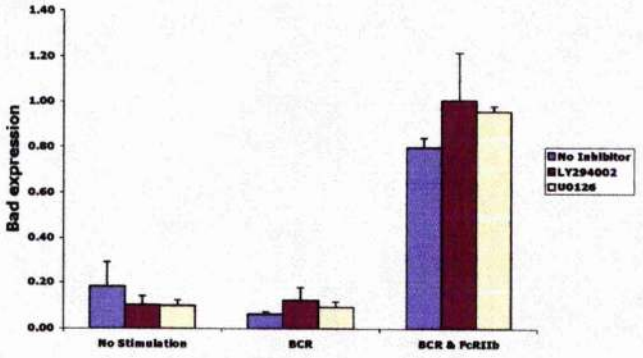
Bad expression
1.40
1.20
1.00
0.80
0.60
0.40
0.20
0.00
No Stimulation
BCR
BCR & FcRIIb
No Inhibitor
LY294002
U0126

Figure 4.24: Coligation of the BCR and FcγRIIb upregulates the activation of p53

(A) Cells were incubated for 24 or 48 h with either media alone (No Stimulation), 56 pg/ml murine IL4 (IL4), 50 μg/ml $F(Ab)_2$' fragments of anti-IgM (BCR) or 50 μg/ml $F(Ab)_2$' fragments of anti-IgM and 75 μg/ml of intact IgM Ab (BCR & FcγRIIb) prior to making nuclear extracts. The nuclear extracts were then used to assess active p53 by a modified ELISA method. The data is displayed as the level of active p53 (optical density at 450 nm) mean value of three wells ± SEM. This data is from a single experiment, representative of 3 experiments.

(B) Cells were incubated for 48 h with 50 μg/ml $F(Ab)_2$' fragments of anti-IgM and 75 μg/ml of intact IgM Ab (BCR & FcγRIIb) in the presence or absence of executioner protease inhibitors (1 μM) prior to making nuclear extracts. The nuclear extracts were then used to assess active p53 by a modified ELISA method. The data is displayed as the level of active p53 (optical density at 450 nm) mean value of three wells ± SEM.

(C) Cells were incubated for 48 h 50 μg/ml $F(Ab)_2$' fragments of anti-IgM and 75 μg/ml of intact IgM Ab (BCR & FcγRIIb) in the presence or absence of 1 μM U0126 or 1 μM LY294002 prior to making nuclear extracts. The nuclear extracts were then used to assess active p53 by a modified ELISA method. The data is displayed as the level of active p53 (optical density at 450 nm) mean value of three wells ± SEM.

A

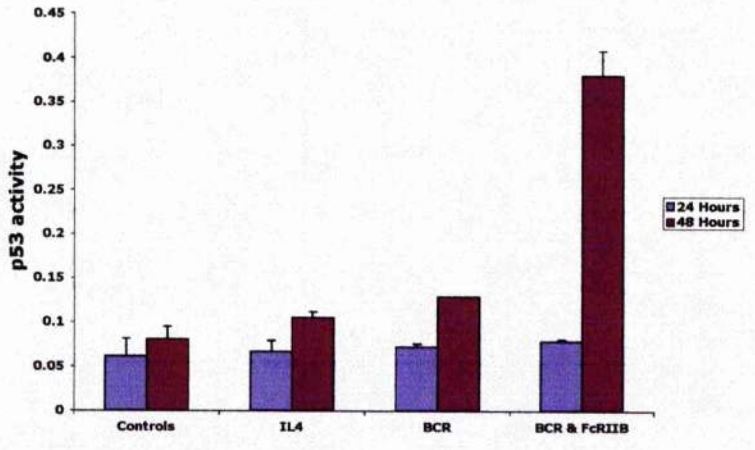
0.45
0.4
0.35
0.3
0.25
0.2
0.15
0.1
0.05
0
p53 activity
24 Hours
48 Hours
Controls
IL4
BCR
BCR & FcRIIB

B

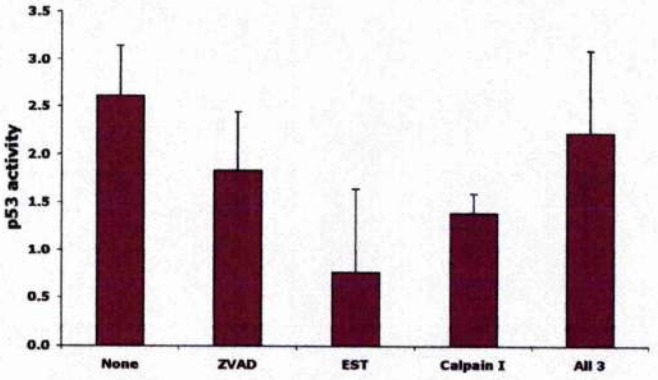
3.5
3.0
2.5
2.0
1.5
1.0
0.5
0.0
p53 activity
None
ZVAD
EST
Calpain I
All 3

C

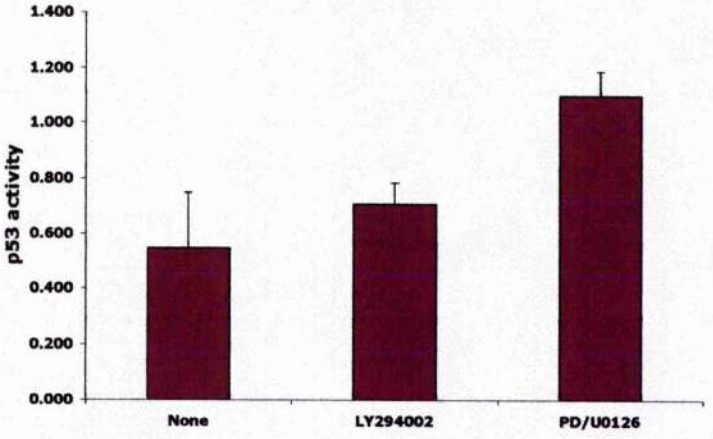
1.400
1.200
1.000
0.800
0.600
0.400
0.200
0.000
p53 activity
None
LY294002
PD/U0126

Figure 4.25: Coligation of the BCR and FcγRIIb differentially modulates individual members of the NF-κB family: cRel , p52 and Rel B have upregulated activation levels at 24 h but not 48 h.

Cells were incubated for 24 or 48 h with either media alone (No Stimulation), 56 pg/ml murine IL4 (IL4), 50 μg/ml $F(Ab)_2$' fragments of anti-IgM (BCR) or 50 μg/ml $F(Ab)_2$' fragments of anti-IgM and 75 μg/ml of intact IgM Ab (BCR & FcγRIIb) prior to making nuclear extracts. The nuclear extracts were then used to measure the activation of the various NF-κB family subunits by a modified ELISA method. The data is displayed as the level of activated NF-κB family member (optical density at 450 nm) mean value of three wells ± SD.

(A) Activation levels of cRel at 24 and 48 hours

(B) Activation levels of p52 at 24 and 48 hours

(C) Activation levels of Rel B at 24 and 48 hours

A

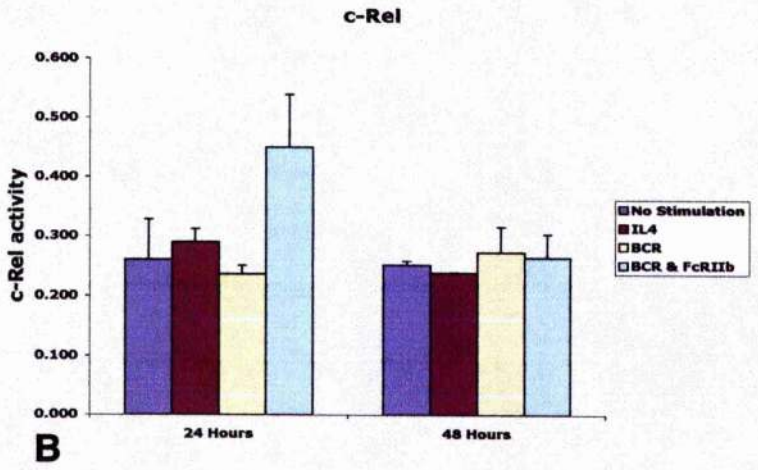
c-Rel
c-Rel activity
0.600
0.500
0.400
0.300
0.200
0.100
0.000
24 Hours
48 Hours
No Stimulation
IL4
BCR
BCR & FcRIIb

B

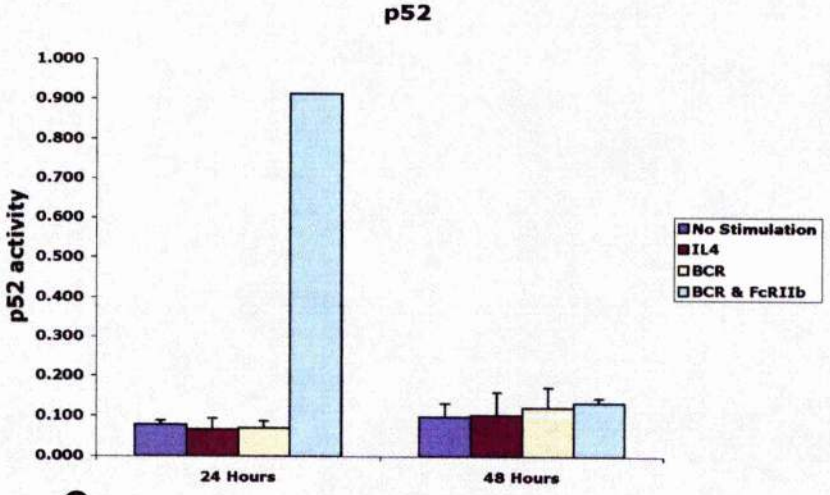
p52
p52 activity
1.000
0.900
0.800
0.700
0.600
0.500
0.400
0.300
0.200
0.100
0.000
24 Hours
48 Hours
No Stimulation
IL4
BCR
BCR & FcRIIb

C

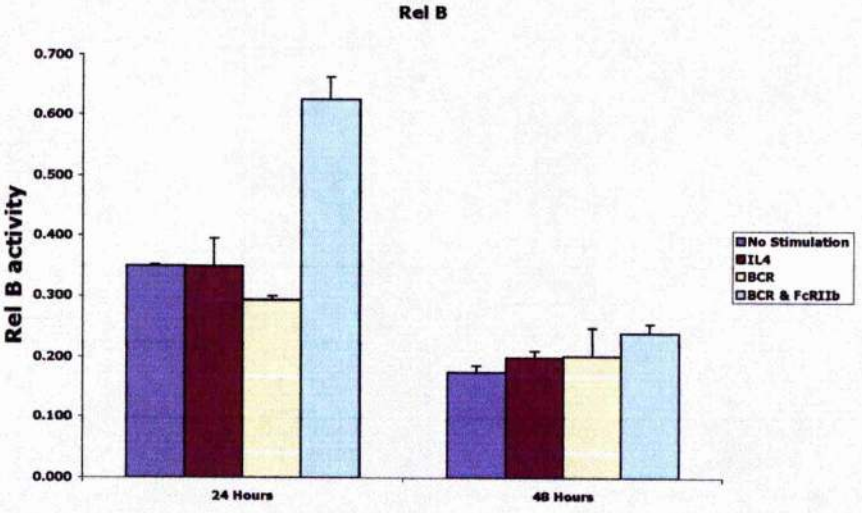
Rel B
Rel B activity
0.700
0.600
0.500
0.400
0.300
0.200
0.100
0.000
24 Hours
48 Hours
No Stimulation
IL4
BCR
BCR & FcRIIb

Figure 4.26: Coligation of the BCR and FcγRIIb differentially modulates the activation of individual members of the NF-KB family: Both p50 and p65 have upregulated activation levels at 48 h but not 24 h.

Cells were incubated for 24 or 48 h with either media alone (No Stimulation), 56 pg/ml murine IL4 (IL4), 50 μg/ml $F(Ab)_2$' fragments of anti-IgM (BCR) or 50 μg/ml $F(Ab)_2$' fragments of anti-IgM and 75 μg/ml of intact IgM Ab (BCR & FcγRIIb) prior to making nuclear extracts. The nuclear extracts were then used to measure the activation of the various NF-KB family subunits by a modified ELISA method. The data is displayed as the level of activated NF-KB family member (optical density at 450 nm) mean value of three wells ± SD.

(A) Activation levels of p50 at 24 and 48 hours

(B) Activation levels of p65 at 24 and 48 hours

A

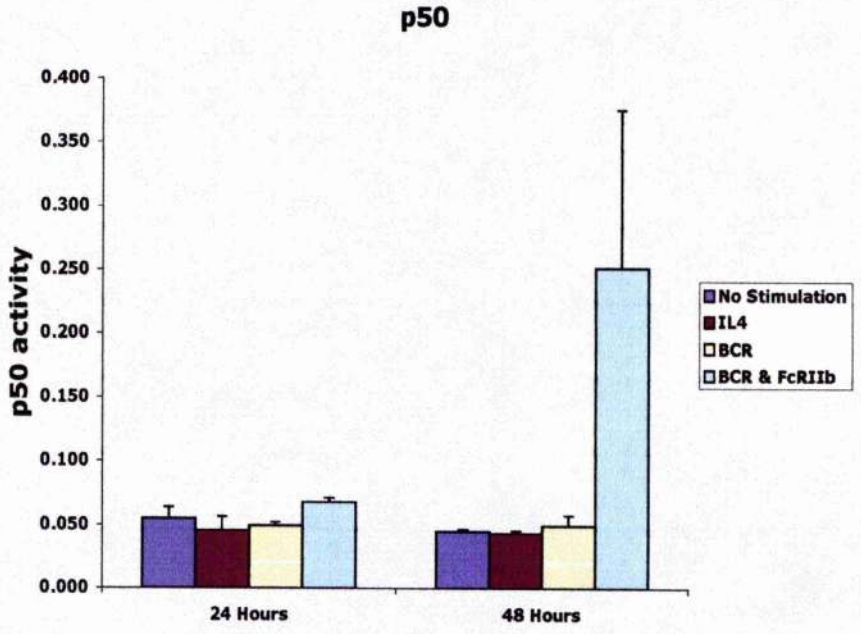
p50
p50 activity
0.400
0.350
0.300
0.250
0.200
0.150
0.100
0.050
0.000
24 Hours
48 Hours
No Stimulation
IL4
BCR
BCR & FcRIIb

B

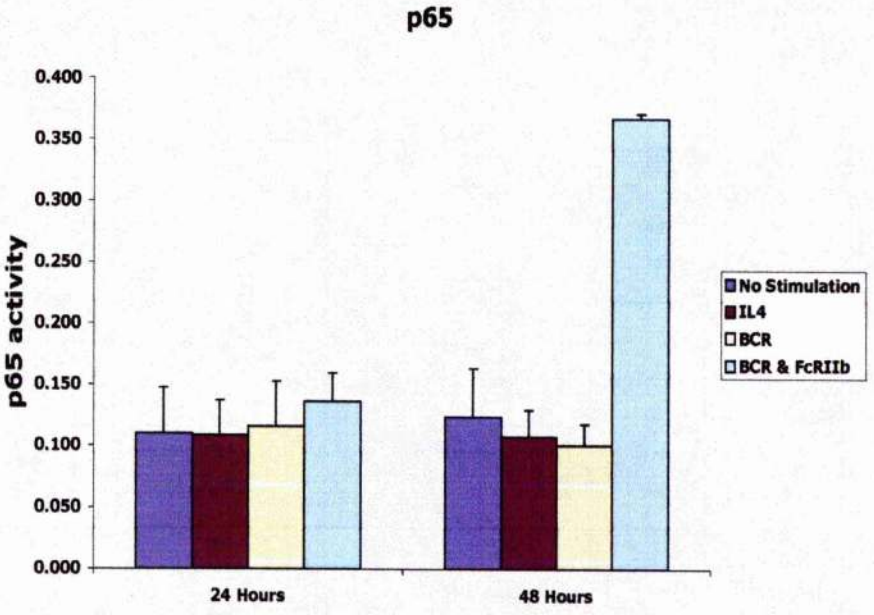
p65
p65 activity
0.400
0.350
0.300
0.250
0.200
0.150
0.100
0.050
0.000
24 Hours
48 Hours
No Stimulation
IL4
BCR
BCR & FcRIIb

Figure 4.27: Current working model for the signals involved in FcγRIIb-mediated growth arrest

BCR mediated proliferation is under the control of both the MAP kinase and PI-3 kinase pathways. Coligation of FcγRIIb induces the activation of the PI-3 kinase antagonist PTEN. FcγRIIb also recruits SHIP which can inhibit both the PI-3 kinase and ERKMAPK pathways. The expression of Pac1 is also induced which acts to switch off the ongoing ERK signalling. Recruitment of these 3 signalling molecules by FcγRIIb results in the abrogation of both PI-3 kinase and ERKMAPK signalling and prevents and proliferation.

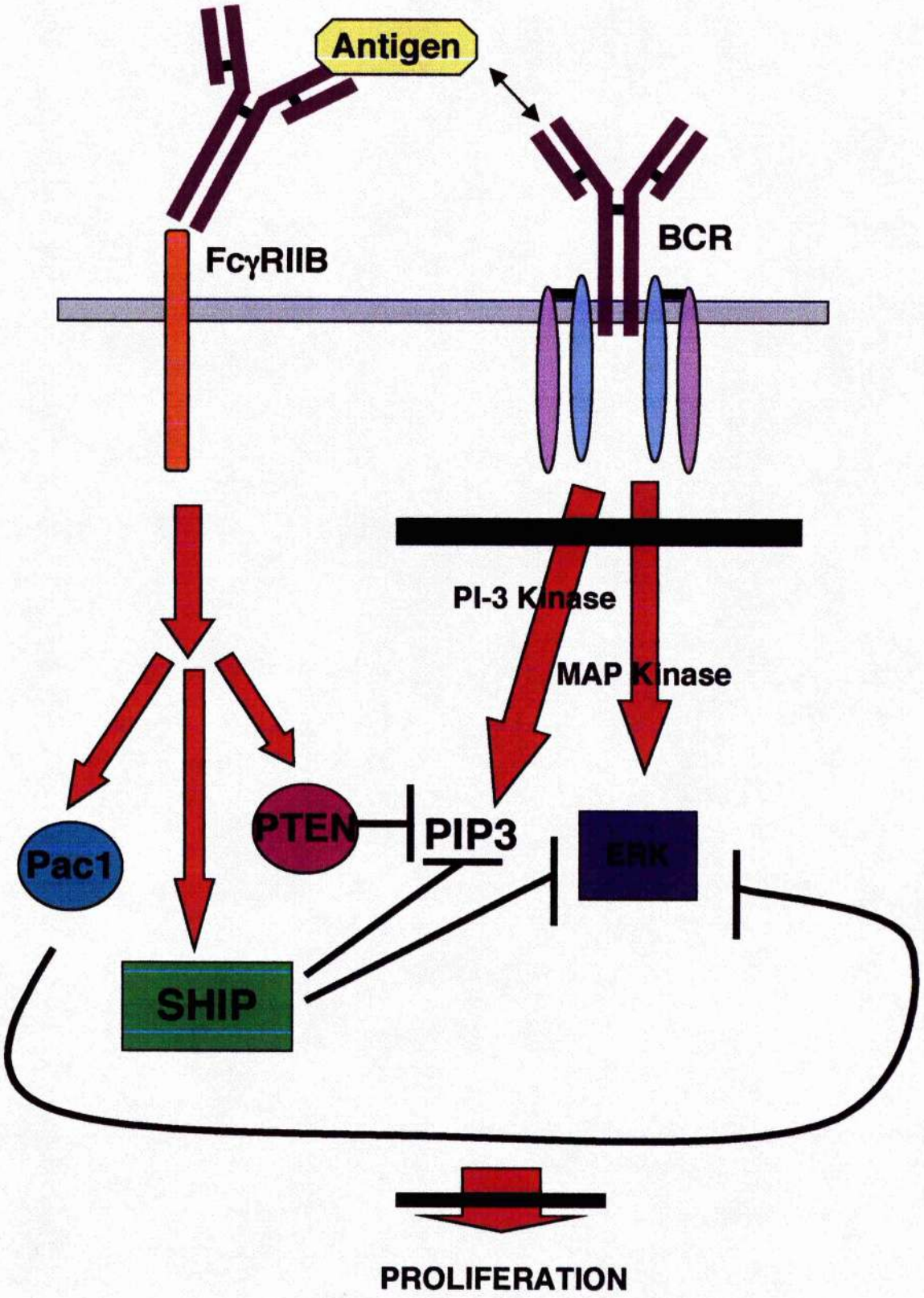
Antigen
FcγRIIB
BCR
PI-3 Kinase
MAP Kinase
Pac1
PTEN
PIP3
ERK
SHIP
PROLIFERATION

Figure 4.28: Current working model for FcγRIIb-mediated apoptosis

We have demonstrated that the dissipation of MMP and hence the breakdown of mitochondrial membrane integrity is essential for FcγRIIb mediated apoptosis. As was discussed in figure 4.28, FcγRIIb acts to inhibit PI-3 kinase and AKT signalling presumably resulting in the sequestration of $BclX_L$ by Bad. This prevents $BclX_L$ homo-dimers from protecting the mitochondrial membrane integrity and hence allows for the opening of the permeability transition pore. Furthermore, caspase 8 is involved in this form of apoptosis. Caspase 8 acts upstream of the loss of mitochondrial membrane integrity and is proximal to the activation of cathepsin B and calpains. We have also demonstrated that the pro-apoptotic Bcl-2 family member Bid is upregulated however we have not provided clear evidence that it is in the active, truncated form. Therefore we cannot comment on the interaction between caspase 8 and Bid. The transcription factor p53 is also activated by FcγRIIb coligation. This molecule is known to act as a pro-apoptotic Bcl-2 family member or may mediate its effects via upregulation of Bax/Bak expression. The loss of mitochondrial membrane integrity is signalled by cytochrome c release, loss of MMP and commitment of the cell to apoptosis.

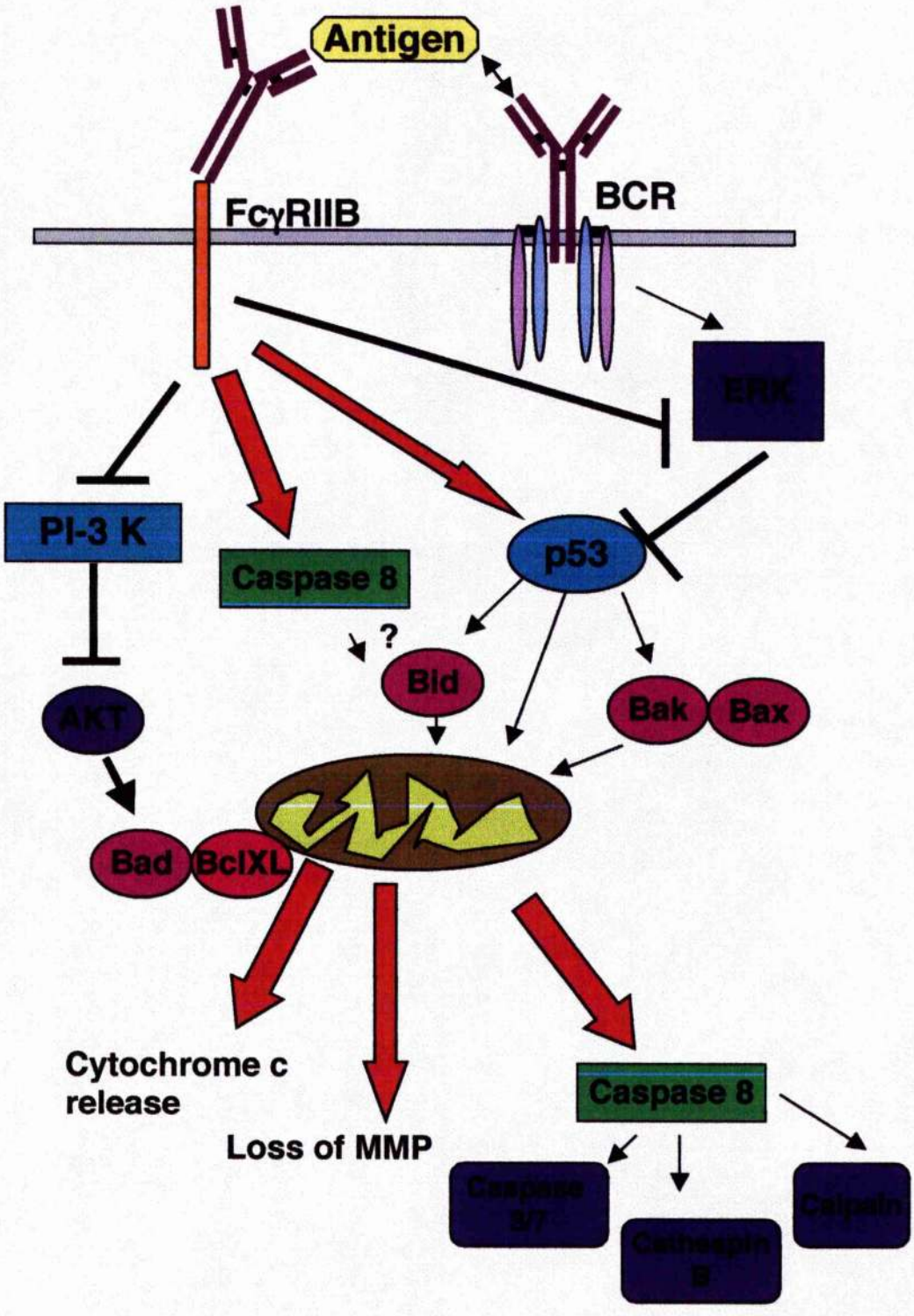
Antigen
FcγRIIB
BCR
ERK
PI-3 K
Caspase 8
p53
?
Bid
AKT
Bak
Bax
Bad
BclXL
Cytochrome c
release
Loss of MMP
Caspase 8
Caspase
3/7
Cathepsin
B
Calpain

Chapter 5: General Discussion

During B cell development there is a dichotomy in BCR signalling. As has been described in chapter 3, ligation of the BCR on immature B cells results in cell cycle arrest and apoptosis whereas BCR ligation in mature B cells, as described in chapter 4, results in growth and proliferation. Furthermore, coligation of the BCR and FcγRIIb in mature B cells mediates negative feedback inhibition, which can induce cell cycle arrest and apoptosis. This dichotomy of BCR signalling is a central question that must be resolved in order to properly understand mammalian B cell development. A full understanding of this process will lead to better vaccine development and an appreciation of how defects in these processes can contribute to diseases, such as leukaemia, and autoimmune syndromes, such as SLE. Moreover, information on apoptotic and proliferative signalling in a central tenet for many areas of biomedical science and is of general scientific interest. Therefore this study aimed to ascertain the main proliferative and apoptotic signalling cascades utilised by BCR signalling during B cell maturation.

5.1 Immature B cell signalling

Firstly, the signalling systems employed by the BCR in the murine lymphoma cell line WEHI 231 were addressed as this cell line provides a model for negative selection of immature B lymphocyte in the bone marrow (20, 406). Previous work in this laboratory, and others, has demonstrated that such BCR ligation results in cell cycle arrest and apoptosis, and that this is used physiologically to prevent the generation of self-reactive B cells (300, 503). The mechanism underlying this form of apoptosis involves loss of mitochondrial membrane integrity and the activation of PLA_2 and translocation of PLA_2 to both mitochondria and the nucleus (156). This study has extended these findings by identifying that the active metabolite during BCR-mediated apoptosis is actually arachidonic acid, generated by PLA_2 action rather than an eicosanoid metabolite (425). Indeed, it has been demonstrated that further metabolism of arachidonic acid to the ecosinoid prostaglandin E_2 (PGE_2) by COX2/ LOX results in anti-apoptotic signalling (425). Therefore arachidonic acid provides an

essential dynamic molecular switch from apoptotic signalling initiated by the BCR (arachidonic acid) to anti-apoptotic signalling mediated by CD40 engagement (conversion of arachidonic acid to PGE_2).

Previous work in this laboratory had also highlighted the importance of dynamic ERK signalling in both proliferation and apoptosis in immature B cells (275). Thus, during BCR-mediated signalling the sustained ERK signalling, found in proliferating WEHI 231 cells, is abrogated (275). A causal role for such ERK signalling in proliferating WEHI 231 cells was therefore investigated in this thesis by manipulating activation of the ERK pathway by expressing Ras mutant constructs in WEHI 231 cells. Interestingly, following expression of constitutively active Ras constructs, although the ERK signal was maintained it continued to be cyclical indicating that the negative regulatory elements that interact with this pathway remained active. The expression of RasV12 did provide rescue from both BCR-mediated growth arrest and apoptosis of WEHI 231 cells for 24 h highlighting the importance of such ERK signalling. However, this capacity was not maintained beyond 24 h, suggesting that there is a complex interplay of many cascades that must be simultaneously activated or inactivated to regulate BCR-stimulated apoptosis. In an attempt to identify these regulatory elements we investigated the BCR response in WEHI 231 cells expressing dominant negative constructs of both SHIP and Dok which have been reported to negativelt regulate Ras/ERK signalling, however these constructs did not provide release from BCR-mediated apoptosis.

Rescue of immature B cells from BCR-mediated growth arrest and apoptosis using anti-CD40 also provides a model for T cell help and such rescue has been associated with both upregulation of the anti-apoptotic Bcl-2 family members $BclX_L$ and A1 as well as a maintenance of the sustained, cycling ERK activation (275, 277, 416, 425). This study demonstrated that upregulation of $BclX_L$ is sufficient to protect from arachidonic acid-mediated loss of mitochondrial membrane integrity and apoptosis. Furthermore, we identified that co-engagement of CD40 increases the association of Bak with $BclX_L$ indicating that $BclX_L$ may act to sequester the pro-apoptotic Bak to inhibit the opening of the mitochondrial permeability pore. In addition, we have identified that upregulation of $BclX_L$ can downmodulate calcium signals providing an additional

mechanism for the downregulation of BCR-coupled $mPLA_2$ activation and hence a reduction in apoptotic signalling.

Another major area of investigation of in this thesis was the investigation of the role of PKC isoforms in immature B cell apoptosis, survival and proliferation. PKC α, β, δ, ε, ζ, η and θ isoforms are all expressed in B lymphocytes (348, 349). However immature B cells have diminished PKC signalling compared to mature B lymphocytes suggesting PKC may contribute to the differential response of distinct developmental stages of B cells to ligation of the BCR. For example, ligation of the BCR on mature B cells leads to PI-(3,4)-P_2 hydrolysis, Ca^{2+} mobilisation and stimulation of PKC. In contrast, ligation of the BCR on immature B cells can mobilise calcium but PI-(3,4)-P_2 hydrolysis and subsequent PKC activation are significantly reduced. Previous work in this laboratory had demonstrated that PKCs α, δ, ε and ζ are all expressed in the immature B cell line WEHI 231. Considering that previous studies have suggested a non-redundant role for PKC isoforms in B lymphocytes it was therefore decided to investigate the role of PKCs α, δ, ε and ζ in proliferation, growth arrest and apoptosis in WEHI 231 cells. However, these results were disappointing as expression of both constitutively active and kinase dead forms of the PKC isoforms in WEHI 231 B cells induced essentially identical functional responses, suggesting that there may be problems in functionality and localization of the PKC constructs in these WEHI 231 cells . However, the PKC family will still provide an interesting area of study as the PKC mutants generated did provide at least partial rescue from BCR-mediated apoptosis and loss of MMP indicating that PKC signalling may be important in these processes.

There are still many interesting potential areas of follow up study within BCR-mediated signalling of immature cells. For example, it would be very interesting to further investigate which Bcl-2 family members are present, how they are activated and their potential binding partners. Furthermore, it would be extremely interesting to relate the calcium signals generated by ligation of the BCR to the localisation and activation of such Bcl-2 family members. Indeed, there have been reports that Bcl-2 family members can themselves acts as calcium channels and that they regulate the relative E.R, mitochondrial and

cytosolic calcium levels (106, 191, 426, 437-441). It would therefore be interesting to investigate the relative calcium levels in these subcellular organelles by utilising differential dye loading and tagging of GFP-FRET pairs to localise them to specific organelles. Pairing this with a study to identify which organelles are the sites for clustering of Bcl-2 family members would be very informative regarding the key mechanism underlying calcium signalling and mitochondrial homeostasis in immature B cell survival and clonal deletion.

5.2 Mature B cell signalling

In contrast to the situation with immature B cells, ligation of the BCR in mature B cells results in growth and proliferation. Previous studies had concentrated on the early signals (within 30 min) associated with BCR signalling focussing on the ERK and PI-3 kinase cascades which are established to be associated with early BCR-mediated proliferative signals (278, 458). This study has extended such findings by indicating mitogenic BCR-mediated ERK and PI-3 kinase signalling are maintained for up to 48 h post BCR-ligation. Moreover, these data suggest that PI-3 kinase maintains a pro-survival signal by activation of AKT and hence maintenance of phospho-Bad signals. Coligation of FcγRIIb results in the inhibition both ERK and PI-3 kinase cascades and induces cell cycle arrest. Parallel studies in this laboratory have indicated that the abrogation of the ERK signal reflects induction of the ERKMAPKinase phosphatase Pac1 (124). Similarly, PI-3 kinase responses are abrogated by both the recruitment of SHIP and the induction of PTEN both of which can antagonize the production of PI-(3,4,5)-P_3 (124, 346, 464, 466).

This present study has also demonstrated that negative feedback inhibition, by coligation of the BCR and FcγRIIb, not only induces cell cycle arrest but also induces an apoptotic phenotype. This is the only study to date that has attempted to characterise this form of apoptosis. It has demonstrated that the dissipation of MMP, and hence the breakdown of mitochondrial membrane integrity, is essential for FcγRIIb-mediated apoptosis. To do this FcγRIIb acts to inhibit PI-3 kinase signalling presumably resulting in the sequestration of $BclX_L$/Bcl-2 by Bad. This would prevent $BclX_L$/Bcl-2 dimers from protecting the mitochondrial membrane integrity and hence allow for the opening of the

permeability transition pore. Furthermore, caspase 8 has been shown to be involved in this form of apoptosis. Caspase 8 acts upstream of the loss of mitochondrial membrane integrity and is proximal to the activation of executioner proteases such as caspase 3, cathepsin B and calpains. In addition, the pro-apoptotic Bcl-2 family member Bid is likely to be upregulated, however there is no clear evidence that the active, truncated form is induced. Therefore it is not yet possible to comment on the potential interaction between caspase 8 and Bid. Finally, the transcription factor p53 is also activated by FcγRIIb coligation and consistent with this, p53 is known to act like a pro-apoptotic Bcl-2 family member or alternatively may mediate its effects via upregulation of Bid, Bax or Bak expression. Collectively these signals result in the loss of mitochondrial membrane integrity which is signalled by cytochrome c release and commitment of the cell to apoptosis via the induction of executioner proteases.

There is obviously much more work to be done to elucidate the exact mechanism and complex interplay of the above components during FcγRIIb mediated-apoptosis. For example, it would be interesting to further investigate the activation status and binding partners of the Bcl-2 family members involved as the activation of p53 implies that the pro-apoptotic Bcl-2 family members may be particularly important. Thus, it would be interesting to investigate which p53 controlled genes are actively transcribed and furthermore assessment of the localization of p53 would identify whether p53 had transcription-independent functions in this form of apoptosis. Moreover, it would be interesting to identify the intermediate targets of caspase 8 and to ascertain whether other non-redundant executioner proteases are involved.

5.3 Concluding Remarks

The finding that two novel mechanisms of apoptosis have been identified at distinct stages of B lymphocyte maturation is not surprising as these cells regularly utilise apoptosis to ensure not only that non-autoreactive and functional BCR are formed but also as part of homeostatic regulation of the immune system. B cells may therefore have evolved different apoptotic mechanisms for use at different differentiation states, as the correct regulation

of B cell function is essential to prevent disease. The BCR-mediated PLA_2-dependent apoptosis utilised in negative selection of immature B cells and FcγRIIb-mediated caspase 8-dependent mechanism observed during negative feedback inhibition of mature B cells both provide interesting areas for further research as dissection of the key regulatory events may provide useful therapeutic targets in health (vaccines) and disease (autoimmunity/cancer).

Bibliography

1. Cory S. Immunology. Wavering on commitment. Nature 1999;401(6753):538-9.
2. Rolink A, Melchers F. Molecular and cellular origins of B lymphocyte diversity. Cell 1991;66(6):1081-94.
3. Tarlinton D. B-cell differentiation in the bone marrow and the periphery. Immunol Rev 1994;137:203-29.
4. Coleclough C, Perry RP, Karjalainen K, Weigert M. Aberrant rearrangements contribute significantly to the allelic exclusion of immunoglobulin gene expression. Nature 1981;290(5805):372-8.
5. Spanopoulou E, Roman CA, Corcoran LM, Schlissel MS, Silver DP, Nemazee D, et al. Functional immunoglobulin transgenes guide ordered B-cell differentiation in Rag-1-deficient mice. Genes Dev 1994;8(9):1030-42.
6. Nagata K, Nakamura T, Kitamura F, Kuramochi S, Taki S, Campbell KS, et al. The Ig alpha/Igbeta heterodimer on mu-negative proB cells is competent for transducing signals to induce early B cell differentiation. Immunity 1997;7(4):559-70.
7. Gong S, Nussenzweig MC. Regulation of an early developmental checkpoint in the B cell pathway by Ig beta. Science 1996;272(5260):411-4.
8. Minegishi Y, Coustan-Smith E, Rapalus L, Ersoy F, Campana D, Conley ME. Mutations in Igalpha (CD79a) result in a complete block in B-cell development. J Clin Invest 1999;104(8):1115-21.
9. Pelanda R, Braun U, Hobeika E, Nussenzweig MC, Reth M. B cell progenitors are arrested in maturation but have intact VDJ recombination in the absence of Ig-alpha and Ig-beta. J Immunol 2002;169(2):865-72.
10. Karasuyama H, Rolink A, Shinkai Y, Young F, Alt FW, Melchers F. The expression of Vpre-B/lambda 5 surrogate light chain in early bone marrow precursor B cells of normal and B cell-deficient mutant mice. Cell 1994;77(1):133-43.
11. Neuberger MS. Antigen receptor signaling gives lymphocytes a long life. Cell 1997;90(6):971-3.
12. Benschop RJ, Cambier JC. B cell development: signal transduction by antigen receptors and their surrogates. Curr Opin Immunol 1999;11(2):143-51.

13. Reth M. Antigen receptors on B lymphocytes. Annu Rev Immunol 1992;10:97-121.
14. Osmond DG. Population dynamics of bone marrow B lymphocytes. Immunol Rev 1986;93:103-24.
15. Goodnow CC, Crosbie J, Adelstein S, Lavoie TB, Smith-Gill SJ, Brink RA, et al. Altered immunoglobulin expression and functional silencing of self-reactive B lymphocytes in transgenic mice. Nature 1988;334(6184):676-82.
16. Hartley SB, Crosbie J, Brink R, Kantor AB, Basten A, Goodnow CC. Elimination from peripheral lymphoid tissues of self-reactive B lymphocytes recognizing membrane-bound antigens. Nature 1991;353(6346):765-9.
17. Hasbold J, Klaus GG. Anti-immunoglobulin antibodies induce apoptosis in immature B cell lymphomas. Eur J Immunol 1990;20(8):1685-90.
18. Nemazee D, Buerki K. Clonal deletion of autoreactive B lymphocytes in bone marrow chimeras. Proc Natl Acad Sci U S A 1989;86(20):8039-43.
19. Radic MZ, Erikson J, Litwin S, Weigert M. B lymphocytes may escape tolerance by revising their antigen receptors. J Exp Med 1993;177(4):1165-73.
20. Norvell A, Mandik L, Monroe JG. Engagement of the antigen-receptor on immature murine B lymphocytes results in death by apoptosis. J Immunol 1995;154(9):4404-13.
21. Sandel PC, Monroe JG. Negative selection of immature B cells by receptor editing or deletion is determined by site of antigen encounter. Immunity 1999;10(3):289-99.
22. Allman DM, Ferguson SE, Lentz VM, Cancro MP. Peripheral B cell maturation. II. Heat-stable antigen(hi) splenic B cells are an immature developmental intermediate in the production of long-lived marrow-derived B cells. J Immunol 1993;151(9):4431-44.
23. Monroe JG. Balancing signals for negative selection and activation of developing B lymphocytes. Clin Immunol 2000;95(1 Pt 2):S8-13.
24. Carsetti R, Kohler G, Lamers MC. Transitional B cells are the target of negative selection in the B cell compartment. J Exp Med 1995;181(6):2129-40.
25. Craxton A, Otipoby KL, Jiang A, Clark EA. Signal transduction pathways that regulate the fate of B lymphocytes. Adv Immunol 1999;73:79-152.
26. Cushley W, Harnett MM. Cellular signalling mechanisms in B lymphocytes. Biochem J 1993;292 (Pt 2):313-32.

27. Campbell KS. Signal transduction from the B cell antigen-receptor. Curr Opin Immunol 1999;11(3):256-64.
28. Kurosaki T. Genetic analysis of B cell antigen receptor signaling. Annu Rev Immunol 1999;17:555-92.
29. Justement LB. The role of the protein tyrosine phosphatase CD45 in regulation of B lymphocyte activation. Int Rev Immunol 2001;20(6):713-38.
30. DeFranco AL, Richards JD, Blum JH, Stevens TL, Law DA, Chan VW, et al. Signal transduction by the B-cell antigen receptor. Ann N Y Acad Sci 1995;766:195-201.
31. Gauld SB, Cambier JC. Src-family kinases in B-cell development and signaling. Oncogene 2004;23(48):8001-6.
32. Tamir I, Cambier JC. Antigen receptor signaling: integration of protein tyrosine kinase functions. Oncogene 1998;17(11 Reviews):1353-64.
33. Gauld SB, Dal Porto JM, Cambier JC. B cell antigen receptor signaling: roles in cell development and disease. Science 2002;296(5573):1641-2.
34. Ishiai M, Sugawara H, Kurosaki M, Kurosaki T. Cutting edge: association of phospholipase C-gamma 2 Src homology 2 domains with BLNK is critical for B cell antigen receptor signaling. J Immunol 1999;163(4):1746-9.
35. Johmura S, Oh-hora M, Inabe K, Nishikawa Y, Hayashi K, Vigorito E, et al. Regulation of Vav localization in membrane rafts by adaptor molecules Grb2 and BLNK. Immunity 2003;18(6):777-87.
36. Baba Y, Hashimoto S, Matsushita M, Watanabe D, Kishimoto T, Kurosaki T, et al. BLNK mediates Syk-dependent Btk activation. Proc Natl Acad Sci U S A 2001;98(5):2582-6.
37. Harnett MM, Katz E, Ford CA. Differential signalling during B-cell maturation. Immunol Lett 2005;98(1):33-44.
38. Fruman DA, Meyers RE, Cantley LC. Phosphoinositide kinases. Annu Rev Biochem 1998;67:481-507.
39. Vanhaesebroeck B, Leevers SJ, Ahmadi K, Timms J, Katso R, Driscoll PC, et al. Synthesis and function of 3-phosphorylated inositol lipids. Annu Rev Biochem 2001;70:535-602.
40. Wymann MP, Pirola L. Structure and function of phosphoinositide 3-kinases. Biochim Biophys Acta 1998;1436(1-2):127-50.

41. Kurosaki T, Maeda A, Ishiai M, Hashimoto A, Inabe K, Takata M. Regulation of the phospholipase C-gamma2 pathway in B cells. Immunol Rev 2000;176:19-29.

42. Katso R, Okkenhaug K, Ahmadi K, White S, Timms J, Waterfield MD. Cellular function of phosphoinositide 3-kinases: implications for development, homeostasis, and cancer. Annu Rev Cell Dev Biol 2001;17:615-75.

43. Koyasu S. The role of PI3K in immune cells. Nat Immunol 2003;4(4):313-9.

44. Okkenhaug K, Vanhaesebroeck B. PI3K in lymphocyte development, differentiation and activation. Nat Rev Immunol 2003;3(4):317-30.

45. Gold MR, Aebersold R. Both phosphatidylinositol 3-kinase and phosphatidylinositol 4-kinase products are increased by antigen receptor signaling in B cells. J Immunol 1994;152(1):42-50.

46. Gold MR, Chan VW, Turck CW, DeFranco AL. Membrane Ig cross-linking regulates phosphatidylinositol 3-kinase in B lymphocytes. J Immunol 1992;148(7):2012-22.

47. Toker A, Cantley LC. Signalling through the lipid products of phosphoinositide-3-OH kinase. Nature 1997;387(6634):673-6.

48. Lemmon MA, Ferguson KM. Pleckstrin homology domains. Curr Top Microbiol Immunol 1998;228:39-74.

49. Isakoff SJ, Cardozo T, Andreev J, Li Z, Ferguson KM, Abagyan R, et al. Identification and analysis of PH domain-containing targets of phosphatidylinositol 3-kinase using a novel in vivo assay in yeast. Embo J 1998;17(18):5374-87.

50. Rawlings DJ. Bruton's tyrosine kinase controls a sustained calcium signal essential for B lineage development and function. Clin Immunol 1999;91(3):243-53.

51. Craxton A, Jiang A, Kurosaki T, Clark EA. Syk and Bruton's tyrosine kinase are required for B cell antigen receptor-mediated activation of the kinase Akt. J Biol Chem 1999;274(43):30644-50.

52. Li HL, Davis WW, Whiteman EL, Birnbaum MJ, Pure E. The tyrosine kinases Syk and Lyn exert opposing effects on the activation of protein kinase Akt/PKB in B lymphocytes. Proc Natl Acad Sci U S A 1999;96(12):6890-5.

53. Hashimoto S, Iwamatsu A, Ishiai M, Okawa K, Yamadori T, Matsushita M, et al. Identification of the SH2 domain binding protein of Bruton's tyrosine

kinase as BLNK--functional significance of Btk-SH2 domain in B-cell antigen receptor-coupled calcium signaling. Blood 1999;94(7):2357-64.

54. Moscat J, Diaz-Meco MT, Rennert P. NF-kappaB activation by protein kinase C isoforms and B-cell function. EMBO Rep 2003;4(1):31-6.

55. Gold MR, Ingham RJ, McLeod SJ, Christian SL, Scheid MP, Duronio V, et al. Targets of B-cell antigen receptor signaling: the phosphatidylinositol 3-kinase/Akt/glycogen synthase kinase-3 signaling pathway and the Rap1 GTPase. Immunol Rev 2000;176:47-68.

56. Astoul E, Watton S, Cantrell D. The dynamics of protein kinase B regulation during B cell antigen receptor engagement. J Cell Biol 1999;145(7):1511-20.

57. Yaffe MB, Rittinger K, Volinia S, Caron PR, Aitken A, Leffers H, et al. The structural basis for 14-3-3:phosphopeptide binding specificity. Cell 1997;91(7):961-71.

58. Brunet A, Bonni A, Zigmond MJ, Lin MZ, Juo P, Hu LS, et al. Akt promotes cell survival by phosphorylating and inhibiting a Forkhead transcription factor. Cell 1999;96(6):857-68.

59. Andjelkovic M, Alessi DR, Meier R, Fernandez A, Lamb NJ, Frech M, et al. Role of translocation in the activation and function of protein kinase B. J Biol Chem 1997;272(50):31515-24.

60. Brennan P, Babbage JW, Burgering BM, Groner B, Reif K, Cantrell DA. Phosphatidylinositol 3-kinase couples the interleukin-2 receptor to the cell cycle regulator E2F. Immunity 1997;7(5):679-89.

61. Ozes ON, Mayo LD, Gustin JA, Pfeffer SR, Pfeffer LM, Donner DB. NF-kappaB activation by tumour necrosis factor requires the Akt serine-threonine kinase. Nature 1999;401(6748):82-5.

62. Arcaro A, Wymann MP. Wortmannin is a potent phosphatidylinositol 3-kinase inhibitor: the role of phosphatidylinositol 3,4,5-trisphosphate in neutrophil responses. Biochem J 1993;296 (Pt 2):297-301.

63. Vlahos CJ, Matter WF, Hui KY, Brown RF. A specific inhibitor of phosphatidylinositol 3-kinase, 2-(4-morpholinyl)-8-phenyl-4H-1-benzopyran-4-one (LY294002). J Biol Chem 1994;269(7):5241-8.

64. Gunther R, Kishore PN, Abbas HK, Mirocha CJ. Immunosuppressive effects of dietary wortmannin on rats and mice. Immunopharmacol Immunotoxicol 1989;11(4):559-70.

65. Bi L, Okabe I, Bernard DJ, Nussbaum RL. Early embryonic lethality in mice deficient in the p110beta catalytic subunit of PI 3-kinase. Mamm Genome 2002;13(3):169-72.
66. Bi L, Okabe I, Bernard DJ, Wynshaw-Boris A, Nussbaum RL. Proliferative defect and embryonic lethality in mice homozygous for a deletion in the p110alpha subunit of phosphoinositide 3-kinase. J Biol Chem 1999;274(16):10963-8.
67. Okkenhaug K, Bilancio A, Farjot G, Priddle H, Sancho S, Peskett E, et al. Impaired B and T cell antigen receptor signaling in p110delta PI 3-kinase mutant mice. Science 2002;297(5583):1031-4.
68. Suzuki H, Terauchi Y, Fujiwara M, Aizawa S, Yazaki Y, Kadowaki T, et al. Xid-like immunodeficiency in mice with disruption of the p85alpha subunit of phosphoinositide 3-kinase. Science 1999;283(5400):390-2.
69. Clayton E, Bardi G, Bell SE, Chantry D, Downes CP, Gray A, et al. A crucial role for the p110delta subunit of phosphatidylinositol 3-kinase in B cell development and activation. J Exp Med 2002;196(6):753-63.
70. Roux PP, Blenis J. ERK and p38 MAPK-activated protein kinases: a family of protein kinases with diverse biological functions. Microbiol Mol Biol Rev 2004;68(2):320-44.
71. Geyer M, Wittinghofer A. GEFs, GAPs, GDIs and effectors: taking a closer (3D) look at the regulation of Ras-related GTP-binding proteins. Curr Opin Struct Biol 1997;7(6):786-92.
72. Chong H, Vikis HG, Guan KL. Mechanisms of regulating the Raf kinase family. Cell Signal 2003;15(5):463-9.
73. Hallberg B, Rayter SI, Downward J. Interaction of Ras and Raf in intact mammalian cells upon extracellular stimulation. J Biol Chem 1994;269(6):3913-6.
74. Chen Z, Gibson TB, Robinson F, Silvestro L, Pearson G, Xu B, et al. MAP kinases. Chem Rev 2001;101(8):2449-76.
75. Gavin AC, Nebreda AR. A MAP kinase docking site is required for phosphorylation and activation of p90(rsk)/MAPKAP kinase-1. Curr Biol 1999;9(5):281-4.
76. Sturgill TW, Ray LB, Erikson E, Maller JL. Insulin-stimulated MAP-2 kinase phosphorylates and activates ribosomal protein S6 kinase II. Nature 1988;334(6184):715-8.

77. Stokoe D, Engel K, Campbell DG, Cohen P, Gaestel M. Identification of MAPKAP kinase 2 as a major enzyme responsible for the phosphorylation of the small mammalian heat shock proteins. FEBS Lett 1992;313(3):307-13.
78. Stokoe D, Campbell DG, Nakielny S, Hidaka H, Leevers SJ, Marshall C, et al. MAPKAP kinase-2; a novel protein kinase activated by mitogen-activated protein kinase. Embo J 1992;11(11):3985-94.
79. Chen RH, Juo PC, Curran T, Blenis J. Phosphorylation of c-Fos at the C-terminus enhances its transforming activity. Oncogene 1996;12(7):1493-502.
80. Chen RH, Abate C, Blenis J. Phosphorylation of the c-Fos transrepression domain by mitogen-activated protein kinase and 90-kDa ribosomal S6 kinase. Proc Natl Acad Sci U S A 1993;90(23):10952-6.
81. Chen RH, Tung R, Abate C, Blenis J. Cytoplasmic to nuclear signal transduction by mitogen-activated protein kinase and 90 kDa ribosomal S6 kinase. Biochem Soc Trans 1993;21(4):895-900.
82. Alvarez E, Northwood IC, Gonzalez FA, Latour DA, Seth A, Abate C, et al. Pro-Leu-Ser/Thr-Pro is a consensus primary sequence for substrate protein phosphorylation. Characterization of the phosphorylation of c-myc and c-jun proteins by an epidermal growth factor receptor threonine 669 protein kinase. J Biol Chem 1991;266(23):15277-85.
83. Lin LL, Wartmann M, Lin AY, Knopf JL, Seth A, Davis RJ. cPLA2 is phosphorylated and activated by MAP kinase. Cell 1993;72(2):269-78.
84. Kyriakis JM, Avruch J. Mammalian mitogen-activated protein kinase signal transduction pathways activated by stress and inflammation. Physiol Rev 2001;81(2):807-69.
85. Reynolds CH, Nebreda AR, Gibb GM, Utton MA, Anderton BH. Reactivating kinase/p38 phosphorylates tau protein in vitro. J Neurochem 1997;69(1):191-8.
86. Kramer RM, Roberts EF, Um SL, Borsch-Haubold AG, Watson SP, Fisher MJ, et al. p38 mitogen-activated protein kinase phosphorylates cytosolic phospholipase A2 (cPLA2) in thrombin-stimulated platelets. Evidence that proline-directed phosphorylation is not required for mobilization of arachidonic acid by cPLA2. J Biol Chem 1996;271(44):27723-9.
87. Choi WS, Eom DS, Han BS, Kim WK, Han BH, Choi EJ, et al. Phosphorylation of p38 MAPK induced by oxidative stress is linked to activation

of both caspase-8- and -9-mediated apoptotic pathways in dopaminergic neurons. J Biol Chem 2004;279(19):20451-60.

88. Bulavin DV, Saito S, Hollander MC, Sakaguchi K, Anderson CW, Appella E, et al. Phosphorylation of human p53 by p38 kinase coordinates N-terminal phosphorylation and apoptosis in response to UV radiation. Embo J 1999;18(23):6845-54.

89. Yee AS, Paulson EK, McDevitt MA, Rieger-Christ K, Summerhayes I, Berasi SP, et al. The HBP1 transcriptional repressor and the p38 MAP kinase: unlikely partners in G1 regulation and tumor suppression. Gene 2004;336(1):1-13.

90. Molnar A, Theodoras AM, Zon LI, Kyriakis JM. Cdc42Hs, but not Rac1, inhibits serum-stimulated cell cycle progression at G1/S through a mechanism requiring p38/RK. J Biol Chem 1997;272(20):13229-35.

91. Zarubin T, Han J. Activation and signaling of the p38 MAP kinase pathway. Cell Res 2005;15(1):11-8.

92. Mizukami Y, Yoshioka K, Morimoto S, Yoshida K. A novel mechanism of JNK1 activation. Nuclear translocation and activation of JNK1 during ischemia and reperfusion. J Biol Chem 1997;272(26):16657-62.

93. Weston CR, Davis RJ. The JNK signal transduction pathway. Curr Opin Genet Dev 2002;12(1):14-21.

94. Tournier C, Hess P, Yang DD, Xu J, Turner TK, Nimnual A, et al. Requirement of JNK for stress-induced activation of the cytochrome c-mediated death pathway. Science 2000;288(5467):870-4.

95. Carpenter G, Ji Q. Phospholipase C-gamma as a signal-transducing element. Exp Cell Res 1999;253(1):15-24.

96. Ji QS, Winnier GE, Niswender KD, Horstman D, Wisdom R, Magnuson MA, et al. Essential role of the tyrosine kinase substrate phospholipase C-gamma1 in mammalian growth and development. Proc Natl Acad Sci U S A 1997;94(7):2999-3003.

97. Wang D, Feng J, Wen R, Marine JC, Sangster MY, Parganas E, et al. Phospholipase Cgamma2 is essential in the functions of B cell and several Fc receptors. Immunity 2000;13(1):25-35.

98. Watanabe D, Hashimoto S, Ishiai M, Matsushita M, Baba Y, Kishimoto T, et al. Four tyrosine residues in phospholipase C-gamma 2, identified as Btk-

dependent phosphorylation sites, are required for B cell antigen receptor-coupled calcium signaling. J Biol Chem 2001;276(42):38595-601.
99. Inoue M, Kishimoto A, Takai Y, Nishizuka Y. Studies on a cyclic nucleotide-independent protein kinase and its proenzyme in mammalian tissues. II. Proenzyme and its activation by calcium-dependent protease from rat brain. J Biol Chem 1977;252(21):7610-6.
100. Takai Y, Kishimoto A, Inoue M, Nishizuka Y. Studies on a cyclic nucleotide-independent protein kinase and its proenzyme in mammalian tissues. I. Purification and characterization of an active enzyme from bovine cerebellum. J Biol Chem 1977;252(21):7603-9.
101. Saito N, Kikkawa U, Nishizuka Y. The family of protein kinase C and membrane lipid mediators. J Diabetes Complications 2002;16(1):4-8.
102. Parekh DB, Ziegler W, Parker PJ. Multiple pathways control protein kinase C phosphorylation. Embo J 2000;19(4):496-503.
103. Miyazaki S. Inositol trisphosphate receptor mediated spatiotemporal calcium signalling. Curr Opin Cell Biol 1995;7(2):190-6.
104. Boittin FX, Macrez N, Halet G, Mironneau J. Norepinephrine-induced Ca(2+) waves depend on InsP(3) and ryanodine receptor activation in vascular myocytes. Am J Physiol 1999;277(1 Pt 1):C139-51.
105. Grafton G, Stokes L, Toellner KM, Gordon J. A non-voltage-gated calcium channel with L-type characteristics activated by B cell receptor ligation. Biochem Pharmacol 2003;66(10):2001-9.
106. Jacobson MD. Apoptosis: Bcl-2-related proteins get connected. Curr Biol 1997;7(5):R277-81.
107. Schievella AR, Regier MK, Smith WL, Lin LL. Calcium-mediated translocation of cytosolic phospholipase A2 to the nuclear envelope and endoplasmic reticulum. J Biol Chem 1995;270(51):30749-54.
108. Squier MK, Miller AC, Malkinson AM, Cohen JJ. Calpain activation in apoptosis. J Cell Physiol 1994;159(2):229-37.
109. Mathiasen IS, Sergeev IN, Bastholm L, Elling F, Norman AW, Jaattela M. Calcium and calpain as key mediators of apoptosis-like death induced by vitamin D compounds in breast cancer cells. J Biol Chem 2002;277(34):30738-45.

110. Tomida T, Hirose K, Takizawa A, Shibasaki F, Iino M. NFAT functions as a working memory of Ca2+ signals in decoding Ca2+ oscillation. Embo J 2003;22(15):3825-32.
111. Chakraborti T, Das S, Mondal M, Roychoudhury S, Chakraborti S. Oxidant, mitochondria and calcium: an overview. Cell Signal 1999;11(2):77-85.
112. Sugawara H, Kurosaki M, Takata M, Kurosaki T. Genetic evidence for involvement of type 1, type 2 and type 3 inositol 1,4,5-trisphosphate receptors in signal transduction through the B-cell antigen receptor. Embo J 1997;16(11):3078-88.
113. Miyakawa T, Maeda A, Yamazawa T, Hirose K, Kurosaki T, Iino M. Encoding of Ca2+ signals by differential expression of IP3 receptor subtypes. Embo J 1999;18(5):1303-8.
114. Schreiber SL, Crabtree GR. The mechanism of action of cyclosporin A and FK506. Immunol Today 1992;13(4):136-42.
115. Venkataraman L, Francis DA, Wang Z, Liu J, Rothstein TL, Sen R. Cyclosporin-A sensitive induction of NF-AT in murine B cells. Immunity 1994;1(3):189-96.
116. Choi MS, Brines RD, Holman MJ, Klaus GG. Induction of NF-AT in normal B lymphocytes by anti-immunoglobulin or CD40 ligand in conjunction with IL-4. Immunity 1994;1(3):179-87.
117. Graves JD, Draves KE, Craxton A, Saklatvala J, Krebs EG, Clark EA. Involvement of stress-activated protein kinase and p38 mitogen-activated protein kinase in mIgM-induced apoptosis of human B lymphocytes. Proc Natl Acad Sci U S A 1996;93(24):13814-8.
118. Malkin D, Li FP, Strong LC, Fraumeni JF, Jr., Nelson CE, Kim DH, et al. Germ line p53 mutations in a familial syndrome of breast cancer, sarcomas, and other neoplasms. Science 1990;250(4985):1233-8.
119. Vogelstein B, Lane D, Levine AJ. Surfing the p53 network. Nature 2000;408(6810):307-10.
120. Clarke AR, Purdie CA, Harrison DJ, Morris RG, Bird CC, Hooper ML, et al. Thymocyte apoptosis induced by p53-dependent and independent pathways. Nature 1993;362(6423):849-52.
121. Lowe SW, Schmitt EM, Smith SW, Osborne BA, Jacks T. p53 is required for radiation-induced apoptosis in mouse thymocytes. Nature 1993;362(6423):847-9.

122. Strasser A, Harris AW, Jacks T, Cory S. DNA damage can induce apoptosis in proliferating lymphoid cells via p53-independent mechanisms inhibitable by Bcl-2. Cell 1994;79(2):329-39.
123. Lohr K, Moritz C, Contente A, Dobbelstein M. p21/CDKN1A mediates negative regulation of transcription by p53. J Biol Chem 2003;278(35):32507-16.
124. Brown KS, Blair D, Reid SD, Nicholson EK, Harnett MM. FcgammaRIIb-mediated negative regulation of BCR signalling is associated with the recruitment of the MAPkinase-phosphatase, Pac-1, and the 3'-inositol phosphatase, PTEN. Cell Signal 2004;16(1):71-80.
125. Stambolic V, MacPherson D, Sas D, Lin Y, Snow B, Jang Y, et al. Regulation of PTEN transcription by p53. Mol Cell 2001;8(2):317-25.
126. Robles AI, Bemmels NA, Foraker AB, Harris CC. APAF-1 is a transcriptional target of p53 in DNA damage-induced apoptosis. Cancer Res 2001;61(18):6660-4.
127. Sax JK, Fei P, Murphy ME, Bernhard E, Korsmeyer SJ, El-Deiry WS. BID regulation by p53 contributes to chemosensitivity. Nat Cell Biol 2002;4(11):842-9.
128. Urano T, Nishimori H, Han H, Furuhata T, Kimura Y, Nakamura Y, et al. Cloning of P2XM, a novel human P2X receptor gene regulated by p53. Cancer Res 1997;57(15):3281-7.
129. Chipuk JE, Green DR. Cytoplasmic p53: bax and forward. Cell Cycle 2004;3(4):429-31.
130. Chipuk JE, Kuwana T, Bouchier-Hayes L, Droin NM, Newmeyer DD, Schuler M, et al. Direct activation of Bax by p53 mediates mitochondrial membrane permeabilization and apoptosis. Science 2004;303(5660):1010-4.
131. Gilmore TD. The Re1/NF-kappa B/I kappa B signal transduction pathway and cancer. Cancer Treat Res 2003;115:241-65.
132. Ghosh S, Karin M. Missing pieces in the NF-kappaB puzzle. Cell 2002;109 Suppl:S81-96.
133. Feuerhake F, Kutok JL, Monti S, Chen W, Lacasce AS, Cattoretti G, et al. NF{kappa}B activity, function and target gene signatures in primary mediastinal large B-cell lymphoma and diffuse large B-cell lymphoma subtypes. Blood 2005.

134. Younes A, Garg A, Aggarwal BB. Nuclear transcription factor-kappaB in Hodgkin's disease. Leuk Lymphoma 2003;44(6):929-35.
135. Gerondakis S, Grumont R, Rourke I, Grossmann M. The regulation and roles of Rel/NF-kappa B transcription factors during lymphocyte activation. Curr Opin Immunol 1998;10(3):353-9.
136. Gerondakis S, Strasser A. The role of Rel/NF-kappaB transcription factors in B lymphocyte survival. Semin Immunol 2003;15(3):159-66.
137. Grumont RJ, Rourke IJ, O'Reilly LA, Strasser A, Miyake K, Sha W, et al. B lymphocytes differentially use the Rel and nuclear factor kappaB1 (NF-kappaB1) transcription factors to regulate cell cycle progression and apoptosis in quiescent and mitogen-activated cells. J Exp Med 1998;187(5):663-74.
138. Doi TS, Takahashi T, Taguchi O, Azuma T, Obata Y. NF-kappa B RelA-deficient lymphocytes: normal development of T cells and B cells, impaired production of IgA and IgG1 and reduced proliferative responses. J Exp Med 1997;185(5):953-61.
139. Bash J, Zong WX, Banga S, Rivera A, Ballard DW, Ron Y, et al. Rel/NF-kappaB can trigger the Notch signaling pathway by inducing the expression of Jagged1, a ligand for Notch receptors. Embo J 1999;18(10):2803-11.
140. D'Abaco GM, Hooper S, Paterson H, Marshall CJ. Loss of Rb overrides the requirement for ERK activity for cell proliferation. J Cell Sci 2002;115(Pt 23):4607-16.
141. Levine AJ. p53, the cellular gatekeeper for growth and division. Cell 1997;88(3):323-31.
142. Lam EW, Choi MS, van der Sman J, Burbidge SA, Klaus GG. Modulation of E2F activity via signaling through surface IgM and CD40 receptors in WEHI-231 B lymphoma cells. J Biol Chem 1998;273(16):10051-7.
143. Harding A, Giles N, Burgess A, Hancock JF, Gabrielli BG. Mechanism of mitosis-specific activation of MEK1. J Biol Chem 2003;278(19):16747-54.
144. Ezhevsky SA, Toyoshima H, Hunter T, Scott DW. Role of cyclin A and p27 in anti-IgM induced G1 growth arrest of murine B-cell lymphomas. Mol Biol Cell 1996;7(4):553-64.
145. Medema RH, Klompmaker R, Smits VA, Rijksen G. p21waf1 can block cells at two points in the cell cycle, but does not interfere with processive DNA-replication or stress-activated kinases. Oncogene 1998;16(4):431-41.

146. Wu M, Bellas RE, Shen J, Sonenshein GE. Roles of the tumor suppressor p53 and the cyclin-dependent kinase inhibitor p21WAF1/CIP1 in receptor-mediated apoptosis of WEHI 231 B lymphoma cells. J Exp Med 1998;187(10):1671-9.
147. Pomerantz J, Schreiber-Agus N, Liegeois NJ, Silverman A, Alland L, Chin L, et al. The Ink4a tumor suppressor gene product, p19Arf, interacts with MDM2 and neutralizes MDM2's inhibition of p53. Cell 1998;92(6):713-23.
148. Zhang Y, Xiong Y, Yarbrough WG. ARF promotes MDM2 degradation and stabilizes p53: ARF-INK4a locus deletion impairs both the Rb and p53 tumor suppression pathways. Cell 1998;92(6):725-34.
149. Earnshaw WC, Martins LM, Kaufmann SH. Mammalian caspases: structure, activation, substrates, and functions during apoptosis. Annu Rev Biochem 1999;68:383-424.
150. Conradt B. With a little help from your friends: cells don't die alone. Nat Cell Biol 2002;4(6):E139-43.
151. Van de Craen M, Van Loo G, Pype S, Van Criekinge W, Van den brande I, Molemans F, et al. Identification of a new caspase homologue: caspase-14. Cell Death Differ 1998;5(10):838-46.
152. Green D, Kroemer G. The central executioners of apoptosis: caspases or mitochondria? Trends Cell Biol 1998;8(7):267-71.
153. Leist M, Jaattela M. Four deaths and a funeral: from caspases to alternative mechanisms. Nat Rev Mol Cell Biol 2001;2(8):589-98.
154. Isahara K, Ohsawa Y, Kanamori S, Shibata M, Waguri S, Sato N, et al. Regulation of a novel pathway for cell death by lysosomal aspartic and cysteine proteinases. Neuroscience 1999;91(1):233-49.
155. Foghsgaard L, Wissing D, Mauch D, Lademann U, Bastholm L, Boes M, et al. Cathepsin B acts as a dominant execution protease in tumor cell apoptosis induced by tumor necrosis factor. J Cell Biol 2001;153(5):999-1010.
156. Katz E, Deehan MR, Seatter S, Lord C, Sturrock RD, Harnett MM. B cell receptor-stimulated mitochondrial phospholipase A2 activation and resultant disruption of mitochondrial membrane potential correlate with the induction of apoptosis in WEHI-231 B cells. J Immunol 2001;166(1):137-47.
157. Palaga T, Osborne B. The 3D's of apoptosis: death, degradation and DIAPs. Nat Cell Biol 2002;4(6):E149-51.

158. Stoka V, Turk B, Schendel SL, Kim TH, Cirman T, Snipas SJ, et al. Lysosomal protease pathways to apoptosis. Cleavage of bid, not pro-caspases, is the most likely route. J Biol Chem 2001;276(5):3149-57.
159. Lawen A. Apoptosis-an introduction. Bioessays 2003;25(9):888-96.
160. Krammer PH. CD95's deadly mission in the immune system. Nature 2000;407(6805):789-95.
161. Boldin MP, Goncharov TM, Goltsev YV, Wallach D. Involvement of MACH, a novel MORT1/FADD-interacting protease, in Fas/APO-1- and TNF receptor-induced cell death. Cell 1996;85(6):803-15.
162. Varfolomeev EE, Schuchmann M, Luria V, Chiannilkulchai N, Beckmann JS, Mett IL, et al. Targeted disruption of the mouse Caspase 8 gene ablates cell death induction by the TNF receptors, Fas/Apo1, and DR3 and is lethal prenatally. Immunity 1998;9(2):267-76.
163. Kang TB, Ben-Moshe T, Varfolomeev EE, Pewzner-Jung Y, Yogev N, Jurewicz A, et al. Caspase-8 serves both apoptotic and nonapoptotic roles. J Immunol 2004;173(5):2976-84.
164. Salmena L, Lemmers B, Hakem A, Matysiak-Zablocki E, Murakami K, Au PY, et al. Essential role for caspase 8 in T-cell homeostasis and T-cell-mediated immunity. Genes Dev 2003;17(7):883-95.
165. Li P, Nijhawan D, Budihardjo I, Srinivasula SM, Ahmad M, Alnemri ES, et al. Cytochrome c and dATP-dependent formation of Apaf-1/caspase-9 complex initiates an apoptotic protease cascade. Cell 1997;91(4):479-89.
166. Hofmann K, Bucher P, Tschopp J. The CARD domain: a new apoptotic signalling motif. Trends Biochem Sci 1997;22(5):155-6.
167. Srinivasula SM, Ahmad M, Fernandes-Alnemri T, Alnemri ES. Autoactivation of procaspase-9 by Apaf-1-mediated oligomerization. Mol Cell 1998;1(7):949-57.
168. Cardone MH, Roy N, Stennicke HR, Salvesen GS, Franke TF, Stanbridge E, et al. Regulation of cell death protease caspase-9 by phosphorylation. Science 1998;282(5392):1318-21.
169. Thornberry NA, Lazebnik Y. Caspases: enemies within. Science 1998;281(5381):1312-6.
170. Kuida K, Haydar TF, Kuan CY, Gu Y, Taya C, Karasuyama H, et al. Reduced apoptosis and cytochrome c-mediated caspase activation in mice lacking caspase 9. Cell 1998;94(3):325-37.

171. Hakem R, Hakem A, Duncan GS, Henderson JT, Woo M, Soengas MS, et al. Differential requirement for caspase 9 in apoptotic pathways in vivo. Cell 1998;94(3):339-52.
172. Borner C. The Bcl-2 protein family: sensors and checkpoints for life-or-death decisions. Mol Immunol 2003;39(11):615-47.
173. Newmeyer DD, Ferguson-Miller S. Mitochondria: releasing power for life and unleashing the machineries of death. Cell 2003;112(4):481-90.
174. Kelekar A, Thompson CB. Bcl-2-family proteins: the role of the BH3 domain in apoptosis. Trends Cell Biol 1998;8(8):324-30.
175. Muchmore SW, Sattler M, Liang H, Meadows RP, Harlan JE, Yoon HS, et al. X-ray and NMR structure of human Bcl-xL, an inhibitor of programmed cell death. Nature 1996;381(6580):335-41.
176. Petros AM, Olejniczak ET, Fesik SW. Structural biology of the Bcl-2 family of proteins. Biochim Biophys Acta 2004;1644(2-3):83-94.
177. Narita M, Shimizu S, Ito T, Chittenden T, Lutz RJ, Matsuda H, et al. Bax interacts with the permeability transition pore to induce permeability transition and cytochrome c release in isolated mitochondria. Proc Natl Acad Sci U S A 1998;95(25):14681-6.
178. Shimizu S, Narita M, Tsujimoto Y. Bcl-2 family proteins regulate the release of apoptogenic cytochrome c by the mitochondrial channel VDAC. Nature 1999;399(6735):483-7.
179. Minn AJ, Kettlun CS, Liang H, Kelekar A, Vander Heiden MG, Chang BS, et al. Bcl-xL regulates apoptosis by heterodimerization-dependent and -independent mechanisms. Embo J 1999;18(3):632-43.
180. Abe T, Takagi N, Nakano M, Furuya M, Takeo S. Altered Bad localization and interaction between Bad and Bcl-xL in the hippocampus after transient global ischemia. Brain Res 2004;1009(1-2):159-68.
181. Mahajan NP, Linder K, Berry G, Gordon GW, Heim R, Herman B. Bcl-2 and Bax interactions in mitochondria probed with green fluorescent protein and fluorescence resonance energy transfer. Nat Biotechnol 1998;16(6):547-52.
182. Capano M, Crompton M. Biphasic translocation of Bax to mitochondria. Biochem J 2002;367(Pt 1):169-78.
183. Reed JC. Bcl-2 family proteins. Oncogene 1998;17(25):3225-36.
184. Aon MA, Cortassa S, Akar FG, O'Rourke B. Mitochondrial criticality: A new concept at the turning point of life or death. Biochim Biophys Acta 2005.

185. Hockenbery DM, Oltvai ZN, Yin XM, Milliman CL, Korsmeyer SJ. Bcl-2 functions in an antioxidant pathway to prevent apoptosis. Cell 1993;75(2):241-51.

186. Hockenbery D, Nunez G, Milliman C, Schreiber RD, Korsmeyer SJ. Bcl-2 is an inner mitochondrial membrane protein that blocks programmed cell death. Nature 1990;348(6299):334-6.

187. Hockenbery DM. bcl-2, a novel regulator of cell death. Bioessays 1995;17(7):631-8.

188. Bellosillo B, Villamor N, Lopez-Guillermo A, Marce S, Bosch F, Campo E, et al. Spontaneous and drug-induced apoptosis is mediated by conformational changes of Bax and Bak in B-cell chronic lymphocytic leukemia. Blood 2002;100(5):1810-6.

189. Tsujimoto Y. Role of Bcl-2 family proteins in apoptosis: apoptosomes or mitochondria? Genes Cells 1998;3(11):697-707.

190. Tsujimoto Y. Prevention of neuronal cell death by Bcl-2. Results Probl Cell Differ 1998;24:137-55.

191. He L, Perkins GA, Poblenz AT, Harris JB, Hung M, Ellisman MH, et al. Bcl-xL overexpression blocks bax-mediated mitochondrial contact site formation and apoptosis in rod photoreceptors of lead-exposed mice. Proc Natl Acad Sci U S A 2003;100(3):1022-7.

192. Chittenden T. BH3 domains: intracellular death-ligands critical for initiating apoptosis. Cancer Cell 2002;2(3):165-6.

193. Eskes R, Desagher S, Antonsson B, Martinou JC. Bid induces the oligomerization and insertion of Bax into the outer mitochondrial membrane. Mol Cell Biol 2000;20(3):929-35.

194. Liu J, Durrant D, Yang HS, He Y, Whitby FG, Myszka DG, et al. The interaction between tBid and cardiolipin or monolysocardiolipin. Biochem Biophys Res Commun 2005;330(3):865-70.

195. Lutter M, Fang M, Luo X, Nishijima M, Xie X, Wang X. Cardiolipin provides specificity for targeting of tBid to mitochondria. Nat Cell Biol 2000;2(10):754-61.

196. Kuwana T, Mackey MR, Perkins G, Ellisman MH, Latterich M, Schneiter R, et al. Bid, Bax, and lipids cooperate to form supramolecular openings in the outer mitochondrial membrane. Cell 2002;111(3):331-42.

197. Kim TH, Zhao Y, Ding WX, Shin JN, He X, Seo YW, et al. Bid-cardiolipin interaction at mitochondrial contact site contributes to mitochondrial cristae reorganization and cytochrome C release. Mol Biol Cell 2004;15(7):3061-72.
198. Chou JJ, Li H, Salvesen GS, Yuan J, Wagner G. Solution structure of BID, an intracellular amplifier of apoptotic signaling. Cell 1999;96(5):615-24.
199. Schendel SL, Montal M, Reed JC. Bcl-2 family proteins as ion-channels. Cell Death Differ 1998;5(5):372-80.
200. Jia L, Dourmashkin RR, Newland AC, Kelsey SM. Mitochondrial ultracondensation, but not swelling, is involved in TNF alpha-induced apoptosis in human T-lymphoblastic leukaemic cells. Leuk Res 1997;21(10):973-83.
201. Mancini M, Anderson BO, Caldwell E, Sedghinasab M, Paty PB, Hockenbery DM. Mitochondrial proliferation and paradoxical membrane depolarization during terminal differentiation and apoptosis in a human colon carcinoma cell line. J Cell Biol 1997;138(2):449-69.
202. Martinou I, Desagher S, Eskes R, Antonsson B, Andre E, Fakan S, et al. The release of cytochrome c from mitochondria during apoptosis of NGF-deprived sympathetic neurons is a reversible event. J Cell Biol 1999;144(5):883-9.
203. Sattler M, Liang H, Nettesheim D, Meadows RP, Harlan JE, Eberstadt M, et al. Structure of Bcl-xL-Bak peptide complex: recognition between regulators of apoptosis. Science 1997;275(5302):983-6.
204. Yang E, Zha J, Jockel J, Boise LH, Thompson CB, Korsmeyer SJ. Bad, a heterodimeric partner for Bcl-XL and Bcl-2, displaces Bax and promotes cell death. Cell 1995;80(2):285-91.
205. Zha J, Harada H, Yang E, Jockel J, Korsmeyer SJ. Serine phosphorylation of death agonist BAD in response to survival factor results in binding to 14-3-3 not BCL-X(L). Cell 1996;87(4):619-28.
206. Datta SR, Dudek H, Tao X, Masters S, Fu H, Gotoh Y, et al. Akt phosphorylation of BAD couples survival signals to the cell-intrinsic death machinery. Cell 1997;91(2):231-41.
207. Datta SR, Katsov A, Hu L, Petros A, Fesik SW, Yaffe MB, et al. 14-3-3 proteins and survival kinases cooperate to inactivate BAD by BH3 domain phosphorylation. Mol Cell 2000;6(1):41-51.

208. Zong WX, Lindsten T, Ross AJ, MacGregor GR, Thompson CB. BH3-only proteins that bind pro-survival Bcl-2 family members fail to induce apoptosis in the absence of Bax and Bak. Genes Dev 2001;15(12):1481-6.
209. Yang CC, Lin HP, Chen CS, Yang YT, Tseng PH, Rangnekar VM. Bcl-xL mediates a survival mechanism independent of the phosphoinositide 3-kinase/Akt pathway in prostate cancer cells. J Biol Chem 2003;278(28):25872-8.
210. Wang Z, Karras JG, Howard RG, Rothstein TL. Induction of bcl-x by CD40 engagement rescues sIg-induced apoptosis in murine B cells. J Immunol 1995;155(8):3722-5.
211. Kelekar A, Chang BS, Harlan JE, Fesik SW, Thompson CB. Bad is a BH3 domain-containing protein that forms an inactivating dimer with Bcl-XL. Mol Cell Biol 1997;17(12):7040-6.
212. Kerr DA, Larsen T, Cook SH, Fannjiang YR, Choi E, Griffin DE, et al. BCL-2 and BAX protect adult mice from lethal Sindbis virus infection but do not protect spinal cord motor neurons or prevent paralysis. J Virol 2002;76(20):10393-400.
213. Middleton G, Davies AM. Populations of NGF-dependent neurones differ in their requirement for BAX to undergo apoptosis in the absence of NGF/TrkA signalling in vivo. Development 2001;128(23):4715-28.
214. Danial NN, Gramm CF, Scorrano L, Zhang CY, Krauss S, Ranger AM, et al. BAD and glucokinase reside in a mitochondrial complex that integrates glycolysis and apoptosis. Nature 2003;424(6951):952-6.
215. Seo SY, Chen YB, Ivanovska I, Ranger AM, Hong SJ, Dawson VL, et al. BAD is a pro-survival factor prior to activation of its pro-apoptotic function. J Biol Chem 2004;279(40):42240-9.
216. Ranger AM, Zha J, Harada H, Datta SR, Danial NN, Gilmore AP, et al. Bad-deficient mice develop diffuse large B cell lymphoma. Proc Natl Acad Sci U S A 2003;100(16):9324-9.
217. Salvesen GS. A lysosomal protease enters the death scene. J Clin Invest 2001;107(1):21-2.
218. Turk B, Stoka V, Rozman-Pungercar J, Cirman T, Droga-Mazovec G, Oresic K, et al. Apoptotic pathways: involvement of lysosomal proteases. Biol Chem 2002;383(7-8):1035-44.

219. Brunk UT, Neuzil J, Eaton JW. Lysosomal involvement in apoptosis. Redox Rep 2001;6(2):91-7.
220. Katunuma N, Matsui A, Le QT, Utsumi K, Salvesen G, Ohashi A. Novel procaspase-3 activating cascade mediated by lysoapoptases and its biological significances in apoptosis. Adv Enzyme Regul 2001;41:237-50.
221. Shibata M, Kanamori S, Isahara K, Ohsawa Y, Konishi A, Kametaka S, et al. Participation of cathepsins B and D in apoptosis of PC12 cells following serum deprivation. Biochem Biophys Res Commun 1998;251(1):199-203.
222. Deussing J, Roth W, Saftig P, Peters C, Ploegh HL, Villadangos JA. Cathepsins B and D are dispensable for major histocompatibility complex class II-mediated antigen presentation. Proc Natl Acad Sci U S A 1998;95(8):4516-21.
223. Sadowski-Debbing K, Coy JF, Mier W, Hug H, Los M. Caspases--their role in apoptosis and other physiological processes as revealed by knock-out studies. Arch Immunol Ther Exp (Warsz) 2002;50(1):19-34.
224. Guicciardi ME, Miyoshi H, Bronk SF, Gores GJ. Cathepsin B knockout mice are resistant to tumor necrosis factor-alpha-mediated hepatocyte apoptosis and liver injury: implications for therapeutic applications. Am J Pathol 2001;159(6):2045-54.
225. Takuma K, Kiriu M, Mori K, Lee E, Enomoto R, Baba A, et al. Roles of cathepsins in reperfusion-induced apoptosis in cultured astrocytes. Neurochem Int 2003;42(2):153-9.
226. Michallet MC, Saltel F, Preville X, Flacher M, Revillard JP, Genestier L. Cathepsin-B-dependent apoptosis triggered by antithymocyte globulins: a novel mechanism of T-cell depletion. Blood 2003;102(10):3719-26.
227. Saido TC, Sorimachi H, Suzuki K. Calpain: new perspectives in molecular diversity and physiological-pathological involvement. Faseb J 1994;8(11):814-22.
228. Arthur JS, Elce JS, Hegadorn C, Williams K, Greer PA. Disruption of the murine calpain small subunit gene, Capn4: calpain is essential for embryonic development but not for cell growth and division. Mol Cell Biol 2000;20(12):4474-81.
229. Molinari M, Carafoli E. Calpain: a cytosolic proteinase active at the membranes. J Membr Biol 1997;156(1):1-8.

230. Wang KK. Calpain and caspase: can you tell the difference?, by kevin K.W. WangVol. 23, pp. 20-26. Trends Neurosci 2000;23(2):59.
231. McCollum AT, Nasr P, Estus S. Calpain activates caspase-3 during UV-induced neuronal death but only calpain is necessary for death. J Neurochem 2002;82(5):1208-20.
232. Choi WS, Lee EH, Chung CW, Jung YK, Jin BK, Kim SU, et al. Cleavage of Bax is mediated by caspase-dependent or -independent calpain activation in dopaminergic neuronal cells: protective role of Bcl-2. J Neurochem 2001;77(6):1531-41.
233. Sarin A, Nakajima H, Henkart PA. A protease-dependent TCR-induced death pathway in mature lymphocytes. J Immunol 1995;154(11):5806-12.
234. Witkowski JM, Zmuda-Trzebiatowska E, Swiercz JM, Cichorek M, Ciepluch H, Lewandowski K, et al. Modulation of the activity of calcium-activated neutral proteases (calpains) in chronic lymphocytic leukemia (B-CLL) cells. Blood 2002;100(5):1802-9.
235. Ruiz-Vela A, Gonzalez de Buitrago G, Martinez AC. Implication of calpain in caspase activation during B cell clonal deletion. Embo J 1999;18(18):4988-98.
236. Ravetch JV, Kinet JP. Fc receptors. Annu Rev Immunol 1991;9:457-92.
237. Hulett MD, Hogarth PM. Molecular basis of Fc receptor function. Adv Immunol 1994;57:1-127.
238. Allen JM, Seed B. Isolation and expression of functional high-affinity Fc receptor complementary DNAs. Science 1989;243(4889):378-81.
239. Muta T, Kurosaki T, Misulovin Z, Sanchez M, Nussenzweig MC, Ravetch JV. A 13-amino-acid motif in the cytoplasmic domain of Fc gamma RIIB modulates B-cell receptor signalling. Nature 1994;369(6478):340.
240. Amigorena S, Bonnerot C, Drake JR, Choquet D, Hunziker W, Guillet JG, et al. Cytoplasmic domain heterogeneity and functions of IgG Fc receptors in B lymphocytes. Science 1992;256(5065):1808-12.
241. Aman MJ, Lamkin TD, Okada H, Kurosaki T, Ravichandran KS. The inositol phosphatase SHIP inhibits Akt/PKB activation in B cells. J Biol Chem 1998;273(51):33922-8.
242. Bolland S, Pearse RN, Kurosaki T, Ravetch JV. SHIP modulates immune receptor responses by regulating membrane association of Btk. Immunity 1998;8(4):509-16.

243. Pearse RN, Kawabe T, Bolland S, Guinamard R, Kurosaki T, Ravetch JV. SHIP recruitment attenuates Fc gamma RIIB-induced B cell apoptosis. Immunity 1999;10(6):753-60.
244. Bolland S, Ravetch JV. Spontaneous autoimmune disease in Fc(gamma)RIIB-deficient mice results from strain-specific epistasis. Immunity 2000;13(2):277-85.
245. Diegel ML, Rankin BM, Bolen JB, Dubois PM, Kiener PA. Cross-linking of Fc gamma receptor to surface immunoglobulin on B cells provides an inhibitory signal that closes the plasma membrane calcium channel. J Biol Chem 1994;269(15):11409-16.
246. Pani G, Kozlowski M, Cambier JC, Mills GB, Siminovitch KA. Identification of the tyrosine phosphatase PTP1C as a B cell antigen receptor-associated protein involved in the regulation of B cell signaling. J Exp Med 1995;181(6):2077-84.
247. Phillips NE, Parker DC. Cross-linking of B lymphocyte Fc gamma receptors and membrane immunoglobulin inhibits anti-immunoglobulin-induced blastogenesis. J Immunol 1984;132(2):627-32.
248. D'Ambrosio D, Hippen KL, Minskoff SA, Mellman I, Pani G, Siminovitch KA, et al. Recruitment and activation of PTP1C in negative regulation of antigen receptor signaling by Fc gamma RIIB1. Science 1995;268(5208):293-7.
249. Siminovitch KA, Neel BG. Regulation of B cell signal transduction by SH2-containing protein-tyrosine phosphatases. Semin Immunol 1998;10(4):329-47.
250. Tamir I, Dal Porto JM, Cambier JC. Cytoplasmic protein tyrosine phosphatases SHP-1 and SHP-2: regulators of B cell signal transduction. Curr Opin Immunol 2000;12(3):307-15.
251. Koncz G, Toth GK, Bokonyi G, Keri G, Pecht I, Medgyesi D, et al. Co-clustering of Fcgamma and B cell receptors induces dephosphorylation of the Grb2-associated binder 1 docking protein. Eur J Biochem 2001;268(14):3898-906.
252. Sarmay G, Koncz G, Pecht I, Gergely J. Fc gamma receptor type IIb induced recruitment of inositol and protein phosphatases to the signal transductory complex of human B-cell. Immunol Lett 1997;57(1-3):159-64.

253. Ono M, Bolland S, Tempst P, Ravetch JV. Role of the inositol phosphatase SHIP in negative regulation of the immune system by the receptor Fc(gamma)RIIB. Nature 1996;383(6597):263-6.
254. Nadler MJ, Chen B, Anderson JS, Wortis HH, Neel BG. Protein-tyrosine phosphatase SHP-1 is dispensable for FcgammaRIIB-mediated inhibition of B cell antigen receptor activation. J Biol Chem 1997;272(32):20038-43.
255. Ono M, Okada H, Bolland S, Yanagi S, Kurosaki T, Ravetch JV. Deletion of SHIP or SHP-1 reveals two distinct pathways for inhibitory signaling. Cell 1997;90(2):293-301.
256. Liu Q, Oliveira-Dos-Santos AJ, Mariathasan S, Bouchard D, Jones J, Sarao R, et al. The inositol polyphosphate 5-phosphatase ship is a crucial negative regulator of B cell antigen receptor signaling. J Exp Med 1998;188(7):1333-42.
257. Ross TS, Jefferson AB, Mitchell CA, Majerus PW. Cloning and expression of human 75-kDa inositol polyphosphate-5-phosphatase. J Biol Chem 1991;266(30):20283-9.
258. Laxminarayan KM, Chan BK, Tetaz T, Bird PI, Mitchell CA. Characterization of a cDNA encoding the 43-kDa membrane-associated inositol-polyphosphate 5-phosphatase. J Biol Chem 1994;269(25):17305-10.
259. Rohrschneider LR, Fuller JF, Wolf I, Liu Y, Lucas DM. Structure, function, and biology of SHIP proteins. Genes Dev 2000;14(5):505-20.
260. Geier SJ, Algate PA, Carlberg K, Flowers D, Friedman C, Trask B, et al. The human SHIP gene is differentially expressed in cell lineages of the bone marrow and blood. Blood 1997;89(6):1876-85.
261. Helgason CD, Damen JE, Rosten P, Grewal R, Sorensen P, Chappel SM, et al. Targeted disruption of SHIP leads to hemopoietic perturbations, lung pathology, and a shortened life span. Genes Dev 1998;12(11):1610-20.
262. Yuasa T, Kubo S, Yoshino T, Ujike A, Matsumura K, Ono M, et al. Deletion of fcgamma receptor IIB renders H-2(b) mice susceptible to collagen-induced arthritis. J Exp Med 1999;189(1):187-94.
263. Damen JE, Liu L, Rosten P, Humphries RK, Jefferson AB, Majerus PW, et al. The 145-kDa protein induced to associate with Shc by multiple cytokines is an inositol tetraphosphate and phosphatidylinositol 3,4,5-triphosphate 5-phosphatase. Proc Natl Acad Sci U S A 1996;93(4):1689-93.

264. Liu Q, Sasaki T, Kozieradzki I, Wakeham A, Itie A, Dumont DJ, et al. SHIP is a negative regulator of growth factor receptor-mediated PKB/Akt activation and myeloid cell survival. Genes Dev 1999;13(7):786-91.
265. Kohn AD, Takeuchi F, Roth RA. Akt, a pleckstrin homology domain containing kinase, is activated primarily by phosphorylation. J Biol Chem 1996;271(36):21920-6.
266. Gingery A, Bradley E, Shaw A, Oursler MJ. Phosphatidylinositol 3-kinase coordinately activates the MEK/ERK and AKT/NFkappaB pathways to maintain osteoclast survival. J Cell Biochem 2003;89(1):165-79.
267. Tridandapani S, Kelley T, Cooney D, Pradhan M, Coggeshall KM. Negative signaling in B cells: SHIP Grbs Shc. Immunol Today 1997;18(9):424-7.
268. Tridandapani S, Pradhan M, LaDine JR, Garber S, Anderson CL, Coggeshall KM. Protein interactions of Src homology 2 (SH2) domain-containing inositol phosphatase (SHIP): association with Shc displaces SHIP from FcgammaRIIb in B cells. J Immunol 1999;162(3):1408-14.
269. Tamir I, Stolpa JC, Helgason CD, Nakamura K, Bruhns P, Daeron M, et al. The RasGAP-binding protein p62dok is a mediator of inhibitory FcgammaRIIB signals in B cells. Immunity 2000;12(3):347-58.
270. Malbec O, Schmitt C, Bruhns P, Krystal G, Fridman WH, Daeron M. Src homology 2 domain-containing inositol 5-phosphatase 1 mediates cell cycle arrest by FcgammaRIIB. J Biol Chem 2001;276(32):30381-91.
271. Ward Y, Gupta S, Jensen P, Wartmann M, Davis RJ, Kelly K. Control of MAP kinase activation by the mitogen-induced threonine/tyrosine phosphatase PAC1. Nature 1994;367(6464):651-4.
272. Rohan PJ, Davis P, Moskaluk CA, Kearns M, Krutzsch H, Siebenlist U, et al. PAC-1: a mitogen-induced nuclear protein tyrosine phosphatase. Science 1993;259(5102):1763-6.
273. Grumont RJ, Rasko JE, Strasser A, Gerondakis S. Activation of the mitogen-activated protein kinase pathway induces transcription of the PAC-1 phosphatase gene. Mol Cell Biol 1996;16(6):2913-21.
274. Deehan MR, Goodridge HS, Blair D, Lochnit G, Dennis RD, Geyer R, et al. Immunomodulatory properties of Ascaris suum glycosphingolipids - phosphorylcholine and non-phosphorylcholine-dependent effects. Parasite Immunol 2002;24(9-10):463-9.

275. Gauld SB, Blair D, Moss CA, Reid SD, Harnett MM. Differential roles for extracellularly regulated kinase-mitogen-activated protein kinase in B cell antigen receptor-induced apoptosis and CD40-mediated rescue of WEHI-231 immature B cells. J Immunol 2002;168(8):3855-64.
276. Choi MS, Boise LH, Gottschalk AR, Quintans J, Thompson CB, Klaus GG. The role of bcl-XL in CD40-mediated rescue from anti-mu-induced apoptosis in WEHI-231 B lymphoma cells. Eur J Immunol 1995;25(5):1352-7.
277. Fang W, Rivard JJ, Ganser JA, LeBien TW, Nath KA, Mueller DL, et al. Bcl-xL rescues WEHI 231 B lymphocytes from oxidant-mediated death following diverse apoptotic stimuli. J Immunol 1995;155(1):66-75.
278. Koncz G, Bodor C, Kovesdi D, Gati R, Sarmay G. BCR mediated signal transduction in immature and mature B cells. Immunol Lett 2002;82(1-2):41-9.
279. Suzuki H, Matsuda S, Terauchi Y, Fujiwara M, Ohteki T, Asano T, et al. PI3K and Btk differentially regulate B cell antigen receptor-mediated signal transduction. Nat Immunol 2003;4(3):280-6.
280. Niiro H, Clark EA. Regulation of B-cell fate by antigen-receptor signals. Nat Rev Immunol 2002;2(12):945-56.
281. Heyman B. Feedback regulation by IgG antibodies. Immunol Lett 2003;88(2):157-61.
282. O'Rourke L, Tooze R, Fearon DT. Co-receptors of B lymphocytes. Curr Opin Immunol 1997;9(3):324-9.
283. Yajima K, Nakamura A, Sugahara A, Takai T. FcgammaRIIB deficiency with Fas mutation is sufficient for the development of systemic autoimmune disease. Eur J Immunol 2003;33(4):1020-9.
284. Shortman K, Cerottini JC, Brunner KT. The separation of sub-populations of T and B lymphocytes. Eur J Immunol 1972;2(4):313-9.
285. von Boehmer H. Direct cell contact is required in the syngeneic mixed lymphocyte reaction. Eur J Immunol 1973;3(2):109-11.
286. Gottschalk AR, Boise LH, Thompson CB, Quintans J. Identification of immunosuppressant-induced apoptosis in a murine B-cell line and its prevention by bcl-x but not bcl-2. Proc Natl Acad Sci U S A 1994;91(15):7350-4.
287. Chang BS, Minn AJ, Muchmore SW, Fesik SW, Thompson CB. Identification of a novel regulatory domain in Bcl-X(L) and Bcl-2. Embo J 1997;16(5):968-77.

288. Gilbert JJ, Pettitt TR, Seatter SD, Reid SD, Wakelam MJ, Harnett MM. Antagonistic roles for phospholipase D activities in B cell signaling: while the antigen receptors transduce mitogenic signals via a novel phospholipase D activity, phosphatidylcholine-phospholipase D mediates antiproliferative signals. J Immunol 1998;161(12):6575-84.
289. Gilbert JJ, Stewart A, Courtney CA, Fleming MC, Reid P, Jackson CG, et al. Antigen receptors on immature, but not mature, B and T cells are coupled to cytosolic phospholipase A2 activation: expression and activation of cytosolic phospholipase A2 correlate with lymphocyte maturation. J Immunol 1996;156(6):2054-61.
290. Garner DL, Thomas CA. Organelle-specific probe JC-1 identifies membrane potential differences in the mitochondrial function of bovine sperm. Mol Reprod Dev 1999;53(2):222-9.
291. Lyons AB, Parish CR. Determination of lymphocyte division by flow cytometry. J Immunol Methods 1994;171(1):131-7.
292. Parish CR. Fluorescent dyes for lymphocyte migration and proliferation studies. Immunol Cell Biol 1999;77(6):499-508.
293. Versteeg HH, Nijhuis E, van den Brink GR, Evertzen M, Pynaert GN, van Deventer SJ, et al. A new phosphospecific cell-based ELISA for p42/p44 mitogen-activated protein kinase (MAPK), p38 MAPK, protein kinase B and cAMP-response-element-binding protein. Biochem J 2000;350 Pt 3:717-22.
294. McCarron JG, MacMillan D, Bradley KN, Chalmers S, Muir TC. Origin and mechanisms of Ca2+ waves in smooth muscle as revealed by localized photolysis of caged inositol 1,4,5-trisphosphate. J Biol Chem 2004;279(9):8417-27.
295. Davis W, Sage SO, Allen JM. Cytosolic calcium elevation in response to Fc receptor cross-linking in undifferentiated and differentiated U937 cells. Cell Calcium 1994;16(1):29-36.
296. Grynkiewicz G, Poenie M, Tsien RY. A new generation of Ca2+ indicators with greatly improved fluorescence properties. J Biol Chem 1985;260(6):3440-50.
297. Ralph P. Functional subsets of murine and human B lymphocyte cell lines. Immunol Rev 1979;48:107-21.

298. Sitia R, Abbott J, Hammerling U. The ontogeny of B lymphocytes. V. Lipopolysaccharide-induced changes of IgD expression on murine B lymphocytes. Eur J Immunol 1979;9(11):859-64.
299. Hammerling U, Chin AF, Abbott J. Ontogeny of murine B lymphocytes: sequence of B-cell differentiation from surface-immunoglobulin-negative precursors to plasma cells. Proc Natl Acad Sci U S A 1976;73(6):2008-12.
300. Jakway JP, Usinger WR, Gold MR, Mishell RI, DeFranco AL. Growth regulation of the B lymphoma cell line WEHI-231 by anti-immunoglobulin, lipopolysaccharide, and other bacterial products. J Immunol 1986;137(7):2225-31.
301. Monroe JG, Seyfert VL, Owen CS, Sykes N. Isolation and characterization of a B lymphocyte mutant with altered signal transduction through its antigen receptor. J Exp Med 1989;169(3):1059-70.
302. Monroe JG. Molecular mechanisms regulating B-cell negative selection. Biochem Soc Trans 1997;25(2):643-7.
303. Wiesner DA, Kilkus JP, Gottschalk AR, Quintans J, Dawson G. Anti-immunoglobulin-induced apoptosis in WEHI 231 cells involves the slow formation of ceramide from sphingomyelin and is blocked by bcl-XL. J Biol Chem 1997;272(15):9868-76.
304. Green DR, Mahboubi A, Nishioka W, Oja S, Echeverri F, Shi Y, et al. Promotion and inhibition of activation-induced apoptosis in T-cell hybridomas by oncogenes and related signals. Immunol Rev 1994;142:321-42.
305. Nossal GJ. Negative selection of lymphocytes. Cell 1994;76(2):229-39.
306. Klinman NR. The "clonal selection hypothesis" and current concepts of B cell tolerance. Immunity 1996;5(3):189-95.
307. Berberich I, Shu G, Siebelt F, Woodgett JR, Kyriakis JM, Clark EA. Cross-linking CD40 on B cells preferentially induces stress-activated protein kinases rather than mitogen-activated protein kinases. Embo J 1996;15(1):92-101.
308. Purkerson JM, Parker DC. Differential coupling of membrane Ig and CD40 to the extracellularly regulated kinase signaling pathway. J Immunol 1998;160(5):2121-9.
309. van Kooten C, Banchereau J. Functional role of CD40 and its ligand. Int Arch Allergy Immunol 1997;113(4):393-9.

310. Kehry MR. CD40-mediated signaling in B cells. Balancing cell survival, growth, and death. J Immunol 1996;156(7):2345-8.
311. Gray D. CD40 signalling in T-dependent B cell responses. In: Harnett MMaR, K. P., editor. Lymphocytes Signalling: Mechanisms, Subversion and Manipulation: John Wiley & Sons Ltd; 1997. p. 77-89.
312. Faris M, Gaskin F, Parsons JT, Fu SM. CD40 signaling pathway: anti-CD40 monoclonal antibody induces rapid dephosphorylation and phosphorylation of tyrosine-phosphorylated proteins including protein tyrosine kinase Lyn, Fyn, and Syk and the appearance of a 28-kD tyrosine phosphorylated protein. J Exp Med 1994;179(6):1923-31.
313. Van Kooten C, Galibert L, Seon BK, Garrone P, Liu YJ, Banchereau J. Cross-linking of antigen receptor via Ig-beta (B29, CD79b) can induce both positive and negative signals in CD40-activated human B cells. Clin Exp Immunol 1997;110(3):509-15.
314. Durie FH, Foy TM, Masters SR, Laman JD, Noelle RJ. The role of CD40 in the regulation of humoral and cell-mediated immunity. Immunol Today 1994;15(9):406-11.
315. Banchereau J, Briere F, Liu YJ, Rousset F. Molecular control of B lymphocyte growth and differentiation. Stem Cells 1994;12(3):278-88.
316. Tsubata T, Wu J, Honjo T. B-cell apoptosis induced by antigen receptor crosslinking is blocked by a T-cell signal through CD40. Nature 1993;364(6438):645-8.
317. Parry SL, Hasbold J, Holman M, Klaus GG. Hypercross-linking surface IgM or IgD receptors on mature B cells induces apoptosis that is reversed by costimulation with IL-4 and anti-CD40. J Immunol 1994;152(6):2821-9.
318. Parry SL, Holman MJ, Hasbold J, Klaus GG. Plastic-immobilized anti-mu or anti-delta antibodies induce apoptosis in mature murine B lymphocytes. Eur J Immunol 1994;24(4):974-9.
319. Tsubata T. Molecular mechanisms for apoptosis induced by signaling through the B cell antigen receptor. Int Rev Immunol 2001;20(6):791-803.
320. Gauld SB. Differential roles of ERK-MAPkinase in WEHI 231 cell apoptosis and growth. Glasgow: University of Glasgow; 2001.
321. Merino R, Grillot DA, Simonian PL, Muthukkumar S, Fanslow WC, Bondada S, et al. Modulation of anti-IgM-induced B cell apoptosis by Bcl-xL and CD40 in WEHI-231 cells. Dissociation from cell cycle arrest and dependence on

the avidity of the antibody-IgM receptor interaction. J Immunol 1995;155(8):3830-8.
322. Craxton A, Chuang PI, Shu G, Harlan JM, Clark EA. The CD40-inducible Bcl-2 family member A1 protects B cells from antigen receptor-mediated apoptosis. Cell Immunol 2000;200(1):56-62.
323. Perez-Sala D, Rebollo A. Novel aspects of Ras proteins biology: regulation and implications. Cell Death Differ 1999;6(8):722-8.
324. Campbell SL, Khosravi-Far R, Rossman KL, Clark GJ, Der CJ. Increasing complexity of Ras signaling. Oncogene 1998;17(11 Reviews):1395-413.
325. Rodriguez-Viciana P, Warne PH, Khwaja A, Marte BM, Pappin D, Das P, et al. Role of phosphoinositide 3-OH kinase in cell transformation and control of the actin cytoskeleton by Ras. Cell 1997;89(3):457-67.
326. Mulcahy LS, Smith MR, Stacey DW. Requirement for ras proto-oncogene function during serum-stimulated growth of NIH 3T3 cells. Nature 1985;313(5999):241-3.
327. Feig LA, Cooper GM. Inhibition of NIH 3T3 cell proliferation by a mutant ras protein with preferential affinity for GDP. Mol Cell Biol 1988;8(8):3235-43.
328. Satoh T, Endo M, Nakafuku M, Akiyama T, Yamamoto T, Kaziro Y. Accumulation of p21ras.GTP in response to stimulation with epidermal growth factor and oncogene products with tyrosine kinase activity. Proc Natl Acad Sci U S A 1990;87(20):7926-9.
329. Taylor SJ, Shalloway D. Cell cycle-dependent activation of Ras. Curr Biol 1996;6(12):1621-7.
330. Gille H, Downward J. Multiple ras effector pathways contribute to G(1) cell cycle progression. J Biol Chem 1999;274(31):22033-40.
331. Aktas H, Cai H, Cooper GM. Ras links growth factor signaling to the cell cycle machinery via regulation of cyclin D1 and the Cdk inhibitor p27KIP1. Mol Cell Biol 1997;17(7):3850-7.
332. Rodriguez-Viciana P, Marte BM, Warne PH, Downward J. Phosphatidylinositol 3' kinase: one of the effectors of Ras. Philos Trans R Soc Lond B Biol Sci 1996;351(1336):225-31; discussion 231-2.
333. Rodriguez-Viciana P, Warne PH, Vanhaesebroeck B, Waterfield MD, Downward J. Activation of phosphoinositide 3-kinase by interaction with Ras and by point mutation. Embo J 1996;15(10):2442-51.

334. Carpino N, Wisniewski D, Strife A, Marshak D, Kobayashi R, Stillman B, et al. p62(dok): a constitutively tyrosine-phosphorylated, GAP-associated protein in chronic myelogenous leukemia progenitor cells. Cell 1997;88(2):197-204.
335. Yamanashi Y, Baltimore D. Identification of the Abl- and rasGAP-associated 62 kDa protein as a docking protein, Dok. Cell 1997;88(2):205-11.
336. Bollag G, McCormick F. Regulators and effectors of ras proteins. Annu Rev Cell Biol 1991;7:601-32.
337. Gold MR, Crowley MT, Martin GA, McCormick F, DeFranco AL. Targets of B lymphocyte antigen receptor signal transduction include the p21ras GTPase-activating protein (GAP) and two GAP-associated proteins. J Immunol 1993;150(2):377-86.
338. Vuica M, Desiderio S, Schneck JP. Differential effects of B cell receptor and B cell receptor-FcgammaRIIB1 engagement on docking of Csk to GTPase-activating protein (GAP)-associated p62. J Exp Med 1997;186(2):259-67.
339. Tang J, Feng GS, Li W. Induced direct binding of the adapter protein Nck to the GTPase-activating protein-associated protein p62 by epidermal growth factor. Oncogene 1997;15(15):1823-32.
340. Di Cristofano A, Niki M, Zhao M, Karnell FG, Clarkson B, Pear WS, et al. p62(dok), a negative regulator of Ras and mitogen-activated protein kinase (MAPK) activity, opposes leukemogenesis by p210(bcr-abl). J Exp Med 2001;194(3):275-84.
341. Zhao M, Schmitz AA, Qin Y, Di Cristofano A, Pandolfi PP, Van Aelst L. Phosphoinositide 3-kinase-dependent membrane recruitment of p62(dok) is essential for its negative effect on mitogen-activated protein (MAP) kinase activation. J Exp Med 2001;194(3):265-74.
342. Yamanashi Y, Tamura T, Kanamori T, Yamane H, Nariuchi H, Yamamoto T, et al. Role of the rasGAP-associated docking protein p62(dok) in negative regulation of B cell receptor-mediated signaling. Genes Dev 2000;14(1):11-6.
343. Zhang J, Somani AK, Siminovitch KA. Roles of the SHP-1 tyrosine phosphatase in the negative regulation of cell signalling. Semin Immunol 2000;12(4):361-78.
344. Scheid MP, Huber M, Damen JE, Hughes M, Kang V, Neilsen P, et al. Phosphatidylinositol (3,4,5)P3 is essential but not sufficient for protein kinase B

(PKB) activation; phosphatidylinositol (3,4)P2 is required for PKB phosphorylation at Ser-473: studies using cells from SH2-containing inositol-5-phosphatase knockout mice. J Biol Chem 2002;277(11):9027-35.

345. Brauweiler AM, Cambier JC. Fc gamma RIIB activation leads to inhibition of signalling by independently ligated receptors. Biochem Soc Trans 2003;31(Pt 1):281-5.

346. Coggeshall KM. Inhibitory signaling by B cell Fc gamma RIIb. Curr Opin Immunol 1998;10(3):306-12.

347. Ingham RJ, Okada H, Dang-Lawson M, Dinglasan J, van Der Geer P, Kurosaki T, et al. Tyrosine phosphorylation of shc in response to B cell antigen receptor engagement depends on the SHIP inositol phosphatase. J Immunol 1999;163(11):5891-5.

348. Mischak H, Kolch W, Goodnight J, Davidson WF, Rapp U, Rose-John S, et al. Expression of protein kinase C genes in hemopoietic cells is cell-type- and B cell-differentiation stage specific. J Immunol 1991;147(11):3981-7.

349. Bras A, Martinez AC, Baixeras E. B cell receptor cross-linking prevents Fas-induced cell death by inactivating the IL-1 beta-converting enzyme protease and regulating Bcl-2/Bcl-x expression. J Immunol 1997;159(7):3168-77.

350. Chen ZZ, Coggeshall KM, Cambier JC. Translocation of protein kinase C during membrane immunoglobulin-mediated transmembrane signaling in B lymphocytes. J Immunol 1986;136(6):2300-4.

351. Nel AE, Wooten MW, Landreth GE, Goldschmidt-Clermont PJ, Stevenson HC, Miller PJ, et al. Translocation of phospholipid/Ca2+-dependent protein kinase in B-lymphocytes activated by phorbol ester or cross-linking of membrane immunoglobulin. Biochem J 1986;233(1):145-9.

352. Liu JL, Chiles TC, Sen RJ, Rothstein TL. Inducible nuclear expression of NF-kappa B in primary B cells stimulated through the surface Ig receptor. J Immunol 1991;146(5):1685-91.

353. Huo L, Rothstein TL. Receptor-specific induction of individual AP-1 components in B lymphocytes. J Immunol 1995;154(7):3300-9.

354. Hashimoto A, Okada H, Jiang A, Kurosaki M, Greenberg S, Clark EA, et al. Involvement of guanosine triphosphatases and phospholipase C-gamma2 in extracellular signal-regulated kinase, c-Jun NH2-terminal kinase, and p38

mitogen-activated protein kinase activation by the B cell antigen receptor. J Exp Med 1998;188(7):1287-95.
355. Krappmann D, Patke A, Heissmeyer V, Scheidereit C. B-cell receptor- and phorbol ester-induced NF-kappaB and c-Jun N-terminal kinase activation in B cells requires novel protein kinase C's. Mol Cell Biol 2001;21(19):6640-50.
356. Li HL, Davis W, Pure E. Suboptimal cross-linking of antigen receptor induces Syk-dependent activation of p70S6 kinase through protein kinase C and phosphoinositol 3-kinase. J Biol Chem 1999;274(14):9812-20.
357. Guinamard R, Signoret N, Ishiai M, Marsh M, Kurosaki T, Ravetch JV. B cell antigen receptor engagement inhibits stromal cell-derived factor (SDF)-1alpha chemotaxis and promotes protein kinase C (PKC)-induced internalization of CXCR4. J Exp Med 1999;189(9):1461-6.
358. Rothstein TL, Zhong X, Schram BR, Negm RS, Donohoe TJ, Cabral DS, et al. Receptor-specific regulation of B-cell susceptibility to Fas-mediated apoptosis and a novel Fas apoptosis inhibitory molecule. Immunol Rev 2000;176:116-33.
359. van Kooyk Y, Figdor CG. Avidity regulation of integrins: the driving force in leukocyte adhesion. Curr Opin Cell Biol 2000;12(5):542-7.
360. Parker PJ, Coussens L, Totty N, Rhee L, Young S, Chen E, et al. The complete primary structure of protein kinase C--the major phorbol ester receptor. Science 1986;233(4766):853-9.
361. Soh JW, Weinstein IB. Roles of specific isoforms of protein kinase C in the transcriptional control of cyclin D1 and related genes. J Biol Chem 2003;278(36):34709-16.
362. Whelan RD, Parker PJ. Loss of protein kinase C function induces an apoptotic response. Oncogene 1998;16(15):1939-44.
363. Dooley NP, Baltuch GH, Groome N, Villemure JG, Yong VW. Apoptosis is induced in glioma cells by antisense oligonucleotides to protein kinase C alpha and is enhanced by cycloheximide. Neuroreport 1998;9(8):1727-33.
364. Ito T, Deng X, Carr B, May WS. Bcl-2 phosphorylation required for anti-apoptosis function. J Biol Chem 1997;272(18):11671-3.
365. Ruvolo PP, Deng X, Carr BK, May WS. A functional role for mitochondrial protein kinase Calpha in Bcl2 phosphorylation and suppression of apoptosis. J Biol Chem 1998;273(39):25436-42.

366. Lee JY, Hannun YA, Obeid LM. Ceramide inactivates cellular protein kinase Calpha. J Biol Chem 1996;271(22):13169-74.
367. Keenan C, Thompson S, Knox K, Pears C. Protein kinase C-alpha is essential for Ramos-BL B cell survival. Cell Immunol 1999;196(2):104-9.
368. Leitges M, Schmedt C, Guinamard R, Davoust J, Schaal S, Stabel S, et al. Immunodeficiency in protein kinase cbeta-deficient mice. Science 1996;273(5276):788-91.
369. King LB, Norvell A, Monroe JG. Antigen receptor-induced signal transduction imbalances associated with the negative selection of immature B cells. J Immunol 1999;162(5):2655-62.
370. Macfarlane DE, Manzel L, Krieg AM. Unmethylated CpG-containing oligodeoxynucleotides inhibit apoptosis in WEHI 231 B lymphocytes induced by several agents: evidence for blockade of apoptosis at a distal signalling step. Immunology 1997;91(4):586-93.
371. Grumont RJ, Strasser A, Gerondakis S. B cell growth is controlled by phosphatidylinosotol 3-kinase-dependent induction of Rel/NF-kappaB regulated c-myc transcription. Mol Cell 2002;10(6):1283-94.
372. Wu M, Lee H, Bellas RE, Schauer SL, Arsura M, Katz D, et al. Inhibition of NF-kappaB/Rel induces apoptosis of murine B cells. Embo J 1996;15(17):4682-90.
373. Siebelt F, Berberich I, Shu G, Serfling E, Clark EA. Role for CD40-mediated activation of c-Rel and maintenance of c-myc RNA levels in mitigating anti-IgM-induced growth arrest. Cell Immunol 1997;181(1):13-22.
374. Barbazuk SM, Gold MR. Protein kinase C-delta is a target of B-cell antigen receptor signaling. Immunol Lett 1999;69(2):259-67.
375. Popoff IJ, Deans JP. Activation and tyrosine phosphorylation of protein kinase C delta in response to B cell antigen receptor stimulation. Mol Immunol 1999;36(15-16):1005-16.
376. Zang Q, Lu Z, Curto M, Barile N, Shalloway D, Foster DA. Association between v-Src and protein kinase C delta in v-Src-transformed fibroblasts. J Biol Chem 1997;272(20):13275-80.
377. Szallasi Z, Denning MF, Chang EY, Rivera J, Yuspa SH, Lehel C, et al. Development of a rapid approach to identification of tyrosine phosphorylation sites: application to PKC delta phosphorylated upon activation of the high

affinity receptor for IgE in rat basophilic leukemia cells. Biochem Biophys Res Commun 1995;214(3):888-94.

378. Denning MF, Dlugosz AA, Threadgill DW, Magnuson T, Yuspa SH. Activation of the epidermal growth factor receptor signal transduction pathway stimulates tyrosine phosphorylation of protein kinase C delta. J Biol Chem 1996;271(10):5325-31.

379. Haleem-Smith H, Chang EY, Szallasi Z, Blumberg PM, Rivera J. Tyrosine phosphorylation of protein kinase C-delta in response to the activation of the high-affinity receptor for immunoglobulin E modifies its substrate recognition. Proc Natl Acad Sci U S A 1995;92(20):9112-6.

380. Konishi H, Tanaka M, Takemura Y, Matsuzaki H, Ono Y, Kikkawa U, et al. Activation of protein kinase C by tyrosine phosphorylation in response to H2O2. Proc Natl Acad Sci U S A 1997;94(21):11233-7.

381. Saxton TM, van Oostveen I, Bowtell D, Aebersold R, Gold MR. B cell antigen receptor cross-linking induces phosphorylation of the p21ras oncoprotein activators SHC and mSOS1 as well as assembly of complexes containing SHC, GRB-2, mSOS1, and a 145-kDa tyrosine-phosphorylated protein. J Immunol 1994;153(2):623-36.

382. Emoto Y, Manome Y, Meinhardt G, Kisaki H, Kharbanda S, Robertson M, et al. Proteolytic activation of protein kinase C delta by an ICE-like protease in apoptotic cells. Embo J 1995;14(24):6148-56.

383. Kikkawa U, Matsuzaki H, Yamamoto T. Protein kinase C delta (PKC delta): activation mechanisms and functions. J Biochem (Tokyo) 2002;132(6):831-9.

384. Mecklenbrauker I, Kalled SL, Leitges M, Mackay F, Tarakhovsky A. Regulation of B-cell survival by BAFF-dependent PKCdelta-mediated nuclear signalling. Nature 2004;431(7007):456-61.

385. Mecklenbrauker I, Saijo K, Zheng NY, Leitges M, Tarakhovsky A. Protein kinase Cdelta controls self-antigen-induced B-cell tolerance. Nature 2002;416(6883):860-5.

386. Miyamoto A, Nakayama K, Imaki H, Hirose S, Jiang Y, Abe M, et al. Increased proliferation of B cells and auto-immunity in mice lacking protein kinase Cdelta. Nature 2002;416(6883):865-9.

387. Hamilton M, Liao J, Cathcart MK, Wolfman A. Constitutive association of c-N-Ras with c-Raf-1 and protein kinase C epsilon in latent signaling modules. J Biol Chem 2001;276(31):29079-90.
388. Tojima Y, Fujimoto A, Delhase M, Chen Y, Hatakeyama S, Nakayama K, et al. NAK is an IkappaB kinase-activating kinase. Nature 2000;404(6779):778-82.
389. Matsumoto M, Ogawa W, Hino Y, Furukawa K, Ono Y, Takahashi M, et al. Inhibition of insulin-induced activation of Akt by a kinase-deficient mutant of the epsilon isozyme of protein kinase C. J Biol Chem 2001;276(17):14400-6.
390. Moriya S, Kazlauskas A, Akimoto K, Hirai S, Mizuno K, Takenawa T, et al. Platelet-derived growth factor activates protein kinase C epsilon through redundant and independent signaling pathways involving phospholipase C gamma or phosphatidylinositol 3-kinase. Proc Natl Acad Sci U S A 1996;93(1):151-5.
391. Olivier AR, Parker PJ. Bombesin, platelet-derived growth factor, and diacylglycerol induce selective membrane association and down-regulation of protein kinase C isotypes in Swiss 3T3 cells. J Biol Chem 1994;269(4):2758-63.
392. Perletti GP, Concari P, Brusaferri S, Marras E, Piccinini F, Tashjian AH, Jr. Protein kinase Cepsilon is oncogenic in colon epithelial cells by interaction with the ras signal transduction pathway. Oncogene 1998;16(25):3345-8.
393. Cai H, Smola U, Wixler V, Eisenmann-Tappe I, Diaz-Meco MT, Moscat J, et al. Role of diacylglycerol-regulated protein kinase C isotypes in growth factor activation of the Raf-1 protein kinase. Mol Cell Biol 1997;17(2):732-41.
394. Cacace AM, Ueffing M, Philipp A, Han EK, Kolch W, Weinstein IB. PKC epsilon functions as an oncogene by enhancing activation of the Raf kinase. Oncogene 1996;13(12):2517-26.
395. Lee YJ, Soh JW, Jeoung DI, Cho CK, Jhon GJ, Lee SJ, et al. PKC epsilon -mediated ERK1/2 activation involved in radiation-induced cell death in NIH3T3 cells. Biochim Biophys Acta 2003;1593(2-3):219-29.
396. Mayne GC, Murray AW. Evidence that protein kinase Cepsilon mediates phorbol ester inhibition of calphostin C- and tumor necrosis factor-alpha-induced apoptosis in U937 histiocytic lymphoma cells. J Biol Chem 1998;273(37):24115-21.

397. Ting HC, Christian SL, Burgess AE, Gold MR. Activation and phosphatidylinositol 3-kinase-dependent phosphorylation of protein kinase C-epsilon by the B cell antigen receptor. Immunol Lett 2002;82(3):205-15.
398. Leitges M, Sanz L, Martin P, Duran A, Braun U, Garcia JF, et al. Targeted disruption of the zetaPKC gene results in the impairment of the NF-kappaB pathway. Mol Cell 2001;8(4):771-80.
399. Martin P, Duran A, Minguet S, Gaspar ML, Diaz-Meco MT, Rennert P, et al. Role of zeta PKC in B-cell signaling and function. Embo J 2002;21(15):4049-57.
400. Chao MV. The p75 neurotrophin receptor. J Neurobiol 1994;25(11):1373-85.
401. Gruss HJ, Duyster J, Herrmann F. Structural and biological features of the TNF receptor and TNF ligand superfamilies: interactive signals in the pathobiology of Hodgkin's disease. Ann Oncol 1996;7 Suppl 4:19-26.
402. Otten U, Ehrhard P, Peck R. Nerve growth factor induces growth and differentiation of human B lymphocytes. Proc Natl Acad Sci U S A 1989;86(24):10059-63.
403. Torcia M, Bracci-Laudiero L, Lucibello M, Nencioni L, Labardi D, Rubartelli A, et al. Nerve growth factor is an autocrine survival factor for memory B lymphocytes. Cell 1996;85(3):345-56.
404. Kronfeld I, Kazimirsky G, Gelfand EW, Brodie C. NGF rescues human B lymphocytes from anti-IgM induced apoptosis by activation of PKCzeta. Eur J Immunol 2002;32(1):136-43.
405. Ford CA. Differential regulation of Erk-MAPK in the control and proliferation of immature B cells. Glasgow: University of Glasgow; 2004.
406. Benhamou LE, Cazenave PA, Sarthou P. Anti-immunoglobulins induce death by apoptosis in WEHI-231 B lymphoma cells. Eur J Immunol 1990;20(6):1405-7.
407. Scott DW. Analysis of B cell tolerance in vitro. Adv Immunol 1993;54:393-425.
408. Doi T, Motoyama N, Tokunaga A, Watanabe T. Death signals from the B cell antigen receptor target mitochondria, activating necrotic and apoptotic death cascades in a murine B cell line, WEHI-231. Int Immunol 1999;11(6):933-41.

409. Metivier D, Dallaporta B, Zamzami N, Larochette N, Susin SA, Marzo I, et al. Cytofluorometric detection of mitochondrial alterations in early CD95/Fas/APO-1-triggered apoptosis of Jurkat T lymphoma cells. Comparison of seven mitochondrion-specific fluorochromes. Immunol Lett 1998;61(2-3):157-63.
410. Chandra D, Liu JW, Tang DG. Early mitochondrial activation and cytochrome c up-regulation during apoptosis. J Biol Chem 2002;277(52):50842-54.
411. Algeciras-Schimnich A, Barnhart BC, Peter ME. Apoptosis-independent functions of killer caspases. Curr Opin Cell Biol 2002;14(6):721-6.
412. Zamzami N, Kroemer G. Apoptosis: mitochondrial membrane permeabilization--the (w)hole story? Curr Biol 2003;13(2):R71-3.
413. Susin SA, Zamzami N, Kroemer G. Mitochondria as regulators of apoptosis: doubt no more. Biochim Biophys Acta 1998;1366(1-2):151-65.
414. Penninger JM, Kroemer G. Mitochondria, AIF and caspases--rivaling for cell death execution. Nat Cell Biol 2003;5(2):97-9.
415. Guo Y, Srinivasula SM, Druilhe A, Fernandes-Alnemri T, Alnemri ES. Caspase-2 induces apoptosis by releasing proapoptotic proteins from mitochondria. J Biol Chem 2002;277(16):13430-7.
416. Kuss AW, Knodel M, Berberich-Siebelt F, Lindemann D, Schimpl A, Berberich I. A1 expression is stimulated by CD40 in B cells and rescues WEHI 231 cells from anti-IgM-induced cell death. Eur J Immunol 1999;29(10):3077-88.
417. Altmeyer A, Simmons RC, Krajewski S, Reed JC, Bornkamm GW, Chen-Kiang S. Reversal of EBV immortalization precedes apoptosis in IL-6-induced human B cell terminal differentiation. Immunity 1997;7(5):667-77.
418. Ghia P, Boussiotis VA, Schultze JL, Cardoso AA, Dorfman DM, Gribben JG, et al. Unbalanced expression of bcl-2 family proteins in follicular lymphoma: contribution of CD40 signaling in promoting survival. Blood 1998;91(1):244-51.
419. Zhang X, Li L, Choe J, Krajewski S, Reed JC, Thompson C, et al. Up-regulation of Bcl-xL expression protects CD40-activated human B cells from Fas-mediated apoptosis. Cell Immunol 1996;173(1):149-54.
420. Herold MJ, Kuss AW, Kraus C, Berberich I. Mitochondria-dependent caspase-9 activation is necessary for antigen receptor-mediated effector caspase activation and apoptosis in WEHI 231 lymphoma cells. J Immunol 2002;168(8):3902-9.

421. Petros AM, Medek A, Nettesheim DG, Kim DH, Yoon HS, Swift K, et al. Solution structure of the antiapoptotic protein bcl-2. Proc Natl Acad Sci U S A 2001;98(6):3012-7.

422. Mikhailov V, Mikhailova M, Degenhardt K, Venkatachalam MA, White E, Saikumar P. Association of Bax and Bak homo-oligomers in mitochondria. Bax requirement for Bak reorganization and cytochrome c release. J Biol Chem 2003;278(7):5367-76.

423. Pawlowski J, Kraft AS. Bax-induced apoptotic cell death. Proc Natl Acad Sci U S A 2000;97(2):529-31.

424. Kharbanda S, Pandey P, Schofield L, Israels S, Roncinske R, Yoshida K, et al. Role for Bcl-xL as an inhibitor of cytosolic cytochrome C accumulation in DNA damage-induced apoptosis. Proc Natl Acad Sci U S A 1997;94(13):6939-42.

425. Katz E, Lord C, Ford CA, Gauld SB, Carter NA, Harnett MM. Bcl-(xL) antagonism of BCR-coupled mitochondrial phospholipase A(2) signaling correlates with protection from apoptosis in WEHI-231 B cells. Blood 2004;103(1):168-76.

426. Distelhorst CW, Shore GC. Bcl-2 and calcium: controversy beneath the surface. Oncogene 2004;23(16):2875-80.

427. Jo DG, Jun JI, Chang JW, Hong YM, Song S, Cho DH, et al. Calcium binding of ARC mediates regulation of caspase 8 and cell death. Mol Cell Biol 2004;24(22):9763-70.

428. Penzo D, Petronilli V, Angelin A, Cusan C, Colonna R, Scorrano L, et al. Arachidonic acid released by phospholipase A(2) activation triggers Ca(2+)-dependent apoptosis through the mitochondrial pathway. J Biol Chem 2004;279(24):25219-25.

429. Franke TF, Cantley LC. Apoptosis. A Bad kinase makes good. Nature 1997;390(6656):116-7.

430. Tanaka Y, Gavrielides MV, Mitsuuchi Y, Fujii T, Kazanietz MG. Protein kinase C promotes apoptosis in LNCaP prostate cancer cells through activation of p38 MAPK and inhibition of the Akt survival pathway. J Biol Chem 2003;278(36):33753-62.

431. Eeva J, Postila V, Matto M, Nuutinen U, Ropponen A, Eray M, et al. Kinetics and signaling requirements of CD40-mediated protection from B cell receptor-induced apoptosis. Eur J Immunol 2003;33(10):2783-91.

432. Janumyan YM, Sansam CG, Chattopadhyay A, Cheng N, Soucie EL, Penn LZ, et al. Bcl-xL/Bcl-2 coordinately regulates apoptosis, cell cycle arrest and cell cycle entry. Embo J 2003;22(20):5459-70.
433. Vander Heiden MG, Chandel NS, Williamson EK, Schumacker PT, Thompson CB. Bcl-xL regulates the membrane potential and volume homeostasis of mitochondria. Cell 1997;91(5):627-37.
434. Gunter TE, Pfeiffer DR. Mechanisms by which mitochondria transport calcium. Am J Physiol 1990;258(5 Pt 1):C755-86.
435. Kinnally KW, Antonenko YN, Zorov DB. Modulation of inner mitochondrial membrane channel activity. J Bioenerg Biomembr 1992;24(1):99-110.
436. Kristal BS, Park BK, Yu BP. 4-Hydroxyhexenal is a potent inducer of the mitochondrial permeability transition. J Biol Chem 1996;271(11):6033-8.
437. Nutt LK, Chandra J, Pataer A, Fang B, Roth JA, Swisher SG, et al. Bax-mediated Ca2+ mobilization promotes cytochrome c release during apoptosis. J Biol Chem 2002;277(23):20301-8.
438. Li C, Fox CJ, Master SR, Bindokas VP, Chodosh LA, Thompson CB. Bcl-X(L) affects Ca(2+) homeostasis by altering expression of inositol 1,4,5-trisphosphate receptors. Proc Natl Acad Sci U S A 2002;99(15):9830-5.
439. He H, Lam M, McCormick TS, Distelhorst CW. Maintenance of calcium homeostasis in the endoplasmic reticulum by Bcl-2. J Cell Biol 1997;138(6):1219-28.
440. Foyouzi-Youssefi R, Arnaudeau S, Borner C, Kelley WL, Tschopp J, Lew DP, et al. Bcl-2 decreases the free Ca2+ concentration within the endoplasmic reticulum. Proc Natl Acad Sci U S A 2000;97(11):5723-8.
441. Nutt LK, Pataer A, Pahler J, Fang B, Roth J, McConkey DJ, et al. Bax and Bak promote apoptosis by modulating endoplasmic reticular and mitochondrial Ca2+ stores. J Biol Chem 2002;277(11):9219-25.
442. Demaurex N, Distelhorst C. Cell biology. Apoptosis--the calcium connection. Science 2003;300(5616):65-7.
443. Pinton P, Ferrari D, Magalhaes P, Schulze-Osthoff K, Di Virgilio F, Pozzan T, et al. Reduced loading of intracellular Ca(2+) stores and downregulation of capacitative Ca(2+) influx in Bcl-2-overexpressing cells. J Cell Biol 2000;148(5):857-62.

444. Wang NS, Unkila MT, Reineks EZ, Distelhorst CW. Transient expression of wild-type or mitochondrially targeted Bcl-2 induces apoptosis, whereas transient expression of endoplasmic reticulum-targeted Bcl-2 is protective against Bax-induced cell death. J Biol Chem 2001;276(47):44117-28.
445. Thomenius MJ, Wang NS, Reineks EZ, Wang Z, Distelhorst CW. Bcl-2 on the endoplasmic reticulum regulates Bax activity by binding to BH3-only proteins. J Biol Chem 2003;278(8):6243-50.
446. Chao DT, Korsmeyer SJ. BCL-2 family: regulators of cell death. Annu Rev Immunol 1998;16:395-419.
447. Bedner E, Li X, Kunicki J, Darzynkiewicz Z. Translocation of Bax to mitochondria during apoptosis measured by laser scanning cytometry. Cytometry 2000;41(2):83-8.
448. Tashiro S, Sumi T, Uozumi N, Shimizu T, Nakamura T. B-Myb-dependent regulation of c-Myc expression by cytosolic phospholipase A2. J Biol Chem 2004;279(17):17715-22.
449. Sheridan AM, Sapirstein A, Lemieux N, Martin BD, Kim DK, Bonventre JV. Nuclear translocation of cytosolic phospholipase A2 is induced by ATP depletion. J Biol Chem 2001;276(32):29899-905.
450. Sheridan AM, Force T, Yoon HJ, O'Leary E, Choukroun G, Taheri MR, et al. PLIP, a novel splice variant of Tip60, interacts with group IV cytosolic phospholipase A(2), induces apoptosis, and potentiates prostaglandin production. Mol Cell Biol 2001;21(14):4470-81.
451. Ferrari G, Scagliotti GV. Serum and urinary vascular endothelial growth factor levels in non-small cell lung cancer patients. Eur J Cancer 1996;32A(13):2368-9.
452. Gomez J, Martinez C, Giry M, Garcia A, Rebollo A. Rho prevents apoptosis through Bcl-2 expression: implications for interleukin-2 receptor signal transduction. Eur J Immunol 1997;27(11):2793-9.
453. Gomez J, Martinez C, Fernandez B, Garcia A, Rebollo A. Ras activation leads to cell proliferation or apoptotic cell death upon interleukin-2 stimulation or lymphokine deprivation, respectively. Eur J Immunol 1997;27(7):1610-8.
454. Sutherland CL, Heath AW, Pelech SL, Young PR, Gold MR. Differential activation of the ERK, JNK, and p38 mitogen-activated protein kinases by CD40 and the B cell antigen receptor. J Immunol 1996;157(8):3381-90.

455. Craxton A, Shu G, Graves JD, Saklatvala J, Krebs EG, Clark EA. p38 MAPK is required for CD40-induced gene expression and proliferation in B lymphocytes. J Immunol 1998;161(7):3225-36.
456. Kawakami Y, Kitaura J, Yao L, McHenry RW, Newton AC, Kang S, et al. A Ras activation pathway dependent on Syk phosphorylation of protein kinase C. Proc Natl Acad Sci U S A 2003;100(16):9470-5.
457. Melendez AJ, Harnett MM, Allen JM. Crosstalk between ARF6 and protein kinase Calpha in Fc(gamma)RI-mediated activation of phospholipase D1. Curr Biol 2001;11(11):869-74.
458. Blair D. Signalling mechanisms regulating proliferation and apoptosis in immature and mature B cells. Glasgow: University of Glasgow; 2004.
459. Schechtman D, Mochly-Rosen D. Adaptor proteins in protein kinase C-mediated signal transduction. Oncogene 2001;20(44):6339-47.
460. Aman MJ, Tosello-Trampont AC, Ravichandran K. Fc gamma RIIB1/SHIP-mediated inhibitory signaling in B cells involves lipid rafts. J Biol Chem 2001;276(49):46371-8.
461. Billadeau DD, Leibson PJ. ITAMs versus ITIMs: striking a balance during cell regulation. J Clin Invest 2002;109(2):161-8.
462. Chan VW, Meng F, Soriano P, DeFranco AL, Lowell CA. Characterization of the B lymphocyte populations in Lyn-deficient mice and the role of Lyn in signal initiation and down-regulation. Immunity 1997;7(1):69-81.
463. Fong DC, Malbec O, Arock M, Cambier JC, Fridman WH, Daeron M. Selective in vivo recruitment of the phosphatidylinositol phosphatase SHIP by phosphorylated Fc gammaRIIB during negative regulation of IgE-dependent mouse mast cell activation. Immunol Lett 1996;54(2-3):83-91.
464. D'Ambrosio D, Fong DC, Cambier JC. The SHIP phosphatase becomes associated with Fc gammaRIIB1 and is tyrosine phosphorylated during 'negative' signaling. Immunol Lett 1996;54(2-3):77-82.
465. Koncz G, Pecht I, Gergely J, Sarmay G. Fcgamma receptor-mediated inhibition of human B cell activation: the role of SHP-2 phosphatase. Eur J Immunol 1999;29(6):1980-9.
466. Jacob A, Cooney D, Tridandapani S, Kelley T, Coggeshall KM. FcgammaRIIb modulation of surface immunoglobulin-induced Akt activation in murine B cells. J Biol Chem 1999;274(19):13704-10.

467. Pritchard NR, Smith KG. B cell inhibitory receptors and autoimmunity. Immunology 2003;108(3):263-73.
468. Stokoe D, Stephens LR, Copeland T, Gaffney PR, Reese CB, Painter GF, et al. Dual role of phosphatidylinositol-3,4,5-trisphosphate in the activation of protein kinase B. Science 1997;277(5325):567-70.
469. Okada H, Bolland S, Hashimoto A, Kurosaki M, Kabuyama Y, Iino M, et al. Role of the inositol phosphatase SHIP in B cell receptor-induced Ca2+ oscillatory response. J Immunol 1998;161(10):5129-32.
470. Dolmetsch RE, Lewis RS, Goodnow CC, Healy JI. Differential activation of transcription factors induced by Ca2+ response amplitude and duration. Nature 1997;386(6627):855-8.
471. Tridandapani S, Chacko GW, Van Brocklyn JR, Coggeshall KM. Negative signaling in B cells causes reduced Ras activity by reducing Shc-Grb2 interactions. J Immunol 1997;158(3):1125-32.
472. Henning SW, Cantrell DA. p56lck signals for regulating thymocyte development can be distinguished by their dependency on Rho function. J Exp Med 1998;188(5):931-9.
473. Yoshino T, Kishi H, Nagata T, Tsukada K, Saito S, Muraguchi A. Differential involvement of p38 MAP kinase pathway and Bax translocation in the mitochondria-mediated cell death in TCR- and dexamethasone-stimulated thymocytes. Eur J Immunol 2001;31(9):2702-8.
474. Lei K, Davis RJ. JNK phosphorylation of Bim-related members of the Bcl2 family induces Bax-dependent apoptosis. Proc Natl Acad Sci U S A 2003;100(5):2432-7.
475. Yamamoto K, Ichijo H, Korsmeyer SJ. BCL-2 is phosphorylated and inactivated by an ASK1/Jun N-terminal protein kinase pathway normally activated at G(2)/M. Mol Cell Biol 1999;19(12):8469-78.
476. Chauhan D, Li G, Hideshima T, Podar K, Mitsiades C, Mitsiades N, et al. JNK-dependent release of mitochondrial protein, Smac, during apoptosis in multiple myeloma (MM) cells. J Biol Chem 2003;278(20):17593-6.
477. Olson NE, Graves JD, Shu GL, Ryan EJ, Clark EA. Caspase activity is required for stimulated B lymphocytes to enter the cell cycle. J Immunol 2003;170(12):6065-72.

478. Woo M, Hakem R, Furlonger C, Hakem A, Duncan GS, Sasaki T, et al. Caspase-3 regulates cell cycle in B cells: a consequence of substrate specificity. Nat Immunol 2003;4(10):1016-22.
479. Degli Esposti M, Ferry G, Masdehors P, Boutin JA, Hickman JA, Dive C. Post-translational modification of Bid has differential effects on its susceptibility to cleavage by caspase 8 or caspase 3. J Biol Chem 2003;278(18):15749-57.
480. Cohen PL, Eisenberg RA. Lpr and gld: single gene models of systemic autoimmunity and lymphoproliferative disease. Annu Rev Immunol 1991;9:243-69.
481. Fisher CL, Eisenberg RA, Cohen PL. Quantitation and IgG subclass distribution of antichromatin autoantibodies in SLE mice. Clin Immunol Immunopathol 1988;46(2):205-13.
482. Trune DR, Craven JP, Morton JI, Mitchell C. Autoimmune disease and cochlear pathology in the C3H/lpr strain mouse. Hear Res 1989;38(1-2):57-66.
483. Piatelli MJ, Wardle C, Blois J, Doughty C, Schram BR, Rothstein TL, et al. Phosphatidylinositol 3-kinase-dependent mitogen-activated protein/extracellular signal-regulated kinase kinase 1/2 and NF-kappa B signaling pathways are required for B cell antigen receptor-mediated cyclin D2 induction in mature B cells. J Immunol 2004;172(5):2753-62.
484. Gold MR, Scheid MP, Santos L, Dang-Lawson M, Roth RA, Matsuuchi L, et al. The B cell antigen receptor activates the Akt (protein kinase B)/glycogen synthase kinase-3 signaling pathway via phosphatidylinositol 3-kinase. J Immunol 1999;163(4):1894-905.
485. Piatelli MJ, Doughty C, Chiles TC. Requirement for a hsp90 chaperone-dependent MEK1/2-ERK pathway for B cell antigen receptor-induced cyclin D2 expression in mature B lymphocytes. J Biol Chem 2002;277(14):12144-50.
486. Fruman DA, Snapper SB, Yballe CM, Alt FW, Cantley LC. Phosphoinositide 3-kinase knockout mice: role of p85alpha in B cell development and proliferation. Biochem Soc Trans 1999;27(4):624-9.
487. Fluckiger AC, Li Z, Kato RM, Wahl MI, Ochs HD, Longnecker R, et al. Btk/Tec kinases regulate sustained increases in intracellular Ca2+ following B-cell receptor activation. Embo J 1998;17(7):1973-85.
488. Takata Y, Imamura T, Yang GH, Takada Y, Sawa T, Morioka H, et al. Pioglitazone attenuates the inhibitory effect of phorbol ester on epidermal

growth factor receptor autophosphorylation and tyrosine kinase activity. Biochim Biophys Acta 1996;1312(1):68-72.
489. Zhuang ZY, Xu H, Clapham DE, Ji RR. Phosphatidylinositol 3-kinase activates ERK in primary sensory neurons and mediates inflammatory heat hyperalgesia through TRPV1 sensitization. J Neurosci 2004;24(38):8300-9.
490. Qiao M, Shapiro P, Kumar R, Passaniti A. Insulin-like growth factor-1 regulates endogenous RUNX2 activity in endothelial cells through a phosphatidylinositol 3-kinase/ERK-dependent and Akt-independent signaling pathway. J Biol Chem 2004;279(41):42709-18.
491. Duca L, Debelle L, Debret R, Antonicelli F, Hornebeck W, Haye B. The elastin peptides-mediated induction of pro-collagenase-1 production by human fibroblasts involves activation of MEK/ERK pathway via PKA- and PI(3)K-dependent signaling. FEBS Lett 2002;524(1-3):193-8.
492. Cauwels A, Janssen B, Waeytens A, Cuvelier C, Brouckaert P. Caspase inhibition causes hyperacute tumor necrosis factor-induced shock via oxidative stress and phospholipase A2. Nat Immunol 2003;4(4):387-93.
493. Vercammen D, Beyaert R, Denecker G, Goossens V, Van Loo G, Declercq W, et al. Inhibition of caspases increases the sensitivity of L929 cells to necrosis mediated by tumor necrosis factor. J Exp Med 1998;187(9):1477-85.
494. Fiers W, Beyaert R, Declercq W, Vandenabeele P. More than one way to die: apoptosis, necrosis and reactive oxygen damage. Oncogene 1999;18(54):7719-30.
495. Agarwal ML, Taylor WR, Chernov MV, Chernova OB, Stark GR. The p53 network. J Biol Chem 1998;273(1):1-4.
496. Villunger A, Michalak EM, Coultas L, Mullauer F, Bock G, Ausserlechner MJ, et al. p53- and drug-induced apoptotic responses mediated by BH3-only proteins puma and noxa. Science 2003;302(5647):1036-8.
497. Gerondakis S, Grossmann M, Nakamura Y, Pohl T, Grumont R. Genetic approaches in mice to understand Rel/NF-kappaB and IkappaB function: transgenics and knockouts. Oncogene 1999;18(49):6888-95.
498. Meffert MK, Chang JM, Wiltgen BJ, Fanselow MS, Baltimore D. NF-kappa B functions in synaptic signaling and behavior. Nat Neurosci 2003;6(10):1072-8.
499. Kontgen F, Grumont RJ, Strasser A, Metcalf D, Li R, Tarlinton D, et al. Mice lacking the c-rel proto-oncogene exhibit defects in lymphocyte

proliferation, humoral immunity, and interleukin-2 expression. Genes Dev 1995;9(16):1965-77.

500. Franzoso G, Carlson L, Poljak L, Shores EW, Epstein S, Leonardi A, et al. Mice deficient in nuclear factor (NF)-kappa B/p52 present with defects in humoral responses, germinal center reactions, and splenic microarchitecture. J Exp Med 1998;187(2):147-59.

501. Sha WC, Liou HC, Tuomanen EI, Baltimore D. Targeted disruption of the p50 subunit of NF-kappa B leads to multifocal defects in immune responses. Cell 1995;80(2):321-30.

502. Weih F, Carrasco D, Durham SK, Barton DS, Rizzo CA, Ryseck RP, et al. Multiorgan inflammation and hematopoietic abnormalities in mice with a targeted disruption of RelB, a member of the NF-kappa B/Rel family. Cell 1995;80(2):331-40.

503. Carman JA, Wechsler-Reya RJ, Monroe JG. Immature stage B cells enter but do not progress beyond the early G1 phase of the cell cycle in response to antigen receptor signaling. J Immunol 1996;156(12):4562-9.

Publications:

Katz. E., Lord. C., Ford. C. A., Gauld. S. B., Carter. N. A. and Harnett. M.M.
Bcl-(xL) antagonism of BCR-coupled mitochondrial phospholipase A(2) signaling correlates with protection from apoptosis in WEHI-231 B cells.
Blood (2003) **103** (1) 168

N.A. Carter. and M.M. Harnett
Dissection of signalling mechanisms underlying FcγRIIb mediated apoptosis of mature B cells.
Biochemical Society Transactions (2004) 32 (6) 973